Development of a Spiroalkylation Method for the Stereoselective Construction of α-Quaternary Carbons, its Application to the Total Synthesis of (*R*)-Puraquinonic Acid, and Efforts Towards HDAC/HIV-1 Protease Hybrid Inhibitors

Adam A. H. Elmehriki

Department of Chemistry, McGill University

Montréal Québec, Canada

August 2020

A thesis submitted to McGill University in partial fulfilment of the requirements

of the degree of Doctor of Philosophy

Abstract

α-Quaternary carbon stereocentres are a common yet challenging motif encountered in the synthesis of many organic molecules, ranging from natural products to molecules employed in medicinal chemistry endeavours. Herein, cyclic α-quaternary carbon stereocentres were prepared from biselectrophilic substrates and an easily prepared chiral bicyclic sulfonyl lactam. This was achieved in two steps by spiroalkylation, employing biphasic reaction conditions with a phase-transfer catalyst, followed by reduction and alkylation with a series of alkyl halide electrophiles. The products of this method were isolated in good yields with high levels of diastereoselectivity. Additionally, the methodology was employed in the enantioselective total synthesis of (*R*)-puraquinonic acid for a late-stage installation of the α-quaternary carbon stereocentre. This enabled the shortest total synthesis of (*R*)-puraquinonic acid to date, an eight-pot sequence providing an overall yield of 14%.

Inspired by reports indicating that inhibition of histone deacetylase (HDAC) promotes reactivation of latent HIV reservoirs, a set of molecules were conceived and prepared which possessed both HDAC and HIV protease inhibitory activity. It was expected that such hybrid inhibitors could provide a means to clear HIV reservoirs by directly inhibiting viral protease function upon reactivation of latent HIV. The design of hybrid inhibitors was based on the known HDAC inhibitor vorinostat and the HIV-1 protease inhibitor darunavir. Initial biological testing proved that molecules of this design maintain their HDAC inhibitory function despite structural modifications made to incorporate HIV-1 protease inhibitory activity. Unfortunately, while the inhibitory activity against cytosolic HDAC6 of one hybrid inhibitor was comparable to the positive control (vorinostat) it was found to be over six-fold less potent against the desired nuclear target, HDAC3.

Résumé

Les stéréocentres de carbone α-quaternaire sont un motif commun mais difficile rencontré dans la synthèse de nombreuses molécules organiques, allant des produits naturels aux molécules utilisées dans les efforts de chimie médicinale. Ici, des stéréocentres de carbone a-quaternaire cycliques ont été synthétisés à partir de substrats bisélectrophiles et d'un sulfonyl lactame bicyclique chiral facilement préparé. Ceci a été réalisé en deux étapes par spiroalkylation, en utilisant des conditions de réaction biphasique avec un catalyseur de transfert de phase, suivi par une réduction et une alkylation avec une série d'électrophiles d'halogénure d'alkyle. Les produits de cette méthode ont été isolés en de bons rendements avec des niveaux élevés de diastéréosélectivité. En outre, la méthodologie a été utilisée dans la synthèse totale énantiosélective de l'acide (*R*) -puraquinonique pour une installation de stade avancé du stéréocentre de carbone α-quaternaire. Cela a permis la synthèse totale la plus courte de l'acide (*R*) -puraquinonique à ce jour; une séquence à huit pots fournissant un rendement global de 14%.

Inspiré par des rapports indiquant que l'inhibition de l'histone désacétylase (HDAC) favorise la réactivation des réservoirs latents du VIH, un ensemble de molécules ayant une activité inhibitrice de HDAC et de protéase du VIH a été préparé. On s'attendait à ce que ces inhibiteurs hybrides puissent fournir un moyen d'éliminer les réservoirs du VIH en inhibant directement la fonction de protéase virale lors de la réactivation du VIH latent. La conception des inhibiteurs hybrides était basée sur l'inhibiteur connu de l'HDAC, le vorinostat et l'inhibiteur de la protéase du VIH-1, le darunavir. Les tests biologiques initiaux ont prouvé que les molécules de cette conception conservent leur fonction inhibitrice d'HDAC, et ce malgré les modifications structurelles apportées pour incorporer l'activité inhibitrice de la protéase du VIH-1. Malheureusement, alors que l'activité inhibitrice contre l'HDAC6 cytosolique d'un inhibiteur

hybride était comparable à celle du contrôle positif (vorinostat), elle s'est avérée être plus de six fois moins puissante contre la cible nucléaire souhaitée, HDAC3.

Acknowledgements

I must start by thanking my supervisor, Prof. James L. Gleason, to whom I owe a debt of gratitude for providing an excellent environment in which to grow as a chemist. I truly enjoyed my time as a member of his group and leave having made many fond memories. Thank you, Jim, for your support and guidance.

Secondly, I would like to express my thanks to the other members of the chemistry faculty with whom I have had the great privilege of interacting with during my time at McGill. Thank you to Professors Lumb, Arndtsen, Tsantrizos, Li, Moitessier, Auclair, and Harpp for sharing your knowledge and experience. I also need to take the opportunity to extend my appreciation to my undergraduate supervisors, Prof. Robert Hudson and Dr Mojmír Suchý, for kindling my interest in organic chemistry.

Thank you to Drs Nadim Saade and Alex Wahba for your ever-dependable assistance with acquiring HRMS data. Dr Robin Stein, thank you for always being a great help with anything NMR related and especially for digging up old, near-forgotten data. A special thanks to Chantal Marotte, for always keeping my forms in order and sending friendly reminders whenever I forgot to register for a semester. Thank you to the department's office staff, Lina, Chelsea, Linda, Jennifer, and Sandra, for always being there to help with a last-minute room booking, extra chalk, and expense reports.

I cannot forget to acknowledge the amazing colleagues I have had the privilege of working alongside in the Gleason group. Thank you to: Rodrigo, for introducing me to chemistry reference resolver; Ben, for leaving me your office desk; Daniel, for showing me where to get the best coffee near campus; Shuo, for always helping me find the exact piece of glassware I needed; Chris, for demonstrating how to regulate the fire on the lab's barbeque; Marx, for sharing all his the

deliciously spicy Mexican candy; Dainis, for the helpful suggestions over the years; Anthony, for understanding my Sci-Fi/obscure pop-culture references and helping with the HDAC assays; Nick, for sharing my enjoyment of language jokes and being great company during late nights in the lab; Jon, for getting me involved in the MCSILS and CGSS and going for two-chow at ungodly late hours; Florent, for sharing your experience; Yiram, for never failing to make the lab a happier and brighter place to be; Sam, for regularly having an amusing story about some chemical I had never heard of; Ryan, for always being around to help; Josie, for generously sharing your cooking with me and helping to keep work in perspective; Ali, for being the only one who knew what I was talking about when describing Egyptian food; Donald, for introducing me to Jay Peak and letting me tag along on your ski trips; Yufei, for keeping me on my toes with all your chemistry question; David, for always being around to chat; and June, for kindly laughing at all my embarrassingly bad jokes. I could not have asked for better lab mates and I wish you all the very best.

I must also mention the many wonderful friends I have made in the department. Liz, Kenn, Naresh, Anna, Haiyan, Allie, Zoe, Vanja, Tim, Shoronia, Fabien, Dustin, Julie, Igor, Dan, Ricky – you all helped make my time at McGill a most memorable adventure. And, thank you to my dear friends unrelated to chemistry. Angus, for reliably indulging my need to barbeque large amounts of meat and vegetables; Lindsey, for sharing my excitement for Bladerunner; Andrew, for always inviting me for Christmas with your family; Chis, for reminding me to enjoy life away from chemistry now and then; and Gianni, for your generosity, and for helping provide the translation of the abstract for this thesis.

Finally, thank you to my family – Mum, Dad, and Nadine; thank you for all your love and support. I love you all very much.

Contributions to Original Knowledge

CHAPTER 2

1. The reactivity of chiral bicyclic sulfonyl lactams and biselectrophilic substrates was investigated to discover a simple biphasic reaction to construct spirocyclic structures system using tetrabutylammonium iodide as phase-transfer catalyst. High levels of stereoselectivity were achieved in cases where the electrophilic sites of the biselectrophilic substrate were electronically or sterically differentiated.
2. α-Quaternary carbon stereocentres were prepared from the chiral spirocycles by reduction followed by alkylation with a series of alkyl halide electrophiles. This method provided novel cyclic products containing challenging quaternary stereocentres in good yields and with high levels of diastereoselectivity.

CHAPTER 3

1. The synthetic utility of the spiroalkylation/reduction/alkylation sequence for the construction of α-quaternary carbon stereocentres was demonstrated through its use as the key step in the total synthesis of (*R*)-puraquinonic acid.
2. Endeavours towards the total synthesis of (*R*)-puraquinonic acid lead to the shortest route to this natural product to date. The synthesis involved an eight-pot sequence providing an overall yield of 14%.
3. The absolute configuration of the synthesised α-quaternary carbon stereocentres was independently achieved using two methods: (i) comparison to an intercepted intermediate on route to (*R*)-puraquinonic acid and (ii) the preparation of the enantiomers of two previously reported compounds.

CHAPTER 4

1. The synthetic efforts described herein resulted in the development of a strategy for the late-stage modification at the para position of the phenyl moiety found in the darunavir skeleton. Modifications were successfully carried out to introduce HDAC inhibitor activity to the structure through Suzuki-Miyaura cross-coupling. Additionally, this work provides a general method for further and underexplored diversification at this site.
2. Results from biological testing have revealed that HDAC/HIV-PR hybrid inhibitors based on the structures of darunavir and vorinostat are able to inhibit HDAC3 and HDAC6 activity *in vitro*.

Contributions by the Author

Other than the exceptions listed below, all original work described in this thesis (chapters two, three, and four) is the sole work of Adam A. H. Elmehriki. Prof. James L. Gleason carried out the DFT calculations for chapter two; Anthony F. Palermo is acknowledged for his collaboration on developing the HDAC inhibitor assay protocol; and Yufei Wang and Donald A. Campbell are acknowledged for acquiring melting point and optical rotation data for some molecules reported herein.

Table of Contents

Abstract i
Résumé ii
Acknowledgements iv
Contributions to Original Knowledge vi
Contributions by the Author viii
Table of Contents ix
List of Schemes xiii
List of Figures xvii
List of Tables xix
List of Abbreviations xx
Nomenclature xxvi
CHAPTER 1 Introduction to Quaternary Carbon Stereocentres, their Construction, and Applications Thereof in the Total Synthesis of Puraquinonic Acid 1
1.1 Introduction to Quaternary Carbon Stereocentre Formation 2
1.1.1 Importance of Quaternary Carbons 2
1.1.2 Construction of Quaternary Carbon Stereocentres 6
1.1.3 α-Quaternary Carbon Stereocentres 7
1.1.3.1 Use of Enolates in Carbon-Carbon Bond Forming Reactions 8
1.1.3.2 Controlling Enolate Geometry 11
1.1.3.3 Controlling Enolate Facial Selectivity 14
1.1.3.4 The Practicality of the Chiral Bicyclic Thioglycolate Lactam Auxiliary 22
1.2 Catalytic Construction of α-Quaternary Carbon Stereocentres 26
1.2.1 Transition Metal Catalysis 26
1.2.2 Organocatalytic Formation of α-Quaternary Carbon Stereocentres 30
1.2.2.1 Phase-Transfer Catalysis 32
1.3 Puraquinonic Acid 36
1.3.1 Isolation, Structure, and Biological Activity 36
1.3.2 Related Natural Products and Proposed Biosynthesis 37
1.3.3 Previous Total Syntheses of Puraquinonic Acid 39
1.3.3.1 Approaches to the Racemic Preparation of Puraquinonic Acid 40
1.3.3.2 Asymmetric Syntheses of Puraquinonic Acid 44
1.4 Construction of α-Quaternary Carbon Stereocentres in Advanced Settings 51

1.4.1 Investigation of Biselectrophilic Substrates in the Alkylation of Bicyclic Lactams. 51
1.4.2 A Novel Approach to (*R*)-Puraquinonic Acid 52
1.5 References 53
CHAPTER 2 Use of Biselectrophilic Substrates in the Stereoselective Formation of α-Quaternary Stereocentres 69
2.1 Overview 70
2.1.1 Project Aim 70
2.1.2 Initial Route of Enquiry 73
2.2 The Model System 75
2.2.1 Selection of Model Substrates and Reaction Optimisation 75
2.2.2 Promoting Spirocycle Formation 78
2.2.3 Stereochemical Assessment 83
2.2.4 Investigation into Enolate Formation 85
2.2.5 Investigation into Electrophile Competence 91
2.3 Substrate Scope 97
2.3.1 Substrate Design and Synthesis 97
2.3.2 Investigation of Substrate Scope 103
2.3.3 Formation of α-Quaternary Stereocentres 105
2.4 Conclusions 114
2.5 References 115
CHAPTER 3 An Asymmetric Total Synthesis of (*R*)-Puraquinonic Acid 118
3.1 Overview 119
3.1.1 Project Aim 119
3.1.2 Outline of The Synthetic Approach 119
3.2 Retrosynthetic Analyses 124
3.3 Synthesis of Dibromide 378 125
3.3.1 Preparation of Diene **378** *via* Cross-Coupling 125
3.3.2 Acylation of 2,3-dihydrofuran 128
3.3.3 Diene Synthesis by Enyne Metathesis 131
3.3.4 Preparation of Dibromide **375** 135
3.4 Formation of the α-Quaternary Carbon Stereocentre 136
3.5 Oxidation to the Paraquinone: Total Synthesis of Puraquinonic Acid 138
3.6 Determination of Absolute Stereochemistry 143
3.7 Comparison to Proline Derivatives 148

3.8 Future Directions 151
3.8 Conclusions 154
3.9 References 157
CHAPTER 4 Design of HDAC/HIV-1 Protease Inhibitor Hybrid Molecules for the Development of Novel HIV Treatments 160
4.1 Current HIV Treatment 161
4.1.1 HIV/AIDS 161
4.1.2 Viral Lifecycle 162
4.1.3 State of the Art Treatment 164
4.1.4 HIV Latency 167
4.1.5 Histones, Histone Deacetylases, and Their Role in HIV-Latency 168
4.1.5.1 Histones 168
4.1.5.2 Histone Deacetylases (HDACs) 170
4.1.5.3 Use of HDAC Inhibitors for Latent HIV Reactivation 172
4.2 Combination Therapy and Hybrid Drugs 173
4.2.1 Combination Therapy 173
4.2.2 Advantages of Hybrid Drug Design 174
4.2.3 Examples of Hybrid Drugs 175
4.3 Design of Novel Hybrid HDAC/HIV-1 Protease Inhibitors 179
4.3.1 Rational for a Hybrid Drug Approach 179
4.3.2 General HDAC Inhibitor Design 180
4.3.3 HIV-1 Protease and Inhibitors Thereof 182
4.3.4 Proposed HDAC/HIV-PR Design 186
4.4 Synthesis of HDAC/HIV-1 Protease Inhibitors Hybrid 190
4.4.1 Retrosynthetic Analysis 190
4.4.2 Chemical Synthesis 192
4.5 Biological Evaluation of Hybrid Molecules 199
4.5.1 HDAC Inhibition Assay 199
4.5.1 Results 201
4.6 Discussion and Future Direction 203
4.7 References 205
Final Conclusions and Future Perspectives 215
CHAPTER 5 Experimental Procedures 218
5. 1 General Experimental 219
5.2 Procedures for Chapter 2 221

5.2.1 General Method for Spiroalkylation 239
5.2.2 General Procedure for Reductive Alkylation 247
5.2.3 DFT Calculations 261
5.3 Procedures for Chapter 3 270
5.4 Procedures for Chapter 4 288
5.4.1 Synthesis of Hybrid Inhibitors 288
5.4.2 Preparation of HDAC Inhibitor Assay Substrate 304
5.4.3 HDAC Inhibitor Assay 309
5.5 References 312
Appendix 315

List of Schemes

Scheme 1.1 Zimmerman-Traxler transition state model for the aldol reaction 10
Scheme 1.2 Ireland model for the enolization selectivity 12
Scheme 1.3 Effects of amide substitution on enolization selectivity 13
Scheme 1.4 Enolization selectivity for α,α-disubstituted esters 13
Scheme 1.5 Chiral amides in selective enolization of chiral α,α-disubstituted esters 14
Scheme 1.6 Evans' oxazolidinone auxiliary directed alkylation 15
Scheme 1.7 Use of diminutive α-substituents to control enolate geometry 17
Scheme 1.8 Meyers' endo-selective bicyclic lactam auxiliary 18
Scheme 1.9 Cyclic enolates *via* chelation 18
Scheme 1.10 Chiral auxiliary directed deprotonation and Michael addition 20
Scheme 1.11 Asymmetric lithium enediolate alkylation 21
Scheme 1.12 Quaternary carbon containing aldol products *via* allyl zinc additions 22
Scheme 1.13 Alkylation of second-generation auxiliary 23
Scheme 1.14 Removal of auxiliary by hydrolysis and reduction 25
Scheme 1.15 Palladium catalysed asymmetric allylic alkylation 28
Scheme 1.16 α-Quaternary carbon stereocentre formation *via* palladium catalysed C-H activation/desymmetrisation 29
Scheme 1.17 Iridium catalysed C-H fictionalisation of methanol 30
Scheme 1.18 Organocatalytic preparation of the Hajos-Parrish and Wieland-Miescher ketones and Barbas' organocatalytic asymmetric aldol reaction 31
Scheme 1.19 Formation of vicinal quaternary and tertiary stereocentres 32
Scheme 1.20 Asymmetric phase-transfer catalysis in the synthesis of (+)-indacrinone 33
Scheme 1.21 Asymmetric dialkylation of malonate esters 34
Scheme 1.22 Asymmetric dialkylation in the synthesis of MK-3207 35
Scheme 1.23 Proposed biosynthesis of the illudalanes 38
Scheme 1.24 Facile conversion from the protoilludalane to illudalane carbon skeleton 39
Scheme 1.25 Clive's first-generation racemic synthesis of puraquinonic acid 41
Scheme 1.26 Clive's second-generation racemic synthesis of puraquinonic acid 42
Scheme 1.27 Kraus' racemic synthesis of puraquinonic acid ethyl ester and deliquinone 43
Scheme 1.28 Baudoin's racemic synthesis of puraquinonic acid methyl ester 44
Scheme 1.29 Clive's synthesis of (*S*)-puraquinonic acid 46

Scheme 1.30 Gleason and Tiong's synthesis of (*R*)-puraquinonic acid 48
Scheme 1.31 Baudoin's synthesis of (*R*)-puraquinonic acid 49
Scheme 2.1 Strategies for α-quaternary carbon stereocentres using lactam **104** 72
Scheme 2.2 Synthesis of model biselectrophile, dibromide **209** 75
Scheme 2.3 Synthesis of lactam **104** 76
Scheme 2.4 Anticipated possible products formed from the alkylation of lactam **104** 77
Scheme 2.5 Isolation of adduct **271** 77
Scheme 2.6 Methods for promoting a second deprotonation 79
Scheme 2.7 Synthesis of sulfone **277** 80
Scheme 2.8 Rationalisation of observed stereochemistry 85
Scheme 2.9 Synthesis of sulfoxides **292a** and **292b** 88
Scheme 2.10 Synthesis and testing of sulfone **297** 90
Scheme 2.11 Synthesis of thioether **269** 91
Scheme 2.12 Investigation of simple, symmetric biselectrophiles 92
Scheme 2.13 Synthesis of diiodide **305** and cyclic sulfonate **307** 92
Scheme 2.14 Possible hydrolysis and subsequent cyclisation of dibromide **209** 93
Scheme 2.15 Identification of facial selectivity for the alkylation of sulfone **310** 96
Scheme 2.16 Synthesis of dibromide **313** 98
Scheme 2.17 Synthesis of dibromide **314** 98
Scheme 2.18 Synthesis of dibromide **315** 99
Scheme 2.19 Attempts to synthesise dibromide **316** and analogues thereof 99
Scheme 2.20 Attempts to synthesise tetrasubstituted olefin containing biselectrophiles 100
Scheme 2.21 Synthesis of dimesylate **329** 101
Scheme 2.22 Synthesis of biaryl dibromide **317** 101
Scheme 2.23 Synthesis of alkyl biselectrophiles 102
Scheme 2.24 Reduction and alkylation of sulfone **251** 105
Scheme 2.25 Reduction and alkylation of cyclic sulfone **347** 106
Scheme 2.26 Allylation with 3,3-dimethylallyl bromide 111
Scheme 3.1 Summary of previous asymmetric approaches to puraquinonic acid and points wherein the quaternary carbon was introduced 122
Scheme 3.2 Comparison to Kraus' racemic preparation of the key α-quaternary stereocentre in puraquinonic acid 123
Scheme 3.3 Retrosynthetic analysis of puraquinonic acid (**164**) 124

Scheme 3.4 Proposed Kumada cross-coupling for the synthesis of diene **378** 125
Scheme 3.5 Su's preparation of iodinated hydrofurans and hydropyrans 125
Scheme 3.6 Attempts to reproduce results disclosed by Su 126
Scheme 3.7 Tanaka's preparation of vinyl stannanes from thioethers 127
Scheme 3.8 Preparation of tributyl dihydrofuryl stannane 127
Scheme 3.9 Hojo's trichloroacylation of 2,3-dihydrofuran 128
Scheme 3.10 Attempts at direct acylation of 2,3-dihydrofuran 129
Scheme 3.11 Preparation of vinylogous ether **397** 129
Scheme 3.12 Trapping of diene **378** with DMAD 130
Scheme 3.13 Retrosynthesis for the formation of diene **378** via an eneyne metathesis 131
Scheme 3.14 Diver's intermolecular eneyne metathesis 132
Scheme 3.15 Hiersemann's alkyne de Mayo reaction 132
Scheme 3.16 Synthesis of vinyl-ether **399** 133
Scheme 3.17 Stepwise and one-pot reparation of diester **376** 134
Scheme 3.18 Enyne metathesis mechanism and off-cycle catalyst sequestration 135
Scheme 3.19 Preparation of dibromide **375** 135
Scheme 3.20 Construction of the key quaternary stereocentre 136
Scheme 3.21 Initial attempts to oxidise the arene core to the *para*-quinone 138
Scheme 3.22 Bromination of arene **417** 139
Scheme 3.23 Possible synthetic route to puraquinonic acid *via* aryl bromide **418** 139
Scheme 3.24 Proposed mechanism for the oxidation of carboxylic acid **417** 140
Scheme 3.25 Oxidation of carboxylic acid **393** to puraquinonic acid 141
Scheme 3.26 Stereochemical determination of alkylation products of lactam **104** 144
Scheme 3.27 Synthesis of *para*-quinones (*R*,*S*)-**433** and (*R*,*R*)-**433** 145
Scheme 3.28 Baudoin's palladium catalysed C-H activation 148
Scheme 3.29 Synthesis of proline derivates of amide **353** 149
Scheme 3.30 Proposed use of alternate alkynes 152
Scheme 3.31 Total synthesis of (*R*)-puraquinonic acid 155
Scheme 4.1 Late stage Suzuki-Miyaura cross-coupling approach 190
Scheme 4.2 Synthesis of enantioenriched epoxide **51** 193
Scheme 4.3 Synthesis of key aryl bromide intermediate **501** 194
Scheme 4.4 Failed Suzuki-Miyaura cross-coupling 194
Scheme 4.5 Successful Suzuki-Miyaura cross-couplings 195

Scheme 4.6 Successful cross coupling of model substate **506** 196
Scheme 4.7 Preparation of hybrid inhibitors **488** and **489** 197
Scheme 4.8 Preparation methyl ester **513** 198
Scheme 4.9 Enzymatic processing of HDAC inhibitor assay substrates 200

List of Figures

Figure 1.1 Quaternary carbons 2

Figure 1.2 Quaternary carbons in the structures of taxol, morphine, strychnine, and cholesterol. 3

Figure 1.3 Isomerisation of thalidomide in human blood 4

Figure 1.4 Structure of lenolidomide, an FDA approved treatment for multiple myeloma 5

Figure 1.5 Thalidomide analogues which do not bear the problematic α-carbon 5

Figure 1.6 Examples of various reactions which produce quaternary carbon stereocentres: a) Diels-Alder cycloaddition, b) Claisen rearrangement, c) asymmetric conjugate addition, and d) desymmetrisation. 7

Figure 1.7 Examples of α-quaternary carbon stereocentres and derivates thereof 8

Figure 1.8 Examples of chiral auxiliaries successfully used in asymmetric allylations 16

Figure 1.9 Enolate geometry resulting from reductive enolisation 24

Figure 1.10 The natural products puraquinonic acid, strobilurin D, and muscarine 36

Figure 1.11 Carbon skeleton and examples of protoilludalanes, illudanes, illudalanes, and norilludalanes 37

Figure 1.12 Natural products structurally related to puraquinonic acid 39

Figure 2.1 Examples of natural products and biologically relevant molecules containing α-quaternary carbon stereocentres 71

Figure 2.2 Structures of a) *ent*-fredericamycin A and b) the most potent member of series of orally bioavailable CGRP receptor antagonists developed by Merck 73

Figure 2.3 Plot of pK_a in DMSO as a function of change in proton affinity and interpolation of the pK_a of sulfone **277** 81

Figure 2.4 Vinyl ether **288** 83

Figure 2.5 Determination of relative stereochemistry by NOESY spectrum analysis 84

Figure 2.6 ^{1}H NMR spectra displaying deuterium incorporation of sulfone **277** 87

Figure 2.7 ^{1}H NMR spectra displaying deuterium incorporation of sulfoxide **292a** 89

Figure 2.8 ^{1}H NMR spectra displaying deuterium incorporation of sulfoxide **292b** 89

Figure 2.9 Proposed electrophiles and predicted relative reactivities 97

Figure 2.10 Final set of test substrates 102

Figure 2.11 DFT optimised structure of spirocycle **350** B3LYP/6-311+G(d,p) 111

Figure 2.12 DFT optimised structures of spirocycle **350** derived enolates 112

Figure 3.1 Natural products containing α-quaternary carbon stereocentres 119

Figure 3.2 Alkylation selectivity for sulfide and sulfone derived α,α-disubstituted enolates ... 121

Figure 3.3 Determination of relative stereochemistry by NOESY spectrum analysis for **374** .. 137

Figure 3.4 Comparison of ^{1}H NMR spectra for *para*-quinones (*R*,*S*)-**433** and (*R*,*R*)-**433**, data for authentic (*R*,*S*)-**433** was only available as a printout and has been manipulated to provide a one-to-one comparison 146

Figure 3.5 Comparison of ^{13}C NMR spectra for *para*-quinones (*R*,*S*)-**433** and (*R*,*R*)-**433** 147

Figure 3.6 Possible natural product and medicinal chemistry targets 153

Figure 4.1 Overall global trends of HIV infection and associated deaths 162

Figure 4.2 The HIV viral lifecycle 164

Figure 4.3 Steps in the HIV lifecycle inhibited by current antiretroviral drugs 165

Figure 4.4 Representative examples of entry inhibitors (maraviroc), nucleoside reverse transcriptase inhibitors (abacavir), non-nucleoside reverse transcriptase inhibitors (efavirenz), integrase strand transfer inhibitors (dolutegravir), and protease inhibitors (atazanavir) 166

Figure 4.5 Dynamic modification of histone lysine residues by HDAC and HAT enzymes 170

Figure 4.6 Mechanism for zinc dependant HDAC cleavage of acetylated lysine residues 171

Figure 4.7 FDA approved kinase inhibitors known to target multiple kinases 175

Figure 4.8 Examples of a) linked and b) joined pharmacophores 177

Figure 4.9 Examples of a) overlapped and b) merged pharmacophores 178

Figure 4.10 HDAC/(N)NRT hybrid inhibitors developed by Doyle and Gleason 179

Figure 4.11 Co-crystal structure of HDAC2 and vorinostat (**469**) illustrating the extension of the linker away from the cap group on the surface of the enzyme allowing the hydroxamic acid to engage the zinc atom at the end of the lipophilic tunnel (PDB: 4LXZ) 181

Figure 4.12 Illustration of the design principles common to most HDAC inhibitors 182

Figure 4.13 X-Ray crystal structure of HIV-1 protease homodimer complexed with gag-pol (blue) (PDB:1KJF) 183

Figure 4.14 HIV-1 protease peptide bond hydrolysis mechanism 184

Figure 4.15 FDA Approved HIV-1 protease inhibitors oriented and arranged to highlight common structural features. 186

Figure 4.16 a) X-ray crystal structure of HIV-1 protease co-crystallised with darunavir (**478**)(PDB:1T3R) and b) schematic of key interactions 188

Figure 4.17 Initial design of darunavir based HDAC/HIV-1 PR hybrid inhibitor 189

Figure 4.18 Final HDAC/HIV-1 protease hybrid inhibitor design 192

Figure 4.19 First and second generation εN-acetyllysine substrates 200

Figure 4.20 Romodepsin, the only HDAC inhibitor shown to have shown clear clinical benefits in decreasing HIV reservoirs 203

Figure 4.21 Structure of HDAC inhibitor fimepinostat 204

List of Tables

Table 2.1 Difference in acid/conjugate base proton affinity for surveyed molecules and their respective acidities in DMSO 81

Table 2.2 Optimisation of spirocycle **287** formation 82

Table 2.3 Levels of deuterium incorporation for sulfone **277** 86

Table 2.4 Levels of deuterium incorporation for sulfoxides **292a** and **292b** 88

Table 2.5 Optimisation of biphasic reaction using phase transfer catalysis 94

Table 2.6 Substrate scope for spirocycle formation 104

Table 2.7 Alkylation of spirocycle **287** derived enolates 109

Table 2.8 Allylation *versus* methylation of sulfone derived enolates 110

Table 3.1 Comparison of (*R*)-puraquinonic acid characterisation data 142

Table 3.2 Comparison of ^{1}H and ^{13}C NMR spectra data for amide **435** 150

Table 4.1 HDAC inhibitor assay results for **488** and **489** 201

List of Abbreviations

Ac	acetyl
AIBN	azobisisobutyronitrile
AIDS	acquired immune deficiency syndrome
AMC	7-amino-4-methylcoumarin
APCI	atmospheric pressure chemical ionization
ART	antiretroviral therapy
aq	aqueous
B3LYP	Becke, 3-parameter, Lee–Yang–Parr
9-BBN	9-borabicyclo[3.3.1]nonane
Bn	benzyl
Boc	*tert*-butyloxycarbonyl
br	broad
Bu	butyl
CAN	cerium ammonium nitrate
cART	combination antiretroviral therapy
CDC	American Centers for Disease Control
CDK	cyclin-dependent kinase
CGRP	calcitonin gene-related peptide
cod	1,5-cyclooctadiene
COSY	correlation spectroscopy
CSA	camphorsulfonic acid
d	doublet
dba	dibenzylideneacetone
DBU	1,8-diazabicyclo[5.4.0]undec-7-ene
DCE	dichloroethane
DCM	dichloromethane

DDQ	2,3-dichloro-5,6-dicyano-1,4-benzoquinone
DFT	density functional theory
DIBAL/DIBAL-H	diisobutylaluminium hydride
DIPEA	N,N-diisopropylethylamine
DIPPA	diphenylphosphorylazide
DMAD	dimethyl acetylenedicarboxylate
DMAP	4-(dimethylamino)pyridine
DMF	N,N-dimethylformamide
DMP	Dess-Martin periodinane
DMPU	N,N′-dimethylpropyleneurea
DMSO	dimethylsulfoxide
d.r.	diasteromeric ratio
EDC	N-ethyl-N′-carbodiimide
EDG	electron donating group
ee	enantiomeric excess
EI	electron ionization
ESI	electron spray ionization
Et	ethyl
Et_2O	diethyl ether
EtOAc	ethyl acetate
EtOH	ethanol
equiv	equivalent(s)
EWG	electron withdrawing group
FDA	United States Food and Drug Administration
gag-pol	group-specific antigen polyprotein
HAART	highly active antiretroviral therapy
HAT	histone acetyl transferase

HDAC	histone deacetylase
HDACi	histone deacetylase inhibitor(s)
HIV	human immunodeficiency virus
HOAt	1-hydroxy-7-azabenzotriazole
HOBt	hydroxybenzotriazole
HOMO	highest occupied molecular orbital
HMBC	heteronuclear multiple bond correlation
HPLC	high-performance liquid chromatography
HRMS	high-resolution mass spectrometry
HSQC	heteronuclear single quantum correlation
hν	light, photon energy
JohnPhos	(2-biphenyl)di-*tert*-butylphosphine
i	iso
IBX	2-iodoxybenzoic acid
IC_{50}	half maximal inhibitory concentration
Im	imidazole
IR	infrared
J	coupling constant
KHMDS	potassium bis(trimethylsilyl)amide
K_i	inhibitor dissociation constant
L. A.	Lewis acid
LDA	lithium diisopropylamide
LiDBB	4,4′-di-tert-butylbiphenylide
LiHMDS	lithium bis(trimethylsilyl)amide
LTR	long terminal repeat
LUMO	lowest unoccupied molecular orbital
m	meta

m	multiplet
m/z	mass to charge ratio
*m*CPBA	meta-chloroperbenzoic acid
Me	methyl
MeCN	acetonitrile
MeOH	methanol
mmol	millimole
mol	mole
MOM	methoxymethyl
MS	molecular sieves
Ms	mesyl, methanesulfonyl
n	normal
NAD^+	nicotinamide adenine dinucleotide
NaHMDS	sodium bis(trimethylsilyl)amide
NBS	N-bromosuccinimide
n.d.	not determined
NMR	nuclear magnetic resonance
NOE	nuclear Overhauser effect
NOESY	nuclear Overhauser effect spectroscopy
n.r.	no reaction
Ns	nosyl, 4-nitrobenzenesulfonyl
o	ortho
p	para
PDB	protein data bank
Ph	phenyl
PI3K	phosphoinositide 3-kinase
PIDA	phenyliodine(III) diacetate

Piv	pivaloyl
pK_a	log of the acid dissociation constant
PMP	para-methoxyphenyl
PR	protease
r.t.	room temperature
RT	reverse transcriptase
PTSA	*para*-toluenesulfonic acid
RNA	ribonucleic acid
s	secondary
s	singlet
SAHA	suberoylanilide hydroxamic acid
SALEN	2,2′-ethylenebis(nitrilomethylidene)diphenol
SAR	structure activity relationship
SM	starting material
t	tertiary
t	triplet
TBAF	tetrabutylamonium fluoride
TBHP	*tert*-butyl hydroperoxide
TBS	*tert*-butyldimethylsilyl
Tf	triflyl, trifluoromethylsulfonyl
TFA	trifluoroacetic acid
THF	tetrahydrofuran
TLC	thin layer chromatography
TMS	trimethylsilyl
TS	transition state
TSA	trichostatin A
v/v	volume/volume

wt%	percentage by weight
XPhos	2-dicyclohexylphosphino-2′,4′,6′-triisopropylbiphenyl

Nomenclature

Regarding the discussion of enolate geometry, the notation (*E/Z*)-enolate is synonymous with *E/Z*(O)-enolate within the text of this thesis.

The numbering convention used herein for the norilludalane puraquinonic acid (**164**), is the same as established by Anke and Sternerin in the original report of the natural product.[1] The convention is illustrated below.

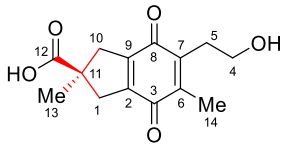

puraquinonic acid (**164**)

[1] Becker, U.; Erkel, G.; Anke, T.; Sterner, O., *Natural Product Letters* **1997**, 9 (3), 229-236.

CHAPTER 1

Introduction to Quaternary Carbon Stereocentres, their Construction, and Applications Thereof in the Total Synthesis of Puraquinonic Acid

1.1 Introduction to Quaternary Carbon Stereocentre Formation

1.1.1 Importance of Quaternary Carbons

Among the myriad structural motifs encountered in chemistry, the quaternary carbon is perhaps one of the most intriguing. Although by definition structurally simple – a carbon atom bonded to four additional carbon atoms – this simplicity facilitates the construction of a staggering array of molecular architectures and leads one to encounter numerous examples of quaternary carbons in any given volume of organic chemistry research journals.[1-3] This diversity also leads to complexity, and indeed quaternary carbons are frequently found nestled within the carbon skeletons of important. and synthetically challenging organic molecules.

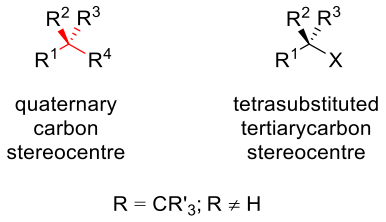

Figure 1.1 Quaternary carbons

Examples of important, naturally occurring, molecules that contain quaternary carbons include taxol[4-6] (**1**), a cancer chemotherapy medication, morphine[7, 8] (**2**), an important analgesic, strychnine[9, 10] (**3**), a famously toxic indole alkaloid, and the sterol cholesterol[11, 12] (**4**), in which quaternary carbons decorate the common gonane structure. The presence of quaternary carbons is also encountered in the pharmaceutical industry with twenty-two of the top two hundred pharmaceuticals sold in 2018 (representing twenty-nine percent of all small molecules included in the list), containing at least one quaternary carbon.[13]

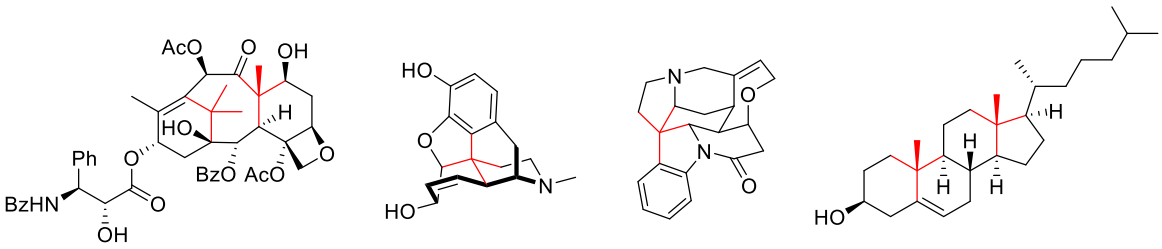

Figure 1.2 Quaternary carbons in the structures of taxol, morphine, strychnine, and cholesterol

Quaternary carbons are frequently employed in the design of novel molecules where they can provide chemical and configurational stability. As carbon-carbon bonds represent the structural foundation of organic molecules, the chemical stability of quaternary carbons makes them inherently robust to all but the harshest of conditions or specifically designed chemical reactions. Additionally, their configurational stability is an acutely critical property as quaternary carbons are a frequent source of stereogenicity in organic structures, with each of the four peripheral carbon atoms able to bear considerable chemical and structural diversity. This structural diversity is on great display in nature wherein natural products of varying class and complexity contain quaternary carbons.

The ability to resist stereochemical alteration is of added importance in the discussion of biologically active molecules. This is a result of the biological function of biomolecules being frequently influenced by the absolute stereochemistry of the molecules (both small and macromolecules) with which they interact. In turn this makes configurationally stable stereocentres (such as those formed by quaternary carbons) desirable features of biologically active molecules, such as pharmaceuticals.

A tragic example of the considerable role stereochemistry plays in biological settings is the widely recounted case of the pharmaceutical thalidomide. First prescribed as a sedative,

thalidomide came to be employed as an antiemetic to control morning sickness in pregnant women. Thought to be safe due to it displaying little activity as a CNS and respiratory depressant, its use proved disastrous, with the use of the drug during the early stages of pregnancy resulting in teratogenicity, causing phocomelia and other severe or life-threatening birth defects. Investigation into the origins of the varying clinical effects of thalidomide revealed a significant importance of stereochemistry, with (*S*)-thalidomide (**6**) responsible for the teratogenic effects while (*R*)-thalidomide (**5**) having sedative effects without significant toxicity.[14] As the stereogenic centre in thalidomide bears an acidic proton, interconversion between the two isomers can be achieved *via* deprotonation and subsequent reprotonation (Figure 1.3). Importantly this stereochemical interconversion occurs under physiological conditions, thus precluding the administration of a single enantiomer as a method of eliminating the negative effects of the medication.[15]

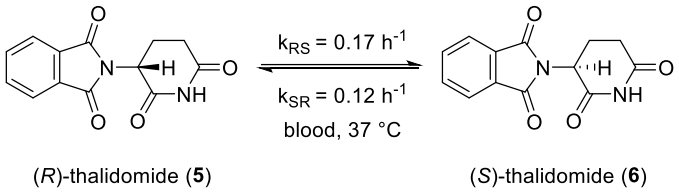

Figure 1.3 Isomerisation of thalidomide in human blood

The stereochemical instability, and accompanying change in biological activity, of thalidomide and its analogues has long retarded the development of this class of pharmaceuticals. Despite thalidomide removal from markets in 1962, research in the past decades has shown that it regulates the activity of tumour necrosis factor-α, rekindling interest in the molecule class for treatment of diseases such as rheumatoid arthritis, Crohn's disease, leprosy, AIDS, and cancer. An informative example is the use of lenolidomide (**7**), which was approved by the FDA in 2005 for the treatment for multiple myeloma[16] and in 2018 had retail sales of $9.9 billion US.[13,17] As a result

of this modern attention, one approach to overcome stereochemical instability has been to leverage the stability of quaternary carbon stereocentres by replacing the α-hydrogen to confer configurational stability.[18]

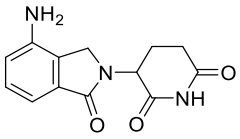

lenolidomide (**7**)

Figure 1.4 Structure of lenolidomide, an FDA approved treatment for multiple myeloma

Attempts to remove the problematic acidic α-hydrogen has led to the synthesis and evaluation of several thalidomide analogues.[19, 20] Unfortunately, while replacement of the hydrogen does result in configurationally stable molecules, some analogues have inferior toxicity profiles; 3'-fuorothalidamide (**8**) has been shown to cause pulmonary oedema, renal tubular degeneration, macerated foetuses, and death in pregnant New Zealand white rabbits.[21] Other analogues, such as glutethimide[22] (**10**) (once used as an alternative to barbiturates in the treatment of insomnia) are less toxic with the more recently reported Gu998[23] (**11**) displaying anti-angiogenic properties. Despite the tragic history, research into the biological uses of this class of molecules remains an active field of research.

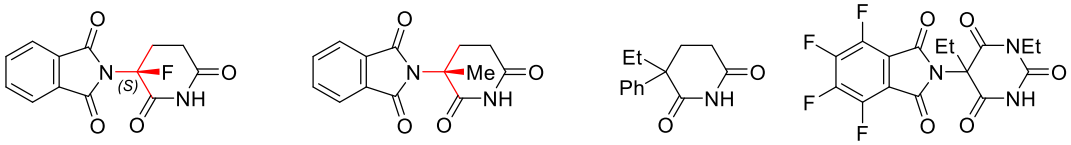

(*S*)-3'-fluorothalidomide (**8**) (*R*)-methylthalidomide (**9**) glutethimide (**10**) Gu998 (**11**)

Figure 1.5 Thalidomide analogues which do not bear the problematic α-carbon

1.1.2 Construction of Quaternary Carbon Stereocentres

Due to their prevalence in organic molecules many classic reactions have been developed to construct quaternary carbons, with several also being able to deliver products with high levels of enantiomeric excess. These include well studied reaction classes such cycloadditions, sigmatropic rearrangements, 1,4-additions, and desymmetrizations.[24, 25] As reactions like the Diels-Alder cycloaddition[26] and Claisen rearrangement[27] can rapidly generate molecular complexity and provide molecules that contain multiple stereogenic centres, it becomes necessary for the reaction products to map reasonably well onto the desired target in order to maximise synthetic efficiency. However, the ability to set multiple stereogenic centres in a single step ensures that such pericyclic reactions remain a favourite strategy among organic chemists. In the past two decades, methods such as conjugate additions[28] and desymmetrisations reactions (exemplified by a C-H activation strategies employed by Yu,[29-31] Figure 1.6d) have become increasingly common with the advent of numerous chiral ligands for transition metal catalysis. Due to the breadth of transformations able to furnish quaternary carbons the remainder of this chapter will focus on the preparation of quaternary carbon stereocentres located α to carbonyl groups with an emphasis on techniques wherein bond formation at the α-carbon is the stereo defining event.

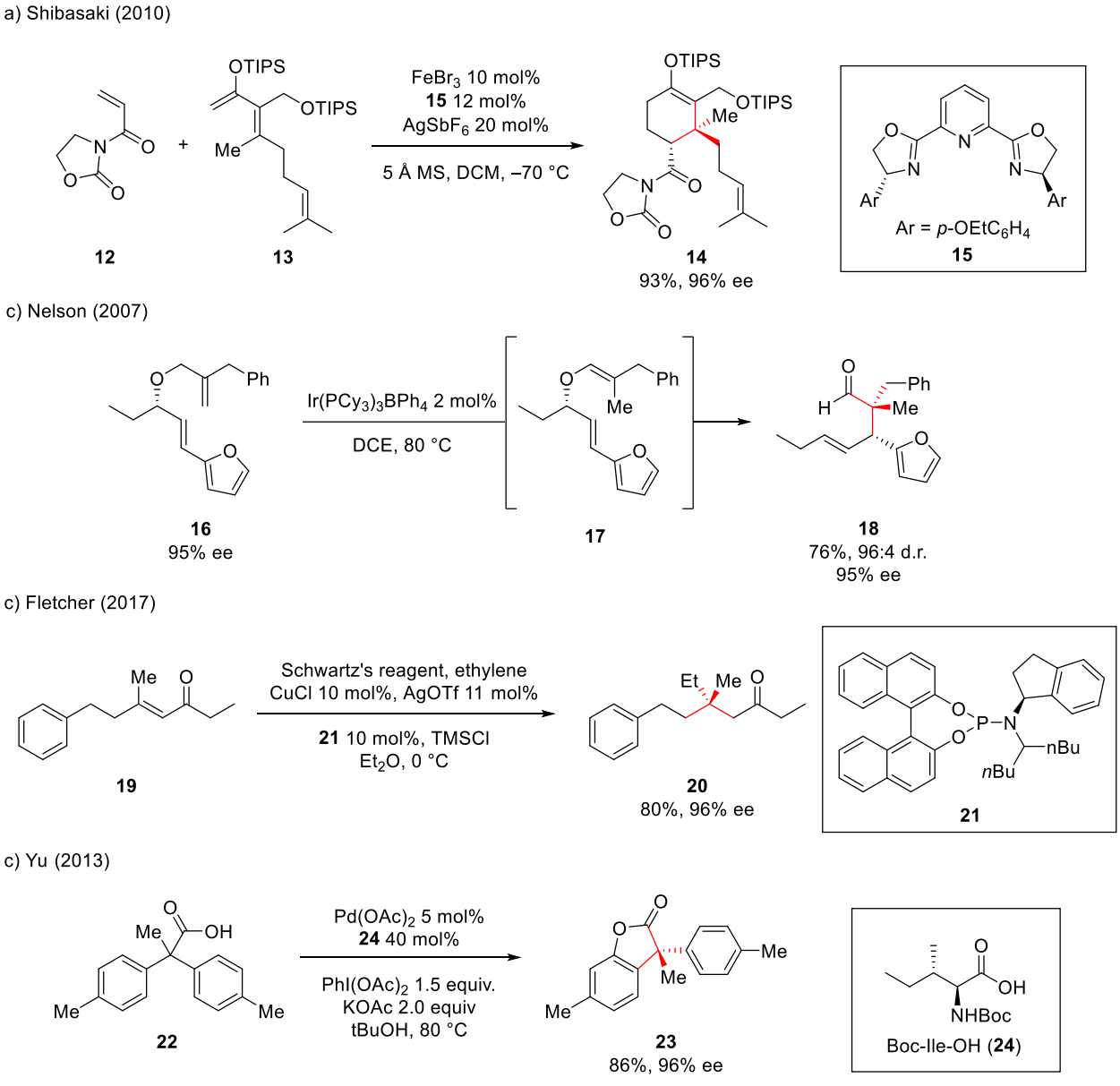

Figure 1.6 Examples of various reactions which produce quaternary carbon stereocentres: a) Diels-Alder cycloaddition, b) Claisen rearrangement, c) asymmetric conjugate addition, and d) desymmetrisation.

1.1.3 α-Quaternary Carbon Stereocentres

Considering the range of structural architectures quaternary carbons are found in, the synthetic challenge of forming any given quaternary carbon can vary. A challenging subset of quaternary carbons are those located at the α-position of carbonyls (or derivatives thereof *e.g.*

quebrachamine (**26**), Figure 1.7) which are otherwise structurally isolated from additional stereocentres or functional groups.[32-37] While common, such carbon stereocentres are not trivial to construct leading to significant research activity into the development of methods for their preparation.

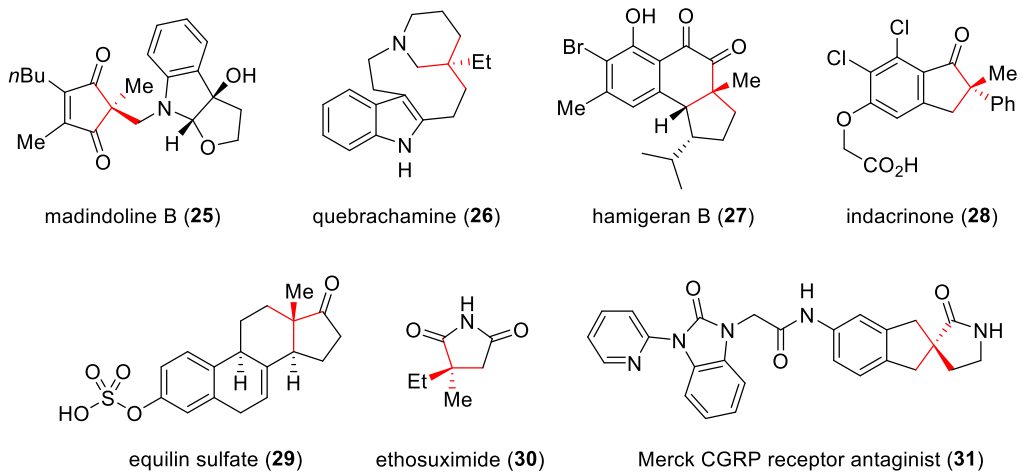

Figure 1.7 Examples of α-quaternary carbon stereocentres and derivates thereof

1.1.3.1 Use of Enolates in Carbon-Carbon Bond Forming Reactions

Several factors are responsible for the synthetic challenge presented in the formation of α-quaternary carbon stereocentres. Being comprised of four carbon-carbon sigma bonds necessitates the construction of the final bond to occur at a highly sterically encumbered tertiary site. The multiple carbon substituents also lead to concerns regarding stereochemistry, as it is not unusual for some of the substituents to be of similar electronic and steric character, making it difficult to differentiate between them. Within the methods employed for the construction of carbon-carbon bonds the use of enolates has long been one of the more popular methods, with numerous carbonyl derivates, such as aldehydes, ketones, imides, esters, amides, and thioesters, forming enolates

capable of reacting with range of electrophiles to form quaternary stereocentres (*e.g.* aldehydes, imines, Michael acceptors, alkyl halides, and Pd(II) aryl/π-allyl species).

As exemplified by the prototypical case of the aldol reaction, enolate geometry governs the stereochemical result of reactions involving enolate substitution. As such, issues surrounding selective enolate formation weigh heavily on any method involving their use in the preparation of α-quaternary carbon stereocentres. It is therefore useful to identify the origins of stereoselectivity for classical systems in some detail.

The effect of enolate geometry on stereochemical outcome of the aldol reaction is conveniently analysed through examination of the Zimmerman-Traxler transition states for the addition of the two possible enolates to a given aldehyde (Scheme 1.1).[38] The cyclic nature of the transition state places emphasis on minimising 1,3-diaxial interactions leading (*E*)-enolates (**33**) to favour the formation of products with *anti*-relative stereochemistry (**36**) while (*Z*)-enolates (**34**) provide *syn*-products (**40**).

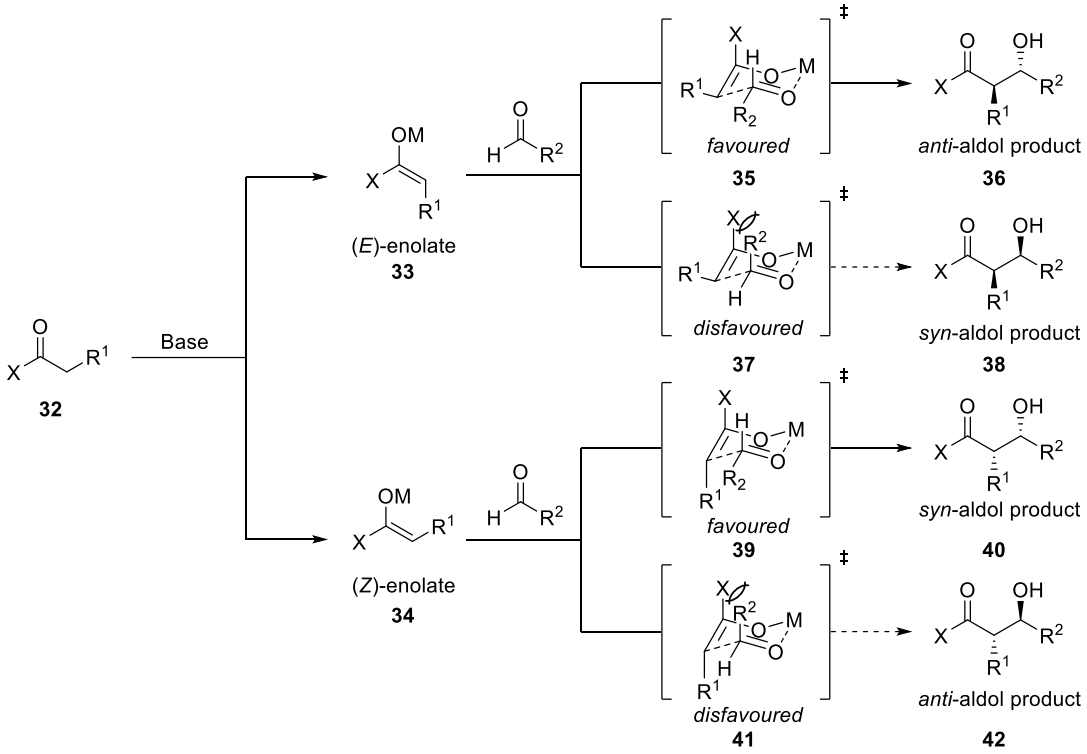

Scheme 1.1 Zimmerman-Traxler transition state model for the aldol reaction

Despite the role of enolate geometry in determining the stereochemical outcome, it is impossible for enolate geometry to alone control absolute stereochemistry, as the set of enantiomers is formed in each case outlined in Figure 1.1. Instead, the prochiral faces (*si* and *re*) of the enolate must also be differentiated to provide absolute stereocontrol, with electrophile addition occurring preferentially on one face. This differentiation can be achieved by adding a stereo directing element to the enolate, commonly achieved by taking advantage of stereochemistry elsewhere on the enolate (*e.g.* chiral auxiliary) or by addition of additional chiral reagents (*e.g.* chiral catalysis). In general, methods of attaining high levels of absolute stereocontrol rely on favouring the formation of a single enolate geometry while concurrently blocking one of the enolate faces. These features remain critical for the substitution of α,α-

disubstituted esters leading to quaternary carbon formation but become more challenging due to the lack of steric differentiation when a carbon atom replaces the α-proton.

1.1.3.2 Controlling Enolate Geometry

Numerous strategies have been developed for the selective formation of a single enolate geometry. Arguably, the most fundamental method is to rely on the steric properties of substituents located at the α-carbon. This is particularly useful for the formation of α-tertiary stereocentres where enolate geometry is dictated by the small relative size of a hydrogen atom (R_S = H, Scheme 1.2) to the other α-substituent (R_L = alkyl).

The Ireland model provides one predictive tool to rationalise the observed enolate geometry for deprotonations using amide bases (*e.g.* LDA). [39, 40] The model assumes a six-membered ring transition state where the lithium cation of the base is coordinated to the carbonyl while the nitrogen lone pair interacts with the α-proton. This geometric arrangement roughly satisfies the stereoelectronic for α-deprotonation where a 90° O-C-C-H dihedral angle is ideal (**48**), while bringing attention to two steric considerations: (i) the 1,3-diaxial interaction between the second α-substituent and the amide base (**44**) and (ii) the 1,2-eclipsing interaction between one α-substituent and the acyl group X (**46**). Changes to the nature of the carbonyl X substituent, solvent, and base influence the relative importance of these interactions and therefore modulate the geometric outcome. In the case of esters and ketones with small X substituents, in THF the 1,2-eclipsing interaction is not substantial and thus a geometry minimising the 1,3-diaxial interactions favours the formation of (*E*)-enolates. The influence of the 1,2-eclipsing steric interaction can be exaggerated to favour the (*Z*)-enolate through the addition of HMPA (or other polar cosolvents), which act to solubilise the lithium cation disrupting the tight six-membered ring conformation, to

reduce the influence of the 1,3-diaxial interaction. The 1,2-eclipsing interaction also dominates in cases where X is large, such as for amides and ketones with large substituents (X = NR_2, *t*Bu).

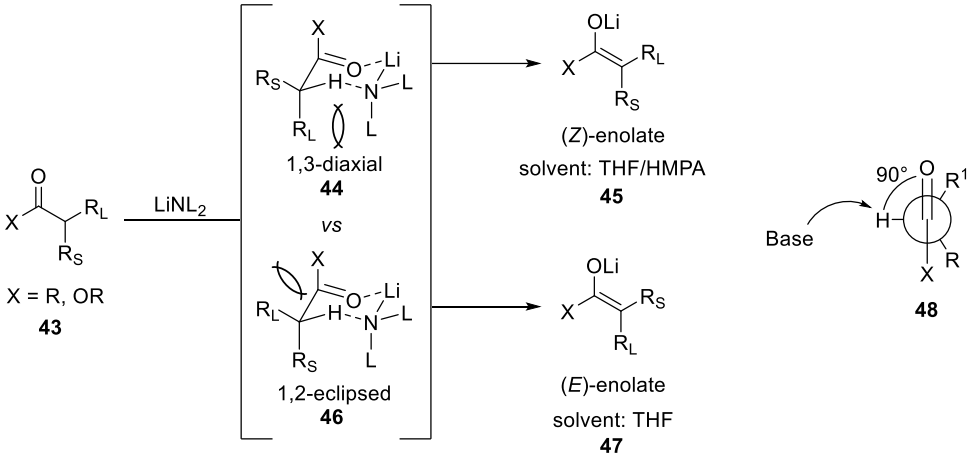

Scheme 1.2 Ireland model for the enolization selectivity

Due to the close association of the amide base and species undergoing deprotonation changes to the substituents on the amide base can have a considerable influence on the observed selectivity. The nature of these effects has been investigated by Xie (Scheme 1.3) and is rationalised on the bases of the Ireland model.[41, 42] The electron withdrawing properties of the phenyl groups in base **52** reduce the electron density on nitrogen. This weakens (*i.e.* lengthens) the nitrogen-lithium bond leading to a late transition state, mimicking the loose transition state traditionally accessed with the addition of HMPA, where 1,2-eclipsing interactions dominate. Xie also noticed a significant temperature dependence on the selectivity of *tert*-butyltrimethylsilylamide (**53**) with deprotonations carried out at room temperature (*E*:*Z* = 92:8) found to be much more selective than when conducted at –78 °C (*E*:*Z* = 77:23). As with all arguments made with reference to the Ireland model, Xie is careful to highlight that despite the model's consistency with their findings is possible that the observations result from changes in the aggregation state of the lithium amides.

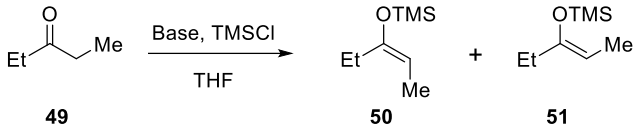

49 **50** **51**

Base	Tempreature	*E*:*Z*
LDA	–70 °C	70:30
LHMDS	–70 °C	34:66
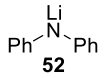 **52**	–78 °C	5:95
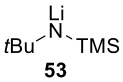 **53**	23 °C	92:8

Scheme 1.3 Effects of amide substitution on enolization selectivity

While the Ireland model is a useful tool, it highlights a dependence on steric differentiation between the two α-substituents (R_L vs. R_S) to provide (*E*/*Z*)-enolate selectivity. Such steric bias works exceptionally well in cases where one of the substituents is hydrogen (R_S = H) but becomes problematic when considering the use of enolates for the formation of quaternary carbon stereocentres. In these cases, the comparative size of the substituents may be very close, such as in the case described in Scheme 1.3 (R_S = Me, R_L = Et).[43] As would be predicted from the Ireland model, deprotonation of ester **54** and trapping the resulting α,α-disubstituted enolates as silyl enol ethers **55** and **56** provides poor selectivity for the formation of the (*Z*)-isomer. The additional steric demands introduced by substituted amides may cause further issues, as in these cases amide bases may be incapable of performing α-deprotonations, with more forcing condition being required (*e.g.* *s*BuLi).

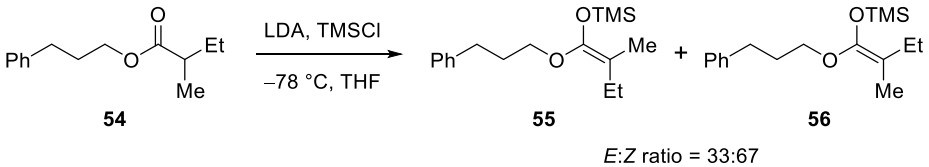

54 **55** **56**

E:*Z* ratio = 33:67

Scheme 1.4 Enolization selectivity for α,α-disubstituted esters

In addition to the electronic and steric properties of the base, the use of chiral bases can have a strong directing influence. Zakarian and co-workers investigated the use of chiral lithium amide base in the context of Ireland-Claisen rearrangements.[43] By employing single enantiomers of α,α-disubstituted esters together with Koga-type chiral amide bases,[44] α,α-disubstituted enolates were accessed with very high levels of selectivity (Scheme 1.5).[45] Use of the enantiomeric form of the base provided the opposite enolate geometry and is consistent with the authors' proposed Ireland deprotonation model, wherein the chirality of the base provides discrimination between the two diastereomeric transition states. Zakarian has successfully demonstrated the utility of this methodology in efforts towards the synthesis of spirolide C[46, 47] and in the total synthesis of (+)-pinnatoxin A.[48]

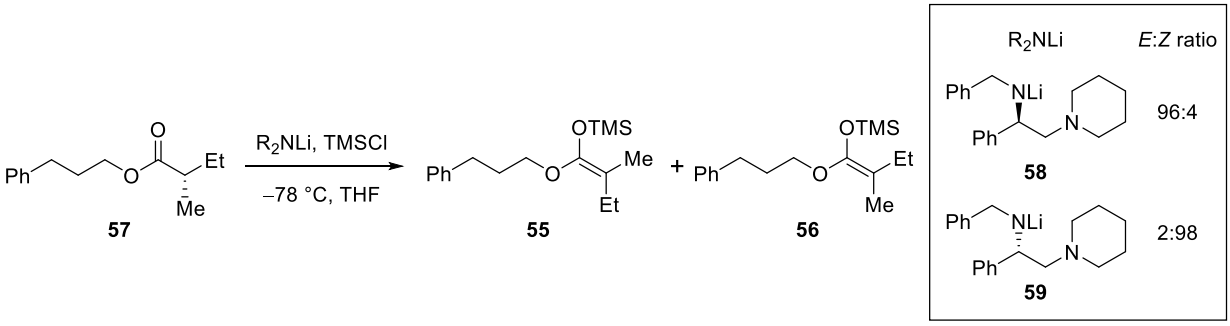

Scheme 1.5 Chiral amides in selective enolization of chiral α,α-disubstituted esters

1.1.3.3 Controlling Enolate Facial Selectivity

A classic method for controlling the absolute stereochemical outcome of reactions is the use of chiral auxiliaries. Chiral auxiliaries are stereogenic groups that are appended to a structure to impose stereocontrol on subsequent reactivity. In many cases, once the auxiliary is removed, it can be recovered and recycled. Naturally, this strategy can be applied to a wide array of chemical reactivity ranging from cycloadditions, aldol additions, Michael additions, allylations, reductions,

ene reactions, *etc*. with many structurally diverse chiral auxiliaries having been developed over the past several decades (Figure 1.8). In the context of enolate allylations the auxiliary serves two functions; (i) control of enolate geometry and (ii) control of the facial approach of the electrophile. In these regards the oxazolidinone based auxiliaries, developed by Evans provide an instructive example (Scheme 1.6).

In 1981 Evans introduced oxazolidinone based auxiliaries which derive their stereochemistry from easily available chiral amino alcohols.[49] As exemplified by the valinol derived oxazolidinone **66**, the A-1,3 interaction introduced by the substituents on the imide allow for selective enolization. As predicted by the Ireland model, this results in high levels of selectivity for (*Z*)-enolates. Chelation of the lithium counter ion locks the enolate into a single conformation (**67**) whereby the electrophile approaches opposite the isopropyl group providing alkylated products in high yield and with high diastereoselectivity.[50]

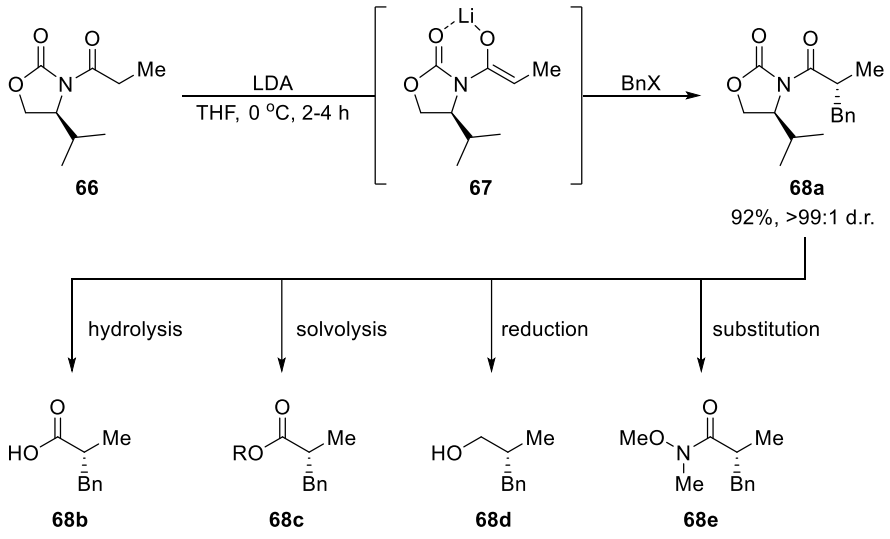

Scheme 1.6 Evans' oxazolidinone auxiliary directed alkylation

The use of chiral auxiliaries in stereoselective enolate alkylation is not limited to Evans type oxazolidinones, with several other groups developing unique frameworks to achieve similar results. Examples of other chiral auxiliaries employed in this regard include Meyers' oxazoline,[51] Myers' pseudoephedrine,[52, 53] Helmchen's camphor alkanolamine,[54] Oppolzer's camphorsultam,[55] Enders' hydrazone (RAMP/SAMP),[56, 57] and Coltart's oxazolidinone[58] auxiliaries (Figure 1.8). Chiral auxiliaries have also played a large role in the development of asymmetric aldol additions where Evans' oxazolidinone auxiliaries again are a classic example. In this application, Evans' auxiliaries display a high degree of absolute and relative stereocontrol for *syn*-aldol products, with stereoinduction being governed by a tight Zimmerman-Traxler transition state formed from the use of boron enolates. The oxazolidinone moiety can be converted into a number of different functional groups *via* hydrolysis (**68b**), solvolysis (**68c**), reduction (**68d**), or substitution (**68e**), allowing the methodology to have broad applicability.[59, 60]

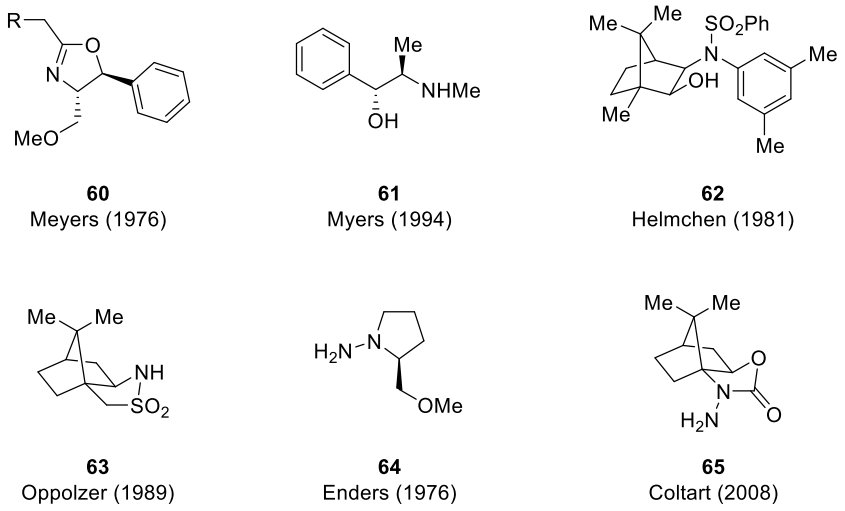

60 Meyers (1976) **61** Myers (1994) **62** Helmchen (1981)

63 Oppolzer (1989) **64** Enders (1976) **65** Coltart (2008)

Figure 1.8 Examples of chiral auxiliaries successfully used in asymmetric allylations

The use of auxiliaries has also been extended to the formation of α-quaternary carbon stereocentres, with these methods designed to overcome issues associated with enolate geometry

in α,α-disubstituted systems. One approach used to address the issue of enolate geometry is to employ a diminutive α-substituent that is reliably smaller than the second alkyl group. This necessarily limits the scope of α-substituents.[61, 62] In this regard, the nitrile group is attractive due to the small steric profile of the sp hybridised carbon atom. Yamaguchi successfully employed this strategy in conjunction with a C_2-symmetric pyrrolidine chiral auxiliary to forge α-cyano quaternary carbon stereocentres (Scheme 1.7).[63] Due to the acidity of the α-proton poor diastereoselectivity in the initial alkylation (**71**) is observed. Unfortunately, the utility of this methodology is also limited due to the lengthy synthesis of the auxiliary.[64]

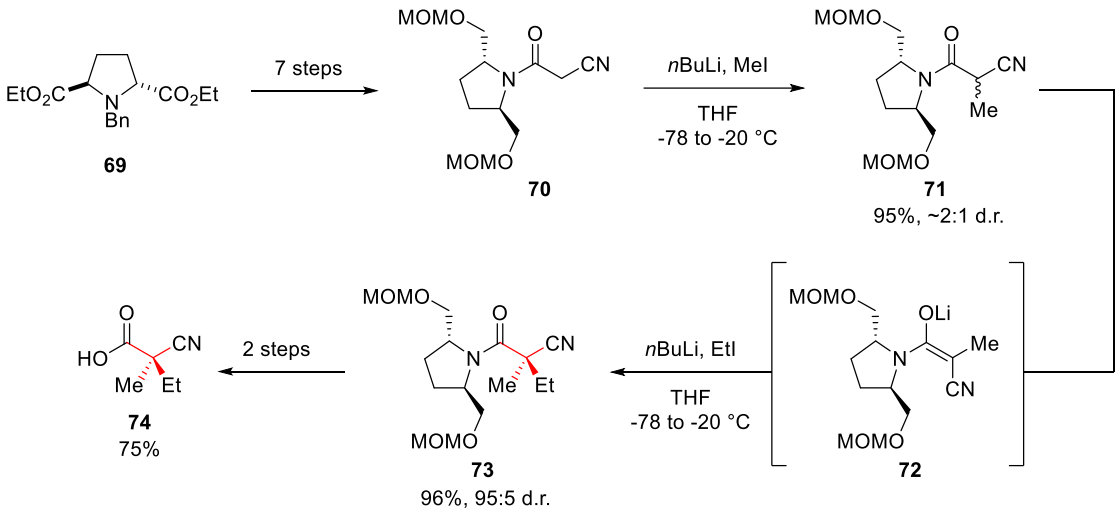

Scheme 1.7 Use of diminutive α-substituents to control enolate geometry

A second method of exerting control on enolate geometry is by employing cyclic systems which limit enolate geometry.[65-69] This is achieved through substrate design, a strategy exemplified by Meyers' use of a bicyclic lactam auxiliary (Scheme 1.8).[70-74] Only the formation of the (*E*)-enolate **76** is possible within the confines of the γ-lactam as the (*Z*)-enolate would require an impossibly strained trans–olefin to be contained in the γ-lactam. Alkylation of enolate **76** provided products with high levels of diastereoselectivity. However, removal of the auxiliary reveals a γ-

ketone as a vestigial element of the auxiliary.[75] Unlike many cyclic lactams, and indeed other [3.3.0] bicyclic lactams,[76] lactam **75** displays *endo* alkylation selectivity. From comparison to similar [3.3.0] bicyclic lactams it was discovered that location of the aminal ether oxygen to be the critical element in driving the observed *endo* electivity. In similar systems where this position is occupied by a methylene carbon, a pseudo-axial hydrogen atom projects directly toward the concave face of the bicyclic enolate, hindering alkylation from the *endo*-face.[77]

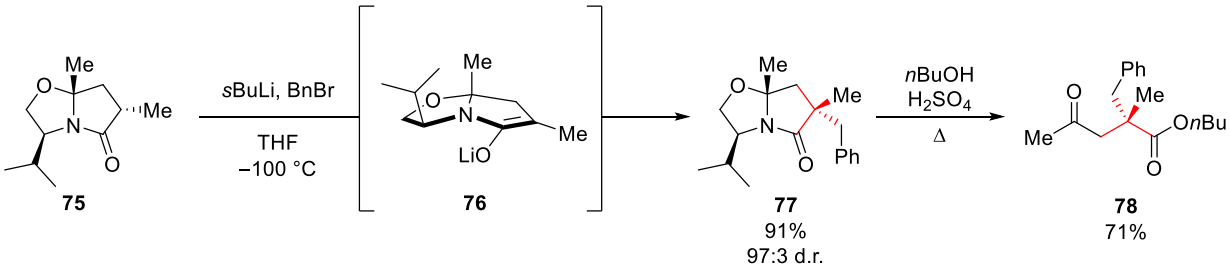

Scheme 1.8 Meyers' endo-selective bicyclic lactam auxiliary

Metal chelation can also be employed in a similar manner to apply stereocontrol in enolate formation. In Frater's work with β-hydroxy esters, the lithium counterion chelates to the β-alkoxide and carbonyl oxygen to form a six-membered metallocycle providing selective formation of enolate **80**.[78-80] Stereoselective alkylation is then achieved with the electrophile approaching anti to the β-alkoxide to provide α-quaternary-β-hydroxy esters with good levels of selectivity.

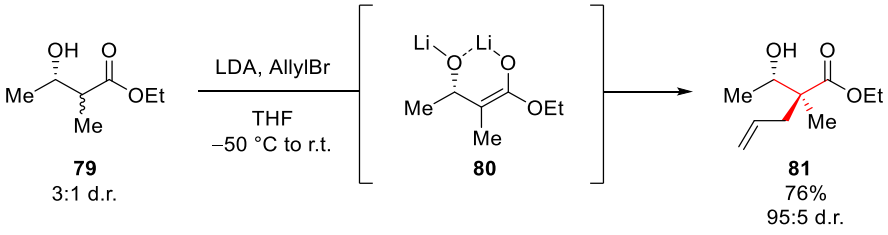

Scheme 1.9 Cyclic enolates *via* chelation

Careful consideration of the O-C-C-H dihedral angle can also prove useful in governing enolate selectivity. Indeed, Myers' use of a pseudoephedrine auxiliary takes advantage of the conformational preference of α,α-disubstituted amides and the requirement that deprotonation occur from a conformer where the O-C-C-H dihedral angle is approximately 90°.[81, 82] This allows for either the *E* or *Z* enolate to be derived selectively from the *R* or *S* configuration of the α-carbon, which can be simply prepared, in a preceding step, using the same pseudoephedrine auxiliary.[53] However, it is worth noting that higher levels of stereoselectivity are obtained through allylation of the (*Z*)-enolate compared to the (*E*)-enolate. Pseudoephedrine auxiliaries can also be employed in directing the enolate geometry resulting from Michael additions providing a complementary method to direct deprotonation. It should be noted that for both methods (deprotonation and Michael addition) the related pseudoephenamine auxiliary provides superior diastereoselectivity to pseudoephedrine, while not compromising yield.

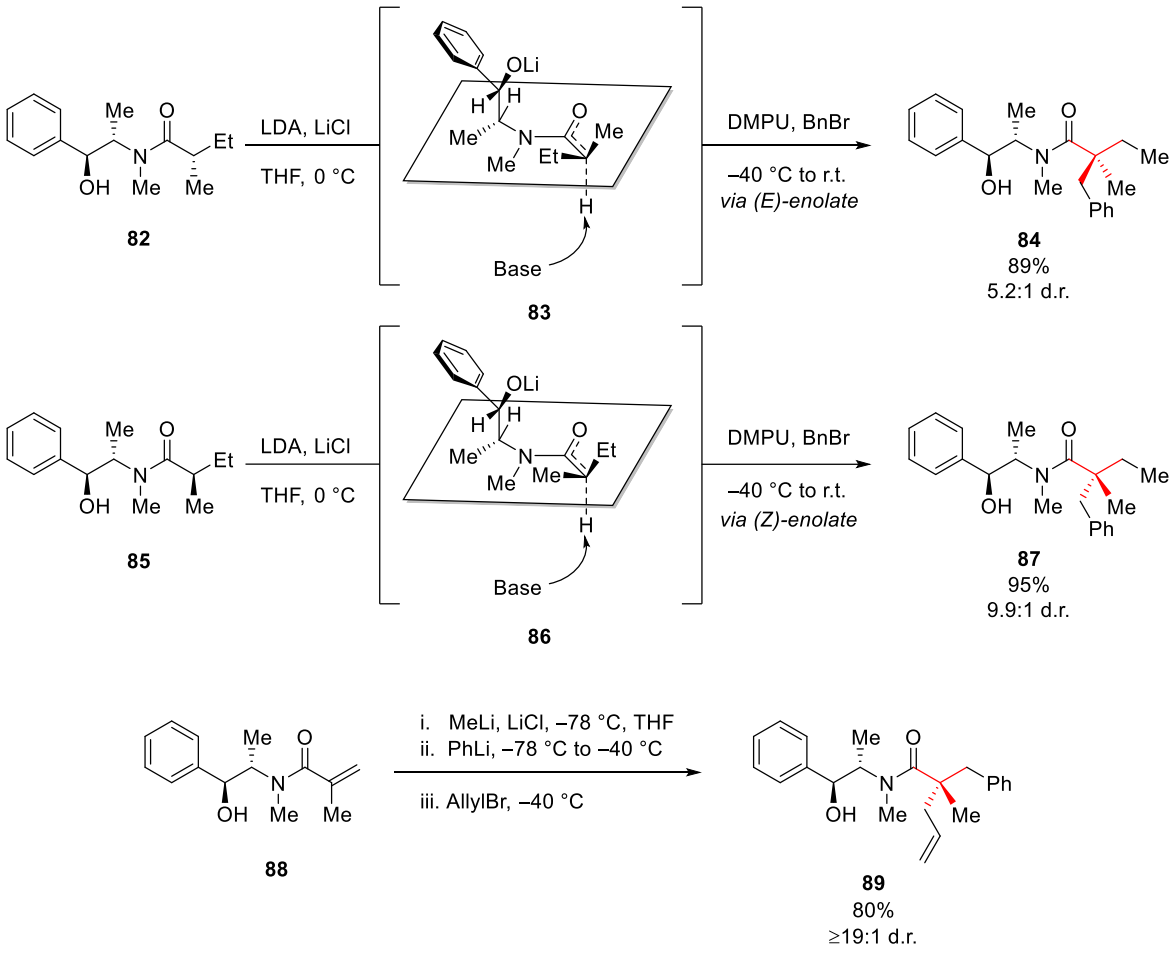

Scheme 1.10 Chiral auxiliary directed deprotonation and Michael addition

In 2017 Zakarian continued the investigation of chiral lithium amides and applied them to the construction of tetrasubstituted carbon stereocentres from α-aryl carboxylic acids.[83] The use of carboxylic acids has two notable advantages: (i) the intermediate enediolates of carboxylic acids are symmetric, removing concerns of enolate geometry, and (ii) their high nucleophilicity. Enantioselectivity is driven by the formation of well-defined mixed aggregates (**95**) of the chiral lithium tetramide and enediolate (Scheme 1.11). Indeed, insufficient aging of the enolate compromises enantioselectivity in these reactions. Although, the scope of the enediolate is largely limited to derivatives of *O*-methylmandelic acid (**90**) a large variety of alkyl halide and Michael-

type electrophiles provide reasonable structural diversity while maintaining good yields, with enantioselectivities usually remaining in excess of 80% ee. This methodology was also found to be reasonably competent in the formation of quaternary carbon stereocentres (with revered facial selectivity) as displayed in the example of carboxylic acid **91**. However, the authors note that in these cases, the generation of the enediolate is problematic with the competitive formation of *n*-butyl ketones observed, resulting in variable yields and enantioselectivity.

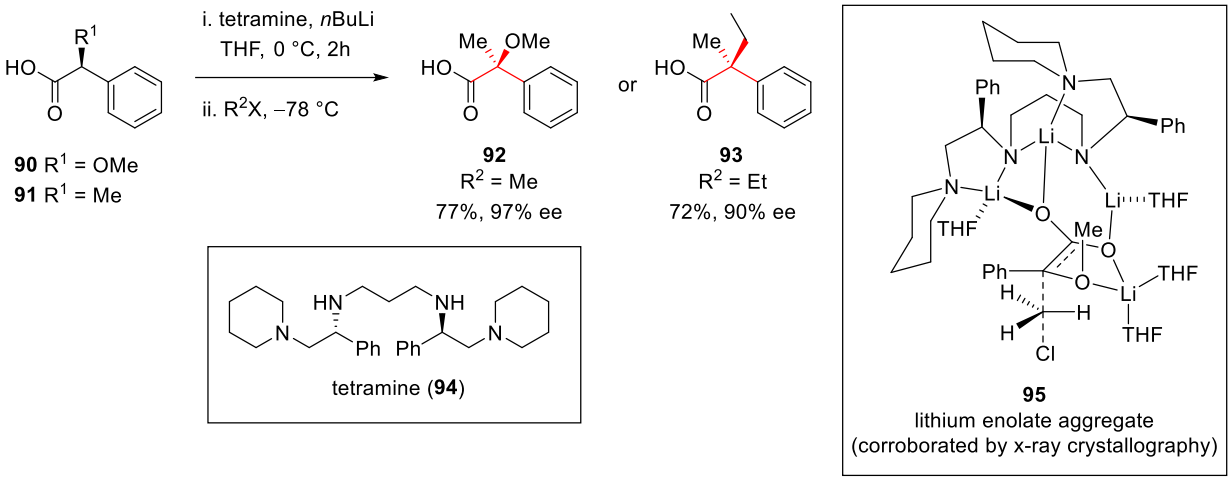

Scheme 1.11 Asymmetric lithium enediolate alkylation

In contrast to methods which rely on the acidity of the α-protons to generate α,α-disubstituted enolates, Marek and colleagues have developed a multicomponent reaction procedure wherein allyl zinc species are generated and employed as enolate surrogates (Scheme 1.12).[84, 85] In a single pot, chiral alkynyl oxazolidinones[86] (*e.g.* **96**; use of alkynyl sulfoxides has also been disclosed[87]) are submitted to a highly selective carbometallation with organocuprates to generate β,β-disubstituted copper enamines (**97**) which are then homologated with the Simmons–Smith–Furukawa zinc carbenoid (generated *in situ*) to generate the desired allyl zinc species (**98**). The allyl zinc reacts diastereoselectively with aldehydes, through a Zimmerman–Traxler-type

transition state (**100**), to give an intermediate zinc alkoxide, which is quickly trapped *in situ* as the silyl ether and is hydrolysed upon purification. This methodology successfully provides rapid access to a range of products containing challenging quaternary carbon stereocentres, including a particularly difficult case wherein the quaternary stereocentre is defined by *n*-hexyl and *n*-butyl alkyl substituents (**101**, in 66% yield, 92:8 d.r.). To further demonstrate the ability of this method to provide products classically synthesised using enolate chemistry, removal of the oxazolidinone auxiliary provides methyl ketone **102**. More recently, this chemistry has been expanded to the preparation of chlorohydrins,[88] homoallylic alcohols,[89] and β-amino amides[90] (through oxidation of the vinyl cuprate to provide stereodefined α,α-disubstituted amide enolates).

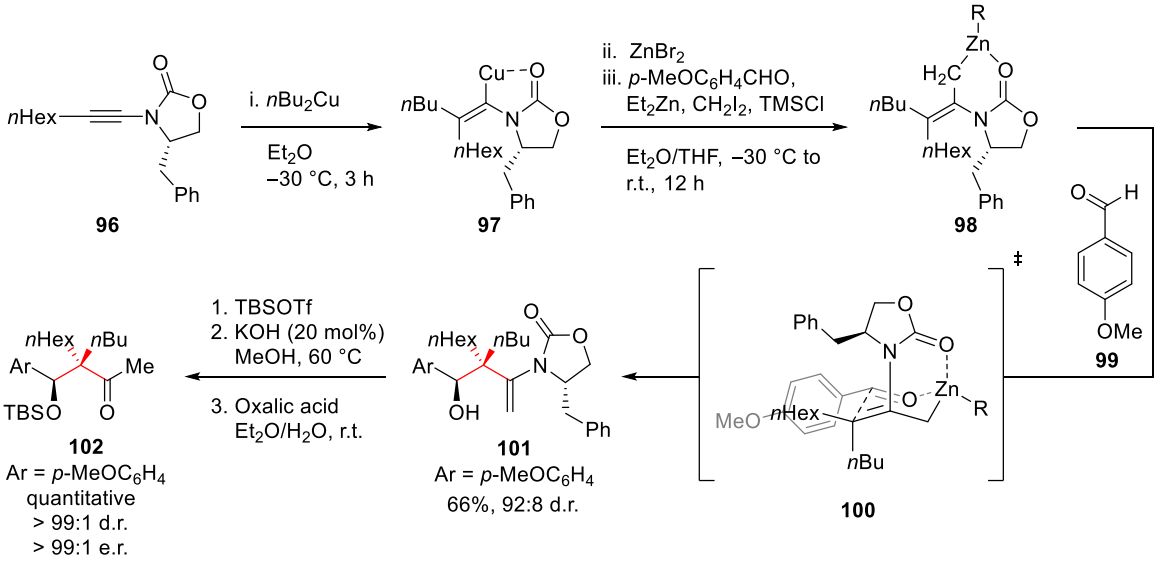

Scheme 1.12 Quaternary carbon containing aldol products *via* allyl zinc additions

1.1.3.4 The Practicality of the Chiral Bicyclic Thioglycolate Lactam Auxiliary

When examined for potential use in more challenging settings, the limitations of the systems discussed above become apparent and may be attributed to one or more of the following drawbacks: (i) the products are decorated with residual functionality (even post auxiliary

cleavage), (ii) not all stereoisomers are accessible, (iii) reactions of *E* and *Z* enolates provide different levels of selectivity, and (iv) the use of specific α-substituents is required, limiting the substrate scope of the method. Many of these issues were addressed in our laboratory through the development of bicyclic thioglycolate lactam auxiliaries **103** and **104** (Scheme 1.13).

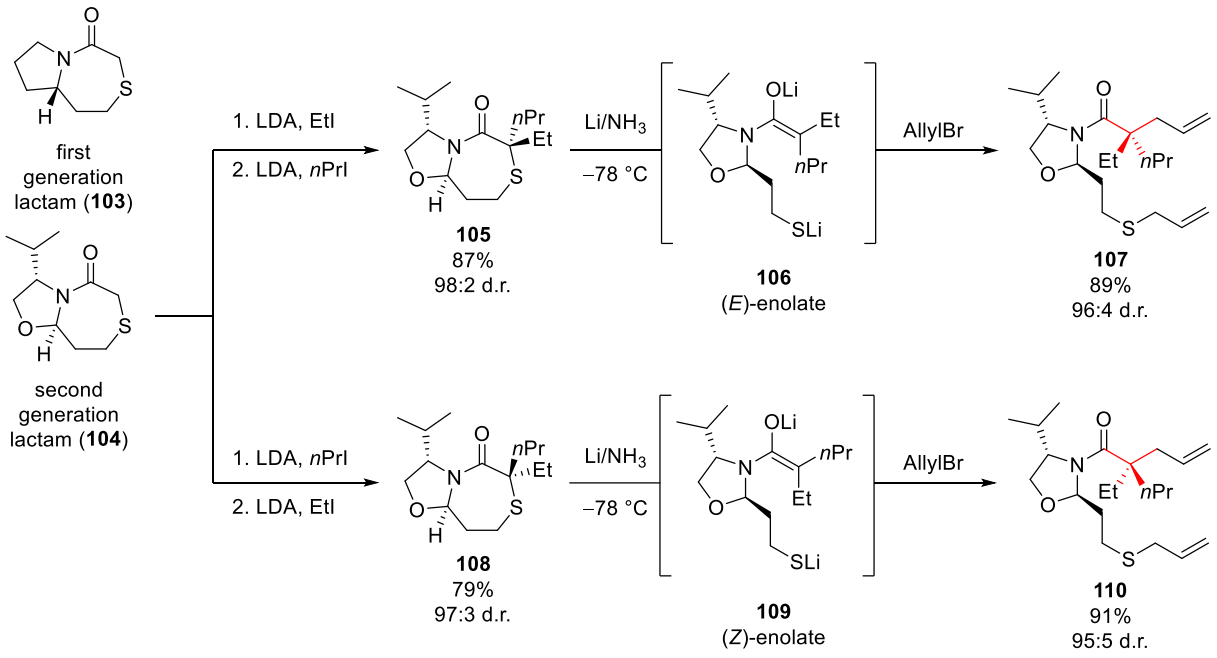

Scheme 1.13 Alkylation of second-generation auxiliary

The first iteration of bicyclic thioglycolate lactam auxiliary (**103**) derived its chirality from L-proline and providing good to high levels of stereoselectivity for α-alkylations for *Z* enolates.[91] However, the second generation lactam **104** is synthetically easier to access, being prepared in only three steps from L-valinol and provided reliably high levels of stereoselectivity for both *E* and *Z* enolates.[92] Selectivity for both lactams is governed by the convex conformation of the bicycle with electrophiles approaching from the *exo* face, as observed for most bicyclic lactam systems (lactam **75** (Scheme 1.8) being an exceptional case, *vide supra*). The third enolate formation is achieved *via* reduction of the carbon-sulfur bond wherein the geometry of the enolate

is dictated by the S-C-C-O dihedral angle, which is influenced by the stereochemistry of the ring fusion. The conformation of the bicycle locks the dihedral angle at approximately 120° (**112**), independent of the α-substituents, and prevents conformational change to a dihedral angle of 240° (*i.e.* − 120°, **111**) (Figure 1.9). This is the central advantage of these bicyclic lactam auxiliaries as the relative positions of the α-substituents (*i.e.* R^1 and R^2) are maintained though reductive enolate formation (as per the least motion principle) and not dependent on relative steric or other distinguishing features. Accordingly, the stereochemical outcome of the reduction (*E* or *Z* enolate) is a function of the starting diastereomer which in turn is dependent on alkylation sequence and not the nature of the electrophiles (Scheme 1.13).

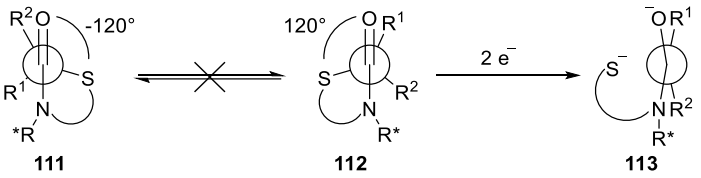

Figure 1.9 Enolate geometry resulting from reductive enolisation

The versatility of the bicyclic thioglycolate lactam auxiliary has been demonstrated in number of reaction classes including: alkylations,[93] aldol additions,[94] and Mannich reactions.[95] The hemiaminal ether moiety of the second-generation auxiliary also lends itself to facile amide hydrolysis though N to O acyl transfer after aminal cleavage, allowing the carboxylic acid to be liberated *via* ester hydrolysis as opposed to the more challenging direct amide hydrolysis (Scheme 1.14). The L-valine derived auxiliary has a second practical advantage over its predecessor: the addition of a second stereogenic centre on the five membered-ring provides a pseudo C_2-symmetric auxiliary upon enolate formation. This provided it with the ability overcome the poor selectivity observed for the alkylation of (*E*)-enolates in the earlier system and is attributed to the ability of

the C_2-symmetry to direct the approach of the electrophile regardless of rotation about the C-N bond. Upon construction of the α-quaternary carbon stereocentre (**114**, Scheme 1.14), the auxiliary may be removed by reduction to furnish the alcohol (**117**) or through acidic hydrolysis (facilitated by N to O acyl transfer) to afford the corresponding carboxylic acid.

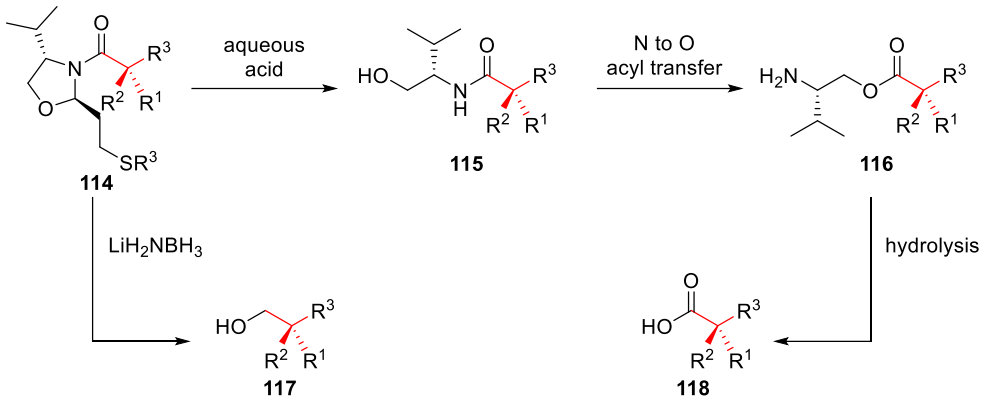

Scheme 1.14 Removal of auxiliary by hydrolysis and reduction

1.2 Catalytic Construction of α-Quaternary Carbon Stereocentres

In the modern conception of organic synthesis, the discussion of almost any topic is incomplete without reference to catalytic methods. Many arguments are made for the superiority of catalytic methods over the use of sociometric reagents; including (i) limiting the generation of stoichiometric waste, (ii) milder reaction conditions, and (ii) recycling of catalysts. However, these advantages do not make catalytic systems universally superior, and many catalytic methods have considerable shortcomings that can range from toxic metal contamination and sensitivity to the presence of water and/or oxygen.

Considering the prevalence of quaternary carbon stereocentres, significant effort has been made in establishing catalytic methods for their formation. The following are notable examples of the preparation of α-quaternary carbon stereocentres adjacent to carbonyls using asymmetric catalytic methods. For a comprehensive examination of the broader field of catalytic enantioselective quaternary carbon stereocentre formation the reader is encouraged to refer to recent reviews by Corey,[96] Overman,[25, 97] Krische,[98] and Stoltz.[99]

1.2.1 Transition Metal Catalysis

A particularly well-developed class of reactions capable of constructing α-quaternary carbon stereocentres is the Tsuji–Trost allylic alkylation.[100, 101] Significant effort over the past decade has allowed this reaction to develop from requiring cyclic systems to the point where quaternary carbon stereocentres can be constructed with high levels of selectivity[102] to generate branched linear systems (Scheme 1.15). In cases employing substituted acyclic enol carbonates (*e.g,* **120**),[103-105] transitioning away from cyclic systems presented a challenge in the synthesis of the starting materials, as questions of enolisation selectivity and enolate geometry once again come

to the fore. However, this is drawback is somewhat tempered as the enol carbonates isomers may be separated prior to allylation (*i.e.* quaternary stereocentre formation). With pure acyclic enol carbonates in hand chiral palladium species can differentiate the *si* and *re* faces of the enol derivatives to derive enantioenriched products, although it should be noted that the chiral ligand frameworks almost always require one of the α-substituents to be aryl in order to achieve high enantioselectivity.

Shimizu and Kanai have shown that *in situ* formation of chiral boron enolates, coupled with palladium catalysed allylation, can provide products with high optical purity in a single step, but again a dependence on a large steric difference between the α-substituents is required.[106] This mode of reactivity has also been explored with lithium amide enolates, employing LiHMDS as the base.[107] Similar allylation methods to those employing palladium catalysis, have also been developed with iridium[108-111] and rhodium[112] to generate quaternary carbon stereocentres. It should be noted that, as with the palladium catalysed examples, these systems also suffer from the requirement that the α-substituents be sterically differentiated to attain high degrees of enantioselectivity (ideally methyl *vs* aryl).

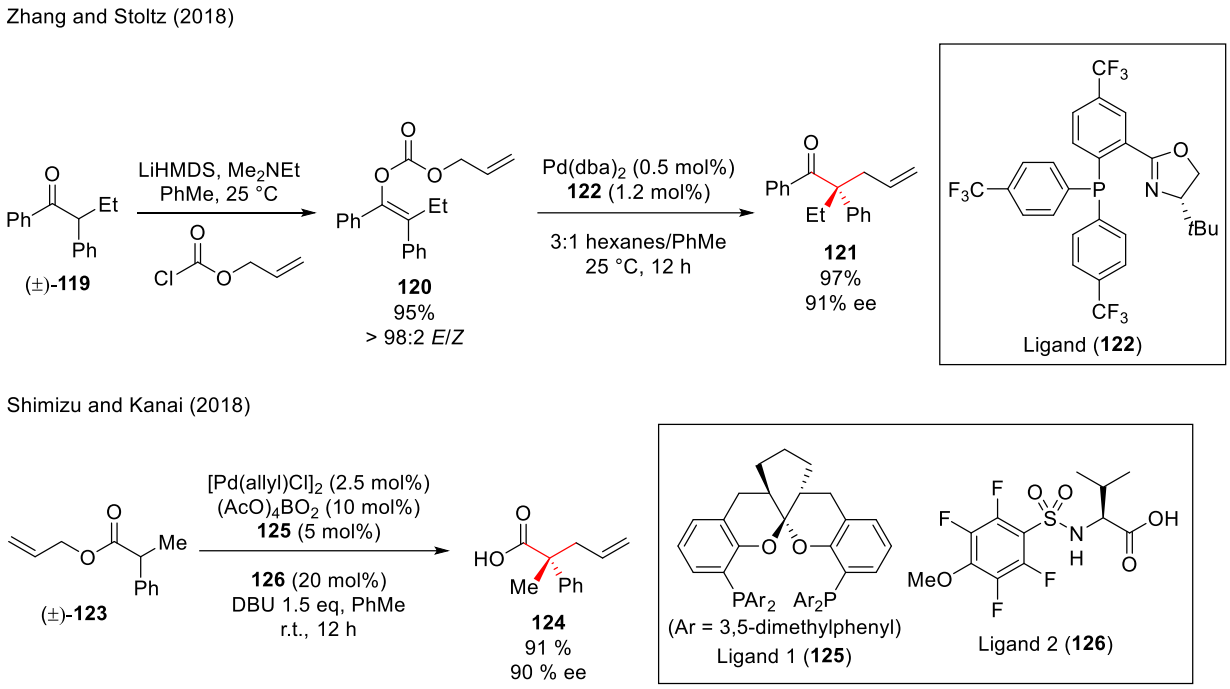

Scheme 1.15 Palladium catalysed asymmetric allylic alkylation

In recent years, activation of carbon-hydrogen bonds classically considered as inert, has become an influential paradigm in organic synthesis.[30, 113, 114] Palladium(II) catalysis has proved to be a powerful tool for engaging carbon-hydrogen bonds located proximal to directing functionality, providing selectivity in the activation step. Notable examples of this chemistry, which provide access to α-quaternary carbon stereocentres, have been reported by Yu. In most cases, the activated bond is located β-[115] (**127**) or γ-[29, 116] (**130**) to a heteroatom-containing functional group, commonly a carbonyl derivative, resulting in methods which routinely depend on desymmetrisation to install asymmetry, as the bond formed is not located α-to the carbonyl. Systems capable of activating sp^3 carbon-hydrogen bonds are well described in the literature yet in the context of enantioselective processes substrates are commonly more specialised, such as cyclopropanes,[117, 118] cyclobutanes,[119] or provide cyclic products,[120, 121] (Scheme 1.16).

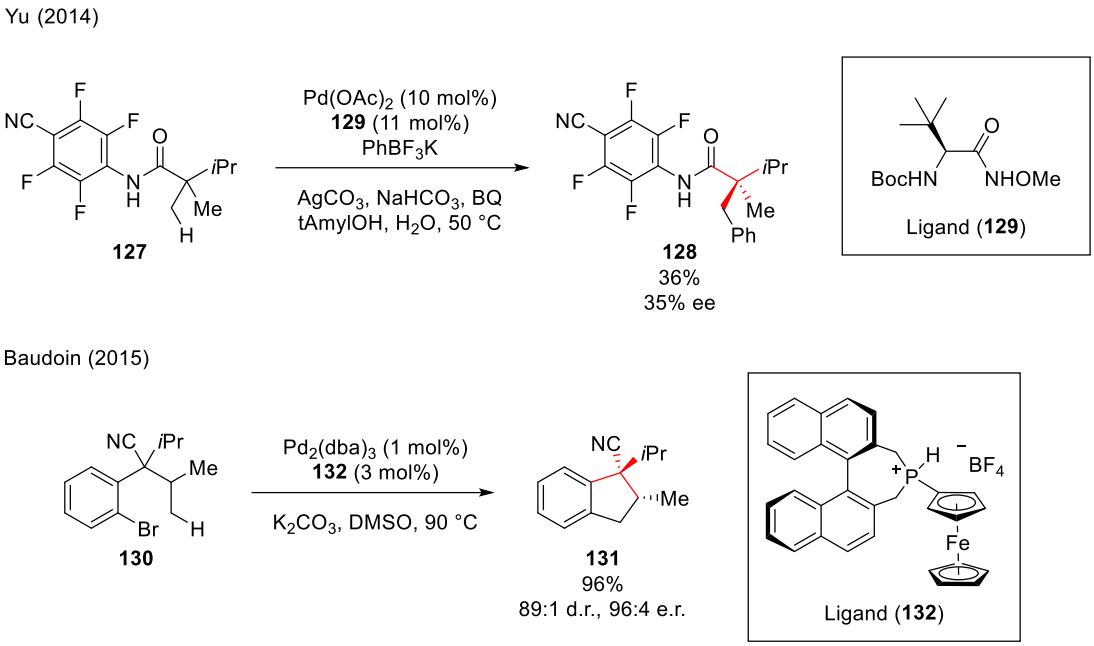

Scheme 1.16 α-Quaternary carbon stereocentre formation *via* palladium catalysed C-H activation/desymmetrisation

Due to the ability of desymmetrisation strategies to address the steric and stereochemical aspects of quaternary carbon stereocentre formation in separate steps it remains an attractive method. The interested reader is directed to the reviews by Yu[122] and Zhou[24] for a detailed discussion of catalytic systems which leverage this approach.

While not directly leading to carbonyl containing products, 1-2 additions to carbonyls by tertiary carbon nucleophiles has also been explored as a method for the generation of quaternary carbon stereocentres. The ability of allyl iridium species to undergo addition at their more substituted position has made them attractive intermediates for the formation of highly substituted structures. Krische has exploited this property in an iridium catalysed transformation which through a transfer hydrogenation mechanism allows for a previously unprecedented C-H activation of methanol.[123] β-hydride elimination of methanol leads to an iridium hydride species which undergoes reversable hydrometallation with a diene (Scheme 1.17). The iridium centre then

engages the equivalent of formaldehyde generated from the β-hydride elimination (**134**) with subsequent carbonyl addition then providing the homoallylic product (**136**). Higher order aldehydes, generated from higher order alcohols, impose greater steric congestion, raising the energy of the transition state and cause the reaction to proceed through a hydrometallation adduct which results in C3 coupling of the diene and a tertiary stereocentre. More recently this chemistry has been expended to the use of trifluoromethyl substituted allenes[124] and/or floral hydrate,[125] the later requiring an equivalent of isopropanol as a sacrificial reductant.

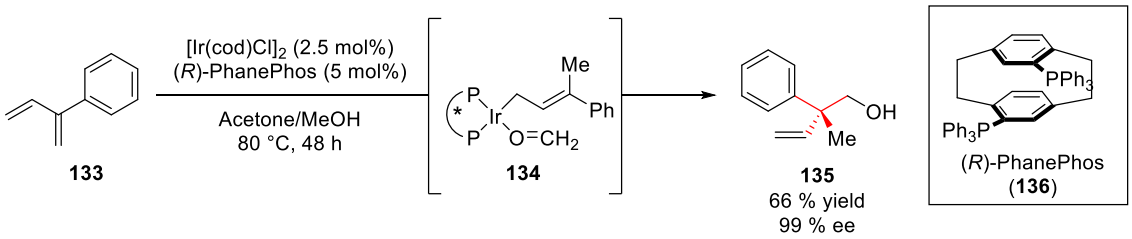

Scheme 1.17 Iridium catalysed C-H fictionalisation of methanol

1.2.2 Organocatalytic Formation of α-Quaternary Carbon Stereocentres

A highly useful example of employing organocatalysis in the preparation of α-quaternary carbon stereocentres is the synthesis of the Hajos-Parrish and Wieland–Miescher ketones (Scheme 1.18).[126, 127] Many methods are available for the preparation of these widely used chiral ketones, with some of the most popular being the use of proline[128, 129] (*i.e.* the Hajos–Parrish–Eder–Sauer–Wiechert reaction) and other chiral amine catalysts.[130] Like reactions discussed previously, these reactions take advantage of pro-chiral substrate desymmetrisation to afford high enantioselectivities. However, in recent years increased development of novel primary and secondary amine catalysis has allowed the use of acyclic and nonsymmetric substrates as well as the ability to form α-quaternary carbon stereocentres *via* intermolecular reactions. Notable

examples include Barbas' intramolecular aldol[131] (Scheme 1.18) and Diels-Alder reactions developed by Gleason[132] and Hayashi.[133]

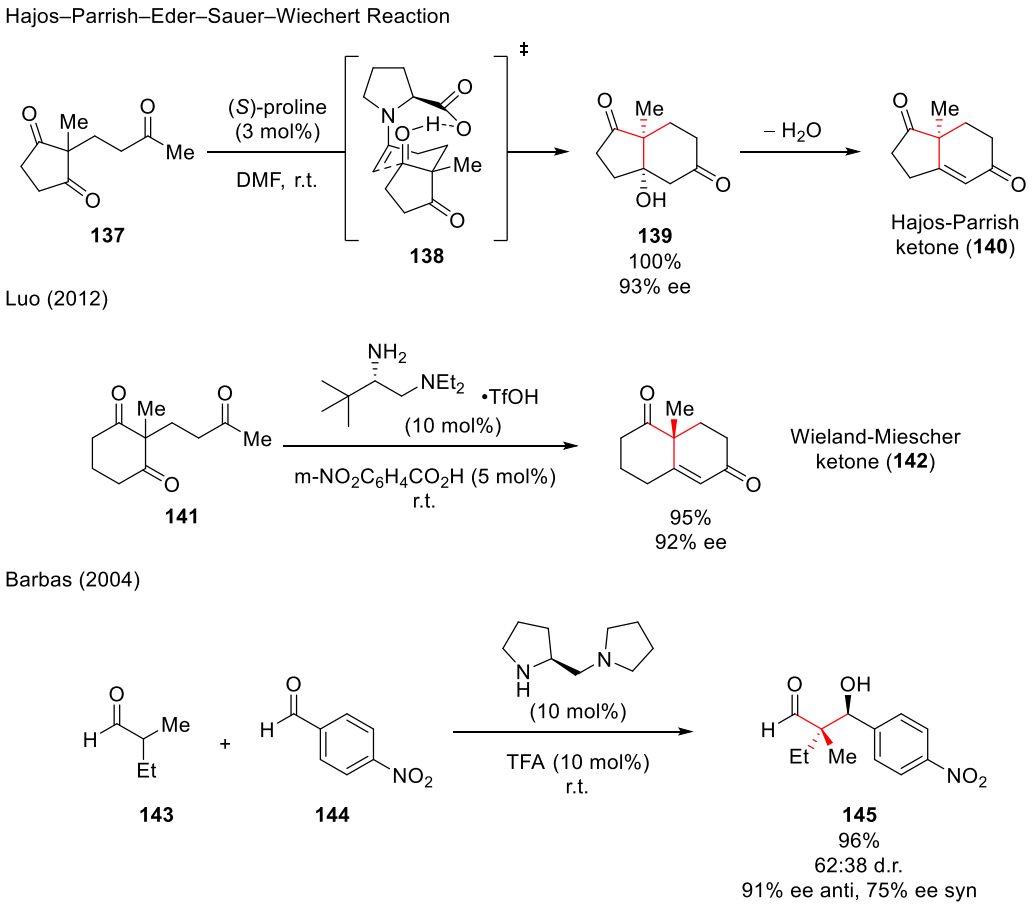

Scheme 1.18 Organocatalytic preparation of the Hajos-Parrish and Wieland-Miescher ketones and Barbas' organocatalytic asymmetric aldol reaction

In 2013, Carreira furthered the use of cinchona amine catalysis[134, 135] by coupling it to iridium-catalysed allylic substitution.[136] Taking advantage of the two distinct reactivity paradigms, the authors could generate chiral imine nucleophiles in the presence of chiral allyl-iridium electrophiles (from racemic aldehydes and allylic alcohols respectively) to form branched aldehyde products possessing α-quaternary and β-tertiary carbon stereocentres. The planar nature of the two intermediates allowed the catalysts to exert stereocontrol largely independent of one

another, allowing all four diastereomers to be accessed by selection of specific amine (**149**) and ligand (**150**) enantiomers (Scheme 1.19). Yields and enantioselectivity for the process remain high throughout the investigated substrate scope with reductions in diastereoselectivity observed in cases where there is little steric bias between the aldehyde α-substituents (*e.g.* methyl *vs n*-propyl 6:1 d.r.). It should be noted that an apparent limitation is the requirement for one α-substituent to be methyl (save for one example where the α-substituents comprise part of an indoline system). This example remains an interesting case of the interplay between organo-and transition metal catalysis.

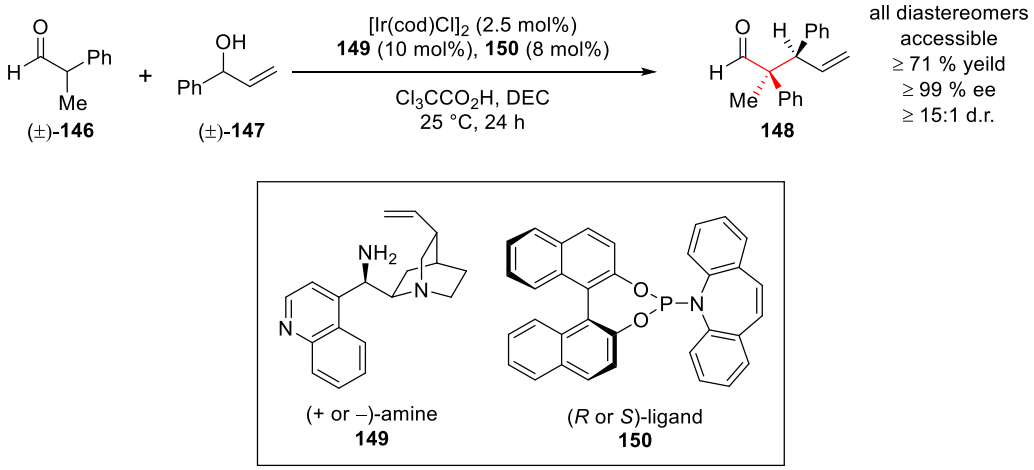

Scheme 1.19 Formation of vicinal quaternary and tertiary stereocentres

1.2.2.1 Phase-Transfer Catalysis

A subclass of organocatalysis, chiral phase-transfer agents, have found success in the stereoselective α-allylation of species containing reasonably acidic α-protons (*e.g.* α-aryl amides).[137, 138] These reactions are characterised by an aqueous phase, containing an inorganic base (*e.g.* NaOH, KOH, *etc.*), and a separate organic phase in which the reagents are isolated and allowed to react with small amounts of base either at the phase interface or transported to the

organic phase through association with the phase-transfer catalyst. Advantages of these reactions, over monophasic/homogeneous reaction conditions, include mild reaction conditions and simple experimental set up and operation.[139] With regard to asymmetric catalysis, chiral, non-racemic, quaternary ammonium salts have been particularly useful, with many of the most widely employed examples being isolated from nature, such as the cinchona alkaloids. A notable example of using cinchona alkaloid derivatives as phase transfer catalysts is O'Donnell's synthesis of chiral amino acids.[140] Although not employed to construct chiral quaternary carbons, this chemistry does highlight the use of such ammonium catalysts for stereoselective enolate alkylation.

A practical example of the use of asymmetric phase-transfer catalysis is found in Merck's synthesis of (+)-indacrinone (**28**),[141] a loop diuretic. Scheme 1.20 shows the interaction of the substrate with *N*-(p-(trifluoro-methyl)benzyl)cinchoninium (**154**), the phase-transfer catalyst, allowing for the discrimination of the *si* and *re* faces of the enolate. This system provided situatable stereo-control to afford the methylated intermediate in 92% ee.[142]

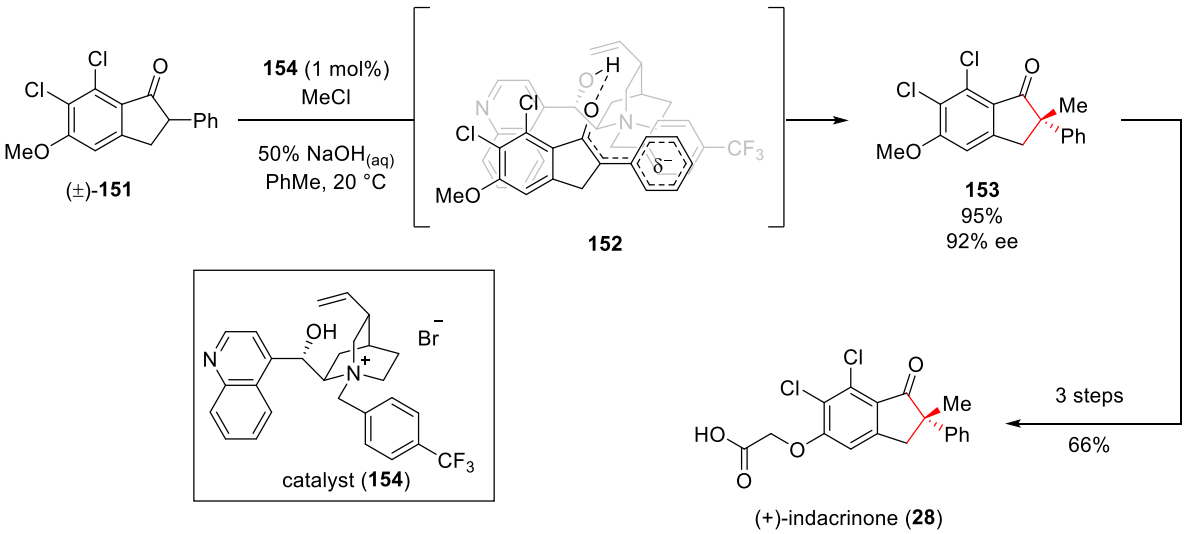

Scheme 1.20 Asymmetric phase-transfer catalysis in the synthesis of (+)-indacrinone

Though many examples of asymmetric phase-transfer catalysis use cyclic systems to control enolate geometry some catalytic systems are competent in linear systems. Conditions developed by Park allow for the one-pot sequential alkylation of malonate esters in high yield and enantiomeric excess (Scheme 1.21).[143]

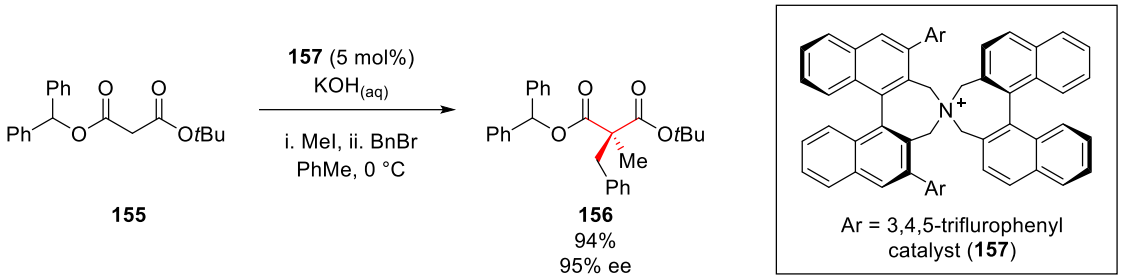

Scheme 1.21 Asymmetric dialkylation of malonate esters

Phase transfer catalysis has also been used to derive α-quaternary carbon stereocentres from intramolecular alkylations. In the large scale (> 1 kg) preparation of MK-3207 – a calcitonin gene-related peptide receptor antagonist under investigation for the treatment of migraine[144] – the challenging α-quaternary carbon stereocentre was set in a single step through the sequential alkylation with aniline **159**.[145] Under the reaction conditions, the highly electrophilic aza-para-quinone methide is generated from aniline **159**, *via* elimination, and is trapped by azaindole **158**. Intermediate **160** then undergoes decarboxylation generating the enolate which may subsequently attack the benzylic chloride to forge chiral spirocycle **161** in good yield and with high levels of enantioselectivity.

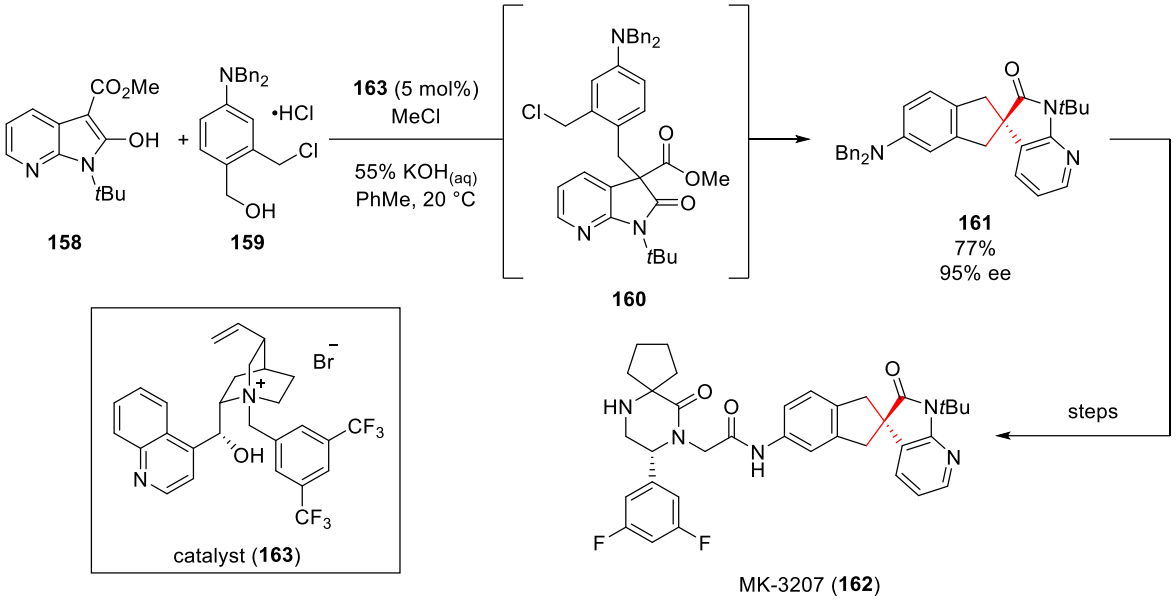

Scheme 1.22 Asymmetric dialkylation in the synthesis of MK-3207

1.3 Puraquinonic Acid

1.3.1 Isolation, Structure, and Biological Activity

Mycena pura (referred to as *Agaricus prunus* until 1871) is a wild mushroom common to the woodlands of Britain, Ireland and most parts of continental Europe.[146] In 1997 Anke and Sterner reported the isolation of two secondary metabolites from *Mycena pura*.[147] These compounds were the known fungicide strobilurin D[148] (**165**) and the novel norilludalane sesquiterpene puraquinonic acid (**164**) (Figure 1.10). While the authors established the structure of puraquinonic acid through MS and NMR spectroscopy the absolute stereochemical configuration was unknown until determined by enantioselective total synthesis by Clive in 2004 (*vide infra*).[149, 150]

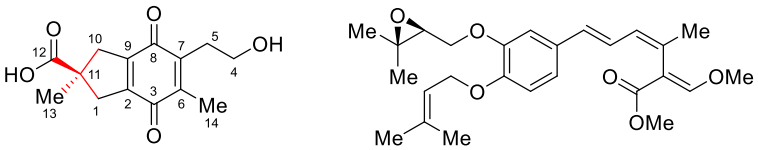

Figure 1.10 The natural products puraquinonic acid, strobilurin D, and muscarine

Puraquinonic acid was identified to be biologically active with doses of 380 µM inducing differentiation to either granulocyte- or monocyte/macrophage-like cells in 30% – 40% of HL-60 cells and 10% – 15% of U-937 cells (a histiocytic lymphoma cell line). At these concentrations the number of cells, in both cell lines, increased to 120% of the inoculum, with a retention in cellular metabolic activity (as measured by XTT reduction[151]). To identify mechanism of action, the influence of puraquinonic acid on transcription factors was investigated. Unfortunately, no effect on transcription factors in HL-60 and U-937 related to cell differentiation or apoptosis was observed. However, when tested for mutagenicity puraquinonic acid was found to have no

mutagenic activity at 380 μM. These intriguing biological properties make it, and related natural products,[152] potentially interesting lead molecules in the development of leukaemia treatments.

1.3.2 Related Natural Products and Proposed Biosynthesis

As a norilludalane (**168, 169**), puraquinonic acid is a member of a larger family of natural products that also includes the protoilludalanes (**166**), illudanes (**167**), and illudalanes (**170**) (Figure 1.11). These molecules share many common structural features including a central six-five fused carbocyclic framework with a the geminal dimethyl moiety at C11. Several oxidation motifs can also be observed with some of the most common being C4 oxidation of the (nor)illudalanes and the oxidation of the one of the geminal dimethyl carbons, providing an α-quaternary carbon stereocentre. Oxidation of the six membered ring is a point of significant variation within the family, with examples such as repraesentin A (**171**)[153] having a mainly saturated core while others contain highly oxidised cores such as the central arene of alcyopterosin A (**172**)[154, 155] and the paraquinone found in puraquinonic acid (**164**).

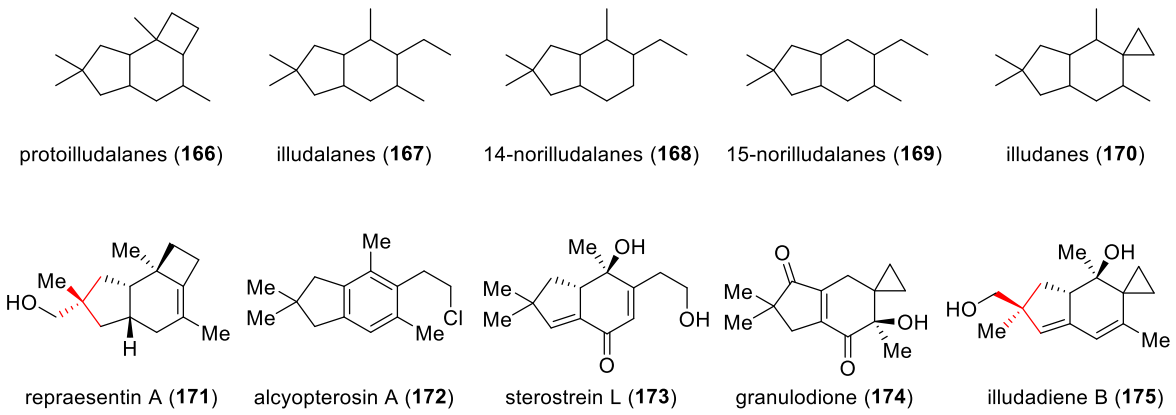

Figure 1.11 Carbon skeleton and examples of protoilludalanes, illudanes, illudalanes, and norilludalanes

The biosynthetic origin of the illudalanes, and related natural products, begins with a C11 to C1 annulation of farnesyl pyrophosphate fungal sesquiterpenoids to afford the humulene-type

macrocycle (**177**). Subsequent transannular ring forming events lead to the tricyclic protoilludyl cation (**180**) which upon deprotonation provides Δ6-protoilludene.[156] From this point in the biosynthesis, a variety of oxidations and ring openings/closures presumably occur to forge the observed frameworks. However, specific enzymes responsible for these transformations are not known.

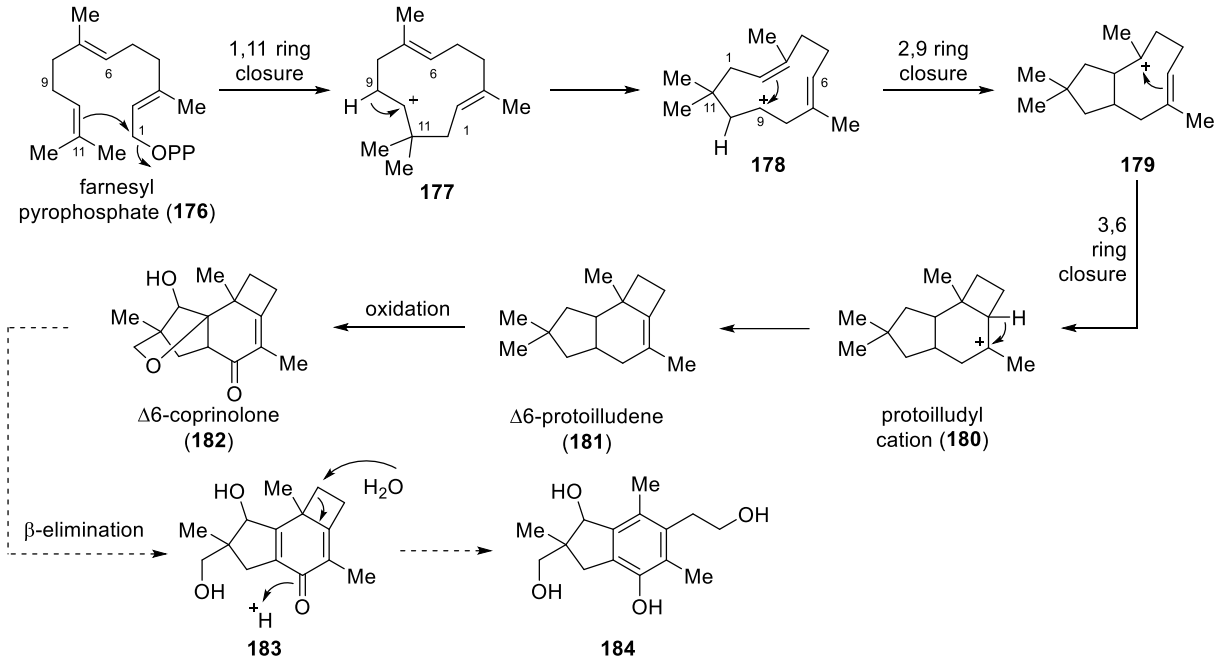

Scheme 1.23 Proposed biosynthesis of the illudalanes

Experiments involving the fungus *Coprinus psychrornorbidus* grown in the presence of ^{13}C enriched sodium acetate demonstrated significant incorporation into the structure of Δ6-coprinolone.[157] Evidence for the further conversion to the illudane framework is poorly documented. However, the protoilludalane stearoyldelicone (**185**) has been shown to undergo a facile addition of water in the presence of SiO_2 to fragment the four membered ring and provide phenol **186** displaying illudane skeleton (Scheme 1.24).[158] It is reasonable to assume that the biosynthesis of the norilludanes proceeded *via* a similar pathway, with the addition of a carbon

dehomologation at some stage, to provide puraquinonic acid (**164**) and related structures (Figure 1.12), but the steps remain unclear.[159]

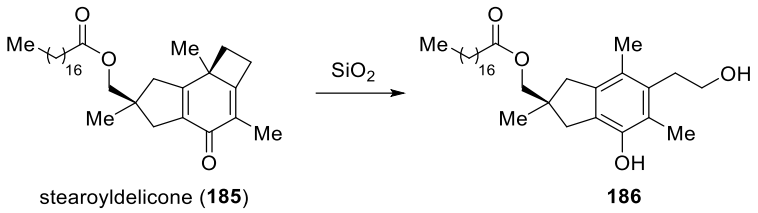

stearoyldelicone (**185**) **186**

Scheme 1.24 Facile conversion from the protoilludalane to illudalane carbon skeleton

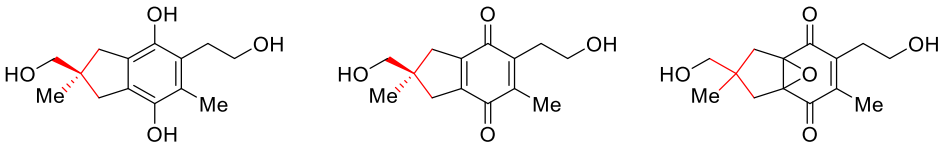

russujaponol L (**187**) deliquinone (**188**) epoxydeliquinone (**189**)

Figure 1.12 Natural products structurally related to puraquinonic acid

1.3.3 Previous Total Syntheses of Puraquinonic Acid

Despite its unassuming structure puraquinonic acid has attracted the attention of synthetic chemists and several approaches to its preparation have been reported in the literature since its isolation. One possible explanation for this dedication is that puraquinonic acid displays a very intriguing α-quaternary carbon stereocentre, wherein the stereo-defining features of the molecule are well removed from the location of the stereocentre. This results in the two of the substituents of the α-carbon to having near identical electronic and steric properties, greatly increasing the challenge of constructing the stereocentre. Additionally, it presents a target with varying degrees of oxidation (primary alcohol, carboxylic acid, and para-quinone) inherently raising questions of chemo- and regioselectivity.

1.3.3.1 Approaches to the Racemic Preparation of Puraquinonic Acid

The first synthesis of puraquinonic acid was disclosed by Clive in 2001.[160] This syntheses brought to the fore several of the challenges present within this molecule (Scheme 1.25). As the starting benzoic acid **190** represents the core of the target's carbon framework and is only one oxidations state below the required quinone, the synthesis focuses on the installation of the missing substituents, with three independent tactics being employed. The first of the carbon-carbon bond is installed *via* a Claisen rearrangement to prepare phenol **194**, taking advantage of a regioselective methyl deprotection to give access to the required aryl-allyl ether. The next substituent to be addressed ultimately becomes the aryl methyl group and is appended by aryl lithium addition to Mander's reagent, which is sufficiently small to overcome the steric demand posed by the two ortho substituents. Functionalisation of the final site on the aryl ring also requires consideration of a crowded steric environment. As such, an intramolecular approach, in the form of an acid promoted Nazarov cyclisation, is used with the substrate being derived from the previously installed allyl group in a four-step sequence. Though this sequence imparts an unnecessary ketone, its location allows for the formation of an α,α-disubstituted enolate which can be quenched with Mander's reagent to complete the carbon skeleton. From this point the remaining steps accomplish the opening and selective reduction of the dihydropyran, saponification of the methyl ester and final oxidation to the paraquinone. CAN is sufficiently oxidising to enable this transformation due to the considerably electron rich nature of the dimethylhydroquinone moiety. This sequence provides a lengthy thirty step sequence which highlights the difficulties encountered by choosing to construct the molecule around an initial aromatic core. Particularly notable is the challenge encountered in the assembly of the five-membered ring, with both additional carbon atoms and functional groups being introduced and later removed in order to complete the synthesis.

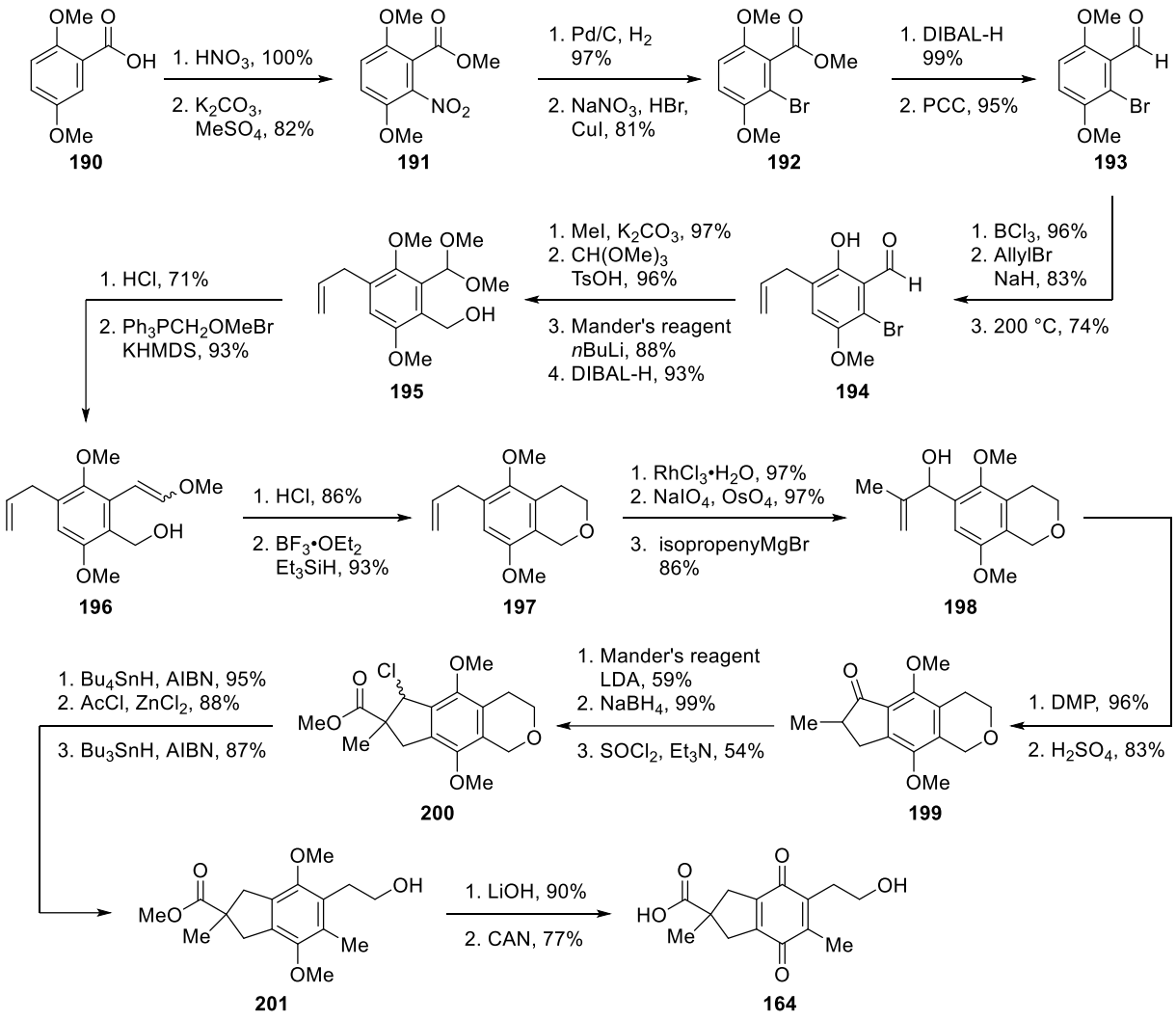

Scheme 1.25 Clive's first-generation racemic synthesis of puraquinonic acid

Shortly after, Clive reported a second racemic synthesis which relies on many of the same tactical steps but manages to cut the number of septs required in half, to fifteen (Scheme 1.26).[161] This was accomplished by selecting a starting material which incorporates the required C14 aryl methyl group and by preparing the Nazarov cyclisation precursor *in situ via* a Fries rearrangement. This allowed use of the allylation-Claisen rearrangement to install the ethyl alcohol sidechain. Overall, the second-generation approach made evolutionary advancements to the author's first synthesis of puraquinonic acid.

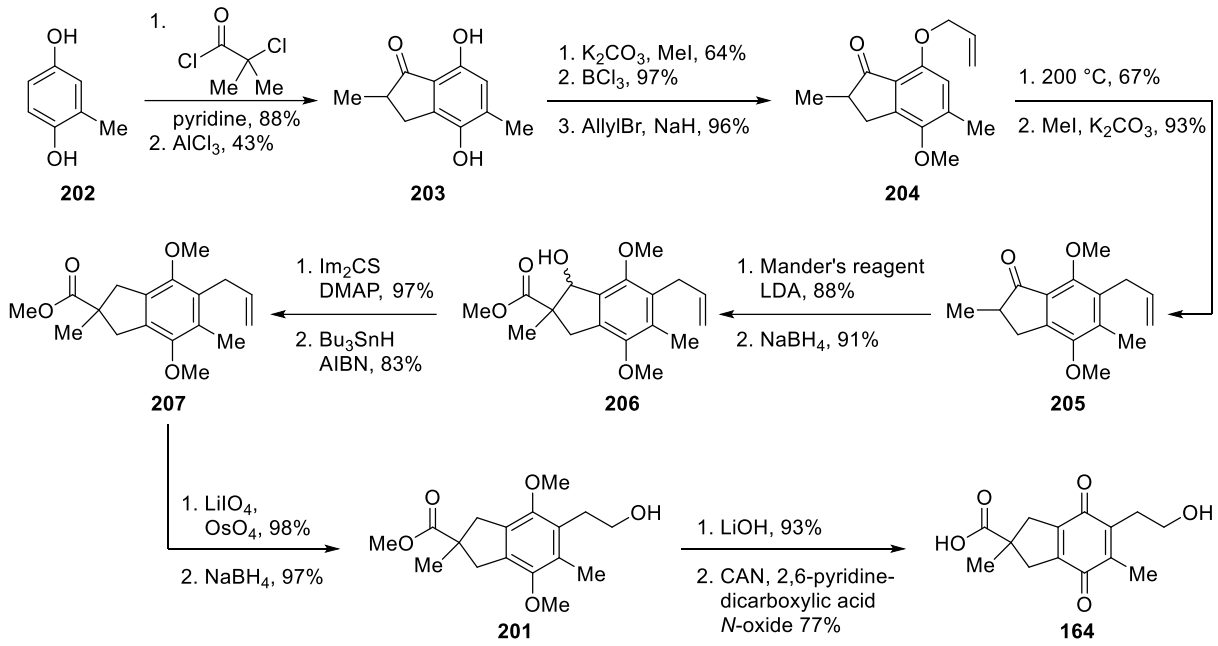

Scheme 1.26 Clive's second-generation racemic synthesis of puraquinonic acid

A year later, in 2002, Kraus published a ten-step divergent total synthesis of puraquinonic acid ethyl ester (**216**) and the related natural product deliquinone (**188**),[162] in which an alternative method for the construction of the cyclopentene portion of target was devised. In the first key step of the synthesis, Meldrum's acid (**210**) was alkylated with dibromide **209** to afford spirocycle **211**. Transesterification and concomitant decarboxylation provided the ethyl ester which was then alkylated with iodomethane to generate the α-quaternary carbon. From here Kraus leveraged the same allylation-Claisen rearrangement followed by Lemieux-Johnson diol cleavage and reduction (as performed by Clive) to attach the ethyl alcohol fragment. Employing sodium borohydride provided chemoselective reduction of the aldehyde while use of lithium aluminium hydride also reduced the ester to the primary alcohol found in deliquinone (**188**). The respective reduction products (**215** and **217**) represent the divergence of the two synthetic routes. Oxidation of the electron rich phenol to the paraquinone was realised, with near quantitative yield for both

substrates, using molecular oxygen and salcomine.[163] Attempts to install the final methyl group using organocuprates and organozincs failed. Ultimately, addition of a methyl radical generated by oxidation of acetic acid completed the synthesis of puraquinonic acid ethyl ester (**216**) and the natural product deliquinone (**188**).

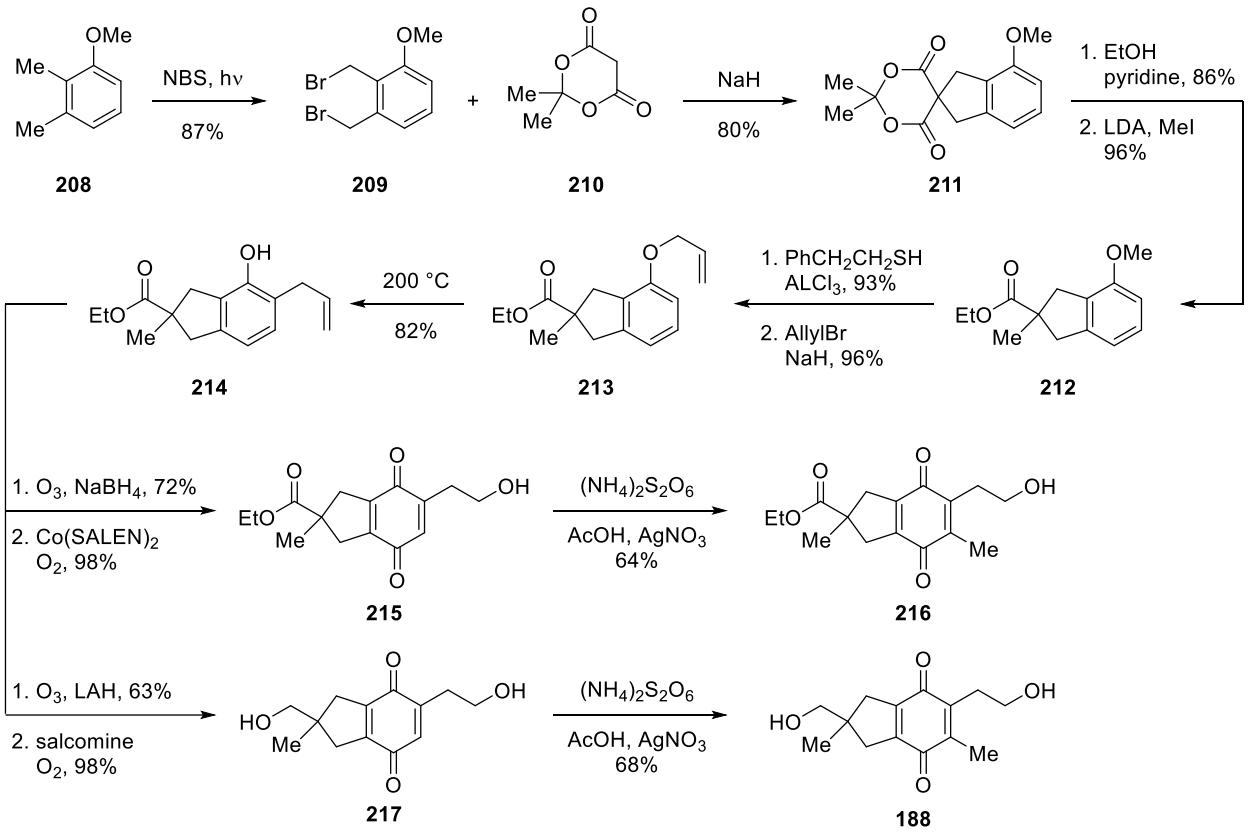

Scheme 1.27 Kraus' racemic synthesis of puraquinonic acid ethyl ester and deliquinone

The final, and most recent, racemic synthesis in this series was the preparation of puraquinonic acid methyl ester (**202**) by Baudoin.[164] The key step involves a palladium(0) catalysed Csp^3-H activation of an α-geminal dimethyl group to form the cylopentene and the α-quaternary centre in a single transformation (Scheme 1.28). Though this synthesis applies a contemporary C-H activation strategy it still focuses on the decoration of a central phenyl ring and continues the use of use of the Claisen rearrangement to install the ethyl alcohol. It also employs

the same salcomine oxidation and methyl radical addition employed by Kraus to complete the synthesis.

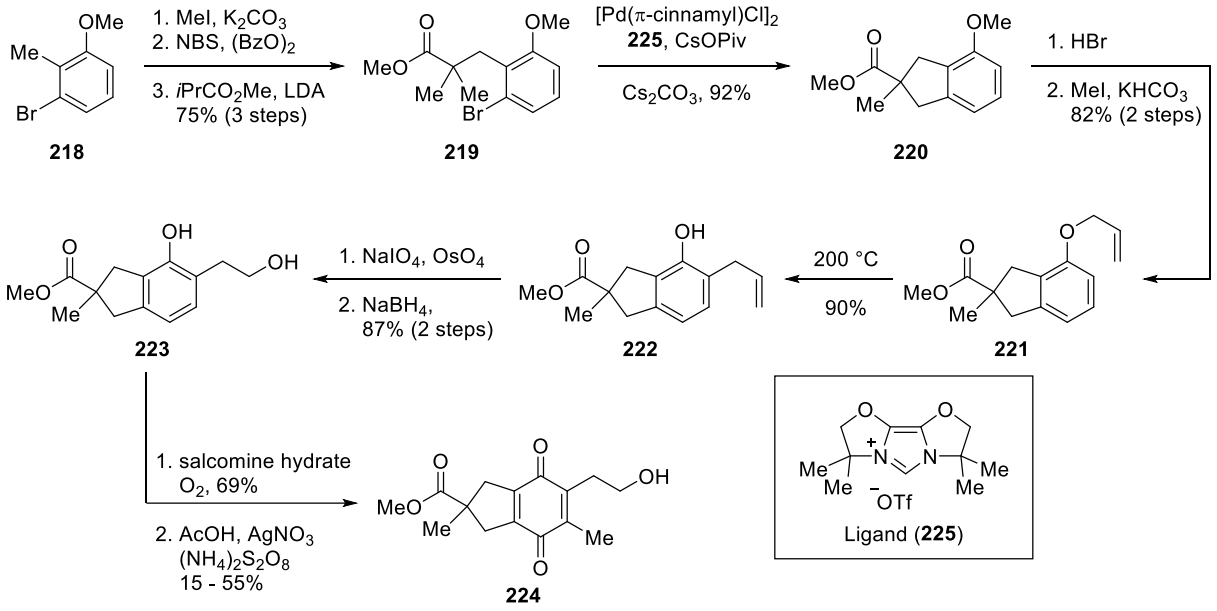

Scheme 1.28 Baudoin's racemic synthesis of puraquinonic acid methyl ester

1.3.3.2 Asymmetric Syntheses of Puraquinonic Acid

The first asymmetric synthesis of puraquinonic acid was published by Clive (Scheme 1.29) shortly following Clive's original work on the racemic synthesis.[149] Considerable portions of this synthesis borrow from the racemic approach with the significant differences resulting from the need to incorporate an element of asymmetry. For this task the Evans' aldol reaction was relied on with the initial eleven steps of the synthesis used to construct the highly decorated benzaldehyde **230**. Due to the problems inherent to forming α-quaternary carbon stereocentres using Evans' oxazolidone based auxiliaries, the stereocentre of puraquinonic acid could not be directly constructed. Instead, in a series of five steps, the authors modified the anti-aldol product to a chiral allylic silyl ether **232**. This proved a suitable substrate for a Grubbs ring closing metathesis to form

the fused bicyclic core. The silyl ether was then converted to the Stork bromo acetal **234** and underwent radical cyclization when treated with tributyltin hydride and AIBN to finally install the chiral quarterly carbon stereocentre. A sequence of seven steps was then used to remove the superfluous functionality associated with the tetrahydrofuran ring to afford dimethyldihydroquinone **236**. In the concluding steps of the synthesis, the protecting groups were removed and a final oxidation with CAN furnished the natural product.

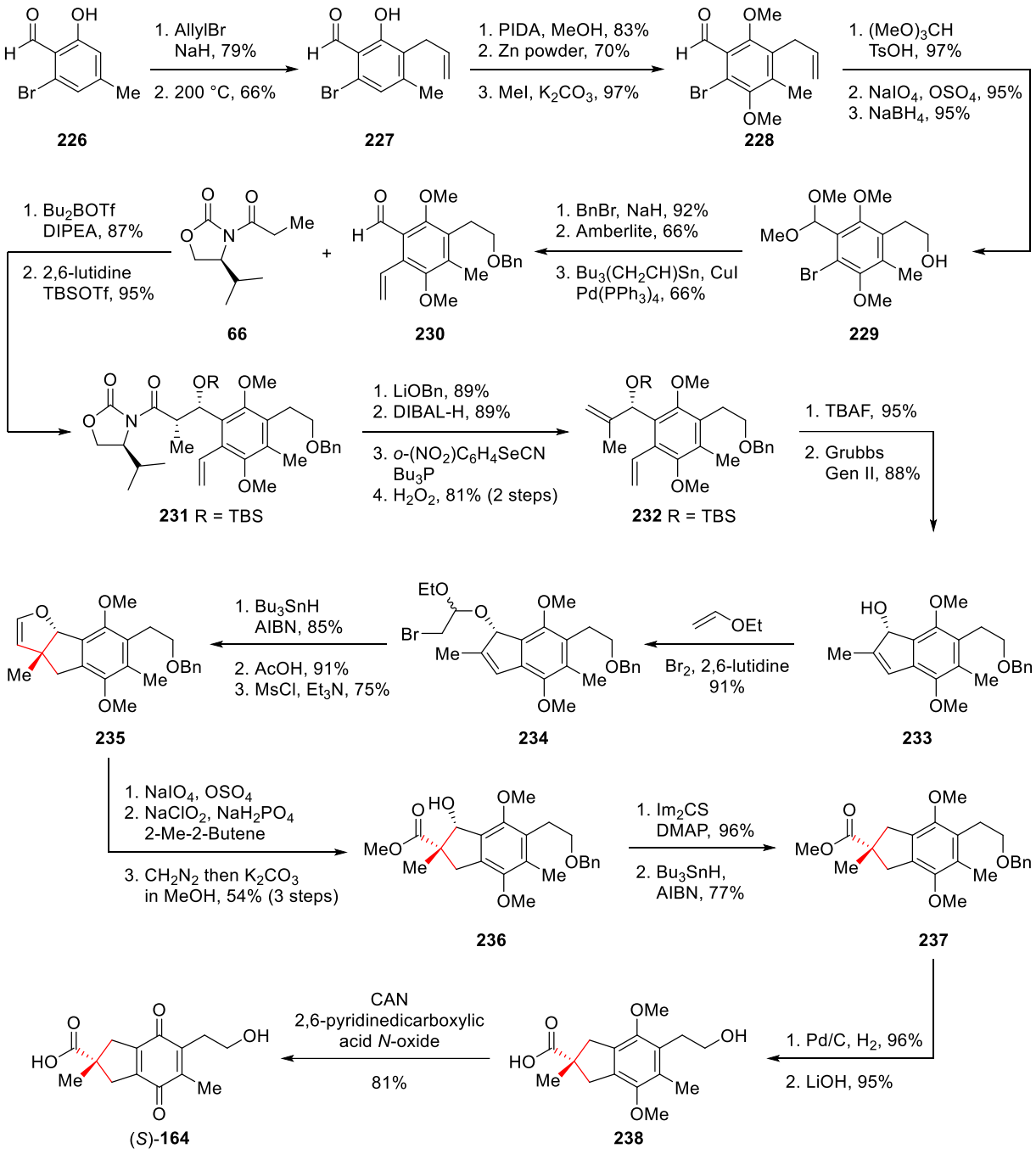

Scheme 1.29 Clive's synthesis of (*S*)-puraquinonic acid

In its entirety, Clive's asymmetric synthesis is thirty-one steps in length and stands as a testament to the difficulty associated with establishing α-quaternary carbon stereocentre with classical approaches. This synthesis was also instrumental in establishing the absolute

stereochemistry of the natural product as (*R*)-puraquinonic acid with comparison of the authentic and synthetic (*R*)-puraquinonic acid shown to be enantiomeric by HPLC.[150] This was of critical importance as the optical rotation of natural puraquinonic acid was reported as +1 [*c* 1.0 $CHCl_3$] but could be correctly reassigned to -2.2 [*c* 0.55, $CHCl_3$].

The ability of our group's methodology to prepare quaternary carbon stereocentres bearing substituents of similar nature suggested it might lead itself to an alternative, more efficient route to (*R*)-puraquinonic acid. Specifically, the group envisioned generating the quaternary stereocentre at an early stage bearing moieties that could be used to construct the aromatic ring.[165] Sequential alkylation of thioglycolate lactam provided rapid access to the quaternary stereocentre with allyl and propargyl substituents proving functional handles to construct the aromatic ring. A one-pot sequence concomitant eneyne/cross metathesis, Diels-Alder cycloaddition, and oxidation furnished the aryl ring with the required substituents installed. Global saponification followed by lactonisation revealed a carboxylic acid, which was transformed to an amine *via* a Curtius rearrangement. This provided a synthetic handle for the eventual oxidation to the paraquinone. Reduction of the lactone with Red-Al resulted in complete reduction to the desired methyl group, through reduction of an intermediate aza-ortho-quinone methide. From here completion of the synthesis simply required hydrolysis of the vestigial auxiliary amide and oxidation, with Fremy's salt, to the paraquinone. This completed the synthesis of puraquinonic acid in only twelve steps from commercially available starting materials; comparable in length to the racemic synthesis of the ethyl ester reported by Kraus.

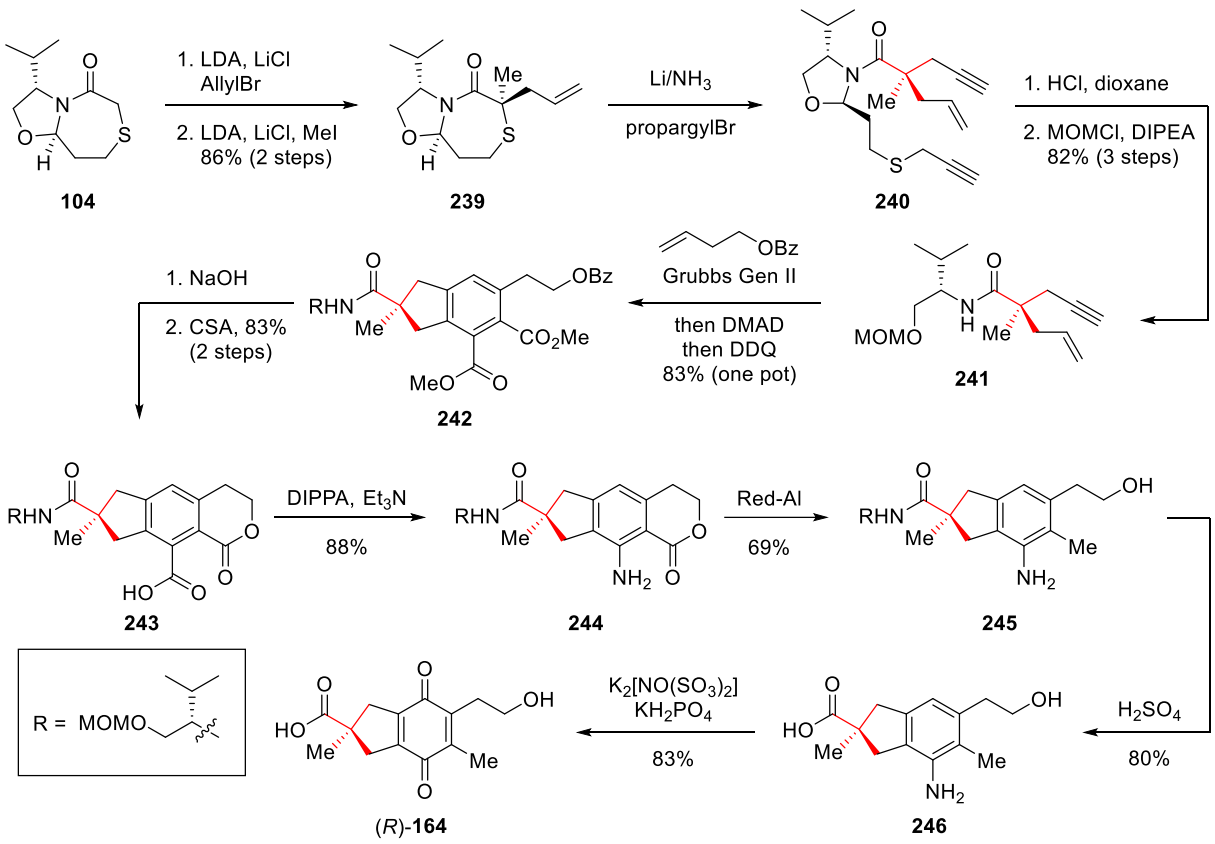

Scheme 1.30 Gleason and Tiong's synthesis of (*R*)-puraquinonic acid

The final total synthesis was reported by Baudoin's who employed a palladium(0) C(sp^3)-H activation.[166] Published prior to the disclosure of the racemic approach[164] the authors clearly describe the development of the two syntheses as part of the same endeavour. As such, the two are very closely linked with the key difference being the need to modify conditions to successfully differentiate the prochiral methyl groups of ester **249**. To accomplish this, a chiral N-heterocyclic carbene ligand (**255**) was used. Unfortunately, use of this ligand on aryl bromide **219**, a model substrate, only provided the C-H activation product **220** in 66:34 e.r. To increase the selectivity, modifications to the substrate were made to replace the ester of aryl bromide **219** with chiral amide derivates. This gave moderate increases in selectivity, with the best selectivity (87:13 d.r.) obtained using a proline derive amide. Use of this ligand and proline auxiliary on aryl bromide **250** afforded

amide **251** in 85:15 d.r. Crystallisation, post amide hydrolysis, provided intermediate **252** in 96:4 e.r. This contrasts with other catalytic systems developed by Baudoin which can generate quaternary carbon stereocentres within similar five-six fused bicyclic systems without the need for a chiral auxiliary.[121] Although this is achieved *via* a similar desymmetrisation strategy (Scheme 1.16, *vide supra*), the quaternary carbon is formed at the benzylic position of the five-six fused bicycle.

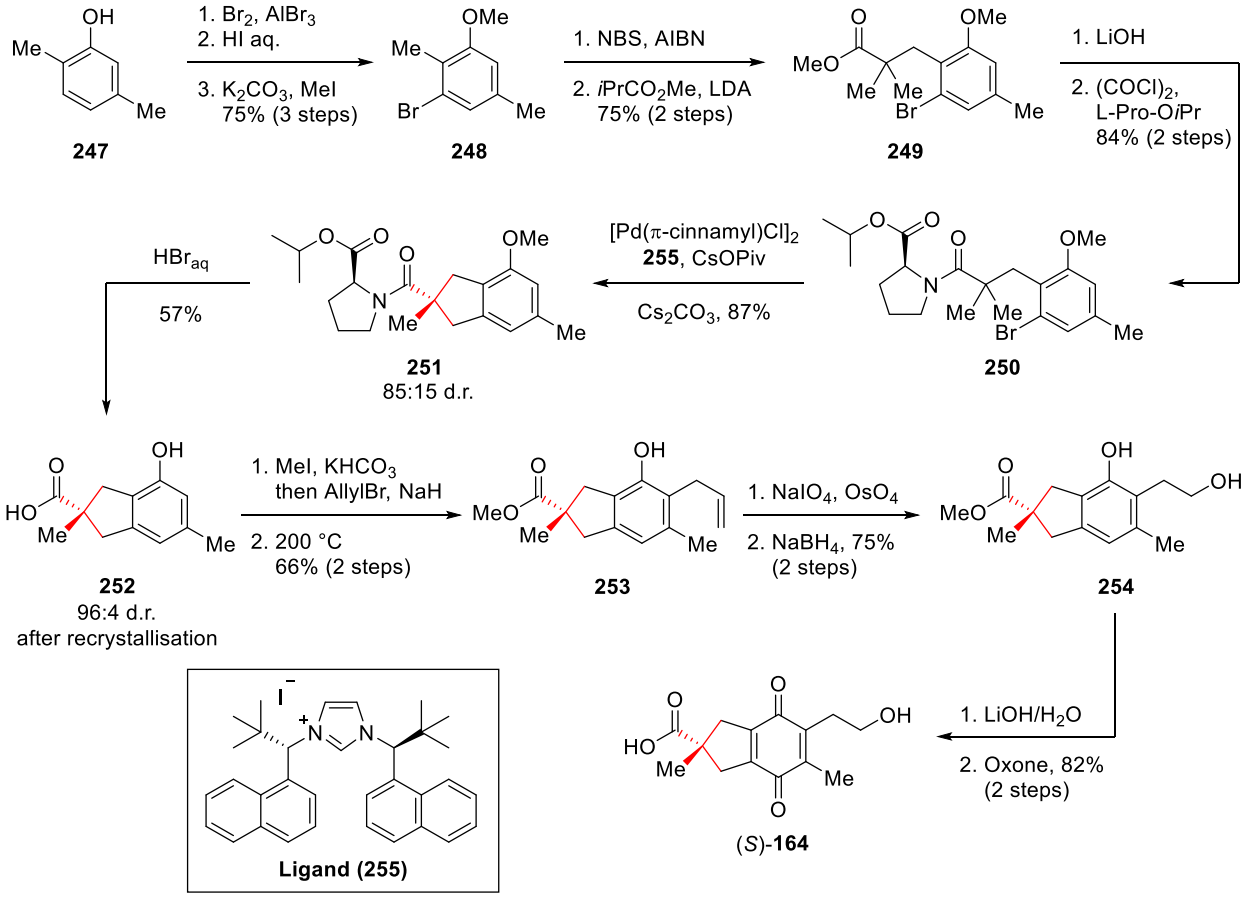

Scheme 1.31 Baudoin's synthesis of (*R*)-puraquinonic acid

Completion of the synthesis followed a similar route to the racemic approach, with the ethyl alcohol side chain installed *via* Claisen rearrangement. However, the final oxidation was performed with Oxone and not salcomine to furnish the natural product in fifteen steps. Baudoin

also took advantage of a common intermediate to complete syntheses of (*R*)-deliquinone (**188**) and (*S*)-russujaponol F using this C-H activation strategy.

1.4 Construction of α-Quaternary Carbon Stereocentres in Advanced Settings

The discussion of the literature concerning construction of isolated α-quaternary carbon stereocentres highlights great interest in general synthetic techniques to reliably form these challenging structures rapidly and reliably at advanced stages of chemical synthesis. Notably, the majority of methods are limited to the use of simple and sterically differentiated α-substituents further limiting their utility in complex settings. The next two chapters of this thesis addresses these challenges in the formation of quaternary carbon stereocentres and highlight the advancements by demonstrating their utility in a second-generation synthesis of puraquinonic acid. Specifically, the two main objectives are (i) the investigation of biselectrophilic substrates for the alkylation of bicyclic lactams and (ii) the use of the strategy in a *de novo* total synthesis of (*R*)-puraquinonic acid.

1.4.1 Investigation of Biselectrophilic Substrates in the Alkylation of Bicyclic Lactams.

In contrast to most methods examined in this chapter, the use of bicyclic thioglycolate lactams does not rely on steric or electronic differentiation for the formation of α,α-disubstituted enolates and, correspondingly, for high levels of stereoselectivity. In chapter two, this property has been further exploited and the chemistry advanced to provide a method amenable to chemically and structurally varied systems including aliphatic, allylic, and benzylic systems in addition to the formation of five- and six-membered ring systems. The chemistry of bicyclic thioglycolate lactam **104** has been explored in relation to more elaborate electrophiles (specifically, those baring multiple electrophilic sites) with the findings outlined in chapter two.

1.4.2 A Novel Approach to (*R*)-Puraquinonic Acid

Demonstrated in the above discussion of the asymmetric syntheses of puraquinonic acid is the significant synthetic challenge imposed by the asymmetric construction of the α-quaternary carbon, requiring the dedication of ten (Clive)[149, 150] to four (Baudoin)[164, 166] steps to successfully install the moiety. Collectively, the syntheses also display generous use of protecting group and functional group manipulations. In the development of a novel synthesis of puraquinonic acid, it is proposed that an approach to the late-stage introduction of α-quaternary carbon stereocentres and applying it to the preparation of puraquinonic acid may address some of the shortcomings of the previously disclosed total syntheses. To this end, the methodology outlined in chapter two shall be tested and validated in the context of the total synthesis documented in chapter three.

1.5 References

1. Büschleb, M.; Dorich, S.; Hanessian, S.; Tao, D.; Schenthal, K. B.; Overman, L. E., Synthetic Strategies toward Natural Products Containing Contiguous Stereogenic Quaternary Carbon Atoms. *Angewandte Chemie International Edition* **2016,** *55* (13), 4156-4186.
2. deVries, J. G., Important Pharmaceuticals and Intermediates. In *Quaternary Stereocenters*, Christoffers, J.; Baro, A., Eds. Wiley: 2005; pp 25-50.
3. Arimoto, H.; Uemura, D., Important Natural Products. In *Quaternary Stereocenters*, Jens Christoffers; Baro, A., Eds. Wiley: 2006; pp 1-24.
4. Nicolaou, K. C.; Roschangar, F.; Vourloumis, D., Chemical Biology of Epothilones. *Angewandte Chemie International Edition* **1998,** *37* (15), 2014-2045.
5. Singla, A. K.; Garg, A.; Aggarwal, D., Paclitaxel and Its Formulations. *International Journal of Pharmaceutics* **2002,** *235* (1), 179-192.
6. Guenard, D.; Gueritte-Voegelein, F.; Potier, P., Taxol and Taxotere: Discovery, Chemistry, and Structure-Activity Relationships. *Accounts of Chemical Research* **1993,** *26* (4), 160-167.
7. Zezula, J.; Hudlicky, T., Recent Progress in the Synthesis of Morphine Alkaloids. *Synlett* **2005,** (3), 388-405.
8. Kalso, E.; Smith, L.; McQuay, H. J.; Moore, A. R., No Pain, No Gain: Clinical Excellence and Scientific Rigour – Lessons Learned from Ia Morphine. *PAIN* **2002,** *98* (3), 269-275.
9. Cannon, J. S.; Overman, L. E., Is There No End to the Total Syntheses of Strychnine? Lessons Learned in Strategy and Tactics in Total Synthesis. *Angewandte Chemie International Edition* **2012,** *51* (18), 4288-4311.
10. Jett, D. A., Chemical Toxins That Cause Seizures. *NeuroToxicology* **2012,** *33* (6), 1473-1475.
11. Albuquerque, H. M. T.; Santos, C. M. M.; Silva, A. M. S., Cholesterol-Based Compounds: Recent Advances in Synthesis and Applications. *Molecules* **2018,** *24* (1), 116-177.
12. Miller, W. L.; Auchus, R. J., The Molecular Biology, Biochemistry, and Physiology of Human Steroidogenesis and Its Disorders. *Endocrine Reviews* **2011,** *32* (1), 81-151.
13. McGrath, N. A.; Brichacek, M.; Njardarson, J. T., A Graphical Journey of Innovative Organic Architectures That Have Improved Our Lives. *Journal of Chemical Education* **2010,** *87* (12), 1348-1349.

14. Teo, S. K.; Colburn, W. A.; Tracewell, W. G.; Kook, K. A.; Stirling, D. I.; Jaworsky, M. S.; Scheffler, M. A.; Thomas, S. D.; Laskin, O. L., Clinical Pharmacokinetics of Thalidomide. *Clinical Pharmacokinetics* **2004,** *43* (5), 311-327.

15. Eriksson, T.; Björkman, S.; Roth, B.; Fyge, Å.; Höuglund, P., Stereospecific Determination, Chiral Inversion in Vitro and Pharmacokinetics in Humans of the Enantiomers of Thalidomide. *Chirality* **1995,** *7* (1), 44-52.

16. Celgene Corporation, United States Food and Drug Administration (2017), Revlimid (Reference ID: 4201579), Summit, NJ.

17. Njarðarson Group website, https://njardarson.lab.arizona.edu/content/top-pharmaceuticals-poster, accessed July 2019.

18. Yadav, S. R.; Tiwari, V. S.; Haq, W., Stereoselective Synthesis of (R)-3-Methylthalidomide by Piperidin-2-One Ring Assembly Approach. *Chirality* **2015,** *27* (9), 619-624.

19. Luzzio, F. A., Chapter 10 - Thalidomide and Analogues. In *Imides,* Luzzio, F. A., Ed. Elsevier: 2019; pp 367-429.

20. Osipov, S. N.; Tsouker, P.; Hennig, L.; Burger, K., 3-Trifluoromethyl- and 3-Difluoromethyl-Thalidomides. *Tetrahedron* **2004,** *60* (2), 271-274.

21. Lee, C. J. J.; Shibata, N.; Wiley, M. J.; Wells, P. G., Fluorothalidomide: A Characterization of Maternal and Developmental Toxicity in Rabbits and Mice. *Toxicological Sciences* **2011,** *122* (1), 157-169.

22. Cookson, J. C., Rebound Exacerbation of Anxiety During Prolonged Tranquilizer Ingestion. *J R Soc Med* **1995,** *88* (9), 544.

23. Beedie, S. L.; Peer, C. J.; Pisle, S.; Gardner, E. R.; Mahony, C.; Barnett, S.; Ambrozak, A.; Gutschow, M.; Chau, C. H.; Vargesson, N.; Figg, W. D., Anticancer Properties of a Novel Class of Tetrafluorinated Thalidomide Analogues. *Mol Cancer Ther* **2015,** *14* (10), 2228-2237.

24. Zeng, X.-P.; Cao, Z.-Y.; Wang, Y.-H.; Zhou, F.; Zhou, J., Catalytic Enantioselective Desymmetrization Reactions to All-Carbon Quaternary Stereocenters. *Chemical Reviews* **2016,** *116* (12), 7330-7396.

25. Quasdorf, K. W.; Overman, L. E., Catalytic Enantioselective Synthesis of Quaternary Carbon Stereocentres. *Nature* **2014,** *516*, 181.

26. Shimizu, Y.; Shi, S.-L.; Usuda, H.; Kanai, M.; Shibasaki, M., Catalytic Asymmetric Total Synthesis of Ent-Hyperforin. *Angewandte Chemie International Edition* **2010,** *49* (6), 1103-1106.

27. Wang, K.; Bungard, C. J.; Nelson, S. G., Stereoselective Olefin Isomerization Leading to Asymmetric Quaternary Carbon Construction. *Organic Letters* **2007,** *9* (12), 2325-2328.

28. Gao, Z.; Fletcher, S. P., Acyclic Quaternary Centers from Asymmetric Conjugate Addition of Alkylzirconium Reagents to Linear Trisubstituted Enones. *Chemical Science* **2017,** *8* (1), 641-646.

29. Cheng, X.-F.; Li, Y.; Su, Y.-M.; Yin, F.; Wang, J.-Y.; Sheng, J.; Vora, H. U.; Wang, X.-S.; Yu, J.-Q., Pd(Ii)-Catalyzed Enantioselective C–H Activation/C–O Bond Formation: Synthesis of Chiral Benzofuranones. *Journal of the American Chemical Society* **2013,** *135* (4), 1236-1239.

30. Saint-Denis, T. G.; Zhu, R.-Y.; Chen, G.; Wu, Q.-F.; Yu, J.-Q., Enantioselective C(Sp^3)–H Bond Activation by Chiral Transition Metal Catalysts. *Science* **2018,** *359* (6377), 4798.

31. Giri, R.; Chen, X.; Yu, J.-Q., Palladium-Catalyzed Asymmetric Iodination of Unactivated C-H Bonds under Mild Conditions. *Angewandte Chemie International Edition* **2005,** *44* (14), 2112-2115.

32. Stump, C. A.; Bell, I. M.; Bednar, R. A.; Bruno, J. G.; Fay, J. F.; Gallicchio, S. N.; Johnston, V. K.; Moore, E. L.; Mosser, S. D.; Quigley, A. G.; Salvatore, C. A.; Theberge, C. R.; Blair Zartman, C.; Zhang, X.-F.; Kane, S. A.; Graham, S. L.; Vacca, J. P.; Williams, T. M., The Discovery of Highly Potent Cgrp Receptor Antagonists. *Bioorganic & Medicinal Chemistry Letters* **2009,** *19* (1), 214-217.

33. Bhavnani, B. R.; Woolever, C. A.; Benoit, H.; Wong, T., Pharmacokinetics of Equilin and Equilin Sulfate in Normal Postmenopausal Women and Men. *The Journal of Clinical Endocrinology & Metabolism* **1983,** *56* (5), 1048-1056.

34. Wellington, K. D.; Cambie, R. C.; Rutledge, P. S.; Bergquist, P. R., Chemistry of Sponges. 19. Novel Bioactive Metabolites from Hamigera Tarangaensis. *Journal of Natural Products* **2000,** *63* (1), 79-85.

35. DeSolms, S. J.; Woltersdorf, O. W.; Cragoe, E. J.; Watson, L. S.; Fanelli, G. M., (Acylaryloxy)Acetic Acid Diuretics. 2. (2-Alkyl-2-Aryl-1-Oxo-5-Indanyloxy)Acetic Acids. *Journal of Medicinal Chemistry* **1978,** *21* (5), 437-443.

36. Witkop, B., Quebrachamine. I. *Journal of the American Chemical Society* **1957,** *79* (12), 3193-3200.

37. Hayashi, M.; Kim, Y. P.; Takamatsu, S.; Enomoto, A.; Shinose, M.; Takahashi, Y.; Tanaka, H.; Komiyama, K.; Omura, S., Madindoline, a Novel Inhibitor of Il-6 Activity from Streptomyces Sp. K93-0711. I. Taxonomy, Fermentation, Isolation and Biological Activities. *The Journal of Antibiotics* **1996,** *49* (11), 1091-1095.

38. Zimmerman, H. E.; Traxler, M. D., The Stereochemistry of the Ivanov and Reformatsky Reactions. I. *Journal of the American Chemical Society* **1957,** *79* (8), 1920-1923.

39. Ireland, R. E.; Willard, A. K., The Stereoselective Generation of Ester Enolates. *Tetrahedron Letters* **1975,** *16* (46), 3975-3978.

40. Ireland, R. E.; Mueller, R. H.; Willard, A. K., The Ester Enolate Claisen Rearrangement. Stereochemical Control through Stereoselective Enolate Formation. *Journal of the American Chemical Society* **1976,** *98* (10), 2868-2877.

41. Xie, L.; Isenberger, K. M.; Held, G.; Dahl, L. M., Highly Stereoselective Kinetic Enolate Formation: Steric Vs Electronic Effects. *The Journal of Organic Chemistry* **1997,** *62* (21), 7516-7519.

42. Xie, L.; Vanlandeghem, K.; Isenberger, K. M.; Bernier, C., Kinetic Enolate Formation by Lithium Arylamide: Effects of Basicity on Selectivity. *The Journal of Organic Chemistry* **2003,** *68* (2), 641-643.

43. Gu, Z.; Herrmann, A. T.; Stivala, C. E.; Zakarian, A., Stereoselective Construction of Adjacent Quaternary Chiral Centers by the Ireland-Claisen Rearrangement: Stereoselection with Esters of Cyclic Alcohols. *Synlett* **2010,** *2010* (11), 1717-1722.

44. Shirai, R.; Tanaka, M.; Koga, K., Enantioselective Deprotonation by Chiral Lithium Amide Bases: Asymmetric Synthesis of Trimethylsilyl Enol Ethers from 4-Alkylcyclohexanones. *Journal of the American Chemical Society* **1986,** *108* (3), 543-545.

45. Qin, Y.-C.; Stivala, C. E.; Zakarian, A., Acyclic Stereocontrol in the Ireland–Claisen Rearrangement of A-Branched Esters. *Angewandte Chemie International Edition* **2007,** *46* (39), 7466-7469.

46. Stivala, C. E.; Gu, Z.; Smith, L. L.; Zakarian, A., Studies toward the Synthesis of Spirolide C: Exploration into the Formation of the 23-Membered All-Carbon Macrocyclic Framework. *Organic Letters* **2012,** *14* (3), 804-807.

47. Stivala, C. E.; Zakarian, A., Studies toward the Synthesis of Spirolides: Assembly of the Elaborated E-Ring Fragment. *Organic Letters* **2009,** *11* (4), 839-842.

48. Stivala, C. E.; Zakarian, A., Total Synthesis of (+)-Pinnatoxin A. *Journal of the American Chemical Society* **2008,** *130* (12), 3774-3776.

49. Evans, D. A.; Bartroli, J.; Shih, T. L., Enantioselective Aldol Condensations. 2. Erythro-Selective Chiral Aldol Condensations Via Boron Enolates. *Journal of the American Chemical Society* **1981,** *103* (8), 2127-2129.

50. Evans, D. A.; Ennis, M. D.; Mathre, D. J., Asymmetric Alkylation Reactions of Chiral Imide Enolates. A Practical Approach to the Enantioselective Synthesis of Alpha-Substituted Carboxylic Acid Derivatives. *Journal of the American Chemical Society* **1982,** *104* (6), 1737-1739.

51. Meyers, A. I.; Knaus, G.; Kamata, K.; Ford, M. E., Asymmetric Synthesis of R and S Alpha-Alkylalkanoic Acids from Metalation and Alkylation of Chiral 2-Oxazolines. *Journal of the American Chemical Society* **1976,** *98* (2), 567-576.

52. Myers, A. G.; McKinstry, L., Practical Syntheses of Enantiomerically Enriched Γ-Lactones and Γ-Hydroxy Ketones by the Alkylation of Pseudoephedrine Amides with Epoxides and Their Derivatives. *The Journal of Organic Chemistry* **1996,** *61* (7), 2428-2440.

53. Myers, A. G.; Yang, B. H.; Chen, H.; Gleason, J. L., Use of Pseudoephedrine as a Practical Chiral Auxiliary for Asymmetric Synthesis. *Journal of the American Chemical Society* **1994,** *116* (20), 9361-9362.

54. Schmierer, R.; Grotemeier, G.; Helmchen, G.; Selim, A., Functional Groups at Concave Sites: Asymmetric Alkylation of Esters with Very High Stereoselectivity and Reversal of Configuration by Change of Solvent. *Angewandte Chemie International Edition in English* **1981,** *20* (2), 207-208.

55. Oppolzer, W.; Moretti, R.; Thomi, S., Asymmetric Alkylation of N-Acylsultams: A General Route to Enantiomerically Pure, Crystalline C(A,A)-Disubstituted Carboxylic Acid Derivatives. *Tetrahedron Letters* **1989,** *30* (41), 5603-5606.

56. Job, A.; Janeck, C. F.; Bettray, W.; Peters, R.; Enders, D., The Samp-/Ramp-Hydrazone Methodology in Asymmetric Synthesis. *Tetrahedron* **2002,** *58* (12), 2253-2329.

57. Enders, D.; Eichenauer, H., Asymmetric Synthesis of A-Substituted Ketones by Metalation and Alkylation of Chiral Hydrazones. *Angewandte Chemie International Edition in English* **1976,** *15* (9), 549-551.

58. Lim, D.; Coltart, D. M., Simple and Efficient Asymmetric A-Alkylation and A,A-Bisalkylation of Acyclic Ketones by Using Chiral N-Amino Cyclic Carbamate Hydrazones. *Angewandte Chemie International Edition* **2008,** *47* (28), 5207-5210.

59. Heravi, M. M.; Zadsirjan, V.; Farajpour, B., Applications of Oxazolidinones as Chiral Auxiliaries in the Asymmetric Alkylation Reaction Applied to Total Synthesis. *RSC Advances* **2016,** *6* (36), 30498-30551.

60. Heravi, M. M.; Zadsirjan, V., Oxazolidinones as Chiral Auxiliaries in Asymmetric Aldol Reactions Applied to Total Synthesis. *Tetrahedron: Asymmetry* **2013,** *24* (19), 1149-1188.

61. Boeckman, R. K.; Boehmler, D. J.; Musselman, R. A., Toward the Development of a General Chiral Auxiliary. 9. Highly Diastereoselective Alkylations and Acylations to Form Tertiary and Quaternary Centers. *Organic Letters* **2001,** *3* (23), 3777-3780.

62. Dalko, P. I.; Langlois, Y., Stereoselective Synthesis of Quaternary Benzylic Carbons Using C2 Symmetric Imidazolines and Tetrahydrofuran as Electrophile. *The Journal of Organic Chemistry* **1998,** *63* (23), 8107-8117.

63. Hanamoto, T.; Katsuki, T.; Yamaguchi, M., Asymmetric Dialkylation of A-Cyanoacetic Acid. *Tetrahedron Letters* **1986,** *27* (22), 2463-2464.

64. Kawanami, Y.; Ito, Y.; Kitagawa, T.; Taniguchi, Y.; Katsuki, T.; Yamaguchi, M., Asymmetric Alkylation of Carboxyamides by Using Trans-2,5-Disubstituted Pyrrolidines as Chiral Auxiliaries. *Tetrahedron Letters* **1984,** *25* (8), 857-860.

65. Romo, D.; Meyers, A. I., Chiral Non-Racemic Bicyclic Lactams. Vehicles for the Construction of Natural and Unnatural Products Containing Quaternary Carbon Centers. *Tetrahedron* **1991,** *47* (46), 9503-9569.

66. Vedejs, E.; Fields, S. C.; Schrimpf, M. R., Asymmetric Transformation in Synthesis: Chiral Amino Acid Enolate Equivalents. *Journal of the American Chemical Society* **1993,** *115* (24), 11612-11613.

67. Vedejs, E.; Fields, S. C.; Hayashi, R.; Hitchcock, S. R.; Powell, D. R.; Schrimpf, M. R., Asymmetric Memory at Labile, Stereogenic Boron: Enolate Alkylation of Oxazaborolidinones. *Journal of the American Chemical Society* **1999,** *121* (11), 2460-2470.

68. Enders, D.; Teschner, P.; Raabe, G.; Runsink, J., Asymmetric Electrophilic Substitutions at the A-Position of Γ- and Δ-Lactams. *European Journal of Organic Chemistry* **2001,** (23), 4463-4477.

69. Schöllkopf, U.; Groth, U.; Deng, C., Enantioselective Syntheses of (R)-Amino Acids Using L-Valine as Chiral Agent. *Angewandte Chemie International Edition in English* **1981,** *20* (9), 798-799.

70. Meyers, A. I.; Harre, M.; Garland, R., Asymmetric Synthesis of Quaternary Carbon Centers. *Journal of the American Chemical Society* **1984,** *106* (4), 1146-1148.

71. Meyers, A. I.; Seefeld, M. A.; Lefker, B. A., Chiral Bicyclic Lactams. A New Study on Facial Alkylation. *The Journal of Organic Chemistry* **1996,** *61* (17), 5712-5713.

72. I. Meyers, A.; P. Brengel, G., Chiral Bicyclic Lactams: Useful Precursors and Templates for Asymmetric Syntheses1. *Chemical Communications* **1997,** (1), 1-8.

73. Meyers, A. I.; Wanner, K. T., Chiral Quaternary Carbon Compounds. Ii. An Asymmetric Synthesis of (R) or (S)-4,4-Dialkyl-2-Cyclopentenones. *Tetrahedron Letters* **1985,** *26* (17), 2047-2050.

74. Meyers, A. I.; Downing, S. V.; Weiser, M. J., Asymmetric Synthesis of 2-Alkyl-Perhydroazepines from [5,3,0]-Bicyclic Lactams. *The Journal of Organic Chemistry* **2001,** *66* (4), 1413-1419.

75. Meyers, A. I.; Seefeld, M. A.; Lefker, B. A.; Blake, J. F.; Williard, P. G., Stereoselective Alkylations in Rigid Systems. Effect of Remote Substituents on Π-Facial Additions to Lactam Enolates. Stereoelectronic and Steric Effects. *Journal of the American Chemical Society* **1998,** *120* (30), 7429-7438.

76. Roth, G. P.; Leonard, S. F.; Tong, L., Complementary Selectivity in the Alkylation of Chiral Bicyclic Lactam Enolates. *The Journal of Organic Chemistry* **1996,** *61* (17), 5710-5711.

77. Groaning, M. D.; Meyers, A. I., Chiral Non-Racemic Bicyclic Lactams. Auxiliary-Based Asymmetric Reactions. *Tetrahedron* **2000,** *56* (51), 9843-9873.

78. Fráter, G.; Müller, U.; Günther, W., The Stereoselective A-Alkylation of Chiral B-Hydroxy Esters and Some Applications Thereof. *Tetrahedron* **1984,** *40* (8), 1269-1277.

79. Fráter, G., Über Die Stereospezifität Der A-Alkylierung Von B-Hydroxycarbonsäureestern. Vorläufige Mitteilung. *Helvetica Chimica Acta* **1979,** *62* (8), 2825-2828.

80. Fráter, G., Stereospezifische Synthese Von (+)-(3r, 4r)-4-Methyl-3-Heptanol, Das Enantiomere Eines Pheromons Des Kleinen Ulmensplintkäfers (Scolytus Multistriatus). *Helvetica Chimica Acta* **1979,** *62* (8), 2829-2832.

81. Kummer, D. A.; Chain, W. J.; Morales, M. R.; Quiroga, O.; Myers, A. G., Stereocontrolled Alkylative Construction of Quaternary Carbon Centers. *Journal of the American Chemical Society* **2008,** *130* (40), 13231-13233.

82. Morales, M. R.; Mellem, K. T.; Myers, A. G., Pseudoephenamine: A Practical Chiral Auxiliary for Asymmetric Synthesis. *Angewandte Chemie International Edition* **2012,** *51* (19), 4568-4571.

83. Yu, K.; Lu, P.; Jackson, J. J.; Nguyen, T.-A. D.; Alvarado, J.; Stivala, C. E.; Ma, Y.; Mack, K. A.; Hayton, T. W.; Collum, D. B.; Zakarian, A., Lithium Enolates in the Enantioselective Construction of Tetrasubstituted Carbon Centers with Chiral Lithium Amides as Noncovalent Stereodirecting Auxiliaries. *Journal of the American Chemical Society* **2017,** *139* (1), 527-533.

84. Koester, D. C.; Werz, D. B., Creating Aldols Differently: How to Build up Aldol Products with Quaternary Stereocenters Starting from Alkynes. *Angewandte Chemie International Edition* **2009,** *48* (43), 7971-7973.

85. Marek, I., A Shift in Retrosynthetic Paradigm. *Chemistry – A European Journal* **2008,** *14* (25), 7460-7468.

86. Das, J. P.; Chechik, H.; Marek, I., A Unique Approach to Aldol Products for the Creation of All-Carbon Quaternary Stereocentres. *Nature Chemistry* **2009,** *1*, 128.

87. Sklute, G.; Marek, I., New Multicomponent Approach for the Creation of Chiral Quaternary Centers in the Carbonyl Allylation Reactions. *Journal of the American Chemical Society* **2006,** *128* (14), 4642-4649.

88. Vabre, R.; Island, B.; Diehl, C. J.; Schreiner, P. R.; Marek, I., Forming Stereogenic Centers in Acyclic Systems from Alkynes. *Angewandte Chemie International Edition* **2015,** *54* (34), 9996-9999.

89. Dutta, B.; Gilboa, N.; Marek, I., Highly Diastereoselective Preparation of Homoallylic Alcohols Containing Two Contiguous Quaternary Stereocenters in Acyclic Systems from Simple Terminal Alkynes. *Journal of the American Chemical Society* **2010,** *132* (16), 5588-5589.

90. Minko, Y.; Pasco, M.; Lercher, L.; Botoshansky, M.; Marek, I., Forming All-Carbon Quaternary Stereogenic Centres in Acyclic Systems from Alkynes. *Nature* **2012,** *490*, 522.

91. Manthorpe, J. M.; Gleason, J. L., Stereoselective Generation of E- and Z-Disubstituted Amide Enolates. Reductive Enolate Formation from Bicyclic Thioglycolate Lactams. *Journal of the American Chemical Society* **2001,** *123* (9), 2091-2092.

92. Arpin, A.; Manthorpe, J. M.; Gleason, J. L., A Practical Chiral Bicyclic Thioglycolate Lactam Auxiliary for Stereoselective Quaternary Carbon Formation. *Organic Letters* **2006,** *8* (7), 1359-1362.

93. Manthorpe, J. M.; Gleason, J. L., Stereoselective Formation of Quaternary Carbon Centers: Alkylation of A,A-Disubstituted Amide Enolates. *Angewandte Chemie International Edition* **2002,** *41* (13), 2338-2341.

94. Burke, E. D.; Gleason, J. L., A,A-Disubstituted Boron Enolates in the Asymmetric Synthesis of Quaternary Carbon Centers. *Organic Letters* **2004,** *6* (3), 405-407.

95. Tiong, E. A.; Gleason, J. L., Stereoselective Formation of A-Quaternary Stereocenters in the Mannich Reaction. *Organic Letters* **2009,** *11* (8), 1725-1728.

96. Corey, E. J.; Guzman-Perez, A., The Catalytic Enantioselective Construction of Molecules with Quaternary Carbon Stereocenters. *Angewandte Chemie International Edition* **1998,** *37* (4), 388-401.

97. Douglas, C. J.; Overman, L. E., Catalytic Asymmetric Synthesis of All-Carbon Quaternary Stereocenters. *Proceedings of the National Academy of Sciences of the United States of America* **2004,** *101* (15), 5363-5367.

98. Feng, J.; Holmes, M.; Krische, M. J., Acyclic Quaternary Carbon Stereocenters Via Enantioselective Transition Metal Catalysis. *Chemical Reviews* **2017,** *117* (19), 12564-12580.

99. Liu, Y.; Han, S.-J.; Liu, W.-B.; Stoltz, B. M., Catalytic Enantioselective Construction of Quaternary Stereocenters: Assembly of Key Building Blocks for the Synthesis of Biologically Active Molecules. *Accounts of Chemical Research* **2015,** *48* (3), 740-751.

100. Trost, B. M.; Crawley, M. L., Asymmetric Transition-Metal-Catalyzed Allylic Alkylations: Applications in Total Synthesis. *Chemical Reviews* **2003,** *103* (8), 2921-2944.

101. Trost, B. M., Metal Catalyzed Allylic Alkylation: Its Development in the Trost Laboratories. *Tetrahedron* **2015,** *71* (35), 5708-5733.

102. Weaver, J. D.; Recio, A.; Grenning, A. J.; Tunge, J. A., Transition Metal-Catalyzed Decarboxylative Allylation and Benzylation Reactions. *Chemical Reviews* **2011,** *111* (3), 1846-1913.

103. Alexy, E. J.; Zhang, H.; Stoltz, B. M., Catalytic Enantioselective Synthesis of Acyclic Quaternary Centers: Palladium-Catalyzed Decarboxylative Allylic Alkylation of Fully Substituted Acyclic Enol Carbonates. *Journal of the American Chemical Society* **2018,** *140* (32), 10109-10112.
104. Alexy, E. J.; Fulton, T. J.; Zhang, H.; Stoltz, Brian M., Palladium-Catalyzed Enantioselective Decarboxylative Allylic Alkylation of Fully Substituted N-Acyl Indole-Derived Enol Carbonates. *Chemical Science* **2019,** *10* (23), 5996-6000.
105. Starkov, P.; Moore, J. T.; Duquette, D. C.; Stoltz, B. M.; Marek, I., Enantioselective Construction of Acyclic Quaternary Carbon Stereocenters: Palladium-Catalyzed Decarboxylative Allylic Alkylation of Fully Substituted Amide Enolates. *Journal of the American Chemical Society* **2017,** *139* (28), 9615-9620.
106. Fujita, T.; Yamamoto, T.; Morita, Y.; Chen, H.; Shimizu, Y.; Kanai, M., Chemo- and Enantioselective Pd/B Hybrid Catalysis for the Construction of Acyclic Quaternary Carbons: Migratory Allylation of O-Allyl Esters to A-C-Allyl Carboxylic Acids. *Journal of the American Chemical Society* **2018,** *140* (18), 5899-5903.
107. Zhang, K.; Peng, Q.; Hou, X.-L.; Wu, Y.-D., Highly Enantioselective Palladium-Catalyzed Alkylation of Acyclic Amides. *Angewandte Chemie International Edition* **2008,** *47* (9), 1741-1744.
108. Hethcox, J. C.; Shockley, S. E.; Stoltz, B. M., Enantioselective Synthesis of Vicinal All-Carbon Quaternary Centers Via Iridium-Catalyzed Allylic Alkylation. *Angewandte Chemie International Edition* **2018,** *57* (28), 8664-8667.
109. Shockley, S. E.; Hethcox, J. C.; Stoltz, B. M., Enantioselective Synthesis of Acyclic A-Quaternary Carboxylic Acid Derivatives through Iridium-Catalyzed Allylic Alkylation. *Angewandte Chemie International Edition* **2017,** *56* (38), 11545-11548.
110. Hethcox, J. C.; Shockley, S. E.; Stoltz, B. M., Iridium-Catalyzed Diastereo-, Enantio-, and Regioselective Allylic Alkylation with Prochiral Enolates. *ACS Catalysis* **2016,** *6* (9), 6207-6213.
111. Liu, W.-B.; Reeves, C. M.; Virgil, S. C.; Stoltz, B. M., Construction of Vicinal Tertiary and All-Carbon Quaternary Stereocenters Via Ir-Catalyzed Regio-, Diastereo-, and Enantioselective Allylic Alkylation and Applications in Sequential Pd Catalysis. *Journal of the American Chemical Society* **2013,** *135* (29), 10626-10629.

112. Turnbull, B. W. H.; Evans, P. A., Enantioselective Rhodium-Catalyzed Allylic Substitution with a Nitrile Anion: Construction of Acyclic Quaternary Carbon Stereogenic Centers. *Journal of the American Chemical Society* **2015,** *137* (19), 6156-6159.

113. Abrams, D. J.; Provencher, P. A.; Sorensen, E. J., Recent Applications of C–H Functionalization in Complex Natural Product Synthesis. *Chemical Society Reviews* **2018,** *47* (23), 8925-8967.

114. Gandeepan, P.; Müller, T.; Zell, D.; Cera, G.; Warratz, S.; Ackermann, L., 3d Transition Metals for C–H Activation. *Chemical Reviews* **2019,** *119* (4), 2192-2452.

115. Xiao, K.-J.; Lin, D. W.; Miura, M.; Zhu, R.-Y.; Gong, W.; Wasa, M.; Yu, J.-Q., Palladium(Ii)-Catalyzed Enantioselective C(Sp3)–H Activation Using a Chiral Hydroxamic Acid Ligand. *Journal of the American Chemical Society* **2014,** *136* (22), 8138-8142.

116. Shi, B.-F.; Zhang, Y.-H.; Lam, J. K.; Wang, D.-H.; Yu, J.-Q., Pd(Ii)-Catalyzed Enantioselective C−H Olefination of Diphenylacetic Acids. *Journal of the American Chemical Society* **2010,** *132* (2), 460-461.

117. Shen, P.-X.; Hu, L.; Shao, Q.; Hong, K.; Yu, J.-Q., Pd(Ii)-Catalyzed Enantioselective C(Sp3)–H Arylation of Free Carboxylic Acids. *Journal of the American Chemical Society* **2018,** *140* (21), 6545-6549.

118. Wasa, M.; Engle, K. M.; Lin, D. W.; Yoo, E. J.; Yu, J.-Q., Pd(Ii)-Catalyzed Enantioselective C–H Activation of Cyclopropanes. *Journal of the American Chemical Society* **2011,** *133* (49), 19598-19601.

119. Hu, L.; Shen, P.-X.; Shao, Q.; Hong, K.; Qiao, J. X.; Yu, J.-Q., Pdii-Catalyzed Enantioselective C(Sp3)−H Activation/Cross-Coupling Reactions of Free Carboxylic Acids. *Angewandte Chemie International Edition* **2019,** *58* (7), 2134-2138.

120. Martin, N.; Pierre, C.; Davi, M.; Jazzar, R.; Baudoin, O., Diastereo- and Enantioselective Intramolecular C(Sp^3)-H Arylation for the Synthesis of Fused Cyclopentanes. *Chemistry – A European Journal* **2012,** *18* (15), 4480-4484.

121. Holstein, P. M.; Vogler, M.; Larini, P.; Pilet, G.; Clot, E.; Baudoin, O., Efficient Pd0-Catalyzed Asymmetric Activation of Primary and Secondary C–H Bonds Enabled by Modular Binepine Ligands and Carbonate Bases. *ACS Catalysis* **2015,** *5* (7), 4300-4308.

122. Giri, R.; Shi, B.-F.; Engle, K. M.; Maugel, N.; Yu, J.-Q., Transition Metal-Catalyzed C-H Activation Reactions: Diastereoselectivity and Enantioselectivity. *Chemical Society Reviews* **2009,** *38* (11), 3242-3272.

123. Nguyen, K. D.; Herkommer, D.; Krische, M. J., Enantioselective Formation of All-Carbon Quaternary Centers Via C–H Functionalization of Methanol: Iridium-Catalyzed Diene Hydrohydroxymethylation. *Journal of the American Chemical Society* **2016,** *138* (43), 14210-14213.

124. Holmes, M.; Nguyen, K. D.; Schwartz, L. A.; Luong, T.; Krische, M. J., Enantioselective Formation of Cf_3-Bearing All-Carbon Quaternary Stereocenters Via C–H Functionalization of Methanol: Iridium Catalyzed Allene Hydrohydroxymethylation. *Journal of the American Chemical Society* **2017,** *139* (24), 8114-8117.

125. Schwartz, L. A.; Holmes, M.; Brito, G. A.; Gonçalves, T. P.; Richardson, J.; Ruble, J. C.; Huang, K.-W.; Krische, M. J., Cyclometalated Iridium–Phanephos Complexes Are Active Catalysts in Enantioselective Allene–Fluoral Reductive Coupling and Related Alcohol-Mediated Carbonyl Additions That Form Acyclic Quaternary Carbon Stereocenters. *Journal of the American Chemical Society* **2019,** *141* (5), 2087-2096.

126. Bradshaw, B.; Bonjoch, J., The Wieland-Miescher Ketone: A Journey from Organocatalysis to Natural Product Synthesis. *Synlett* **2012,** *23* (03), 337-356.

127. Eagan, J. M.; Hori, M.; Wu, J.; Kanyiva, K. S.; Snyder, S. A., Synthesis and Applications of Hajos–Parrish Ketone Isomers. *Angewandte Chemie International Edition* **2015,** *54* (27), 7842-7846.

128. Hajos, Z. G.; Parrish, D. R., Asymmetric Synthesis of Bicyclic Intermediates of Natural Product Chemistry. *The Journal of Organic Chemistry* **1974,** *39* (12), 1615-1621.

129. Eder, U.; Sauer, G.; Wiechert, R., New Type of Asymmetric Cyclization to Optically Active Steroid Cd Partial Structures. *Angewandte Chemie International Edition in English* **1971,** *10* (7), 496-497.

130. Zhou, P.; Zhang, L.; Luo, S.; Cheng, J.-P., Asymmetric Synthesis of Wieland–Miescher and Hajos–Parrish Ketones Catalyzed by an Amino-Acid-Derived Chiral Primary Amine. *The Journal of Organic Chemistry* **2012,** *77* (5), 2526-2530.

131. Mase, N.; Tanaka, F.; Barbas III, C. F., Synthesis of B-Hydroxyaldehydes with Stereogenic Quaternary Carbon Centers by Direct Organocatalytic Asymmetric Aldol Reactions. *Angewandte Chemie* **2004,** *116* (18), 2474-2477.

132. Häggman, N. O.; Zank, B.; Jun, H.; Kaldre, D.; Gleason, J. L., Diazepane Carboxylates as Organocatalysts in the Diels–Alder Reaction of A-Substituted Enals. *European Journal of Organic Chemistry* **2018,** *2018* (39), 5412-5416.

133. Hayashi, Y.; Bondzic, B. P.; Yamazaki, T.; Gupta, Y.; Ogasawara, S.; Taniguchi, T.; Monde, K., Asymmetric Diels–Alder Reaction of A-Substituted and B,B-Disubstituted A,B-Enals Via Diarylprolinol Silyl Ether for the Construction of All-Carbon Quaternary Stereocenters. *Chemistry – A European Journal* **2016,** *22* (44), 15874-15880.

134. Melchiorre, P., Cinchona-Based Primary Amine Catalysis in the Asymmetric Functionalization of Carbonyl Compounds. *Angewandte Chemie International Edition* **2012,** *51* (39), 9748-9770.

135. McCooey, S. H.; Connon, S. J., Readily Accessible 9-Epi-Amino Cinchona Alkaloid Derivatives Promote Efficient, Highly Enantioselective Additions of Aldehydes and Ketones to Nitroolefins. *Organic Letters* **2007,** *9* (4), 599-602.

136. Krautwald, S.; Sarlah, D.; Schafroth, M. A.; Carreira, E. M., Enantio- and Diastereodivergent Dual Catalysis: A-Allylation of Branched Aldehydes. *Science* **2013,** *340* (6136), 1065-1068.

137. Hashimoto, T.; Maruoka, K., Recent Development and Application of Chiral Phase-Transfer Catalysts. *Chemical Reviews* **2007,** *107* (12), 5656-5682.

138. Kaneko, S.; Kumatabara, Y.; Shirakawa, S., A New Generation of Chiral Phase-Transfer Catalysts. *Organic & Biomolecular Chemistry* **2016,** *14* (24), 5367-5376.

139. Shirakawa, S.; Maruoka, K., Recent Developments in Asymmetric Phase-Transfer Reactions. *Angewandte Chemie International Edition* **2013,** *52* (16), 4312-4348.

140. O'Donnell, M. J., The Enantioselective Synthesis of A-Amino Acids by Phase-Transfer Catalysis with Achiral Schiff Base Esters. *Accounts of Chemical Research* **2004,** *37* (8), 506-517.

141. Dolling, U. H.; Davis, P.; Grabowski, E. J. J., Efficient Catalytic Asymmetric Alkylations. 1. Enantioselective Synthesis of (+)-Indacrinone Via Chiral Phase-Transfer Catalysis. *Journal of the American Chemical Society* **1984,** *106* (2), 446-447.

142. Hughes, D. L.; Dolling, U. H.; Ryan, K. M.; Schoenewaldt, E. F.; Grabowski, E. J. J., Efficient Catalytic Asymmetric Alkylations. 3. A Kinetic and Mechanistic Study of the Enantioselective Phase-Transfer Methylation of 6,7-Dichloro-5-Methoxy-2-Phenyl-1-Indanone. *The Journal of Organic Chemistry* **1987,** *52* (21), 4745-4752.

143. Hong, S.; Lee, J.; Kim, M.; Park, Y.; Park, C.; Kim, M.-h.; Jew, S.-s.; Park, H.-g., Highly Enantioselective Synthesis of A,A-Dialkylmalonates by Phase-Transfer Catalytic Desymmetrization. *Journal of the American Chemical Society* **2011,** *133* (13), 4924-4929.

144. Bell, I. M.; Gallicchio, S. N.; Wood, M. R.; Quigley, A. G.; Stump, C. A.; Zartman, C. B.; Fay, J. F.; Li, C.-C.; Lynch, J. J.; Moore, E. L.; Mosser, S. D.; Prueksaritanont, T.; Regan, C. P.; Roller, S.; Salvatore, C. A.; Kane, S. A.; Vacca, J. P.; Selnick, H. G., Discovery of Mk-3207: A Highly Potent, Orally Bioavailable Cgrp Receptor Antagonist. *ACS Medicinal Chemistry Letters* **2010,** *1* (1), 24-29.

145. Tan, J.; Yasuda, N., Contemporary Asymmetric Phase Transfer Catalysis: Large-Scale Industrial Applications. *Organic Process Research & Development* **2015,** *19* (11), 1731-1746.

146. English Names for Fungi (July 2019). https://www.britmycolsoc.org.uk/library/english-names (accessed July 2019).

147. Becker, U.; Erkel, G.; Anke, T.; Sterner, O., Puraquinonic Acid, a Novel Inducer of Differentiation of Human Hl-60 Promyelocytic Leukemia Cells from Mycena Pura (Pers. Ex Fr.). *Natural Product Letters* **1997,** *9* (3), 229-236.

148. Weber, W.; Anke, T.; Bross, M.; Steglich, W., Strobilurin D and Strobilurin F: Two New Cytostatic and Antifungal (E)-B-Methoxyacrylate Antibiotics Fromcyphellopsis Anomala. *Planta Medica* **1990,** *56* (05), 446-450.

149. Clive, D. L. J.; Yu, M., Synthesis of (+)-Puraquinonic Acid. *Chemical Communications* **2002,** (20), 2380-2381.

150. Clive, D. L. J.; Yu, M.; Sannigrahi, M., Synthesis of Optically Pure (+)-Puraquinonic Acid and Assignment of Absolute Configuration to Natural (−)-Puraquinonic Acid. Use of Radical Cyclization for Asymmetric Generation of a Quaternary Center. *The Journal of Organic Chemistry* **2004,** *69* (12), 4116-4125.

151. Zapf, S.; Hossfeld, M.; Anke, H.; Velten, R.; Steglich, W., Darlucins a and B, New Isocyanide Antibiotics from Sphaerellopsis Filum (Darluca Filum). *The Journal of Antibiotics* **1995,** *48* (1), 36-41.

152. Finkielsztein, L. M.; Bruno, A. M.; Renou, S. G.; Moltrasio Iglesias, G. Y., Design, Synthesis, and Biological Evaluation of Alcyopterosin a and Illudalane Derivatives as Anticancer Agents. *Bioorganic & Medicinal Chemistry* **2006,** *14* (6), 1863-1870.

153. Hirota, M.; Shimizu, Y.; Kamo, T.; Makabe, H.; Shibata, H., New Plant Growth Promoters, Repraesentins a, B and C, from Lactarius Repraesentaneus. *Bioscience, Biotechnology, and Biochemistry* **2003,** *67* (7), 1597-1600.

154. Hoang, T. T.; Birepinte, M.; Kramer, N. J.; Dudley, G. B., Six-Step Synthesis of Alcyopterosin a, a Bioactive Illudalane Sesquiterpene with a Gem-Dimethylcyclopentane Ring. *Organic Letters* **2016,** *18* (14), 3470-3473.

155. Palermo, J. A.; Rodríguez Brasco, M. F.; Spagnuolo, C.; Seldes, A. M., Illudalane Sesquiterpenoids from the Soft Coral Alcyonium Paessleri: The First Natural Nitrate Esters. *The Journal of Organic Chemistry* **2000,** *65* (15), 4482-4486.

156. Quin, M. B.; Flynn, C. M.; Schmidt-Dannert, C., Traversing the Fungal Terpenome. *Natural Product Reports* **2014,** *31* (10), 1449-1473.

157. Starratt, A. N.; Ward, E. W. B.; Stothers, J. B., Coprinolone and Δ6-Coprinolone: New Sesquiterpenes from Coprinus Psychromorbidus. *Canadian Journal of Chemistry* **1989,** *67* (3), 417-427.

158. Clericuzio, M.; Pan, F.; Han, F.; Pang, Z.; Sterner, O., Stearoyldelicone, an Unstable Protoilludane Sesquiterpenoid from Intact Fruit Bodies of Russula Delica. *Tetrahedron Letters* **1997,** *38* (47), 8237-8240.

159. Clericuzio, M.; Han, F. G.; Pan, F. S.; Pang, Z. J.; Sterner, O., The Sesquiterpenoid Contents of Fruit Bodies of Russula Delica. *Acta Chemica Scandinavica* **1998,** *52* (11), 1333-1337.

160. Clive, D. L. J.; Sannigrahi, M.; Hisaindee, S., Synthesis of (±)-Puraquinonic Acid: An Inducer of Cell Differentiation. *The Journal of Organic Chemistry* **2001,** *66* (3), 954-961.

161. Hisaindee, S.; Clive, D. L. J., A Synthesis of Puraquinonic Acid. *Tetrahedron Letters* **2001,** *42* (12), 2253-2255.

162. Kraus, G. A.; Choudhury, P. K., Synthesis of Puraquinonic Acid Ethyl Ester and Deliquinone Via a Common Intermediate. *The Journal of Organic Chemistry* **2002,** *67* (16), 5857-5859.

163. Bloomer, J. L.; Stagliano, K. W., Directable Regiochemistry in Naphthazarins Via the Use of Masked Derivatives. *Tetrahedron Letters* **1993,** *34* (5), 757-760.

164. Melot, R.; Craveiro, M. V.; Baudoin, O., Total Synthesis of (nor)Illudalane Sesquiterpenes Based on a C(Sp^3)–H Activation Strategy. *The Journal of Organic Chemistry* **2019,** *84* (20), 12933-12945.

165. Tiong, E. A.; Rivalti, D.; Williams, B. M.; Gleason, J. L., A Concise Total Synthesis of (R)-Puraquinonic Acid. *Angewandte Chemie International Edition* **2013,** *52* (12), 3442-3445.

166. Melot, R.; Craveiro, M. V.; Bürgi, T.; Baudoin, O., Divergent Enantioselective Synthesis of (nor)Illudalane Sesquiterpenes Via Pd^0-Catalyzed Asymmetric C(Sp^3)–H Activation. *Organic Letters* **2019,** *21* (3), 812-815.

CHAPTER 2

Use of Biselectrophilic Substrates in the Stereoselective Formation of α-Quaternary Stereocentres

2.1 Overview

2.1.1 Project Aim

As discussed in chapter one, α-quaternary carbon stereocentres are a common yet challenging structural element routinely encountered in organic synthesis. While many methods have been developed that can reliably introduce the motif when there exists a reasonable steric difference between at least two of the substitutes (*vide supra*) fewer examples are known for preparing compounds wherein little steric bias is present. While methods which can successfully prepare this subclass of quaternary carbon stereocentres remain sparse, such stereocentres are well represented in the structures of natural products and other biologically relevant molecules (Figure 2.1). To address the need for additional methods to tackle the synthesis of these types of molecules this research project aims to extend the Gleason Group's chemistry of bicyclic lactam auxiliaries to electrophiles possessing sterically similar but electronically differentiated electrophilic sites. This chapter traces the development of this approach from reaction scouting through optimisation and the investigation of substrate scope.

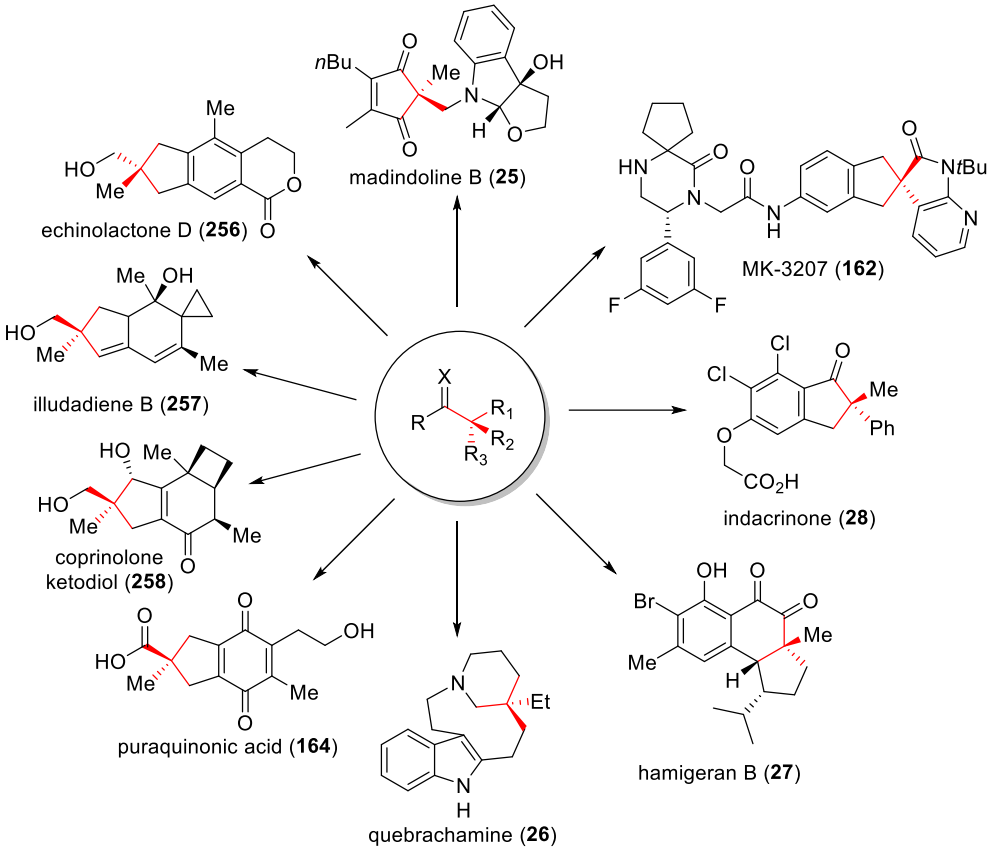

Figure 2.1 Examples of natural products and biologically relevant molecules containing α-quaternary carbon stereocentres

The Gleason group has previously demonstrated the use and practicality of lactam **104** for the preparation of α-quaternary carbon stereocentres through stereocontrolled enolate formation (Scheme 2.1a). The enolate geometry resulting from the reductive enolization event is dependent on the relative α-carbon stereochemistry of the bicyclic lactam, thus providing access to either (*E*)- or (*Z*)-enolates. This eliminates the need to consider the relative electronic or steric properties of the substituents for the purposes of enolate formation. Importantly, the configuration of the α-stereocentre is controlled by the sequence of alkylation, allowing for facile entry to either diastereomer. The versatility of this method has allowed it to be employed in alkylation,[1, 2] aldol,[3] and Mannich[4] chemistry. In the case of alkylation, the nature of the electrophile has remained

relatively underexplored, with the majority being simple alkyl substituents (methyl, ethyl, allyl, benzyl, *etc.*). As such, the introduction of more complex electrophiles represented an interesting avenue to further expand the synthetic utility of lactam **104**.

Considering previous reports established the introduction of simple α-substituents (*e.g.* alkyl, allyl and propargyl), this project focused on extending the scope of compatible electrophiles to include alkylating agents possessing two electrophilic sites (Scheme 2.1b). After the initial alkylation, such *biselectrophilic* molecules would be able to participate in a second intramolecular alkylation affording spirocyclic compounds such as lactam **261**. These spirocyclic lactams could then be converted to the corresponding α,α-disubstituted enolates and allowed to react with a variety of electrophiles to generate α-quaternary carbon stereocentres on cyclic frameworks (**262**). It was conceived that this strategy would provide opportunity for the use of structurally complex and diverse electrophiles thereby permitting it to be employed for the introduction of α-quaternary carbon stereocentres late within synthetic routes.

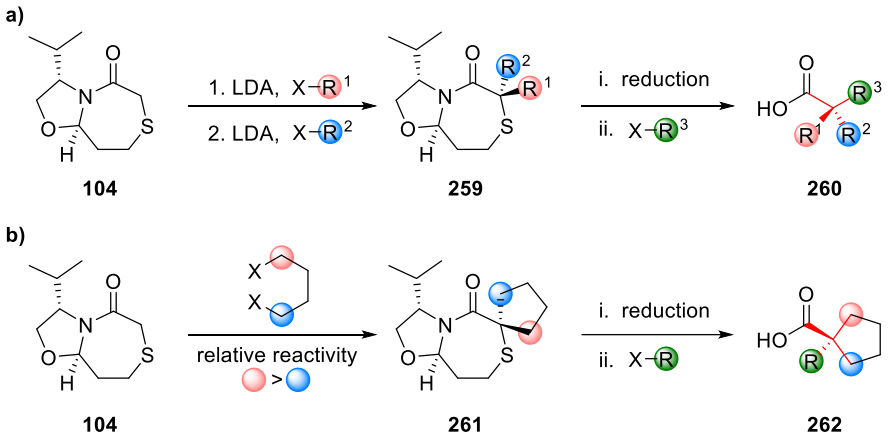

Scheme 2.1 Strategies for α-quaternary carbon stereocentres using lactam **104**

By establishing a means to rapidly construct α-quaternary carbon stereocentres within cyclic systems, the methodology advanced herein provides a powerful tool for simplifying the

synthesis of complex molecules. This is especially advantageous as the construction of carbon–carbon bonds alpha to carbonyls is a common and powerful retrosynthetic disconnection but is difficult to achieve in the context of α-quaternary carbon stereocentres. This challenge can lead to the unfortunate need for chiral separations of racemic mixtures, as observed in the case of the Merck's development of orally bioavailable CGRP receptor antagonists[5, 6] and Boger's synthesis of fredericamycin A (Figure 2.2).[7] In both cases, α-alkylation provided a facile synthetic route to the desired carbon framework with chiral HPLC relied upon to provide enantioenriched products.

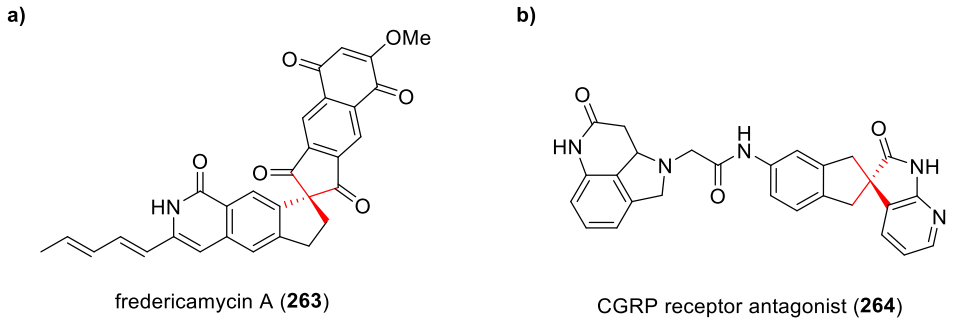

Figure 2.2 Structures of a) *ent*-fredericamycin A and b) the most potent member of series of orally bioavailable CGRP receptor antagonists developed by Merck

2.1.2 Initial Route of Enquiry

To establish a method capable of employing biselectrophiles, the central query is the extent to which alkylation occurs preferentially at one of the two electrophilic sites. This question is inherently entwined with the diastereoselectivity of the transformation, as alkylation order was expected to determine the stereochemical outcome. (Scheme 2.1b). It was reasoned that if the relative rate of alkylation at each electrophilic site was sufficiently different, high levels of diastereoselectivity would be achieved. By differentiating the reactivity of the two sites was predicted to provide analogous selectivity of that observed for simple electrophiles (Scheme 2.1a)

wherein the outcome was governed by sequential addition. Therefore, work on this project commenced with efforts to discriminate between the relative reactivity of each electrophilic site.

2.2 The Model System

2.2.1 Selection of Model Substrates and Reaction Optimisation

In order to probe the effect of electronic or steric influences on alkylation selectivity, a biselectrophile with general structure **265** was conceived. It was hypothesised that varying the nature of the aryl substituent 'R' would provide a means to modulate the electronic nature of the system while the two benzylic sites would be sterically differentiated by the virtue of having either one or two flanking groups. After investigating possible candidates, dibromide **209** was selected as the model substrate as benzylic bromides are known to be competent in the alkylation of lactam **104**[1] and the methoxy group provides strong electron-donating character. Dibromide **209** could be prepared quickly in two steps.[8] 2,3-Dimethylphenol (**266**) was alkylated with iodomethane in a slurry of acetone and potassium carbonate. This provided 2,3-Dimethylanisole (**208**) as a clear colourless liquid which could be brominated with NBS and AIBN in refluxing carbon tetrachloride or chloroform to yield dibromide **209** in 63% yield after recrystallisation.

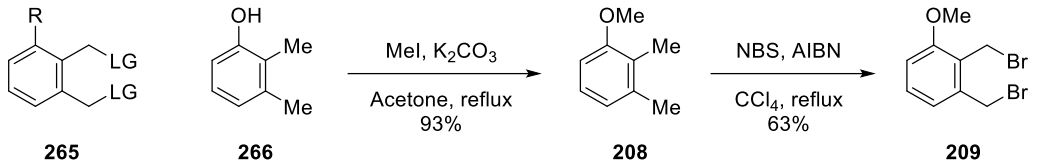

265 **266** **208** **209**

Scheme 2.2 Synthesis of model biselectrophile, dibromide **209**

Lactam **104** could be prepared on multi gram scale based on the reaction sequence established previously in our laboratory.[1] This was accomplished by alkylating methyl thioglycolate (**268**) with 2-(2-bromoethyl)-1,3-dioxolane (**267**) to provide thioether **269**. Subsequent treatment with the lithium alkoxide of (*S*)-valinol proceeds via transesterification and subsequent N→O acyl shift to prepare the valinol amide. The sequence concludes with a boron

trifluoride promoted transketalisation allowing lactam **104** to be crystallised from diethyl ether as slightly off-white crystals.

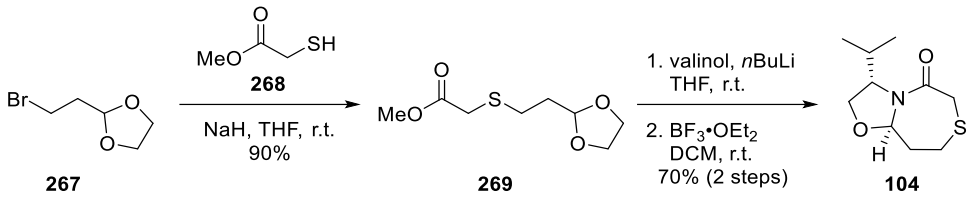

Scheme 2.3 Synthesis of lactam **104**

To investigate the alkylation, lactam **104** was subjected to deprotonation with LDA, using the conditions developed for simple electrophiles.[1] Dibromide **209** was then slowly added to the deprotonated lactam at –78 °C and allowed to stir for 4 h. It was expected that the relative distribution of products would give insight into which benzylic site is more reactive and if the assumption made regarding facial selectivity was correct (Scheme 2.4). Unfortunately, the reaction failed to yield any of the anticipated products. However, upon careful inspection of products isolated *via* column chromatography revealed a product resulting for the addition of two enolates to a single dibromide – a 2:1 adduct (**271**) of lactam **104** to dibromide **209** (Scheme 2.5). While such an observation was unexpected, it did indicate alkylation of the dibromide was possible. The occurrence of this product likely indicates that during the addition of the dibromide the initial large excess of enolate deprives the reaction the opportunity to provide single addition products, even when taking care to add the THF solution of dibromide at low temperature. Changes to reaction time, temperature, and amount of LDA likewise had no positive influence on the results. To supress the formation of adduct **271** an increased stochiometric ratio of dibromide **209** to lactam **104** and quicker addition of were examined but provided no benefit. To provide the greatest proportion of dibromide **209** to enolate the addition of reagents was inverted, with the enolate

added slowly to a cooled solution of dibromide. Ultimately, this also failed to provide any monoalkylated (**270a-d**) products with reactions again only providing small amounts of adduct **271**.

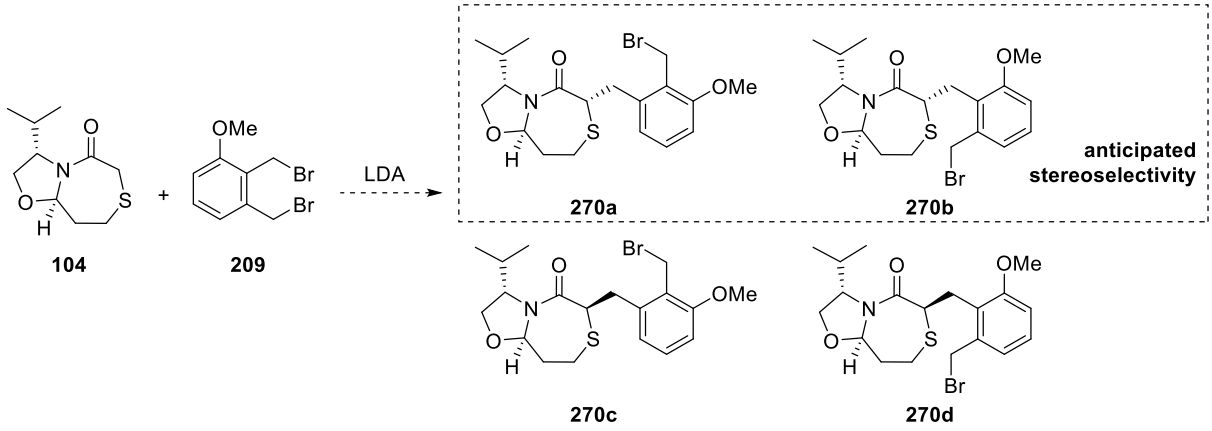

Scheme 2.4 Anticipated possible products formed from the alkylation of lactam **104**

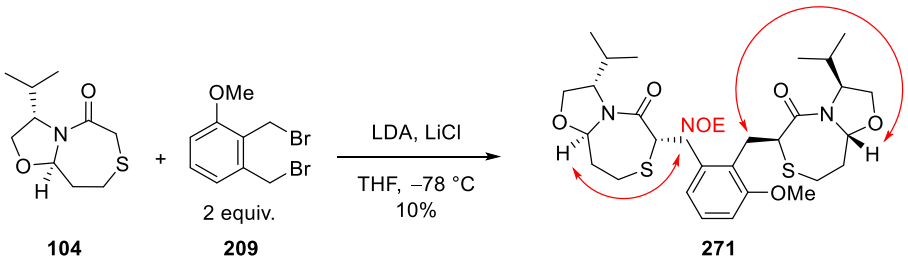

Scheme 2.5 Isolation of adduct **271**

Despite adduct **271** not being the intended product, the observation of **271** presented some promising aspects. The first (perhaps trivial) point is that both electrophilic sites could participate in the alkylation of lactam **104**. The second, and more critical aspect, was the formation of **271** as a single diastereomer, as indicated by ^{1}H and ^{13}C NMR (Scheme 2.4). This suggests that the exo-facial selectivity observed for lactam **104** with simple monoelectrophiles was retained. With these

observation in mind it appeared reasonable to investigate the possibility of engaging the second benzylic site in an intramolecular alkylation to outcompete the formation of adduct **271**.

2.2.2 Promoting Spirocycle Formation

As it was proving difficult to prevent a second intermolecular alkylation event, attempts were undertaken to engage the second electrophilic site through intramolecular alkylation. For the intramolecular addition to occur a second deprotonation must take place immediately following the first alkylation event. This requires a second equivalent of base to be present in the reaction medium; two sets of conditions were investigated to accomplish this. The first, excess LDA, provided none of the expected spirocycle **249** and was detrimental to the recovery of unreacted dibromide **209**, suggesting a sensitivity of dibromide **209** to basic conditions. The second option was to employ excess lactam **104**, relative to dibromide **209** and LDA, with the intention of using the excess enolate generated to perform the second deprotonation (Scheme 2.6). Perhaps unsurprisingly, this stoichiometry favoured the formation of the 2:1 adduct with no concurrent formation of the desired spirocyclic products.

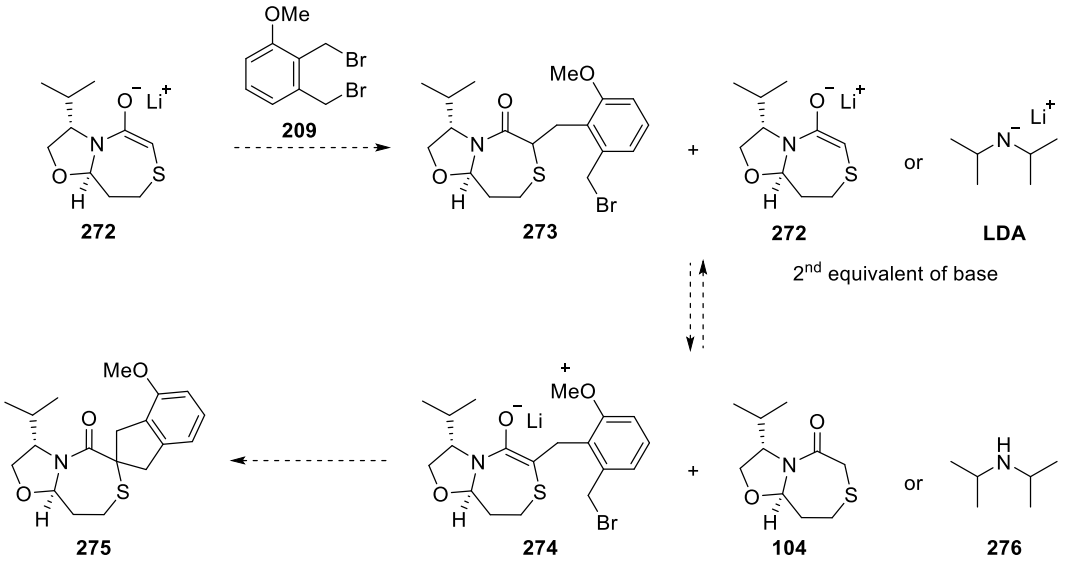

Scheme 2.6 Methods for promoting a second deprotonation

At this juncture it became necessary to survey of a wider range of reaction conditions. One significant limitation to such an enterprise was the poor α-proton acidity of lactam **104**. With a pK_a of around 26 for α-thio amides,[9] the generation of the amide enolate requires the use of strong base. It was hypothesised that by conducting the reaction under condition in which only a small percentage of the lactam exists as the enolate would provide opportunity for a second deprotonation and intermolecular alkylation to occur in advance of the addition of a second enolate. However, reactions which maintain such an equilibrating balance, between enolate and carbon acid, frequently require the use of weaker bases which are unlikely to be sufficiently basic to deprotonate lactam **104**.

To overcome the limitation of low acidity, it was reasoned that the acidity of the α-protons may be increased by amplifying the electron withdrawing character of the sulfur atom, a task which could be accomplished through oxidation to the sulfoxide or sulfone. Use of the sulfoxide was initially dismissed, in favour of the sulfone, as introduction of the additional stereochemical

element would add an unnecessary level of complexity. Lactam **104** was promptly oxidised to sulfone **250** with *m*CPBA in excellent (96% to quantitative) yield (Scheme 2.7). The sulfone was isolated as a fine white non-hygroscopic crystalline powder which could be stored on the bench top under ambient atmosphere for extended periods of time without any detectable decomposition.

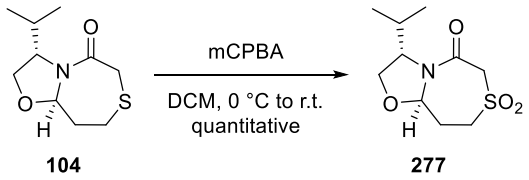

Scheme 2.7 Synthesis of sulfone **277**

With sulfone **277** in hand, the pressing question was to what extent had the α-protons been acidified (*i.e.* measurement of their pK_a). Direct experimental measurement of sulfone **277**'s acidity proved impossible due to complete insolubility in water. Efforts were made to use DMSO as a cosolvent however the proportion of DMSO required was incompatible with the instrumentation available. Having encountered this obstacle *in silico* methods were employed to provide an estimate of the acidity.

To estimate the pK_a, proton affinities for sulfone **277** and a diverse series of carbon acids were calculated, consisting of calculations for both the protonated and deprotonated acid (Table 2.1). The absolute difference in proton affinity, for each pair, was then plotted against their known experimental pK_a in DMSO, revealing a data set with a clear linear correlation (Figure 2.3). Interpolation of these data gave an estimated pK_a of 15.9 for lactam **277**, a value low enough for the consideration of weaker bases (*e.g.* alkoxides, carbonates, DBU, *etc.*). With this more acidic lactam now available, and with a reasonable approximation for the pK_a value of the α-protons, a new round of reaction screening could be undertaken.

Table 2.1 Difference in acid/conjugate base proton affinity for surveyed molecules and their respective acidities in DMSO

Acid	Δ Proton Affinity (kcal/mol)[a]	Experimental pK_a in DMSO[b]	Acid	Δ Proton Affinity (kcal/mol)[a]	Experimental pK_a in DMSO[b]
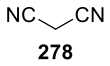 **278**	330.2	11.1[10]	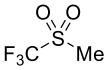 **283**	347.4	18.8[11]
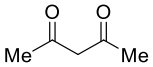 **279**	338.2	13.3[12]	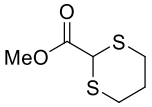 **284**	350.5	20.9[13]
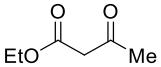 **280**	339.1	14.2[14]	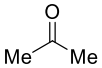 **285**	368.9	26.5[15]
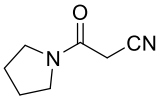 **281**	343.5	17.2[9]	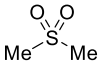 **286**	368.3	31.1[15]
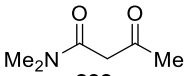 **282**	346.8	18.2[16]	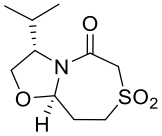 **277**	341.7	–

[a] DFT calculations performed at the B3LYP/6-31+G** level of theory; [b] Values from D.H. Ripin and D. A. Evans' pK_a table with citations for the specific examples given.

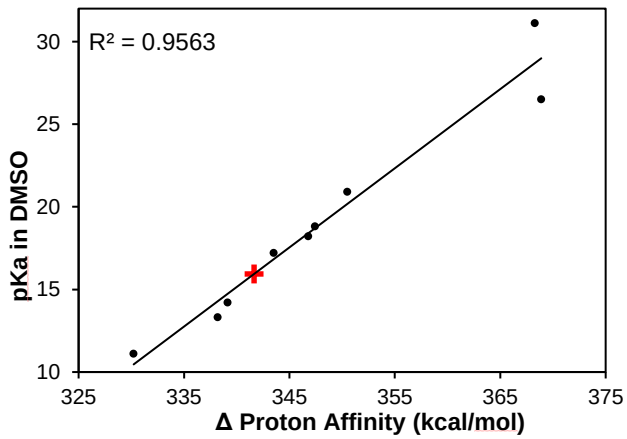

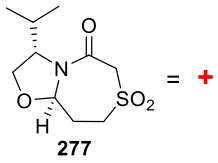

Figure 2.3 Plot of pK_a in DMSO as a function of change in proton affinity and interpolation of the pK_a of sulfone **277**

The examination of alternate bases in the alkylation reaction commenced with carbonate bases (K_2CO_3 and Cs_2CO_3). This provided no product formation even at elevated temperatures. Using amine bases, such as triethylamine and DBU also did not give the desired product with DBU only providing products resulting from DBU addition to the dibromide. The stronger organic base TMG also failed to promote the reaction. Gratifyingly, it was discovered that hydride and alkoxide bases could furnish the desired product, spirocyclic **287,** in low yields (Table 2.2).

Table 2.2 Optimisation of spirocycle **287** formation

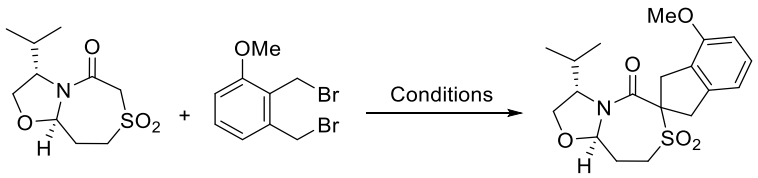

Entry	209 (equiv)	Base	Base (equiv)	Solvent	Temp.	Time	287 (yield)
1	1	K_2CO_3	2.5	DMF	reflux	16 h	n.r.
2	1	C_2CO_3	2.5	DMF	reflux	16 h	n.r.
3	2	Et_3N	3	THF	r.t.	16 h	n.r.
4	2	DBU	3	THF	r.t.	16 h	0
5	2	TMG	3	THF	r.t.	16 h	0
6	1	NaH	2.5	THF/DMF (1:1)	−78 °C to r.t	16 h	23
7	1	NaH	2.5	DMF	−20 °C to 0	3 h	47
8	1	KH	2.5	DMF	−15 °C to 0	2 h	54
9	1	KO*t*Bu	2.5	DMF	−10 °C	16 h	0
10	1	KO*t*Bu	2.5	THF	−20 °C	16 h	21
11	1	KO*t*Bu	2.5	THF/DMF (2:1)	−78 °C to r.t	16 h	32
12	1.5	KO*t*Bu	2.5	THF	−78 °C to r.t	16 h	58
13	2	KO*t*Bu	2.5	THF	−78 °C to r.t	16 h	33
14	1.5	KO*t*Bu	4	THF	−78 °C to r.t	16 h	0
15	2	KO*t*Bu	2.5	Et_2O (4% DMSO)	−78 °C to r.t	12 h	<10
16	3	KO*t*Bu	2.5	THF/DMPU (4:1)	−78 °C to r.t	16 h	<5
17	1.2	KH	2.5	THF	−78 °C to r.t	16 h	58

Reactions conduced at 50 mM in anhydrous solvent under an argon atmosphere.

Initially, DMF proved a reasonably good solvent (or cosolvent), for this transformation, providing a 47% yield of spirocycle with the use of sodium hydride. However, a vinyl ether side

product (**288**), arising from enolate O-alkylation, was also produced in non-trivial quantities (Figure 2.4); its regiochemistry was confirmed through analysis of HSQC and HMBC spectra.

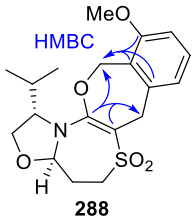

Figure 2.4 Vinyl ether **288**

O-Alkylation likely arises due to the greater nucleophilicity of the enolate oxygen owing to the ability of the polar environment to dissociate the metal counter ion. Formation of the vinyl ether **288** was suppressed when non-polar solvents such as THF and diethyl ether were used, with THF providing comparable yields when the reactions were conducted at −78 °C and allowed to slowly warm to room temperature overnight. Yields in the range or 50% to 60% could be achieved with a slight excess of dibromide (58%, entry 12) while higher loadings of base (entry 13) led to no product formation (entry 14). After considerable effort it was found that the most reliable conditions were the use of potassium hydride in THF at –78 °C. This provided the desired product as a single diastereomer and in a modest yield of 58%; requiring only a 20% excess of dibromide **209**.

2.2.3 Stereochemical Assessment

Although the reaction provided spirocycle **287** in only moderate yield, this granted the first opportunity to examine the stereoselectivity of the transformation. Pleasingly the reaction afforded the product as a single diastereomer, as observed in the ^{1}H NMR spectrum of the crude reaction mixture as well as in the product after chromatographic separation. The relative stereochemistry

of spirocycle was investigated using NMR spectroscopy with the two sets of benzylic methylene signals being easily identified and differentiated by inspection of the HSQC and HMBC spectra thus allowing for the relative *R*-configuration of the α-carbon to be identified through signals corresponding to NOE interactions (NOESY spectrum, Figure 2.5) between one set of benzylic protons and the aminal proton on the convex face of the bicycle.

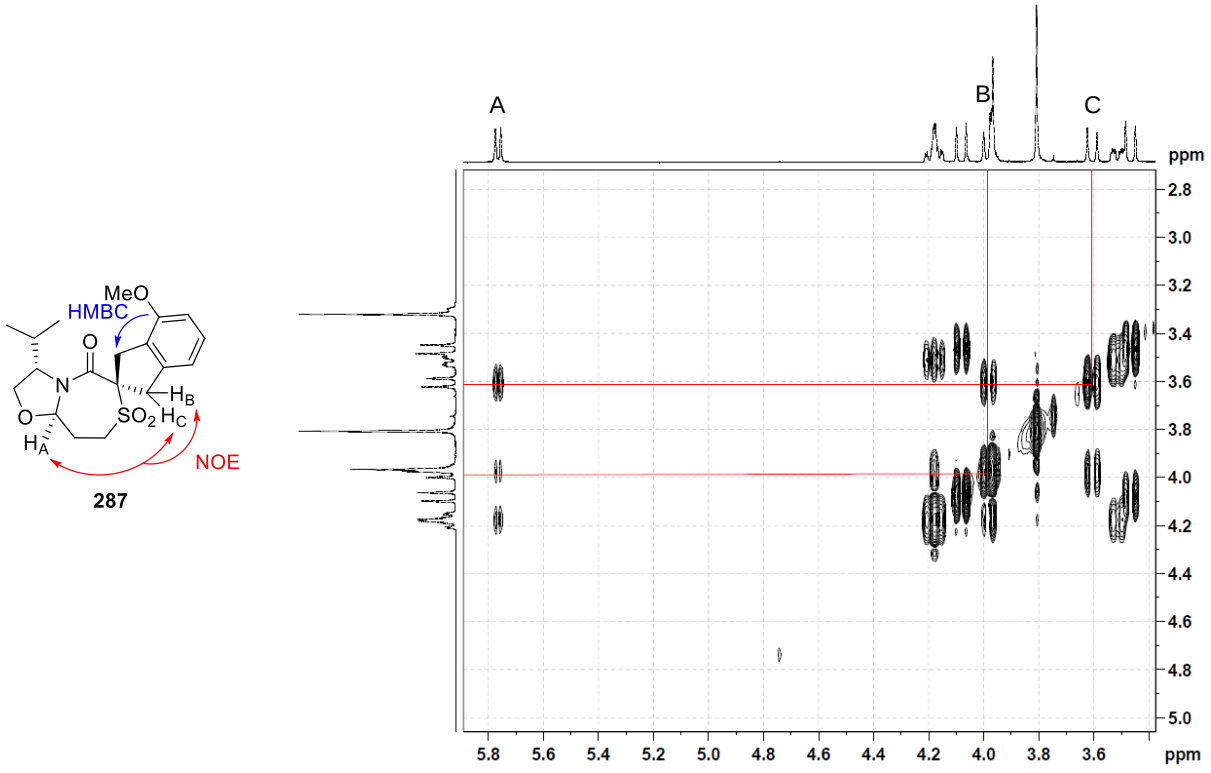

Figure 2.5 Determination of relative stereochemistry by NOESY spectrum analysis

The order of alkylation of the dibromide can be inferred from the stereochemistry of the alkylation product. Alkylation of bicyclic lactam **104** takes place on the convex face of the bicycle (please see section 2.2.6 for investigations into the facial selectivity of sulfone **277** derivatives). In the spirocyclisation, it is reasonable to assume that the final stereochemistry is set in the second alkylation step. Assuming alkylations of sulfone **290** also occur on the convex face, this implies

that substitution of **209** proceeds first at the bromide *ortho* to the methoxy group, followed by intramolecular alkylation at the *meta* position (Scheme 2.8). This order of operations suggests that the relative reactivity is a result of electronic activation of the *ortho* methyl bromide and not due to any steric influence of the flanking-substituents. The electronic bias is rationalised by the stabilisation of the incipient positive charge in the transition state by the ortho methoxy group. Having identified this reactivity profile opens avenues of interest regarding substrate scope, which shall be discussed in section 2.3.

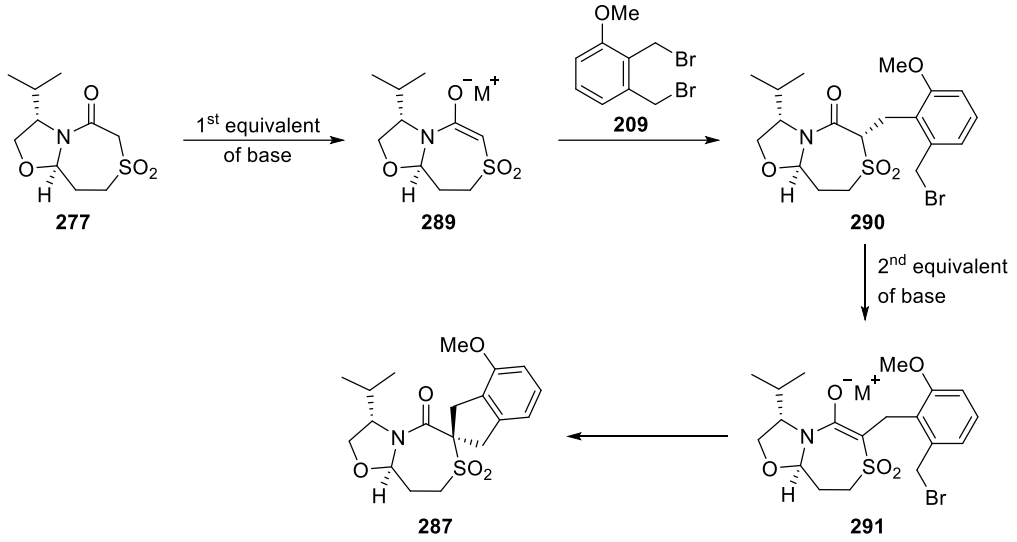

Scheme 2.8 Rationalisation of observed stereochemistry

2.2.4 Investigation into Enolate Formation

As the 58% yield of **287** can hardly be considered optimal, a more fundamental understanding of the reaction became necessary. A possible issue with the reaction was the formation of the desired enolate in insufficient quantities to provide high yields. To examine the enolisation, deuterium labelling experiments were performed. Enolisation was carried out using potassium hydride, as it provided the most consistent yield of spirocycle **287**. Sulfone **277** was

subjected to deprotonation at room temperature, at reflux, and in the presence of substoichiometric H_2O and quenched with several deuteron sources (D_2O, MeOH-d_4, and TFA-d_1). The results, summarised in table 2.3, indicated that sulfone **277** can be deprotonated at two positions with significant deuterium incorporation at C6 and variable incorporation at C8. Deuterium incorporation at C8 was particularly significant when the reaction was quenched with MeOH-d_4 suggesting the presence of KOMe-d_3 (formed when the reaction is quenched) leads to further deprotonation and correspondingly high levels of deuterium incorporation (*i.e.* greater than 100%). These results contrasted with the selective C6 deprotonation observed using LDA at −78 °C and TFA-d_1 used as a deuteron source. While excess deprotonation is still observed, deuterium is only incorporated at C6 signifying selective enolate formation.

Table 2.3 Levels of deuterium incorporation for sulfone **277**

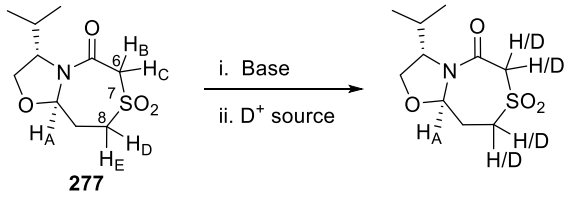

277

Entry	Conditions		Relative Integration[a]				
	Base	D^+ Source	H_A	H_B	H_C	H_D	H_E
1	KH, THF, r.t.	D_2O	1.00	0.49	0.44	0.93	0.67
2	KH, THF, reflux	D_2O	1.00	0.25	0.22	0.87	– [b]
3	KH, 15 mol% H_2O, r.t.	D_2O	1.00	0.44	0.42	0.88	0.52
4	KH, THF, reflux	MeOH-d_4	1.00	0.83	0.84	0.25	– [b]
5	LDA, −78 °C	MeOH-d_4	1.00	0.96	0.95	0.99	0.94
6	LDA, −78 °C	MeOH-d_4/TFA-d_1	1.00	0.22	0.28	1.05	1.12

[a] Proton A used for reference; [b] integration value for H_E could not be measured due to coalescence with other peaks.

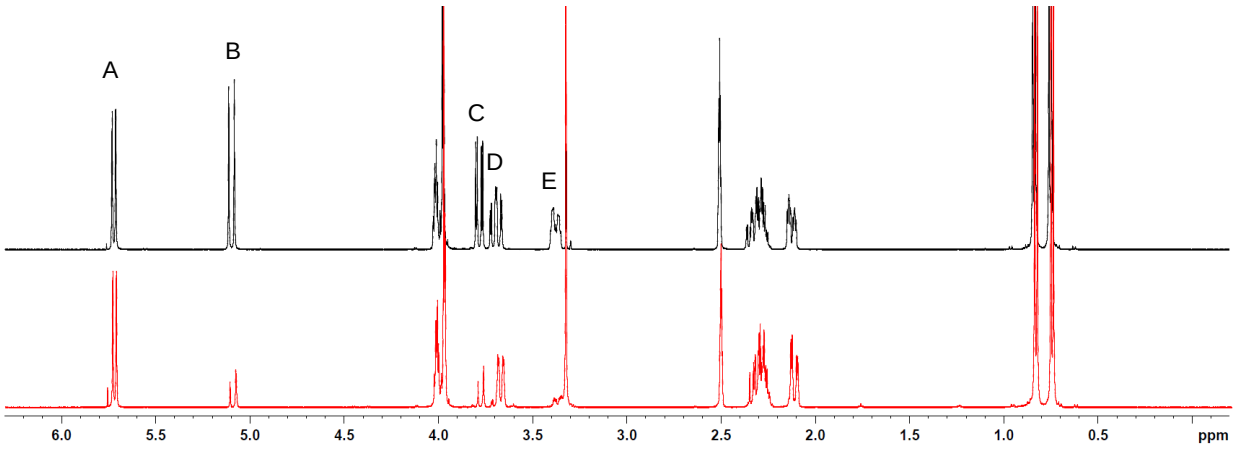

Figure 2.6 ^{1}H NMR spectra displaying deuterium incorporation of sulfone **277**

The deprotonation of C8 was considered undesirable and was thought to be a complicating factor that may be leading to complex mixtures and low yields. As such, two attempts were made to mitigate the acidity of the C8 protons: (i) limiting oxidisation of lactam **104** to provide the corresponding sulfoxide (**265**), and (ii) substituting C8 with a geminal dimethyl moiety to remove the C8 protons from the system. In addition to lowering the acidity of the C8 protons it was thought that use of the sulfoxide analogues would provide a more nucleophilic enolate, when compared to the sulfone, due to the decreased electron withdrawing capabilities of sulfoxides when compared to sulfones.

Beginning with the simpler task of synthesising sulfoxide **292**, lactam **104** was treated with a limiting amount (0.95 equivalents) of mCPBA to provide sulfoxides **292a** and **92b** as a 7:2 diastereomeric ratio as white powders in a combined yield of 82%. Determination of the stereochemical configuration at S7 was not carried out due to the need for analysis by x-ray crystallography and for the purposes of initial investigation, knowledge of the relative stereochemistry was unnecessary.

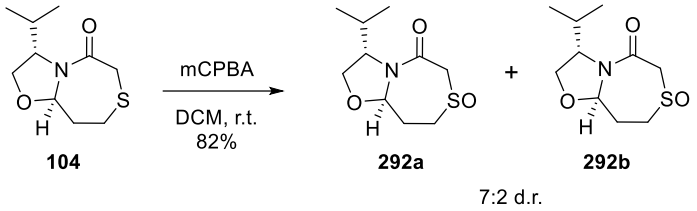

Scheme 2.9 Synthesis of sulfoxides **292a** and **292b**

Gratifyingly, when sulfoxide **292a** and **292b** were independently subjected to deprotonation and deuterium incorporation both displayed high levels of incorporation at C6 while no deuterium was observed at C8 as determined by ^{1}H and ^{2}H NMR (Table 2.4, Figures 2.7 and 2.8).

Table 2.4 Levels of deuterium incorporation for sulfoxides **292a** and **292b**

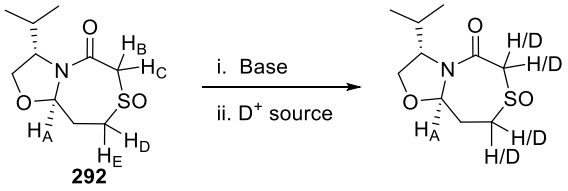

Entry	Acid	Conditions		Relative Integration[a]				
		Base	D^+ Source	H_A	H_B	H_C	H_D	H_E
1	**292a**	KH, THF, r.t.	D_2O	1.00	0.06	0.00	1.07	1.05
2	**292b**	KH, THF, r.t.	D_2O	1.00	0.16	0.00	1.03	– [b]

[a] Proton A used for reference; [b] integration value for H_E could not be measured due to coalescence with other peaks.

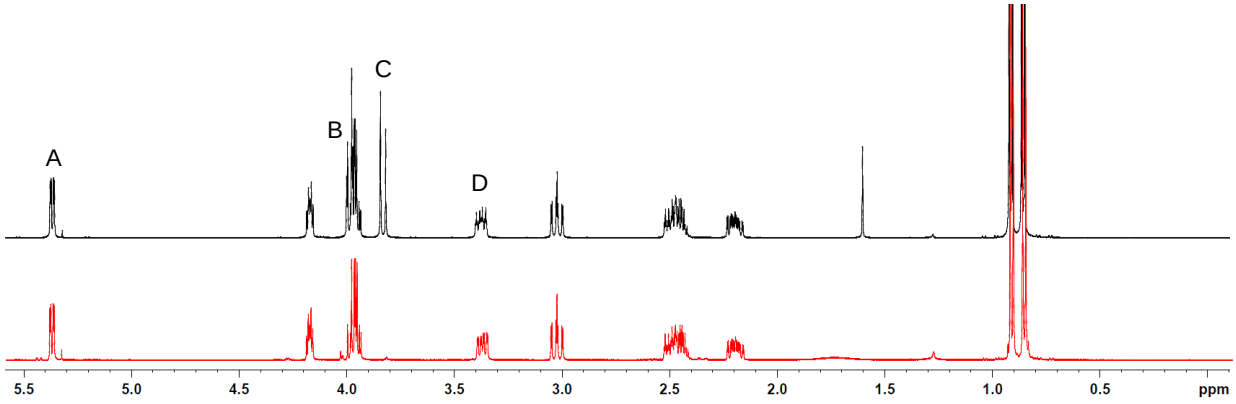

Figure 2.7 ^{1}H NMR spectra displaying deuterium incorporation of sulfoxide **292a**

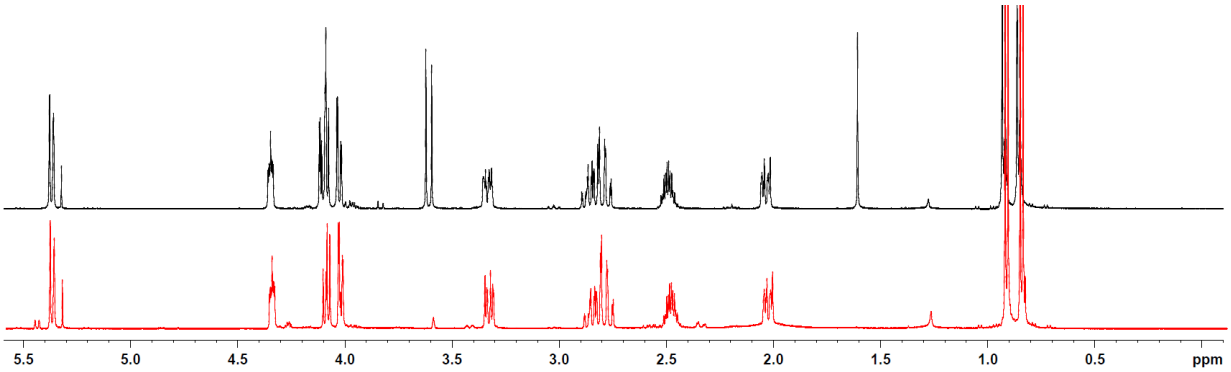

Figure 2.8 ^{1}H NMR spectra displaying deuterium incorporation of sulfoxide **292b**

Unfortunately, when either diastereomer was subjected to alkylation with dibromide **209**, the reactions returned complex mixtures of products. Upon subjection to column chromatography, mixtures of products appearing to be stereochemically related were only isolated as mixtures and in small quantities (less than 10%). This further discouraged investigation of the sulfoxide as useful solution to the encountered reactivity issues. Attention was therefore directed to the synthesis of the geminal methyl substituted sulfoxide (**297**, Scheme 2.10).

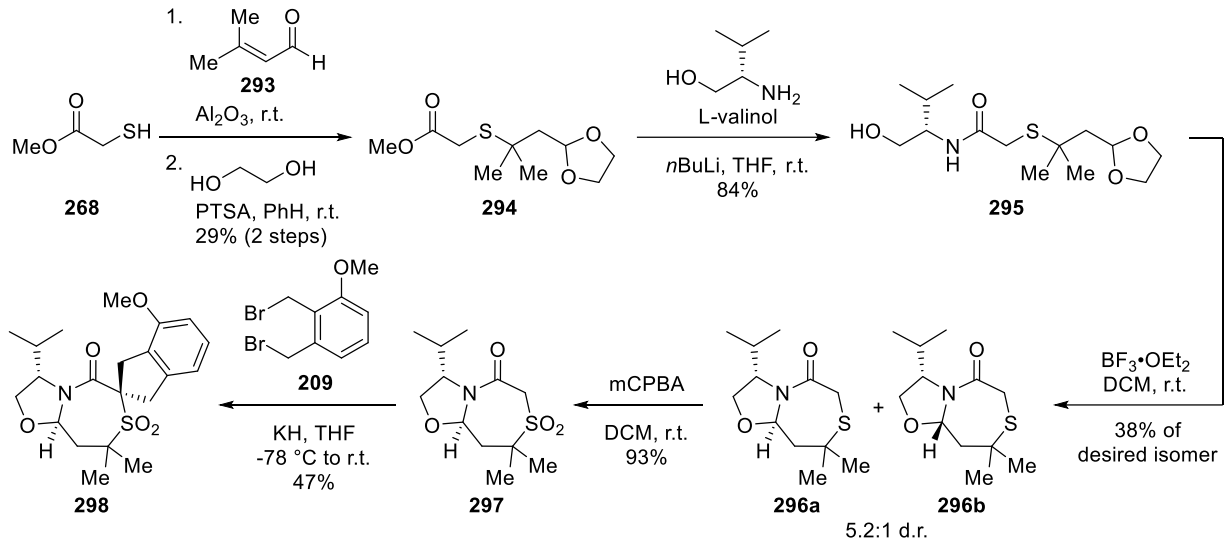

Scheme 2.10 Synthesis and testing of sulfone **297**

Sulfone **297** was synthesised beginning with the addition of methyl thioglycolate to 2-methyl-2-butenal neat on neutral aluminium oxide. Upon completion of the reaction, the aluminium oxide was filtered off and the filtrate concentrated to provide the crude adduct. The aldehyde was then protected as the dioxolane with ethylene glycol, providing ester **294** in 29% yield. Amide **295** was then generated in 84% by transacylation with L-valinol and *n*BuLi in THF. Lactam formation was successfully achieved, albeit in poor 38% yield, with boron trifluoride. Oxidation with mCPBA proceeded well and afforced sulfone **297** in 93% yield. Notably, a similar strategy may be employed to prepare ester **269** (from methyl thioglycolate, acrolein, and ethylene glycol, Scheme 2.11) for the synthesis of lactam **104**. Though the procedure provides only an overall 45% yield, it has the significant benefit of not producing a similar putrid odour due to the limiting amount of methyl thioglycolate employed.

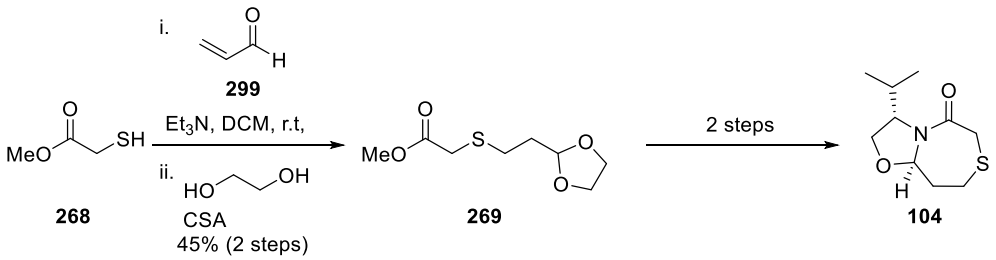

Scheme 2.11 Synthesis of thioether **269**

Subjecting sulfone **297** to alkylation with dibromide **209** and potassium hydride in THF gave a modest 47% yield of the expected spirocycle as a single diastereomer along with recovered sulfone **297** and 8% of a 2:1 adduct. As these results provided no improvement over the use of sulfone **277** further investigations concentrated on the use of sulfone **277**, due to its simpler and higher yielding preparation.

2.2.5 Investigation into Electrophile Competence

Having failed to produce a more efficient reaction through modification the enolate, attention was redirected to investigating the nature of the electrophile. As a starting point it seemed prudent to examine whether more, or less reactive electrophiles would provide higher alkylation yields. To this end, it was pleasing to discover that subjecting sulfone **277** to alkylation with iodomethane and potassium hydride provided the α-geminal dimethyl sulfone (**302**) in 84% yield. However, the use of 1,4-dibromobutane provided spirocyclic product **303** in only 37% yield. Similarly, symmetric dibromide **301** did not provide improved yields of the corresponding spirocycle **204**. These results indicated that perhaps a dibromide based biselectrophile was not suitable for this transformation. As such, two alternative systems were investigated: diiodide **305** and cyclic sulfate **307**.

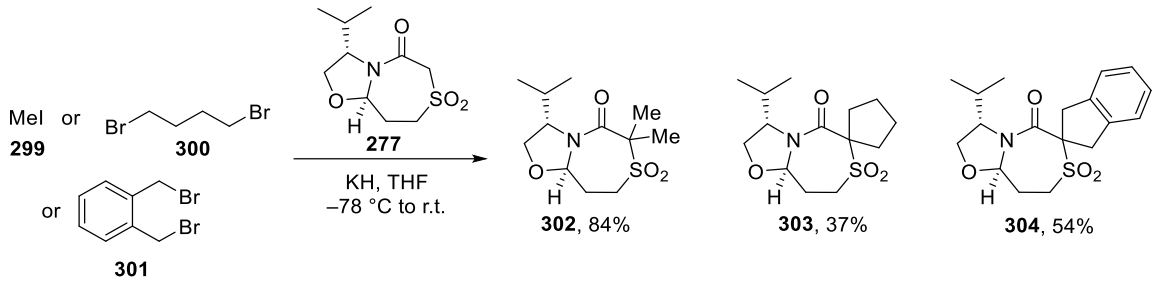

Scheme 2.12 Investigation of simple, symmetric biselectrophiles

Diiodide **305** was easily was prepared in 88% yield from dibromide **209** *via* a Finkelstein reaction with sodium iodide in refluxing acetone. Sulfate **307** required three steps to prepare. Beginning again with dibromide **209**, diol **306** was prepared by introducing acetate substituents using potassium acetate in acetic acid. Transesterification with potassium carbonate in methanol provided diol **279** in 54% yield, over two steps. Formation of cyclic sulfate **307** was then achieved in 57% yield by treating diol **279** with sulfuryl chloride and triethylamine.

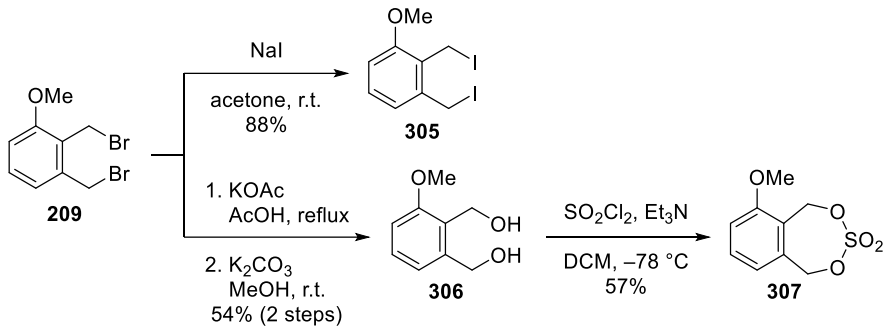

Scheme 2.13 Synthesis of diiodide **305** and cyclic sulfonate **307**

With these two new biselectrophiles in hand, each was subjected to alkylation with sulfone **277** with the aim of improving conversion. The results were disappointing with diiodide **305** providing a modest 33% yield while cyclic sulfonate **307** failed to provide any of the desired product.

With the examination of numerous conditions to this point, it started to become clear that a ceiling in the yield of spirocycle **287** was being reached. A common observation in the experiments was the full consumption of biselectrophile (either **209** or **305**), despite it being added in excess, relative to sulfone **277**. This characteristic was particularly troublesome as one goal of this work was to develop a reaction in which a complex biselectrophile substrate (*i.e.* one of significant value and perhaps requiring considerable effort to prepare) could be employed. The fate of dibromide **209** was an important aspect of the reaction which warranted investigation. Based on observations from previous reactions, it was perhaps unsurprising to discover that upon subjecting dibromide **209** to the reaction conditions, in the absence of sulfone **277**, resulted in complete decomposition as observed by ^{1}H NMR, with no identifiable decomposition products observable. It was initially thought that this may have been due to deleterious water present in the reaction causing hydrolysis of the electrophile and/or formation of cyclic ether **308**. However, attempts to examine such base promoted hydrolysis by exposing dibromide **209** to aqueous base resulted in no reaction. Further consideration led to entertaining the possibility that under the reaction conditions dibromide **209** may eliminate bromide and form a highly reactive ortho quinone methide species. Such a species could undergo numerous rapid reactions (*e.g.* nonspecific cycloadditions) leading to general decomposition and hindering further analysis of the crude reaction mixture.

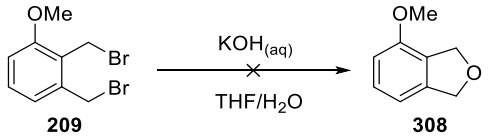

209 **308**

Scheme 2.14 Possible hydrolysis and subsequent cyclisation of dibromide **209**

The identification of the significant instability of dibromide **209** towards the normal alkylation conditions coupled to its stability to aqueous base suggested use of the latter for the alkylation. Moreover, the insolubility of both sulfone **277** and **209** in water naturally lead to the consideration of biphasic reaction conditions. As similar α-carbon alkylations of amides, esters, and ketones[17-19] have been performed with aqueous base by employing phase transfer agents, investigations commenced using tetrabutylammonium iodide in concert with aqueous potassium hydroxide (Table 2.5).

Table 2.5 Optimisation of biphasic reaction using phase transfer catalysis

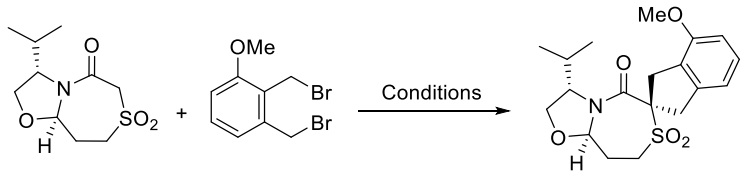

277 **209** **287**

Entry	277 (equiv)	209 (equiv)	*n*Bu$_4$NI (equiv)	[KOH] (wt% in H$_2$O)	Solvent	Temp.	Time	287 (yield)
1	1	1.2	0.5	50	THF/H$_2$O (2:1)	r.t.	16 h	46%
2	1	1.2	0.5	25	THF/H$_2$O (2:1)	r.t.	5 h	54%
3	1	1.2	0.5	50	THF/H$_2$O (2:1)	0 °C	12 h	59%
4	1	1.2	0.5	50	$CHCl_3$/H$_2$O (2:1)	0 °C	12 h	decomp.
5	1	1.2	0.25	25	THF/H$_2$O (2:1)	0 °C	24 h	Incomplete
6	1	1.5	0.5	50	THF/H$_2$O (2:1)	0 °C	18 h	72%
7	1.5	1	0.5	50	THF/H$_2$O (2:1)	0 °C	18 h	74%
8[a]	1	1.5	0.5	50	THF/H$_2$O (8:1)	0 °C	18 h	51%
9[a,b]	1.5	1	0.5	50	THF/H$_2$O (8:1)	0 °C	18 h	71%
10[c]	1.5	1	0.5	50	THF/H$_2$O (8:1)	0 °C	18 h	66%

Reactions conduced at 50 mM unless otherwise stated; [a] 1 mmol scale; [b] reaction conducted at 25 mM; c reaction conducted at 25 mM.

Reaction screening commenced with the treatment of sulfone **277** and dibromide **209**, in THF, with aqueous potassium hydroxide in the presence of tetrabutylammonium iodide. This proved to be a promising starting point as it provided a comparable 46% isolated yield of the

desired spirocycle while not exhibiting the facile degradation of dibromide **209** previously observed. Having obtained this result a more thorough investigation of reaction conditions was undertaken. It was quickly identified that the reaction did not require sixteen hours to reach completion at room temperature and that the yield of spirocycle **287** could be improved by lowering the temperature or decreasing the concentration of potassium hydroxide (entries 2 and 3). Lowering the loading of tetrabutylammonium iodide slowed the reaction, requiring more than twenty-four hours to reach completion (entry 5). It was eventually found that the reaction provided higher yields (72%) by slightly increasing the equivalents of dibromide **209** from 1.2 to 1.5. As discussed above, requiring such an excess of electrophile is far from ideal. Fortuity, use of the dibromide as the limiting reagent, with 1.5 equivalents of sulfone **277**, provides a comparably good yield of 74% (entry 7).

The biphasic reaction conditions have many advantages over the systems that were studied to this point. In addition to tolerating the dibromide as the limiting reagent they also benefited from a far simpler reaction set-up, not requiring dry solvent, inert atmosphere, or water sensitive strong bases. These reactions were also much more robust, providing greater reproducibility in yield. The only serious issue encountered using these conditions was regarding scale up; initial attempts to scale the reaction to 1 mmol gave only a 50% yield. Thankfully this was quickly solved by pre-cooling of the organic phase, dilution of the reaction, and using a smaller relative volume of base. Under these conditions, a 71% yield at a 1 mmol scale could be achieved. It is thought that these modifications have the effect of maintaining the reaction's temperature at 0 °C, a task that is harder to achieve with larger volumes. With reliable conditions established the project moved onto the task of investigating the facial selectivity of the transformation and by extension confirm the relative reactivity of the electrophilic sites of dibromide **209**.

2.2.6 Alkylation facial selectivity

With conditions for the alkylation of sulfone **277** successfully identified it became possible to directly determine the facial selectivity of the intermolecular alkylation by examining the reaction of sulfone **277** derivatives with only one α-proton. To accomplish this α-Benzyl sulphide **309** was prepared from lactam **104** (a known alkylation product[1]) and subjected to oxidation in diastereomerically pure form. Under the oxidation conditions epimerisation at the α-carbon was observed to give a six-to-five ratio of sulfones **310a** and **310b**. This mixture of diastereomers could then be alkylated under the biphasic reaction conditions to provide the methyl (**311**) or ethyl (**312**) alkylation products as single diastereomers, with the relative configuration of the α-carbon established by examination of NOESY NMR spectra. This stereoselectivity is indicative of enolate alkylation proceeding from the convex face (*i.e. exo* face) of the lactam bicycle, the same selectivity as previously observed for lactam **104**. These results provide further evidence that the sequence of events delineated in Scheme 2.8 is indeed correct. With experimental evidence now in hand to support the assumptions outlined in section 2.1.2, work on investigating the substrate scope of the reaction could commence.

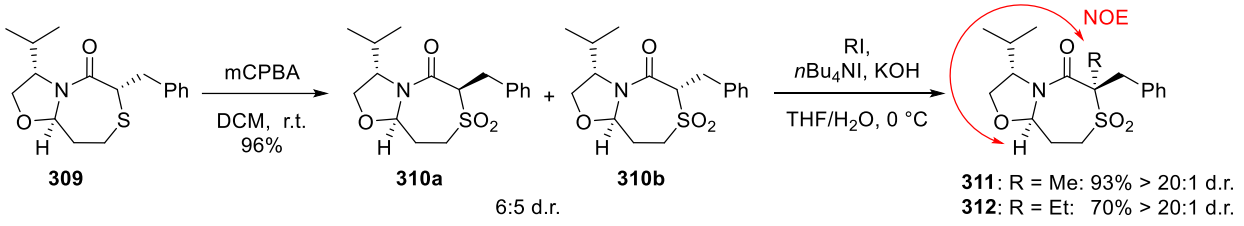

Scheme 2.15 Identification of facial selectivity for the alkylation of sulfone **310**

2.3 Substrate Scope

2.3.1 Substrate Design and Synthesis

Alkylation with dibromide **209** proceeded with excellent stereoselectivity, presumably arising from electronic differences between the two electrophilic positions. As such, an investigation seeking to explore the efficiency and stereoselectivity for a range of dihalides bearing electron donating/withdrawing groups at various positions (Figure 2.9), relative to the electrophilic carbon, was undertaken.

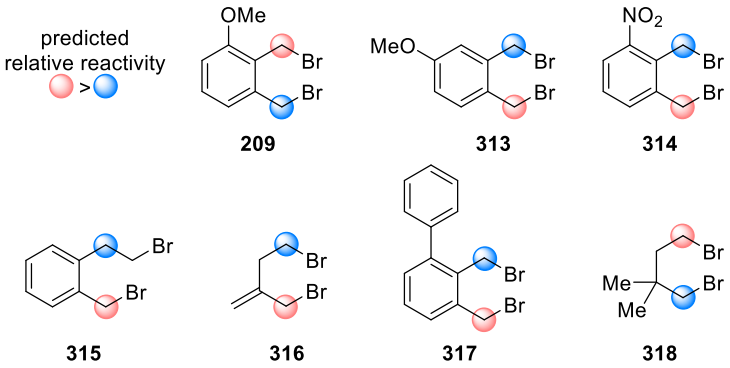

Figure 2.9 Proposed electrophiles and predicted relative reactivities

The placement of the methoxy group in dibromide **313** is expected to activate the electrophilic site in *para* relation to it by stabilisation of the positive charge in the same fashion as was achieved at the *ortho* position in dibromide **209**. The preparation of this substrate proved more troublesome than dibromide **209**. AIBN promoted bromination of 3,4-dimethylanisole only provided the desired product in 31% yield (28% from the available phenol). However, a more efficient synthesis was achieved in three steps from dimethyl 4-bromophthalate by initial Buchwald-Hartwig cross-coupling with methanol followed by reduction with LAH and a final bromination with phosphorus tribromide to yield dibromide **313** in 60% over three steps.

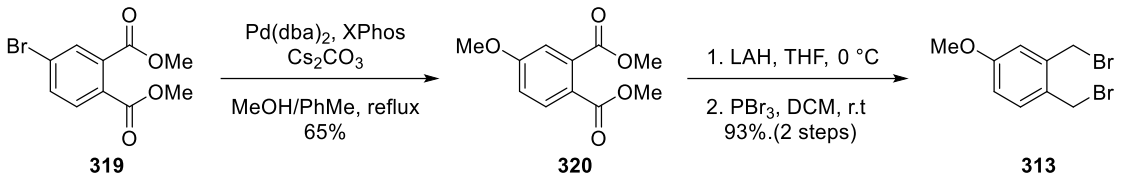

Scheme 2.16 Synthesis of dibromide **313**

The decoration of the arene with the strongly withdrawing nitro group is proposed to act in the opposite manner to the methoxy group of dibromide **209**. By destabilising the alkylation transition state for the *ortho* substituent, this substrate is theoretically prone to faster alkylation at the *meta* electrophilic site relative to the *ortho* electrophilic site. A similar strategy to that employed for dibromide **313** was relied upon for the synthesis of the nitro containing arene **314**. 3-Nitrophthalic acid was dimethylated with iodomethane and sodium bicarbonate providing dimethyl phthalate **295**. Reduction of the ester functionality to the corresponding diol proved difficult in the presence of the nitro group; DIBAL was marginally successful at the task providing diol **296** in 38% yield. Finally, an Appel reaction, with triphenylphosphine and NBS afforded 73% of the desired dibromide **287**.

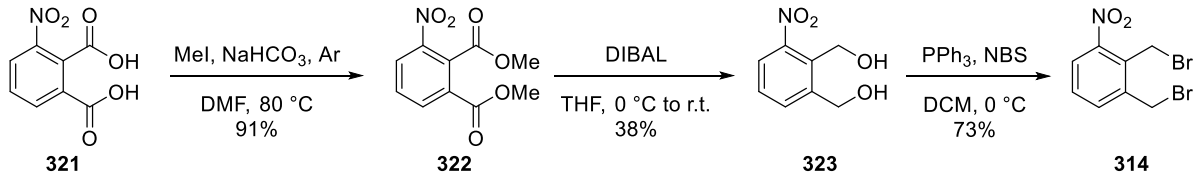

Scheme 2.17 Synthesis of dibromide **314**

Arene **315** presents benzylic and homobenzylic electrophilic sites as the sites for alkylation selectivity. From the stability granted by the arene in the alkylation transition state it may be predicted that this biselectrophile should alkylate first at the benzylic position with alkylation at the homobenzylic site following to provide access a six-membered ring product. Dibromide **315**

was provided in 76% overall yield in two steps from homophthalic acid *via* an initial global reduction with LAH followed by Appel bromination with triphenylphosphine and NBS.

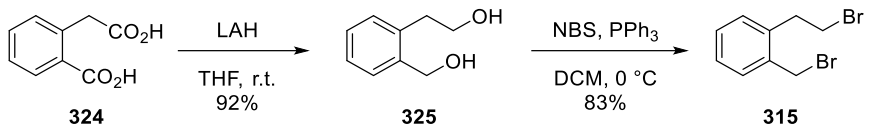

Scheme 2.18 Synthesis of dibromide **315**

Dibromide **316** is expected to behave in an analogous manner to dibromide **315** with the allylic bromide being displaced preferentially over the homoallylic bromide. Synthesis of this molecule proved much more challenging than the preparation of any substrates to this point. Direct reduction of itaconic acid with LAH to provide the diol failed and first required Fisher esterification with methanol to give the corresponding methyl ester. Reduction of the ester at 0 °C provided modest quantities of diol **327.** However, Appel bromination provided less than 5% of the desired dibromide. Attempts were also made to synthesise the dichloride and the dimesylate from diol **327** using thionyl chloride or methanesulfonyl chloride respectively, these too failed.

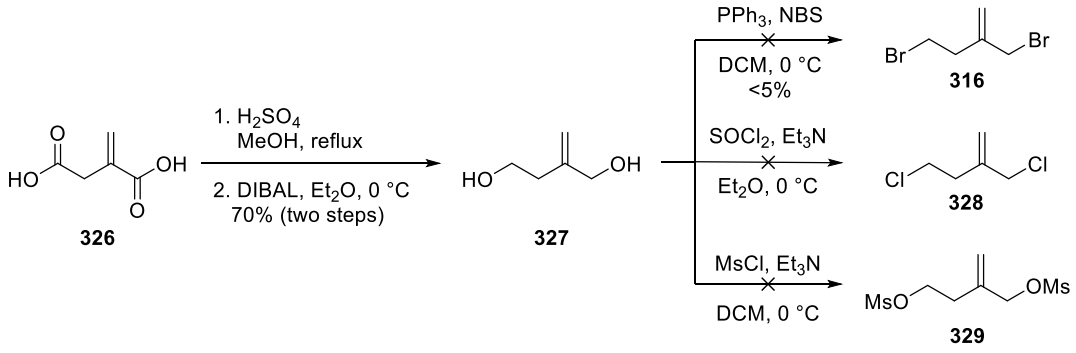

Scheme 2.19 Attempts to synthesise dibromide **316** and analogues thereof

At this point it was suspected that much of the difficulty encountered may be overcome by substituting the terminal olefin to suppress competing reactions involving the olefin.

Tetrasubstituted olefin **331** could be synthesised using a literature procedure by aldol condensation of diethyl succinate with acetone.[20] Reduction of the diethyl ester with LAH proceeded much more smoothly, likely due to the suppression of 1,4-conjugate reduction chemistry owing to the presence of the methyl groups. However, the location of the methyl groups proved problematic in attempting to manipulate the hydroxyl functionality; triphenylphosphine and NBS, phosphorus tribromide, and methanesulfonyl chloride all manage to functionalise the homoallylic alcohol but the increased steric hindrance imposed by the tetrasubstituted olefin prevented facile manipulation of the allylic alcohol. Considering the possibility that this steric issue may complicate alkylation selectivity, no further effort was expended in synthesising a tetrasubstituted olefin containing biselectrophile.

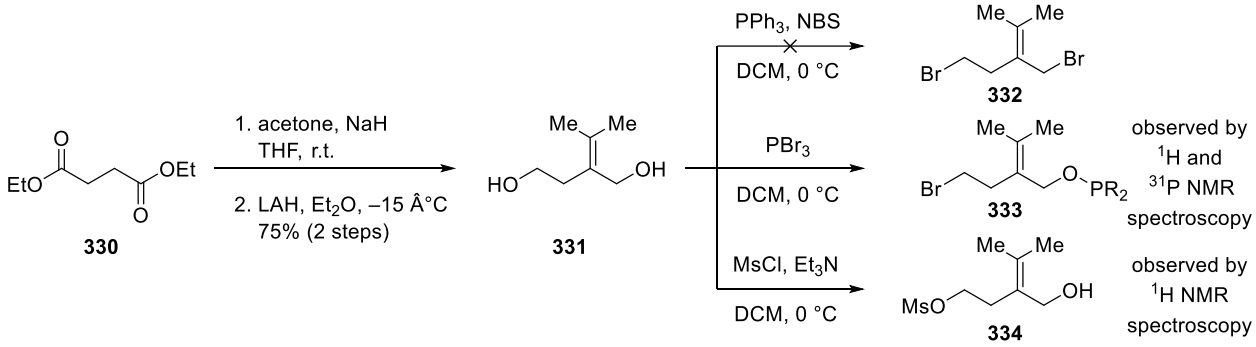

Scheme 2.20 Attempts to synthesise tetrasubstituted olefin containing biselectrophiles

Having exhausted several routes to biselectrophiles of the allylic *versus* homoallylic type a final effort was made to prepare the dimesylate analogue *via* a reported thermal rearrangement of substituted cyclopropanes.[21] The requisite cyclopropane **336** was synthesised from dimethyl malonate and 1,2-dichloroethane,[22] then modified by reduction to the diol by LAH followed by mesylation with methanesulfonyl chloride to give dimesylate **337** in 26% overall yield. Dimesylate **337** was then heated neat at 110 °C for only fifteen minutes to provide a black tar from which dimesylate **329** could be isolated as a slightly off-white solid in 77% yield.

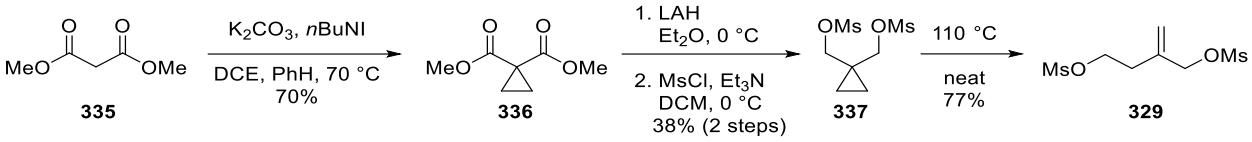

Scheme 2.21 Synthesis of dimesylate **329**

The last two substrates were intended to determine if steric hindrance would be adequate to drive alkylation selectivity. The first substrate introduces a phenyl *ortho* substituent to provide steric hindrance and discourage substitution at the proximal benzylic site. To this end, a phenyl group was introduced to 1-bromo-2,3-dimethylbenzene through a Kumada cross-coupling with bromobenzene. This proceeded well, in 80% yield, and subsequent radical bromination with AIBN and NBS gave 84% of the desired biaryl dibromide (Scheme 2.22).

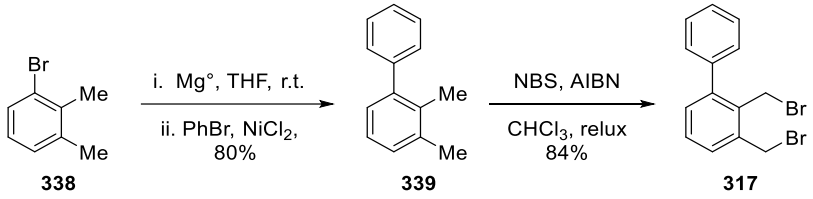

Scheme 2.22 Synthesis of biaryl dibromide **317**

The second sterically biased substrate was designed with a geminal dimethyl group to slow alkylation at the neopentylic site. This substrate is also interesting in that neither electrophilic site is activated by proximal functionality. The preparation this molecule begins with the reduction of 2,2-dimethylsuccinic acid to diol **341** in 86% yield. Attempts to brominate the diol with triphenyl phosphene and NBS failed, likely owing to slow displacement adjacent to the geminal dimethyl moiety. Diol **341** could be efficiently transformed to the corresponding dimesylate **342**. However, attempts to perform Finkelstein reactions with either lithium bromide or sodium iodide only provided reasonable amounts of the monohalogenated products **343** and **344**. Attempts to force the

reactions to completion, with elevated temperatures, excess halide salt, and extended reaction times failed to garner the desired dibromide.

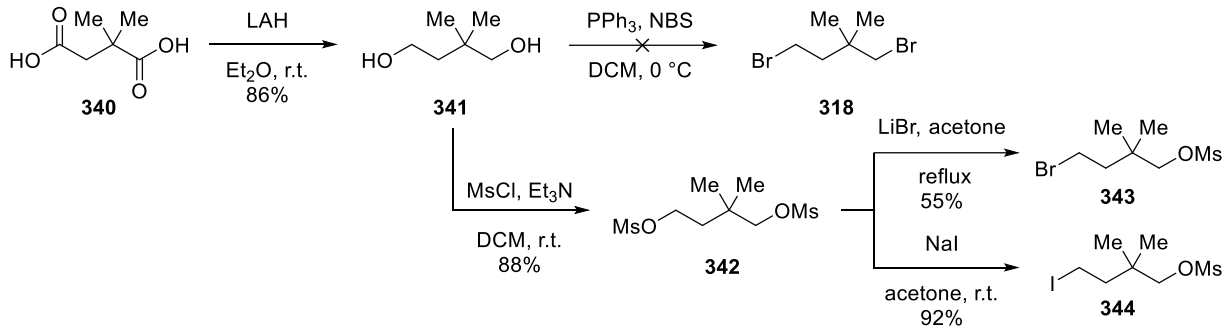

Scheme 2.23 Synthesis of alkyl biselectrophiles

Despite not synthesising exactly the desired dibromides **316** and **318**, dimesylates **329** and **342** were expected to be competent replacements. As the biphasic reaction conditions contain a sizable proportion of iodide it is not unreasonable to propose that a Finkelstein type iodination may occur. This would provide halogen-based electrophile *in situ* promoting the first alkylation with the second alkylation being facilitated by intramolecular displacement, perhaps overcoming the steric hindrance which prevented the preparation of dibromide **318**.

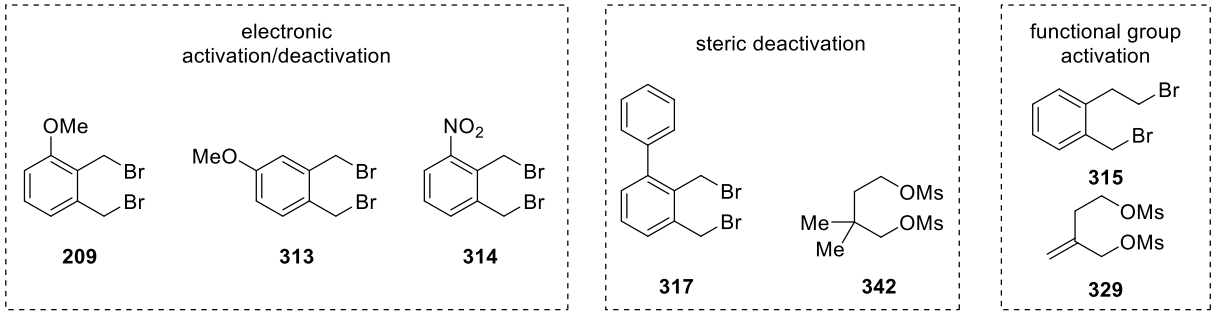

Figure 2.10 Final set of test substrates

2.3.2 Investigation of Substrate Scope

The substrates prepared above were subjected to the reaction conditions outlined in entry 7 of table 2.5. Pleasantly, most of the substrates provided good to excellent yields of the alkylated products (Table 2.7). The highest yields were observed for dibromide **315** and mesylate **329** which both display one activated and one nonactivated electrophilic site. The reason for these high yields is attributed to their less reactive nature when compared to dibromide **209** and therefore higher stability to the reaction conditions. Similarly, moderately activated substrates **313** and **317** provided yields in line with those observed for dibromide **209**, with spirocycles **319** and **323** being isolated in 85% and 68% respectively.

The cases of nitro substituted dibromide **314** and alkyl dimesylate **342** did not perform well under the standard set of conditions. In the case of dibromide **314**, the electrophile was completely consumed but no product was identified or isolated while sulfone **277** remained the major component of the reaction mixture. The reaction was therefore attempted again at −20 °C, with the addition of brine to prevent freezing of the aqueous phase. This allowed for isolation of the alkylated product in an improved 40% yield. Under standard conditions, use of dimesylate **342** could afford a 25% yield, with the remaining mass balance being accounted for in the form of unreacted starting materials (**277** and **342**). This observation lends credence to the suggestion that nonactivated primary electrophiles react slowly and are more stable under the reaction conditions (*vide supra*).

Unsatisfied with the low yield efforts were made to modify the conditions. Use the mono iodinated biselectrophile **344** provided an identical 25% yield thus investigations remained focused on dimesylate **342**. Excess dimesylate **342** provided higher conversions, but it was eventually discovered that the highest yields were obtained by employing a limiting amount of dimesylate

342 with room temperature reaction conditions, two equivalents of sulfone **277**, and four equivalents tertbutyl ammonium iodide. After a protracted reaction time of four days, this resulted in a 63% yield with no erosion of diastereoselectivity.

Table 2.6 Substrate scope for spirocycle formation

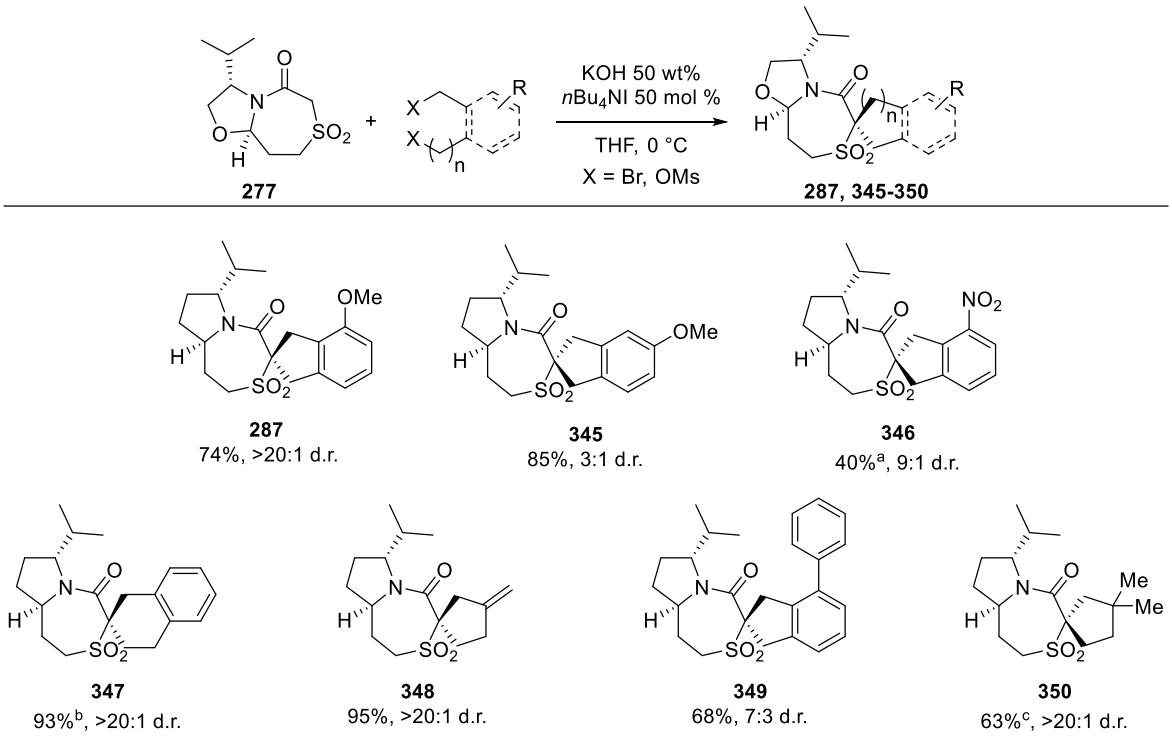

Reactions conducted at 0.3 mmol scale, 50 mM, and 0 °C with 1.5 equivalents of sulfone **250** under ambient atmosphere unless otherwise stated; [a] −20 °C and aqueous NaCl; [b] 1.0 mmol scale at 25 mM; [c] reaction performed at r.t. for 96 h with 2.0 equiv of sulfone **250** and 4.0 equiv of *n*Bu_4NI.

As with spirocycle **287**, interpretation of NOESY and HMBC spectra was sufficient to determine the configuration of the α-carbon for all cases. Dibromide **215**, and dimesylates **329** and **342** provided products with greater than twenty-to-one diastereoselectivity in the preparation of spirocycles **347**, **348**, and **350**. Notably the selectivity bias for dimesylate **342** is large enough to tolerate room temperature reaction conditions without any observable loss in diastereoselectivity. The three-to-one selectivity of spirocycle **345** indicates that the activating effect of the methoxy

group is less strongly communicated when attempting to activate a substituent at the *para*-position. The electron withdrawing properties of the nitro group in dibromide **314** provided a reasonable nine-to-one diastereomeric ratio with the major isomer resulting from the second alkylation occurring proximal to the nitro moiety. The poorest selectivity observed in the series was for the biaryl dibromide **317**, wherein the phenyl group was insufficient to provide selectivity for alkylation at the distal electrophilic site. In fact, alkylation still preferentially occurred at the proximal site, likely due to the electronic stabilisation provided by the phenyl group. Thus, the low seven-to-three diastereomeric ratio is a direct result of conflicting electronic and steric considerations.

2.3.3 Formation of α-Quaternary Stereocentres

With several spirocycle products now ion hand, the next task was to demonstrate their competency in the formation of α-quaternary stereocentres. An experiment previously conducted in the laboratory demonstrated that sulfones are successfully reduced, generating enolates that can be selectivity alkylated (Scheme 2.24).[23]

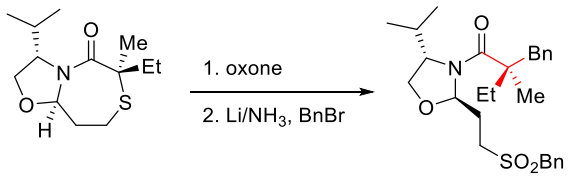

351 **352**
51 %, 88:12 d.r.

Scheme 2.24 Reduction and alkylation of sulfone **251**

Prototypical spirocycle **287** was subjected to the same lithium in ammonia reduction conditions and the resulting enolate quenched with benzyl bromide. The resulting alkylated product was immediately hydrolysed with aqueous hydrochloric acid to afford amide **353** in 34%

yield. Though the product was isolated as a single diastereomer (as observed in the ^{1}H NMR spectrum of the reaction mixture prior to purification) the yield was disappointingly low. Spirocycle **347** was alkylated with iodomethane using the same enolisation conditions and similarly provided the desired amide (**363**) as a single diastereomer in a low 41% yield.

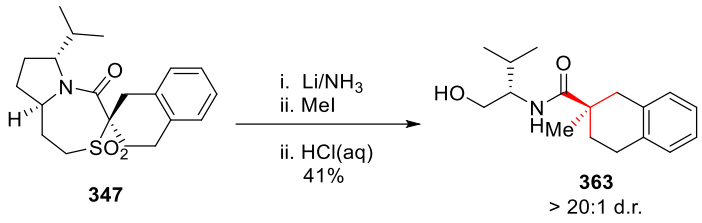

Scheme 2.25 Reduction and alkylation of cyclic sulfone **347**

Three main variables of the reaction were considered as possible central causes for the low yields. In order of occurrence these were; (i) the reduction of the sulfone to provide the corresponding α,α-disubstituted enolate, (ii) the alkylation of the α,α-disubstituted enolate, and (iii) hemiaminal ether hydrolysis. Due to the intricate nature of the reaction it proved difficult to directly monitor each aspect in real time (by NMR or TLC). However, issues arising with each step would provide characteristic evidence allowing for appropriate changes to be made.

The first issue to be addressed was the formation of the α,α-disubstituted enolate. Curiously, analysis of the ^{1}H NMR spectra of the crude product indicated a large proportion of the starting spirocycle to be present. The survival of the hemiaminal ether under the hydrolytic conditions is ascribed to its bicyclic nature, precluding complete excision of the propanal fragment. This observation indicated that the reduction conditions were leading to incomplete conversion to the α,α-disubstituted enolate, despite the use of up to eight equivalents of lithium. To remedy this, lithium-in-ammonia was replaced with the use of LiDBB, a powerful single electron reductant. LiDBB has been established to be a useful method for the reductive enolisation of lactam **104**

derivatives in the context of Mannich type additions to imines.[4] By employing LiDBB the progress of the reduction could be visualised colourimetrically as LiDBB may be titrated directly into the reaction mixture. This visual indication of complete reduction would ensure that the sulfone substrates would be completely reduced prior to the addition of the electrophile. To this end, the use of LiDBB ensured that the spirocycle completely consumed but it failed to significantly improve the yield of the reaction, providing only a 41% yield in the methylation of spirocycle **287**.

To fully interrogate the reduction step, it was of interest to identify amount of LiDBB required to provide complete conversion to the enolate. The method initially used for the preparation of LiDBB, used a 20% excess of lithium metal to 4,4′-di-tert-butylbiphenyl and would provide a theoretical 0.4 M solution of LiDBB. However, when employed, reactions would consume a volume well in excess of the two equivalents necessary. As such, experimental verification of LiDBB concentration was the logical next step. Reduction of a known quantity of trityl bromide provided an experimental concentration of only 0.1 M. An alternative and well evaluated procedure from Hill and Rychnovsky was used for the preparation of LiDBB. This procedure uses a large excess of lithium (10 equiv) relative to 4,4′-di-tert-butylbiphenyl.[24] When LiDBB, prepared in this manner, was used for spirocycle reduction only a slight excess (2.1 equivalents relative to the sulfone) was required for complete reduction providing amide **353** in an improved 61% yield, after alkylation with iodomethane, from spirocycle **287**.

The failure of the α,α-disubstituted enolate to alkylate was only a slight problem in this system. In some cases, protonation of the enolate provided the α-tertiary amide as a minor side product. This issue could be eliminated by careful removal of water from the substrate though azeotropic drying with toluene and the use of freshly distilled THF. Additionally, all electrophiles

were passed through basic alumina immediately prior to being added to the reaction, removing any small quantities of acid or water they may contain.

The hydrolysis of the alkylated products, to cleave the hemiaminal ether, presented a possible complication as the resulting amide products are suspectable to acid catalysed intramolecular N→O acyl transfer. Though this process is reversable under basic conditions, under the acidic conditions of the hydrolysis the product amino ester species exist as the cationic ammonium ion. This form of the product is more difficult to extract and purify and can easily lead to depressed yields. To prevent product loss as a result of acyl transfer the reaction were adjusted to pH 7 and allowed to stir for one hour before proceeding with the extractive workup. Prolonged stirring at pH 7 or 8 did not have a further positive effect on isolated yields.

Screening of electrophiles provided moderate to good yields of the expected α-quaternary amides with the enolate derived from spirocycle **287** (Table 2.8). Highest yields were observed for alkylation with active electrophiles, such as methyl iodide, and allylic/propargylic/benzylic halides. In contrast, less reactive n-alkyl halides, such as 1-iodopropane, gave low yields. Except for the case of allyl bromide, the amides were prepared as single diastereomers. Curiously, a slightly lower diastereomeric ratio was obtained for the allylation product.

Table 2.7 Alkylation of spirocycle **287** derived enolates

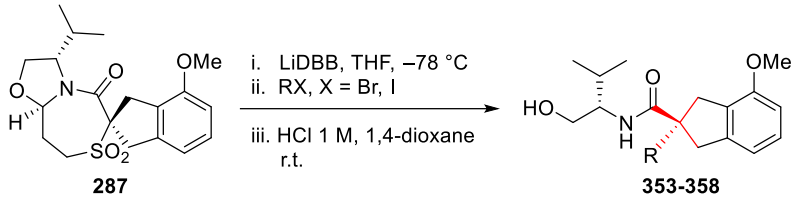

287 **353-358**

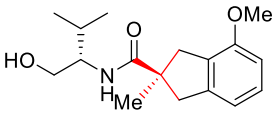

353
61%, >20:1 d.r.

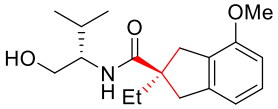

354
57%, >20:1 d.r.

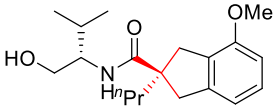

355
30%, >20:1 d.r.

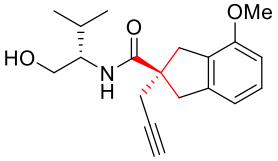

356
63%, >20:1 d.r.

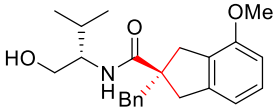

357
60%, >20:1 d.r.

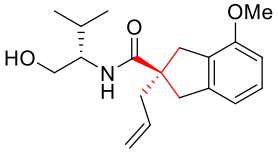

358
72%, 9:1 d.r.

This stereoselectivity trend was again observed for the other sulfones of the series (**347-350**, Table 2.8). Methylation selectivity remained above twenty-to-one for sulfone **347** and **349** while decreasing only slightly to ten-to-one for sulfone **348**. On the other hand, allylations were consistently low throughout the series, with the best result being only a four-to-one diastereomeric ratio for sulfone **348**. Interestingly the most structurally similar sulfone to **348**, sulfone **350** also suffers from poor selectivity with allylation proceeding equally poorly in a four-to-one diastereomeric ratio (amide **362**) and methylation yielding the lowest selectivity in the series at a ratio of only two-to-one (amide **366**).

Table 2.8 Allylation *versus* methylation of sulfone derived enolates

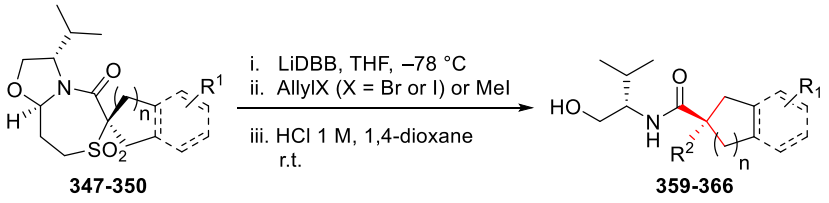

347-350 **359-366**

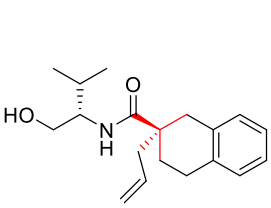

359
53%, 9:1 d.r.

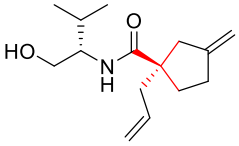

360
57%, 4:1 d.r.

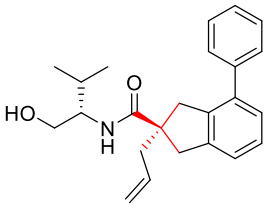

361
63 %, 13:1 d.r.

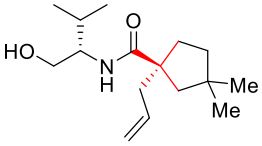

362
73%, 4:1 d.r.

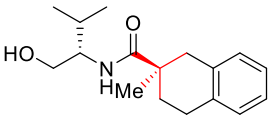

363
76%, >20:1 d.r.

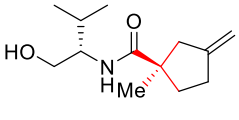

364
87%, 10:1 d.r.

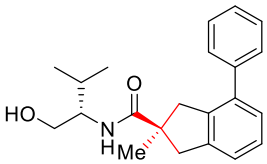

365
62%, >20:1 d.r.

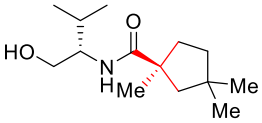

366
45%, 2:1 d.r.

One consideration that was thought may be causing the electrophile dependant selectivity was ability of allyl electrophiles to undergo substitution *via* an S_N2 or S_N2` mechanism. To test this spirocycle **350** was subjected to reduction and alkylation with 3,3-dimethylallyl bromide as the added methyl substitution should supress $S_N2$` type reactivity (Scheme 2.23). Though allylation with 3,3-dimethylallyl bromide only yielded 12% of the expected alkylated product (**366**), it was isolated in a poor two-to-one diastereomeric ratio. Moreover, along with continuing the trend of poor selectivity in allylic systems, this experiment further demonstrated the low selectivity observed for spirocycle **350**. To attempt an explanation the geometry of spirocycle **350** was examined using computational methods to determine if the O-C-C-S dihedral angle is indeed close to the 120° required for selective enolate formation (Figure 211).

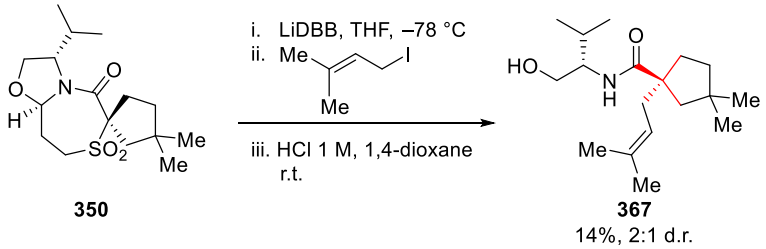

Scheme 2.26 Allylation with 3,3-dimethylallyl bromide

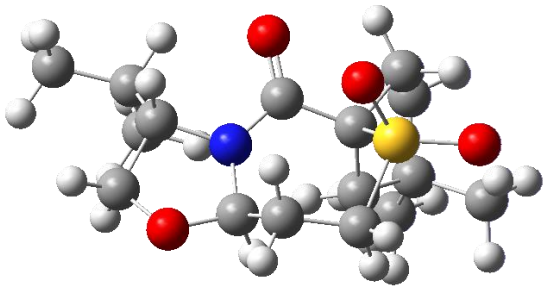

Figure 2.11 DFT optimised structure of spirocycle **350** B3LYP/6-311+G(d,p)

The DFT calculations indicated that the key O-C-C-S dihedral is 106°, perfectly suitable for selective enolate formation. As such, further computational studies were undertaken to examine the conformation of the resulting enolate. While the methyl groups are in proximity to the nucleophilic carbon in both conformers, they were found to be similar in energy and presumably equilibrate rapidly even at −78 °C. Additionally the Curtin–Hammett principle would suggest that the relative energies of these conformers is inconsequential to product formation. A possible explanation for the poor selectivity arising from the presence of the geminal methyl groups may be their influence on the overall reactivity of the enolate. The increased steric demand may be leading to a decrease in overall reactivity that results in the alkylation not occurring until the reaction is quickly warmed to room temperature immediately before the hydrolytic phase of the

reaction. The elevated temperatures would thus have a deleterious impact on the selectivity of the reaction.

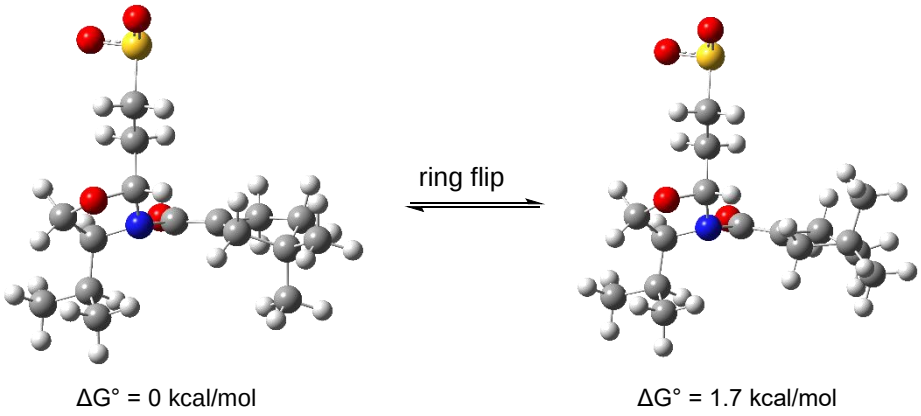

Figure 2.12 DFT optimised structures of spirocycle **350** derived enolates

While spirocycle **350** represents a significant outlier in terms of diastereoselectivity the examples summarised in tables 2.8 and 2.9 illustrate the ability of this methodology to quickly construct quaternary carbon stereocentres. In the majority of examples α-quaternary amides can be prepared in above ten-to-one diastereoselectivity with many instances providing single diastereomers. This method may be employed to generate α-quaternary carbon amide derivates with even greater levels of stereoselectivity by employing conventional chromatographic techniques to first separate the diastereomers. This is a characteristic advantage over enantioselective methods, which generally provide poor selectivity when provided with similarly small steric bias and rely on favourable crystallisation conditions and/or chiral HLPC for further enantio-enrichment. Additionally, the ability to directly synthesis 5,6- and 6,6-fused carbocyclic systems (amides **327**-**333**, **335**, **337**, and **339**) which incorporate α-quaternary carbons at positions distal to the ring fusion is an important strength of this work as, while the structural motif is

common within the literature, molecules possessing this feature are seldom synthesised stereoselectivity.

2.4 Conclusions

This chapter has outlined the development of a stereoselective double alkylation of a chiral bicyclic lactam auxiliary for the formation of α,α-disubstituted enolates which then may be alkylated to generate α-quaternary stereocentres. This effort has involved the exploration of synthetic routes for the preparation of suitable biselectrophiles as well as an examination of enolisation conditions permitting multiple alkylations to occur sequentially in one operation.

Unlike classic chiral auxiliary methods developed to date, the approach described, leverages biselectrophilic substrates and exploits inherent differences in reactivity of distinct electrophilic sites to dictate the stereochemical outcome of the reaction. In addition to expanding the scope of electrophiles which can be used with this bicyclic lactam auxiliary system, the oxidation of the sulfide has allowed for initial alkylations to be conducted at higher temperatures (0 °C in place of −78 °C) and without the need for inert atmosphere or anhydrous conditions. Additionally, the α-carbon of the auxiliary is alkylated twice in a single transformation, providing a shorter (by one step) procedure in comparison to the use of simple/classic electrophiles.

A variety of electrophiles have been demonstrated to provide high levels of diastereoselectivity in the transformation, including benzyl, allyl, and alkyl, with selectivity guided by steric or electronic consideration, though competing electronic and steric influences were shown to erode selectivity. The second intramolecular alkylation provided access to substituted cyclopentanes, and cyclohexanes. The spirocyclic intermediates were then shown to undergo reduction with LiDBB to form the corresponding α,α-disubstituted enolates, which could be alkylated with methyl, ethyl, *n*-propyl, allyl, propargyl, and benzyl electrophiles to form α-quaternary stereocentres. Products were isolated in good yield and in most cases with high (nine-to-one) to excellent (greater than twenty-to-one) diastereoselectivity.

2.5 References

1. Arpin, A.; Manthorpe, J. M.; Gleason, J. L., A Practical Chiral Bicyclic Thioglycolate Lactam Auxiliary for Stereoselective Quaternary Carbon Formation. *Organic Letters* **2006,** *8* (7), 1359-1362.

2. Manthorpe, J. M.; Gleason, J. L., Stereoselective Formation of Quaternary Carbon Centers: Alkylation of A,A-Disubstituted Amide Enolates. *Angewandte Chemie International Edition* **2002,** *41* (13), 2338-2341.

3. Burke, E. D.; Gleason, J. L., A,A-Disubstituted Boron Enolates in the Asymmetric Synthesis of Quaternary Carbon Centers. *Organic Letters* **2004,** *6* (3), 405-407.

4. Tiong, E. A.; Gleason, J. L., Stereoselective Formation of A-Quaternary Stereocenters in the Mannich Reaction. *Organic Letters* **2009,** *11* (8), 1725-1728.

5. Bell, I. M.; Bednar, R. A.; Corcoran, H. A.; Fay, J. F.; Gallicchio, S. N.; Johnston, V. K.; Hershey, J. C.; Miller-Stein, C. M.; Moore, E. L.; Mosser, S. D.; Roller, S. A.; Salvatore, C. A.; Theberge, C. R.; Wong, B. K.; Blair Zartman, C.; Kane, S. A.; Williams, T. M.; Graham, S. L.; Vacca, J. P., The Identification of Potent, Orally Bioavailable Tricyclic Cgrp Receptor Antagonists. *Bioorganic & Medicinal Chemistry Letters* **2009,** *19* (16), 4740-2.

6. Stump, C. A.; Bell, I. M.; Bednar, R. A.; Bruno, J. G.; Fay, J. F.; Gallicchio, S. N.; Johnston, V. K.; Moore, E. L.; Mosser, S. D.; Quigley, A. G.; Salvatore, C. A.; Theberge, C. R.; Blair Zartman, C.; Zhang, X. F.; Kane, S. A.; Graham, S. L.; Vacca, J. P.; Williams, T. M., The Discovery of Highly Potent Cgrp Receptor Antagonists. *Bioorganic & Medicinal Chemistry Letters* **2009,** *19* (1), 214-217.

7. Dale L. Boger, O. H., Kapiamba Mbiya, Minsheng Zhang, Total Synthesisof Natural and Ent-Fredericamycin A. *Journal of the American Chemical Society* **1995,** *117*, 10.

8. Kraus, G. A.; Choudhury, P. K., Synthesis of Puraquinonic Acid Ethyl Ester and Deliquinone Via a Common Intermediate. *The Journal of Organic Chemistry* **2002,** *67* (16), 5857-5859.

9. Bordwell, F. G.; Fried, H. E., Acidities of the Hydrogen-Carbon Protons in Carboxylic Esters, Amides, and Nitriles. *The Journal of Organic Chemistry* **1981,** *46* (22), 4327-4331.

10. Matthews, W. S.; Bares, J. E.; Bartmess, J. E.; Bordwell, F. G.; Cornforth, F. J.; Drucker, G. E.; Margolin, Z.; McCallum, R. J.; McCollum, G. J.; Vanier, N. R., Equilibrium Acidities of

Carbon Acids. Vi. Establishment of an Absolute Scale of Acidities in Dimethyl Sulfoxide Solution. *Journal of the American Chemical Society* **1975,** *97* (24), 7006-7014.

11. Bordwell, F. G.; Vanier, N. R.; Matthews, W. S.; Hendrickson, J. B.; Skipper, P. L., Acidities of Carbon Acids. Vii. Conjugation and Strain in Some Cyclopropyl Anions. *Journal of the American Chemical Society* **1975,** *97* (24), 7160-7162.

12. Olmstead, W. N.; Bordwell, F. G., Ion-Pair Association Constants in Dimethyl Sulfoxide. *The Journal of Organic Chemistry* **1980,** *45* (16), 3299-3305.

13. Bordwell, F. G.; Drucker, G. E.; Andersen, N. H.; Denniston, A. D., Acidities of Hydrocarbons and Sulfur-Containing Hydrocarbons in Dimethyl Sulfoxide Solutions. *Journal of the American Chemical Society* **1986,** *108* (23), 7310-7313.

14. Bordwell, F. G.; Harrelson Jr, J. A., Acidities and Homolytic Bond Dissociation Energies of the Ac—H Bonds in Ketones in Dmso. *Canadian Journal of Chemistry* **1990,** *68* (10), 1714-1718.

15. Bordwell, F. G., Equilibrium Acidities in Dimethyl Sulfoxide Solution. *Accounts of Chemical Research* **1988,** *21* (12), 456-463.

16. Bordwell, F. G.; Fried, H. E., Heterocyclic Aromatic Anions with 4n+2 Pi-Electrons. *The Journal of Organic Chemistry* **1991,** *56* (13), 4218-4223.

17. Lygo, B.; Andrews, B. I., Asymmetric Phase-Transfer Catalysis Utilizing Chiral Quaternary Ammonium Salts: Asymmetric Alkylation of Glycine Imines. *Acc Chem Res* **2004,** *37* (8), 518-25.

18. Shirakawa, S.; Maruoka, K., Recent Developments in Asymmetric Phase-Transfer Reactions. *Angewandte Chemie International Edition* **2013,** *52* (16), 4312-4348.

19. Xiang, B.; Belyk, K. M.; Reamer, R. A.; Yasuda, N., Discovery and Application of Doubly Quaternized Cinchona-Alkaloid-Based Phase-Transfer Catalysts. *Angewandte Chemie International Edition* **2014,** *53* (32), 8375-8378.

20. Lee, W.-W. W.; Gan, L.-M.; Loh, T.-P., Synthesis and Photochromic Properties of Cycloalkylidene Fulgides. *Synlett* **2005,** *16* (16), 2473-2477.

21. Wade, P. A.; Kondracki, P. A., Thermolytic Rearrangements of 1,1-Cyclopropanedimethanol Disulfonates: Cyclopropylcarbinyl Cations Revisited. *The Journal of Organic Chemistry* **1993,** *58* (11), 3140-3147.

22. Heiszman, J.; Bitter, I.; Harsányi, K.; Töke, L., A Facile Synthesis of Dialkyl Cyclopropane-1,1-Dicarboxylates and Alkyl 1-Cyanocyclopropanecarboxylates by Phase-Transfer Alkylation. *Synthesis* **1987,** (08), 738-739.

23. Arpin, A. Development of a Practical Method for the Asymmetric Synthesis of Quaternary Carbon Centers: A Second Generation Auxiliary. McGill University, Montreal, Canada, 2005.

24. Hill, R. R.; Rychnovsky, S. D., Generation, Stability, and Utility of Lithium 4,4′-Di-Tert-Butylbiphenylide (Lidbb). *The Journal of Organic Chemistry* **2016,** *81* (22), 10707-10714.

CHAPTER 3

An Asymmetric Total Synthesis of (*R*)-Puraquinonic Acid

3.1 Overview

3.1.1 Project Aim

In chapter two, a spiroalkylation/reductive alkylation method for the formation of quaternary carbon stereocentres on carbocyclic ring systems was developed. Notable advantages of this method include (i) using electronic instead of steric discriminating factors between electrophilic sites to drive selectivity, (ii) implementing biselectrophilic substrates to forge two key bonds in a single synthetic step, and (iii) the use of simple biphasic reaction conditions, eliminating the need for anhydrous and cryogenic conditions for two of the three carbon-carbon bond forming steps. In this chapter it is demonstrated that this novel methodology is applicable in total synthesis of natural products which possess such α-quaternary carbon stereocentres (Figure 3.1). Specifically, the method is applied to the highly challenging quaternary stereocentre found in the noroilludalane natural product puraquinonic acid (**164**).[1] The method allows for the late-stage incorporation of the stereocentre, resulting in a short and efficient synthesis.

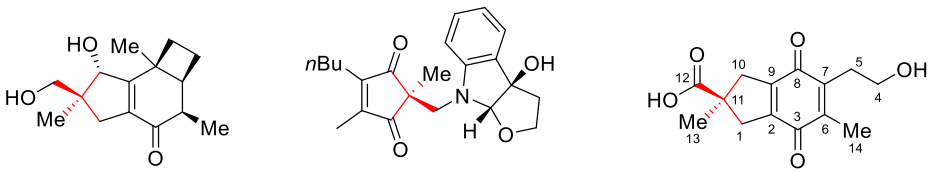

coprinolone ketodiol (**368**) madindoline B (**25**) puraquinonic acid (**164**)

Figure 3.1 Natural products containing α-quaternary carbon stereocentres

3.1.2 Outline of The Synthetic Approach

As discussed in Section 1.3, puraquinonic acid holds a particularly interesting stereochemical challenge within its modest fourteen carbon skeleton. As with many illudalane natural products, carbons twelve and thirteen have been differentiated, through selective oxidation,

to endow puraquinonic acid with a α-quaternary carbon stereocentre. However, what makes this feature special is that the structural elements which define the stereocentre are the C6 methyl and C7 ethyl alcohol, located on the opposite side of puraquinonic acid from the α-carbon. Importantly, this means that they are nearly identical in both steric and electronic terms, greatly increasing the synthetic challenge associated with setting the stereocentre with high levels of control.

An added benefit of selecting puraquinonic acid as a target relates to the stereoselectivity of alkylation of α,α-disubstituted enolates derived from sulfone **277**. Although, high levels of diastereoselectivity could generally be achieved for this alkylation (Section 2.3.3) the absolute stereochemistry of the resulting α-quaternary stereocentre was not directly assigned. Instead, the relative stereochemical configuration was simply inferred by analogy to lactam **104**, for which the selectivity previously has been confirmed. This assumption, though reasonable, due to the near identical pseudo C2 symmetry of the chiral auxiliaries in both cases (Figure 3.2), required experimental confirmation. It was thought that a synthesis of **164** would be ideal for this purpose as stereoisomers of known intermediates from prior work in the Gleason group could be intercepted and compared to assign absolute stereochemistry. This approach to stereochemical determination was necessary due to the novel nature of the products generated, preventing the stereochemical outcome to be confirmed by comparison to independent literature reports. However, upon near completion of the project new work by Baudoin and coworkers[2, 3] allowed for the comparison of one product, amide **435** (section 3.7).

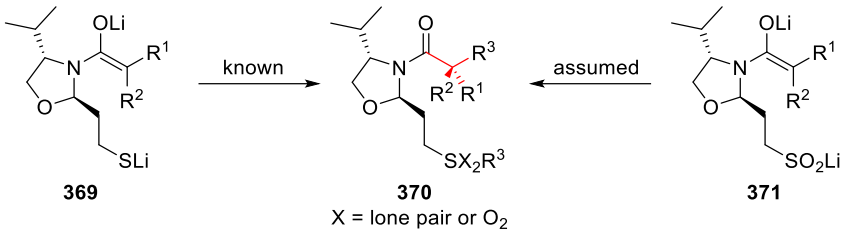

Figure 3.2 Alkylation selectivity for sulfide and sulfone derived α,α-disubstituted enolates

It was anticipated that in revisiting the total synthesis of *R*-puraquinonic acid some of the less desirable aspects of previous synthetic approaches could be addressed to provide an improved route to the molecule. Chiefly among these aspects was the point in which the formation of the quaternary stereocentre takes place. In the three prior enantioselective syntheses, the quaternary stereocentre was introduced either midway or at the outset of the synthetic route (Scheme 3.1). It may be argued that that Clive's strategy does pursue the construction of the stereocentre as the last structural element of the molecule to be introduced.[4] However, any advantage the late-stage introduction presents is obscured by the numerous steps required to remove structural features introduced exclusively for the installation of the quaternary carbon. In choosing to form the quaternary stereocentre earlier, the synthesis of Baudoin[2, 3] and our work[5] required significant elaboration of their respective chiral intermediates (**251** and **240** respectively).

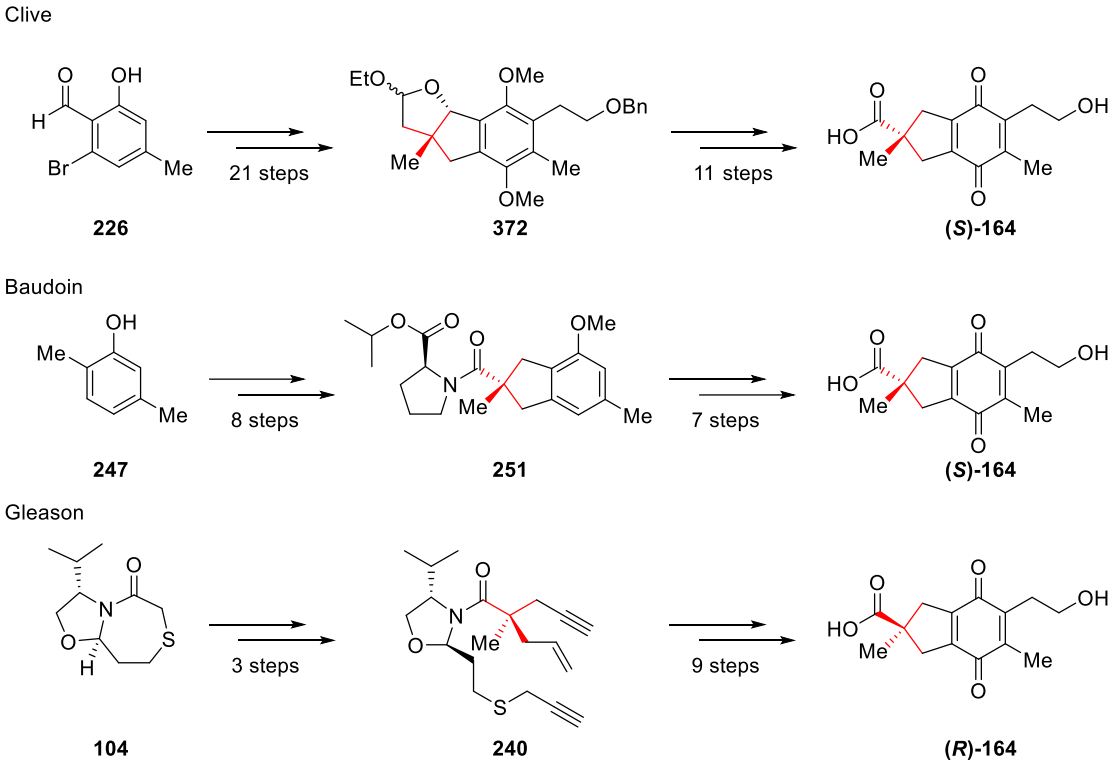

Scheme 3.1 Summary of previous asymmetric approaches to puraquinonic acid and points wherein the quaternary carbon was introduced

It was envisioned that a more efficient synthesis may be possible by addressing the quaternary stereocentre in the final steps of a new synthetic strategy. Inspired by Kraus' use of dibromide **209** to quickly construct of the racemic α-stereocentre of puraquinonic acid through a sequential dialkylation step,[6] it was thought that the use of sulfone **277** could render a similar strategy asymmetric (Scheme 3.2). This notion was further reinforced by the observation that dibromide **209** reacts with high levels of stereoselectivity with sulfone **277**.

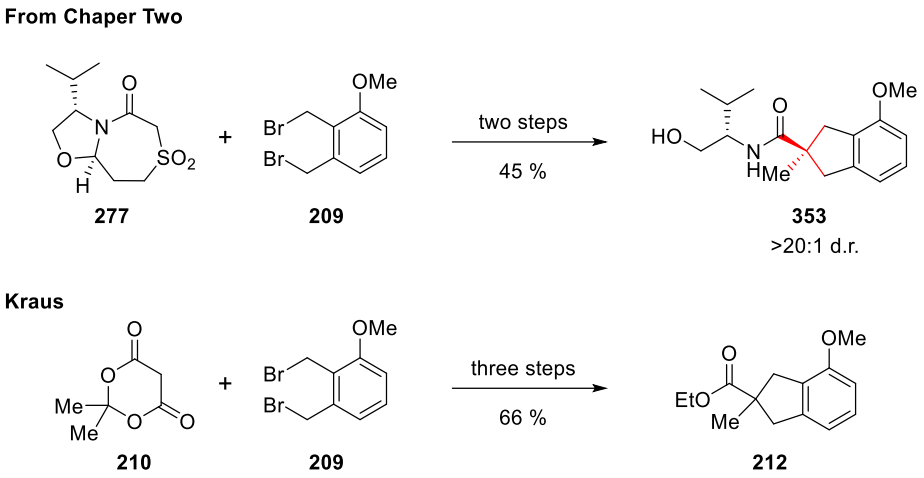

Scheme 3.2 Comparison to Kraus' racemic preparation of the key α-quaternary stereocentre in puraquinonic acid

3.2 Retrosynthetic Analyses

Following from the methodology developed in chapter two, a retrosynthetic strategy for accessing puraquinonic acid involving the late-stage introduction of the quaternary stereocentre was devised (Scheme 3.3). It was envisioned that employing sulfone **277** to construct the key stereocentre using a *bis*-electrophile with the reactivity of the two electrophilic sites appropriately differentiated. This differentiation could be introduced electronically *via* suitable substitution of the aryl ring, in a similar manner to that which was achieved in the case of dibromide **209**. This leads back to an aryl ether and therefore necessitates oxidation of the arene to the paraquinone post introduction of the stereocentre. Importantly, by combining the aryl ether with protection of the ethyl alcohol allows the alcohol to be revealed in the oxidation process. Construction of dibromide **375** might be achieved *via* a Diels-Alder reaction of dimethyl acetylene-dicarboxylate (DAMD, **377**) and diene **378**. It was initially envisioned that diene **378** could be constructed through a palladium mediated cross coupling of a vinyl nucleophile (accessible from olefin **354**) and the accompanying halogenated dihydrofuran (**380**). As such, initial investigations centred on affecting a Kumada type cross-coupling between dihydrofuran **381** and vinyl Grignard **382**.

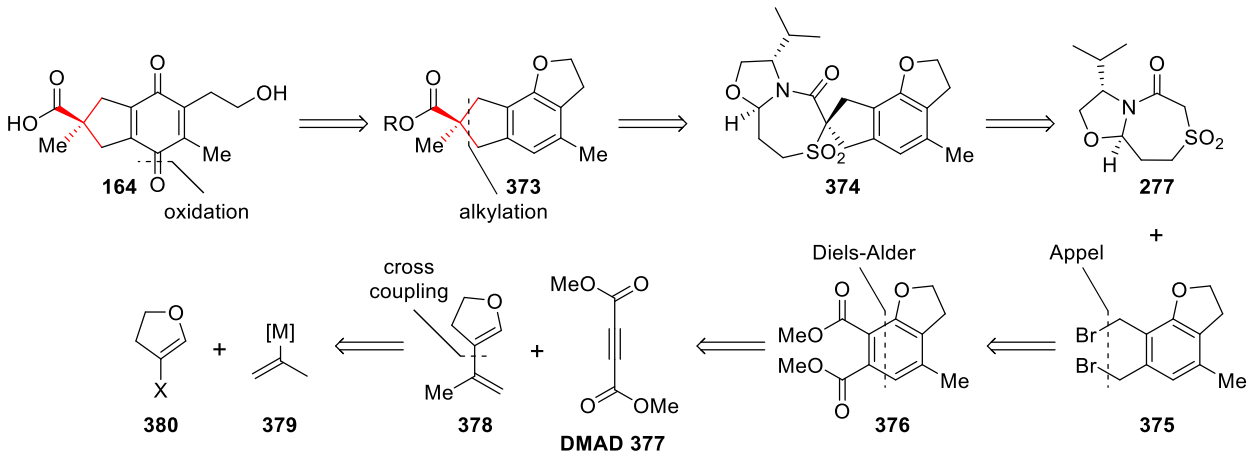

Scheme 3.3 Retrosynthetic analysis of puraquinonic acid (**164**)

3.3 Synthesis of Dibromide 378

3.3.1 Preparation of Diene **378** *via* Cross-Coupling

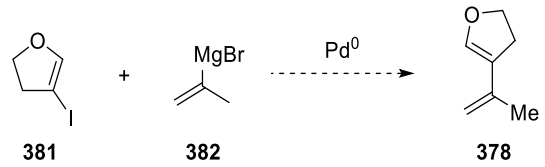

381 **382** **378**

Scheme 3.4 Proposed Kumada cross-coupling for the synthesis of diene **378**

To avoid the need to manipulate a volatile vinyl halide reagent, the commercially available vinyl Grignard reagent **382** was selected as the nucleophilic coupling partner in the initial cross coupling. This necessitated the preparation of a 4-halo-2,3-dihydrofuran fragment. Reports of such mono-functionalised dihydrofurans are uncommon. However, one report for the preparation of 4-iodo-2,3-dihydrofuran (**381**) proposed activation of molecular iodine with iron(III) chloride to promote a five-endo-trig cyclisation of homopropargyl alcohol (**383**).[7] Disappointingly, in our hands this procedure failed to give any of the reported dihydrofuran **381**. However, given the known reactivity of alkynes towards activated electrophilic iodine species and the authors' proposed mechanism (involving activation of the alkyne *via* formation of an iodonium) it was believed that other electrophilic iodine sources might provide the desired product.

Su (2011)

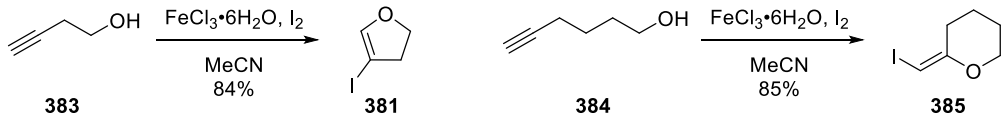

383 **381** **384** **385**

Scheme 3.5 Su's preparation of iodinated hydrofurans and hydropyrans

Homopropargyl alcohol (**383**) was subjected to conditions with the aim of affecting the desired cyclisation. Conditions tested included: use of anhydrous iron(III) chloride and the use of NIS as an alternate electrophilic iodine source. From inspection of the ^{1}H NMR spectrum of the crude reaction mixture it was ultimately found that all attempts failed to provide the desired product, even in trace amounts, with only the *bis*-iodinated homoallylic alcohol **386** observed by ^{1}H and ^{13}C NMR. With this initial failure attention was turned to investigating the possibility of preparing a nucleophilic dihydrofuran coupling partner.

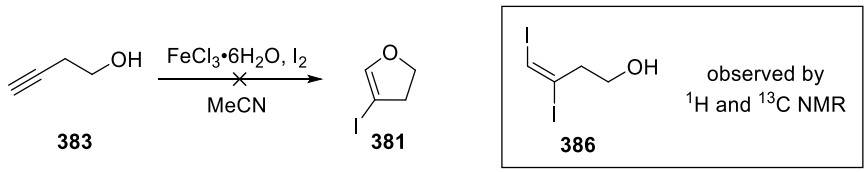

Scheme 3.6 Attempts to reproduce results disclosed by Su

As with the case of the desired case of 4-haloginated dihydrofurans, suitably substituted nucleophilic dihydrofurans were also discovered to be uncommon. One report, was the use of dihydrofuran (**389**) as a model system for the stannation of nucleosides (Scheme 3.7).[8] Tanaka reported that dihydrofuran (**389**) could be selectively functionalised by leveraging the nucleophilicity of the enol ether in concert with highly electrophilic benzenesulfenyl chloride (**390**). This provided phenyl-vinyl thioether **391** which could be transformed to the tributylstannane derivative through treatment with AIBN and tributyltin hydride (Scheme 3.7).

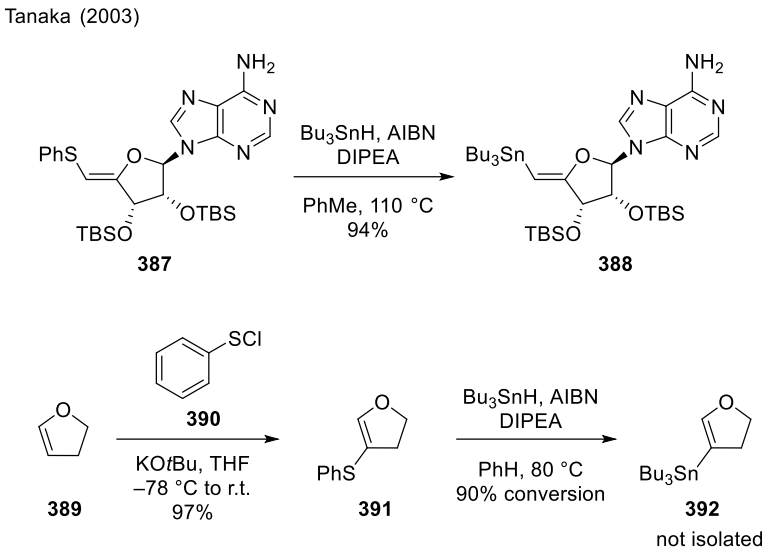

Scheme 3.7 Tanaka's preparation of vinyl stannanes from thioethers

Benzenesulfenyl chloride (**390**) required preparation using a procedure established by Taylor[9] and provided high yields of thioether **391** when reacted with dihydrofuran in THF (Scheme 3.8). Under the reported conditions (AIBN and tributylstannane) the expected dihydrofuryl tributylstannane could be obtained, albeit in low yield. Unfortunately, it was found that the four-fold excess of tributylstannane, described by Tanaka, was necessary to provide complete consumption of the thioether. The excess stannane was impossible to remove *via* chromatography on Florisil, basic/neutral alumina, or silica. With this second approach also unable to provide useful quantities of the required coupling partner an alternative to the cross-coupling approach was devised.

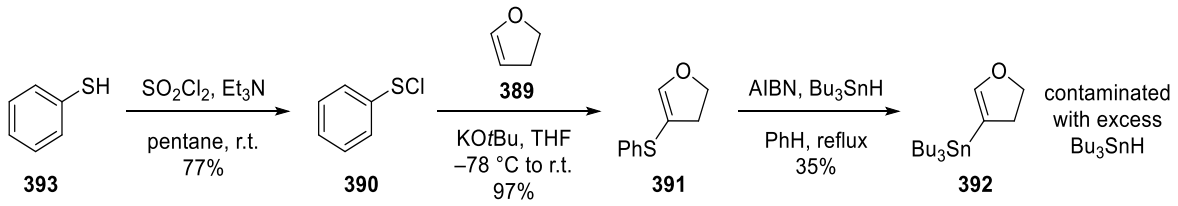

Scheme 3.8 Preparation of tributyl dihydrofuryl stannane

3.3.2 Acylation of 2,3-dihydrofuran

Inspired by the relative ease with which benzenesulfenyl chloride could functionalise dihydrofuran, it was thought that a suitably activated carbon-centred electrophile might exploit the nucleophilicity of the enol ether to provide a route to diene **378**. Indeed, a report by Hojo described the facile acylation of dihydrofuran with trichloroactyl chloride (**369**).[10]

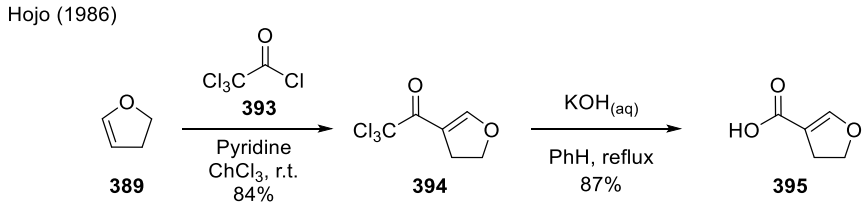

Scheme 3.9 Hojo's trichloroacylation of 2,3-dihydrofuran

Considering this, attempts were made to extend this reactivity to unsubstituted acetyl electrophiles; this would allow for diene **378** to be accessed *via* a subsequent Wittig olefination. Initial investigations were carried out to determine if commercially available acetyl chloride or acetyl bromide were indeed suitably electrophilic. Efforts were made to promote the reaction between acyl chloride and dihydrofuran with the addition of Lewis acids: aluminium(III) chloride or boron trifluoride, magnesium chloride/bromide, iron(III) chloride, zinc iodide, scandium triflate, and ytterbium triflate. However, all reactions failed to produce the desired vinylogous ether **397**. As these results illustrate the poor electrophilicity of **396a**, and **396b** when compared to trichloroacetyl chloride (**393**), an attempt was made to overcome this disadvantage by turning to acetyl iodide as the acetylating agent. The use of acetyl iodide was investigated using a known protocol by Hoffmann, subjecting acetyl chloride to Finkelstein reaction conditions with sodium iodide prior to the addition of dihydrofuran.[11] Despite the increased electrophilicity of acetyl iodide it also proved inert toward acylation.

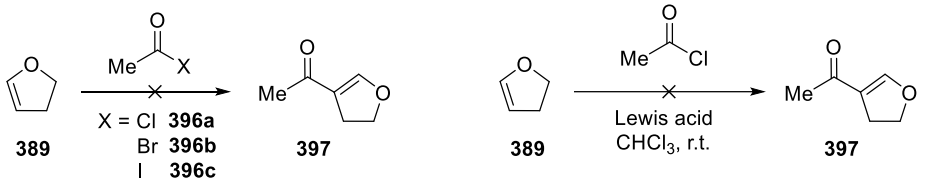

Scheme 3.10 Attempts at direct acylation of 2,3-dihydrofuran

With the inability to directly acetylate dihydrofuran (**389**), it was decided that reduction of the trichloromethyl group to produce the desired ketone (**397**) would be performed. Gratifyingly, this was easily achieved using zinc in acetic acid and could also be achieved with milder conditions employing ammonium chloride as the proton source (Scheme 3.11). This two-step trichloroacylation-dehalogenation sequence thus provided quick entry to vinylogous ester **397** as a white solid in 98% overall yield.

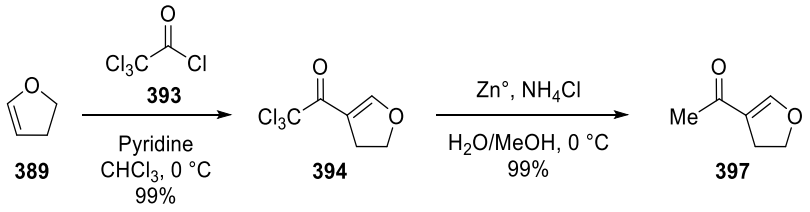

Scheme 3.11 Preparation of vinylogous ether **397**

With sufficient quantities of vinylogous ester **397** in hand, conditions to affect the olefination of the carbonyl commenced. Typical Wittig conditions provided poor conversion to desired olefin, likely to do with the reduced electrophilicity of vinylogous esters relative to ketones. This led to the consideration of more nucleophilic olefination reagents, principally titanium carbenes. Vinylogous ester **397** was exposed to both Tebbe's and Petasis' reagents with Petasis' reagent providing cleaner conversion to the olefin, as determined by ^{1}H NMR. However, isolation of pure diene proved impossible, with samples subjected to purification by thorough

aqueous work up and/or chromatography on silica (or alumina) providing either no product or large amounts of titanocene oxide contamination. These issues were attributed to both the volatility and inherent instability of diene **378**. Thus, is was necessary to quickly trap the diene as the Diels-Alder adduct after the olefination was complete. This provided the desired product in low yield which could be increased to a maximum of 29% (over two steps) by thorough removal of the titanocene by-products followed by reaction with freshly distilled DMAD in a toluene-acetonitrile mixture. The removal of the titanocene by-products was achieved through precipitation with pentane, subsequent filtration through celite, and removal of pentane, resulting in a solution of diene **378** in toluene that was employed without further purification. The addition of acetonitrile provided a noticeable increase in yield due to an increase in reaction rate overcoming some of the background decomposition of diene **378**. Further yield optimisation proved impossible due to diene losses during the required manipulations. These loses were attributed to the volatility and instability of diene **378**. Trapping of diene **378** was also able to provide diester **398** when Tebbe's reagent was employed but only in 12% yield.

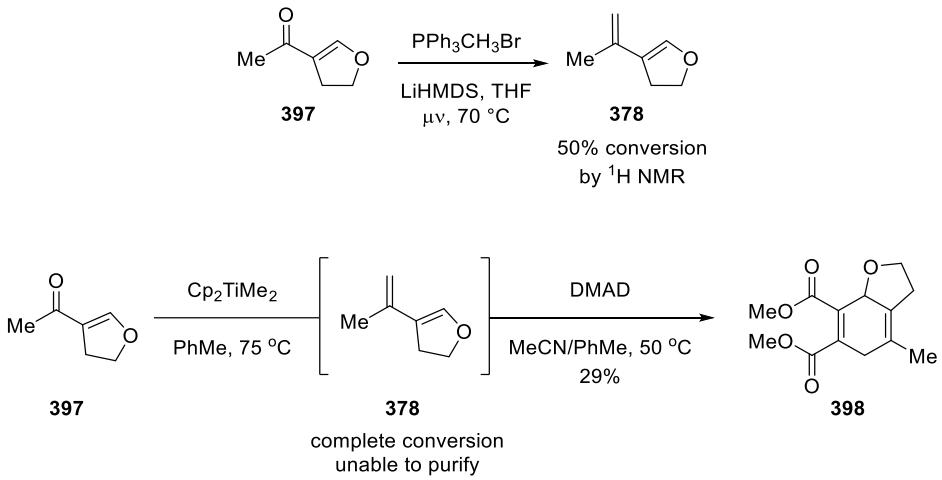

Scheme 3.12 Trapping of diene **378** with DMAD

3.3.3 Diene Synthesis by Enyne Metathesis

While the sequence developed at this point did provide access to the required diester intermediate (**398**) it suffered from many inadequacies, primarily poor yield and low atom economy. While acylation with trichloroactyl chloride and the subsequent reduction are high yielding the need to remove three chlorine atoms is inefficient. The poor conversion of the vinylogous ester **397** to the Diels-Adler adduct exacerbates the issues with this synthetic approach. Unsatisfied with the developed sequence, an alternative, highly atom economic approach based on eneyne metathesis was examined.

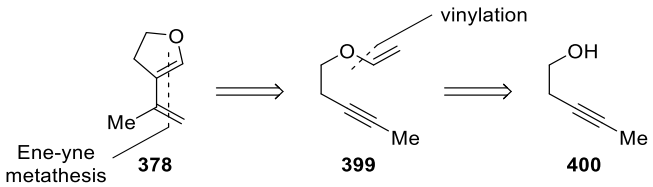

Scheme 3.13 Retrosynthesis for the formation of diene **378** via an eneyne metathesis

Enyne metathesis is a well-established method of rapidly generating 1,3-dienes and has found significant use in the preparation of substrates for Diels-Alder reaction.[12, 13] Using this transformation, diene **378** leads retrosynthetically back to homopropargyl-vinyl ether **399** (Scheme 3.13). The suitability of a vinyl ether containing substrate was initially questionable. Vinyl ethers are frequently introduced to arrest the activity of Grubbs' type ruthenium catalysts,[14, 15] with Schrock's catalyst often necessary to carry out ring-closing metathesis reactions of vinyl ethers.[16] Examples of ring-closing metathesis reactions of vinyl ethers with Grubbs' ruthenium catalysts are known, yet tend to lack the generality frequently associated with analogous metathesis reactions.[17, 18] Despite the apparent limitations, intermolecular eneyne metathesis reactions of ethyl vinyl ether have been described by Diver wherein Grubbs' second generation catalyst was able to

furnish the desired product in high yield provided an excess of the vinyl ether is used (Scheme 3.14).[19] Interestingly, examples of intramolecular eneyne metathesis, of the type outlined in Scheme 3.13, are not known. However, vaguely similar products have been obtained through intramolecular de Mayo reactions with alkynes (Scheme 3.15).[20] Similar photochemical methods may prove useful to access diene **378** in the event the eneyne metathesis strategy were to fail.

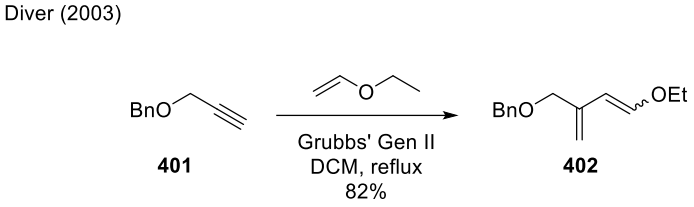

Scheme 3.14 Diver's intermolecular eneyne metathesis

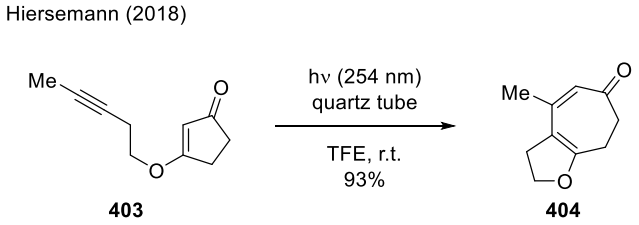

Scheme 3.15 Hiersemann's alkyne de Mayo reaction

Studies towards effecting the desired eneyne metathesis commenced with the vinylation of the commercially available homopropargyl alcohol **403**, using mercury(II) acetate in ethyl-vinyl ether. While high loading of mercury(II) acetate (15 mol%) was initially used, to ensure the reaction quickly reached equilibrium, loadings as low as 5 mol% were eventually used in concert with long reaction times to reduce the amount of mercury(II) acetate required. This provided access to multi gram quantities of vinyl-ether **399** after purification by distillation.

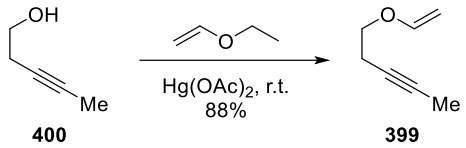

Scheme 3.16 Synthesis of vinyl-ether **399**

With easy access to eneyne **399** achieved, focus could be placed on identifying conditions to effect the eneyne metathesis. Grubbs' first-generation catalyst failed to provide any conversion to diene **378**. Fortunately, Grubbs' second-generation catalyst succeeded in providing 16% yield (observed by ^{1}H NMR) with loadings of 1 mol% in DCM. Increasing the reaction temperature to reflux did not contribute to greater conversion. Importantly, tracking the reaction by ^{1}H NMR over extended periods of time showed product yield to reach a maximum prior to complete conversion of eneyne **399**. Additionally, steady degradation of diene **378** was also observed. This was is in line with previous observations of diene **378**'s instability in the context of the olefination of ketone **397** (*vide supra*). These results suggested cessation of catalytic activity was preventing further product generation while background degradation of diene **378** was leading to product loss. Indeed, if the reaction stirred for longer than forty-eight hours, none of the desired diene (**353**) could be identified by ^{1}H NMR spectroscopy.

As the incomplete consumption of eneyne **399** was attributed to catalyst degradation and/or inhibition, increasing catalyst loadings was identified as a possible remedy to the low yields. Raising loadings to 4 mol% provided complete consumption of eneyne **399**. As with previous preparations of diene **378** it was necessary to directly trap the diene as the Diels-Alder adduct. Addition of DMAD to the reaction mixture provided diester **398** in 66% isolated yield. The success of this two-step eneyne-Diels-Alder sequence suggested the possibility of performing the two reactions as a cascade. Disappointingly, the presence of DMAD completely inhibited the reactivity

of the catalyst, necessitating the reaction be run in a stepwise fashion. This sequence could be further extended to incorporate oxidation of **398** with DDQ to afford dihydrobenzofuran **376** in 42% yield over the three transformations. However, a much higher yield of 93% was obtained when the oxidation was conducted as a discrete step.

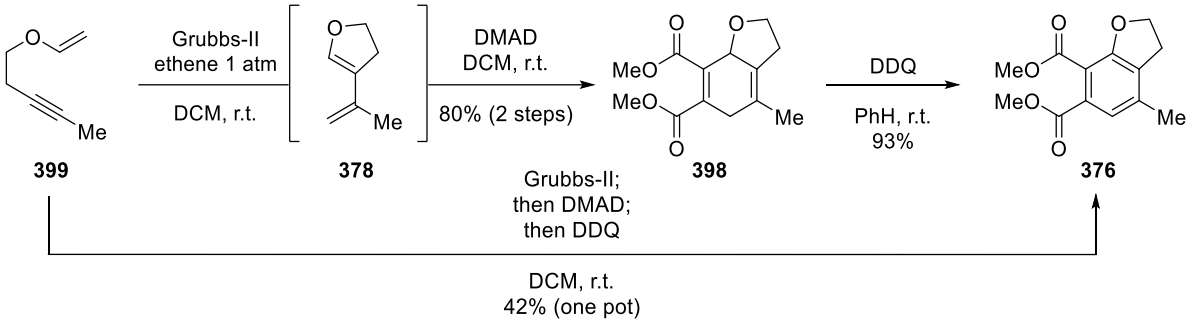

Scheme 3.17 Stepwise and one-pot reparation of diester **376**

Unsatisfied with the high catalyst loadings and far from optimal yields further effort was made to optimise the eneyne metathesis step. Catalyst loadings could be reduced to 2 mol% by replacing the argon atmosphere with ethylene to provide an 80% yield of diester **398**. The use of ethylene was introduced by Mori to allow for the eneyne metathesis of terminal alkynes.[21] In this case, the 1,3-diene product **411** contains a reactive mono-substituted olefin which rapidly engages with catalytic ruthenium carbene **406** and undergoes olefin metathesis to expel ethylene and form carbene **411** which is non catalytically active and limits the efficacy of the ruthenium catalyst (Scheme 3.18).[21, 22] Although carbene **411** could theoretically engage with the olefin of the starting eneyne to regenerate the 1,3-diene and carbene **406**, the coordination of the endocyclic olefin in carbene **411** limits its reactivity. This may be particularly problematic in the case of eneyne **399** due to the more Lewis-basic vinyl ether (**414**). The introduction of ethylene allows for excess olefinic substrate to accelerate the reformation of carbene **406** from carbene **411**, thus maintaining higher concentrations of the active catalyst. Attempts to reduce catalyst loadings further to 0.5 or

1 mol% resulted in incomplete starting material consumption with a minimum catalyst loading of 2 mol% being identified as the minimum possible catalyst loading.

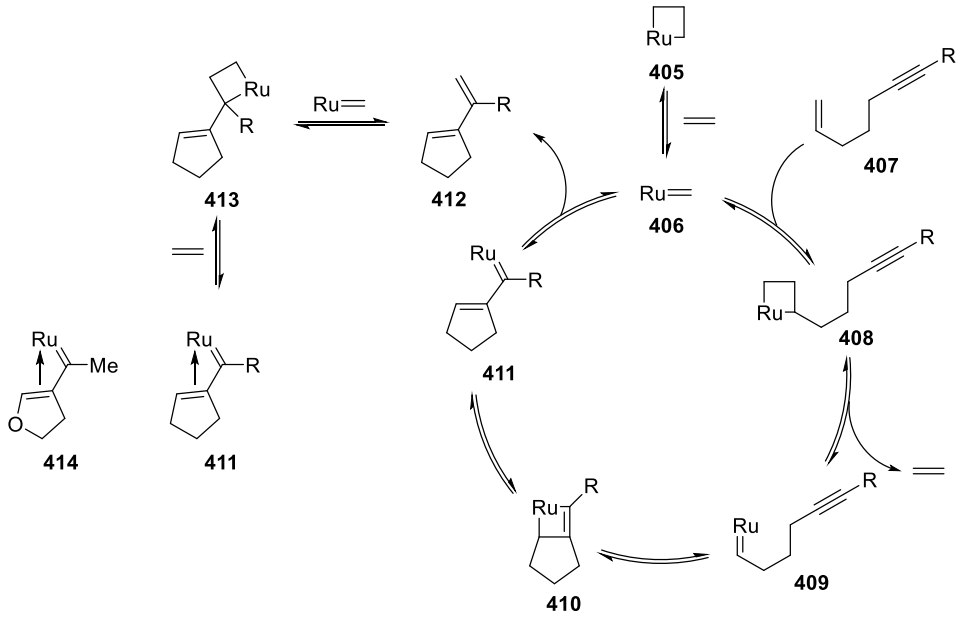

Scheme 3.18 Enyne metathesis mechanism and off-cycle catalyst sequestration

3.3.4 Preparation of Dibromide **375**

With a route established for the preparation of diester **376** synthesis of dibromide **375** was quickly achieved. Global reduction of diester **376** with lithium aluminium hydride provided clean conversion to diol **415** in 95% yield. Treating diol **415** with phosphorus tribromide efficiently transformed it to the key dibromide in quantitative yield. With dibromide **375** successfully synthesised, the crucial introduction of the α-quaternary carbon stereocentre could now take place.

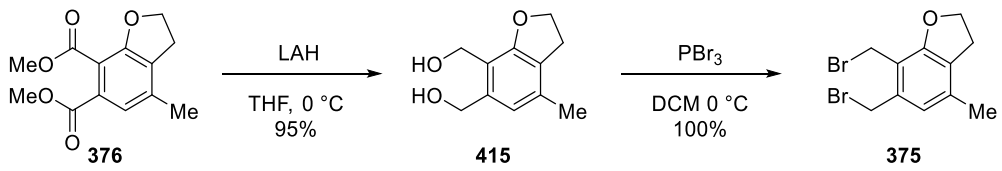

Scheme 3.19 Preparation of dibromide **375**

3.4 Formation of the α-Quaternary Carbon Stereocentre

Spiroalkylation of sulfone **277** with dibromide **375** using the biphasic conditions described in chapter two, employing tetrabutylammonium iodide, provided the desired spirocycle **374** in 70% yield. As with the alkylation with dibromide **209**, the reaction affords the spirocycle as a single diastereomer with the relative stereochemistry governed by the ability of the aryl ether to activate the methylene at the *ortho* position toward S_N2 displacement. Akin to the stereochemical determination of spirocycle **287** (section 2.2.3) HSQC, HMBS, and NOESY NMR spectra were acquired and examined to determine the configuration of the α-carbon of spirocycle **374**.

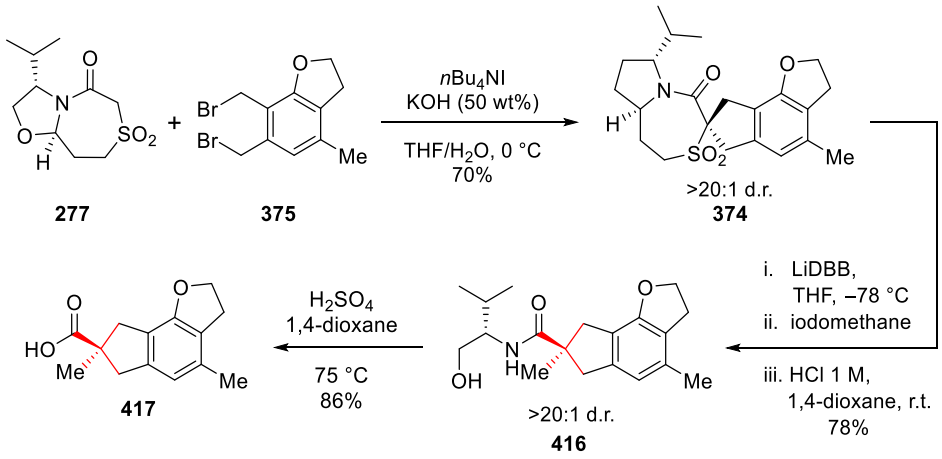

Scheme 3.20 Construction of the key quaternary stereocentre

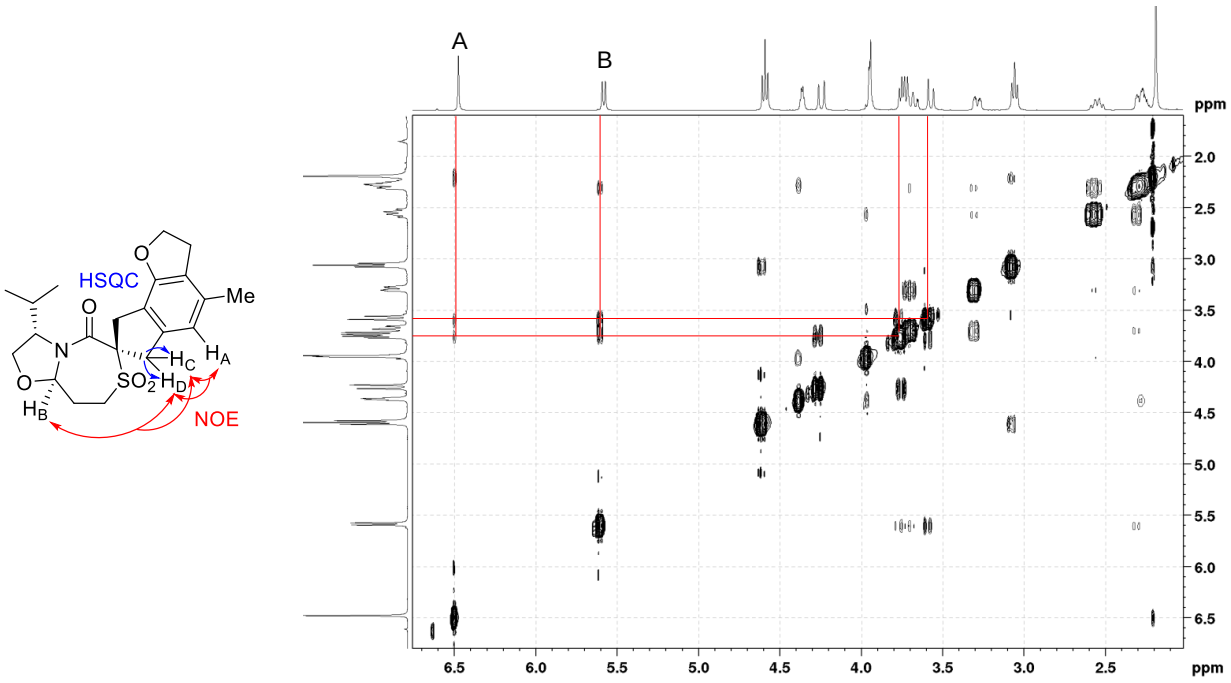

Figure 3.3 Determination of relative stereochemistry by NOESY spectrum analysis for **374**

Reductive enolization of spirolactam **374** with LiDBB, followed by methylation of the α,α-disubstituted enolate likewise proceeded without difficulty providing amide **416**, bearing the anticipated quaternary stereocentre, in 78% yield and in greater than 20:1 diastereoselectivity. From this point the remaining valinol portion of the auxiliary could be removed *via* hydrolysis with sulfuric acid in refluxing dioxane to give the corresponding carboxylic acid (**417**) in 86% yield. As this sequence entails hydrolysis with hydrochloric acid followed by sulfuric acid, an attempt was made to subject the initial alkylation product directly to the more vigorous sulfuric acid hydrolysis condition. This would remove a step from the final count. However, this proved unsuccessful and returned none of the desired carboxylic acid, or other useful products, after purification.

3.5 Oxidation to the Paraquinone: Total Synthesis of Puraquinonic Acid

With carboxylic acid **417** in hand, the final task was the seemingly simple oxidation of the arene core to the *para*-quinone. Although not a classical precursor for paraquinone synthesis, due to the lack of an unsubstituted heteroatom (*i.e.* phenol or aniline) or suitably disposed 1,4-subsituents (*e.g.* methoxy), the first oxidants tried were those described for the oxidation of arenes to quinones; such as Fremy's salt, PIDA and CAN. None of these provided any discernible oxidation products (Scheme 3.21).

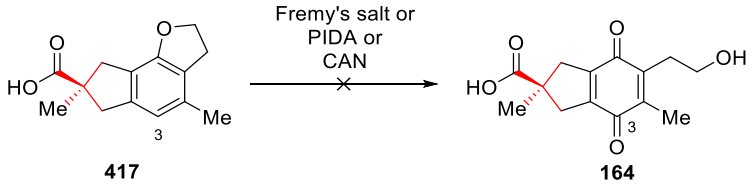

Scheme 3.21 Initial attempts to oxidise the arene core to the *para*-quinone

Disappointed by the lack of any oxidation products the challenge at hand was examined from a more fundamental perspective. The task presented was twofold: 1) an oxidation of the arene to the paraquinone and 2) by extension, introduce an oxygen atom at C3. It was thought that a process proceeding through such an oxidation would allow for opening of the dihydrofuran ring through formation and subsequent hydrolysis of an oxonium intermediate. Considering direct oxidation to the paraquinone failed, efforts were directed at the functionalisation of C3 to provide a handle for subsequent oxidation.

Due to the electron rich nature of the arene, the most attractive strategy was to functionalise the arene by engaging an appropriate electrophile. Happily, it was discovered that C3 could be very easily brominated simply using bromine in chloroform to provide aryl bromide **418**. As aryl bromide **418** is, formally a two-electron oxidation product of carboxylic acid **417**, it was thought

that a further two-electron oxidation may be achieved using CAN. Unfortunately, oxidation to the paraquinone was not observed. Instead, treatment with CAN led to formation of benzofuran **419**, with distinctive C4 and C5 proton signals indicating the fate of the reaction.

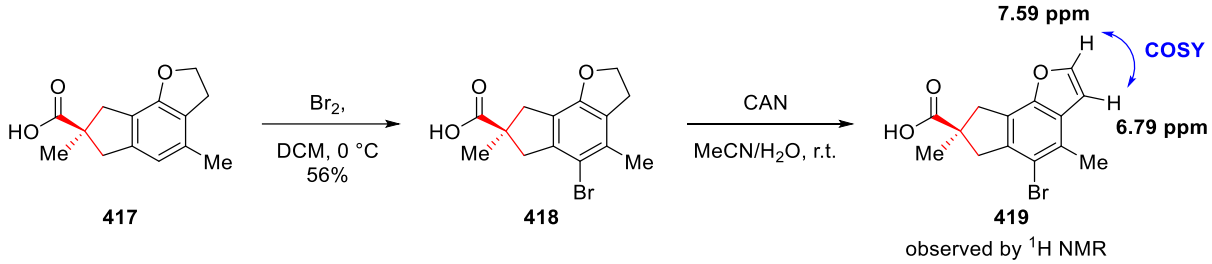

Scheme 3.22 Bromination of arene **417**

Using the aryl bromide as a synthetic handle, it may have been possible to perform a Buchwald–Hartwig coupling to install a second aryl ether and ultimately facilitate the oxidation to the paraquinone (Scheme 3.23). This was determined to be an unacceptably long sequence and the idea was abandoned in favour of direct oxidative functionalisation.

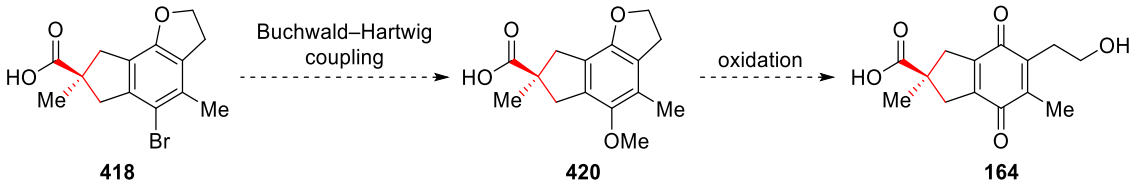

Scheme 3.23 Possible synthetic route to puraquinonic acid *via* aryl bromide **418**

Undeterred and convinced that leverage of the nucleophilic properties of the arene held the key to completing the synthesis, a series of electrophilic oxidants were screened on both carboxylic acid **417** and diol **415**. Several including DMDO, Oxone®, and mCPBA returned only starting material but peracetic acid in chloroform proved able to not only install the required oxygen but also oxidised the arene to the paraquinone in 58% yield, completing the total synthesis of

puraquinonic acid. A possible mechanism for this transformation is provided in Scheme 3.24. The reaction initiates with an electrophilic aromatic substitution with peracetic acid. Loss of a proton generates an equivalent of acetic acid while also aromatizing to phenol **422**. This process repeats a second time. However, lacking the ability to quench the oxonium (**423**) *via* aromatization and proton loss, the oxonium is hydrolysed to break the dihydrofuran ring. Finally, dehydration furnishes the *para*-quinone (**164**).

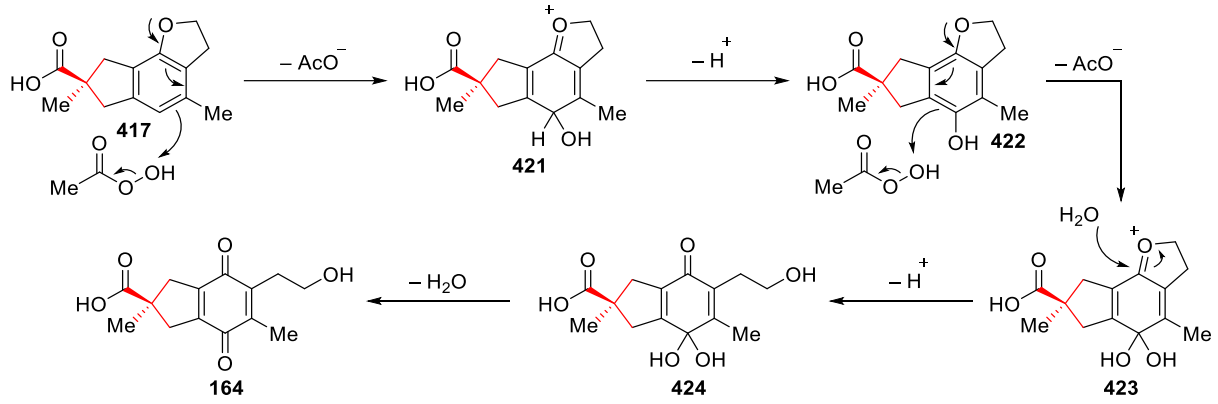

Scheme 3.24 Proposed mechanism for the oxidation of carboxylic acid **417**

The mediocre yield required that time be taken to optimise the reaction conditions. The selection of peracid was investigated with both trifluoroperacetic acid and magnesium monoperoxyphthalate screened. The use of trifluoroperacetic acid resulted in complete decomposition while treatment of carboxylic acid **417** with magnesium monoperoxyphthalate in acetonitrile and water provided slow and affected incomplete conversion to puraquinonic acid. Acetonitrile, water, dioxane, and DCM were all examined as possible replacements for chloroform. The reaction failed to proceed in dioxane or water (in the case of water due to the insolubility of carboxylic acid **417** in aqueous media) while the use of acetonitrile resulted in increased degradation, as observed by ^{1}H NMR. Addition of water to reagent chloroform, to ensure

the solvent was saturated with water, provided no positive change. Pleasingly, a two-to-one solution of DCM to 39% peracetic acid in acetic acid (approximately seventy equivalents of peracetic acid) gave an increased yield of 73% and with the reaction achieving full conversion in ninety minutes. This was considerably more rapid when compared to the two days required to achieve full conversion if carboxylic acid **417** is treated with five equivalents of peracetic acid in chloroform.

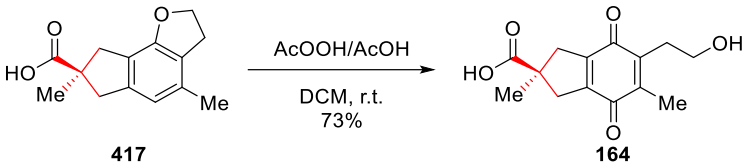

417 **164**

Scheme 3.25 Oxidation of carboxylic acid **393** to puraquinonic acid

With the optimisation of the final step complete, the total synthesis of puraquinonic acid comprised eight steps and with an overall yield of 14% (see Table 3.1 for comparison of characterisation data to known literature values). The physical appearance of the synthesised puraquinonic acid matched the physical description of a yellow oil previously reported. Additionally, the ^{1}H and ^{13}C NMR spectra agreed with the literature data. Importantly the direction of the optical rotation was consistent with literature values indicating that the *R*-enantiomer had been prepared by the route herein described.

Table 3.1 Comparison of (*R*)-puraquinonic acid characterisation data

Method	Experimental Value	Literature Value[1]
^{1}H NMR 500 MHz, $CDCl_3$ (ppm)	3.77, 2H, t, *J* = 6.4 Hz 3.39, 2H, m 2.80, 2H, t, *J* = 6.4 Hz 2.76, 2H, m 2.08, 3H, s 1.43, 3H, s	3.75, 2H, t, *J* = 6.5 Hz 3.37, 2H, m 2.78, 2H, t, *J* = 6.5 Hz 2.74, 2H, m 2.07, 3H, s 1.41, 3H, s
^{13}C NMR 500 MHz, $CDCl_3$ (ppm)	186.2 185.7 180.0 145.7 145.3 142.8 141.4 61.5 46.7 43.4 42.3 29.9 25.7 12.2	186.2 185.7 181.5 145.7 145.4 142.8 141.4 61.4 46.9 42.3 42.3 29.9 25.7 12.1
IR (cm^{-1})	3393, 2968, 1702, 1647, 1462, 1430, 1376, 1333, 1276, 1210, 1022, 736	3450, 2965, 1705, 1650, 1460, 1425, 1375, 1330, 1285, 1210, 1045, 720
HRMS (*m/z*) **$[C_{14}H_{16}O_5Na]^+$ = 287.0890** **$[C_{14}H_{16}O_5]^+$ = 264.0998**	287.0899 $[C_{14}H_{16}O_5Na]^+$	264.0999 $[C_{14}H_{16}O_5]^+$
Optical Rotation (Na lamp 589 nm)	+3.5 $[\alpha]_D^{22}$ (*c* 0.5, $CHCl_3$)	+1 $[\alpha]_D^{22}$ (*c* 1.0, $CHCl_3$)
Physical Appearance	yellowish oil	yellowish oil

3.6 Determination of Absolute Stereochemistry

With the total synthesis of puraquinonic acid complete, the central question of absolute stereochemistry was addressed next. Due to the near symmetric nature of the α-quaternary carbon stereocentre the magnitude of the optical rotation is particularly small. In fact, the optical rotation of opposite enantiomers has been reported with the same direction of rotation; Clive's report of (*S*)-puraquinonic acid $[\alpha]_D^{22}$ +3.1 (*c* 0.7, CH_2Cl_3) [*sic*],[4] Gleason and Tiong's report of (*R*)-puraquinonic acid $[\alpha]_D^{22}$ +1.5 (*c* 0.3, $CHCl_3$),[5] Clive's report of (*S*)-puraquinonic acid $[\alpha]_D^{22}$ +3.1 (*c* 0.7, CH_2Cl_3) [*sic*],[4] and Baudoin's report of (*S*)-puraquinonic acid $[\alpha]_D^{23}$ +1.4 (*c* 0.5, $CHCl_3$).[3] This inconsistency necessitated an alternative method for unambiguous method for stereochemical determination.

To provide definitive evidence for the absolute stereochemical outcome of their synthesis, Gleason and Tiong directly compared the stereochemistry of products formed from the alkylation of lactam **104** to the derivative of Mannich product **427**, for which the stereochemistry had been unambiguously determined by X-ray crystallography (Scheme 3.26).[5] By employing this generic method to prove the alkylation selectivity, Gleason and Tiong were able to assert that the alkylation of lactam **104** had indeed resulted in the formation of the (*S*)-α stereocentre and, by analogy, the total synthesis of (*R*)-puraquinonic acid. The cyclic alkylation products in our new route lack any easily accessible structures for comparison to prove the stereochemical outcome of the alkylation process. Instead, we intercepted an intermediate in the prior synthesis of (*R*)-puraquinonic acid by preparing two diastereomeric paraquinones, (*R*,*S*)-**433** and (*R*,*R*)-**433**.

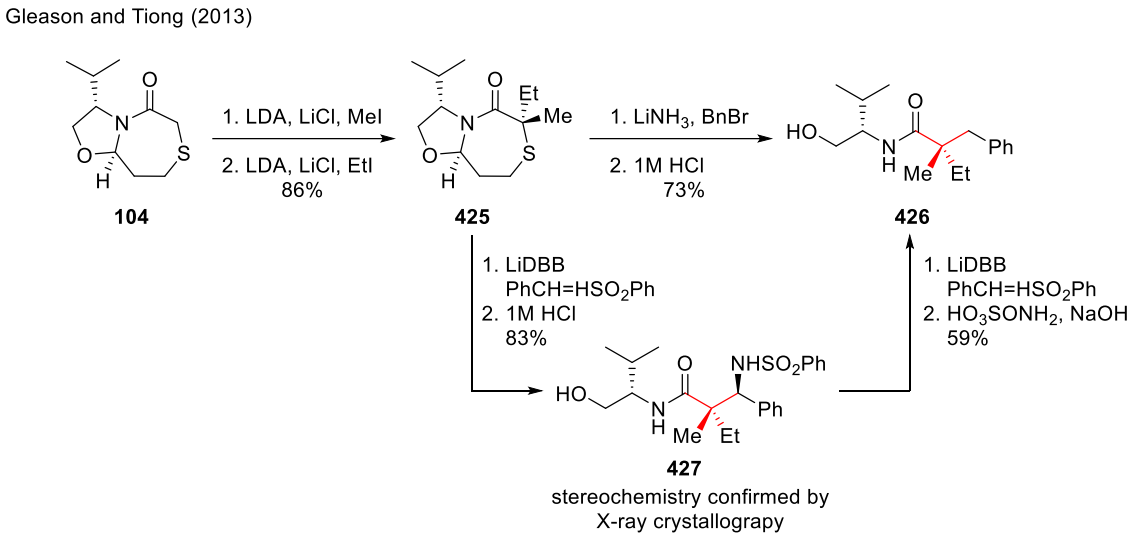

Scheme 3.26 Stereochemical determination of alkylation products of lactam **104**

To prepare (*R*,*S*)-**433** and (*R*,*R*)-**433** (Scheme 3.27), the hydroxyl group in amide **416** was first protected with methoxymethyl chloride, producing (*R*,*S*)-**432** in essentially quantitative yield. Oxidation of (*R*,*S*)-**432** to the corresponding paraquinone was achieved though treatment with peracetic acid. The preparation (*R*,*R*)-**433** required slightly more synthetic work. (*R*)-Valinol was obtained from the reduction of unnatural valine with sodium borohydride and iodine in 70% yield after purification by distillation. (*R*)-Valinol could then be orthogonally protected in a two-step one-pot procedure involving initial amine protection with benzyl chloroformate followed by treatment with methoxymethyl chloride to yield carbamate **430** in 94% yield. Removal of the benzyl carbamate *via* hydrogenolysis with palladium on carbon furnished the requisite primary amine **431** in a low but adequate 46% yield. Next, EDC mediated peptide coupling with carboxylic acid **393** afforded a 98% yield of (*R*,*R*)-**432**. As in the case of (*R*,*S*)-**433**, (*R*,*R*)-**433** was oxidised to the analogues paraquinone with the use of peracetic acid.

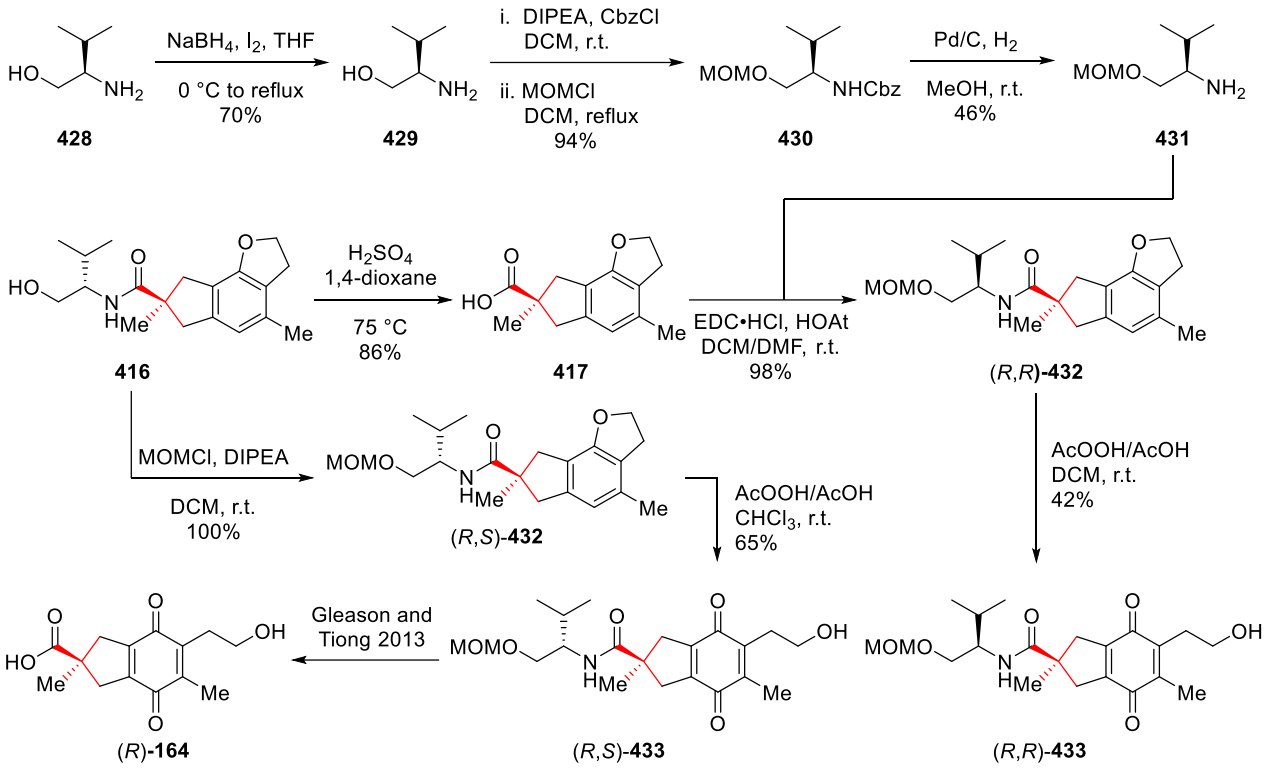

Scheme 3.27 Synthesis of *para*-quinones (*R*,*S*)-**433** and (*R*,*R*)-**433**

With the two diastereomers of *para*-quinone **433** in hand their ^{1}H and ^{13}C NMR spectra were compared to the spectra of authentic (*R*,*S*)-**433** from the Gleason/Tiong synthesis; the results are displayed in Figures 3.4 and 3.5. As predicted, from analogy to the alkylation of lactam **104**, the reduction and alkylation of sulfone **250** does indeed lead to the synthesis of (*R*,*S*)-**433** and the generation of the (*R*)-α-stereocentre in puraquinonic acid. This was confirmed by both ^{1}H and ^{13}C NMR spectroscopy (Figures 3.4 and 3.5). While the ^{1}H NMR spectra for both diastereomers share many similarities the signals at 2.72 and 2.69 ppm are the most dissimilar with second order coupling effects leading to a large tenting effect in the spectra of (*R*,*S*)-**433** which is mostly absent in the spectra of (*R*,*R*)-**433**. As the original ^{1}H NMR FID data were unavailable for high resolution comparison, greater weight was placed on the comparison of ^{13}C NMR spectral analysis. These data again supported the conclusion that the (*S*)-valinol derivative was indeed (*R*,*S*)-**433**. To reach

this conclusion the resonance of 42.7 was taken to be diagnostic, with (*R*,*R*)-**433** having a resonance of 42.8 ppm for this carbon signal (Figure 3.5). This provides clear evidence that (*R*)-puraquinonic has been successfully prepared by the synthesis outlined in this chapter.

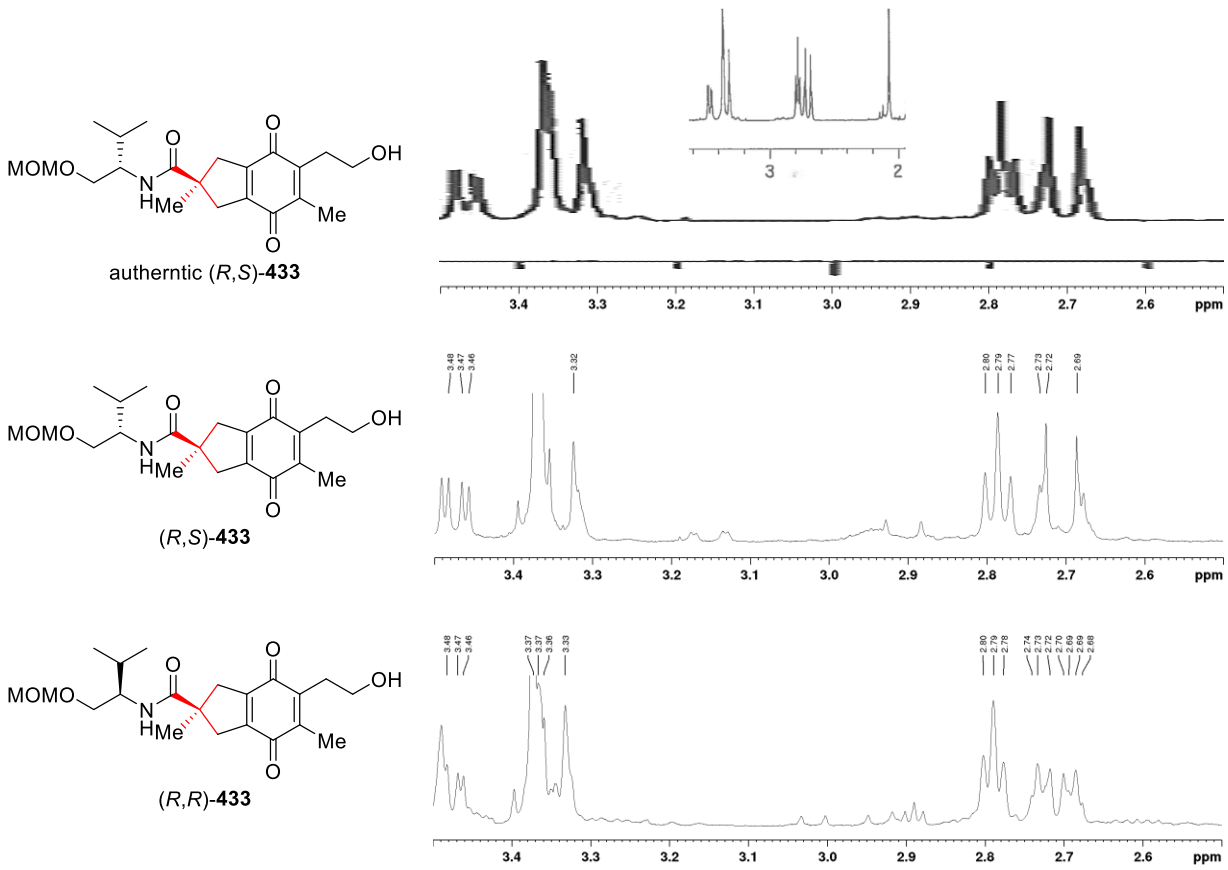

Figure 3.4 Comparison of ^{1}H NMR spectra for *para*-quinones (*R*,*S*)-**433** and (*R*,*R*)-**433**, data for authentic (*R*,*S*)-**433** was only available as a printout and has been manipulated to provide a one-to-one comparison

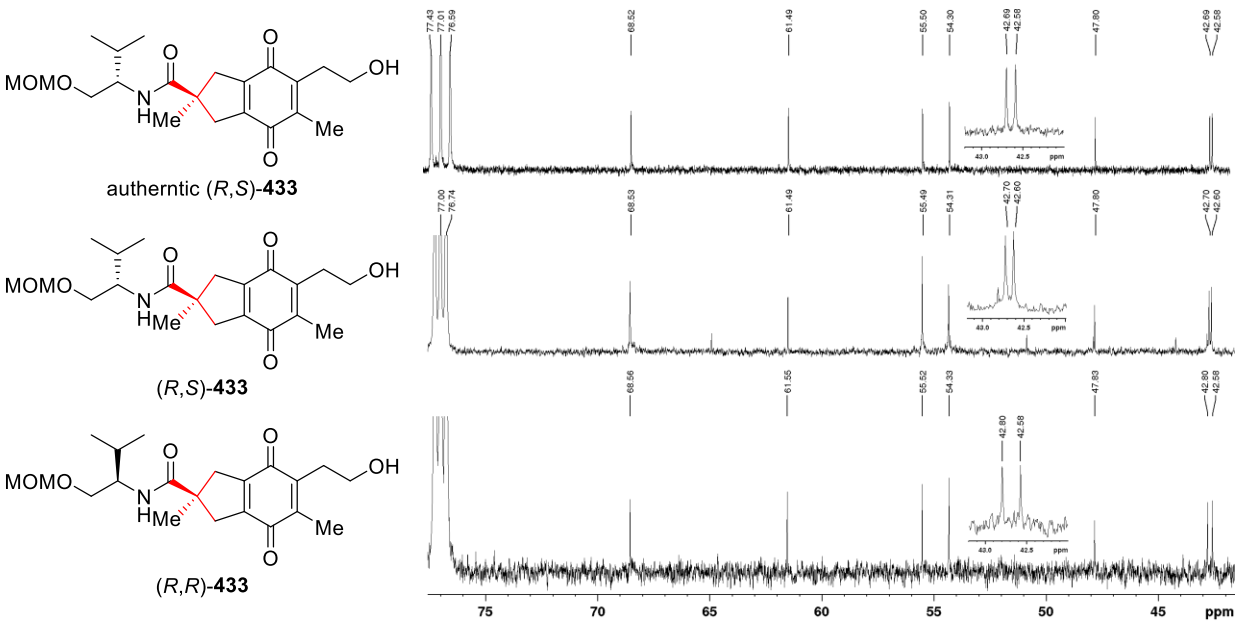

Figure 3.5 Comparison of ^{13}C NMR spectra for *para*-quinones (*R*,*S*)-**433** and (*R*,*R*)-**433**

3.7 Comparison to Proline Derivatives

At the outset of this project, the synthesis of (*R*)-puraquinonic and the interception of related synthetic intermediates provided the most direct route to establishing the stereochemistry of the quaternary stereocentres synthesised in chapter two. However, towards the culmination of the project, Baudoin reported the use of chiral palladium catalysis in the preparation of a variety of amides related to **353** *via* a C-H activation approach.[3] Among these were (*R*)- and (*S*)-proline derivates (*R*,*S*)-**435** and (*S*,*S*)-**435** (Scheme 3.28) which provided attractive species for stereochemical comparison and further confirmation of the absolute stereochemistry of the products described in section 2.3.3.

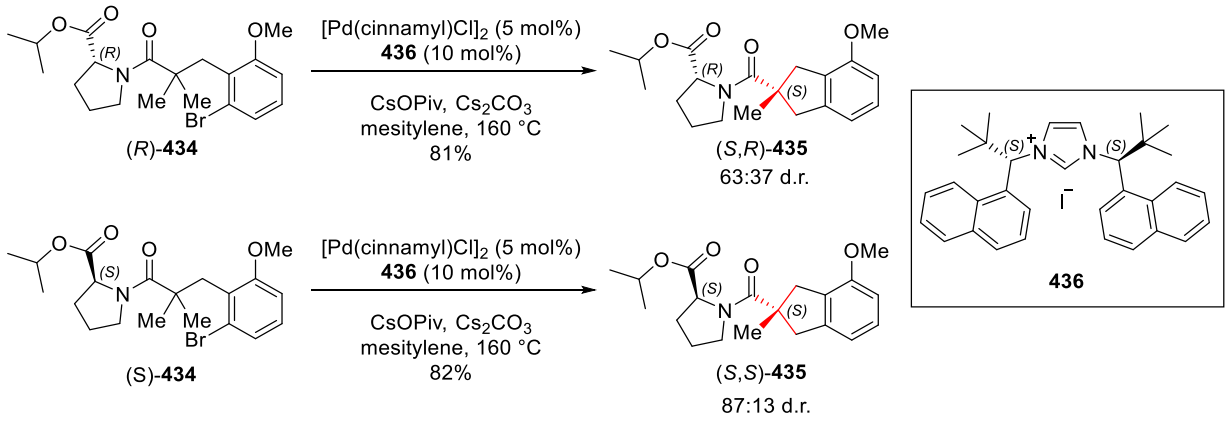

Scheme 3.28 Baudoin's palladium catalysed C-H activation

To make the necessary spectroscopic comparisons, the enantiomers of (*R*,*S*)-**435** and (*S*,*S*)-**435** were prepared from amide **353**. This was accomplished through initial amide hydrolysis with warm sulfuric acid followed by EDC-mediated peptide coupling with either (*R*)- or (*S*)-proline isopropyl ester (Scheme 3.29). This sequence afforded (*R*,*S*)-**435** and (*R*,*R*)-**435** in 98% and 75% yield respectively.

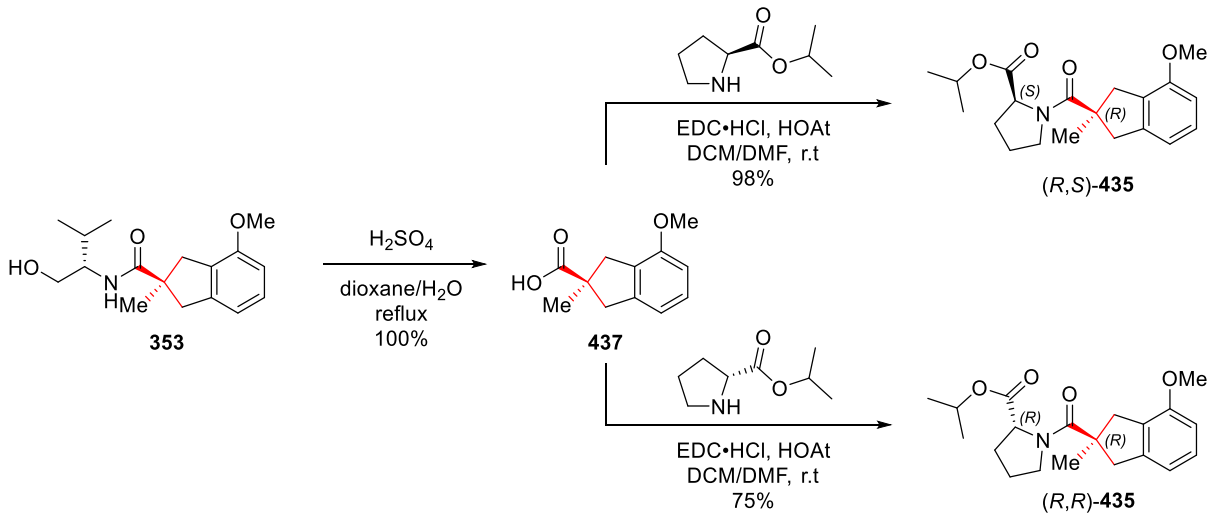

Scheme 3.29 Synthesis of proline derivates of amide **353**

At this stage the quaternary stereocentre was assigned by analogy to the stereochemical outcome observed in the synthesis of (*R*)-puraquinonic acid. By extension this indicated that derivatisation of amide **353** had resulted in the preparation of the enantiomers of Baudoin's two products. Fortunately, this still enabled comparison of the ^{1}H and ^{13}C NMR spectra; the results are outlined in Table 3.2. The most diagnostic differences in the ^{1}H NMR spectra were found to be signals at 3.33/3.39 ppm and 1.21/1.19 ppm. The ^{13}C NMRs spectra were close to identical, a characteristic also observed in the data reported by Baudoin, with the largest change being a 0.4 ppm difference in the signal at 40.1/40.5 ppm. While the spectra of diastereomers only differed subtly, these experiments indeed reconfirmed that the absolute stereochemistry of the quaternary carbon is the (*R*)-isomer.

Table 3.2 Comparison of ^{1}H and ^{13}C NMR spectra data for amide **435**

	Experimental Value	Literature Value[3]	Experimental Value	Literature Value[3]
	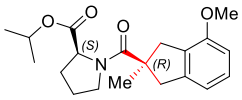 (*R*,*S*)-**435**	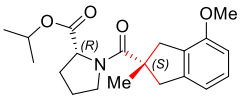 (*S*,*R*)-**435**	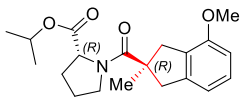 (*R*,*R*)-**435**	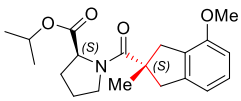 (*S*,*S*)-**435**
^{1}H NMR 500 MHz, $CDCl_3$ (ppm)	7.15, 1H, dd, *J* = 8.1, 7.4 Hz 6.82,1H, d, *J* = 7.4 Hz 6.68, 1H, d, *J* = 8.1 Hz 5.03, 1H, qq, *J* = 6.3, 6.2 4.50, 1H, dd, *J* = 8.4, 4.8 Hz 3.82, 1H, s 3.75, 1H, m; 3.69, 1H, m 3.61, 1H, d, *J* = 16.3 Hz 3.33, 1H, d, *J* = 16.1 Hz 2.95, 1H, d, *J* = 16.1 Hz 2.87, 1H, d, *J* = 16.3 Hz 2.15,1H, m 2.06,1H, m 1.96, 1H, m; 1.90, 1H, m 1.37, 3H, s 1.26, 3H, d, *J* = 6.3 Hz 1.21, 3H, d, *J* = 6.2 Hz	7.15, 1H, t, *J* = 7.8 Hz 6.82, 1H, d, *J* = 7.8 Hz 6.68, 1H, d, *J* = 7.8 Hz 5.04, 1H, hept, *J* = 6.2 Hz 4.49, 1H, dd, *J* = 8.6, 4.8 Hz 3.81, 3H, s 3.76-3.60, 2H, m 3.61, 1H, d, *J* = 16.2 Hz 3.33, 1H, d, *J* = 16.2 Hz 2.95, 1H, d, *J* = 16.4 Hz 2.86, 1H, d, *J* = 16.2 Hz 2.21-2.11, 1H, m 2.12-2.00, 1H, m 1.99-1.83, 2H, m 1.37, 3H, s 1.26, 3H, d, *J* = 6.2 Hz 1.21, 3H, d, *J* = 6.2 Hz	7.15, 1H, dd, *J* = 8.1, 7.5 Hz 6.82, 1H, d, *J* = 7.5 Hz 6.68, 1H, d, *J* = 8.1 Hz 5.03, 1H, qq, *J* = 6.3, 6.2 Hz 4.50, 1H, dd, *J* = 8.6, 4.8 Hz 3.82, 3H, s 3.73, 1H, m; 3.64, 1H, m 3.61, 1H, d, *J* = 16.3 Hz 3.39, 1H, d, *J* = 16.3 Hz 2.94, 1H, d, *J* = 16.3 Hz 2.87, 1H, d, *J* = 16.3 Hz 2.17, 1H, m 2.06, 1H, m 1.97-1.85, 2H, m 1.36, 3H, s 1.26, 3H, d, *J* = 6.3 Hz 1.19, 3H, d, *J* = 6.2 Hz	7.15, 1H, t, *J* = 7.8 Hz 6.81, 1H, d, *J* = 7.8 Hz 6.68, 1H, d, *J* = 7.8 Hz 5.03, 1H, hept, *J* = 6.2 Hz 4.49, 1H, dd, *J* = 8.6, 4.8 Hz 3.81, 3H, s 3.76-3.60, 2H, m 3.60, 1H, d, *J* = 16.2 Hz 3.39, 1H, d, *J* = 16.4 Hz 2.94, 1H, d, *J* = 16.4 Hz 2.86, 1H, d, *J* = 16.2 Hz 2.21-2.11, 1H, m 2.12-2.00, 1H, m 1.99-1.83, 2H, m 1.35, 3H, s 1.26, 3H, d, *J* = 6.2 Hz 1.19, 3H, d, *J* = 6.2 Hz
^{13}C NMR 500 MHz, $CDCl_3$ (ppm)	175.8 172.1 156.1 143.0 128.3 128.0 117.1 107.8 68.1 60.7 55.1 49.7 47.6 44.8 40.1 28.1 25.6 25.0 21.8 21.7	175.9 172.2 156.3 143.2 128.5 128.2 117.2 108.0 68.3 60.9 55.2 49.9 47.8 45.0 40.3 28.3 25.8 25.1 21.9 21.8	175.8 172.1 156.2 143.0 128.5 128.0 117.1 107.9 68.1 60.8 55.1 49.5 47.6 44.6 40.5 28.1 25.7 25.2 21.8 21.7	175.9 172.3 156.4 143.2 128.6 128.2 117.2 108.1 68.3 61.0 55.3 49.7 47.8 44.7 40.7 28.3 25.9 25.4 21.9 21.8

Highlighted entries correspond to differences between the diastereomers of greater than 0.02 ppm in the ^{1}H NMR spectrum and greater than 0.2 ppm in the ^{13}C spectrum; discrepancies between experimental and literature data are attributed to refencing the residual chloroform peak to 77.00 ppm and 77.16 ppm respectively.

3.8 Future Directions

With the synthesis of (*R*)-puraquinonic acid complete, room exists for the contemplation of future directions that may follow from this work. Potential goals might include the following: 1) further reduction in step count by eliminating redox manipulations and functional group interconversions, 2) find suitable conditions for the direct hydrolysis to carboxylic acid **393**, and 3) application of the methodology to additional natural product targets.

Stated at the outset, one of the central goals of the synthesis was to provide as rapid as possible access to the carbon framework of puraquinonic acid. Though the synthesis described in the chapter represents a marked improvement over previous approaches, it consists of a few non-constructive steps; mainly the reduction of diester **376** and the subsequent bromination of diol **415**. These steps may be rendered unnecessary if the electrophilic functionality was introduced directly as part of the dienophile. To accomplish this, a suitably electron deficient, and appropriacy decorated, alkyne would be needed to replace DMAD and may take the form of dimesylate **436** by employing cobalt catalysis, which has been shown to tolerate electron rich dienes and dienophiles in the same reaction.[23, 24] Considering that nonactivated alkyl mesylates were shown to have been competent electrophiles in chapter two, it is reasonable to assume that dimesylate **438** may be a suitable replacement for dibromide **375**. Such a modification may encounter issues with the stability of the Diels-Alder adduct, as the allylic leaving groups may be prone to elimination resulting in aromatisation.

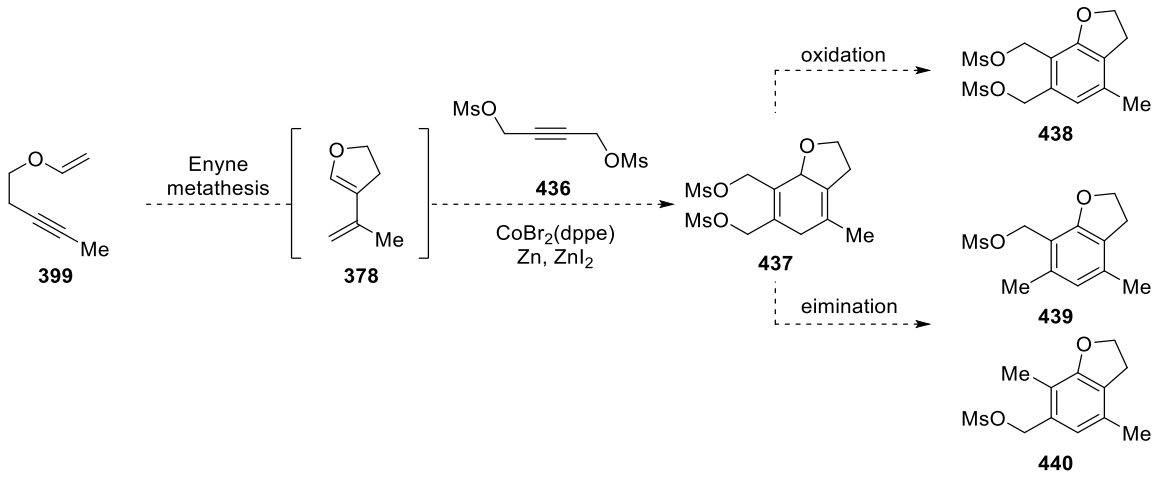

Scheme 3.30 Proposed use of alternate alkynes

The second proposed improvement would be to screen hydrolysis conditions to directly provide carboxylic acid **417** without the need for the isolation of amide **416**. Considering the similarities between the conditions of the two sequential hydrolysis steps it appears eminently reasonable that hydrolytic conditions should exist to accomplish this transformation. This study would take the form of a solvent and acid screen and hopefully not require an excess amount of investigation to complete.

Finally, this work naturally leads to proposing continued efforts in total synthesis. Some ideas for future targets are provide in Figure 3.6 and display quaternary carbon stereocentres that may otherwise be challenging to introduce. Another possible arena for this chemistry may be in the preparation of molecules for the purposes of drug discovery and development; an area the Gleason Group is active in.

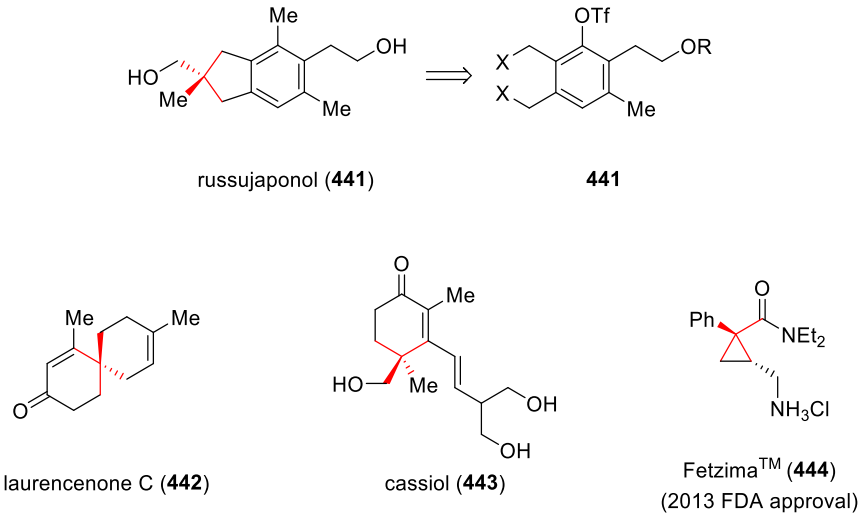

Figure 3.6 Possible natural product and medicinal chemistry targets

3.8 Conclusions

To conclude, the work put forth in this chapter has demonstrated the utility and practicality of sulfone **277** in providing a rapid and efficient means for the construction of challenging α-quaternary carbon stereocentres. The synthesis of (*R*)-puraquinonic acid was completed in only eight steps though the rapid construction of a key bis-electrophile with much of the carbon framework rapidly constructed with a one-pot enyne/Diels-Alder/oxidation sequence. Use of sulfone **277** allowed for the α-quaternary carbon stereocentre to be introduced in the final carbon-carbon bond forming step of the synthesis. Finally, oxidation to the para-quinone was achieved in a single step through leveraging the inherently nucleophilic arene in conjunction with electrophilic oxidants.

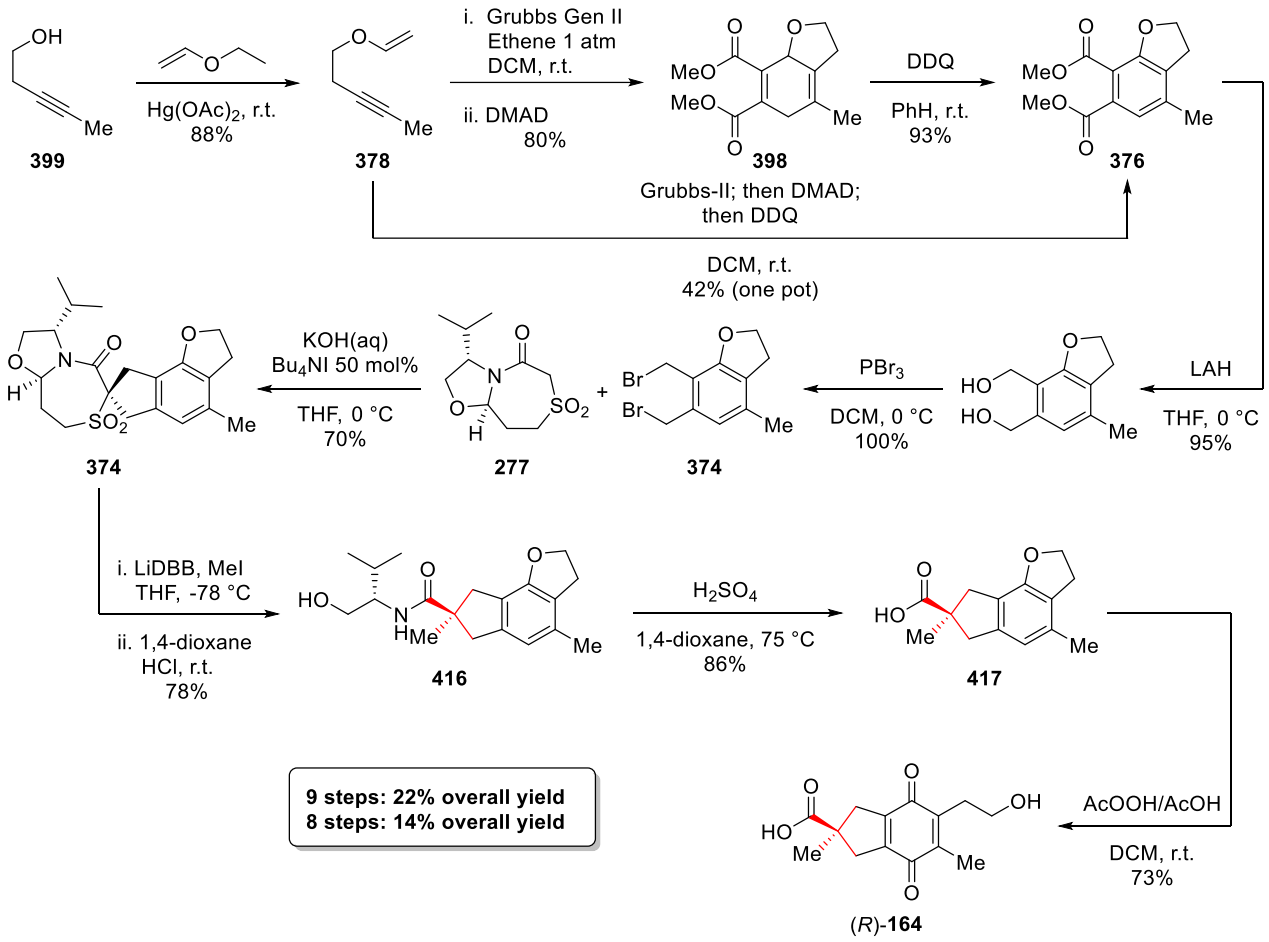

Scheme 3.31 Total synthesis of (*R*)-puraquinonic acid

This work provides a highly useful advancement in the chemistry of bicyclic thioglycolate lactam-based auxiliaries as it allows of the chemistry to be performed late within a synthetic route. This is critical for the use of chiral auxiliaries as they are inherently an atom inefficient endeavour best employed late within a synthesis to limit the amount of auxiliary consumed in each synthesis. The efficacy of this synthetic route is particularly striking when its 8-steps are compared to the twelve-steps previously required for the construction of puraquinonic acid using lactam **104** or the ten-step racemic synthesis of puraquinonic acid ethyl ester. Additionally, at 22.3% overall yield in its 9-step incarnation, it is the highest yielding synthesis to date (*i.e.* when the DDQ oxidation is

conducted separate of the enyne-metathesis-Diels-Alder sequence); this is again comparable to the synthesis of racemic puraquinonic acid ethyl ester in 23% overall yield.

3.9 References

1. Becker, U.; Erkel, G.; Anke, T.; Sterner, O., Puraquinonic Acid, a Novel Inducer of Differentiation of Human Hl-60 Promyelocytic Leukemia Cells from Mycena Pura (Pers. Ex Fr.). *Natural Product Letters* **1997,** *9* (3), 229-236.

2. Melot, R.; Craveiro, M. V.; Baudoin, O., Total Synthesis of (nor)Illudalane Sesquiterpenes Based on a C(Sp^3)–H Activation Strategy. *The Journal of Organic Chemistry* **2019,** *84* (20), 12933-12945.

3. Melot, R.; Craveiro, M. V.; Bürgi, T.; Baudoin, O., Divergent Enantioselective Synthesis of (nor)Illudalane Sesquiterpenes Via Pd^0-Catalyzed Asymmetric C(Sp^3)–H Activation. *Organic Letters* **2019,** *21* (3), 812-815.

4. Clive, D. L. J.; Yu, M.; Sannigrahi, M., Synthesis of Optically Pure (+)-Puraquinonic Acid and Assignment of Absolute Configuration to Natural (−)-Puraquinonic Acid. Use of Radical Cyclization for Asymmetric Generation of a Quaternary Center. *The Journal of Organic Chemistry* **2004,** *69* (12), 4116-4125.

5. Tiong, E. A.; Rivalti, D.; Williams, B. M.; Gleason, J. L., A Concise Total Synthesis of (R)-Puraquinonic Acid. *Angewandte Chemie International Edition* **2013,** *52* (12), 3442-3445.

6. Kraus, G. A.; Choudhury, P. K., Synthesis of Puraquinonic Acid Ethyl Ester and Deliquinone Via a Common Intermediate. *The Journal of Organic Chemistry* **2002,** *67* (16), 5857-5859.

7. Su, L.; Lei, C.-Y.; Fan, W.-Y.; Liu, L.-X., $Fecl_3$-Mediated Reaction of Alkynols with Iodine: An Efficient and Convenient Synthetic Route to Vinyl Iodides. *Synthetic Communications* **2011,** *41* (8), 1200-1207.

8. Kumamoto, H.; Onuma, S.; Tanaka, H., Sulfur Extrusion with Tin Radical: Synthesis of 4‘,5‘-Didehydro-5‘-Deoxy-5‘-(Tributylstannyl)Adenosine, an Intermediate for Potential Inhibitors against S-Adenosyl Homocysteine Hydrolase. *The Journal of Organic Chemistry* **2004,** *69* (1), 72-78.

9. Barrett, A. G. M.; Dhanak, D.; Graboski, G. G.; Taylor, S. J., (Phenylthio)Nitromethane. *Organic Syntheses* **1990,** *68* (68).

10. Hojo, M.; Masuda, R.; Sakaguchi, S.; Takagawa, M., A Convenient Synthetic Method for B-Alkoxy- and B-Phenoxyacrylic Acids and 3,4-Dihydro-2h-Pyran-5- and 2,3-Dihydrofuran-4-Carboxylic Acids. *Synthesis* **1986,** (12), 1016-1017.

11. Hoffmann, H. M. R.; Haase, K., The Synthesis of Acyl Iodides. *Synthesis* **1981,** (09), 715-719.

12. Mori, M., Recent Progress on Enyne Metathesis: Its Application to Syntheses of Natural Products and Related Compounds. *Materials* **2010,** *3* (3), 2087-2140.

13. Fischmeister, C.; Bruneau, C., Ene-Yne Cross-Metathesis with Ruthenium Carbene Catalysts. *Beilstein Journal of Organic Chemistry* **2011,** *7*, 156-66.

14. Sanford, M. S.; Love, J. A.; Grubbs, R. H., Mechanism and Activity of Ruthenium Olefin Metathesis Catalysts. *Journal of the American Chemical Society* **2001,** *123* (27), 6543-6554.

15. Minenkov, Y.; Occhipinti, G.; Jensen, V. R., Complete Reaction Pathway of Ruthenium-Catalyzed Olefin Metathesis of Ethyl Vinyl Ether: Kinetics and Mechanistic Insight from Dft. *Organometallics* **2013,** *32* (7), 2099-2111.

16. Stephen; Clark, J.; Kettle, J. G., Synthesis of Brevetoxin Sub-Units by Sequential Ring-Closing Metathesis and Hydroboration. *Tetrahedron Letters* **1997,** *38* (1), 123-126.

17. Grubbs, R. H.; Chang, S., Recent Advances in Olefin Metathesis and Its Application in Organic Synthesis. *Tetrahedron* **1998,** *54* (18), 4413-4450.

18. Sturino, C. F.; Wong, J. C. Y., The Ring-Closing Metathesis of Vinyl Ethers with Grubbs' Catalyst for the Synthesis of Dihydropyrans. *Tetrahedron Letters* **1998,** *39* (52), 9623-9626.

19. Giessert, A. J.; Snyder, L.; Markham, J.; Diver, S. T., Intermolecular Enol Ether−Alkyne Metathesis. *Organic Letters* **2003,** *5* (10), 1793-1796.

20. Tymann, D.; Tymann, D. C.; Bednarzick, U.; Iovkova-Berends, L.; Rehbein, J.; Hiersemann, M., Development of an Alkyne Analogue of the De Mayo Reaction: Synthesis of Medium-Sized Carbacycles and Cyclohepta[B]Indoles. *Angewandte Chemie International Edition* **2018,** *57* (47), 15553-15557.

21. Mori, M.; Sakakibara, N.; Kinoshita, A., Remarkable Effect of Ethylene Gas in the Intramolecular Enyne Metathesis of Terminal Alkynes. *The Journal of Organic Chemistry* **1998,** *63* (18), 6082-6083.

22. Kinoshita, A.; Mori, M., Ruthenium Catalyzed Enyne Metathesis. *Synlett* **1994,** (12), 1020-1022.

23. Hilt, G.; Erver, F.; Harms, K., Cobalt(I) Catalysis in the Diastereoselective Two-Step Synthesis of Tricyclic Systems. *Synthesis* **2011,** (06), 972-978.

24. Hilt, G.; Kuttner, J., Synthesis of Acyclic Polycarbonyl Compounds Via Ozonolysis of Cyclohexa-1,4-Dienes. *Synthesis* **2015,** *47* (08), 1170-1180.

CHAPTER 4

Design of HDAC/HIV-1 Protease Inhibitor Hybrid Molecules for the Development of Novel HIV Treatments

4.1 Current HIV Treatment

4.1.1 HIV/AIDS

Acquired immune deficiency syndrome (AIDS) was first clinically reported on June 5, 1981 as a cluster of five cases in Los Angeles, California.[1] While initially not providing a name for the new disease, the American Centers for Disease Control (CDC) coined it the "4H disease", a reference to the disease's prevalence among heroin users, homosexuals, haemophiliacs, and Haitians.[2] The term 4H disease was replaced by the CDC in 1982 with AIDS as the disease was frequently referred to in the press as GRID (gay-related immune deficiency) which was considered misleading as it had become clear that the disease was not isolated to the gay community. By 1983 the independent groups of Gallo[3] and Montagnier[4] had discovered that AIDS was caused by a novel retrovirus. It was later established that the viruses identified by the two groups were in fact the same virus. As such, the virus was renamed the human immunodeficiency virus (HIV).

In the years following the identification of the disease, it spread quickly across the globe with the number of new cases raising to 2.7 million by 2000 and HIV-related deaths reaching a peak of 1.7 million in 2005. Today HIV/AIDS remains endemic to many parts of the world and populations and by World Health Organization (WHO) estimates, some 38 million people currently live with the disease (2019 numbers).[5]

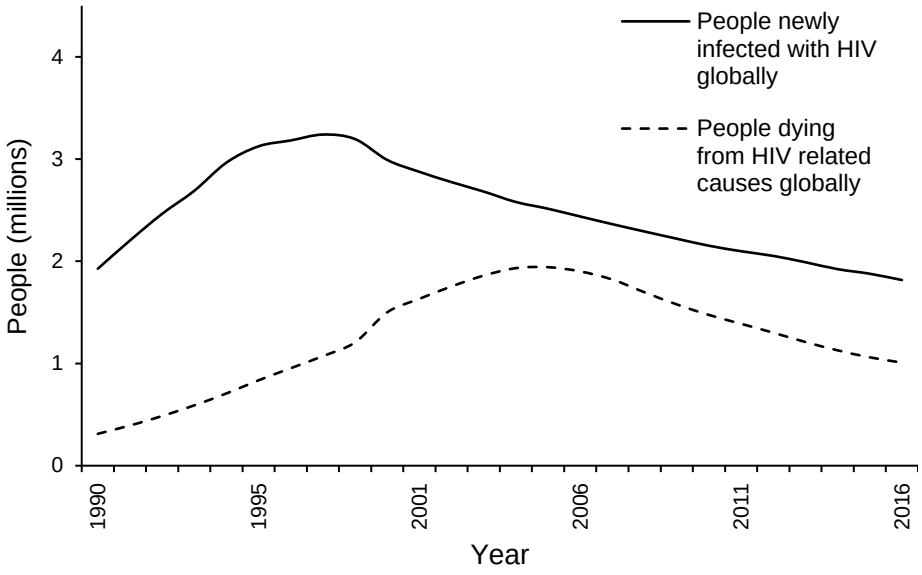

Figure 4.1 Overall global trends of HIV infection and associated deaths

Acute HIV infection may result in no symptoms but is often associated with a brief phase characterised by fever, generalized lymphadenopathy, a nonspecific rash, myalgias, and/or malaise. As the infection continues progressive loss of $CD4^+$ T cells is observed. As these so-called T helper cells play a critical role in the overall function and regulation of the immune system their loss eventually results in overwhelming immunodeficiency. Infected individuals thus succumb to characteristic infections and/or oncological complications which define AIDS. Although timelines may vary, with some cases proceeding rapidly or never progressing, infected individuals typically progress to death within ten years.[6]

4.1.2 Viral Lifecycle

HIV is a diverse collection of retroviruses with the two most encountered bring HIV-1 and HIV-2. HIV-1 is both more prevalent and more pathogenic than HIV-2 and is the major focus of research and discussion as it is responsible for most cases worldwide. From genetic analyses it has

been discovered that HIV arose as a result of cross-species transmission of strains of simian immunodeficiency virus found in chimpanzees and sooty mangabeys.

The primary cellular target of HIV-1 is the CD4 receptor found on the surface of T lymphocytes, monocytes, macrophages, and dendritic cells, all of which are critical components of the host's immune system. To enter the cell the virus engages co-receptors such as CCR5 and CXCR4 and once inside uses its viral proteins to incorporate its genome into that of the host. As a retrovirus this process is achieved through the reverse transcription of the virus' RNA genome into HIV-DNA with the process mediated by the HIV reverse transcriptase enzyme. The HIV-DNA is then imported to the host cell nucleus where HIV integrase inserts it into the genome of the host.

Once the HIV-DNA is fully incorporated, the host's enzymes transcribe and/or translate the viral genome into the enzymes, genome, and structural components necessary for the formation of new virions.[7] Finally, for the new virions to mature and become capable of infecting new cells, viral proteins must be cleaved by specific HIV protease enzymes. Specifically, HIV-1 protease is responsible for site selective peptide hydrolysis of the Gag polyprotein (gag-pol) which results in mature, functional proteins such as HIV-reverse transcriptase and HIV-integrase.[8]

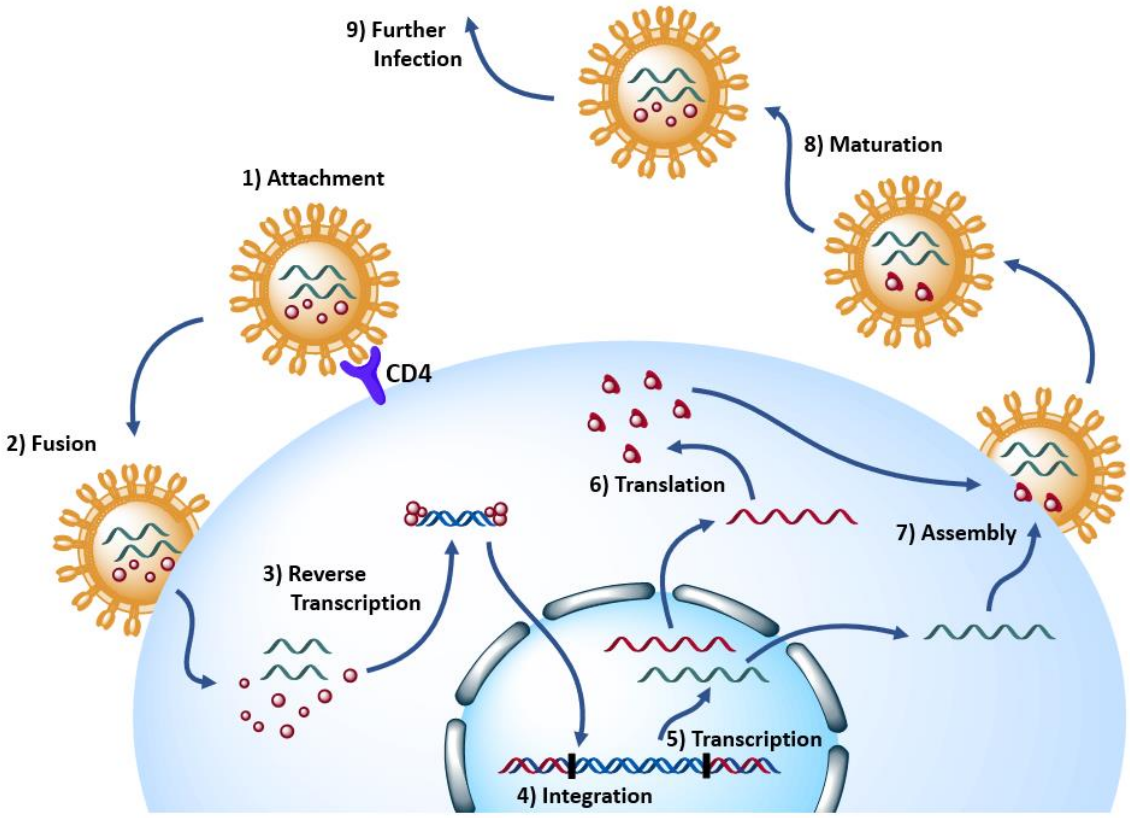

Figure 4.2 The HIV viral lifecycle

4.1.3 State of the Art Treatment

While no cure for HIV infection exists, the herculean efforts made in its management have led to the development of numerous antiretroviral drugs with around twenty-five unique antiretroviral drugs having been approved for use in adults in America and Europe. These drugs belong to five classes, with each class targeting a different step in the viral life cycle.[9] These include: (i) entry inhibitors, (ii) nucleoside reverse transcriptase inhibitors, (iii) non-nucleoside reverse transcriptase inhibitors (iv) integrase strand transfer inhibitors, and (v) protease inhibitors (Figure 4.3).[10]

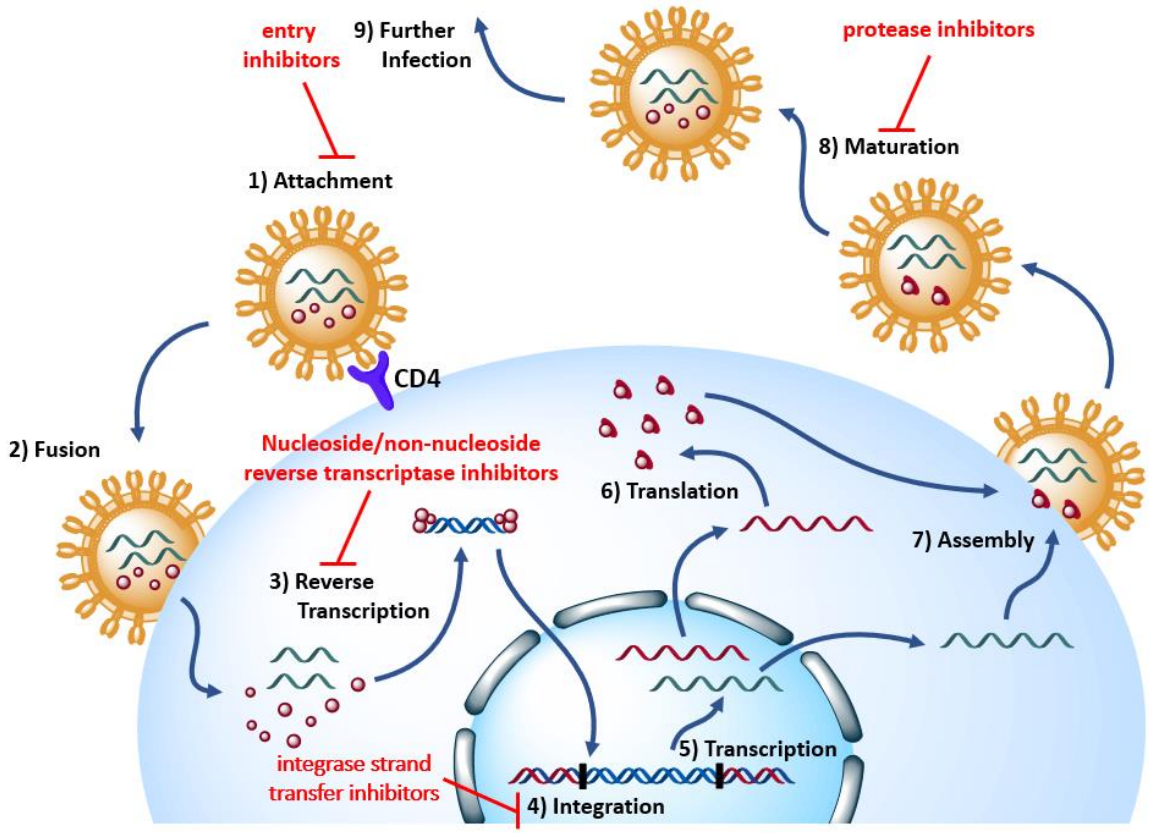

Figure 4.3 Steps in the HIV lifecycle inhibited by current antiretroviral drugs

Entry inhibitors, such as maraviroc (**445**), act by binding to receptor protein (CCR5 in the case of maraviroc) and prevent the virus from entering host cells. To date only a few entry inhibitors have been approved. Once the virus has made it into a host cell both nucleoside and non-nucleoside reverse transcriptase inhibitors prevent the viral RNA's conversion to DNA. In the case of nucleoside reverse transcriptase inhibitors this is achieved by preferential incorporation into growing viral DNA which leads to premature termination of DNA synthesis. As nucleoside reverse transcriptase inhibitors must be suitable substrates for HIV-reverse transcriptase these drugs are typically analogues of natural nucleosides and nucleotides (*e.g.* abacavir, **446**) that lack the 3′ hydroxyl group. Non-nucleoside reverse transcriptase inhibitors inhibit the same enzyme but bind to an allosteric site and thus are structurally unrelated (*e.g.* efavirenz, **447**) to nucleoside reverse

transcriptase inhibitors. Integrase strand transfer inhibitors such as dolutegravir (**448**), can prevent HIV-DNA from being incorporated into the host genome ultimately preventing the macronodular components of new virions from ever being produced by the host cell. Lastly, protease inhibitors, such as atazanavir (**449**), inhibit the HIV-PR enzymes responsible for cleaving newly synthesised long viral polypeptides into the active proteins necessary for new virions to mature and become infective.

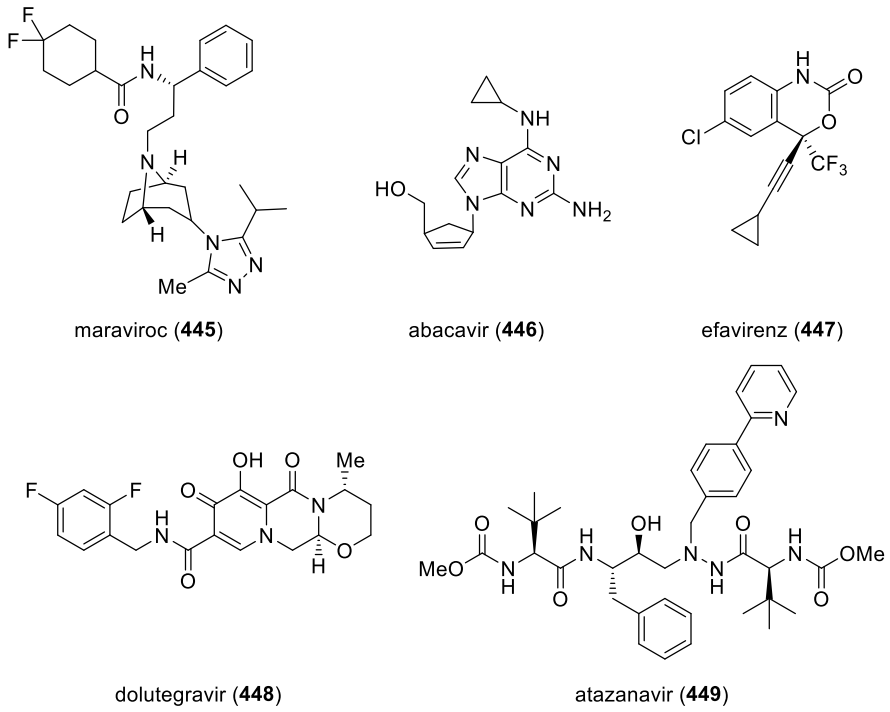

Figure 4.4 Representative examples of entry inhibitors (maraviroc), nucleoside reverse transcriptase inhibitors (abacavir), non-nucleoside reverse transcriptase inhibitors (efavirenz), integrase strand transfer inhibitors (dolutegravir), and protease inhibitors (atazanavir)

While anti-HIV drugs of any class can on their own lower the viral load of infected individuals, they are overwhelmingly prescribed in combination treatment regimens known as highly active antiretroviral therapy (HAART, frequently simplified to as ART or cART). A common drug combination will consist of two nucleoside reverse transcriptase inhibitors and one

drug of another class such as the use of raltegravir (an integrase inhibitor) in combination with tenofovir and emtricitabine). In extreme cases six or more dugs may be used simultaneously in treatment regimens termed mega-HAART.[11]

The use of drug combinations in HAART allow for multiple viral targets to be inhibited simultaneously leading to a high level of viral suppression and allows for recovery of the immune system. Additionally, the low levels of viral replication that are achieved with HAART reduce the risk of viral evolution/the emergence of drug-resistant mutations, and the further infection of virus free cells or healthy individuals. In principle, HAART regimens should be able to supress the infection indefinitely. Sadly, this is not the case; it is not always fully effective at restoring optimal immune function, leads to long-term toxicity (due to the life-long need for treatment), and presents the constant possibility of the development and/or transmission of drug resistant strains of HIV.

4.1.4 HIV Latency

The question remains: with so many available drugs targeting multiple druggable viral enzymes why do none of them provide a route to curative treatment? The answer lies in HIV's ability to remain within a host cell's genome yet remain transcriptionally silent.[12] In this state the infected cell expresses no viral proteins depriving antiretroviral drugs from their targets. In this state, termed latency, no viral proteins are expressed causing antiretroviral drugs to have no effect as there are no druggable targets within an infected cell.

As infected $CD4^+$ T cells can remain in this quiescent state for many years and may live for as long as non-infected cells, continuous HAART treatment is unable to clear the infection despite nearly inhibiting all viral replication. The resulting viral reservoirs thus become a source of viral recrudescence among individuals who stop/interrupt HAART or where drug resistance

develops. Owing to limited host clearance mechanisms[13] and viral sanctuaries (such as the lymph nodes where antiretroviral drug penetration is limited[14]) current estimates suggest it would take several decades for the low levels of natural reservoir decay to completely eliminate the infection.[15] Considering that infection models have demonstrated that viral reservoirs can be established in a short a time as three days post infection[16] efforts to develop a cure must address latency as a central concern.

A promising method in the targeting of latently infected cells is the so-called 'shock and kill' approach to treatment design.[17] In this paradigm, viral revisors are targeted for reactivation such that they begin to produce druggable targets which may allow for new or established antiretrovirals to eradicate the infection. Such a strategy needs to address the molecular factors which inhibit infected cells from exiting latency. These epigenetic factors include histone modification of the long terminal repeat unit (LTR) of the viral DNA by methylation and deacetylation,[18] translational restriction by host mRNAs,[19] and lack of necessary transcription factors.[20] Due to the extensive research conducted in this field this chapter will focus on efforts to activate infected cells by modulating histone acetylation. However, the reader is directed to reviews by Verdin,[21] Davenport,[22] and Palmer[23] for an overview of other methods being investigated.

4.1.5 Histones, Histone Deacetylases, and Their Role in HIV-Latency

4.1.5.1 Histones

Histones are a collection of proteins located within the nucleus of eukaryotic cells which play a critical role in determining the transcriptional activity of discrete sections of DNA within a genome. In general, covalent modifications made to histone tails by an array of endonuclear

enzymes, modulate gene expression by influencing the level of chromatin condensation. The extent of chromatin condensation is achieved through the modulation of several molecular interaction: electrostatic interactions between positively charged histones and negatively charged DNA phosphate groups, hydrogen bonds, salt bridges, and nonpolar interactions with the deoxyribose portion of the DNA backbone. Many of these interactions are facilitated by post translational modifications such as methylation, citrullination, acetylation, phosphorylation, SUMOylation, ubiquitination, and ADP-ribosylation. At the macromolecular level, sections of the genome that are bound less to histones are transcriptionally active with inactive genes being bound tightly to associated histones.

Due to the prevalence of phosphate groups contained in the backbone of DNA strands, and their propensity to be negatively charged under physiological conditions, post translational changes influencing the overall charge of histones play a significant part in gene regulation. The main loci of these modifications are protein residues displaying amino or carboxyl functional groups as at physiological pH; these groups can provide histones with positive and negative charges respectively.

A common modification made to histones is the acetylation of lysine residues, a process modulated by histone acetyltransferases (HATs) and histone deacetylase (HDAC) enzymes. By acetylating the ε-amino group of lysine residues the basic amines are converted to the corresponding acetamides. At physiological pH the significantly lower basicity of amides prevents the residue from forming interactions as in the cationic ammonium. In turn, this results in weaker DNA binding and promotes DNA transcription. This dynamic process provides an avenue for small molecular inhibitors to influence the levels of gene expression through selective inhibition of HDACs and HATs, respectively leading to up and down regulation of genes. The remainder of

this chapter will focus on the inhibition of HDACs as the chemistry of HAT inhibition falls beyond the purview of this work.

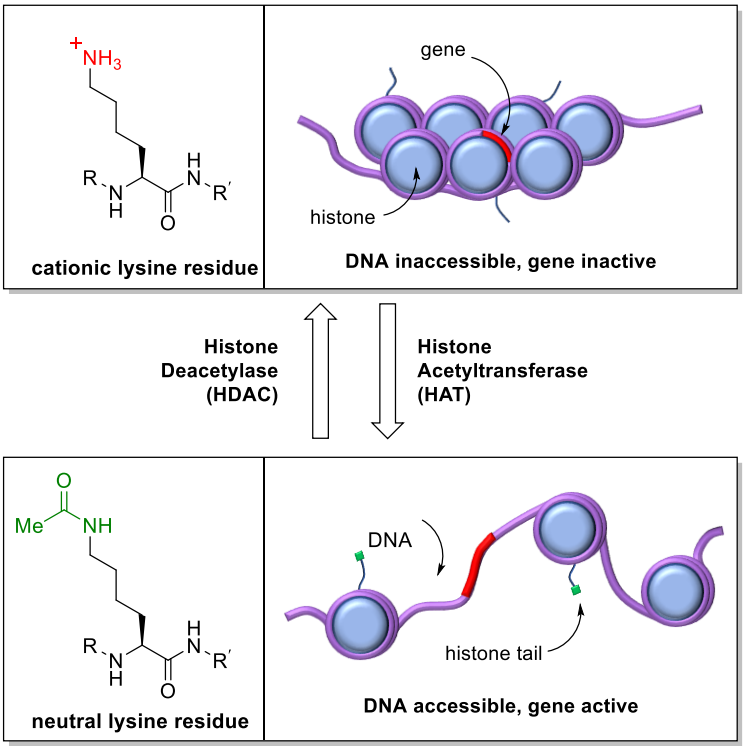

Figure 4.5 Dynamic modification of histone lysine residues by HDAC and HAT enzymes

4.1.5.2 Histone Deacetylases (HDACs)

Although the primary function of HDACs is the regulation of gene transcription, acetylation of lysine residues is also an observed post-translation modification of other proteins.[24] However, it is less well studied than protein phosphorylation regulated by kinases and phosphatases. Within humans there are a total of eighteen HDAC enzymes which are organised into four classes based on their homology to yeast proteins.[25] Class I HDACs (HDAC 1, 2, 3, and 8) display high homology to the yeast transcriptional regulator RPD3 are expressed in all tissues and are predominantly localised in the cell nucleus. As such, they play critical roles in fundamental cellular processes such as cell proliferation/apoptosis (HDACs 1 and 2)[26] and DNA damage

response (HDAC 3).[27] HDAC 8 is the outlier of the class, being found in the cytosol of cells showing smooth muscle differentiation.[28] Class II HDACs are subdivided into class IIa (HDACs 4, 5, 7, and 9) and class IIb (HDACs 6 and 10). Class II HDACs are expressed in a tissue-specific manner and can be found in both the nucleus and cytoplasm[29] where they are responsible for signal transduction and other functions in the cytoplasm.[30, 31] Class III HDACs are the most dissimilar due to their active site not containing a catalytic Zn^{2+} centre (Figure 4.6) which is conserved in all three other HDAC classes. Also, unlike HDACs of other classes, class III enzymes are NAD^{+} dependent. Owing to these fundamental differences, class III HDACs are known as sirtuins (SIRT1, 2, 3, 4, 5, 6, and 7) but perform a similarly broad range of biological function as class I, II and III HDACs, such as regulation of oxidative stress, DNA repair, regulation of metabolism and aging.[32, 33] Class IV is the smallest class consisting of only HDAC 11. HDAC 11 is not well studied but displays homology to both class I and II HDACs and is thus categorised separately.[34] Its exact functions are unknown but has been found expressed in kidney, brain, testis, heart and skeletal muscle tissues.[35]

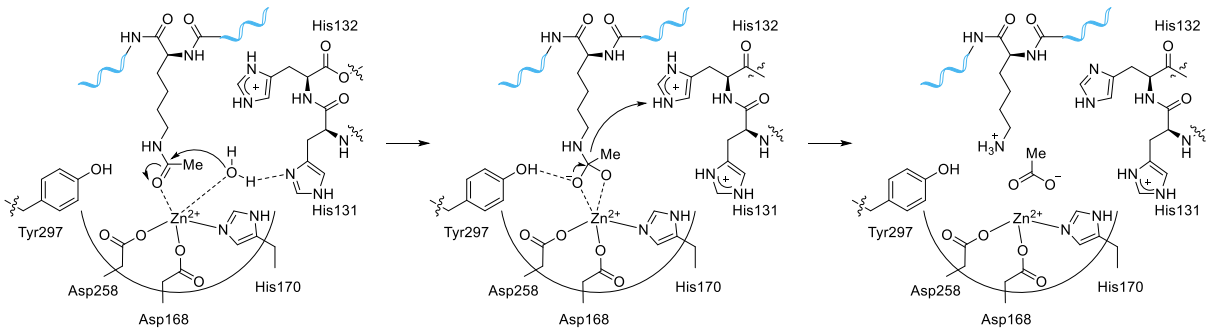

Figure 4.6 Mechanism for zinc dependant HDAC cleavage of acetylated lysine residues

4.1.5.3 Use of HDAC Inhibitors for Latent HIV Reactivation

Due to the ubiquitous presence of HDACs and their critical role in gene regulation, it is unsurprising that they are implicated in aspects of the HIV lifecycle.[36] Specifically, Class I HDACs (HDACs 1, 2, and 3[37]) are recruited to the HIV LTR by transcription factors and remodel the nucleosome nuc-1 by removal of acetyl groups on lysine residues. This leads to down regulation of enhancer and promoter elements contained within the LTR allowing the virus to remain in its latent state.[38] Inhibition of HDACs by small molecule inhibitors has been demonstrated to supress the level of histone acetylation and reactivate latently infected $CD4^+$ cells. In hopes of leveraging this activity into novel treatments for HIV infection, HDAC inhibitors vorinostat,[39-41] panobinostat,[42] and romidepsin[43] have all been studied in clinical trials while many others have been tested *in vetro*.[44-46] For discussions on other classes of agents designed to promote latent HIV reactivation kindly see reviews by Kim,[47] Spivak,[48] and Sadowski.[49]

It is important to acknowledge that inhibition of HDAC activity has effects beyond latent HIV reactivation. In addition to general toxicity associated with non-specific HDAC inhibitors (a direct consequence of the involvement of HDACs in normal/healthy cellular function) HDAC inhibitors have been shown to preferentially induce apoptosis in diseased cells such as cancer cells. Indeed, a similar response was observed to treatment of latently infected cell lines with HDAC inhibitors (valproic acid, oxamflatin and metacept-1).[50] More subtle effects are have also been documented such as the decreased expression of co-receptors (CXCR4 and CCR5) on $CD4^+$ lymphocytes and monocyte upon treatment with gavinostat.[51] This is significant as these co-receptors are necessary for viral fusion to uninfected cells. In all, the effects of HDAC inhibitors, beyond straightforward HIV reactivation, provide compelling reasons to investigate their use in novel HIV treatment.

4.2 Combination Therapy and Hybrid Drugs

4.2.1 Combination Therapy

The use of multiple drugs in concert to address a single condition has been used to great success in many diseases beyond HIV/AIDS. The use of multiple drugs in this way is termed combination therapy and is distinguished from monotherapies where a single drug is enough to treat or manage a given disease. Examples where combination therapy is routinely used include artemisinin-based combination therapies (ACT) for malaria,[52] the use of ethambutol, isoniazid, pyrazinamide, rifampicin, and streptomycin in first line tuberculosis treatment,[53] and the numerous treatment regimens designed to combat specific cancers.[54] Combination therapies have found such varied use, be that in vial (HIV) parasitic (malaria), bacterial (TB), or cancerous disease states, as they are an excellent method of proactively countering drug resistance. Under combination treatment, mutations conferring resistance to most or all drugs being used must develop simultaneously for resistance to arise. Considering this invariably requires an unlikely set of mutations in multiple proteins/enzymes, combination therapy greatly reduces the risk of developing drug resistant strains of the disease.

While combination therapy has its advantages, it suffers from several disadvantages including increased risk of drug-drug interactions, complex dosing protocols, increased research and development time, and increased cost. A strategy commonly employed to exploit some of the benefits of combination therapy while minimising its drawbacks, is the design of hybrid drugs and inhibitors, wherein a single molecule is responsible for the multiple desired biological effects.

4.2.2 Advantages of Hybrid Drug Design

While upon brief inspection the use of a hybrid drug would appear to have a similar/identical impact to combination therapy, the development and use of hybrid drugs has several advantages over such combination treatment regimens. These advantages include eliminating the need to develop and gain approval for multiple drugs, predictable pharmacokinetic properties, limiting negative drug-drug interactions, convenient dosing regimens, decreased prevalence of drug resistance, and spatial/temporal homogeneity of activity (*i.e.* prevents the need for multiple different drug molecules to be present in the same place at the same time and at the necessary concentrations to elicit the desired synergistic effects). Additionally, hybrid drugs can take advantage of a Trojan Horse strategy where one structural element can induce the molecule's translocation (*e.g.* by exploiting endogenous cellular transportation mechanisms) to locations where one of its intended targets is localised.

Several examples of hybrid drugs have been approved for use in humans, mainly in the field of anti-cancer treatment. The simplest examples are those where promiscuity in enzymatic targets leads to the interaction with multiple similar targets. Example of this approach include imatinib (**450**) approved for the treatment of myelogenous leukaemia, sorafenib (**451**) used in the treatment of primary liver and kidney cancer, and lapatinib (**452**) which obtained FDA in 2007 for treatment of metastatic breast cancer (Figure 4.7). In these three cases at least two kinases are inhibited by each drug leading to more effective treatments.

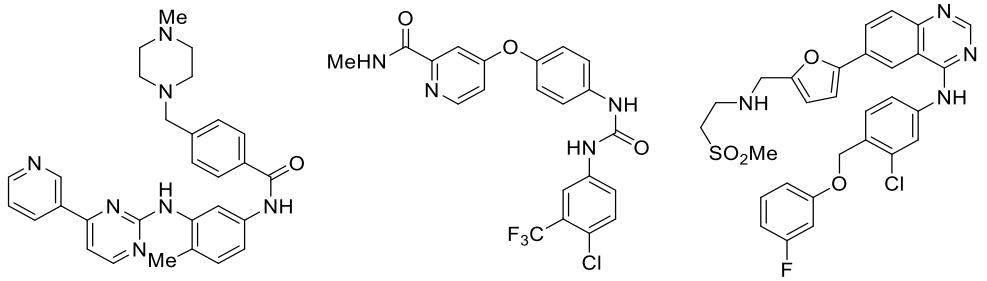

Figure 4.7 FDA approved kinase inhibitors known to target multiple kinases

4.2.3 Examples of Hybrid Drugs

The synthetic development of drugs which can interact with multiple unrelated targets allows for the design of single molecules which can have effects on multiple biochemical pathways. Ideally this will lead to synergistic effects to treat the underlying disease state. As enzymatic promiscuity is not a reliable method to specifically interact with/inhibit multiple targets, molecules intended to function in this manner require greater efforts towards their design. Accordingly, several strategies and molecule classes have emerged to tackle this challenge. Four main methods have emerged for successfully incorporating multiple pharmacophores into a single molecular scaffold.

The four methods routinely encountered in hybrid drug development can be organised by the spatial relationship between two pharmacophores. This leads to the following classes of molecules: (i) linked pharmacophores, (ii) joined pharmacophores, (iii) overlapped pharmacophores, and (iv) merged pharmacophores. However, it should be noted that this purely structural classification system is not the only method encountered with classification based on the activity of the two pharmacophores is also advanced in the literature. In this regard molecules are split into two families, molecules wherein the two pharmacophores act through the same

mechanism (*e.g.* imatinib, sorafenib, and lapatinib, *vide supra*) and molecules with each pharmacophore acting through distinct mechanisms (*e.g.* estramustine, *vide infra*).

Linked and joined pharmacophore molecules are perhaps the most easily designed approach to hybrid drugs. In the linked case two known pharmacophores are linked with a covalent linker of variable size and length. Common molecular motifs such as (poly)ethers, esters, amides, peptides, and carbamates may be employed as the linking unit. The linker may be permanent or may be designed to hydrolyse under biological conditions to allow each pharmacophore to act independently. While this allows for the use of known pharmacophores and minimises the need for pharmacophore structural optimisation, optimisation of the linker type and location is necessary. This is a significant design challenge as pharmacophores are invariably optimised to occupy the limited space of an enzyme active site, leaving few (in any) avenues to introduce additional structural complexity. Additionally, molecules of this design tend to be large and violate Lipinski's rule of five, specifically having a molecular weight over 500 Da, more than five hydrogen bond donors, and more than ten hydrogen bond acceptors.

The requirement of linker optimisation may be eliminated by use of a joined hybrid approach, but this strategy retains many of the same issues inherent in linked hybrid design. Use of a joined design is only suitable in situations where each pharmacophore can tolerate the proximity of the other as to not reduce potency against either target. As with linked hybrids, the inclusion of two full pharmacophores frequently leads to molecules of this design having high molecular weights which may have detrimental impacts on bioavailability, pharmacodynamics, and methods of administration; the resulting designs again often violating one or more of Lipinski's rules. An illustrative example of a joined hybrid is the anti-prostate cancer drug extramustine[55] (**457**). Here the pharmacophore of estradiol (**458**, an oestrogen receptor modulator) and mustine

(**456**, an alkylating agent) are joined though a minor alternation to the oxidation state of the methyl group found in mustine (Figure 4.8b).

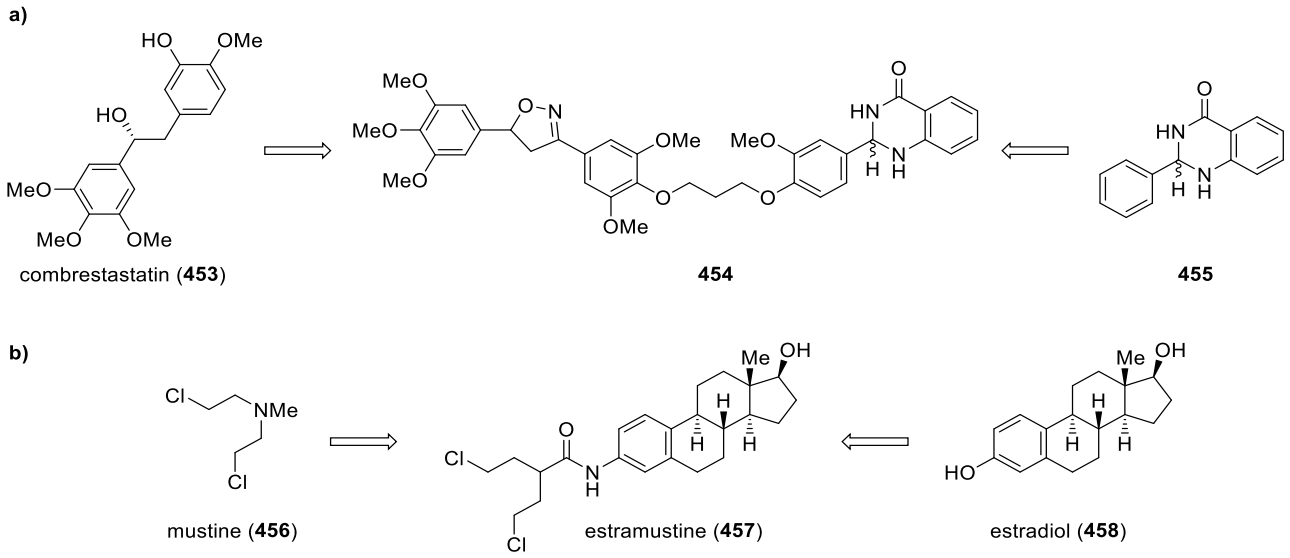

Figure 4.8 Examples of a) linked and b) joined pharmacophores

The final two structural classes of hybrid drugs address the tendency of linked and joined molecules to quickly balloon in molecular weight. To make economic use of structural elements, designs employing overlapped or merged pharmacophores attempt to have structural motifs perform multiple biologic roles. If these is some structural similarity between both pharmacophores the common elements may be overlapped to minimise the size of the final molecule, such as in the case of triciferol[56] (**460**, Figure 4.10a). In some cases, this overlapping of pharmacophores can be taken further to a point where one pharmacophore is almost entirely encompassed by the second, leading to a merged pharmacophore design. To accomplish this without loss of activity generally requires considerable structural similarity between the two pharmacophores but can produce remarkable results such has azatoxin[57] (**463**) where similarity

between the two constitutive pharmacophores of ellipticine (**462**) and etoposide (**464**) can be clearly observed (Figure 4.10b).

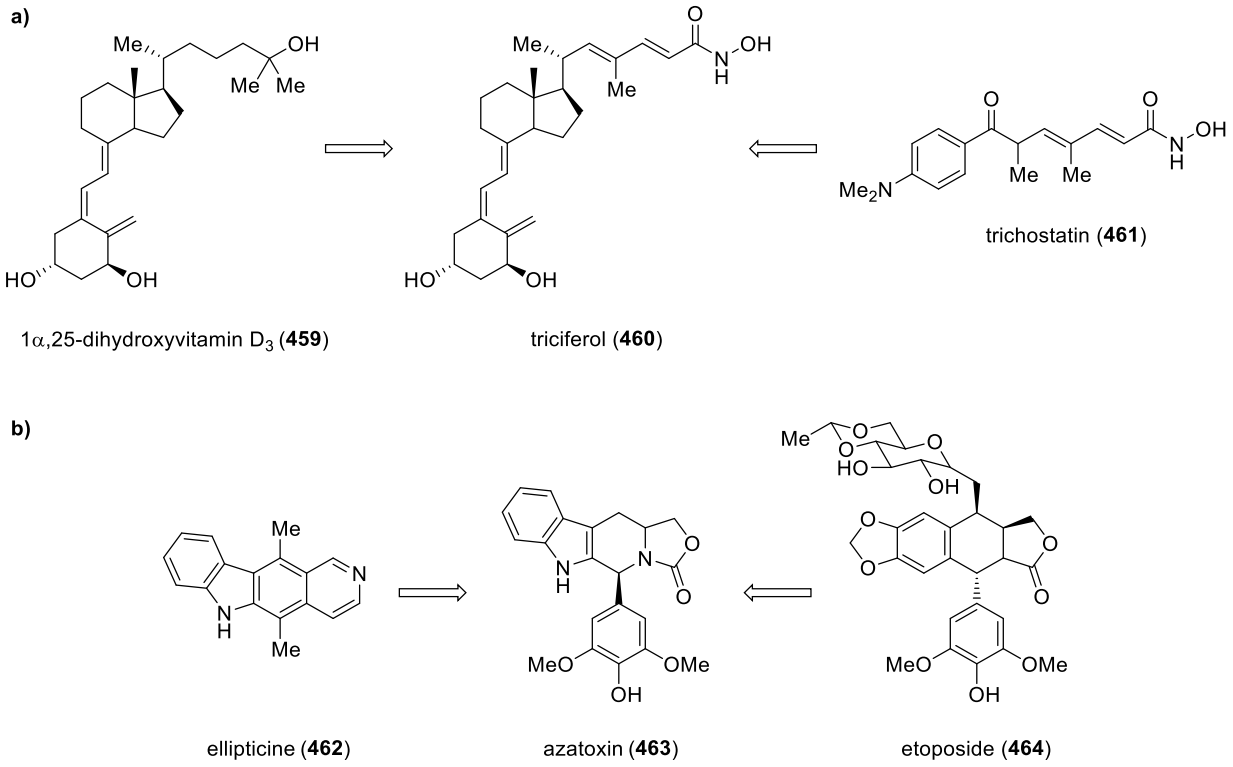

Figure 4.9 Examples of a) overlapped and b) merged pharmacophores

4.3 Design of Novel Hybrid HDAC/HIV-1 Protease Inhibitors

4.3.1 Rational for a Hybrid Drug Approach

Considering the early promise associated with the use of HDAC inhibitors in HIV treatment and our groups long standing interest in the development of hybrid HDAC inhibitor molecules, it was envisioned that we could design a hybrid inhibitor to introduce the advantages of hybrid drug design (*vide supra*) to the arena of HIV treatment. It should be noted that the work outlined in this chapter does not represent the first attempt by the Gleason group to develop a hybrid inhibitor to target latent HIV infection. Investigations by C. Doyle resulted in the preparation of several HDAC/NNRT (**465**, **466**, and **467**) hybrid inhibitors and a single HDAC/NRT (**468** hybrid inhibitor (Figure 4.10).[58] While the HDAC/NNRT hybrid inhibitors were successfully shown to both inhibit HDAC and reverse transcriptase activity their further development was abandoned due to their failure to lead to latent HIV reactivation. Similarly, the HDAC/NRT hybrid inhibitor was also not investigated further as it demonstrated poor HDAC inhibitor activity.

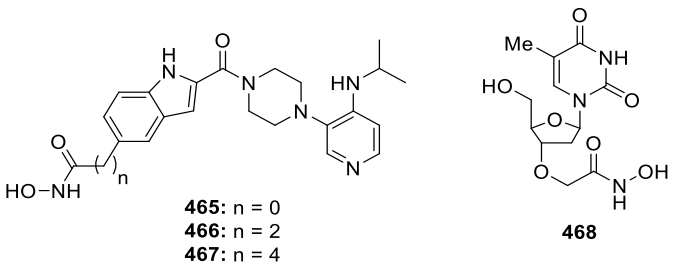

Figure 4.10 HDAC/(N)NRT hybrid inhibitors developed by Doyle and Gleason

In tackling HIV infection for a second time, a different tactic was proposed for reducing viral reservoirs and preventing undesired post reactivation infection of healthy cells. It was hypothesised that replacing reverse transcriptase inhibitor activity with HIV-1 PR inhibitor activity

would prevent the maturation of infectious virions by the newly activated cells, thus supressing the spread of infection. This downstream inhibition of the HIV lifecycle is in contrast to the function of HDAC/RT hybrid inhibitor where inhibition of RT must take place in a separate, newly infected cell and not in it the latently infected cell undergoing reactivation by HDAC inhibition. By targeting the inhibition of two enzymatic processes within the same cell, a HDAC/HIV-PR hybrid inhibitor can take full advantage of a hybrid drug's ability to ensure inhibitors of both enzymes are present in the same location at the same time to perhaps provide superior results to combination therapies.

4.3.2 General HDAC Inhibitor Design

The design of HDAC inhibitors is largely dictated by the relative simplicity of zinc dependant HDAC active site. The HDAC ligand binding pocket is an 11 Å tunnel at the base of which is located a catalytically active Zn^{2+} cation (Figure 4.11).[59] The entrance to the tunnel is a narrow opening of 5.5 by 4.5 Å, evolved for the to accommodate the aliphatic chain of lysine residues, with the walls of the binding pocket being lipophilic. These features are reflected in the molecular structures of HDAC inhibitors with HDAC inhibitors being constructed of complementary structural motifs (Figure 4.12).

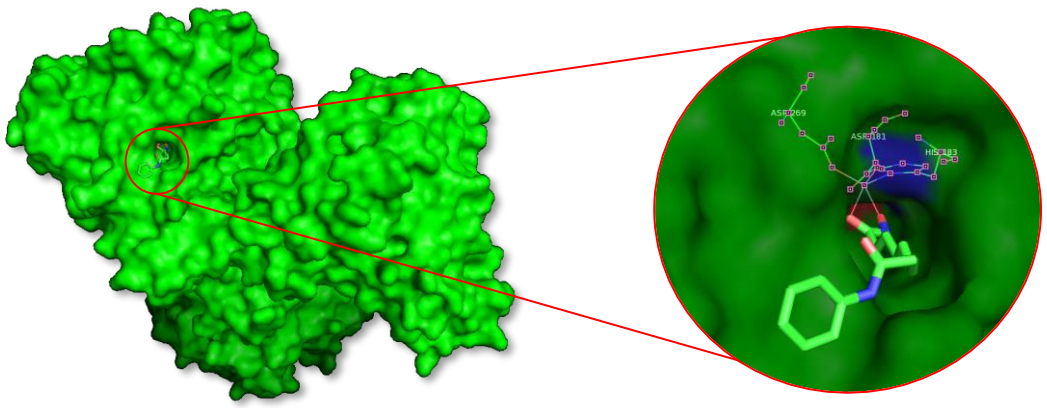

Figure 4.11 Co-crystal structure of HDAC2 and vorinostat (**469**) illustrating the extension of the linker away from the cap group on the surface of the enzyme allowing the hydroxamic acid to engage the zinc atom at the end of the lipophilic tunnel (PDB: 4LXZ)

There are three central structural units in the majority of HDAC inhibitors. They are (i) a cap group, (ii) a lipophilic linker, and (iii) the key zinc binding group. A large degree of structural diversity may be tolerated in the cap group as it rests on the surface of the enzyme. However, some level of isoform selectivity can be derived through careful cap group design. Significantly less variation is tolerated in the linker. Due to the hydrophobic nature of the enzyme pocket the linker is invariably nonpolar. Although, this demand does not limit it to only aliphatic structures, with olefins and aromatic rings successfully employed to increase rigidity and/or participate in π-π interactions. Finally, at the end of the linker is the zinc binding group which is responsible for chelation to the catalytically active Zn^{2+}. Many chemical functional groups can perform this role with their common feature being at least one Lewis basic atom. Such functional groups include: *ortho*-amino anilides, *N*-formyl hydroxylamines, epoxy ketones, carboxylic acids, thiols, and mercapto amides. In most cases these act as bidentate ligands for zinc.

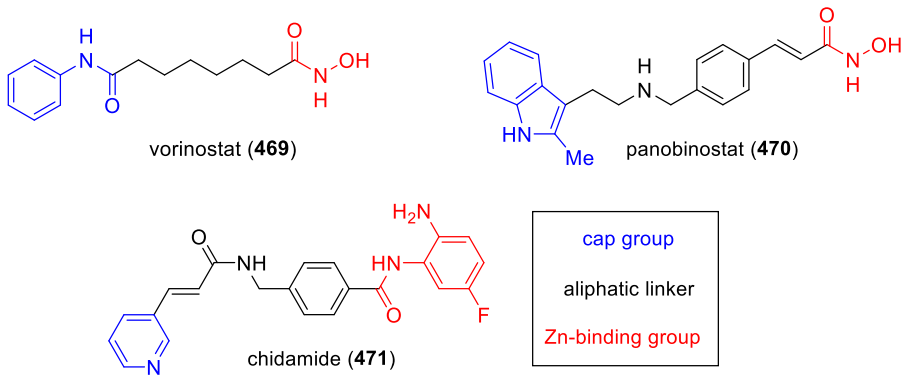

Figure 4.12 Illustration of the design principles common to most HDAC inhibitors

While the use of HDAC inhibitors for the treatment of HIV infection is of great interest, HDAC inhibitors have to date found the greatest utility in the management of cancer. Examples of FDA approved drugs in this class include vorinostat (**469**) for the treatment of cutaneous T-cell lymphoma, romidepsin for cutaneous and peripheral T-cell lymphoma, belinostat for the management of refractory peripheral T-cell lymphoma, panobinostat (**470**) for use in the treatment of multiple myeloma, and chidamide (**471**) for peripheral T-cell lymphoma.[60] Currently there are no HDAC inhibitors approved for use in humans for the treatment of HIV infection.

4.3.3 HIV-1 Protease and Inhibitors Thereof

HIV-1 Protease is a 22 kDa homo-dimeric retroviral aspartyl protease.[61, 62] As stated in section 4.1.2, its function is integral to the formation of functional viral enzymes, which are key to producing new infectious HIV virions. Interestingly, HIV-1 PR is synthesised as part of the Gag-Pol which contains the other viral enzymes (*i.e.* reverse transcriptase, RNase H, and integrase).[63] This necessitates an initial auto-processing step wherein the protease portion of the polyprotein preforms an intramolecular peptide bond cleavage to assemble the more active HIV-1 PR homodimer. This homodimer is then able to carry out a series of intermolecular peptide bond cleavages to facilitate the maturation of reverse transcriptase and integrase.[64]

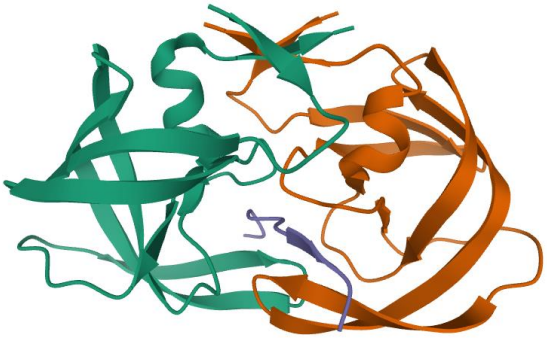

Figure 4.13 X-Ray crystal structure of HIV-1 protease homodimer complexed with gag-pol (blue) (PDB:1KJF)

At the centre of the HIV-1 PR C_2-symmetric dimer are two Asp25-Thr26-Gly27 triads, one found on each polypeptide monomer. While the Asp25 and Asp25′ residues are catalytically active, Thr26, Thr26′, Gly27, and Gly27′ are evolutionarily conserved but their role is unknown.[65] In the active site the two aspartate residues are brought into proximity along with a proton and a molecule of water (Figure 4.14). This monoprotonated state is supported by the pH-rate profile of the enzyme[66] and the key role of the water molecule has been established by ^{18}O labelling studies.[67] Once the enzyme binds to the peptide substate , the aspartic acid residue (Asp25) activates the amide carbonyl while the complementary aspartate residue (Asp25′) activates the water molecule towards 1,2-addition to the carbonyl. Subsequent proton transfer to the amide nitrogen is facilitated by Asp25 and Asp25′ with collapse of the tetrahedral intermediate affording the hydrolysed peptide products. In total, nine sites within the Gag-Pol polyprotein, are cleaved by HIV-1 PR in order to produce a mature HIV virion.

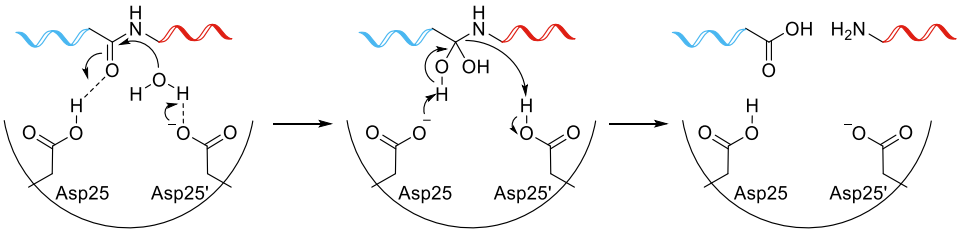

Figure 4.14 HIV-1 protease peptide bond hydrolysis mechanism

It has been shown that the immature PR embedded within the Gag-Pol is as much as ten thousand-fold less sensitive to inhibition by competitive PR inhibitors (specifically ritonavir) when compared to the free mature enzyme.[68] The indispensable nature of mature HIV-1 PR to the HIV life cycle as made it a popular target for HAART.

To date the FDA has approved ten HIV-1 PR inhibitors for use in humans. They are saquinavir (1996), indinavir (1996), ritonavir (1996), nelfinavir (1997), amprenavir (1999), lopinavir (2000), fosamprenavir (2003), atazanavir (2003), tipranavir (2005), and darunavir (2006).[8] All ten are competitive inhibitors of HIV-1 PR and accordingly all bind to the Asp25 and Asp 25' catalytic residues. To accomplish this, each possess a hydroxyl group at the core of the active molecule, able to hydrogen-bond to the active site and thus function as transition state mimics (Figure 4.15). Additionally, PR inhibitors take advantage of non-covalent interactions with the generally conserved residues Gly27, Asp29, Asp30, and Gly48 to increase their binding potential. This along with the development of more recent PR inhibitors through modification of approved drugs has led to several structural motifs appearing repeatedly in PR inhibitor design (*e.g.* benzyl groups, *para*-aminophenylsulfonamides).

Upon first inspection, there appears to be little requirement for the large number of approved HIV-1 PR inhibitors. They all target the same enzyme and it is the only protease HIV-1 encodes for and produces. The issue successive generations of HIV-1 PR inhibitors attempt to

address is the development of PR inhibitor resistance. As result of HIV reverse transcriptase lacking any editing function, HIV can mutate at a rapid rate, resulting in a viral pool containing species with almost any conceivable mutation.[69] This coupled with lifelong treatment with PR inhibitors provides the perfect Darwinian environment for resistance to develop and treatments to rapidly become ineffective.[70] What makes this issue most alarming is that as these mutations for drug resistance are fostered in the wider infected population it becomes increasingly likely that newly infected individuals will become infected with a resistant HIV strains making frontline HAART less effective. This perennial problem makes a strong argument for the need to investigation new PR inhibitor designs and to continue to work towards a cure, despite the proven success of HAART over the past few decades.

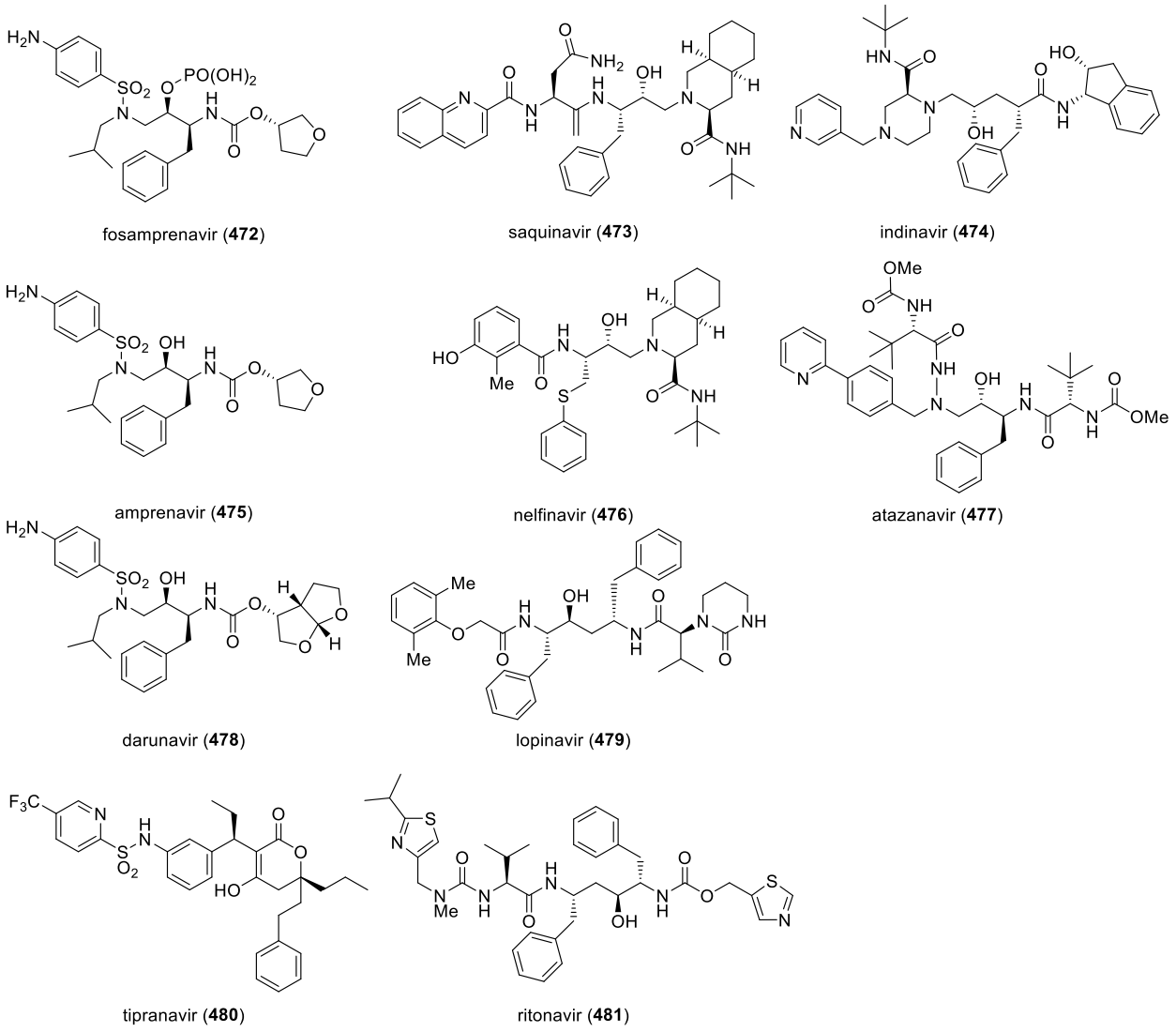

Figure 4.15 FDA Approved HIV-1 protease inhibitors oriented and arranged to highlight common structural features.

4.3.4 Proposed HDAC/HIV-PR Design

As it was intended that the HDAC/HIV-1 RP hybrid inhibitors designed in this project would provide a proving ground for combining these specific biological functions and a possible launch point for SAR studies, it was reasoned an overlapped hybrid design approach would be best suited. This would allow for some degree of independent variation to be made to each pharmacophore while minimising the overall size of the structure. Since HDAC inhibitors can

accommodate a large degree of variation in the structure of the HDAC inhibitor's cap group, attention was initially focused on where modification to a known HIV-1 PR inhibitor skeleton could be made. With darunavir representing the most recently approved PR inhibitor it was selected to be the central scaffold for the HIV-1 PR inhibitor pharmacophore. To determine where modifications to the darunavir structure could be made, the X-ray crystal structures of HIV-1 PR co-crystallised with darunavir was examined.

Upon inspection of the structure it was clear that the heteroatom functionality of darunavir is key to its activity, with the molecule forming many hydrogen bonds to residues Asp25, Asp 25', Gly27', Asp 29', and Asp30, within the active site. Wishing for the design not to interfere with these hydrogen bonds and due to these sites being located deep within the active site, attention was placed on the benzyl fragment. While C-H–π interactions are observed with Val82 and Pro81 at distances of between 3.3 and 4.0 Å, the group lies with the *p*-hydrogen orientated to the outside of the active site. This observation lead to the assertion that the phenyl group would be a suitable site for structural modification and could provide a suitable replacement for the cap group of the HDAC inhibitor pharmacophore.

To complete the HDAC inhibitor pharmacophore, inspiration was lifted from the structure of vorinostat, as its phenyl amide cap group is closely mimicked by darunavir's phenyl group. Additionally, vorinostat's ability to inhibit a broad spectrum of HDAC isoforms made it an attractive selection as any observed isoform selectivity could be attributed to the presence of the HIV-PR pharmacophore. By placing a saturated aliphatic linker at the *para* position of the phenyl ring and terminating the linker with a hydroxamic acid, the overlapped hybrid molecule **482** containing both the requisite HDAC and HIV-PR inhibitor pharmacophores was envisioned

(Figure 4.17)**.** Critically, this design fully incorporates the cap, lipophilic linker, and zinc binding group elements of classic HDAC inhibitors while retaining all darunavir's key structural features.

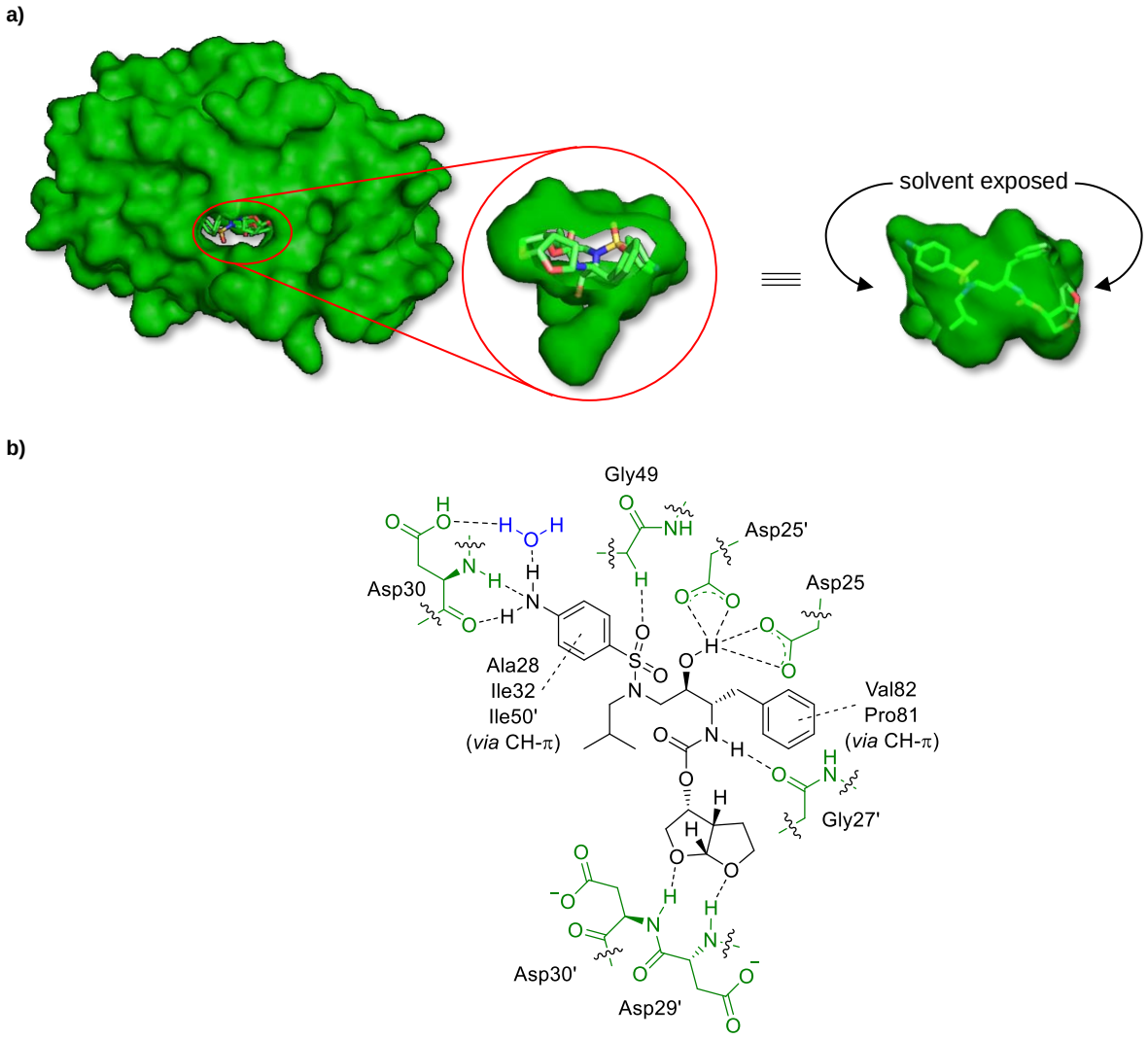

Figure 4.16 a) X-ray crystal structure of HIV-1 protease co-crystallised with darunavir (**478**)(PDB:1T3R) and b) schematic of key interactions

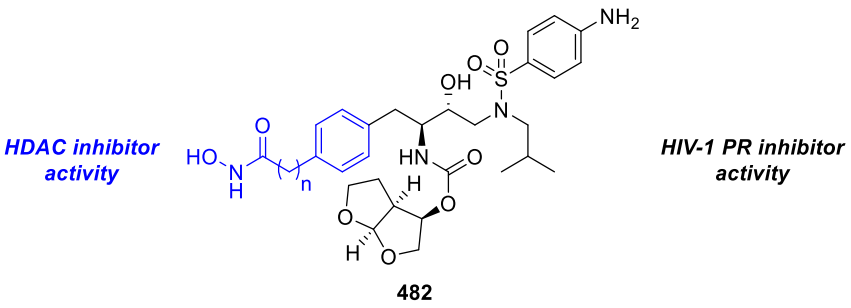

Figure 4.17 Initial design of darunavir based HDAC/HIV-1 PR hybrid inhibitor

Looking at the proposed structure from an HDAC inhibitor viewpoint, the benzyl group is a reasonable replacement for the phenyl amide cap group of vorinostat and leads this design squarely into the realm of overlapped hybrid drug design. The use of a long, flexible, linear linker was selected for several reasons beyond its similarity to vorinostat. The flexibility of the linker allows for it to easily adopt a conformation least detrimental to PR inhibition. Its location at the periphery of the active site and length provides some similarity to the polypeptide fragments that extend from either side of the PR active site when it engages Gag-Pol. Finally, this placement of the terminal hydroxamic acid allows it to be solvent exposed to minimise deleterious interactions within the PR binding site. Being convinced that this design approach was a highly suitable starting point attention shifted to retrosynthetic analysis.

4.4 Synthesis of HDAC/HIV-1 Protease Inhibitors Hybrid

4.4.1 Retrosynthetic Analysis

Owing to its status as an FDA approved drug, many syntheses of darunavir and its derivatives are to be found in the organic synthesis literature. Many of the approaches begin with the commercially available epoxide **484** (Scheme 4.1). Unfortunately, epoxide **484** lacks a synthetic handle for the installation of the HDAC inhibitor unit and the corresponding aliphatic linker. As such, a surrogate of epoxide **484** displaying a bromide at the *para*-position (epoxide **485**) was envisioned as to allow for Suzuki-Miyaura cross-coupling of the alkyl chain at a late stage in the synthesis.

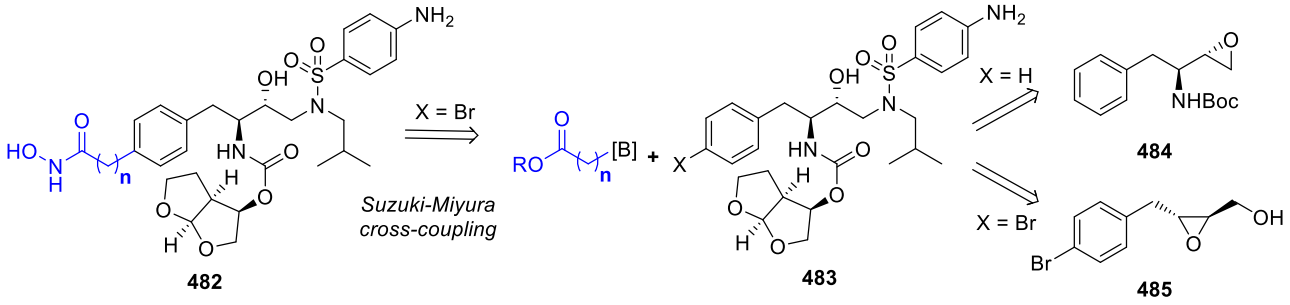

Scheme 4.1 Late stage Suzuki-Miyaura cross-coupling approach

Confident in being able to prepare chiral epoxide **485** through a Sharpless epoxidation, attention was turned to addressing the synthesis of hexahydrofuran[2,3-*b*]furan portion of darunavir. Literature procedures for the enantioselective construction this moiety requires nine steps,[71] greatly increasing the complexity of the synthesis necessary to prepare the target hybrids. To simplify the task at hand other, more synthetically tractable side chains were investigated. Fortunately, there exists a large body of work on the development of HIV-1 protease analogues for the purposes of overcoming emergent viral drug resistance. Many of these studies investigate

the replacement of the hexahydrofuran[2,3-*b*]furan allowing for the reported data on the activity of these analogues to inform the selection of simpler substituent.

Efforts reported by Tidor examined the effects of various amides, benzamides, and peptides on activity of several drug resistant strains of HIV-1 protease.[72] A highly potent subset of these molecules where those decorated with an α-N-acetyl valine in place of the hexahydrofuran[2,3-*b*]furan. The most potent member of the series, MIT-2-KB-86 (**486**), was reported to have a subnanomolar binding affinity of 0.084 nM against wild-type HIV-1 protease. Although this is more than an order of magnitude greater than for darunavir (K_i = 0.008 nM) it is well in the range of other effective HIV-1 protease inhibitors such as atazanavir (K_i = 0.046 nM), tipranavir (K_i = 0.088 nM), and saquinavir (K_i = 0.065 nM) while performing better than indinavir (K_i = 0.18 nM), nelfinavir (K_i = 0.28 nM), and amprenavir (K_i = 0.10 nM). From these results target structure **482** was revised to incorporate the αN-acetyl valine fragment giving the final HDAC/HIV-1 protease hybrid inhibitor design (**487**, **488**, **489**; Figure 4.18).

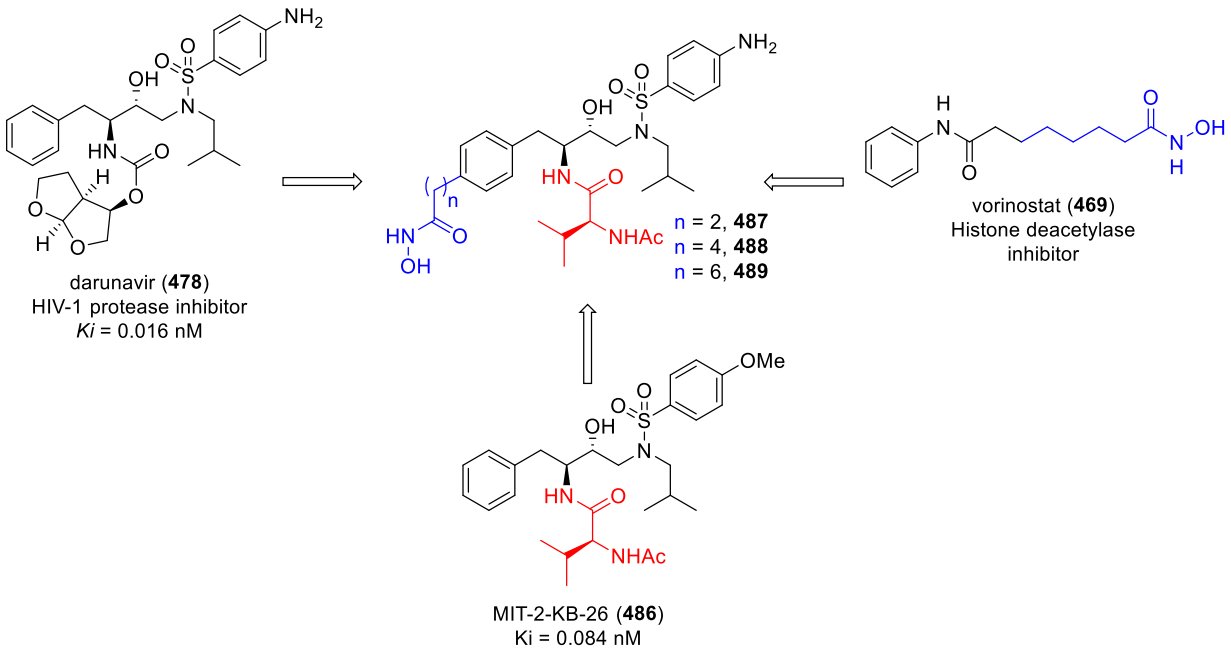

Figure 4.18 Final HDAC/HIV-1 protease hybrid inhibitor design

4.4.2 Chemical Synthesis

The synthesis commenced with the preparation of enantioenriched epoxide **495**. *Para*-bromophenyl magnesium bromide was prepared from 1,4-dibromobenzene and treated with allyl bromide to afford arene **491** contaminated with 1,4-diallylbenzene. As separation of the two products proved difficult, the mixture was subjected to ozonolysis after which short path distillation afforded an 82% yield of aldehyde **492** which solidified as a white solid upon standing. Wittig olefination with (ethoxycarbonylmethyl)triphenylphosphonium bromide in DCM followed by DIBAL reduction of the α,β-unsaturated ester gave allylic alcohol **493** in 91% yield. Finally, subjecting allylic alcohol to standard Sharpless asymmetric epoxidation conditions provided the key epoxide intermediate **495** in 75% yield and 97% ee.

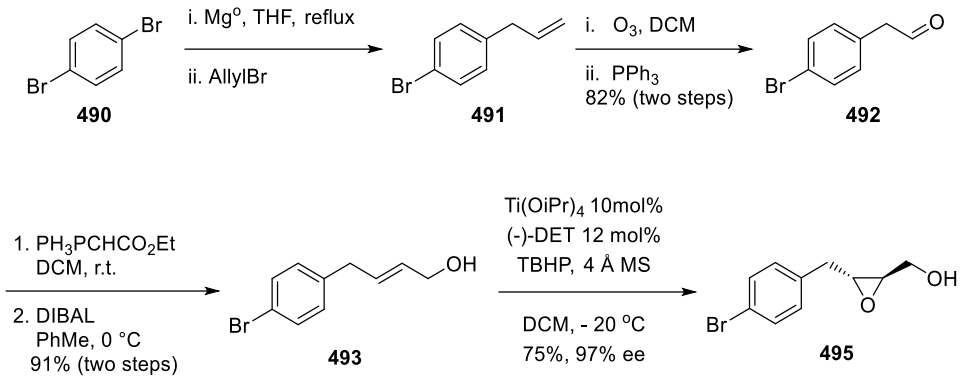

Scheme 4.2 Synthesis of enantioenriched epoxide **51**

From epoxide **495**, azide **496** was synthesised through regioselective epoxide opening with TMS-azide mediated by titanium tetraisopropoxide, providing the product as a single regioisomer in 82% yield. Selective tosylation of the primary alcohol was achieved using catalytic dibutyltin oxide and proceeded in yield of 94%. Subsequent nucleophilic displacement with isobutyl amine and installation of the sulfonimide with *para*-nitrobenzenesulfonyl chloride afforded sulfonimide **499** in a good yield of 81%. Staudinger reduction followed by EDC peptide coupling with N-acetyl valine provided access to aryl bromide **501** in 57% yield over two steps. Introduction of the peptide fragment also provided a point where diastereomers could be separated by column chromatography for batches of epoxide prepared with low enantioselectivity. With intermediate **501** in hand it was decided that investigations into the introduction of the linker group could commence.

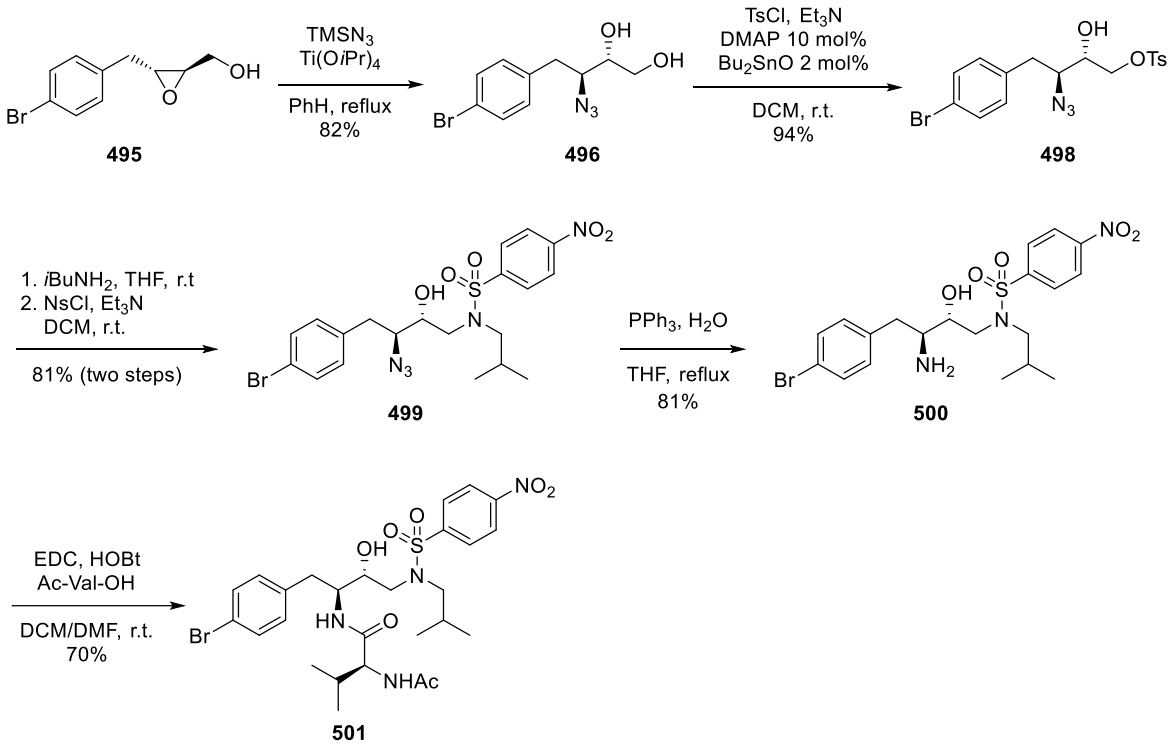

Scheme 4.3 Synthesis of key aryl bromide intermediate **501**

Initial investigations employing standard conditions for alkyl Suzuki-Miyaura cross-couplings failed to provide the desired product (Scheme 4.4). These failures continued despite changes to reaction temperature (r.t. to 50 °C), base (Cs_2CO_3, K_2CO_3, K_3PO_4), solvent (THF, DMF, PhMe, H_2O) and ligand (dppf, PPh_3, OAc), with the desired product **57** never being identified even in trace amounts.

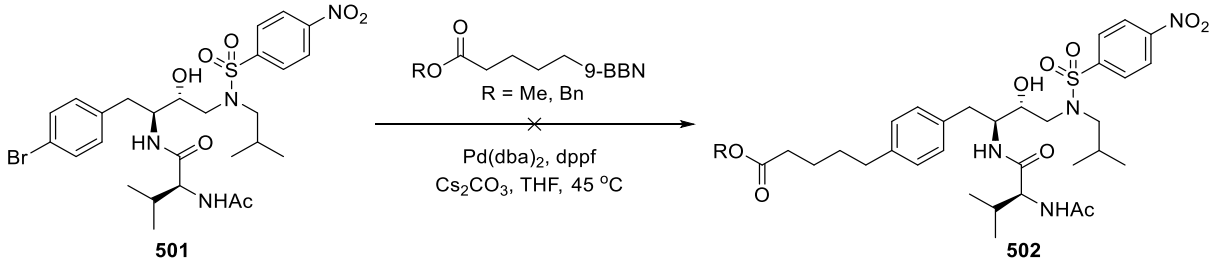

Scheme 4.4 Failed Suzuki-Miyaura cross-coupling

Frustrated by the lack of progress, intermediates earlier in the synthetic route were examined for suitability towards cross-coupling. While epoxide **495** provided a reasonable 59% yield of the expected product (**503**) the most informative reaction was that of azide **499.** Here it was observed that the intended cross-coupling had been achieved to yield benzyl ester **504**. However, this was complicated by the observation of a concomitant Smiles rearrangement, likely prompted by the presence of the para-nitro group decorating the aryl sulfonimide. As the use of a late-stage Suzuki-Miyaura cross-coupling was intended to allow for easy diversification of the HDAC inhibitor portion of the hybrid, the preparation of epoxide **503** was not viewed as a viable alternative synthetic route and instead efforts were made to suppress the undesired Smiles rearrangement.

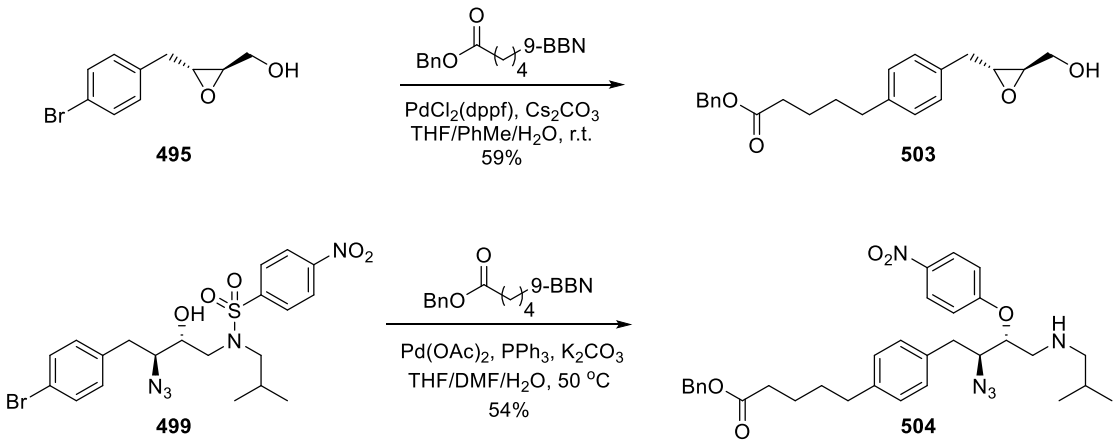

Scheme 4.5 Successful Suzuki-Miyaura cross-couplings

To examine if it was in fact the nitro group which was leading to issues, a simplified system, phenylsulfonamide **506**, lacking the *para*-nitro group, was quickly prepared from amine **505**. Additionally, reduction of the azide and protection of the resulting primary was also carried out as the acetamide was thought to be more comparable to the valine moiety in the original

substrate. Gratifyingly, subjecting sulfonimide **506** to palladium(0) cross-coupling conditions with JohnPhos afforded the expected cross-coupled product **507** in a reasonable 68% yield.

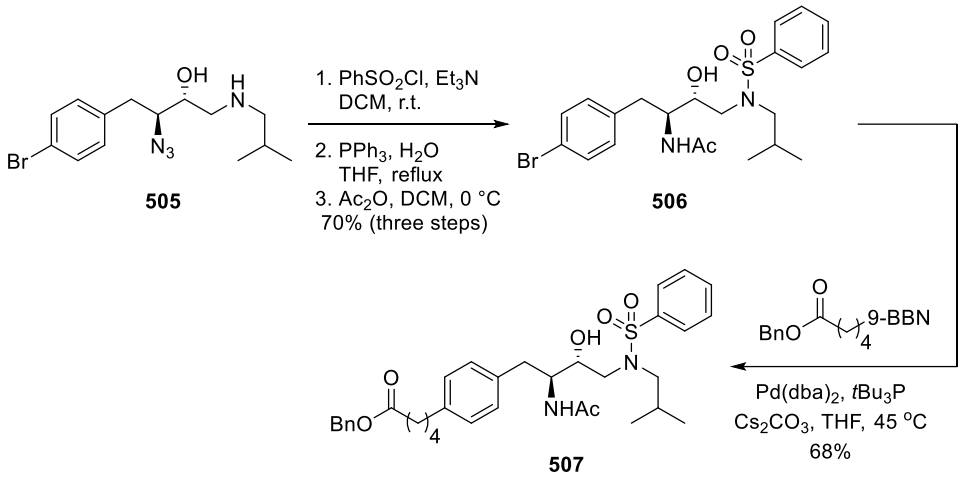

Scheme 4.6 Successful cross coupling of model substate **506**

With the successful cross-coupling of sulfonimide **506** achieved it was decided that reduction of the *para*-nitro group would be conducted prior to subjecting intermediate **501** to cross-coupling conditions. It was reasoned that by reducing the electrophilicity of the *ipso*-carbon the Smiles rearrangement could be inhibited. The use of aniline **508** was initially discounted as amines are occasionally problematic substates in transition metal catalysed transformations as they may compete for ligand binding sites on the metal leading to reaction inhibition. However, in this case it was believed that the *para*-sulfonimide could be enough to deactivate the aniline towards coordination.

Reaction of the nitro group with tin dichloride proceeded in quantitative yield with the subsequent cross-coupling giving the long-sought ester products **509**, and **510** in 65%, and 61% yield respectively. From this point introduction of the hydroxamic acid moiety through treatment

with hydroxylamine under alkaline conditions, afforded hybrid inhibitors **488** and **489** in 59% and 63% yield respectively.

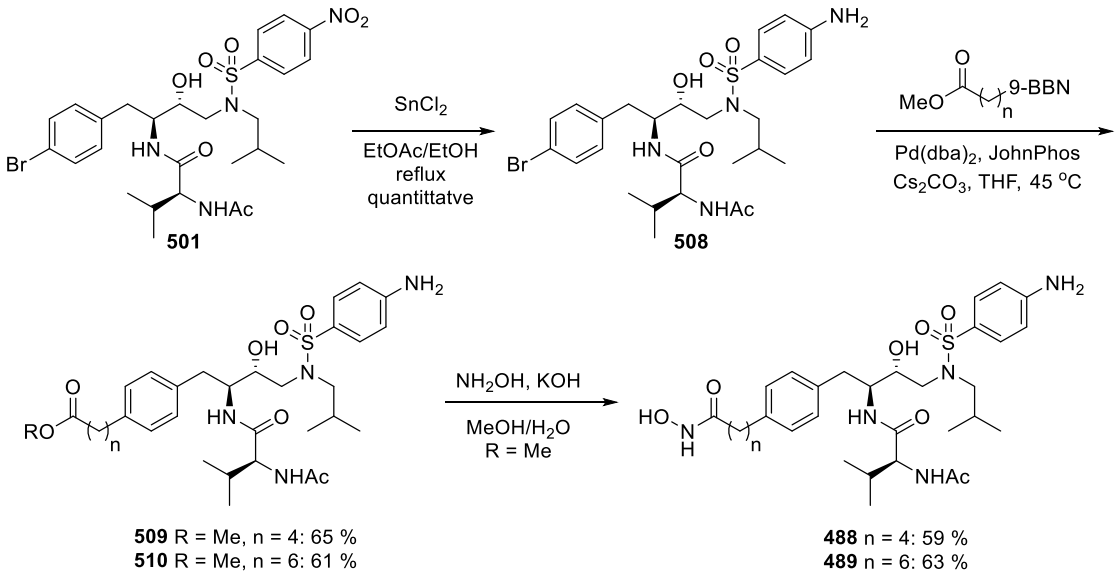

Scheme 4.7 Preparation of hybrid inhibitors **488** and **489**

The preparation of the final inhibitor in the series (**487**) required that a different strategy be employed as the hydroboration of the necessary unsaturated ester (methyl acrylate) was not possible. Instead, a Grubbs' cross-metathesis between olefin **511** (prepared *via* Suzuki-Miyaura coupling with potassium vinyltrifluoroborate[73]) and excess methyl acrylate was performed to introduce the requisite methyl ester. Subsequent hydrogenation of α,β-unsaturated ester **512** afforded the necessary aliphatic ester **70** in a low 31% yield for the two steps. Ester **513** was not taken on further to the hydroxamic acid due both to the very small amounts of ester **513** synthesized in the first successful attempt and the poor initial biological data acquired (*vide infra*) for inhibitors **488** and **489**.

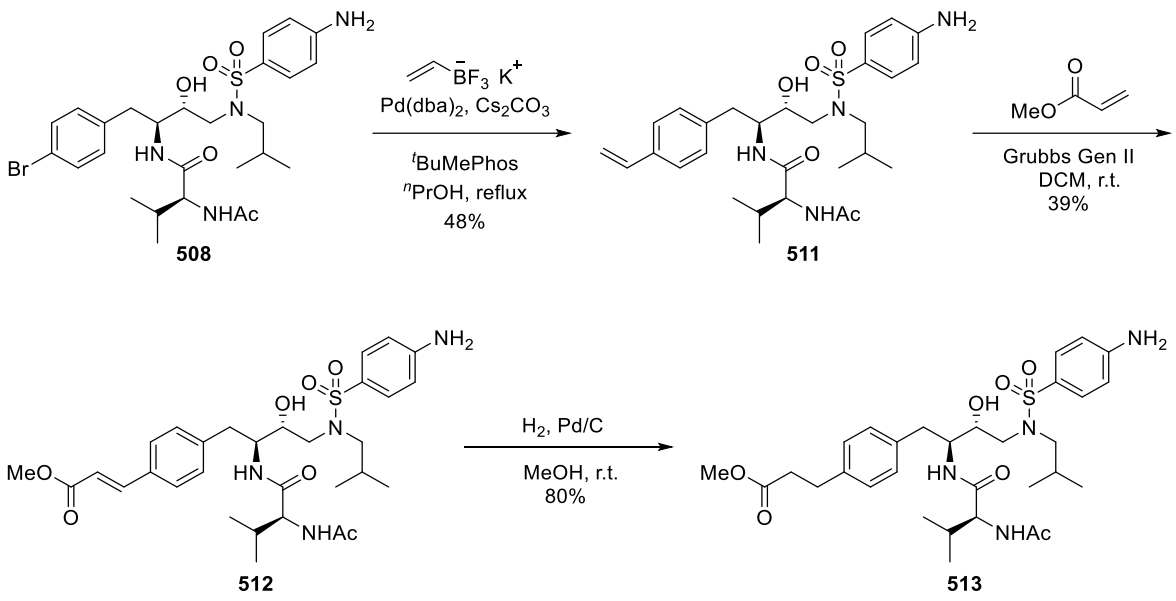

Scheme 4.8 Preparation methyl ester **513**

4.5 Biological Evaluation of Hybrid Molecules

4.5.1 HDAC Inhibition Assay

With a HDAC/PR hybrid inhibitors **488** and **489** in hand their HDAC inhibition activity was investigated by fluorogenic assay. The methodology for this *in vitro* assay was adapted from methods developed by Schwienhorst,[74] Mazitschek,[75] and Olsen[76] and is designed around a two-step enzymatic process outlined in Scheme 4.9. In the assay a small peptide surrogate substrate (*e.g.* Boc-Lys(Ac)-AMC, **514**) containing an acylated lysine residue and a covalently linked fluorophore (*e.g.* 7-amino-4-methylcoumarin, AMC, **516**), is used to report enzymatic activity. The assay is designed such that the fluorophore is quenched in the absence of HDAC activity. To accomplish this a two-step protocol is used wherein in step one HDAC cleaves the ε-N-acetyl group of the lysine residue which allows it to be recognised and processed by trypsin in step two. Trypsin then cleaves the fluorophore from the peptide substate thus activating the fluorophore. In the case of AMC the switch controlling its fluorescent properties is the amide bond used to covalently link it to the substate. As the amide is electron withdrawing it disrupts the electronic push-pull character of the amine-lactone system the chromophore has smaller dipole and correspondingly poor fluorescence. Once the amide is cleaved by trypsin the amine may donate electron density through the conjugated system to the lactone increasing the dipole and affording greatly improved fluorescent properties. In the presence of HDAC inhibitors the lysine residue cannot be cleaved by HDAC and is thus not subsequently processed by trypsin resulting in low fluorescence.

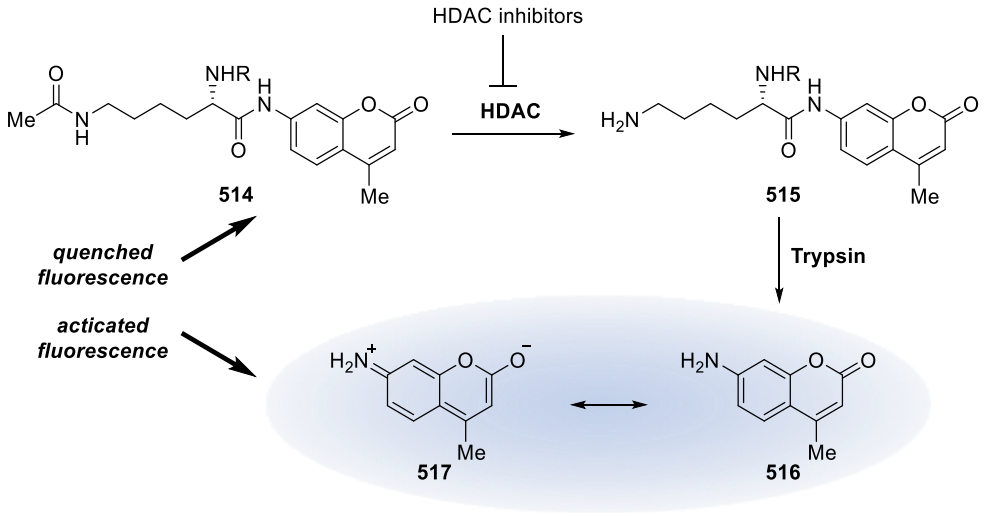

Scheme 4.9 Enzymatic processing of HDAC inhibitor assay substrates

While substrate **514** has been routinely used by the Gleason group it has been shown to perform poorly and require large assay concentration of HDAC. To address this Mazitschek developed a tripeptide substrate where the Boc group of substrate **514** has been replaced by Ac-Leu-Gly.[75] This new substrate was described to have higher HDAC affinity and allowed for the concentration of HDAC in the assay to be lowered. As this work represented first use of substate **518** in the Gleason group, a synthesis for its preparation from lysine was developed by adapting literature routes. Please refer to section 5.4.2 for details regarding its synthesis.

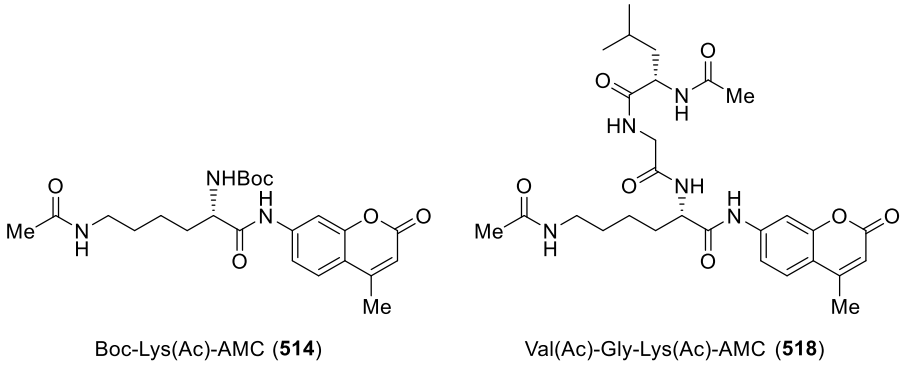

Figure 4.19 First and second generation εN-acetyllysine substrates

4.5.1 Results

Inhibitors **488** and **489** were tested for HDAC inhibition activity against HDACs 3 and 6, a class I HDAC (HDAC3) and class IIB (HDAC6) to investigate if the inhibitors displayed any isoform selectivity. This is important as it is desired that these inhibitors provide inhibition of nuclear HDACs (class I) to reactivate latent HIV while allowing HDACs in the cytoplasm (class IIB) to continue to function normally. To conduct the assays vorinostat was used as a control and eight inhibitor concentrations were used to generate a dose-response curve. K_i values were determined by approximation with the Cheng-Prusoff equation by using the results of two assays run at different substrate concentrations.

Unfortunately, it was found that compound **488** failed to inhibit HDAC3 or 6 within the measurable range of the assay. Inhibitor **489** was observed to inhibit both HDAC3 and 6 with a K_i of 25 nM for HDAC6, roughly equivalent to the K_i of the vorinostat control (20 nM). However, it was six-fold less potent against the intended target nuclear HDAC3 (K_i = 166 nM). These results indicate that hybrid inhibitor design outlined in this chapter are capable of HDAC inhibitory activity but that challenges remain in endowing them with the necessary class I HDAC isoform selectivity.

Table 4.1 HDAC inhibitor assay results for **488** and **489**

HDAC isoform	**Inhibitor**		
	vorinostat	**488**	**489**
HDAC 3	28 nM	Not Active	166 nM
HDAC 6	20 nM	Not Active	25 nM

In addition to the setback caused by the poor activity and isoform selectivity of hybrids **488** and **489**, reports disclosing the disappointing results of HDAC inhibitors began to appear in the literature as the syntheses described in this chapter were reaching completion.[42] As such, only preliminary biological investigations (*vide supra*) were carried out and attention was redirected to other projects (chapters 2 and 3).

4.6 Discussion and Future Direction

Dishearteningly, towards the end of the investigations outlined in this chapter, clinical studies began to demonstrate that HDAC inhibitors consistently failed to reduce the size of the viral reservoirs *in vivo*. In fact, this inability to eliminate viral reservoirs was not limited to studies investigating HDAC inhibitors. Drug/treatment classes targeting other parts of the HIV reactivation pathway (*e.g.* PKC agonists,[77] MAPK agonists,[78] CCR5 antagonists,[79] Tat vaccines,[80] second mitochondria-derived activator of caspases mimetics,[81] inducers of P-TEFb release,[82] activators of Akt pathway,[83] benzotriazole derivatives,[84] epigenetic modifiers,[85] and immunoregulators[86]) all fail to achieve the desired results. A significant divide remains between the potent effects many of these compounds have *in vitro* and the failure of clinical trials to show deceases in the size of latent reservoirs. To date, only studies with nivolumab[87] (an immune check point inhibitor) and romidepsin (**519**)[88] in combination with an immuovaccine have shown a clear change in plasma HIV-1 RNA with a subsequent decrease in viral reservoirs. However, in neither case was the time to viral rebound extended after interruption of HAART.

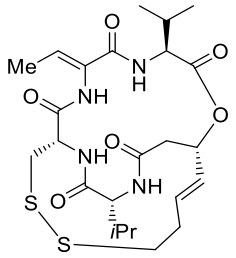

romidepsin (**519**)

Figure 4.20 Romodepsin, the only HDAC inhibitor shown to have shown clear clinical benefits in decreasing HIV reservoirs

Current perspectives on the consistently poor performance of HIV reactivations as a treatment vector are that targeting a single mechanism is insufficient to reactivate the majority of

latent cells. This coupled with the need for treatments to penetrate all tissue sites where HIV reservoirs are located provide issues that significantly complicate the rational design of hybrid reactivation/antiretroviral agents. However, the recent observation that the HDAC/PI3K hybrid inhibitor fimepinostat (**520**, an anticancer drug currently undergoing phase II trials for the treatment of diffuse large B cell lymphoma and thyroid cancer) effectively reverses HIV latency *ex vivo* may indicate a path forward in the use of hybrid drug design to target viral reactivation alone.[89] Such findings suggest that future endeavours into anti-HIV hybrid drug design should focus on the development of reactivation agents with the aim to use them in combination with classic HAART antiretrovirals in a curative treatment regimen.

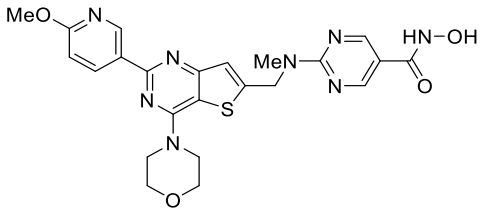

fimepinostat (**520**)

Figure 4.21 Structure of HDAC inhibitor fimepinostat

Ultimately, the present lack of an intimate understanding of all cellular pathways and molecular mechanisms impacting HIV gene expression, productive viral replication, and/or silencing prevent the organic chemist from constructively engaging in this arena through rational drug design.[90] In the short to medium term efforts in organic synthesis may be put to better use in the development of molecular probes for more detailed exploration of the implicated biochemical pathways.

4.7 References

1. M. S. Gottlieb, H. M. S., P. T. Fan, A. Saxon, J. D. Weisman, Pneumocystis Pneumonia. *Morbidity and Mortality Weekly Report* **1981,** *30*, 250-252.

2. Gilman, S. L., Aids and Syphilis: The Iconography of Disease. *October* **1987,** *43*, 87-107.

3. Gallo, R.; Sarin, P.; Gelmann, E.; Robert-Guroff, M.; Richardson, E.; Kalyanaraman, V.; Mann, D.; Sidhu, G.; Stahl, R.; Zolla-Pazner, S.; Leibowitch, J.; Popovic, M., Isolation of Human T-Cell Leukemia Virus in Acquired Immune Deficiency Syndrome (Aids). *Science* **1983,** *220* (4599), 865-867.

4. Barre-Sinoussi, F.; Chermann, J.; Rey, F.; Nugeyre, M.; Chamaret, S.; Gruest, J.; Dauguet, C.; Axler-Blin, C.; Vezinet-Brun, F.; Rouzioux, C.; Rozenbaum, W.; Montagnier, L., Isolation of a T-Lymphotropic Retrovirus from a Patient at Risk for Acquired Immune Deficiency Syndrome (Aids). *Science* **1983,** *220* (4599), 868-871.

5. Organization, W. H., *Consolidated Hiv Strategic Information Guidelines: Driving Impact through Programme Monitoring and Management*. World Health Organization: 2020.

6. Barré-Sinoussi, F.; Ross, A. L.; Delfraissy, J.-F., Past, Present and Future: 30 Years of Hiv Research. *Nature Reviews Microbiology* **2013,** *11* (12), 877-883.

7. Freed, E. O., Hiv-1 Assembly, Release and Maturation. *Nature Reviews Microbiology* **2015,** *13* (8), 484-496.

8. Lv, Z.; Chu, Y.; Wang, Y., Hiv Protease Inhibitors: A Review of Molecular Selectivity and Toxicity. *HIV AIDS (Auckl)* **2015,** *7*, 95-104.

9. Laskey, S. B.; Siliciano, R. F., A Mechanistic Theory to Explain the Efficacy of Antiretroviral Therapy. *Nature Reviews Microbiology* **2014,** *12* (11), 772-780.

10. Arts, E. J.; Hazuda, D. J., Hiv-1 Antiretroviral Drug Therapy. *Cold Spring Harbor perspectives in medicine* **2012,** *2* (4), a007161-a007161.

11. Miller, V.; Cozzi-Lepri, A.; Hertogs, K.; Gute, P.; Larder, B.; Bloor, S.; Klauke, S.; Rabenau, H.; Phillips, A.; Staszewski, S., Hiv Drug Susceptibility and Treatment Response to Mega-Haart Regimen in Patients from the Frankfurt Hiv Cohort. *Antiviral Therapy* **2000,** *5* (1), 49-55.

12. Churchill, M. J.; Deeks, S. G.; Margolis, D. M.; Siliciano, R. F.; Swanstrom, R., Hiv Reservoirs: What, Where and How to Target Them. *Nature Reviews Microbiology* **2016,** *14* (1), 55-60.

13. Fukazawa, Y.; Lum, R.; Okoye, A. A.; Park, H.; Matsuda, K.; Bae, J. Y.; Hagen, S. I.; Shoemaker, R.; Deleage, C.; Lucero, C.; Morcock, D.; Swanson, T.; Legasse, A. W.; Axthelm, M. K.; Hesselgesser, J.; Geleziunas, R.; Hirsch, V. M.; Edlefsen, P. T.; Piatak, M., Jr.; Estes, J. D.; Lifson, J. D.; Picker, L. J., B Cell Follicle Sanctuary Permits Persistent Productive Simian Immunodeficiency Virus Infection in Elite Controllers. *Nature Medicine* **2015,** *21* (2), 132-9.

14. Fletcher, C. V.; Staskus, K.; Wietgrefe, S. W.; Rothenberger, M.; Reilly, C.; Chipman, J. G.; Beilman, G. J.; Khoruts, A.; Thorkelson, A.; Schmidt, T. E.; Anderson, J.; Perkey, K.; Stevenson, M.; Perelson, A. S.; Douek, D. C.; Haase, A. T.; Schacker, T. W., Persistent Hiv-1 Replication Is Associated with Lower Antiretroviral Drug Concentrations in Lymphatic Tissues. *Proceedings of the National Academy of Sciences* **2014,** *111* (6), 2307-12.

15. Siliciano, J. D.; Kajdas, J.; Finzi, D.; Quinn, T. C.; Chadwick, K.; Margolick, J. B.; Kovacs, C.; Gange, S. J.; Siliciano, R. F., Long-Term Follow-up Studies Confirm the Stability of the Latent Reservoir for Hiv-1 in Resting Cd4+ T Cells. *Nature Medicine* **2003,** *9* (6), 727-8.

16. Whitney, J. B.; Hill, A. L.; Sanisetty, S.; Penaloza-MacMaster, P.; Liu, J.; Shetty, M.; Parenteau, L.; Cabral, C.; Shields, J.; Blackmore, S.; Smith, J. Y.; Brinkman, A. L.; Peter, L. E.; Mathew, S. I.; Smith, K. M.; Borducchi, E. N.; Rosenbloom, D. I. S.; Lewis, M. G.; Hattersley, J.; Li, B.; Hesselgesser, J.; Geleziunas, R.; Robb, M. L.; Kim, J. H.; Michael, N. L.; Barouch, D. H., Rapid Seeding of the Viral Reservoir Prior to Siv Viraemia in Rhesus Monkeys. *Nature* **2014,** *512* (7512), 74-77.

17. Thorlund, K.; Horwitz, M. S.; Fife, B. T.; Lester, R.; Cameron, D. W., Landscape Review of Current Hiv 'Kick and Kill' Cure Research - Some Kicking, Not Enough Killing. *BMC Infectious Diseases* **2017,** *17* (1), 595.

18. Easley, R.; Van Duyne, R.; Coley, W.; Guendel, I.; Dadgar, S.; Kehn-Hall, K.; Kashanchi, F., Chromatin Dynamics Associated with Hiv-1 Tat-Activated Transcription. *Biochimica et Biophysica Acta* **2010,** *1799* (3-4), 275-85.

19. Huang, J.; Wang, F.; Argyris, E.; Chen, K.; Liang, Z.; Tian, H.; Huang, W.; Squires, K.; Verlinghieri, G.; Zhang, H., Cellular Micrornas Contribute to Hiv-1 Latency in Resting Primary $Cd4^+$ T Lymphocytes. *Nature Medicine* **2007,** *13* (10), 1241-7.

20. Williams, S. A.; Greene, W. C., Regulation of Hiv-1 Latency by T-Cell Activation. *Cytokine* **2007,** *39* (1), 63-74.

21. Dahabieh, M. S.; Battivelli, E.; Verdin, E., Understanding Hiv Latency: The Road to an Hiv Cure. *Annual review of medicine* **2015,** *66*, 407-421.

22. Petravic, J.; Rasmussen, T. A.; Lewin, S. R.; Kent, S. J.; Davenport, M. P., Relationship between Measures of Hiv Reactivation and Decline of the Latent Reservoir under Latency-Reversing Agents. *Journal of virology* **2017,** *91* (9), e02092-16.

23. Dahl, V.; Josefsson, L.; Palmer, S., Hiv Reservoirs, Latency, and Reactivation: Prospects for Eradication. *Antiviral Research* **2010,** *85* (1), 286-94.

24. Glozak, M. A.; Sengupta, N.; Zhang, X.; Seto, E., Acetylation and Deacetylation of Non-Histone Proteins. *Gene* **2005,** *363*, 15-23.

25. Barneda-Zahonero, B.; Parra, M., Histone Deacetylases and Cancer. *Molecular Oncology* **2012,** *6* (6), 579-589.

26. Segré, C. V.; Chiocca, S., Regulating the Regulators: The Post-Translational Code of Class I Hdac1 and Hdac2. *Journal of Biomedicine and Biotechnology* **2011,** *2011*, 690848.

27. Reichert, N.; Choukrallah, M. A.; Matthias, P., Multiple Roles of Class I Hdacs in Proliferation, Differentiation, and Development. *Cellular and Molecular Life Sciences* **2012,** *69* (13), 2173-2187.

28. Waltregny, D.; Glénisson, W.; Tran, S. L.; North, B. J.; Verdin, E.; Colige, A.; Castronovo, V., Histone Deacetylase Hdac8 Associates with Smooth Muscle Alpha-Actin and Is Essential for Smooth Muscle Cell Contractility. *The FASEB Journal* **2005,** *19* (8), 966-968.

29. Yang, X.-J.; Seto, E., The Rpd3/Hda1 Family of Lysine Deacetylases: From Bacteria and Yeast to Mice and Men. *Nature Reviews Molecular Cell Biology* **2008,** *9* (3), 206-218.

30. Hubbert, C.; Guardiola, A.; Shao, R.; Kawaguchi, Y.; Ito, A.; Nixon, A.; Yoshida, M.; Wang, X. F.; Yao, T. P., Hdac6 Is a Microtubule-Associated Deacetylase. *Nature* **2002,** *417* (6887), 455-458.

31. Yang, X. J.; Seto, E., The Rpd3/Hda1 Family of Lysine Deacetylases: From Bacteria and Yeast to Mice and Men. *Nature Reviews Molecular Cell Biology* **2008,** *9* (3), 206-218.

32. Bosch-Presegué, L.; Vaquero, A., The Dual Role of Sirtuins in Cancer. *Genes Cancer* **2011,** *2* (6), 648-62.

33. Saunders, L. R.; Verdin, E., Sirtuins: Critical Regulators at the Crossroads between Cancer and Aging. *Oncogene* **2007,** *26* (37), 5489-5504.

34. Gao, L.; Cueto, M. A.; Asselbergs, F.; Atadja, P., Cloning and Functional Characterization of Hdac11, a Novel Member of the Human Histone Deacetylase Family. *Journal of Biological Chemistry* **2002,** *277* (28), 25748-25755.

35. Villagra, A.; Cheng, F.; Wang, H. W.; Suarez, I.; Glozak, M.; Maurin, M.; Nguyen, D.; Wright, K. L.; Atadja, P. W.; Bhalla, K.; Pinilla-Ibarz, J.; Seto, E.; Sotomayor, E. M., The Histone Deacetylase Hdac11 Regulates the Expression of Interleukin 10 and Immune Tolerance. *Nature Immunology* **2009,** *10* (1), 92-100.

36. Williams, S. A.; Chen, L.-F.; Kwon, H.; Ruiz-Jarabo, C. M.; Verdin, E.; Greene, W. C., Nf-Kb P50 Promotes Hiv Latency through Hdac Recruitment and Repression of Transcriptional Initiation. *The EMBO Journal* **2006,** *25* (1), 139-149.

37. Keedy, K. S.; Archin, N. M.; Gates, A. T.; Espeseth, A.; Hazuda, D. J.; Margolis, D. M., A Limited Group of Class I Histone Deacetylases Acts to Repress Human Immunodeficiency Virus Type 1 Expression. *Journal of virology* **2009,** *83* (10), 4749-4756.

38. Rohr, O.; Marban, C.; Aunis, D.; Schaeffer, E., Regulation of Hiv-1 Gene Transcription: From Lymphocytes to Microglial Cells. *Journal of Leukocyte Biology* **2003,** *74* (5), 736-749.

39. Elliott, J. H.; Wightman, F.; Solomon, A.; Ghneim, K.; Ahlers, J.; Cameron, M. J.; Smith, M. Z.; Spelman, T.; McMahon, J.; Velayudham, P.; Brown, G.; Roney, J.; Watson, J.; Prince, M. H.; Hoy, J. F.; Chomont, N.; Fromentin, R.; Procopio, F. A.; Zeidan, J.; Palmer, S.; Odevall, L.; Johnstone, R. W.; Martin, B. P.; Sinclair, E.; Deeks, S. G.; Hazuda, D. J.; Cameron, P. U.; Sékaly, R.-P.; Lewin, S. R., Activation of Hiv Transcription with Short-Course Vorinostat in Hiv-Infected Patients on Suppressive Antiretroviral Therapy. *PLOS Pathogens* **2014,** *10* (11), e1004473.

40. Archin, N. M.; Liberty, A. L.; Kashuba, A. D.; Choudhary, S. K.; Kuruc, J. D.; Crooks, A. M.; Parker, D. C.; Anderson, E. M.; Kearney, M. F.; Strain, M. C.; Richman, D. D.; Hudgens, M. G.; Bosch, R. J.; Coffin, J. M.; Eron, J. J.; Hazuda, D. J.; Margolis, D. M., Administration of Vorinostat Disrupts Hiv-1 Latency in Patients on Antiretroviral Therapy. *Nature* **2012,** *487* (7408), 482-485.

41. Archin, N. M.; Kirchherr, J. L.; Sung, J. A. M.; Clutton, G.; Sholtis, K.; Xu, Y.; Allard, B.; Stuelke, E.; Kashuba, A. D.; Kuruc, J. D.; Eron, J.; Gay, C. L.; Goonetilleke, N.; Margolis, D. M., Interval Dosing with the Hdac Inhibitor Vorinostat Effectively Reverses Hiv Latency. *The Journal of Clinical Investigation* **2017,** *127* (8), 3126-3135.

42. Rasmussen, T. A.; Tolstrup, M.; Brinkmann, C. R.; Olesen, R.; Erikstrup, C.; Solomon, A.; Winckelmann, A.; Palmer, S.; Dinarello, C.; Buzon, M.; Lichterfeld, M.; Lewin, S. R.; Østergaard, L.; Søgaard, O. S., Panobinostat, a Histone Deacetylase Inhibitor, for Latent-Virus Reactivation in Hiv-Infected Patients on Suppressive Antiretroviral Therapy: A Phase 1/2, Single Group, Clinical Trial. *The Lancet HIV* **2014,** *1* (1), e13-e21.

43. Søgaard, O. S.; Graversen, M. E.; Leth, S.; Olesen, R.; Brinkmann, C. R.; Nissen, S. K.; Kjaer, A. S.; Schleimann, M. H.; Denton, P. W.; Hey-Cunningham, W. J.; Koelsch, K. K.; Pantaleo, G.; Krogsgaard, K.; Sommerfelt, M.; Fromentin, R.; Chomont, N.; Rasmussen, T. A.; Østergaard, L.; Tolstrup, M., The Depsipeptide Romidepsin Reverses Hiv-1 Latency in Vivo. *PLOS Pathogens* **2015,** *11* (9), e1005142.

44. Hashemi, P.; Sadowski, I., Diversity of Small Molecule Hiv-1 Latency Reversing Agents Identified in Low- and High-Throughput Small Molecule Screens. *Medicinal research reviews* **2020,** *40* (3), 881-908.

45. Maxwell, J. W.; Falcinelli, S. D.; Nefedov, A.; Dorfmeier, C.; Wu, G.; Dewey, M.; Webber, A. L.; Archin, N. M.; Margolis, D. M.; Hazuda, D. J.; Barnard, R. J. O.; Howell, B. J., Cellular Gene Modulation of Hiv-Infected Cd4 T Cells in Response to Serial Treatment with the Histone Deacetylase Inhibitor Vorinostat. *Journal of virology* **2020,** *94* (13), e00351-20.

46. Divsalar, D. N.; Simoben, C. V.; Schonhofer, C.; Richard, K.; Sippl, W.; Ntie-Kang, F.; Tietjen, I., Novel Histone Deacetylase Inhibitors and Hiv-1 Latency-Reversing Agents Identified by Large-Scale Virtual Screening. *Frontiers in pharmacology* **2020,** *11*, 905-905.

47. Kim, Y.; Anderson, J. L.; Lewin, S. R., Getting the "Kill" into "Shock and Kill": Strategies to Eliminate Latent Hiv. *Cell Host & Microbe* **2018,** *23* (1), 14-26.

48. Spivak, A. M.; Planelles, V., Novel Latency Reversal Agents for Hiv-1 Cure. *Annual review of medicine* **2018,** *69* (1), 421-436.

49. Sadowski, I.; Hashemi, F. B., Strategies to Eradicate Hiv from Infected Patients: Elimination of Latent Provirus Reservoirs. *Cellular and Molecular Life Sciences* **2019,** *76* (18), 3583-3600.

50. Shehu-Xhilaga, M.; Rhodes, D.; Wightman, F.; Liu, H. B.; Solomon, A.; Saleh, S.; Dear, A. E.; Cameron, P. U.; Lewin, S. R., The Novel Histone Deacetylase Inhibitors Metacept-1 and Metacept-3 Potently Increase Hiv-1 Transcription in Latently Infected Cells. *AIDS* **2009,** *23* (15), 2047-2050.

51. Matalon, S.; Palmer, B. E.; Nold, M. F.; Furlan, A.; Kassu, A.; Fossati, G.; Mascagni, P.; Dinarello, C. A., The Histone Deacetylase Inhibitor Itf2357 Decreases Surface Cxcr4 and Ccr5 Expression on Cd4(+) T-Cells and Monocytes and Is Superior to Valproic Acid for Latent Hiv-1 Expression in Vitro. *Journal of Acquired Immune Deficiency Syndromes* **2010,** *54* (1), 1-9.

52. Cui, L.; Su, X.-z., Discovery, Mechanisms of Action and Combination Therapy of Artemisinin. *Expert review of anti-infective therapy* **2009,** *7* (8), 999-1013.

53. Sotgiu, G.; Centis, R.; D'Ambrosio, L.; Migliori, G. B., Tuberculosis Treatment and Drug Regimens. *Cold Spring Harbor perspectives in medicine* **2015,** *5* (5), a017822-a017822.

54. Bayat Mokhtari, R.; Homayouni, T. S.; Baluch, N.; Morgatskaya, E.; Kumar, S.; Das, B.; Yeger, H., Combination Therapy in Combating Cancer. *Oncotarget* **2017,** *8* (23), 38022-38043.

55. Erichsen, H. G.; Nygaard, E., [Prostatic Cancer--Treatment with Extramustine Phosphate(Estracyt). An Easier Application Form]. *Tidsskr Nor Laegeforen* **1974,** *94* (28), 1901-2.

56. Tavera-Mendoza, L. E.; Quach, T. D.; Dabbas, B.; Hudon, J.; Liao, X.; Palijan, A.; Gleason, J. L.; White, J. H., Incorporation of Histone Deacetylase Inhibition into the Structure of a Nuclear Receptor Agonist. *Proceedings of the National Academy of Sciences* **2008,** *105* (24), 8250-8255.

57. Cline, S. D.; Macdonald, T. L.; Osheroff, N., Azatoxin Is a Mechanistic Hybrid of the Topoisomerase Ii-Targeted Anticancer Drugs Etoposide and Ellipticine. *Biochemistry* **1997,** *36* (42), 13095-13101.

58. Doyle, C. Design, Synthesis and Testing of Novel Hybrid Drug Moleules. McGill University, Montreal 2014.

59. Lauffer, B. E.; Mintzer, R.; Fong, R.; Mukund, S.; Tam, C.; Zilberleyb, I.; Flicke, B.; Ritscher, A.; Fedorowicz, G.; Vallero, R.; Ortwine, D. F.; Gunzner, J.; Modrusan, Z.; Neumann, L.; Koth, C. M.; Lupardus, P. J.; Kaminker, J. S.; Heise, C. E.; Steiner, P., Histone Deacetylase (Hdac) Inhibitor Kinetic Rate Constants Correlate with Cellular Histone Acetylation but Not Transcription and Cell Viability. *Journal of Biological Chemistry* **2013,** *288* (37), 26926-26943.

60. Eckschlager, T.; Plch, J.; Stiborova, M.; Hrabeta, J., Histone Deacetylase Inhibitors as Anticancer Drugs. *International journal of molecular sciences* **2017,** *18* (7), 1414.

61. Brik, A.; Wong, C. H., Hiv-1 Protease: Mechanism and Drug Discovery. *Organic and Biomolecular Chemistry* **2003,** *1* (1), 5-14.

62. Prabu-Jeyabalan, M.; Nalivaika, E.; Schiffer, C. A., Substrate Shape Determines Specificity of Recognition for Hiv-1 Protease: Analysis of Crystal Structures of Six Substrate Complexes. *Structure* **2002,** *10* (3), 369-381.

63. Wondrak, E. M.; Nashed, N. T.; Haber, M. T.; Jerina, D. M.; Louis, J. M., A Transient Precursor of the Hiv-1 Protease: Isolation, Characterization, and Kinetics of Maturation. *Journal of Biological Chemistry* **1996,** *271* (8), 4477-4481.

64. Louis, J. M.; Nashed, N. T.; Parris, K. D.; Kimmel, A. R.; Jerina, D. M., Kinetics and Mechanism of Autoprocessing of Human Immunodeficiency Virus Type 1 Protease from an Analog of the Gag-Pol Polyprotein. *Proceedings of the National Academy of Sciences* **1994,** *91* (17), 7970-7974.

65. Mager, P. P., The Active Site of Hiv-1 Protease. *Medicinal research reviews* **2001,** *21* (4), 348-53.

66. Hofmann, T.; Hodges, R. S.; James, M. N. G., Effect of Ph on the Activities of Penicillopepsin and Rhizopus Pepsin and a Proposal for the Productive Substrate Binding Mode in Penicillopepsin. *Biochemistry* **1984,** *23* (4), 635-643.

67. Hyland, L. J.; Tomaszek, T. A.; Roberts, G. D.; Carr, S. A.; Magaard, V. W.; Bryan, H. L.; Fakhoury, S. A.; Moore, M. L.; Minnich, M. D., Human Immunodeficiency Virus-1 Protease. 1. Initial Velocity Studies and Kinetic Characterization of Reaction Intermediates by Oxygen-18 Isotope Exchange. *Biochemistry* **1991,** *30* (34), 8441-8453.

68. Pettit, S. C.; Everitt, L. E.; Choudhury, S.; Dunn, B. M.; Kaplan, A. H., Initial Cleavage of the Human Immunodeficiency Virus Type 1 Gagpol Precursor by Its Activated Protease Occurs by an Intramolecular Mechanism. *Journal of virology* **2004,** *78* (16), 8477-8485.

69. Wlodawer, A., Rational Approach to Aids Drug Design through Structural Biology. *Annual review of medicine* **2002,** *53* (1), 595-614.

70. Liu, F.; Kovalevsky, A. Y.; Tie, Y.; Ghosh, A. K.; Harrison, R. W.; Weber, I. T., Effect of Flap Mutations on Structure of Hiv-1 Protease and Inhibition by Saquinavir and Darunavir. *Journal of Molecular Biology* **2008,** *381* (1), 102-115.

71. Moore, G. L.; Stringham, R. W.; Teager, D. S.; Yue, T.-Y., Practical Synthesis of the Bicyclic Darunavir Side Chain: (3r,3as,6ar)-Hexahydrofuro[2,3-B]Furan-3-Ol from Monopotassium Isocitrate. *Organic Process Research & Development* **2017,** *21* (1), 98-106.

72. Altman, M. D.; Ali, A.; Kumar Reddy, G. S. K.; Nalam, M. N. L.; Anjum, S. G.; Cao, H.; Chellappan, S.; Kairys, V.; Fernandes, M. X.; Gilson, M. K.; Schiffer, C. A.; Rana, T. M.; Tidor, B., Hiv-1 Protease Inhibitors from Inverse Design in the Substrate Envelope Exhibit Subnanomolar Binding to Drug-Resistant Variants. *Journal of the American Chemical Society* **2008,** *130* (19), 6099-6113.

73. Molander, G. A.; Brown, A. R., Suzuki−Miyaura Cross-Coupling Reactions of Potassium Vinyltrifluoroborate with Aryl and Heteroaryl Electrophiles. *The Journal of Organic Chemistry* **2006,** *71* (26), 9681-9686.

74. Wegener, D.; Wirsching, F.; Riester, D.; Schwienhorst, A., A Fluorogenic Histone Deacetylase Assay Well Suited for High-Throughput Activity Screening. *Chemistry & Biology* **2003,** *10* (1), 61-68.

75. Bradner, J. E.; West, N.; Grachan, M. L.; Greenberg, E. F.; Haggarty, S. J.; Warnow, T.; Mazitschek, R., Chemical Phylogenetics of Histone Deacetylases. *Nature Chemical Biology* **2010,** *6* (3), 238-243.

76. Villadsen, J. S.; Stephansen, H. M.; Maolanon, A. R.; Harris, P.; Olsen, C. A., Total Synthesis and Full Histone Deacetylase Inhibitory Profiling of Azumamides a–E as Well as B2-Epi-Azumamide E and B3-Epi-Azumamide E. *Journal of Medicinal Chemistry* **2013,** *56* (16), 6512-6520.

77. Spivak, A. M.; Bosque, A.; Balch, A. H.; Smyth, D.; Martins, L.; Planelles, V., Ex Vivo Bioactivity and Hiv-1 Latency Reversal by Ingenol Dibenzoate and Panobinostat in Resting $Cd4^+$ T Cells from Aviremic Patients. *Antimicrobial Agents and Chemotherapy* **2015,** *59* (10), 5984-5991.

78. Cary, D. C.; Peterlin, B. M., Procyanidin Trimer C1 Reactivates Latent Hiv as a Triple Combination Therapy with Kansui and Jq1. *PLOS ONE* **2018,** *13* (11), e0208055.

79. López-Huertas, M. R.; Jiménez-Tormo, L.; Madrid-Elena, N.; Gutiérrez, C.; Rodríguez-Mora, S.; Coiras, M.; Alcamí, J.; Moreno, S., The Ccr5-Antagonist Maraviroc Reverses Hiv-1 Latency in Vitro Alone or in Combination with the Pkc-Agonist Bryostatin-1. *Scientific Reports* **2017,** *7* (1), 2385.

80. Geng, G.; Liu, B.; Chen, C.; Wu, K.; Liu, J.; Zhang, Y.; Pan, T.; Li, J.; Yin, Y.; Zhang, J.; Huang, F.; Yu, F.; Chen, J.; Ma, X.; Zhou, J.; Kuang, E.; Liu, C.; Cai, W.; Zhang, H., Development of an Attenuated Tat Protein as a Highly-Effective Agent to Specifically Activate Hiv-1 Latency. *Molecular Therapy* **2016,** *24* (9), 1528-1537.

81. Hattori, S. I.; Matsuda, K.; Tsuchiya, K.; Gatanaga, H.; Oka, S.; Yoshimura, K.; Mitsuya, H.; Maeda, K., Combination of a Latency-Reversing Agent with a Smac Mimetic Minimizes Secondary Hiv-1 Infection in Vitro. *Frontiers in Microbiology* **2018,** *9*, 2022.

82. Liang, T.; Zhang, X.; Lai, F.; Lin, J.; Zhou, C.; Xu, X.; Tan, X.; Liu, S.; Li, L., A Novel Bromodomain Inhibitor, Cpi-203, Serves as an Hiv-1 Latency-Reversing Agent by Activating Positive Transcription Elongation Factor B. *Biochemical Pharmacology* **2019,** *164*, 237-251.

83. Spivak, A. M.; Andrade, A.; Eisele, E.; Hoh, R.; Bacchetti, P.; Bumpus, N. N.; Emad, F.; Buckheit, R., III; McCance-Katz, E. F.; Lai, J.; Kennedy, M.; Chander, G.; Siliciano, R. F.; Siliciano, J. D.; Deeks, S. G., A Pilot Study Assessing the Safety and Latency-Reversing Activity of Disulfiram in Hiv-1–Infected Adults on Antiretroviral Therapy. *Clinical Infectious Diseases* **2013,** *58* (6), 883-890.

84. Bosque, A.; Nilson, K. A.; Macedo, A. B.; Spivak, A. M.; Archin, N. M.; Van Wagoner, R. M.; Martins, L. J.; Novis, C. L.; Szaniawski, M. A.; Ireland, C. M.; Margolis, D. M.; Price, D. H.; Planelles, V., Benzotriazoles Reactivate Latent Hiv-1 through Inactivation of Stat5 Sumoylation. *Cell Reports* **2017,** *18* (5), 1324-1334.

85. Banga, R.; Procopio, F. A.; Cavassini, M.; Perreau, M., <Em>in Vitro</Em> Reactivation of Replication-Competent and Infectious Hiv-1 by Histone Deacetylase Inhibitors. *Journal of virology* **2016,** *90* (4), 1858-1871.

86. Evans, V. A.; van der Sluis, R. M.; Solomon, A.; Dantanarayana, A.; McNeil, C.; Garsia, R.; Palmer, S.; Fromentin, R.; Chomont, N.; Sékaly, R.-P.; Cameron, P. U.; Lewin, S. R., Programmed Cell Death-1 Contributes to the Establishment and Maintenance of Hiv-1 Latency. *AIDS* **2018,** *32* (11).

87. Guihot, A.; Marcelin, A. G.; Massiani, M. A.; Samri, A.; Soulié, C.; Autran, B.; Spano, J. P., Drastic Decrease of the Hiv Reservoir in a Patient Treated with Nivolumab for Lung Cancer. *Annals of Oncology* **2018,** *29* (2), 517-518.

88. Leth, S.; Schleimann, M. H.; Nissen, S. K.; Højen, J. F.; Olesen, R.; Graversen, M. E.; Jørgensen, S.; Kjær, A. S.; Denton, P. W.; Mørk, A.; Sommerfelt, M. A.; Krogsgaard, K.; Østergaard, L.; Rasmussen, T. A.; Tolstrup, M.; Søgaard, O. S., Combined Effect of Vacc-4x, Recombinant Human Granulocyte Macrophage Colony-Stimulating Factor Vaccination, and Romidepsin on the Hiv-1 Reservoir (Reduc): A Single-Arm, Phase 1b/2a Trial. *The Lancet HIV* **2016,** *3* (10), e463-e472.

89. Gunst, J. D.; Kjær, K.; Olesen, R.; Rasmussen, T. A.; Østergaard, L.; Denton, P. W.; Søgaard, O. S.; Tolstrup, M., Fimepinostat, a Novel Dual Inhibitor of Hdac and Pi3k, Effectively Reverses Hiv-1 Latency Ex Vivo without T Cell Activation. *Journal of Virus Eradication* **2019,** *5* (3), 133-137.

90. Ait-Ammar, A.; Kula, A.; Darcis, G.; Verdikt, R.; De Wit, S.; Gautier, V.; Mallon, P. W. G.; Marcello, A.; Rohr, O.; Van Lint, C., Current Status of Latency Reversing Agents Facing the Heterogeneity of Hiv-1 Cellular and Tissue Reservoirs. *Frontiers in Microbiology* **2019,** *10*, 3060.

Final Conclusions and Future Perspectives

CHAPTER 2

In Chapter 2 the development of a convenient strategy for the preparation of α-quaternary carbon stereocentres has been described and evaluated. The methodology developed employs biselectrophiles and an easily prepared bicyclic sulfone to construct these challenging centres in only two steps, in good yield, and generally high diastereoselectivity. Despite the overall success of the method, the exploration of substrate scope and the accompanying chemistry leaves avenues of inquiry open to further investigation.

Among the possible lines of inquiry is the comparatively poor stereoselectivity observed in the allylation of the key α,α-disubstituted enolates, in contrast to alkylation and propargylation. These contrasting outcomes may point to a possible change in mechanism, a notion put forward in Section 2.3.3. However, with additional time and resources this hypothesis could be further explored beyond the S_N2' mechanism considered herein and may include the consideration of single electron processes and the investigation of different classes of allylic electrophiles (*e.g.* halide, sulphates, *etc.*). Additionally, imines and aldehydes could be explored to extend the chemistry to Mannich and aldol type chemistry, as these have previously been shown to be competent electrophiles for use with similar α,α-disubstituted amide enolates.

While allylation provides poor yet potentially useful levels diastereoselectivity, the use of sulfone **350** in alkylation reactions provided products with diastereomeric ratios of as low as two-to-one. This low level of diastereoselectivity appears to suggest that the steric hindrance of the geminal dimethyl group, located at the γ-carbon is detrimental to stereoselective alkylation of the enolate. While initial computational studies were carried out and referenced herein, they fail to provide a convincing reason for this dramatic loss of selectivity. The preparation and alkylation of

additional sterically hindered substrates (*e.g.* congeners with larger carbocyclic rings) may provide insight into if the poor selectivity is a general feature of sterically larger systems or if it is unique to the exact placement of the geminal dimethyl group. This line of investigation (and the others delineated above) would also be well served through development of a more generally method for the preparation of larger library of biselectrophiles, as considerable time and effort was devoted to the synthesis of the small library synthesised for this thesis.

CHAPTER 3

The total synthesis of (*R*)-puraquinonic acid described in Chapter 3 provides a strong demonstration of the synthetic utility of the method developed in Chapter 2. The robust and reliable nature of the alkylation procedure is evidenced by the absence of any need to optimise the reaction conditions for the key spiroalkylation/reductive alkylation step to achieve good yield and high diastereoselectivity. This experience suggests that this methodology may be relied upon for critical late-stage quaternary carbon stereocentre formation in future total synthesis and medicinal chemistry endeavours. Possible targets are outlined at the end of Chapter 3. However, the value of this mythology could be greatly increased by exploring the use additional classes of electrophiles. These classes could include secondary halides to install contiguous stereocentres or aryl/vinyl halides through application of transition metal catalysis.

CHAPTER 4

While continued research in the field of latent HIV reactivation has dampened hopes that HDAC/HIV-protease hybrid inhibitors may be enough to clear viral reservoirs from infected individuals, the project outlined in Chapter 4 provides advancements in the preparation of HIV-proteases inhibitor analogues. The need to functionalise the benzyl moiety of the darunavir scaffold has led to the development of a synthetic strategy wherein a highly useful aryl bromide

was installed to facilitate late-stage diversification. Due to the near guaranteed appearance of novel strains of HIV, which are immune to the current line-up of approved protease inhibitors, there exists a constant need to develop ever more advanced inhibitors. In this is regard, the functionalisation of darunavir may be particularly important as in 2006 it became the most recent protease inhibitor to gain approved from the FDA. Leveraging the aryl bromide functionality allows for the rapid functionalisation of the darunavir scaffold and would provide facile access to new libraries of protease inhibitors. Such libraries would be an asset in researching the next generation of HIV protease inhibitors.

CHAPTER 5

Experimental Procedures

5. 1 General Experimental

All reactions were performed using magnetic stirring. Reactions employing dry solvents were conducted using oven or flame-dried round bottom flasks. Reactions requiring controlled atmospheres were fitted with rubber septa unless otherwise stated. Oil baths were used for reactions performed at temperatures in excess of room temperature. The cooling of reactions below room temperature was accomplished using one of the following techniques: ice/water bath (0 °C), dry ice/acetone bath (–78 °C), or by placement in an *i*PrOH bath within a cryostat (variable temperature). Liquids and solutions were transferred *via* syringe or stainless-steel cannula under inert conditions. Thin-layer chromatography (TLC) was carried out on glass plates, coated with 250 μm of 230 – 400 mesh silica gel that had been saturated with F-254 indicator. TLC plates were visualised using ultraviolet light and/or by exposure to an acidic solution of cerium(IV) ammonium molybdate followed by heating, a basic solution of potassium permanganate followed by heating, an acidic solution of *p*-anisaldehyde followed by heating, or exposure to I_2 vapours. Flash column chromatography was carried out utilising 230 – 400 mesh silica gel (Silicycle) with reagent grade solvents. In some instances, a CombiFlash Rf automated column system was employed. In such cases the solvent gradient and flow rate are indicated. Room temperature (r.t.) indicates a temperature of 22 °C. All commercial reagents were used without further purification with the following exceptions: tetrahydrofuran (THF) and diethyl ether (Et_2O) were distilled from sodium/benzophenone ketyl radical under an atmosphere of nitrogen; dichloromethane (DCM), toluene (PhMe), triethylamine, and diisopropylamine were distilled from calcium hydride under a dry air atmosphere; or unless otherwise stated. Alkyl halides were purified immediately prior to use by passing neat through activated, basic, Brockmann I aluminum oxide. Infrared (IR) spectra were obtained using a Perkin-Elmer Spectrum One FT-IR spectrophotometer. NMR spectra were

recorded on a 500 MHz Varian or 400, 500 MHz Bruker spectrometers. Chemical shifts (δ) were internally referenced to the residual solvent resonance; $CDCl_3$ (δH 7.26 ppm, δC 77.0 ppm) and DMSO-d_6 (δH 2.50 ppm, δC 39.5 ppm). The following abbreviations were used to describe NMR signal multiplicities: singlet (s), doublet (d), triplet (t), quartet (q), and multiplet (m). Coupling constants (*J*) are reported in Hertz (Hz). Optical rotations were measured on a JASCO DIP-40 digital polarimeter using a Na lamp (589 nm). High resolution mass spectrometry (HRMS) was conducted by Dr. Alexander Wahba or Dr. Nadim Saadé in the Mass Spectrometry Facility in the Department of Chemistry, McGill University. High resolution, accurate mass measurements were made using the a Thermo Exactive Plus Orbitrap-API or Bruker Maxis API QqTOF mass spectrometer. Low resolution mass spectrometry (LRMS) were measured on a Thermo Polaris Q CI quadrupole in trap mass spectrometer. Chemical names were assigned using ChemDraw Professional 18.1.2.18 using the rules and recommendations of International Union of Pure and Applied Chemistry (IUPAC).

5.2 Procedures for Chapter 2

Lithium 4,4′-Di-tert-butylbiphenylide (LiDBB): LiDBB was prepared from a procedure described by Hill and Rychnovsky.[1] 4,4′-Di-tert-butylbiphenyl was purified *via* recrystallisation from hot Et_2O and dried under high vacuum prior to use. Following purification 4,4′-Di-tert-butylbiphenyl (1.50 g, 5.63 mmol, 1 equiv) was placed in a dry flask equipped with a stir bar and fused under vacuum. Once cooled to r.t. 4,4′-di-tert-butylbiphenyl was dissolved in THF (14 mL, dry and degassed freeze-pump-thaw, three cycles) Li° (390 mg, 56.4 mmol, 10 equiv) was pressed into thin sheets then rinsed with hexanes, MeOH, hexanes, and finally THF, then quickly added to the solution of 4,4′-di-tert-butylbiphenyl under a stream of argon. The reaction was cooled to 0 °C and left to stir for 5 hours under an atmosphere of argon. Excess reagent was stored at 0 °C, under an argon atmosphere for up to one week.

(*R*)-Valinol:

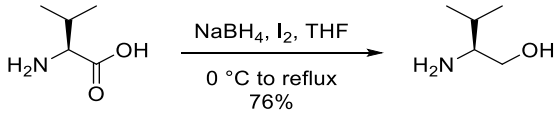

A solution of iodine (50.8 g, 200 mmol, 1 equiv) in dry THF (140 mL) was added drop-wise to a solution of L-valine (23.4 g, 200 mmol, 1 equiv) and $NaBH_4$ (18.2 g, 480 mmol, 2.4 equiv) in dry THF (500 mL) over the course of 1 hour at 0 °C under an atmosphere of argon. Once the addition was complete the flask was then equipped with a reflux condenser then heated to reflux and left to stir overnight. The reaction was then cooled to r.t. and quenched with MeOH until effervescence ceased then concentrated by rotary evaporation to afford a white paste which was dissolved in 25% $KOH_{(aq)}$ (400 mL), left to stir for 4 hours at r.t. then extracted with DCM (3 × 400 mL). Combined organic extracts were then dried over Na_2SO_4, filtered, and concentrated to afford a clear colourless

liquid. The liquid was purified *via* distillation (4 mmHg, 58 – 61 °C) to afford (*R*)-valinol as a clear colourless viscous liquid (15.64 g, 76%) which solidified to give a white solid upon cooling. The solid gave off an odour reminiscent of corn chips or hay. Spectra agreed with previous reports.[2] **^{1}H NMR** (500 MHz, $CDCl_3$) δH 3.63 (1H, dd, *J* = 10.4, 3.64 Hz), 3.26 (1H, dd, *J* = 10.3, 10.0 Hz), 2.75 (1H, br. s, D_2O exch.), 2.54 (1H, ddd, *J* = 9.0, 6.5, 4.1 Hz), 1.55 (1H, qqd, *J* = 6.9, 6.9, 6.9 Hz), 1.11 (2H, br. s, D_2O exch.), 0.93 (3H, d, *J* = 7.4 Hz), 0.91 (3H, d, *J* = 7.1 Hz). **^{13}C NMR** (126 MHz, $CDCl_3$) δC 63.0, 58.7, 30.3, 19.0, 18.7.

(*S*)-Valinol:

(*S*)-valinol was prepared in the same fashion as described for (*R*)-valinol, from D-valine (5.86 g, 50.0 mmol, 1 equiv), iodine (12.7 g, 50 mmol, 1 equiv), and $NaBH_4$ (4.54 g, 120 mmol, 2.4 equiv) in THF (160 mL). Purification via distillation (4 mmHg, 58 – 61 °C) to afford (*S*)-valinol as a clear colourless viscous liquid (3.60 g, 70%) that has a more pronounced amine odour than (*R*)-valinol and is reminiscent of the smell found within a barn. **^{1}H NMR** (500 MHz, $CDCl_3$) δH 3.61 (1H, dd, *J* = 10.4, 3.64 Hz), 3.26 (1H, dd, *J* = 10.3, 10.0 Hz), 2.61 (1H, br. s, D_2O exch.), 2.55 (1H, ddd, *J* = 9.0, 6.5, 4.1 Hz), 1.55 (1H, qqd, *J* = 6.9, 6.9, 6.9 Hz), 1.26 (2H, br. s, D_2O exch.), 0.93 (3H, d, *J* = 7.4 Hz), 0.91 (3H, d, *J* = 7.1 Hz). **^{13}C NMR** (126 MHz, $CDCl_3$) δC 63.0, 58.7, 30.3, 19.0, 18.7.

7,7-Dioxide (3*S*,9*aR*)-3-isopropyltetrahydro-8*H*-oxazolo[3,2-*d*][1,4]thiazepin-5(6*H*)-one (277):

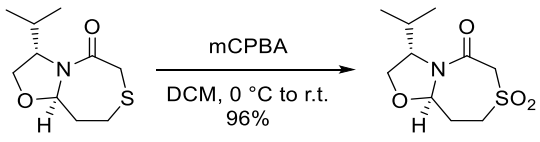

mCPBA (77% wt%, 11.45 g, 51.09 mmol, 2.2 equiv) was added in small portions to a solution of lactam **104**[3] (5.00 g, 23.2 mmol, 1 equiv) in DCM (150 mL) at 0 °C. To this was added and the

reaction stirred at r.t. overnight. Sat. $NHCO_3$ (150 mL) was then added to the reaction and phases separated. The aqueous phase was extracted with DCM (2 × 150 mL). Combined organic extracts were dried over Na_2SO_4, filtered, and concentrated to afford a white solid. The solid was triturated with Et_2O and provided sulfone **6** as a white solid upon filtration (5.51 g, 96%). **^{1}H NMR** (500 MHz, $CDCl_3$) δH 5.45 (1H, d, *J* = 9.0 Hz), 4.27, (1H, d, *J* = 15.0 Hz), 4.25 (1H, m), 3.89 (3H, m), 3.39 (1H, m), 3.35 (1H, m), 2.57 (1H, m), 2.46 (1H, m), 2.33 (1H, m), 0.91 (3H, d, *J* = 7.1 Hz), 0.82 (3H, d, *J* = 7.0); **^{1}H NMR** (500 MHz, DMSO-d_6) δH 5.71 (1H, d, *J* = 9.4 Hz), 5.09 (1H, d, *J* = 14.8 Hz), 4.01 (1H, m), 3.97 (1H, m), 3.78 (1H, dd, *J* = 14.8, 4.1 Hz), 3.69 (1H, dd, *J* = 13.2, 3.2 Hz), 3.37 (1H, m), 2.24 – 2.36 (2H, m), 2.12 (1H, dt, *J* = 14.3, 4.1 Hz), 0.83 (3H, d, *J* = 7.0 Hz), 0.74 (3H, d, *J* = 7.0 Hz); **^{13}C NMR** (126 MHz, $CDCl_3$) δC 157.2, 88.7, 65.6, 62.1, 61.2, 53.0, 32.0, 27.5, 19.2, 15.8; **^{13}C NMR** (126 MHz, DMSO-d_6) δC 157.8, 87.6, 64.7, 61.0, 60.8, 52.2, 31.9, 27.1, 18.9, 15.6; **HRMS (ESI/QqTOF) m/z**: $[M+Na]^+$ calculated for $[C_{10}H_{17}NO_4SNa]^+$ 270.0770, found 270.0764; **IR** (neat) $\tilde{\nu}$ = 2992, 2962, 2932, 2893, 2869, 1661, 1487, 1463, 1438, 1420, 1392, 1372, 1337, 1313, 1295, 1239, 1225, 1192, 1169, 1158, 1115, 1110, 1092, 1036, 1007, 977, 967, 954, 853, 826, 790, 759, 709, 686 cm^{-1}; $[\boldsymbol{\alpha}]_{\mathbf{D}}^{\mathbf{22}}$ −74.6 (*c* 0.5, 9:1 MeOH/DMSO); **Mp** 261-263 °C.

(3S,3'S,6S,6'S,9aR,9a'R)-6,6'-((3-Methoxy-1,2-phenylene)bis(methylene))bis(3-isopropyl tetrahydro-8H-oxazolo[3,2-d][1,4]thiazepin-5(6H)-one) (271):

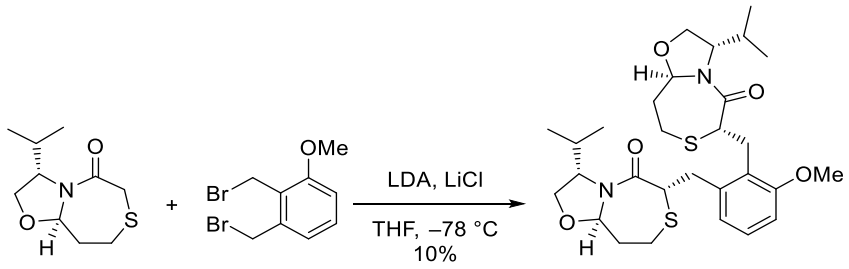

*n*BuLi (0.23 mL, 0.55 mmol, 1.1 equiv) was added to a solution of diisopropylamine (0.80 mL, 0.58 mmol, 1.15 equiv) and flame dried lithium chloride (106 mg, 2.5 mmol, 5.0 equiv) in dry THF (5 mL) at −78 °C under an atmosphere of argon. After stirring at −78 °C for 15 min, lactam **104** (108 mg, 0.50 mmol, 1 equiv) was added drop-wise as a solution dry THF (2.5 mL). The reaction was stirred at −78 °C for 20 min before dibromide **209** (294 mg, 1.0 mmol, 2.0 equiv) was added drop-wise as a solution in dry THF (2.5 mL). The reaction was then left to stir at −78 °C for 4 h. At this time the reaction was quenched with sat $NH_4Cl_{(aq)}$ (10 mL) and then extracted with EtOAc (2 × 15 mL). Combined organic extracts were dried over Na_2SO_4 and concentrated to afford a yellow solid which was purified by column chromatography (15 g SiO_2, 0-40% EtOAc in hexanes) affording arene **12** was as a white solid (28 mg, 10%). **^{1}H NMR** (500 MHz, $CDCl_3$) δH 7.16 (1H, t, *J* = 7.9 Hz), 6.89 (1H, d, *J* = 7.8 Hz), 6.77 (1H, d, *J* = 7.9 Hz), 5.48 (1H, d, *J* = 6.9 Hz), 5.46 (1H, d, *J* = 6.6 Hz), 4.29 (2H, m), 3.92 – 3.97 (2H, m), 3.75 – 3.87 (4H, m), 3.81 (3H, s), 3.63 (1H, dd, , *J* = 14.8, 6.0 Hz), 3.56 (1H, dd, 14.3, 4.6 Hz), 3.15 (1H, dd, 14.2, 9.3 Hz), 3.02 (1H, m), 2.88 (1H, m), 2.72 (1H, dt, 14.2, 4.6 Hz), 2.65 (1H, dt, 14.3, 4.3 Hz), 2.30 – 2.44 (4H, m), 2.06 (2H, m), 0.88 (6H, d, 6.7 Hz), 0.56 (3H, d, 7.0 Hz), 0.84 (3H, d, 6.9 Hz); **^{13}C NMR** (126 MHz, $CDCl_3$) δC 170.1, 169.6, 158.0, 138.3, 127.4, 126.1, 122.2, 109.1, 88.8, 88.7, 64.5, 64.2, 62.4, 62.2, 55.4, 48.6, 47.9, 34.7, 34.4, 33.8, 28.0, 27.7, 26.8, 24.4, 24.3, 19.1, 19.1, 16.1, 15.9;

HRMS (ESI/QqTOF) m/z: $[M+Na]^+$ calculated for $[C_{29}H_{42}O_5N_2NaS_2]^+$ 585.2437, found 585.2438; **IR** (neat) $\tilde{\nu}$ = 3049, 2959, 2874, 2837, 1626, 1583, 1462, 1404, 1369, 1314, 1263, 1191, 1162, 1119, 1095, 1080, 1045, 987, 952, 822, 775, 753, 731, 701, 668, 619, 582, 495, 427 cm^{-1}.

1-Methoxy-2,3-dimethylbenzene (208):

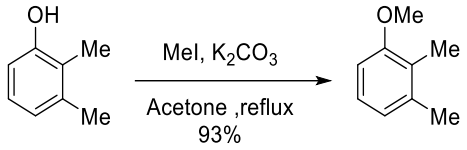

2,3-Dimethylphenol (9.16 g, 75.0 mmol, 1 equiv), iodomethane (6.1 mL, 97.5 mmol, 1.3 equiv) and K_2CO_3 (25.90 g, 187.5 mmol, 2.5 equiv) were added to a flask containing acetone (100 mL). The resulting slurry was left to reflux overnight. The reaction was quenched with MeOH (10 mL) then cooled to r.t. and filtered; washing with excess acetone. The filtrate was concentrated to one half its volume then H_2O (100 mL) added and the solution extracted with hexanes (3 × 125 mL). Combined organic extracts were dried over Na_2SO_4, filtered, and concentrated to afford the crude product as a liquid. The liquid was purified by passing it through a plug of SiO_2 eluting with hexanes. Removal of the hexanes by rotary evaporator gave anisole **208** as a clear colourless liquid (9.52 g, 93%). Spectra agreed with previous reports.[4] **^{1}H NMR** (500 MHz, $CDCl_3$) δH 7.09 (1H, t, *J* = 7.9 Hz), 6.80 (1H, d, *J* = 7.5 Hz), 6.74 (1H, d, *J* = 8.2 Hz), 3.83 (3H, s), 2.29 (3H, s), 2.17 (3H, s). **^{13}C NMR** (126 MHz, $CDCl_3$) δC 157.5, 137.8, 125.8, 125.0, 122.2, 107.8, 55.5, 20.0, 11.5.

1,2-Bis(bromomethyl)-3-methoxybenzene (209):

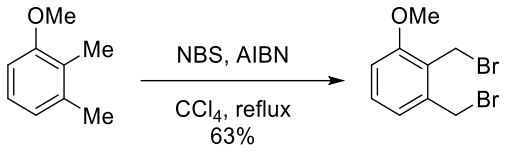

NBS (5.34 g, 30.0 mmol, 2 equiv) and AIBN (99 mg, 0.6 mmol, 4 mol%) were added to a solution of anisole **S1** (2.04 g, 15.0 mmol, 1 equiv) in CCl_4 (50 mL). The reaction was refluxed for 1 hour at which point an additional portion of AIBN (49 mg, 0.3 mmol, 2 mol%) was added and the reaction continued to reflux for another 4 hours. The solution was then cooled to 0 °C, filtered, and the filtrate concentrated to afford a yellow oil. Dibromide **209** was obtained by crystallisation from Et_2O and hexanes providing two crops of a white solid (2.92 g, 63%). Spectra agreed with previous reports.[5] **^{1}H NMR** (400 MHz, $CDCl_3$) δH 7.30 (1H, t, *J* = 8.0 Hz), 7.0 (1H, d, *J* = 7.6 Hz), 6.9 (1H, t, *J* = 8.3 Hz), 4.81 (2H, s), 4.65 (2H, s), 3.9 (3H, s); **^{13}C NMR** (126 MHz, $CDCl_3$) δC 157.9, 138.0, 130.1, 125.1, 122.8, 111.5, 56.0, 29.9, 23.8 **LRMS (CI) m/z:** 214.9 (M−Br, 94.1), 213.9 (M−Br, 100.0), 134.0 (27.3), 105.0 (60.9) .

(3*S*,6(*R*/*S*),9a*R*)-6-Benzyl-3-isopropyltetrahydro-8*H*-oxazolo[3,2-d][1,4]thiazepin-5(6*H*)-one 7,7-dioxide (310a and 310b):

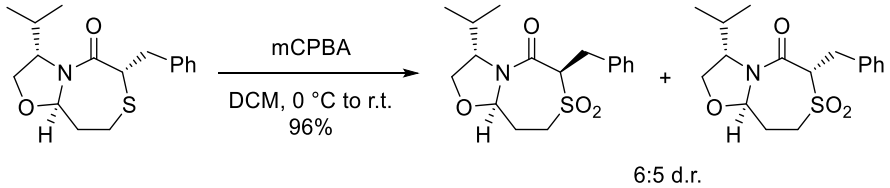

mCPBA (83 wt%, 363 mg, 1.74 mmol, 2.1 equiv) was added to a solution of (3*S*,6*S*,9a*R*)-6-benzyl-3-isopropyltetrahydro-8*H*-oxazolo[3,2-d][1,4]thiazepin-5(6*H*)-one[3] (252 mg 0.83 mmol, 1 equiv) in dry DCM (10 mL) at 0 °C under a stream of argon. The reaction was then warmed to r.t. and

left to stir overnight under an atmosphere of argon. Sat. $NaHCO_{3(aq)}$ (25 mL) was added and the resulting solution extracted with DCM (3 × 40 mL). Combined organic extracts were dried over Na_2SO_4, filtered, and concentrated to afford a mixture of sulfones **310a** and **310b** as a white solid (6:5 d.r.). The product was used in further reaction without additional purification, however small amounts of each diastereomer were isolated for characterisation purposes.

(3*S*,6*R*,9a*R*)-6-Benzyl-3-isopropyltetrahydro-8H-oxazolo[3,2-d][1,4]thiazepin-5(6H)-one 7,7-dioxide (310a):

^{1}H NMR (500 MHz, $CDCl_3$) δH 7.27 (3H, m), 7.22 (2H, m), 5.38 (1H, dd, *J* = 7.5, 2.0 Hz), 4.28 (1H, m), 4.08 (1H, dd, *J* = 10.7, 2.3 Hz), 4.00 (1H, dd, *J* = 9.2, 6.9 Hz), 3.88 (1H, dd, *J* = 9.2, 3.4 Hz), 3.70 (1H, dd, *J* = 13.8, 10.7 Hz), 3.39 (3H, m), 2.56 (1H, m), 2.39 (1H, m), 2.26 (1H, m), 0.76 (3H, d, *J* =7.0 Hz), 0.60 (3H, d, *J* = 6.9 Hz); **^{13}C NMR** (126 MHz, $CDCl_3$) δC 159.3, 137.4, 129.1, 128.6, 126.9, 88.0, 68.5, 65.8, 61.9, 52.2, 31.6, 27.9, 27.6, 18.9, 15.7; **HRMS (ESI) m/z**: $[M+Na]^+$ calculated for $[C_{17}H_{23}NO_4NaS]^+$ 360.1240, found 360.1232; **IR** (neat) $\tilde{\nu}$ = 2958, 2927, 2858, 1725, 1673, 1600, 1580, 1462, 1378, 1269, 1222, 1121, 1071, 1040, 957, 861, 834, 743, 704, 651, 488, 471 cm^{-1}.

(3*S*,6*S*,9a*R*)-6-Benzyl-3-isopropyltetrahydro-8*H*-oxazolo[3,2-d][1,4]thiazepin-5(6*H*)-one 7,7-dioxide (310b):

^{1}H NMR (500 MHz, $CDCl_3$) δH 7.33 (2H, m), 7.24 – 7.38 (3H, m), 5.65 (1H, d, *J* = 9.9 Hz), 4.32 (1H, ddd, *J* = 12.1, 4.5, 2.9 Hz), 4.26 (1H, m), 3.93 (1H, dd, *J* = 9.2, 1.8 Hz), 3.88 (1H, dd, *J* = 9.2, 6.3 Hz), 3.60 (2H, m), 3.28 (1H, dd, *J* = 14.3, 12.1 Hz), 3.24 (1H, m), 2.55 (1H, m), 2.32 (1H, m), 2.04 (1H, d of septet, *J* = 7.1, 3.7 Hz), 0.77 (3H, d, *J* = 7.0 Hz), 0.67 (3H, d, *J* = 6.9 Hz); **^{13}C NMR** (126 MHz, $CDCl_3$) δC 160.4, 134.4, 129.0, 128.5, 127.8, 86.9, 74.1, 64.3, 63.2, 47.8, 32.8,

32.1, 27.9, 19.4, 16.0; **HRMS (ESI) m/z**: $[M+Na]^+$ calculated for $[C_{17}H_{23}NO_4NaS]^+$ 360.1240, found 360.1235; **IR** (neat) $\tilde{\nu}$ = 3063, 3031, 2960, 2931, 2898, 2874, 1660, 1630, 1456, 1422, 1390, 1372, 1315, 1292, 1232, 1166, 1120, 1098, 1031, 952, 878, 843, 757, 738, 697, 571, 540, 492, 473 cm^{-1}.

(3*S*,6*R*,9a*R*)-6-Benzyl-3-isopropyl-6-methyltetrahydro-8*H*-oxazolo[3,2-d][1,4]thiazepin-5(6*H*)-one 7,7-dioxide (311):

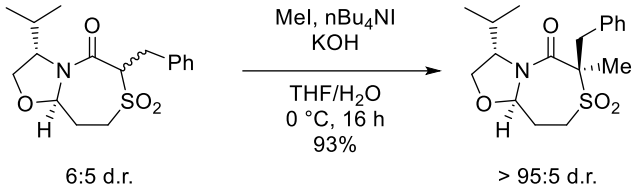

$KOH_{(aq)}$ (50 wt%, 1.5 mL) was added drop-wise to a solution of sulfones **310a** and **310b** (6:5 d.r., 50 mg, 0.15 mmol, 1 equiv), iodomethane (23 µl, 0.37 mmol, 2.5 equiv), and TBAI (27 mg, 0.075 mmol, 0.5 equiv) in THF (6 mL) at 0 °C. The reaction was then vigorously stirred for 18 hours. The solution was then diluted with H_2O (15 mL) and extracted with DCM (3 × 15 mL). Combined organic extracts were dried over Na_2SO_4, filtered, and concentrated to afford a white solid. The solid was subjected to column chromatography (10 g SiO_2, 4% EtOAc in DCM) and afforded sulfone **311** as a white solid and as a single diastereomer (49 mg, 93%). **^{1}H NMR** (500 MHz, $CDCl_3$) δH 7.39 – 7.42 (2H, m), 7.22 – 7.29 (3H, m), 5.49 (1H, d, *J* = 10.8 Hz), 4.49 (1H, m), 3.95 (1H, dd, *J* = 9.0, 6.0 Hz), 3.88 (1H, d, *J* = 13.7 Hz), 3.82 (1H, dd, *J* = 9.0, 4.3 Hz), 2.05 (1H, m), 3.35 (1H, d, *J* = 13.7 Hz), 3.18 (1H, dt, *J* = 15.2, 4.3 Hz), 2.24 (2H, m), 2.18 (1H, m), 1.58 (3H, s), 0.85 (3H, d, *J* = 7.0 Hz), 0.85 (3H, d, *J* = 7.0 Hz); **^{13}C NMR** (126 MHz, $CDCl_3$) δC 165.1, 135.4, 131.7, 128.2, 127.2, 87.5, 72.3, 64.6, 63.6, 48.5, 35.9, 31.0, 28.1, 18.9, 18.6, 16.2; **HRMS (ESI) m/z**: $[M+Na]^+$ calculated for $[C_{18}H_{25}NO_4NaS]^+$ 374.1396, found 374.1387; **IR** (neat) $\tilde{\nu}$ = 3088, 3064, 3030, 2960, 2932, 2896, 2874, 1620, 1495, 1456, 1402, 1390, 1377, 1370, 1358, 1310,

1286, 1229, 1207, 1185, 1168, 1129, 1083, 1054, 1032, 898, 957, 935, 840, 796, 783, 773, 754,737,700, 609, 594, 560, 540, 530, 513, 474, 458, 416 cm^{-1}; $[\alpha]_D^{22}$ −0.2 (*c* 1.0, $CHCl_3$); **Mp** 208-209 °C.

Dimethyl 4-methoxyphthalate (320):

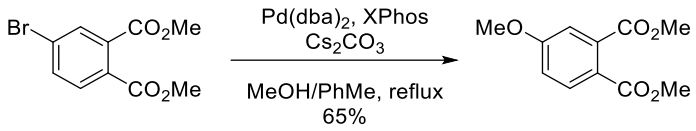

MeOH (810 µl, 20.0 mmol, 5 equiv) was added to a solution of dimethyl 4-bromophthalate (1.09 g, 4.00 mmol, 1 equiv) in dry, degassed (sparged with argon), PhMe (20 mL). To this was added Cs_2CO_3 (1.56 g, 4.80 mmol, 1.2 equiv), $Pd(dba)_2$ (11.5 mg, 0.02 mmol, 0.5 mol%), and XPhos (9.5 mg, 0.02 mmol, 0.5 mol%,). The reaction left to reflux, under an atmosphere of argon, for 5 hours then cooled to r.t. and filtered; washing with DCM. The filtrate was concentrated to afford a yellow liquid. The liquid was purified by column chromatography (24 g SiO_2, 10 – 20% EtOAc in hexanes, 30 mL/min, 15 min) to afford the anisole **320** as a clear colourless liquid (581 mg, 65%). Spectra agreed with previous reports.[6] **^{1}H NMR** (400 MHz, $CDCl_3$) δH 7.83 (1H, d, *J* = 8.7 Hz), 7.08 (1H, d, *J* = 2.3 Hz), 7.01 (1H, dd, *J* = 8.7, 2.3 Hz), 3.94 (3H, s), 3.89 (3H, s), 2.06 (3H, s).

(4-Methoxy-1,2-phenylene)dimethanol (521):

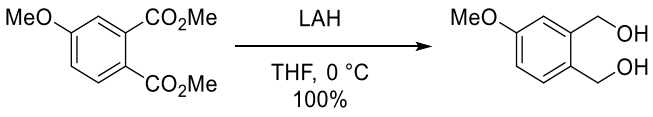

LAH (197 mg, 5.18 mmol, 2 equiv) was added in small portions, to a solution of anisole **320** (581 mg, 2.59 mmol, 1 equiv) in dry THF (26 mL) at 0 °C under a stream of argon. Once the addition

was complete the reaction was left to stir at 0 °C under argon, for 2 hours. The reaction was then slowly quenched with water (200 µl) and 15% $KOH_{(aq)}$ (200 µl). An additional portion of water (600 µl) was then added and the solution warmed to r.t. Vigorous stirring was maintained for 1 hour at which point a white solid had formed. The solution was dried with Na_2SO_4 and flirted through Celite-®; washing with excess THF. The filtrate was concentrated to afford diol **521** as a clear colourless liquid (435 mg, 100%). Spectra agreed with previous reports.[7] **^{1}H NMR** (500 MHz, $CDCl_3$) δH 7.27 (1H, d, *J* = 8.2 Hz), 6.93 (1H, s), 6.83 (1H, d, *J* = 8.2 Hz), 4.69 (4H, m), 3.82 (3H, s), 3.15 (1H, br. s), 2.85 (1H, br. s); **^{13}C NMR** (126 MHz, $CDCl_3$) δC 159.7, 141.2, 131.5, 131.2, 115.6, 113.0, 64.4, 63.8, 55.4.

1,2-Bis(bromomethyl)-4-methoxybenzene (313):

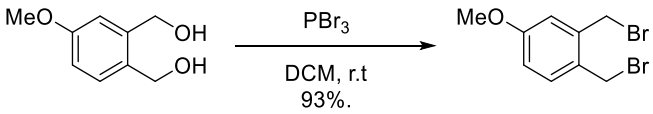

Phosphorus tribromide (180 µl, 2.0 mmol, 2 equiv) was added drop-wise, *via* syringe, to a solution of diol **521** (168 mg, 1 mmol, 1 equiv) in dry DCM (10 mL) at 0 °C under an argon atmosphere. The reaction was left to stir at 0 °C overnight then quenched at 0 °C with sat. $NaHCO_3$ (10 mL) and vigorously stirred for 10 minutes. The solution was then extracted with DCM (3 × 15 mL) with the combined organic extracts then dried over $MgSO_4$, filtered, and concentrated to afford dibromide **313** as a white waxy solid (273 mg, 93%). Spectra agreed with previous reports.[8] **^{1}H NMR** (500 MHz, $CDCl_3$) δH 7.29 (1H, d, *J* = 8.5 Hz), 6.90 (1H, d, *J* = 2.6 Hz), 6.83 (1H, dd, *J* = 8.4, 2.7 Hz), 4.66 (2H, s), 4.62 (2H, s), 3.82 (3H, s); **^{13}C NMR** (126 MHz, $CDCl_3$) δC 160.1, 138.0, 132.5, 128.5, 116.5, 114.6, 114.4, 55.4, 30.5, 30.0; **IR** (neat) $\tilde{\nu}$ = 3003, 2959, 2933, 2836, 1720, 1606, 1576, 1502, 1461, 1438, 1425, 1322, 1292, 1260, 1202, 1166, 1141, 1075, 1034, 937, 857, 818, 767, 740, 728,718, 649, 597,577, 547, 524, 457, 439 cm^{-1}.

Dimethyl 3-nitrophthalate (322):

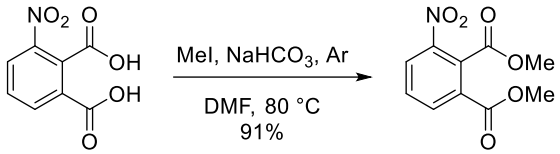

Iodomethane (930 µl, 15.0 mmol, 2.7 equiv) was added to a solution of 3-nitrophthalic acid (1.20 g 5.66 mmol, 1equiv) and $NaHCO_3$ (1.68 g, 20 mmol, 3.5 equiv) in DMF (10 mL). The reaction was then warmed to 60 °C and left to stir overnight. The reaction was quenched with MeOH (2 mL) and after being allowed to stir at 60 °C for an additional 1 hour the solution was diluted with a 1:1 solution of sat. $NaCl_{(aq)}$ to H_2O (125 mL). The resulting mixture was extracted with EtOAc (150 mL) with the organic then being washed with a 1:1 solution of sat. $NaCl_{(aq)}$ to H_2O (125 mL) before the organic phase being dried over Na_2SO_4, filtered, and concentrated to afford a yellow residue. The residue was purified by column chromatography (24 g SiO_2, 0 – 55% EtOAc in hexanes, 30 mL/min, 20 min) to afford diester **322** as a slightly yellow solid (1.23 g, 91%). Spectra agreed with previous reports.[9] **^{1}H NMR** (500 MHz, $CDCl_3$) δH 8.38 (1H, dd, *J* = 8.3, 1.2 Hz), 8.34 (1H, dd, *J* = 7.9, 1.2 Hz), 7.68 (1H, dd, *J* = 8.1, 8.1 Hz), 4.03 (3H, s), 3.95 (3H, s); **^{13}C NMR** (126 MHz, $CDCl_3$) δC 165.8, 164.1, 146.3, 135.7, 131.1, 130.1, 130.0, 128.3, 53.5, 53.2.

(3-Nitro-1,2-phenylene)dimethanol (323):

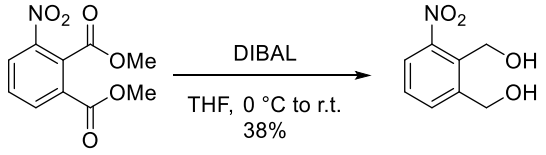

DIBAL (1 M in THF, 19.9 mL, 19.9 mmol, 4.1 equiv) was added drop-wise to a solution of diester **322** (1.16 g, 4.86 mmol, 1 equiv) in dry THF (20 mL) at 0 °C under argon. The reaction was then allowed to warm to r.t. and left to stir overnight. The reaction was then quenched with H_2O (780

μl) and 15% $KOH_{(aq)}$ (780 μl) followed by a second portion of H_2O (1.95 mL) and then left to vigorously stir at r.t. for 2 hours. The solution was then dried over Na_2SO_4 and filtered through a pad of celite; washing with excess THF. Concentration of the filtrate afforded a viscous orange liquid which was purified by column chromatography (24 g SiO_2, 10 – 90% EtOAc in hexanes, 30 mL/min, 15 min) to afford diol **323** as a yellow solid (341 mg, 38%). Spectra agreed with previously reported data.[22] **^{1}H NMR** (500 MHz, $CDCl_3$) δH 7.81 (1H, dd, *J* = 8.2, 1.1 Hz), 7.70 (1H, d, *J* = 7.6 Hz), 7.48 (1H, dd, *J* = 7.9, 7.9 Hz), 4.88 (2H, s), 4.80 (2H, s), 2.97 (1H, s, D_2O exch.), 2.81 (1H, s, D_2O exch.); **^{13}C NMR** (126 MHz, $CDCl_3$) δC 150.9, 142.9, 133.8, 132.7, 129.3, 123.9, 63.3, 57.6.

1,2-Bis(bromomethyl)-3-nitrobenzene (314):

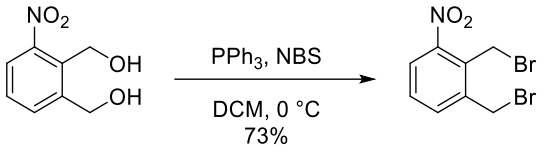

NBS (727 mg, 4.08 mmol, 2.2 equiv) was added in portions to a solution of diol **S323** (340 mg, 1.86 mmol, 1 equiv) and triphenylphosphine (1.07 g, 4.08 mmol, 2.2 equiv) in dry DCM (10 mL) at 0 °C. The reaction was then allowed to stir at 0 °C for 2 hours before being diluted with excess Et_2O and then filtered. The filtrate was concentrated to afford a yellow residue which was subjected to column chromatography (20 g SiO_2, 20% hexanes in DCM) to afford dibromide **314** as a yellow solid (420 mg, 73%). Spectra agreed with previous reports.[10] **^{1}H NMR** (500 MHz, $CDCl_3$) δH 7.88 (1H, dd, *J* = 8.2, 1.2 Hz), 7.64 (1H, dd, *J* = 7.7, 1.2 Hz), 7.47 (1H, d, *J* = 8.0 Hz), 4.86 (2H, s), 4.69 (2H, s); **^{13}C NMR** (126 MHz, $CDCl_3$) δC 150.0, 139.5, 135.4, 131.0, 129.8, 125.4, 28.4, 22.4; **LRMS (CI) m/z:** 229.8 (M−Br, 98.2), 227.9 (M−Br, 100.0), 149.0 (10.6), 120.0 (40.0), 118.0 (25.3), 91.0 (90.2), 90.0 (27.1); **IR** (neat) $\tilde{\nu}$ = 3086, 3042, 2960, 2873, 1730, 1656, 1607, 1527,

1455, 1433, 1346, 1308, 1265, 1215, 1186, 1164, 1131, 1075, 942, 878, 854, 832, 816, 782, 749, 703, 621, 566, 542, 482 cm^{-1}; **Mp** 67-69 °C.

Dimethyl cyclopropane-1,1-dicarboxylate (336):

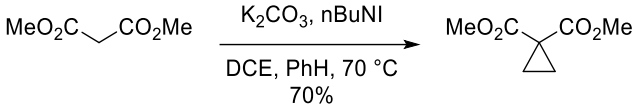

Dimethyl cyclopropane-1,1-dicarboxylate was synthesised according to the procedure reported by Heiszman *et. al.*[11] H_2O (250 μl) was added to a slurry of dimethyl malonate (5.74 mL, 50.0 mmol, 1 equiv), 1,2-dichloroethane (6.68 mL, 100 mmol, 2 equiv), K_2CO_3 (17.3 g, 125 mmol, 2.5 equiv), and tetrabutylammonium iodide (923 mg, 2.50 mmol, 5 mol%) in PhH (25 mL). The reaction was warmed to 70 °C and vigorously stirred overnight. The reaction was then filtered and washed with excess PhH. The filtrate was collected and concentrated to afford a liquid contaminated with solid tetrabutylammonium iodide. The liquid was again filtered and washed with hexanes to remove the tetrabutylammonium iodide prior to being subjected to short path distillation (98 °C, 15 mmHg). This afforded diester **336** as a clear colourless liquid (5.55 g, 70%). Spectra agreed with previously reported data.[12] **^{1}H NMR** (500 MHz, $CDCl_3$) δH 3.76 (6H, s), 1.48 (4H, s); **^{13}C NMR** (126 MHz, $CDCl_3$) δC 170.2, 52.6, 27.9, 16.7.

Cyclopropane-1,1-diyldimethanol (522):

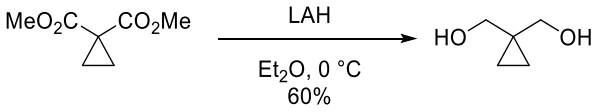

LAH (408 mg, 10.8 mmol, 1.7 equiv) was added in small portions to a solution of diester **336** (1.0 g, 6.3 mmol, 1 equiv) in dry Et_2O (30 mL) then cooled to 0 °C under an argon atmosphere. Once the addition was complete the reaction was stirred at 0 °C for 1 hour. At this point the reaction was

carefully quenched with H_2O (400 µl) and 15% $KOH_{(aq)}$ (400 µl). An additional portion of H_2O (1.2 mL) was then added before the solution was left to vigorously stir at r.t. for 15 min before being dried with Na_2SO_4 and filtered through a pad of celite; washing with excess Et_2O. The filtrate was collected and concentrated to afford diol **522** as a clear colourless liquid (390 mg, 60%). Spectra agreed with previously reported data.[13] **^{1}H NMR** (500 MHz, $CDCl_3$) δH 3.63 (4H, s), 2.52 (2H, s, D_2O exch.), 0.54 (4H, s); **^{13}C NMR** (126 MHz, $CDCl_3$) δC 69.3, 24.4, 8.7.

Cyclopropane-1,1-diylbis(methylene) dimethanesulfonate (337):

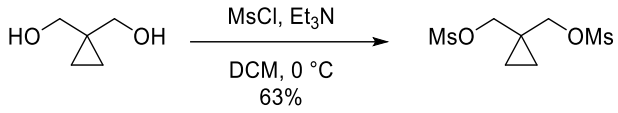

Methanesulfonyl chloride (890 µl, 11.5 mmol, 3 equiv) was added drop-wise to a solution of diol **522** (390 mg, 3.82 mmol, 1 equiv) and triethylamine (2.1 mL, 15 mmol, 4 equiv) in dry DCM (9 mL) at 0 °C under an argon atmosphere. The reaction was stirred at 0 °C for 15 minutes before being warmed to r.t. and left to stir at 2 hours. The reaction was quenched with 1 M $HCl_{(aq)}$ (50 mL) and the resulting solution extracted with EtOAc (2 × 75 mL). Combined orgaknic extracts were dried over Na_2SO_4, filtered, and concentrated to afford an off-while solid. The solid was triturated with warm DCM and filtered to afford a first crop of white crystals (456 mg). The filtrate was concentrated, triturated with DCM, and filtered to afford a second crop of dimesylate **337** (170 mg, 626 mg total, 63%). Spectra agreed with previously reported data.[14] **^{1}H NMR** (500 MHz, $CDCl_3$) δH 4.17 (4H, s), 3.07 (6H, s), 0.84. (4H, s).

4-methoxy-2-methylenebutyl methanesulfonate (329):

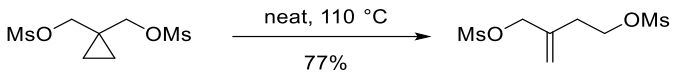

Neat dimesylate **337** (258 mg, 1 mmol) was heated in a small vail at an external temperature of 110 °C for 15 min affording a black residue which was purified by column chromatography (12 g SiO_2, 50 – 80% EtOAc in hexanes, 30 mL/min, 10 min) to afford olefin **329** as a viscous liquid (200 mg, 77%). Please note that extended reaction times result in dramatically lower yields. Reactions performed at 120 °C for 10 minutes resulted in complete decomposition. Spectra agreed with previously reported data.[15] **^{1}H NMR** (500 MHz, $CDCl_3$) δH 5.38 (1H, s), 5.26 (1H, s), 4.73 (2H, s), 4.40 (2H, t, *J* = 6.5 Hz), 3.07 (3H, s), 3.05 (3H, s), 2.63 (2H, t, *J* = 6.4 Hz); **^{13}C NMR** (126 MHz, $CDCl_3$) δC 137.2, 119.3, 71.8, 67.2, 37.9, 37.6, 32.5.

2-(2-(Hydroxymethyl)phenyl)ethan-1-ol (325):

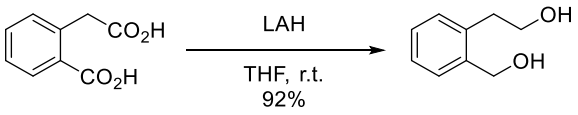

LAH (5.77 g, 150 mmol, 6 equiv) was added in small portions to a solution of homophthalic acid (4.5 g, 25 mmol, 1 equiv) in dry THF (100 mL) under a stream of argon at 0 °C. Once the addition was complete the reaction was warmed to r.t. and left to stir overnight. The reaction was quenched with 2 M $HCl_{(aq)}$ (150 mL) followed by the addition of conc. HCl (25 mL). The resulting solution was extracted with DCM (2 × 150 mL). Combined organic extracts were dried with Na_2SO_4, filtered, and concentrated to afford a viscous light-brown liquid. The liquid was purified by column chromatography (60 g SiO_2, 50% EtOAc in hexanes) to afford diol **325** as a clear yellow viscous liquid (3.51g, 92%). Spectra agreed with previous reports.[16] **^{1}H NMR** (400 MHz, $CDCl_3$) δH 7.27

– 7.32 (2H, m), 7.20 – 7.24 (2H, m), 4.62 (2H, s), 3.85 (2H, t, *J* = 5.9 Hz), 3.65 (2H, br. s, D_2O exch.), 2.93 (2H, t, *J* = 5.9 Hz). **^{13}C NMR** (126 MHz, $CDCl_3$) δC 139.1, 138.2, 130.0, 129.7, 128.5, 126.6, 63.1, 62.9, 35.0.

1-(2-Bromoethyl)-2-(bromomethyl)benzene (315):

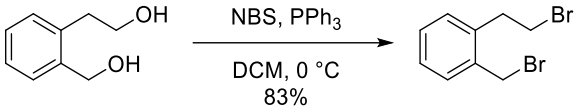

NBS (1.93 g, 10.8 mmol, 2.2 equiv) was added, in small portions, to a solution of diol **325** (750 mg, 4.93 mmol, 1 equiv) and triphenylphosphine (2.84 g, 10.8 mmol, 2.2 equiv) at 0 °C. The reaction was then left to stir at 0 °C for 2 hours then concentrated to one third its volume, *via* rotary evaporation. Excess Et_2O was added causing precipitation. The solution was filtered, washed with excess Et_2O, and the filtrate concentrated to afford a yellow residue, which was purified by column chromatography (24 g SiO_2, 0 – 5% EtOAc in hexanes, 30 mL/min, 10 min) to afford dibromide **315** as white solid (1.13 g, 83%). Spectra agreed with previous reports.[17] **^{1}H NMR** (500 MHz, $CDCl_3$) δH 7.37 (1H, d, *J* = 7.6 Hz), 7.32 (1H, m), 7.26 (2H, m), 4.57 (2H, s), 3.66 (2H, t, *J* = 7.7 Hz), 3.32 (2H, t, *J* = 7.8 Hz); **^{13}C NMR** (126 MHz, $CDCl_3$) δC 137.8, 135.9, 130.9, 130.2, 129.3, 127.7, 35.7, 31.7, 31.2.

2,3-Dimethyl-1,1'-biphenyl (339):

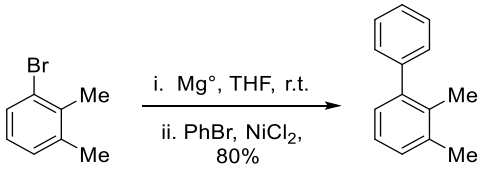

Under a stream of argon, THF (15 mL), a small chip of I_2, and (1 equiv, 1.35 mL, 10 mmol) were added to a dry flask contacting Mg° turnings (243 mg, 10.0 mmol, 1 equiv), which had been flame-

dried. Following the resulting exotherm, the solution was stirred at r.t. for 30 min (at which point no Mg° was visible) and solution was transferred to a phial containing a solution of bromobenzene (1.10 mL, 10.5 mmol, 1.05 equiv) and $NiCl_2$ (26 mg, 0.20 mmol, 0.02 equiv) in dry THF (1 mL) under argon. The phial was sealed and heated to 66 °C and left to stir for 3 hours. The reaction was then cooled to r.t. and diluted with 1M HCl (100 mL). The resulting solution was extracted with Et_2O (3 × 100 mL). Combined organic extracts were dried over $MgSO_4$, filtered, and concentrated to afford a yellow-orange liquid. The liquid was purified by column chromatography (24 g SiO_2, 0 – 5% EtOAc in hexanes, 30 mL/min, 12 min) to afford biphenyl **339** as a clear colourless liquid (1.46 g, 80%). Spectra agreed with previous reports.[18] **^{1}H NMR** (500 MHz, $CDCl_3$) δH 7.41 (2H, m), 7.30 – 7.35 (3H, m), 7.14 – 7.18 (2H, m), 7.09 (1H, dd, *J* = 7.1, 1.8 Hz), 2.35 (3H, s), 2.16 (3H, s); **^{13}C NMR** (126 MHz, $CDCl_3$) δC 142.6, 142.2, 137.2, 134.0, 129.4, 128.8, 127.9, 127.6, 126.6, 125.2, 20.7, 16.9.

2,3-Bis(bromomethyl)-1,1'-biphenyl (317):

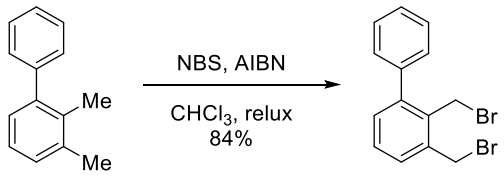

NBS (1.6 g, 9.0 mmol, 2.25 equiv) and AIBN (53 mg, 0.32 mmol, 8 mol%) were added to a solution of biphenyl **339** (729 mg, 4.00 mmol, 1 equiv) in $CHCl_3$ (40 mL) under an argon atmosphere. The reaction was heated to reflux and left to stir overnight. The solvent was then removed by rotary evaporation and Et_2O added which resulted in precipitation of a white solid (succinimide). The precipitate was filtered off and the filtrate concentrated to afford a yellow reside which was purified by column chromatography (24 g SiO_2, 0 – 5% DCM in hexanes, 30 mL/min, 12 min) to afford dibromide **317** as a slightly opaque colourless viscous liquid (1.14 g, 84%). **^{1}H**

NMR (500 MHz, $CDCl_3$) δH 7.40 – 7.47 (6H, m), 7.35 (1H, t, *J* = 7.5 Hz), 7.24 (1H, dd, *J* = 7.6, 1.5 Hz), 4.79 (2H, s), 4.60 (2H, s). **^{13}C NMR** (126 MHz, $CDCl_3$) δC 144.0, 139.9, 137.5, 133.8, 131.1, 130.5, 128.8 (2C), 128.2, 127.6, 30.6, 28.2; **LRMS (CI) m/z:** 260.8 (M−Br, 13.7), 258.9 (M−Br, 12.7), 179.1 (100.0), 178.2 (30.4); **IR** (neat) $\tilde{\nu}$ = 3058, 3028, 2980, 1951, 1890, 1817, 1606, 1589, 1574, 1496, 1460, 1441, 1290, 1264, 1215, 1191, 1178, 1155, 1114, 1073, 1026, 1001, 972, 913, 876, 837, 806, 761, 737, 701, 682 cm^{-1}; **Mp** 46-47 °C.

2,2-Dimethylbutane-1,4-diol (341):

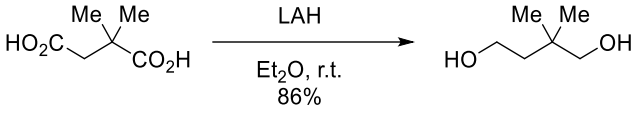

2,2-Dimethylsuccinic acid (1.46 g, 10.0 mmol, 1 equiv) was added in small portions, under a stream of argon, to a suspension of LAH (, 2.24 g, 60.0 mmol, 6 equiv) in dry Et_2O (100 mL) at 0 °C. The reaction was then warmed to r.t. and left to stir for 2 hours before being cooled to 0 °C and slowly quenched with water (2.24 mL) and 15% $KOH_{(aq)}$ (2.24 mL). An additional portion of water (6.72 mL) was then added and the solution warmed to r.t and vigorously stirred for 1 hour at which point a white solid had formed. The solution was dried with Na_2SO_4, filtered, and then flirted through a pad of celite; washing with excess Et_2O. The filtrate was concentrated to afford diol **341** as a clear colourless liquid (1.12 g, 86%). Spectra agreed with previous reports.[19] **^{1}H NMR** (400 MHz, $CDCl_3$) δH 3.73, (2H, t, *J* = 5.6 Hz), 3.36 (2H, s), 2.92 (1H, br. s, D_2O exch.), 2.49 (1H, br. s, D_2O exch.), 1.56 (2H, t, *J* = 5.5 Hz), 0.92 (6H, s); **^{13}C NMR** (126 MHz, $CDCl_3$) δC 71.6, 59.2, 42.7, 34.9, 25.0.

2,2-Dimethylbutane-1,4-diyl dimethanesulfonate (342):

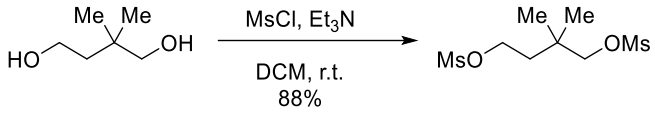

Triethylamine (915 µl, 6.6 mmol, 2.2 equiv) and MsCl (464 µl, 6.0 mmol, 2.0 equiv) were added to a solution of diol **341** (354 mg, 3.0 mmol, 1 equiv) in DCM (10 mL) at 0 °C. The reaction was then allowed to warm to r.t. and left to stir for 2 hours, then diluted with DCM (50 mL) and washed with 1M HCl (50 mL), The aqueous phase was then extracted with DCM (2 × 150 mL). Combined organic extracts were dried over Na_2SO_4, filtered, and concentrated to afford dimesylate **342** as a clear colourless oil (728 mg, 88%). **^{1}H NMR** (500 MHz, $CDCl_3$) δH 4.30, (2H, t, *J* = 6.9 Hz), 3.93 (2H, s), 3.02 (3H, s), 3.01 (3H, s), 1.82 (2H, t, *J* = 6.9 Hz), 1.03 (6H, s); **^{13}C NMR** (126 MHz, $CDCl_3$) δC; 76.7, 66.3, 37.4, 37.1, 37.0, 33.6, 24.1; **HRMS (ESI) m/z**: $[M+Na]^+$ calculated for $[C_8H_{18}O_6S_2Na]^+$ 297.0442, found 297.0437; **IR** (neat) $\tilde{\nu}$ = 2958, 2927, 2858, 1725, 1673, 1600, 2580, 1462, 1378, 1269, 1222, 1121, 1071, 1040, 957, 861, 834, 742, 705, 651, 488, 471 cm^{-1}.

5.2.1 General Method for Spiroalkylation

(2*R*,3'*S*,9a'*R*)-3'-Isopropyl-4-methoxy-1,2',3,3',9',9a'-hexahydro-5'*H*, 8'*H*-spiro[indene-2,6'-oxazolo[3,2-d][1,4]thiazepin]-5'-one 7',7'-dioxide (287):

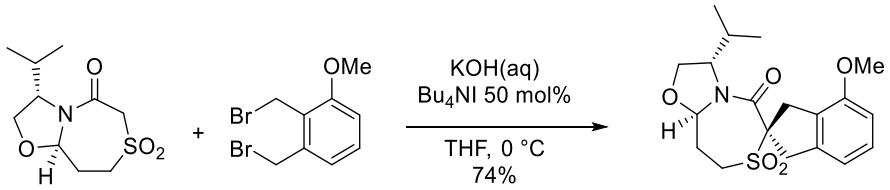

$KOH_{(aq)}$ (50 wt%, 3 mL) was added drop-wise to a solution of sulfone **277** (111 mg, 0.45 mmol, 1.5 equiv), 1,2-bis(bromomethyl)-3-methoxybenzene (**209**, 88 mg, 0.30 mmol, 1 equiv), and tetrabutylammonium iodide (55 mg, 0.15 mmol, 0.5 equiv) in THF (6 mL) at 0 °C. The reaction

was then vigorously stirred for 18 hours. The solution was then diluted with H_2O (10 mL) and extracted with DCM (3 × 20 mL). Combined organic extracts were dried over Na_2SO_4, filtered, and concentrated to afford a yellow solid. The solid was subjected to column chromatography (10 g SiO_2, 0 – 6% EtOAc in DCM) to afforded spirocycle **287** as a white solid (>95:5 d.r., 84 mg, 74%). **^{1}H NMR** (500 MHz, $CDCl_3$) δH 7.16 (1H, dd, *J* = 8.1, 7.6 Hz), 6.76 (1H, d, *J* = 7.6 Hz), 6.70 (1H, d, *J* = 8.1 Hz), 5.59 (1H, d, *J* = 9.3 Hz), 4.39 (1H, m), 1H (1H, d, *J* = 17.9 Hz), 3.95 (2H, m), 3.83 (1H, d, *J* = 16.1 Hz), 3.82 (3H, s), 3.80 (1H, d, *J* = 17.9 Hz), 3.64, (1H, m), 3.69 (1H, m), (1H, d, *J* = 16.1 Hz), 3.31 (1H, ddd, *J* = 15.3, 5.4, 2.9 Hz), 2.57 (1H, m), 2.31 (1H, m), 2.26 (1H, dqq, *J* = 7.0, 7.0, 4.2 Hz), 0.82 (3H, d, *J* = 7.0 Hz), 0.75 (3H, d, *J* = 7.0 Hz); **^{13}C NMR** (126 MHz, $CDCl_3$) δC 163.1, 155.8, 138.4, 128.7, 127.8, 115.7, 109.0, 87.8, 76.8, 64.5, 63.4, 55.2, 48.1, 40.5, 33.9, 31.8, 27.7, 19.1, 16.1; **HRMS (APCI) m/z**: $[M+H]^+$ calculated for $[C_{19}H_{26}NO_5S]^+$ 380.1532, found 380.1539; **IR** (neat) $\tilde{\nu}$ = 2963, 2937, 2889, 2873, 2837, 1624, 1592, 1472, 1451, 1438, 1398, 1389, 1372, 1330, 1316, 1293, 1278, 1265, 1238, 1221, 1187, 1172, 1134, 1096, 1066, 1050, 1035, 992, 955, 943, 931, 912, 892, 848, 838, 800, 770, 754, 731, 711, 706, 691 cm^{-1}; **Mp** 242-245 °C.

(2*S*/*R*,3'*S*,9a'*R*)-3'-Isopropyl-5-methoxy-1,2',3,3',9',9a'-hexahydro-5'H,8'H-spiro[indene-2,6'-oxazolo[3,2-d][1,4]thiazepin]-5'-one 7',7'-dioxide (345):

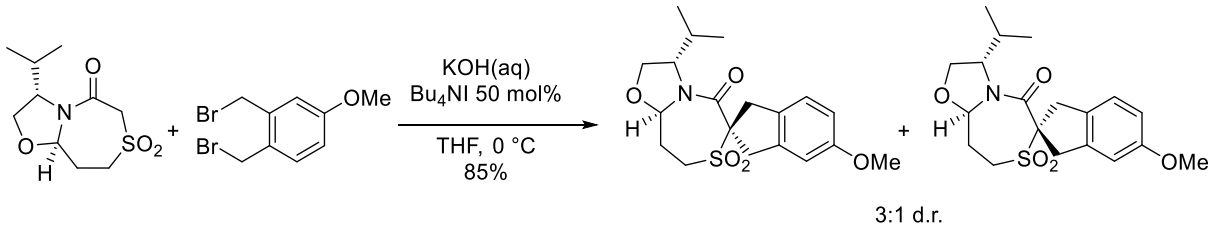

Spirocycle **345** was synthesised according to the example procedure from dibromide **313** (294 mg, 1.0 mmol, 1 equiv), sulfone **277** (371 mg, 1.5 mmol, 1.5 equiv), tetrabutylammonium iodide (185 mg, 0.5 mmol, 0.5 equiv), THF (40 mL), and $KOH_{(aq)}$ (50 wt%, 5 mL). Once complete, the reaction

was diluted with H_2O (50 mL) and extracted with DCM (3 × 50 mL). Combined organic extracts were dried over $MgSO_4$, filtered, and concentrated to afford a white solid. The solid was subjected to column chromatography (40 g SiO_2, 4% EtOAc in DCM) to afford spirocycle **345** as a white solid (3:1 d.r., 321 mg, 85%) however, the diastereomers proved completely inseparable. **HRMS (APCI) m/z**: $[M+H]^+$ calculated for $[C_{19}H_{26}NO_5S]^+$ 380.1532, found 380.1545; **IR** (neat) $\tilde{\nu}$ = 2961, 2932, 2901, 2873, 2835, 1621, 1594, 1497, 1463, 1439, 1409, 1389, 1372, 1354, 1331, 1313, 1290, 1257, 1229, 1201, 1185, 1169, 1147, 1128, 1098, 1063, 1031, 1009, 988, 952, 931, 909, 879, 840, 802, 765, 754, 732, 702 cm^{-1}.

(2*S*,3'*S*,9a'*R*)-345:

^{1}H NMR (500 MHz, $CDCl_3$) δH 7.17 (1H, d, *J* = 8.4 Hz), 6.77 (1H, dd, *J* = 8.4, 2.4 Hz), 6.70 (1H, d, *J* = 2.1 Hz), 5.60 (1H, d, *J* = 9.1 Hz), 4.38 (1H, m), 4.27 (1H, d, *J* = 17.0 Hz), 3.96 (2H, m), 3.80 (1H, d, *J* = 17.0 Hz), 3.79 (1H, d, *J* = 16.1 Hz), 3.77 (3H, s), 3.69 (1H, m), 3.61 (1H, d, *J* = 16.0 Hz), 3.31 (1H, ddd, *J* = 15.3, 6.0, 2.7 Hz), 2.58 (1H, m), 2.32 (1H, m), 2.25 (1H, m), 0.82 (3H, d, *J* = 7.2 Hz), 0.75 (3H, d, *J* = 6.9 Hz); **^{13}C NMR** (126 MHz, $CDCl_3$) δC 163.1, 159.2, 137.9, 131.8, 125.0, 113.7, 109.3, 87.9, 77.5, 64.6, 63.5, 55.5, 48.2, 40.3, 35.7, 31.9, 27.8, 19.1, 16.2.

(2*R*,3'*S*,9a'*R*)-345:

^{1}H NMR (500 MHz, $CDCl_3$) δH 7.04 (1H, d, *J* = 8.4 Hz), 6.81 (1H, d, *J* = 2.1 Hz), 6.73 (1H, dd, *J* = 8.3, 2.4 Hz), 5.60 (1H, d, *J* = 9.1 Hz), 4.37 (1H, m), 4.31 (1H, d, *J* = 17.4 Hz), 3.96 (2H, m), 3.84 (1H, d, *J* = 17.5 Hz), 3.78 (3H, s), 3.75 (1H, d, *J* = 14.5 Hz), 3.69 (1H, m), 3.57 (1H, d, *J* = 15.4 Hz), 3.31 (1H, m), 2.58 (1H, m), 2.32 (1H, m), 2.25 (1H, m), 0.81 (3H, d, *J* = 7.0 Hz), 0.75 (3H, d, *J* = 6.8 Hz); **^{13}C NMR** (126 MHz, $CDCl_3$) δC163.1, 159.8, 141.4, 128.2, 124.4, 113.9, 109.0, 87.9, 77.6, 64.6, 63.5, 55.4, 48.2, 39.4, 36.6, 32.0, 27.8, 19.1, 16.2.

(2*S*,3'*S*,9a'*R*)-3'-isopropyl-4-nitro-1,2',3,3',9',9a'-hexahydro-5'*H*,8'*H*-spiro[indene-2,6'-oxazolo[3,2-d][1,4]thiazepin]-5'-one 7',7'-dioxide (346):

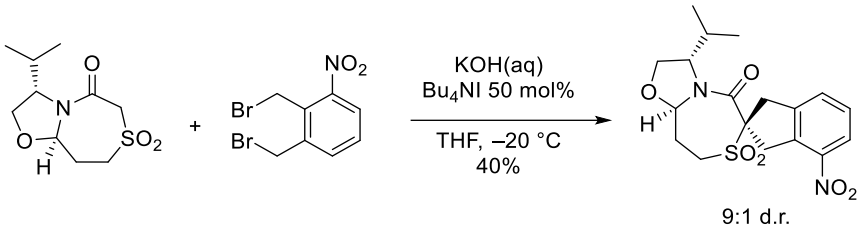

Spirocycle **346** was synthesised according to the example procedure from dibromide **314** (93 mg, 0.3 mmol, 1 equiv), sulfone **277** (111 mg, 0.45 mmol, 1.5 equiv), tetrabutylammonium iodide (110 mg, 0.3 mmol, 1.0 equiv), THF (6 mL), $KOH_{(aq)}$ (50 wt%, 1.5 mL) and sat. NaCl (1.5 mL). Once complete, the reaction was diluted with H_2O (10 mL) and extracted with DCM (3 × 20 mL). Combined organic extracts were dried over $MgSO_4$, filtered, and concentrated to afford a white solid. The solid was subjected to column chromatography (10 g SiO_2, 5% EtOAc in DCM) to afford spirocycle **346** as a white solid (9:1 d.r., 47 mg, 40%). The major isomer could, in large part, be separated, by column chromatography (10 g SiO_2, 50 to 80% EtOAc in hexanes). **^{1}H NMR** (500 MHz, $CDCl_3$) δH 8.09 (1H, d, *J* = 8.2 Hz), 7.62 (1H, d, *J* = 7.5 Hz), 7.45 (1H, dd, *J* = 8.2, 7.5 Hz), 5.71 (1H, d, *J* = 9.4 Hz), 4.50 (1H, d, *J* = 18.0 Hz), 4.38 (1H, m), 4.29 (1H, d, *J* = 18.3 Hz), 4.14 (1H, d, *J* = 18.3 Hz), 3.95 – 4.01 (3H, m), 3.82 (1H, ddd, *J* = 15.6, 13.3, 3.1 Hz), 3.35 (1H, ddd, *J* = 15.6, 5.5, 2.9 Hz), 2.57 – 2.65 (1H, m), 2.38 (1H, m), 2.27 (1H, dqq, *J* = 7.0, 7.0, 4.1 Hz), 0.84 (3H, d, *J* = 7.0 Hz), 0.77 (3H, d, *J* = 7.0 Hz); **^{13}C NMR** (126 MHz, $CDCl_3$) δC 162.3, 144.7, 144.0, 133.3, 130.4, 129.3, 123.0, 87.8, 64.6, 65.7, 47.8, 40.9, 36.5, 31.9, 27.8, 19.1, 16.2; **HRMS (APCI) m/z**: $[M+H]^+$ calculated for $[C_{18}H_{23}N_2O_6S]^+$ 395.1277, found 395.1284; **IR** (neat) $\tilde{\nu}$ = 2959, 2929, 2874, 1629, 1528, 1483, 1462, 1407, 1391, 1352, 1326, 1312, 1293, 1226, 1187,

1164, 1128, 1098, 1068, 1051, 1032, 989, 950, 837, 801, 756, 732, 703, 536, 512, 499, 485, 473 cm^{-1}; $[\alpha]_D^{22}$ −206.5 (*c* 1.0, $CHCl_3$); **Mp** 245-246 °C.

(2*R*,3'*S*,9a'*R*)-3'-Isopropyl-2',3,3',4,9',9a'-hexahydro-1*H*,5'*H*,8'*H*-spiro[naphthalene-2,6'-oxazolo[3,2-d][1,4]thiazepin]-5'-one 7',7'-dioxide (347):

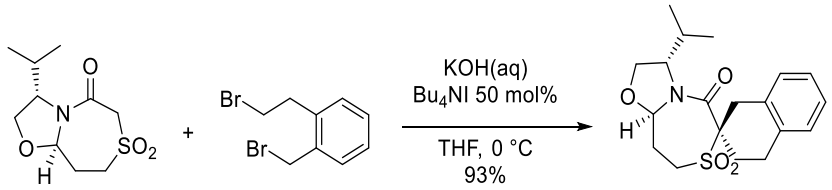

Spirocycle **347** was synthesised according to the example procedure from dibromide **288** (278 mg, 1.0 mmol, 1 equiv), sulfone **277** (371 mg, 1.5 mmol, 1.5 equiv), tetrabutylammonium iodide (185 mg, 0.5 mmol, 0.5 equiv), THF (40 mL), and $KOH_{(aq)}$ (50 wt%, 5 mL). Once complete, the reaction was diluted with H_2O (50 mL) and extracted with DCM (3 × 50 mL). Combined organic extracts were dried over $MgSO_4$, filtered, and concentrated to afford a white solid. The solid was subjected to column chromatography (40 g SiO_2, 2 – 6% EtOAc in DCM) to afford spirocycle **13e** as a white solid (>95:5 d.r., 337 mg, 93%). **^{1}H NMR** (500 MHz, $CDCl_3$) δH 7.24 (1H, d, *J* = 7.7 Hz), 7.17 (1H, t, 7.3 Hz), 7.10 (1H, t, *J* = 7.3 Hz), 7.03 (1H, d, *J* = 7/5 Hz), 5.67 (1H, d, *J* = 10.0 Hz), 4.37 (1H, m), 3.87 – 3.96 (2H, m), 3.77 (1H, d, *J* = 16.1 Hz), 3.71 (1H, m), 3.48 (1H, d, *J* = 15.9 Hz), 3.28 (1H, ddd, *J* = 15.5, 5.5, 2.7 Hz), 2.98 (1H, dt, *J* = 16.8, 4.4 Hz), 2.76 (1H, m), 2.51 – 2.66 (2H, m), 2.41 (1H, td, *J* = 12.8, 5.0 Hz), 2.29 (1H, m), 2.15 (1H, qqd, *J* = 6.8, 6.8, 3.3 Hz), 0.80 (3H, d, *J* = 7.0, Hz), 0.79 (3H, d, *J* = 7.0 Hz); **^{13}C NMR** (126 MHz, DMSO-d_6) δC 162. 2, 133.9, 132.6, 128.9, 127.9, 126.9, 125.9, 87.7, 71.7, 63.9, 63.7, 47.5, 32.3, 29.3, 27.8, 26.2, 25.9, 19.4, 16.1; **HRMS (APCI) m/z**: $[M+H]^+$ calculated for $[C_{19}H_{26}NO_4S]^+$ 364.1583, found 364.1586; **IR** (neat) $\tilde{\nu}$ = 3021, 2962, 2930, 2897, 2847, 1620, 1586, 1496, 1463, 1438, 1401, 1387, 1371, 1360,

1309, 1284, 1255, 1228, 1181, 1169, 1128, 1109, 1067, 1055, 1033, 1015, 990, 958, 917, 899, 883,842, 817, 794, 778, 753, 738, 705, 692, 603, 561, 541, 528, 512, 489, 472, 454, 436, 424 cm^{-1}; $[\boldsymbol{\alpha}]_{\mathbf{D}}^{\mathbf{22}}$ −199.1 (*c* 1.0, $CHCl_3$); **Mp** 248-251 °C.

(1*R*,3'*S*,9a'*R*)-3'-Isopropyl-3-methylenetetrahydro-5'*H*,8'*H*-spiro[cyclopentane-1,6'-oxazolo[3,2-d][1,4]thiazepin]-5'-one 7',7'-dioxide (348):

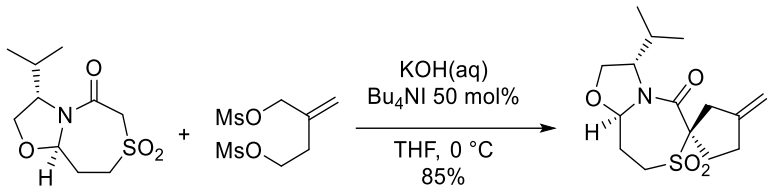

Spirocycle **348** was synthesised according to the example procedure from dimesylate **311** (75 mg, 0.30 mmol, 1 equiv), sulfone **277** (111 mg, 0.45 mmol, 1.5 equiv), tetrabutylammonium iodide (55 mg, 0.15 mmol, 0.5 equiv), THF (6 mL), and $KOH_{(aq)}$ (50 wt%, 3 mL). Once complete, the reaction was diluted with H_2O (10 mL) and extracted with DCM (3 × 20 mL). Combined organic extracts were dried over $MgSO_4$, filtered, and concentrated to afford a yellow solid. The solid was subjected to column chromatography (10 g SiO_2, 0 – 4% EtOAc in DCM) to afforded spirocycle **348** as a white solid (>95:5 d.r., 95 mg, 95%). **^{1}H NMR** (500 MHz, $CDCl_3$) δH 5.56 (1H, d, *J* = 9.1 Hz), 5.03 (1H, tt, *J* = 1.9, 1.9 Hz), 4.93 (1H, tt, *J* = 2.1, 2.1 Hz), 4.39 (1H, m), 3.91 – 3.96 (2H, m), 3.61 (1H, dd, *J* = 16.8, 1.6 Hz), 3.55 (1H, ddd, *J* = 16.1, 13.3, 3.0 Hz), 3.27 (1H, ddd, *J* = 15.3, 5.7, 2.8 Hz), 3.20 (1H, dd, *J* = 16.8, 1.4 Hz), 2.66 (1H, m), 2.26 – 2.56 (6H, m), 0.88 (3H, d, *J* = 7.0 Hz), 0.81 (3H, d, *J* = 6.7 Hz); **^{13}C NMR** (126 MHz, $CDCl_3$) δC 162.7, 145.8, 107.4, 87.9, 77.1, 64.4, 63,7, 48.4, 35.8, 32.6, 31.9, 31.7, 27.9, 19.2, 16.2; **HRMS (APCI) m/z**: $[M+H]^+$ calculated for $[C_{15}H_{24}NO_4S]^+$ 314.1421, found 314.1430; **IR** (neat) $\tilde{\nu}$ = 3075, 2958, 2931, 2897, 2873, 1738, 1661, 1623, 1485, 1463, 1438, 1404, 1388, 1373, 1364, 1316, 1300, 1288, 1253, 1229, 1206, 1186,

1171, 1127, 1097, 1050, 1033, 1007, 991, 965, 954, 934, 912, 878, 841, 802, 784, 776, 754, 730, 701 cm^{-1}; $[\alpha]_D^{22}$ −206.0 (*c* 1.0, $CHCl_3$); **Mp** 285-286 °C.

(2*R*,3'*S*,9a'*R*)-3'-Isopropyl-4-phenyl-1,2',3,3',9',9a'-hexahydro-5'*H*,8'*H*-spiro[indene-2,6'-oxazolo[3,2-d][1,4]thiazepin]-5'-one 7',7'-dioxide (349):

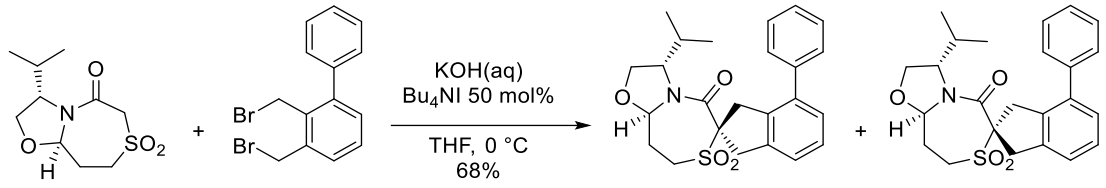

Spirocycle **349** was synthesised according to the example procedure from dibromide **290** (102 mg, 0.3 mmol, 1 equiv), sulfone **277** (111 mg, 0.45 mmol, 1.5 equiv), tetrabutylammonium iodide (55 mg, 0.5 mmol, 0.5 equiv), THF (6 mL), and $KOH_{(aq)}$ (50 wt%, 3 mL). Once complete, the reaction was diluted with H_2O (10 mL) and extracted with DCM (3 × 20 mL). Combined organic extracts were dried over $MgSO_4$, filtered, and concentrated to afford a white solid. The solid was subjected to column chromatography (10 g SiO_2, 5% EtOAc in DCM) to afford spirocycle **349** as a white solid (4:1 d.r., 87 mg, 68%). The major isomer ((*R*,*S*,*R*)- **349**) could, in large part, be separated, by column chromatography (12 g SiO_2, 20 – 50% EtOAc in hexanes, at 20 mL/min over 15 min). **^{1}H NMR** (500 MHz, $CDCl_3$) δH 7.50 (2H, m), 7.43 (2H, m), 7.35 (1H, tt, *J* = 7.3, 1.2 Hz), 7.24 – 7.29 (2H, m), 7.15 (1H, d, *J* = 7.2 Hz), 5.63 (1H, d, *J* = 9.4 Hz), 4.43 (1H, d, *J* = 17.5 Hz), 4.36 (1H, dt, *J* = 4.3, 4.3 Hz), 3.95 (2H, d, *J* = 4.4 Hz), 3.89 (1H, d, *J* = 17.1 Hz), 3.89 (1H, d, *J* = 17.1 Hz), 3.71 (1H, d, *J* = 16.0 Hz), 3.70 (1H, m), 3.30 (1H, ddd, *J* = 15.3, 5.5, 2.7 Hz), 2.57 (1H, m), 2.31 (1H, m), 2.26 (1H, m), 0.82 (3H, d, *J* = 7.0 Hz), 0.76 (3H, d, *J* = 6.9 Hz); **^{13}C NMR** (126 MHz, $CDCl_3$) δC 162.9, 140.1, 138.7, 137.7, 137.1, 128.5 128.3, 127.6, 127.3, 122.6, 87.8, 76.8, 64.5, 63.4, 48.1, 40.2, 36.2, 31.9, 27.7, 19.1, 16.1; **HRMS (APCI) m/z**: $[M+H]^+$ calculated for

$[C_{24}H_{28}NO_4S]^+$ 426.1739, found 426.172; **IR** (neat) $\tilde{\nu}$ = 3058, 2962, 2929, 2875, 1641, 1466, 1431, 1391, 1369, 1311, 1292, 1266, 1226, 1187, 1162, 1129, 1098, 1065, 1034, 989, 954, 910, 835, 791, 758, 731, 700, 649, 612, 586, 567, 539, 497, 476, 446 cm^{-1}; $[\boldsymbol{\alpha}]_{\mathbf{D}}^{\mathbf{22}}$ −207.9 (*c* 1.0, $CHCl_3$); **Mp** 200-204 °C.

(1*S*,3'*S*,9a'*R*)-3'-Isopropyl-3,3-dimethyltetrahydro-5'*H*,8'*H*-spiro[cyclopentane-1,6'-oxazolo[3,2-d][1,4]thiazepin]-5'-one 7',7'-dioxide (350):

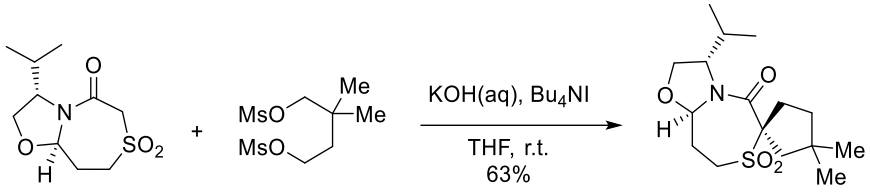

$KOH_{(aq)}$ (50 wt%, 3 mL) was added drop-wise to a solution of sulfone **277** (74 mg, 0.3 mmol, 1 equiv), dimesylate **329** (184 mg, 0.60 mmol, 2.0 equiv), and tetrabutylammonium iodide (442 mg, 1.2 mmol, 4 equiv) in THF (6 mL) at r.t. The reaction was then vigorously stirred for 4 days. The solution was diluted with H_2O (10 mL) and extracted with DCM (3 × 30 mL). Combined organic extracts were dried over $MgSO_4$, filtered, and concentrated to afford a yellow solid. The solid was subjected to column chromatography (10 g SiO_2, 2% EtOAc in DCM) to afforded spirocycle **350** as a white solid (62 mg, 63%). **^{1}H NMR** (500 MHz, $CDCl_3$) δH 5.54 (1H, d, *J* = 9.6 Hz), 4.38 (1H, m), 3.90 – 3.98 (2H, m), 3.63 (1H, ddd, *J* = 15.3, 13.4, 3.0 Hz), 3.11 – 3.22 (2H, m), 2.46 – 2.61 (2H, m), 2.34 (1H, qqd, *J* = 7.0, 7.0, 3.9 Hz), 2.18 (1H, m), 2.15 (2H, s), 1.57 – 1.70 (2H, m), 1.15 (3H, s), 0.95 (3H, s), 0.89 (3H, d, *J* = 7.0 Hz), 0.82 (3H, d, *J* = 7.0 Hz); **^{13}C NMR** (126 MHz, $CDCl_3$) δC 164.2, 88.0, 77.8, 64.4, 63.4, 48.2, 47.9, 41.4, 39.9, 32.1, 29.3, 28.8, 27.9, 27.8, 19.3, 16.2; **HRMS (APCI) m/z**: $[M+H]^+$ calculated for $[C_{16}H_{28}NO_4S]^+$ 330.1739 found 330.1741; **IR** (neat) ν = 2958, 2933, 2870, 1710, 1622, 1487, 1463, 1437, 1405, 1389, 1370, 1352, 1334, 1309,

1289, 1228, 1201, 1172, 1129, 1096, 1050, 1032, 1021, 985, 953, 882, 848, 836, 798, 777, 754, 731 cm^{-1}; $[\alpha]_D^{22}$ −212.4 (*c* 1.0, $CHCl_3$); **Mp** 227-229 °C.

5.2.2 General Procedure for Reductive Alkylation

(*R*)-*N*-((*S*)-1-Hydroxy-3-methylbutan-2-yl)-4-methoxy-2-methyl-2,3-dihydro-1*H*-indene-2-carboxamide (353):

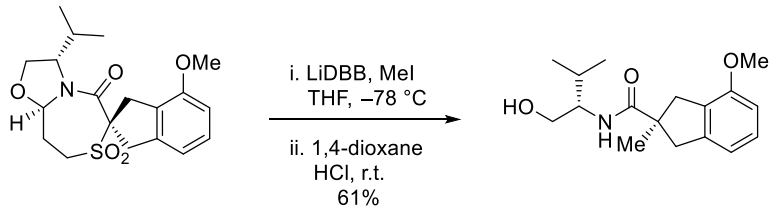

LiDBB (0.4 M, 2.1 equiv, 2.6 mL) drop-wise to a solution of spirocycle **287** (159 mg, 0.42 mmol, 1 equiv), that had been azeotropically dried with PhMe (2 × 15 mL), in dry and degassed THF (10 mL) at –78 °C. Following the addition, the solution left to stir at –78 °C for 20 min. Iodomethane (157 µl, 2.51 mmol, 6 equiv), which had been passed through a column of activated, basic, Brockmann I aluminium oxide, was then added drop-wise *via* glass syringe and the reaction allowed to stir at –78 °C for 4 hours. The reaction was warmed to r.t. and all volatiles removed under reduced pressure. The resulting residue was dissolved in 1,4-dioxane (10 mL) and 1 M $HCl_{(aq)}$ (10 mL) added. After stirring at r.t. for 12 hours the solution was adjusted to pH 7 with $NaOH_{(aq)}$ (15% w.t.) and allowed to stir at r.t for 1 hour before being extracted with EtOAc (3 × 50 mL). Combined organic extracts were dried over Na_2SO_4, filtered, and concentrated to afford a yellow solid which was purified by column chromatography (20 g SiO_2, 40-50% EtOAc in hexanes). Amide **353** was isolated as a white solid (74 mg, 61%). **^{1}H NMR** (500 MHz, $CDCl_3$) δH 7.16 (1H, dd, *J* = 7.8, 7.8 Hz), 6.83 (1H, d, *J* = 7.5 Hz), 6.70 (1H, d, *J* = 8.1 Hz), 5.75 (1H, br. d, *J* = 7.0 Hz, D_2O exch.), 3.82 (3H, s), 3.61 – 3.76 (3H, m), 3.42 (1H, d, *J* = 15.9 Hz), 3.28 (1H, d,

J = 16.1 Hz), 2.87 (1H, d, *J* = 715.8 Hz), 2.87 (1H, d, *J* = 15.8 Hz), 2.65 (1H, t, *J* = 5.1 Hz, D_2O exch.), 1.86 (1H, qqd, *J* = 6.8, 6.8, 6.8 Hz), 1.40 (3H, s), 0.91 (3H, d, *J* = 6.8 Hz), 0.85 (3H, d, *J* = 6.8 Hz); **^{13}C NMR** (126 MHz, $CDCl_3$) δC 178.9, 156.2, 143.4, 128.7, 128.4, 117.2, 108.3, 64.7, 57.3, 55.2, 50.2, 44.8, 41.0, 29.0, 25.8, 19.6, 18.5; **HRMS (APCI) m/z**: $[M+H]^+$ calculated for $[C_{17}H_{26}NO_3]^+$ 292.1913, found 292.1911; **IR** (neat) $\tilde{\nu}$ = 3311, 3261, 3079, 2960, 2933, 2877, 2833, 1624, 1590, 1556, 1483, 1470, 1464, 1439, 1389, 1371, 1351, 1328, 1316, 1299, 1274, 1262, 1241, 1189, 1171, 1155, 1116, 1075, 1033, 970, 900, 888, 864, 827, 813, 771, 750, 725, 704 cm^{-1}; $[\alpha]_D^{22}$ +44.9 (*c* 1.0, $CHCl_3$); **Mp** 140-141 °C.

(*R*)-2-Ethyl-*N*-((*S*)-1-hydroxy-3-methylbutan-2-yl)-4-methoxy-2,3-dihydro-1*H*-indene-2-carboxamide (354):

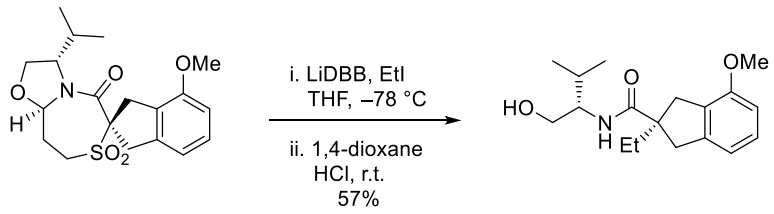

Amide **354** was synthesised according to the example procedure using LiDBB (0.4 M, 2.4 mL, 0.94 mmol, 2.1 equiv), spirocycle **287** (170 mg, 0.45 mmol, 1 equiv), degassed dry THF (12 mL), iodoethane (145 μl, 1.8 mmol, 4 equiv), which had been passed through a column of activated, basic, Brockmann I aluminium oxide, 1,4-dioxane (12 mL) and 1 M $HCl_{(aq)}$ (6 mL). EtOAc (3 × 30 mL) was employed for the aqueous work up with combined organic extracts dried over Na_2SO_4, filtered, and concentrated to afford a yellow oil which was purified by column chromatography (20 g SiO_2, 40 – 50% EtOAc in hexanes). Amide **353** was isolated as a colourless oil (79 mg, 57%). **^{1}H NMR** (500 MHz, $CDCl_3$) δH 7.14 (1H, t, *J* = 7.8 Hz), 6.81 (1H, d, *J* = 7.5 Hz), 6.68 (1H, d, *J* = 8.1 Hz), 5.73 (1H, d, *J* = 7.7 Hz, D_2O exch.), 3.82 (3H, s), 3.74 (1H, m), 3.67 (1H, m), 3.61

(1H, m), 3.36 (1H, d, *J* = 16.1 Hz), 3.24 (1H, d, *J* = 16.2 Hz), 2.94 (1H, d, *J* = 16.2 Hz), 2.92 (1H, d, *J* = 16.2 Hz), 2.79 (1H, br. s, D_2O exch.), 1.84 (1H, m), 1.73 (1H, m), 0.93 (3H, t, *J* = 7.4 Hz), 0.87 (3H, d, *J* = 6.8 Hz), 0.83 (3H, d, *J* = 6.9 Hz); **^{13}C NMR** (126 MHz, $CDCl_3$) δC 177.9, 155.9, 143.6, 128.7, 128.3, 117.0, 108.2, 64.7, 57.3, 55.2(4), 55.2(0), 42.9, 38.4, 32.1, 28.9, 18.4, 9.8; **HRMS (ESI) m/z**: $[M+Na]^+$ calculated for $[C_{18}H_{27}NO_3Na]^+$ 328.1883, found 328.1879; **IR** (neat) $\tilde{\nu}$ = 3306, 3260, 3070, 2962, 2936, 2901, 2874, 2837, 1716, 1619, 1591, 1551, 1482, 1467, 1385, 1371, 1353, 1338, 1316, 1298, 1262, 1230, 1185, 1168, 1149, 1109, 1074, 1056, 1022, 1009, 967, 939, 885, 858, 828, 814, 765, 736, 703 cm^{-1}; $[\alpha]_D^{22}$ −0.3 (*c* 1.0, $CHCl_3$); **Mp** 123-125 °C.

(*R*)-*N*-((*S*)-1-Hydroxy-3-methylbutan-2-yl)-4-methoxy-2-propyl-2,3-dihydro-1*H*-indene-2-carboxamide (335):

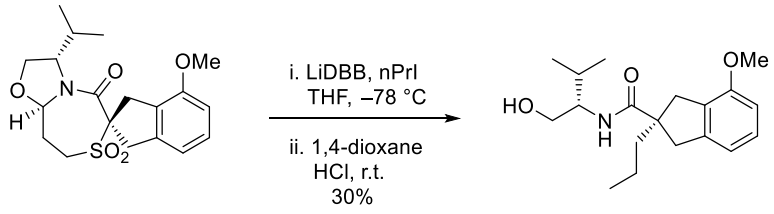

Amide **335** was synthesised according to the example procedure using LiDBB (0.4 M, 1.65 mL, 0.664 mmol, 2.1 equiv), spirocycle **287** (120 mg, 0.316 mmol, 1 equiv), degassed dry THF (6 mL), 1-iodopropane (123 µl, 1.26 mmol, 4 equiv), which had been passed through a column of activated, basic, Brockmann I aluminium oxide, 1,4-dioxane (6 mL) and 1 M $HCl_{(aq)}$ (2.5 mL). EtOAc (3 × 20 mL) was employed for the aqueous work up with combined organic extracts dried over Na_2SO_4, filtered, and concentrated to afford a yellow oil which was purified by column chromatography (15 g SiO_2, 40 – 60% EtOAc in hexanes). Amide **335** was isolated as a colourless oil (30 mg, 30%). **^{1}H NMR** (500 MHz, $CDCl_3$) δH 7.15 (1H, dd, *J* = 7.8, 7.8 Hz), 6.81 (1H, d, *J* = 7.5 Hz), 6.68 (1H, d, *J* = 8.1 Hz), 5.71 (1H, br. d, *J* = 7.3 Hz, D_2O exch.), 3.82 (3H, s), 3.71 (1H, m), 3.59

– 3.68 (2H, m), 3.36 (1H, d, *J* = 16.1 Hz), 3.25 (1H, d, *J* = 16.2 Hz), 2.95 (1H, d, *J* = 16.0 Hz), 2.92 (1H, d, *J* = 16.1 Hz), 2.69 (1H, br. s, D_2O exch.), 1.83 (1H, m), 1.61 – 1.78 (2H, m), 1.34 (2H, m), 0.90 (3H, t, 7.3), 0.87 (3H, d, *J* = 6.8 Hz), 0.82 (3H, d, *J* = 6.8 Hz); **^{13}C NMR** (126 MHz, $CDCl_3$) δC 178.1, 155.9, 143.5, 128.7, 128.3, 117.0, 108.2, 64.8, 57.3, 55.2, 54.9, 43.0, 41.8, 38.7, 28.9, 19.5, 18.7, 18.3, 14.5; **HRMS (APCI) m/z**: $[M+H]^+$ calculated for $[C_{19}H_{30}NO_3]^+$ 320.2226, found 320.2228; **IR** (neat) $\tilde{\nu}$ = 3302, 3253, 3068, 2958, 2937, 29.05, 2872, 2837, 1717, 1619, 1591, 1552, 1482, 1467, 1441, 1388, 1372, 1353, 1335, 1324, 1297, 1284, 1262, 1225, 1184, 1167, 1151, 1132, 1119, 1081, 1057, 1041, 1017, 993, 966, 940, 898, 888, 874, 862, 832, 817, 766, 736, 704 cm^{-1}; $[\alpha]_D^{22}$ −3.4 (*c* 1.0, $CHCl_3$) **Mp** 114-115 °C.

(*R*)-*N*-((*S*)-1-Hydroxy-3-methylbutan-2-yl)-4-methoxy-2-(prop-2-yn-1-yl)-2,3-dihydro-1*H*-indene-2-carboxamide (356):

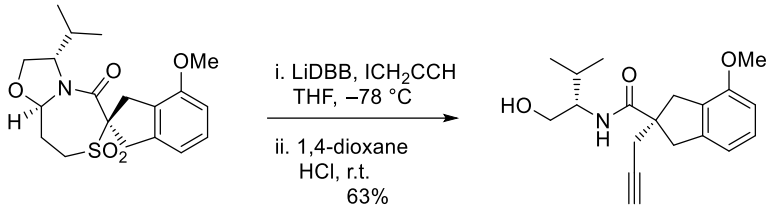

Amide **356** was synthesised according to the example procedure using LiDBB (0.4 M, 690 µl, 0.28 mmol, 2.1 equiv), spirocycle **287** (50 mg, 0.13 mmol, 1 equiv), degassed dry THF (5 mL), propargyl bromide (80% in PhMe, 50 µl, 0.53 mmol, 4 equiv), which had been passed through a column of activated, basic, Brockmann I aluminium oxide, 1,4-dioxane (5 mL) and 1 M $HCl_{(aq)}$ (2.5 mL). EtOAc (3 × 20 mL) was employed for the aqueous work up with combined organic extracts dried over Na_2SO_4, filtered, and concentrated to afford a yellow oil which was purified by column chromatography (15 g SiO_2, 40-60% EtOAc in hexanes). Amide **356** was isolated as a slightly yellow oil (26 mg, 63%). **^{1}H NMR** (500 MHz, $CDCl_3$) δH 7.16 (1H, dd, *J* = 8.2, 7.6 Hz),

6.83 (1H, *J* = 7.6 Hz), 6.70 (1H, d, *J* = 8.2 Hz), 6.04 (1H, d, *J* = 7.9 Hz, D_2O exch.), 3.82 (3H, s), 3.78 (1H, m), 3.69 (1H, dd, *J* = 11.2, 2.9 Hz), 3.62 (1H, dd, *J* = 11.2, 6.3 Hz), 3.20 (1H, d, *J* = 16.2 Hz), 3.23 (1H, d, *J* = 16.2 Hz), 3.16 (1H, d, *J* = 16.3 Hz), 3.07 (1H, d, *J* = 16.2 Hz), 2.59 (2H, m), 2.13 (1H, t, *J* = 2.3 Hz), 1.86 (1H, dqq, *J* = 6.9, 6.7, 6.7 Hz), 0.91 (1H, d, *J* = 6.7 Hz), 0.86 (1H, d, *J* = 6.9 Hz); **^{13}C NMR** (126 MHz, $CDCl_3$) δC 176.3, 156.2, 142.7, 128.6, 128.0, 117.2, 108.4, 81.9, 71.6, 64.2, 57.4, 55.2, 53.4, 42.4, 38.2, 29.0, 27.3, 19.5, 18.3; **HRMS (ESI) m/z**: $[M+Na]^+$ calculated for $[C_{19}H_{25}NO_3Na]^+$ 338.1727, found 338.1717; **IR** (neat) $\tilde{\nu}$ = 3380, 3299, 2960, 2937, 2874, 2838, 1720, 1641, 1591, 1523, 1482, 1468, 1440, 1389, 1369, 1335, 1264, 1180, 1150, 1110, 1070, 976, 939, 911, 769, 735, 704, 638, 525 cm^{-1}; $[\alpha]_D^{22}$ −3.2 (*c* 1.0, $CHCl_3$).

(*R*)-2-Benzyl-*N*-((*S*)-1-hydroxy-3-methylbutan-2-yl)-4-methoxy-2,3-dihydro-1*H*-indene-2-carboxamide (357):

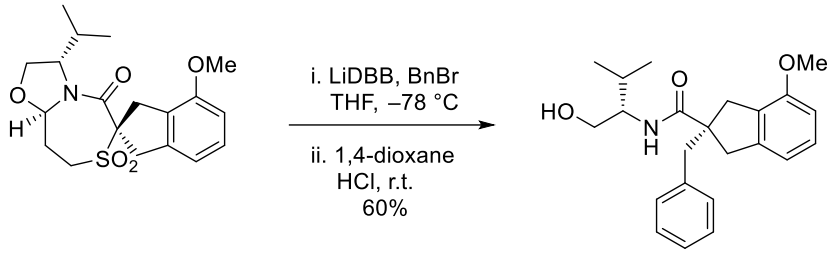

Amide **357** was synthesised according to the example procedure using LiDBB (0.4 M, 1.65 mL, 0.664 mmol, 2.1 equiv), spirocycle **287** (115 mg, 0.316 mmol, 1 equiv), degassed dry THF (6 mL), benzyl bromide (150 µl, 1.26 mmol, 4 equiv), which had been passed through a column of activated, basic, Brockmann I aluminium oxide, 1,4-dioxane (6 mL) and 1 M $HCl_{(aq)}$ (2.5 mL). EtOAc (3 × 20 mL) was employed for the aqueous work up with combined organic extracts dried over Na_2SO_4, filtered, and concentrated to afford a yellow oil which was purified by column chromatography (15 g SiO_2, 40 – 60% EtOAc in hexanes). Amide **357** was isolated as a white solid (69 mg, 60%). **^{1}H NMR** (500 MHz, $CDCl_3$) δH 7.22 – 7.33 (5H, m), 7.19 (1H, t, *J* = 7.8

Hz), 6.88 (1H, d, *J* = 7.4 Hz), 6.73 (1H, d, *J* = 8.2 Hz), 5.79 (1H, d, *J* = 7.7 Hz, D_2O exch.), 3.86 (3H, s), 3.64 (1H, m), 3.52 (2H, m), 3.34 (1H, d, *J* = 15.8 Hz), 3.17 (1H, d, *J* = 13.3 Hz), 3.14 (1H, d, *J* = 14.8 Hz), 3.10 (1H, d, *J* = 16.2 Hz), 3.05 (1H, d, *J* = 15.9 Hz), 2.98 (1H, d, *J* = 13.4 Hz), 2.40 (1H, br. s, D_2O exch.), 1.70 (1H, m), 0.76 (3H, d, *J* = 6.8 Hz), 0.67 (3H, d, *J* = 6.8 Hz); **^{13}C NMR** (126 MHz, $CDCl_3$) δC 176.8, 156.0, 143.4, 138.1, 130.1, 128.5, 128.2, 128.2, 126.7, 117.2, 108.4, 64.1, 57.4, 56.8, 55.2, 43.6, 43.3, 37.3, 28.9, 19.3, 18.2; **HRMS (APCI) m/z**: $[M+H]^+$ calculated for $[C_{23}H_{30}NO_3]^+$ 368.22267, found 368.2231; **IR** (neat) $\tilde{\nu}$ = 3421, 3303, 3254, 3067, 3029, 2957, 2933, 2901, 2873, 2833, 1622, 1591, 1520, 1497, 1483, 1470, 1455, 1443, 1388, 1370, 1354, 1334, 1300, 1263, 1225, 1181, 1165, 1150, 1111, 1086, 1070, 1048, 1029, 998, 966, 942, 923, 984, 881, 835, 819, 764, 735, 701, 674 cm^{-1}; $[\alpha]_D^{22}$ −2.6 (*c* 1.0, $CHCl_3$); **Mp** 146-147 °C.

(*R*)-2-Allyl-*N*-((*S*)-1-hydroxy-3-methylbutan-2-yl)-4-methoxy-2,3-dihydro-1*H*-indene-2-carbox amide (358):

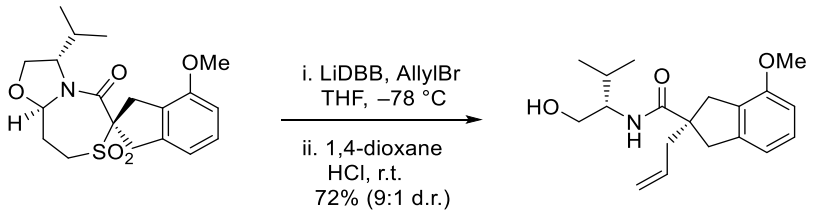

Amide **358** was synthesised according to the example procedure using LiDBB (0.4 M, 3.3 mL, 1.3 mmol, 2.1 equiv), spirocycle **287** (224 mg, 0.590 mmol, 1 equiv), degassed dry THF (13 mL), allyl bromide (205 µl, 2.36 mmol, 4 equiv), which had been passed through a column of activated, basic, Brockmann I aluminium oxide, 1,4-dioxane (8 mL) and 1 M $HCl_{(aq)}$ (4 mL). EtOAc (3 × 30 mL) was employed for the aqueous work up with combined organic extracts dried over Na_2SO_4, filtered, and concentrated to afford a yellow oil which was purified by column chromatography (20 g SiO_2, 40-60% EtOAc in hexanes). Amide **358** was isolated as a colourless oil (135 mg, 72%).

^{1}H NMR (500 MHz, $CDCl_3$) δH 7.15 (1H, dd, *J* = 8.2, 7.5 Hz), 6.82 (1H, *J* = 7.5 Hz), 6.69 (1H, d, *J* = 8.2 Hz), 5.82 (1H, m), 5.71 (1H, d, *J* = 7.5 Hz, D_2O exch.), 5.09 (2H, m), 3.82 (3H, s), 3.73 (1H, m), 3.59 – 3.67 (2H, m), 3.35 (1H, d, *J* = 16.2 Hz), 3.19 (1H, d, *J* = 16.2 Hz), 2.99 (1H, d, *J* = 16.2 Hz), 2.99 (1H, d, *J* = 16.2 Hz), 2.64 (1H, br. s, D_2O exch.), 2.52 (1H, dd, *J* = 14.0, 7.3 Hz), 2.43 (1H, dd, *J* = 14.0, 7.2 Hz), 1.83 (1H, m), 0.88 (3H, d, *J* = 6.7 Hz), 0.83 (3H, d, *J* = 6.9 Hz); **^{13}C NMR** (126 MHz, $CDCl_3$) δC 177.4, 156.0, 143.3, 134.3, 128.4 (2C), 118.4, 117.1, 108.3, 64.5, 57.3, 55.2, 54.2, 42.9, 42.5, 39.0, 29.0, 19.6, 18.4; **HRMS (ESI) m/z**: $[M+Na]^+$ calculated for $[C_{19}H_{28}NO_3]^+$ 318.2062, found 318.2064; **IR** (neat) $\tilde{\nu}$ = 33012, 2157, 3074, 3000, 2960, 2937, 2905, 2873, 2836, 1621, 1591, 1551, 1482, 1468, 1449, 1388, 1372, 1353, 1336, 1305, 1263, 1223, 1183, 1167, 1149, 1102, 1083, 1057, 1130,993, 966, 919, 886, 862, 834, 818, 765, 736, 704, 655 cm^{-1}; $[\boldsymbol{\alpha}]_{\mathbf{D}}^{\mathbf{22}}$ −1.6 (*c* 1.0, $CHCl_3$); **Mp** 102-103 °C.

(*R*)-2-Allyl-N-((*S*)-1-hydroxy-3-methylbutan-2-yl)-4-phenyl-2,3-dihydro-1H-indene-2-carboxamide (361)

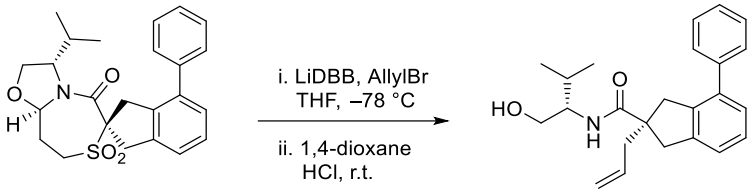

^{1}H NMR (500 MHz, $CDCl_3$) δH 7.39 – 7.45 (4H, m), 7.35 (1H, m), 7.19 – 7.28 (4H, m), 5.78 (1H, m), 5.67 (1H, d, *J* = 7.8 Hz, D_2O exch.), 5.08 (1H, s), 5.05 (1H, d, *J* = 2.9 Hz), 3.70 (1H, m), 3.62 (1H, dd, *J* = 11.0, 3.3 Hz), 3.56 (1H, dd, *J* = 11.0, 6.2 Hz), 3.39 (1H, d, *J* = 15.9 Hz), 3.34 (1H, d, *J* = 16.2 Hz), 3.07 (1H, d, *J* = 15.8 Hz), 3.05 (1H, d, *J* = 16.1 Hz), 2.66 (1H, br. s, D_2O exch.), 2.51 (1H, dd, *J* = 14.0, 7.3 Hz), 2.44 (1H, dd, *J* = 14.0, 7.2 Hz), 1.80 (1H, qqd, *J* = 6.8, 6.8, 6.8 Hz), 0.85 (3H, d, *J* = 6.8 Hz), 0.77 (3H, d, *J* = 6.8 Hz); **^{13}C NMR** (126 MHz, $CDCl_3$) δC 177.0, 142.0,

140.6, 138.7, 138.7, 134.2, 128.4 (two signals), 127.3, 127.2, 127.1, 123.5, 118.3, 64.1, 57.2, 54.5, 42.3, 42.2, 41.5, 28.8, 19.5, 18.4; **HRMS m/z**: $[M+Na]^+$ calculated for $[C_{24}H_{29}NO_2Na]^+$ 386.2090, found 386.2090; **IR** (neat) ν = 3289, 3240, 3083, 3067, 3052, 3032, 3000, 2962, 2944, 2907, 2874, 2849, 1619, 1557, 1500, 1466, 1449, 1428, 1388, 1372, 1353, 1336, 1306, 1278, 1265, 1244, 1224, 1179, 1154, 1136, 1099, 1078, 1062, 1048, 1026, 996, 964, 922, 891, 881, 851, 834, 821, 793, 757, 737, 700, 655.

(*R*)-1-Allyl-*N*-((*S*)-1-hydroxy-3-methylbutan-2-yl)-3,3-dimethylcyclopentane-1-carbox amide (362):

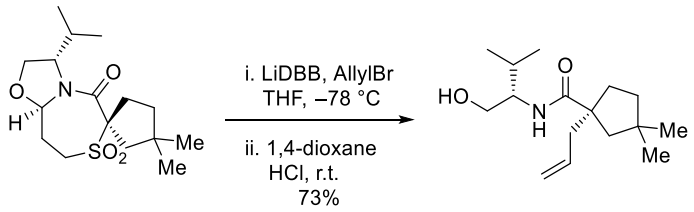

Amide **362** was synthesised according to the example procedure using LiDBB (0.4 M, 2.8 mL, 1.1 mmol, 2.1 equiv), sulfone **350** (176 mg, 0.53 mmol, 1 equiv), degassed dry THF (10 mL), allyl brmoide (185 µl, 2.14 mmol, 4 equiv), which had been passed through a column of activated, basic, Brockmann I aluminium oxide, 1,4-dioxane (12 mL) and 1 M $HCl_{(aq)}$ (6 mL). EtOAc (4 × 20 mL) was employed for the aqueous work up with combined organic extracts dried over Na_2SO_4, filtered, and concentrated to afford a yellow oil which was purified by column chromatography (20 g SiO_2, 45% EtOAc in hexanes). Amide **362** was isolated as a colourless oil as 4:1 mixture of diastereomers (104 mg, 73%). Major isomer: **^{1}H NMR** (500 MHz, $CDCl_3$) δH 5.78 (1H, m, D_2O exch.), 5.72 (1H, m), 5.06 (1H, dd, *J* = 10.2, 1.2 Hz), 5.03, (1H, d, *J* = 1.0 Hz), 3.71 (1H, m), 3.63 (2H, m), 3.05 (1H, broad s D_2O exch.), 2.38 (1H, dd, *J* = 14.0, 2.4 Hz), 2.31 (1H, dd, *J* = 14.0, 2.3 Hz), 2.11 (1H, dt, *J* = 13.0, 7.5 Hz), 2.04 (1H, d, *J* = 13.7 Hz), 1.88 (1H, dqq, *J* = 6.8, 6.8, 6.8 Hz),

1,69 (1H, dt, *J* = 13.2, 6.8 Hz), 1.48 (1H, t, *J* = 6.3 Hz), 1.42 (1H, d, *J* = 13.7 Hz), 1.04 (3H, d), 0.98 (3H, s), 0.94 (3H, d, *J* = 6.8 Hz), 0.91 (3H, d, *J* = 6.8 Hz); **^{13}C NMR** (126 MHz, $CDCl_3$) δC 178.3, 134.7, 117.8, 64.2, 57.2, 54.7, 50.2, 45.4, 40.3, 39.0, 34.7, 30.4, 29.6, 29.0, 19.7, 18.8; Minor isomer: **^{1}H NMR** (500 MHz, $CDCl_3$) δH 5.78 (1H, m, D_2O exch.), 5.72 (1H, m), 5.06 (1H, dd, *J* = 10.2, 1.2 Hz), 5.03, (1H, d, *J* = 1.0 Hz), 3.71 (1H, m), 3.63 (2H, m), 3.05 (1H, broad s D_2O exch.), 2.38 (1H, dd, *J* = 14.0, 2.4 Hz), 2.31 (1H, dd, *J* = 14.0, 2.3 Hz), 2.18 (1H, dt, *J* = 13.1, 7.6 Hz), 1.97 (1H, d, *J* = 13.6 Hz), 1.88 (1H, dqq, *J* = 6.8, 6.8, 6.8 Hz), 1.69 (1H, dt, *J* = 13.2, 6.8 Hz), 1.48 (1H, t, *J* = 6.3 Hz), 1.42 (1H, d, *J* = 13.7 Hz), 1.04 (3H, d), 0.98 (3H, s), 0.94 (3H, d, *J* = 6.8 Hz), 0.91 (3H, d, *J* = 6.8 Hz); **^{13}C NMR** (126 MHz, $CDCl_3$) δC 178.4, 134.7, 117.8, 64.2, 57.2, 54.7, 50.3, 45.5, 40.2, 39.1, 34.7, 30.4, 29.6, 29.0, 19.7, 18.8; **HRMS m/z**: $[M+Na]^+$ calculated for $[C_{16}H_{29}NO_2Na]^+$ 290.2096, found 290.2086; **IR** (neat) ν = 3433, 3359, 3079, 3056, 3008, 2956, 2937, 2868, 1638, 1512, 1464, 1415, 1387, 1366, 1329, 1310, 1275, 1265, 1233, 1175, 1150, 1120, 1075, 995, 917, 764, 739, 703 cm^{-1}.

(*R*)-*N*-((*S*)-1-Hydroxy-3-methylbutan-2-yl)-2-methyl-1,2,3,4-tetrahydronaphthalene-2-carboxamide (363):

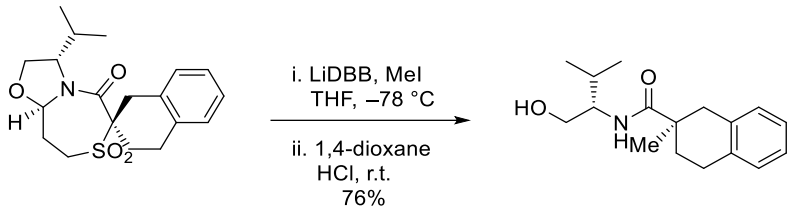

Amide **363** was synthesised according to the example procedure using LiDBB (0.4 M, 500 µl, 0.20 mmol, 2.1 equiv), spirocycle **347** (35 mg, 0.10 mmol, 1 equiv), degassed dry THF (24 mL), methyl iodide (60 µl, 1.0 mmol, 10 equiv), which had been passed through a column of activated, basic, Brockmann I aluminium oxide, 1,4-dioxane (10 mL) and 1 M $HCl_{(aq)}$ (5 mL). EtOAc (3 × 20 mL)

was employed for the aqueous work up with combined organic extracts dried over Na_2SO_4, filtered, and concentrated to afford a colourless residue which was purified by column chromatography (12 g SiO_2, 40 – 50% EtOAc in hexanes). Amide **363** was isolated as a colourless oil (20 mg, 76%). **^{1}H NMR** (500 MHz, $CDCl_3$) δH 7.12 (4H, m), 5.73 (1H, d, *J* = 6.6 Hz, D_2O exch.), 3.71 (1H, ddd, *J* = 7.2, 6.7, 3.5 Hz), 3.64 9 (1H, dd, *J* = 11.0, 3.5 Hz), 3.56 (1H, dd, *J* = 11.0, 6.7 Hz), 3.07 (1H, d, *J* = 17.5 Hz), 2.77 – 2.88 (2H, m), 2.62 (1H, broad s, D_2O exch), 2.22 (1H, m), 1.66 – 1.77 (2H, m), 1.33 (3H, s), 0.69 (3H, d, *J* = 6.8 Hz), 0.60 (3H, d, *J* = 6.8 Hz); **^{13}C NMR** (126 MHz, $CDCl_3$) δC 178.3, 135.8, 134.3, 129.1, 128.8, 126.4, 126.2, 65.0, 57.2, 42.0, 39.1, 33.2, 28.7, 26.5, 25.9, 19.4, 17.7; **HRMS (ESI) m/z**: $[M+Na]^+$ calculated for $[C_{17}H_{25}O_2NNa]^+$ 298.1778, found 298.1775; **IR** (neat) $\tilde{\nu}$ = 3309, 3046, 3019, 2960, 2929, 2878, 2846, 2259, 1627, 1581, 1540, 1495, 1463, 1440, 1418, 1389, 1371, 1347, 1215m 1292, 1273, 1250, 1236, 1215, 1189, 1149, 1125, 1088, 1056, 1032, 1021, 998, 973, 958, 922, 910, 824, 799, 743, 661, 589, 566, 5515, 502, 484, 449, 439 cm^{-1}; $[\alpha]_D^{22}$ +55.7 (*c* 1.0, $CHCl_3$); **Mp** 117-118 °C.

(*R*)-*N*-((*S*)-1-Hydroxy-3-methylbutan-2-yl)-1-methyl-3-methylenecyclopentane-1-carboxamide (364):

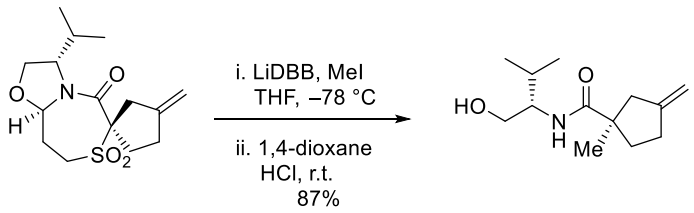

Amide **364** was synthesised according to the example procedure using LiDBB (0.4 M, 530 µl, 0.21 mmol, 2.1 equiv), spirocycle **348** (31 mg, 0.10 mmol, 1 equiv), degassed dry THF (20 mL), methyl iodide (62 µl, 1.0 mmol, 10 equiv), which had been passed through a column of activated, basic, Brockmann I aluminium oxide, 1,4-dioxane (10 mL) and 1 M $HCl_{(aq)}$ (5 mL). EtOAc (3 × 20 mL)

was employed for the aqueous work up with combined organic extracts dried over Na_2SO_4, filtered, and concentrated to afford a colourless residue which was purified by column chromatography (10 g SiO_2, 50 – 60% EtOAc in hexanes). Amide **364** was isolated as a colourless oil (20 mg, 87%). **^{1}H NMR** (500 MHz, $CDCl_3$) δH 5.79 (1H, s, D_2O exch), 4.96 (1H, s), 4.89 (1H, s), 3.73 (2H, m), 3.64 (1H, m), 2.73 (1H, d, *J* = 16.1 Hz), 2.67 (1H, s, D_2O exch), 2.44 (2H, m), 2.26 (1H, d, *J* = 16.0 Hz), 2.13 (1H, dt, *J* = 12.6, 8.3 Hz), 1.90 (1 H, d of septets, *J* = 6.8, 6.8 Hz), 1.67 (1H, dt, *J* = 12.7, 7.3 Hz), 1.28 (3H, s), 0.96 (3H, d, *J* = 6.8 Hz), 0.92 (3H, d, *J* = 6.8 Hz); **^{13}C NMR** (126 MHz, $CDCl_3$) δC 178.7, 150.4, 107.1, 64.5, 57.1, 49.7, 44.6, 37.1, 30.5, 29.1, 24.2, 19.6, 18.6; **HRMS (APCI) m/z**: $[M+H]^+$ calculated for $[C_{13}H_{24}O_2N]^+$ 226.1801, found 226.1806; **IR** (neat) $\tilde{\nu}$ = 3351, 3069, 2961, 2929, 2873, 1724, 1636, 1522, 1464, 1388, 1370, 1304, 1267, 1228, 1174, 1127, 1072, 1034, 950, 925, 879, 734, 702, 609, 479, 423 cm^{-1}; $[\alpha]_D^{22}$ +48.1 (*c* 1.0, $CHCl_3$).

(*R*)-*N*-((*S*)-1-Hydroxy-3-methylbutan-2-yl)-2-methyl-4-phenyl-2,3-dihydro-1*H*-indene-2-carboxamide (365):

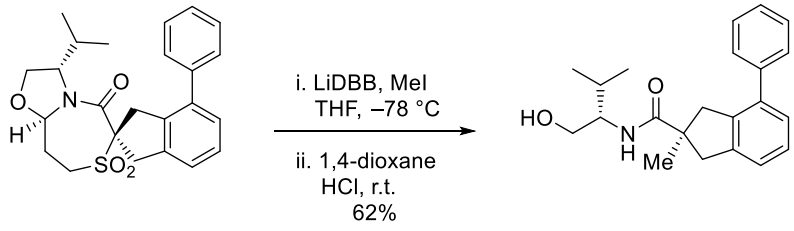

Amide **365** was synthesised according to the example procedure using LiDBB (0.4 M, added until colour persisted), spirocycle **349** (43 mg, 0.10 mmol, 1 equiv), degassed dry THF (5 mL), iodomethane (25 µl, 0.40 mmol, 4 equiv), which had been passed through a column of activated, basic, Brockmann I aluminium oxide, 1,4-dioxane (10 mL) and 1 M $HCl_{(aq)}$ (5 mL). EtOAc (3 × 20 mL) was employed for the aqueous work up with combined organic extracts dried over Na_2SO_4,

filtered, and concentrated to afford a yellow oil which was purified by column chromatography (8 g SiO_2, 10-60% EtOAc in hexanes). Amide **365** was isolated as a slightly yellow solid (21 mg, 62%). **^{1}H NMR** (500 MHz, $CDCl_3$) δH 7.42 (4H, m), 7.34 (1H, m), 2.27 (1H, m), 7.22 (2H, m), 5.71 (1H, d, *J* = 7.1 Hz, D_2O exch.), 3.59 – 3.73 (2H, m), 3.6 (1H, m), 3.49 (1H, d, *J* = 16.0 Hz), 3.48 (1H, d, *J* = 15.6 Hz), 2.94 (1H, d, *J* = 15.4 Hz), 2.92 (1H, d, *J* = 16.0 Hz), (1H, broad s, D_2O exch.), 1.84 (1H, d of septets, *J* = 6.8, 6.8 Hz), 1.37 (3H, s), 0.88 (3H, d, *J* = 6.8 Hz), 0.81 (3H, d, *J* = 6.8 Hz); **HRMS (ESI) m/z**: $[M+Na]^+$ calculated for $[C_{22}H_{27}NO_2Na]^+$ 338.2115, found 338.2118; **^{13}C NMR** (126 MHz, $CDCl_3$) δC 178.7, 142.3, 140.7, 139.1, 138.8, 128.5, 128.4, 127.4, 127.3, 127.1, 123.8, 64.6, 57.3, 50.5, 44.8, 44.0, 29.0, 25.1, 19.6, 18.4; **IR** (neat) $\tilde{\nu}$ = 3348, 3058, 2959, 2928, 2872, 1638, 1519, 1465, 1426, 1386, 1370, 1312, 1265, 1142, 1072, 1027, 978, 920, 889, 789, 757, 736, 700, 670, 590, 569, 519, 444 cm^{-1}; $[\alpha]_D^{22}$ −4.1 (*c* 1.0, $CHCl_3$); **Mp** 140-142 °C.

(*S*)-N-((*S*)-1-Hydroxy-3-methylbutan-2-yl)-1,3,3-trimethylcyclopentane-1-carboxamide (366):

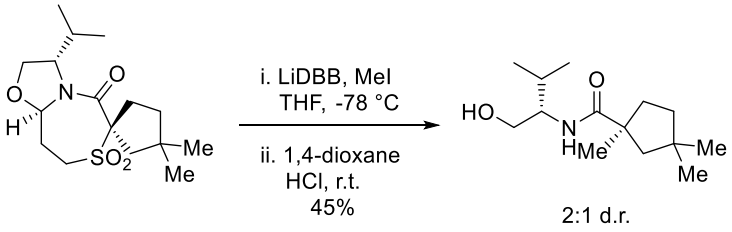

Amide **366** was synthesised according to the example procedure using LiDBB (0.4 M, 640 µl, 0.25 mmol, 2.1 equiv), sulfone **350** (40 mg, 0.12 mmol, 1 equiv), degassed dry THF (4 mL), iodomethane (30 µl, 0.49 mmol, 4 equiv), which had been passed through a column of activated, basic, Brockmann I aluminium oxide, 1,4-dioxane (5 mL) and 1 M $HCl_{(aq)}$ (5 mL). EtOAc (15 × 30 mL) was employed for the aqueous work up with combined organic extracts dried over Na_2SO_4,

filtered, and concentrated to afford a yellow oil which was purified by column chromatography (10 g SiO_2, 30% EtOAc in hexanes). Amide **366** was isolated as a colourless oil as 2:1 mixture of diastereomers (13 mg, 45%). Major isomer: **^{1}H NMR** (500 MHz, $CDCl_3$) δH 5.71 (1H, broad s, D_2O exch.), 3.72 (2H, m), 3.66 (1H, m), 2.66 (1H, broad s, D_2O exch.), 2.23 (1H, m), 2.06 (1H, d, *J* = 13.4 Hz), 1.9 (1H, dqq, *J* = 6.8, 6.8, 6.8 Hz), 1.51 – 1.63 (4H, m), 1.37 (1H, d, *J* = 13.4 Hz), 1.31 (3H, s), 1.07 (3H, s), 1.01 (3H, s), 0.97 (3H, d, *J* = 6.8 Hz), 0.94 (3H, d, *J* = 6.8 Hz); **^{13}C NMR** (126 MHz, $CDCl_3$) δC 180.2, 64.8, 57.3, 52.3, 50.6, 40.7, 39.5, 37.2, 30.6, 29.7, 29.1, 27.8, 19.7, 18.8; Minor isomer: **^{1}H NMR** (500 MHz, $CDCl_3$) δH 5.71 (1H, broad s, D_2O exch.), 3.72 (2H, m), 3.66 (1H, m), 2.66 (1H, broad s, D_2O exch.), 2.23 (1H, m), 2.07 (1H, d, *J* = 13.4 Hz), 1.9 (1H, dqq, *J* = 6.8, 6.8, 6.8 Hz), 1.51 – 1.63 (4H, m), 1.36 (1H, d, *J* = 13.4 Hz), 1.31 (3H, s), 1.07 (3H, s), 1.01 (3H, s), 0.97 (3H, d, *J* = 6.8 Hz), 0.94 (3H, d, *J* = 6.8 Hz); **^{13}C NMR** (126 MHz, $CDCl_3$) δC 180.3, 64.8, 57.3, 52.2, 50.6, 40.7, 39.5, 37.3, 30.6, 29.7, 29.1, 27.9, 19.7, 18.8; **HRMS m/z**: $[M+Na]^+$ calculated for $[C_{14}H_{27}O_2NNa]^+$ 264.1934, found 264.1943.

(*R*)-N-((*S*)-1-Hydroxy-3-methylbutan-2-yl)-3,3-dimethyl-1-(3-methylbut-2-en-1-yl)cyclo pentane-1-carboxamide (367):

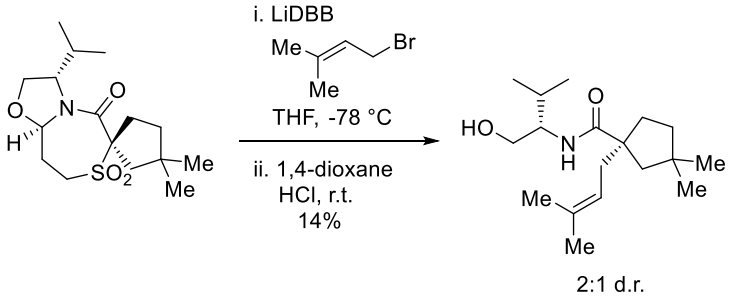

Amide **367** was synthesised according to the example procedure using LiDBB (0.4 M, 620 µl, 0.25 mmol, 2.1 equiv), sulfone **350** (39 mg, 0.12 mmol, 1 equiv), degassed dry THF (4 mL), iodomethane (55 µl, 0.48 mmol, 4 equiv), which had been passed through a column of activated,

basic, Brockmann I aluminium oxide, 1,4-dioxane (5 mL) and 1 M $HCl_{(aq)}$ (5 mL). EtOAc (15 × 30 mL) was employed for the aqueous work up with combined organic extracts dried over Na_2SO_4, filtered, and concentrated to afford a yellow oil which was purified by column chromatography (10 g SiO_2, 25% EtOAc in hexanes). Amide **367** was isolated as a colourless oil as 2:1 mixture of diastereomers (5 mg, 14%). Major isomer: **^{1}H NMR** (500 MHz, $CDCl_3$) δH 5.72 (1H, d, *J* = 7.0 Hz, D_2O exch.), 5.11 (1H, tt, *J* = 7.1, 1.3 Hz), 3.71 (2H, m), 3.60 (1H, dd, *J* = 10.9, 6.5 Hz), 2.76 (1H, broad s, D_2O exch.), 2.32 (2H, m), 2.14 (1H, dt, *J* = 13.0, 7.5 Hz), 2.05 (1H, d, *J* = 13.6 Hz), 1.88 (1H, dqq, , *J* = 6.8, 6.8, 6.8 Hz), 1.70 (3H, s), 1.67 (1H, m), 1.62 (3H, s), 1.51 (2H, t, , *J* = 7.1 Hz), 1.43 (1H, d, , *J* = 13.6 Hz), 1.06 (3H, s), 1.01 (3H, s), 0.95 (3H, d, *J* = 6.8 Hz), 0.92 (3H, d, *J* = 6.8 Hz); **^{13}C NMR** (126 MHz, $CDCl_3$) δC 179.1, 134.5, 120.7, 64.9, 57.5, 55.0, 50.6, 40.5, 39.3, 39.1, 35.0, 30.5, 29.7, 29.2, 26.0, 19.6, 18.6, 18.1; Minor isomer: **^{1}H NMR** (500 MHz, $CDCl_3$) δH 5.72 (1H, d, *J* = 7.0 Hz, D_2O exch.), 5.11 (1H, tt, *J* = 7.1, 1.3 Hz), 3.71 (2H, m), 3.60 (1H, dd, *J* = 10.9, 6.5 Hz), 2.78 (1H, broad s, D_2O exch.), 2.32 (2H, m), 2.19 (1H, dt, *J* = 13.1, 7.5 Hz), 2.00 (1H, d, *J* = 13.4 Hz), 1.88 (1H, dqq, , *J* = 6.8, 6.8, 6.8 Hz), 1.70 (3H, s), 1.67 (1H, m), 1.62 (3H, s), 1.51 (2H, t, , *J* = 7.1 Hz), 1.45 (1H, d, , *J* = 13.4 Hz), 1.06 (3H, s), 1.00 (3H, s), 0.95 (3H, d, *J* = 6.8 Hz), 0.92 (3H, d, *J* = 6.8 Hz); **^{13}C NMR** (126 MHz, $CDCl_3$) δC 179.2, 134.5, 120.7, 65.0, 57.6, 54.9, 50.6, 40.4, 39.3, 39.2, 35.0, 30.5, 29.7, 29.1, 26.0, 19.6, 18.6, 18.1; **HRMS m/z**: $[M+H]^+$ calculated for $[C_{18}H_{34}O_2N]^+$ 296.2584, found 296.2580.

5.2.3 DFT Calculations

All DFT calculations were conducted using Gaussian 16, Revision B.01. Calculations were run at the B3LYP/6-311+G(d,p) with THF solvation. All thermochemistry was determined using frequency calculations on stationary points.

Spirocycle 350:

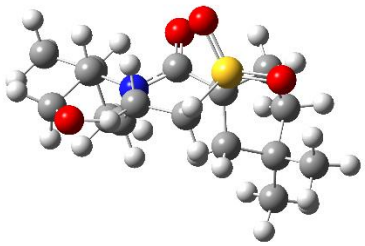

C	0.62618	-1.38118	-0.18881
C	-0.02929	-0.91849	1.15102
C	-0.13531	0.64927	1.33721
H	0.25097	-0.7791	-0.98977
H	0.54427	-1.35061	1.94403
H	0.38536	-2.40798	-0.36915
H	-1.03716	-1.2763	1.18403
H	-0.85684	1.00829	0.63341
C	-0.48782	2.54362	2.58020
H	-0.70833	3.1003	3.46716
H	-1.11554	2.91897	1.79924
C	2.40453	0.92865	1.26986
N	1.09334	1.5148	1.13182
S	2.40852	-1.29361	-0.05473
O	3.03097	0.88433	2.36071
O	2.84946	-2.00998	1.38808
O	3.11771	-2.09686	-1.33553
C	2.95041	0.36451	-0.02632
C	4.49496	0.36804	-0.24184
C	2.45064	1.2979	-1.16835
C	4.73836	1.59986	-1.08935
H	4.75257	-0.45297	-0.87778
H	5.04923	0.28431	0.66955
C	3.61622	1.32666	-2.13113
H	2.38598	2.29722	-0.79112
H	1.49553	1.01648	-1.55963
H	4.56955	2.5118	-0.55606
H	5.7253	1.64501	-1.49997
C	3.48223	2.41031	-3.21755
H	4.3722	2.43176	-3.81163
H	2.64227	2.1875	-3.84168
H	3.33969	3.36429	-2.75452
C	3.82435	-0.01734	-2.85298

H	2.98468	-0.21556	-3.48596
H	4.71431	0.02976	-3.44545
H	3.91856	-0.80006	-2.12963
C	0.976	2.55831	2.19844
H	1.51904	2.23199	3.06093
C	1.5233	3.92735	1.75492
H	2.56045	3.8341	1.50901
C	0.74397	4.41306	0.51854
H	1.12376	5.36412	0.20855
H	0.86022	3.7061	-0.27645
H	-0.29321	4.5058	0.76469
C	1.357	4.94377	2.89968
H	1.89904	4.6061	3.75824
H	1.73624	5.89509	2.58985
H	0.31992	5.03635	3.14645
O	-0.6237	1.03262	2.72760

Enolates derived from Spirocycle 350:

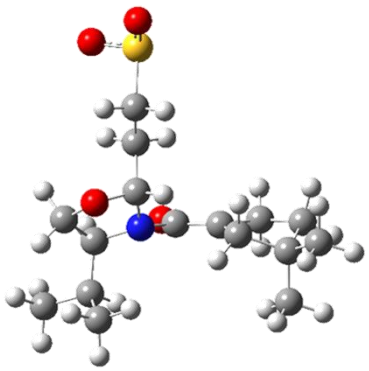

$\Delta G° = 0$ kcal/mol

C	-1.89391	-0.24052	0.14975
H	-2.365	0.60109	0.66654
H	-1.43786	-0.87624	0.91732
C	-2.95705	-1.01816	-0.62228
H	-2.54413	-1.92272	-1.08219
H	-3.43427	-0.40957	-1.39512
C	-0.75915	0.27563	-0.75770
H	-0.37631	-0.55257	-1.36084
N	0.34848	0.97532	-0.09696
C	1.05797	0.33811	1.01978
O	0.9834	0.89251	2.14377
O	-1.26287	1.25903	-1.68314
C	-0.9833	2.55485	-1.15406
C	-0.11432	2.34496	0.10481
C	1.03558	3.36188	0.29372
H	1.51014	3.06093	1.23211
H	-0.74148	2.41757	1.00586
H	-0.45442	3.12555	-1.92801
H	-1.92028	3.07693	-0.92263

S	-4.40049	-1.62348	0.43000
O	-5.08533	-0.3032	0.81378
O	-5.19753	-2.42228	-0.61806
C	1.78082	-0.78982	0.72184
C	2.54806	-1.54375	1.78772
H	3.29499	-0.90695	2.29490
H	1.91204	-1.93392	2.59586
C	2.06886	-1.3841	-0.63582
H	2.78159	-0.78934	-1.22381
H	1.17503	-1.5044	-1.28098
C	3.23744	-2.6895	1.01233
C	2.62243	-2.80469	-0.32500
C	0.48253	4.78419	0.47098
H	1.28581	5.49041	0.71362
H	-0.00756	5.14614	-0.44174
H	-0.25231	4.82211	1.28205
C	2.09877	3.30715	-0.81094
H	2.95348	3.94392	-0.55058
H	2.45278	2.28334	-0.94251
H	1.71065	3.65609	-1.77579
H	4.28073	-2.47533	0.90949
H	3.11137	-3.60894	1.54490
C	1.47585	-3.83247	-0.30025
H	0.88143	-3.72502	-1.18343
H	1.8837	-4.82098	-0.26290
H	0.86577	-3.6655	0.56279
C	3.68134	-3.20674	-1.36840
H	4.08527	-4.1648	-1.11571
H	3.22795	-3.25487	-2.33640
H	4.46652	-2.4799	-1.37805

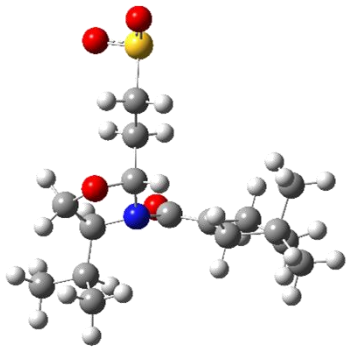

ΔG° = 1.7 kcal/mol

C	-1.89391	-0.24052	0.14975
H	-2.365	0.60109	0.66654
H	-1.43786	-0.87624	0.91732
C	-2.95705	-1.01816	-0.62228
H	-2.54413	-1.92272	-1.08219
H	-3.43427	-0.40957	-1.39512
C	-0.75915	0.27563	-0.75770
H	-0.37631	-0.55257	-1.36084
N	0.34848	0.97532	-0.09696
C	1.05797	0.33811	1.01978

O	0.9834	0.89251	2.14377
O	-1.26287	1.25903	-1.68314
C	-0.9833	2.55485	-1.15406
C	-0.11432	2.34496	0.10481
C	1.03558	3.36188	0.29372
H	1.51014	3.06093	1.23211
H	-0.74148	2.41757	1.00586
H	-0.45442	3.12555	-1.92801
H	-1.92028	3.07693	-0.92263
S	-4.40049	-1.62348	0.43000
O	-5.08533	-0.3032	0.81378
O	-5.19753	-2.42228	-0.61806
C	1.78082	-0.78982	0.72184
C	2.54806	-1.54375	1.78772
H	3.29499	-0.90695	2.29490
H	1.91204	-1.93392	2.59586
C	2.06886	-1.3841	-0.63582
H	2.78159	-0.78934	-1.22381
H	1.17503	-1.5044	-1.28098
C	3.23744	-2.6895	1.01233
C	2.62243	-2.80469	-0.32500
C	0.48253	4.78419	0.47098
H	1.28581	5.49041	0.71362
H	-0.00756	5.14614	-0.44174
H	-0.25231	4.82211	1.28205
C	2.09877	3.30715	-0.81094
H	2.95348	3.94392	-0.55058
H	2.45278	2.28334	-0.94251
H	1.71065	3.65609	-1.77579
H	4.28073	-2.47533	0.90949
H	3.11137	-3.60894	1.54490
C	1.47585	-3.83247	-0.30025
H	0.88143	-3.72502	-1.18343
H	1.8837	-4.82098	-0.26290
H	0.86577	-3.6655	0.56279
C	3.68134	-3.20674	-1.36840
H	4.08527	-4.1648	-1.11571
H	3.22795	-3.25487	-2.33640
H	4.46652	-2.4799	-1.37805

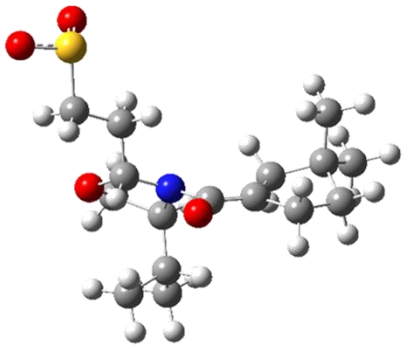

ΔG° = 0.9 kcal/mol

C	-1.2443	-0.30366	-0.65219
H	-1.86119	0.18556	0.10708

H	-0.67059	-1.0862	-0.14477
C	-2.13	-0.91661	-1.73020
H	-1.53519	-1.4229	-2.49717
H	-2.77608	-0.17794	-2.21310
C	-0.23132	0.70718	-1.22762
N	0.1187	1.026	0.41244
C	1.1236	0.37925	1.25753
O	1.91285	-0.46614	0.69158
O	-0.89368	1.86422	-1.74941
C	-1.0321	2.77899	-0.65303
C	0.1511	2.48821	0.29657
C	1.53092	3.004	-0.18366
H	2.2528	2.59513	0.53324
H	-0.03843	2.94983	1.27249
H	-1.0267	3.78836	-1.06765
H	-1.99362	2.62214	-0.15047
S	-3.29715	-2.21139	-1.08547
O	-4.24412	-1.3799	-0.19367
O	-4.00721	-2.64701	-2.38824
C	1.12935	0.7214	2.58812
C	2.1448	0.16219	3.56917
H	2.07371	-0.93453	3.66441
H	3.18768	0.35959	3.28372
C	0.12704	1.57805	3.33567
H	-0.90347	1.44709	2.98094
H	0.33357	2.66259	3.26648
C	1.79185	0.84377	4.90858
H	2.04363	0.23865	5.78760
H	2.34138	1.78899	4.99810
C	0.27747	1.15819	4.82482
C	-0.54623	-0.11227	5.10586
H	-1.61827	0.08884	5.00358
H	-0.28961	-0.9124	4.40668
H	-0.3689	-0.47914	6.12346
C	-0.14185	2.26419	5.80076
H	0.01608	1.95779	6.84152
H	0.43523	3.17871	5.62930
H	-1.20326	2.51234	5.68700
C	1.60478	4.53513	-0.09586
H	2.60616	4.89582	-0.35127
H	0.90009	5.01108	-0.78774
H	1.36953	4.88699	0.91349
C	1.92441	2.50621	-1.57997
H	2.95886	2.78206	-1.80941
H	1.83751	1.41957	-1.64396
H	1.29114	2.94308	-2.36005
H	0.575	0.29353	-1.79652

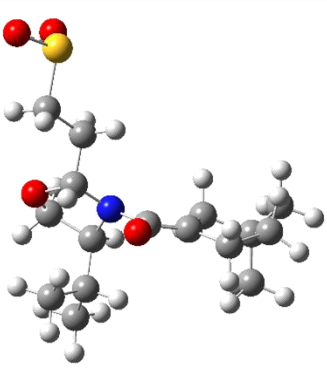

ΔG° = 1.0 kcal/mol

C	2.1503	-0.32047	0.02764
H	2.0303	-0.58534	-1.02685
H	1.75223	-1.15107	0.62249
C	3.62279	-0.10087	0.35457
H	3.76876	0.13597	1.41308
H	4.06884	0.69262	-0.25203
C	1.28064	0.90863	0.32266
N	-0.13517	0.66077	0.05514
C	-0.92467	0.03134	1.10963
O	-0.45089	0.09247	2.30584
O	1.64447	2.01053	-0.52855
C	0.58866	2.22575	-1.46728
C	-0.68124	1.76089	-0.75114
C	-1.44789	2.86418	0.02807
H	-2.20328	2.32475	0.61135
H	-1.38248	1.35984	-1.49112
H	0.58677	3.28478	-1.73380
H	0.75946	1.6365	-2.37772
S	4.68346	-1.59449	0.04029
O	4.57751	-1.75706	-1.49187
O	6.07826	-1.06104	0.44297
C	-2.18945	3.79746	-0.94112
H	-2.81939	4.50555	-0.39362
H	-1.4929	4.38497	-1.55016
H	-2.83604	3.23578	-1.62322
C	-0.58456	3.6646	1.01276
H	-1.20688	4.36964	1.57437
H	-0.09224	3.00739	1.73143
H	0.18752	4.24394	0.49639
H	1.44599	1.23241	1.35578
C	-2.0811	-0.57335	0.74412
C	-2.91913	-1.37456	1.72566
C	-2.6926	-0.67995	-0.64442
H	-2.31319	-2.03266	2.36027
H	-3.48653	-0.73674	2.42533
C	-3.88453	-2.17509	0.82956
H	-2.11365	-1.34691	-1.30650
H	-2.78047	0.26951	-1.18842
C	-4.1053	-1.28991	-0.42100
H	-3.40538	-3.11223	0.51900
H	-4.82709	-2.43996	1.32329
C	-5.11805	-0.17264	-0.10485

C	-4.59951	-2.09588	-1.62836
H	-5.25376	0.48517	-0.96992
H	-6.09692	-0.59095	0.15612
H	-4.7805	0.44493	0.73158
H	-5.5831	-2.53983	-1.43487
H	-4.69322	-1.46084	-2.51666
H	-3.90578	-2.90801	-1.86952

Enolates derived from Spirocycle 287:

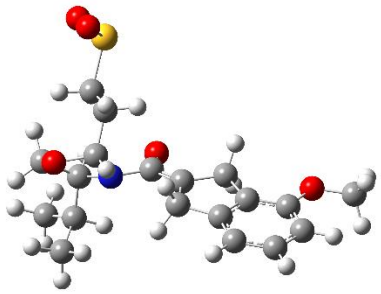

$\Delta G° = 0$ kcal/mol

C	2.22699	-0.87402	-0.17094
H	3.03983	-0.42884	-0.75144
H	1.488	-1.24836	-0.88773
C	2.75755	-2.01607	0.68736
H	1.95635	-2.48973	1.26400
H	3.54452	-1.69222	1.37416
C	1.53899	0.22042	0.66995
H	0.79121	-0.24754	1.31787
N	0.95979	1.32744	-0.09235
C	0.13281	1.06503	-1.26601
O	0.54413	1.52331	-2.39390
O	2.46929	0.86424	1.54603
C	3.04477	1.94581	0.80108
C	1.94918	2.40846	-0.18018
C	1.32014	3.79099	0.12373
H	0.47915	3.87769	-0.57425
H	2.35834	2.45798	-1.19474
H	3.35001	2.71055	1.51697
H	3.93743	1.60156	0.26572
S	3.53402	-3.39116	-0.29642
O	4.76014	-2.6909	-0.91998
O	3.96681	-4.35737	0.83085
C	-1.03575	0.36928	-1.06427
C	-1.37374	-0.25973	0.27580
H	-0.51983	-0.787	0.72598
H	-1.70337	0.46094	1.04638
C	-2.06799	-0.03213	-2.10643
H	-1.62238	-0.41498	-3.03554
H	-2.74777	0.77808	-2.43086
C	-2.50023	-1.21474	-0.05383
C	-2.87692	-1.09044	-1.39139
C	2.30443	4.92634	-0.19081

H	1.83149	5.90445	-0.05801
H	3.17901	4.89453	0.46930
H	2.66376	4.86563	-1.22304
C	0.75937	3.91093	1.54587
H	0.20221	4.8461	1.66321
H	0.08538	3.07997	1.76558
H	1.55595	3.90933	2.29807
C	-3.14143	-2.12761	0.78910
C	-4.16423	-2.9179	0.26995
H	-2.84935	-2.22199	1.83007
H	-4.67276	-3.63588	0.90524
C	-3.91005	-1.88446	-1.90503
C	-4.55449	-2.80547	-1.07070
H	-5.35179	-3.43373	-1.44516
C	-5.26378	-2.4802	-3.79910
H	-5.33844	-2.16654	-4.83920
H	-5.02697	-3.54856	-3.75888
H	-6.22041	-2.30117	-3.29732
O	-4.22236	-1.69524	-3.22798

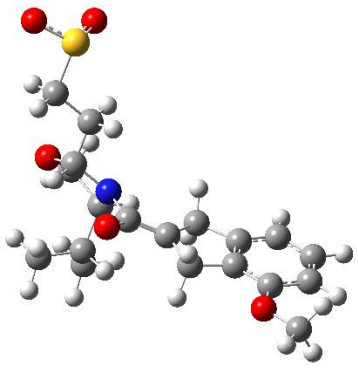

ΔG° = 1.2 kcal/mol

C	2.4524	-1.61426	0.37447
H	2.33279	-1.82636	-0.69193
H	1.89444	-2.3799	0.92644
C	3.92598	-1.65921	0.76164
H	4.06622	-1.47928	1.83206
H	4.52534	-0.93802	0.19843
C	1.79329	-0.26258	0.67871
N	0.36825	-0.25678	0.35199
C	-0.55985	-0.76947	1.35560
O	-0.13248	-0.82248	2.56955
O	2.37434	0.78298	-0.12148
C	1.41036	1.20105	-1.09009
C	0.05132	0.94183	-0.43631
C	-0.54783	2.139	0.35106
H	-1.40752	1.72169	0.88827
H	-0.67674	0.68688	-1.21418
H	1.59986	2.25146	-1.32098
H	1.51585	0.61578	-2.01293
S	4.72889	-3.30362	0.43624
O	4.66029	-3.40461	-1.10333
O	6.17629	-3.02818	0.90673
C	-1.0789	3.21117	-0.61262

H	-1.60116	4.00191	-0.06493
H	-0.26788	3.68662	-1.17608
H	-1.7829	2.78711	-1.33606
C	0.39769	2.75294	1.39254
H	-0.11818	3.53897	1.95449
H	0.74075	2.00208	2.10620
H	1.27785	3.20491	0.92410
H	1.96847	0.00032	1.72739
C	-1.78623	-1.15693	0.92847
C	-2.81916	-1.76587	1.86045
C	-2.31759	-1.17419	-0.49091
H	-2.47365	-2.71488	2.30418
H	-3.07347	-1.12376	2.71548
C	-4.04728	-2.00855	0.95712
H	-1.5548	-1.43739	-1.23511
H	-2.73544	-0.20377	-0.81856
C	-3.47703	-2.20942	-0.46895
C	-5.43427	-2.43204	1.47531
C	-4.13848	-2.85799	-1.69917
C	-6.20004	-3.07589	0.37763
C	-5.5145	-3.27903	-1.35060
H	-3.49692	-2.90834	-2.58914
H	-7.1892	-3.37789	0.74718
H	-5.98621	-3.74158	-2.22794
C	-6.82093	-2.92577	3.49770
H	-7.01015	-2.68242	4.57136
H	-7.76188	-2.73646	2.92598
H	-6.58078	-4.01432	3.42380
O	-5.69473	-2.09607	2.95547

5.3 Procedures for Chapter 3

5-(Vinyloxy)pent-2-yne (399):

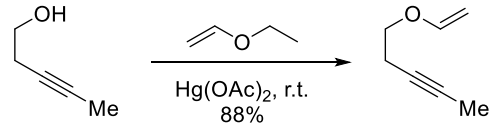

3-pentyn-1-ol (1.84 mL, 20.0 mmol, 1 equiv) and $Hg(OAc)_2$ (319 mg, 1.0 mmol, 0.05 equiv) were dissolved in ethyl vinyl ether (39.4 mL, 400 mmol, 20 equiv) and left to stir at r.t. for 12 days. The reaction solution was then washed with sat. $NaHCO_3$ (20 mL) and the organic phase dried over Na_2SO_4 and filtered. Excess ethyl vinyl ether by simple distillation. Ene-yne **399** was purified by fractional distillation (45 mmHg, 60-63 °C) and isolated as a clear colourless sweet-smelling liquid (1.93 g, 88%). **^{1}H NMR** (500 MHz, $CDCl_3$) δH 6.49 (1H, dd, *J* = 14.4, 6.6 Hz), 4.22 (1H, dd, *J* = 14.4, 2.0 Hz), 4.04 (1H, dd, *J* = 6.7, 2.0 Hz), 3.78 (2H, t, *J* = 7.0 Hz), 2.52 (2H, tq, *J* = 7.0, 2.4 Hz), 1.81 (3H, t, *J* = 2.5 Hz); **^{13}C NMR** (126 MHz, $CDCl_3$) δC 151.5, 86.8, 77.1, 75.1, 66.5, 19.5, 3.5; **HRMS (APCI) m/z**: $[M+H]^+$ calculated for $[C_7H_{11}O_1]^+$ 111.0804, found 111.0806; **IR** (neat) $\tilde{\nu}$ = 3118, 2944, 2921, 2879, 2861, 1637, 1615, 1423, 1374, 1340, 1321, 1290, 1197, 1152, 1079, 1018, 998, 963, 945, 816, 700 cm^{-1}.

Dimethyl 4-methyl-2,3,5,7*a*-tetrahydrobenzofuran-6,7-dicarboxylate (398):

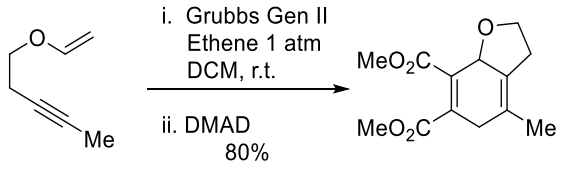

Ethylene was bubbled through a solution of ene-yne **399** (220 mg, 2.0 mmol, 1 equiv) in DCM (12 mL) before Grubbs generation two catalyst (17 mg, 0.020 mmol, 0.01 equiv) was added as a solution in DCM (3 mL) *via* canula. The flask was then fitted with a balloon of ethylene and stirred

at r.t overnight. Activated charcoal was added to the reaction and the solution filtered through a small pad of celite. The filtrate was transferred to a vial and freshly distilled dimethyl acetylenedicarboxylate (0.98 mL, 8.0 mmol, 4 equiv) added before the vial was sealed and the reaction left to still at r.t. overnight. Solvent was removed by rotary evaporator and the resulting residue purified by column chromatography (24 g SiO_2, 0 – 45% EtOAc in hexanes, 30 mL/min, 15 min) to afford dihydroarene **398** as a white solid (400 mg, 80%). **^{1}H NMR** (500 MHz, $CDCl_3$) δH 4.77 (1H, m), 4.00 (2H, m), 3.86 (3H, s), 3.78 (3H, s), 3.11 (1H, dd, *J* = 22.0, 5.6 Hz), 2.90 (1H, dd, *J* = 22.1, 9.7 Hz), 2.64 (1H, m), 2.54 (1H, m), 1.79 (3H, s); **^{13}C NMR** (126 MHz, $CDCl_3$) δC 167.6, 166.4, 137.8, 131.0, 129.3, 122.2, 74.5, 66.9, 52.4 (2C), 34.0, 27.7, 18.9; **HRMS (ESI) m/z**: $[M+Na]^+$ calculated for $[C_{13}H_{16}O_5Na]^+$ 275.0890, found 275.0881; **IR** (neat) $\tilde{\nu}$ = 2952, 2913, 2859, 2813, 1721, 1648, 1434, 1385, 1350, 1259, 1212, 1147, 1114, 1086, 1013, 977, 956, 913, 844, 788, 763, 681 cm^{-1}; **Mp** 107-109 °C.

Dimethyl 4-methyl-2,3-dihydrobenzofuran-6,7-dicarboxylate (376):

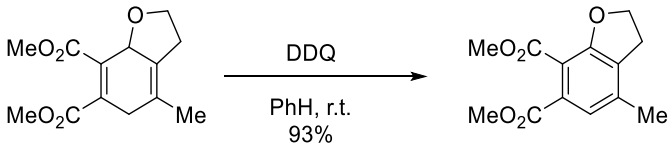

DDQ (1.24 g, 5.45 mmol, 1 equiv) was added to a solution of dimethyl dihydroarene **398** (1.38 g, 5.45 mmol, 1 equiv) in benzene (36 mL). The solution was stirred at r.t. for 1 hour then filtered through celite. The filtrate was concentrated to afford a solid residue which was purified by column chromatography (24 g SiO_2, 20 – 60% EtOAc in hexanes, 30 mL/min, 15 min) to afford dihydrobenzofuran **376** as an off white solid (1.273 g, 93%). **^{1}H NMR** (500 MHz, $CDCl_3$) δH 7.22 (1H, s), 4.70 (2H, t, *J* = 8.7 Hz), 3.90 (3H, s), 3.85 (3H, s), 3.16 (2H, t, *J* = 8.7 Hz), 2.28 (3H, s); **^{13}C NMR** (126 MHz, $CDCl_3$) δC 167.0, 167.0, 157.7, 136.4, 131.7, 129.3, 123.4, 113.4, 72.2,

52.6, 52.5, 28.5, 19.0; **HRMS (ESI) m/z**: $[M+Na]^+$ calculated for $[C_{13}H_{14}O_5Na]^+$ 273.0733, found 273.0725. **IR** (neat) $\tilde{\nu}$ = 3044, 3004, 2957, 2921, 2849, 1715, 1615, 1589, 1483, 1456, 1429, 1411, 1386, 1367, 1348, 1280, 1226, 1191, 1174, 1142, 1066, 1023, 1004, 978, 937, 928, 864, 808, 786, 773, 736, 701 cm^{-1}; **Mp** 104-105 °C.

One-Pot Procedure:

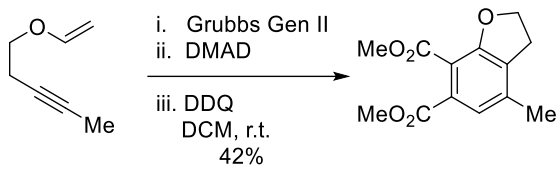

Grubbs generation two catalyst (68 mg, 0.080 mmol, 0.04 equiv) was added, as a solution in DCM (2 mL), *via* canula to a solution of ene-yne **399** (220 mg, 2.0 mmol, 1 equiv) in DCM (8 mL) under an atmosphere for argon. The reaction was stirred at r.t. for 14 hours at which point freshly distilled dimethyl acetylenedicarboxylate (0.98 mL, 8.0 mmol, 4 equiv) was added and the resulting solution allowed to stir at r.t. for 24 hours. DDQ (1.24 g, 5.45 mmol, 1 equiv) was then added and the reaction stirred for an additional 3 hours. At this point volatiles were removed under reduced pressure and the resulting black residue subjected to purification by column chromatorgraphy (30 g SiO_2, 25% EtOAc in hexanes). Fractions in interest were combined and concentrated to afford a solid which was taken up in a small volume of DCM and filtered through celite to remove remaining 2,3-dichloro-5,6-dicyano hydroquinone. Concentration of the filtrate provided dihydrobenzofuran **376** as a brown solid (210 mg, 42%).

(4-Methyl-2,3-dihydrobenzofuran-6,7-diyl)dimethanol (415):

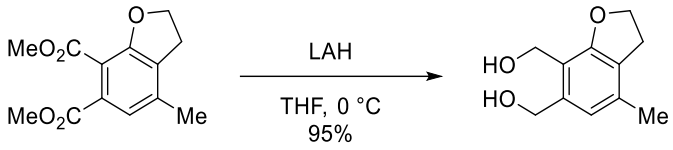

LAH (141 mg, 3.72 mmol, 3 equiv) was added, in small portions, to a solution of dihydrobenzofuran **376** (310 mg, 1.24 mmol, 1 equiv) in dry THF (20 mL), under argon at 0 °C. The reaction was left to stir at 0 °C for 70 min. The reaction was then carefully quenched with water (0.14 mL) and 15% $KOH_{(aq)}$ (0.14 mL) followed by a second portion of water (0.42 mL). The solution was warmed to r.t. and left to stir vigorously for 45 min at which point a white solid had formed. The solution was dried with Na_2SO_4 and flirted through a pad of Celite-®. The filtrate was concentrated to afford diol **415** as a white solid (229 mg, 95%). **^{1}H NMR** (500 MHz, DMSO-d_6) δH 6.71 (1H, s), 5.01 (1H, t, *J* = 5.5 Hz, D_2O exch.), 4.69 (1H, t, *J* = 5.4 Hz, D_2O exch.), 4.53 (2H, d, *J* = 5.4 Hz), 4.52 (2H, t, *J* = 8.6 Hz), 4.43 (2H, d, *J* = 5.4 Hz), 3.08 (2H, t, *J* = 8.6 Hz), 2.81 (3H, s); **^{1}H NMR** (500 MHz, $CDCl_3$) δH 6.68 (1H, s), 4.76 (2H, s), 4.67 (2H, s), 4.61 (2H, t, *J* = 8.7 Hz), 3.13 (2H, t, *J* = 8.7 Hz), 2.63 (2H, broad s, D_2O exch.), 2.23 (3H, s); **^{13}C NMR** (126 MHz, DMSO-d_6) δC 158.2, 141.5, 133.1, 124.9, 121.1, 118.2, 71.0, 61.2, 54.7, 28.7, 19.1; **^{13}C NMR** (126 MHz, $CDCl_3$) δC 158.6, 139.7, 134.5, 126.2, 122.9, 118.3, 71.4, 64.1, 56.9, 28.9, 18.8; **HRMS (ESI) m/z**: $[M+Na]^+$ calculated for $[C_{11}H_{14}O_3Na]^+$ 217.0835, found 217.0831. **IR** (neat) $\tilde{\nu}$ = 3315, 3238, 2960, 2915, 1625, 1595, 1477, 1445, 1411, 1371, 1356, 1328, 1278, 1256, 1201, 1082, 1060, 1027, 1000, 949, 871, 847, 761, 726, 691 cm^{-1}; **Mp** 123-124 °C

6,7-Bis(bromomethyl)-4-methyl-2,3-dihydrobenzofuran (375):

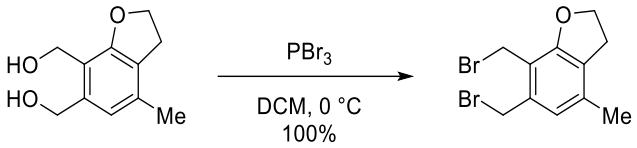

Phosphorus tribromide (51 μl, 0.54 mmol, 1 equiv) was added to a solution of diol **415** (104 mg, 0.535 mmol, 1 equiv) in dry DCM (10 mL) under argon at 0 °C. The reaction was left to stir at 0 °C for 6 hours then quenched with sat. $NaHCO_3$ (3 mL) and stirred at 0 °C for 5 min before being diluted with water (7 mL). The phases were separated, and the aqueous phase extracted with DCM (1 × 15 mL). Combined organic extracts were dried over Na_2SO_4, filtered, and concentrated to afford dibromide **375** as a slightly off-white solid (172 mg, 100%). **^{1}H NMR** (500 MHz, $CDCl_3$) δH 6.70 (1H, s), 4.69 (2H, s), 4.67 (2H, t, *J* = 8.6 Hz), 4.60 (2H, s), 3.13 (2H, t, *J* = 8.6 Hz), 2.22 (3H, s); **^{13}C NMR** (126 MHz, $CDCl_3$) δC 159.1, 136.1, 135.7, 127.5, 124.2, 115.6, 71.9, 30.4, 28.9, 24.4, 18.9; **LRMS (CI) m/z:** 240.9 (M−Br, 100.0), 238.9 (M−Br, 100.0), 195.1 (16.1), 161.1 (18.7), 160.1 (85.1); **IR** (neat) $\tilde{\nu}$ = 3028, 2972, 2915, 2853, 1723, 1622, 1585, 1478, 1450, 1439, 1412, 1379, 1334, 1291, 1263, 1244, 1221, 1149, 1116, 1088, 1040, 999, 976, 911, 864, 824, 737, 676 cm^{-1}; **Mp** 139-140 °C.

(*3*'S,7*R*,9a'*R*)-3'-Isopropyl-4-methyl-2,2',3,3',6,8,9',9a'-octahydro-5'*H*,8'*H*-spiro[indeno[4,5-b]furan-7,6'-oxazolo[3,2-d][1,4]thiazepin]-5'-one 7',7'-dioxide (374):

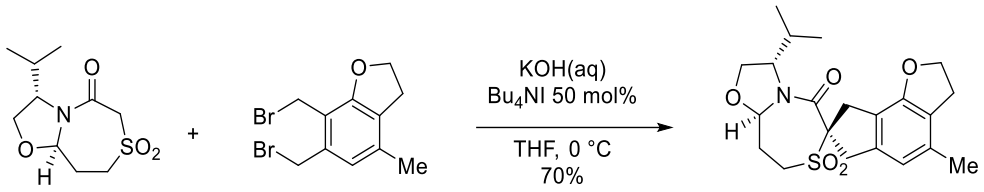

$KOH_{(aq)}$ (50 wt%, 2 mL) was added drop-wise to a solution of sulfone **277** (80 mg, 0.32 mmol, 1.5 equiv), dibromide **375** (69 mg, 0.22 mmol, 1 equiv), and TBAI (40 mg, 0.11 mmol, 0.5 equiv) in THF (4 mL) at 0 °C. The reaction was then vigorously stirred for 18 hours then diluted with H_2O (10 mL) and extracted with DCM (3 × 20 mL). Combined organic extracts were dried over Na_2SO_4, filtered, and concentrated to afford a yellow solid. The solid was subjected to column chromatography (10 g SiO_2, 0 – 5% EtOAc in DCM, R_f = 0.22 in 5% EtOAc in DCM) and afforded spirocycle **374** as a white solid (61 mg, 70%). **^{1}H NMR** (500 MHz, $CDCl_3$) δH 6.48 (1H, s), 5.58 (1H, *J* = 9.6 Hz), 4.60 (2H, t, *J* = 8.7 Hz), 4.39 (1H, q, *J* = 4.4 Hz), 4.24 (1H, d, *J* = 17.4 Hz), 3.96 (2H, d, *J* = 4.6 Hz), 3.75 (1H, d, *J* = 16.0 Hz), 3.74 (1H, d, *J* = 17.4 Hz), 3.68 (1H, m), 5.57 (1H, d, *J* = 16.0 Hz), 3.32 (1H, dq, *J* = 15.3, 2.8 Hz), 3.06 (2H, t, *J* = 8.7 Hz), 2.57 (1H, m), 2.23 – 2.31 (2H, m), 2.19 (3H, s), 0.82 (3H, d, *J* = 7.0 Hz), 0.75 (3H, d, *J* = 6.9 Hz); **^{13}C NMR** (126 MHz, $CDCl_3$) δC 163.0, 155.2, 137.8, 133.7, 125.1, 118.0, 116.0, 87.7, 77.4, 71.6, 64.5, 63.4, 48.1, 40.1, 33.0, 31.8, 28.6, 27.6, 19.1, 18.9, 16.0; **HRMS (ESI) m/z**: $[M+Na]^+$ calculated for $[C_{21}H_{27}NO_5SNa]^+$ 428.1508, found 428.1483; **IR** (neat) $\tilde{\nu}$ = 2961, 2930, 2873, 1732, 1623, 1600, 1483, 1457, 1445, 1406, 1389, 1372, 1312, 1292, 1264, 1227, 1202, 1185, 1167, 1129, 1096, 1085, 1050, 1030, 1000, 969, 952, 910, 899, 888, 878, 840, 811, 797, 756, 732, 702 cm^{-1}; $[\boldsymbol{\alpha}]_{\mathbf{D}}^{\mathbf{22}}$ –212.1 (*c* 1.0, $CHCl_3$); **Mp** 229-231 °C.

(*R*)-*N*-((*S*)-1-Hydroxy-3-methylbutan-2-yl)-4,7-dimethyl-3,6,7,8-tetrahydro-2*H*-indeno[4,5-b]furan-7-carboxamide (416):

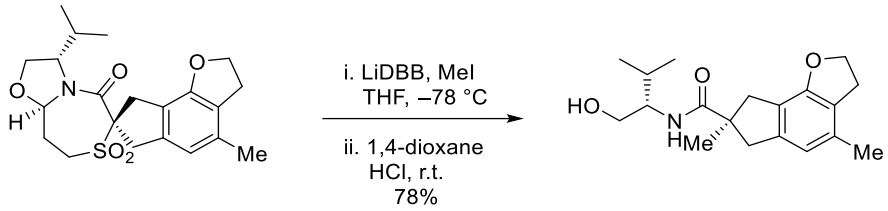

LiDBB (0.4 M, 2.1 equiv, 2.6 mL) drop-wise to a solution of spirocycle **374** (190 mg, 0.47 mmol, 1 equiv), that had been azeotropically dried with PhMe (2 × 15 mL), in dry and degassed THF (12 mL) at –78 °C. Following the addition, the solution left to stir at –78 °C for 20 min. Iodomethane (117 µl, 1.87 mmol, 4 equiv), which had been passed through a column of basic Al_2O_3, was then added drop-wise *via* glass syringe and the reaction allowed to stir at –78 °C for 6 hours. The reaction was warmed to r.t. and all volatiles removed under reduced pressure. The resulting residue was dissolved in 1,4-dioxane (10 mL) and 1 M $HCl_{(aq)}$ (5 mL) added. After stirring at r.t. for 12 hours the solution was adjusted to pH 7 with $NaOH_{(aq)}$ (15% w.t.) and allowed to stir at r.t for 1 hour before being extracted with EtOAc (3 × 15 mL). Combined organic extracts were dried over Na_2SO_4, filtered, and concentrated to afford a yellow solid which was purified by column chromatography (10 g SiO_2, 40-50% EtOAc in hexanes, R_f = 0.20 in 50% EtOAc in hexanes). Amide **416** was isolated as a white solid (116 mg, 78%). **^{1}H NMR** (500 MHz, $CDCl_3$) δH 6.55 (1H, s), 5.75 (1H, d, *J* = 7.5 Hz, D_2O exch.), 4.58 (2H, dd, *J* = 9.8, 1.2 Hz), 3.61-3.75 (3H, m), 3.33 (1H, d, *J* = 15.7 Hz), 3.23 (1H, d, *J* = 15.6 Hz), 3.09 (2H, t, *J* = 8.7 Hz), 2.78 (1H, d, *J* = 15.7 Hz), 2.78 (1H, d, *J* = 15.6 Hz), 2.75 (1H, d, *J* = 5.2 Hz, D_2O exch.), 2.14 (3H, s), 1.89 (1H, m), 1.38 (3H, s), 0.91 (3H, d, *J* = 6.8 Hz), 0.86 (3H, d, *J* = 6.8 Hz); **^{13}C NMR** (126 MHz, $CDCl_3$) δC 178.9, 155.7, 142.8, 133.4, 124.1, 119.0, 117.5, 71.5, 64.6, 57.3, 50.7, 44.4, 40.3, 29.0, 28.7, 25.7, 19.6, 19.0, 18.5; **HRMS (ESI) m/z**: $[M+Na]^+$ calculated for $[C_{19}H_{27}NO_3Na]^+$ 340.1889, found

340.1873; **IR** (neat) $\tilde{\nu}$ = 3340, 3001, 2960, 2926, 2869, 2853, 1637, 1596, 1524, 1481, 1458, 1417, 1386, 1369, 1320, 1292, 1256, 1188, 1140, 1126, 1075, 1034, 1005, 976, 961, 933, 895, 841, 731 cm^{-1}; $[\boldsymbol{\alpha}]_{\mathbf{D}}^{\mathbf{22}}$ +54.8 (*c* 1.0, $CHCl_3$); **Mp** 149-152 °C.

(*R*)-4,7-Dimethyl-3,6,7,8-tetrahydro-2*H*-indeno[4,5-b]furan-7-carboxylic acid (417):

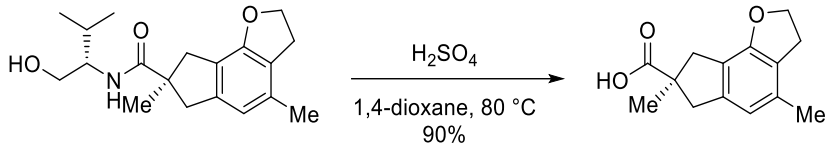

4 M $H_2SO_{4(aq)}$ (1 mL) was added dropwise to a solution of amide **416** (27 mg, 0.085 mmol) in 1,4-dioxane (2 mL). The solution stirred at 80 °C for 8 hours. The reaction was cooled to r.t., diluted with H_2O (5 mL), and extracted with Et_2O (3 × 15 mL). Combined organic extracts were dried over Na_2SO_4, filtered, and concentrated to afford a brown solid which was purified by column chromatography (5 g SiO_2, 3% EtOAc, 1% AcOH in DCM, R_f = 0.20 in 1% AcOH in DCM). Carboxylic acid **417** was isolated as a white solid (26.4 mg, 90%). **^{1}H NMR** (500 MHz, $CDCl_3$) δH 11.57 (1H, br. s, D_2O exch.), 6.55 (1H, s), 4.59 (2H, t, *J* = 8.6 Hz), 3.44 (1H, d, *J* = 15.9 Hz), 3.38 (1H, d, *J* = 15.8 Hz), 3.09 (2H, t, *J* = 8.6 Hz), 2.77 (1H, d, *J* = 15.9 Hz), 2.77 (1H, d, *J* = 15.8 Hz), 2.22 (3H, s), 1.40 (3H, s); **^{13}C NMR** (126 MHz, $CDCl_3$) δC 184.1, 155.7, 142.5, 133.2, 124.0, 119.0, 117.3, 71.5, 49.9, 43.8, 39.8, 28.7, 25.0, 19.0; **HRMS m/z**: $[M-H]^-$ calculated for $[C_{14}H_{15}O_3]^-$ 231.1027, found 231.1017; **IR** (neat) $\tilde{\nu}$ = 3036, 2970, 2915, 2855, 2695, 2675, 2590, 2524, 1734, 1694, 1636, 1590, 1536, 1480, 1457, 1432, 1414, 1383, 1368, 1354, 1307, 1295, 1254, 1231, 1178, 1140, 1116, 1090, 1071, 1029, 1003, 977, 965, 938, 895, 868, 845, 795, 769, 739, 706 cm^{-1}.

(*R*)-Puraquinonic acid (164):

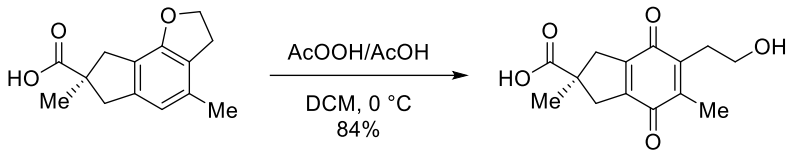

Peracetic acid (39 wt. % in acetic acid, 500 µl) was added dropwise to a solution of carboxylic acid **417** (5.0 mg, 0.022 mmol) in DCM (1.0 mL) at 0 °C. The reaction was stirred at 0 °C for 2 hours then diluted with H_2O (5 mL) and extracted with Et_2O (2 × 5 mL). Combined organic extracts were washed with an additional portion of H_2O (5 mL). The phases were separated, and the aqueous phase extracted with Et_2O (5 mL). All organic extracts were dried over Na_2SO_4, filtered, and concentrated to afford a yellowish residue. The residue was purified by column chromatography (2 g SiO_2, 0 to 5% MeOH in DCM) to provide (R)-puraquinonic acid as a yellow film (4.9 mg, 84%). Characterisation was consistant with previous reports of (*R*)-Puraquinonic acid.[20, 21] **^{1}H NMR** (500 MHz, $CDCl_3$) δH 3.77 (2H, t, *J* = 6.4 Hz), 3.39 (2H, m), 2.80 (2H, t, *J* = 6.4 Hz), 2.76 (2H, m), 2.08 (3H, s), 1.43 (3H, s); **^{13}C NMR** (101 MHz, $CDCl_3$) δC 186.2, 185.7, 180.5, 145.7, 145.3, 142.8, 141.4, 61.5, 46.8, 42.3, 42.3, 29.9, 25.7, 12.2; **HRMS (ESI) m/z**: $[M+Na]^+$ calculated for $[C_{14}H_{16}O_5Na]^+$ 287.0890, found 287.0899; **IR** (neat) $\tilde{\nu}$ = 3440, 2925, 1707, 1647, 1607, 1431, 1376, 1334, 1265, 1209, 1110, 1037, 1021, 908, 801, 733, 702 cm^{-1}; $[\boldsymbol{\alpha}]_{\mathbf{D}}^{\mathbf{22}}$ +3.5 (*c* 0.5, $CHCl_3$).

Benzyl (*R*)-(1-(methoxymethoxy)-3-methylbutan-2-yl)carbamate (430):

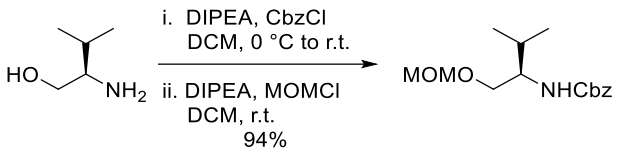

DIPEA (870 µl, 5.0 mmol, 1 equiv) and benzyl chloroformate (896 µl, 5.25 mmol, 1.05 equiv) were added to a solution of (*R*)-valinol (515 mg, 5.00 mmol, 1 equiv) in DCM (25 mL) at 0 °C. The reaction was then warmed to r.t. and left to stir overnight. At this time TLC inspection showed no (*R*)-valinol. A second portion of DIPEA (1.74 mL, 10.0 mmol, 2 equiv) was added followed by chloromethyl methyl ether (570 µl, 7.50 mmol, 1.5 equiv). The reaction was then left to stir at r.t. for 24 hours before being diluted with sat. $NH_4Cl_{(aq)}$ (30 mL) and extracted with DCM (2 × 50 mL). Combined organic extracts were dried over $MgSO_4$, filtered, and concentrated to afford a yellow-orange liquid. The liquid was purified by column chromatography (24 g SiO_2, 0 – 60% EtOAc in hexanes, 30 mL/min, 15 min) to afford carbamate **430** as a clear colourless viscous liquid (1.32 g, 94%). **^{1}H NMR** (500 MHz, $CDCl_3$) δH 7.31 – 7.39 (5H, m), 5.13 (2H, s), 4.97 (1H, d, *J* = 8.2 Hz, D_2O exch.), 4.62 (2H, s), 3.64 (1H, m), 3.54 (1H, dd, *J* = 9.8, 3.7 Hz), 3.36 (3H, s) 1.92 (1H, m), 0.99 (3H, d, *J* = 6.8 Hz), 0.96 (3H, d, *J* = 6.8 Hz); **^{1}H NMR** (500 MHz, DMSO-d_6) δH 7.35 (4H, m), 7.30 (1H, m), 7.13 (1H, d, *J* = 8.6 Hz, D_2O exch.), 5.02 (2H, s), 4.54 (2H, m), 3.47 (2H, m), 3.40 (1H, m), 3.23 (3H, s), 1.78 (1H, dqq, *J* = 6.8, 6.8, 6.7 Hz), 0.86 (3H, d, *J* = 6.8 Hz), 0.84 (3H, d, *J* = 6.8 Hz); **^{13}C NMR** (126 MHz, $CDCl_3$) δC 156.14, 136.7, 128.5, 128.1, 96.7, 68.1, 66.7, 56.2, 55.4, 29.6, 19.5, 18.7; **^{13}C NMR** (126 MHz, DMSO-d_6) δC 156.2, 137.4, 128.3, 127.7, 127.6, 95.7, 67.5, 65.0, 55.8, 54.6, 29.0, 19.3, 18.0; **HRMS (ESI) m/z**: $[M+Na]^+$ calculated for $[C_{15}H_{23}NO_4Na]^+$ 304.1519, found 304.1516; **IR** (neat) $\tilde{\nu}$ = 3335, 3067, 3033, 2959, 2933, 2882,

2824, 2770, 1698, 1587, 1529, 1466, 1455, 1403, 1389, 1370, 1334, 1310, 1280, 1230, 1152, 1109, 1026, 956, 918, 846, 824, 775, 738, 697 cm^{-1}.

(*R*)-1-(Methoxymethoxy)-3-methylbutan-2-amine (431):

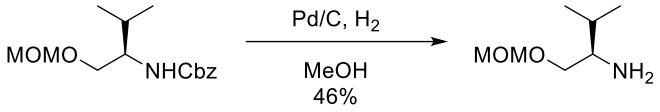

Pd/C (5 wt%, 10 mg, 4.7 nmol, 5 mol%) was added to a solution of carbamate **430** (200 mg, 0.71 mmol, 1 equiv) in MeOH (1 mL) under an argon atmosphere at r.t. The flask was then equipped with a balloon of H_2 with the H_2 allowed to bubble through the solution for 5 min to remove argon. The reaction was then allowed to stir at r.t. under a H_2 atmosphere for 40 min at which point TLC indicated the reaction was complete. The solution was filtered through a small pad of celite and rinsed with Et_2O. The filtrate was diluted with sat. $NaHCO_3$ (10 mL) then extracted with Et_2O (3 × 20 mL). Combined organic extracts were dried over Na_2SO_4, filtered, and concentrated to afford amine **431** as a slightly yellow liquid (48 mg, 46%) which was used without further purification. **^{1}H NMR** (500 MHz, $CDCl_3$) δH 4.58 (2H, m), 3.53 (1H, dd, , *J* = 9.3, 3.5 Hz), 3.31 (3H, s), 3.28 (1H, dd, , *J* = 9.5, 8.2 Hz), 2.68 (1H, ddd, *J* = 8.2, 5.9, 3.7 Hz), 1.59 (1H, dq, *J* = 6.8 Hz) 1.58 (2H, br. s, D_2O exch.); **^{13}C NMR** (126 MHz, $CDCl_3$) δC 96.6, 71.3 56.2, 30.8, 19.2, 18.0; **HRMS (APCI) m/z**: $[M+H]^+$ calculated for $[C_7H_{18}NO_2]^+$ 148.1332, found 148.1326; **IR** (neat) $\tilde{\nu}$ = 3381, 3302, 2955, 2929, 2877, 2825, 2774, 1728, 1611, 1592, 1566, 1466, 1437, 1388, 1368, 1297, 1268, 1218, 1193, 1143, 1108, 1041, 999, 917, 858, 840, 793, 770, 735, 699 cm^{-1}.

(*R*)-*N*-((*R*)-1-(Methoxymethoxy)-3-methylbutan-2-yl)-4,7-dimethyl-3,6,7,8-tetrahydro-2*H*-indeno[4,5-b]furan-7-carboxamide ((*R*,*R*)-432):

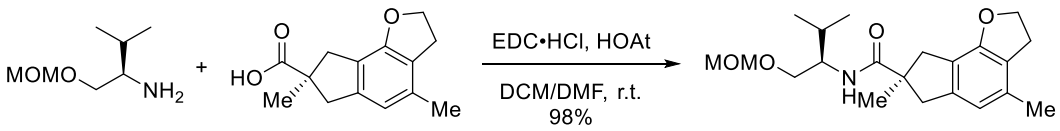

EDC·HCl (19 mg, 0.097 mmol, 1.5 equiv), and HOAt (13 mg, 0.097 mmol, 1.5 equiv) were added to a solution of carboxylic acid **417** (15 mg, 0.065 mmol, 1 equiv) in 6:1 DCM/DMF (1.75 mL) at 0 °C. The solution was stirred at 0 °C for 15 minutes before amine **431** (29 mg, 0.20 mmol, 3 equiv) was added as a solution in DCM (1 mL) *via* syringe. The reaction was then warmed to r.t. and left to stir overnight. The reaction was diluted with H_2O (8 mL) and then extracted with Et_2O (3 × 20 mL). Combined organic extracts were dried over Na_2SO_4, filtered, and concentrated to afford a yellowish residue. The residue was purified by column chromatography (8 g SiO_2, 40% EtOAc in hexanes) to afford amide **(*R*,*R*)-432** as a colourless liquid (25 mg, 98%). **^{1}H NMR** (500 MHz, $CDCl_3$) δH 6.57 (1H, s), 5.88 (1H, d, *J* = 9.0 Hz, D_2O exch.), 4.60 (2H, t, *J* = 8.5 Hz), 4.60 (2H, s), 3.90 (1H, m), 3.73 (1H, dd, *J* = 10.2, 3.7 Hz), 3.47 (1H, dd, *J* = 10.2, 3.9 Hz), 3.37(1) (1H, d, *J* = 15.7 Hz), 3.37(0) (3H, s), 3.25 (1H, d, *J* = 15.7 Hz), 3.11 (2H, t, *J* = 8.7 Hz), 2.79 (1H, d, *J* = 15.6 Hz), 2.78 (1H, d, *J* = 15.8 Hz), 2.24 (3H, s), 1.91 (1H, qqd, *J* = 7.5, 7.5, 7.5 Hz), 1.38 (3H, s), 0.97 (3H, d, *J* = 6.8 Hz), 0.91 (3H, d, *J* = 6.9 Hz); **^{13}C NMR** (126 MHz, $CDCl_3$) δC 177.1, 155.8, 143.0, 133.2, 124.0, 119.1, 117.4, 96.9, 71.5, 68.4, 55.4, 53.9, 50.7, 44.1, 40.2, 29.5, 28.8, 25.8, 19.6, 19.0, 18.8; **HRMS (ESI) m/z**: $[M+Na]^+$ calculated for $[C_{21}H_{31}O_4NNa]^+$ 384.2145, found 384.2148; **IR** (neat) $\tilde{\nu}$ = 3448, 3346, 2958, 2927, 2821, 1728, 1641, 1595, 1522, 1479, 1459, 1417, 1386, 1370, 1318, 1290, 1258, 1214, 1187, 1141, 111, 1075, 1035, 1005, 976, 963, 920, 895, 840, 776, 733, 702 cm^{-1}.

(*R*)-5-(2-Hydroxyethyl)-N-((*R*)-1-(methoxymethoxy)-3-methylbutan-2-yl)-2,6-dimethyl-4,7-dioxo-2,3,4,7-tetrahydro-1*H*-indene-2-carboxamide ((*R*,*R*)-433):

Peracetic acid (39% in AcOH, 500 µl) was added to a solution of amide **(*R*,*R*)-432** (5.0 mg, 0.014 mmol) in DCM (1 mL). The reaction stirred at r.t. for 1 hour. The reaction was then diluted with H_2O (5 mL) and extracted with DCM (2 × 10 mL). Combined organic extracts were dried over Na_2SO_4, filtered, and concentrated to afford a yellow residue. The residue was purified by preparative TLC (230-400 mesh silica, 2% MeOH in DCM) to afford the desired quinone **(*R*,*R*)-433** as a yellow film (2.1 mg, 42%). **^{1}H NMR** (400 MHz, $CDCl_3$) δH 5.95 (1H, d, *J* = 9.2 Hz, D_2O exch.), 4.61 (2H, m), 3.86 (1H, m), 3.76 (2H, m), 3.65 (1H, m), 3.48 (1H, m), 3.37 (3H, s), 3.36 (1H, m), 3.33 (1H, m), 2.79 (2H, t, *J* = 6.6 Hz) 2.73 (1H, m), 2.69 (1H, m), 2.08 (3H, s), 1.91 (1H, m), 1.61 (1H, t, *J* = 5.3 Hz, D_2O exch.), 1.38 (3H, s), 0.97 (3H, d, *J* = 6.7 Hz), 0.93 (3H, d, *J* = 6.8 Hz); **^{13}C NMR** (126 MHz, $CDCl_3$) δC 186.4, 185.9, 175.7, 145.9, 145.6, 142.8, 141.4, 97.0, 68.6, 61.5, 55.5, 54.3, 47.8, 42.8, 42.6, 29.9, 29.6, 26.6, 19.6, 19.2, 12.2; **HRMS (ESI) m/z**: $[M+Na]^+$ calculated for $[C_{21}H_{31}O_6NNa]^+$ 416.2044, found 416.2052; **IR** (neat) $\tilde{\nu}$ = 3352, 2959, 2926, 2874, 2855, 1725, 1639, 1530, 1462, 1377, 1267, 1215, 1148, 1110, 1035, 955, 920, 735, 702, 603, 541 cm^{-1}.

(*R*)-*N*-((*S*)-1-(Methoxymethoxy)-3-methylbutan-2-yl)-4,7-dimethyl-3,6,7,8-tetrahydro-2*H*-indeno[4,5-*b*]furan-7-carboxamide ((*R*,*R*)-433):

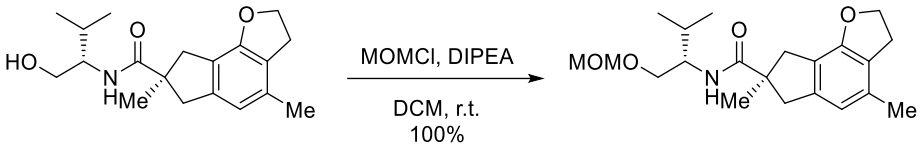

DIPEA (54 µl, 0.32 mmol, 10 equiv) followed by MOMCl (20 µl, 0.15 mmol, 8 equiv) were added to a solution of amide **416** (10 mg, 0.032 mmol, 1 equiv) in DCM (3 mL) at r.t. and left to stir at overnight. The reaction was quenched with sat. NH_4Cl (5 mL) and the resulting solution extracted with DCM (3 × 10 mL). Combined organic extracts were dried over Na_2SO_4, filtered, and concentrated to afford a yellow residue which was purified by column chromatography (3 g SiO_2, 40% EtOAc in hexanes) affording amide **(*R*,*S*)-432** as a white film (11 mg, 97%). **^{1}H NMR** (500 MHz, $CDCl_3$) δH 6.55 (1H, s), 5.85 (1H, d, *J* = 9.1 Hz, D_2O exch.), 4.58 (2H, t, *J* = 8.7 Hz), 4.58 (s, 2H), 3.88 (1H, m), 3.70 (1H, dd, *J* = 3.8, 10.2 Hz), 3.46 (1H, dd, *J* = 3.8, 10.2 Hz), 3.35 (1H, d, 15.6 Hz), 3.35 (3H, s), 3.24 (1H, d, *J* = 15.5 Hz), 3.09 (2H, t, *J* = 8.2 Hz), 2.76 (1H, d, *J* = 15.5 Hz), 2.76 (1H, d, *J* = 15.5 Hz), 2.22 (3H, s), 1.88 (1H, m), 1.36 (3H, s), 0.94 (3H, d, *J* = 6.8 Hz), 0.88 (3H, d, *J* = 6.9 Hz); **^{13}C NMR** (126 MHz, $CDCl_3$) δC 177.1, 155.7, 142.9, 133.2, 123.9, 119.1, 117.5, 96.9, 71.5, 68.4, 55.4, 53.8, 50.7, 44.1, 40.2, 29.5, 28.7, 25.8, 19.6, 19.0, 18.8; **HRMS (ESI) m/z**: $[M+Na]^+$ calculated for $[C_{21}H_{31}NO_4Na]^+$ 384.2145, found 384.2133. **IR** (neat) $\tilde{\nu}$ = 3345, 2958, 2967, 1639, 1595, 1525, 1460, 1417, 1386, 1290, 1256, 1214, 1187, 1143, 1112, 1075, 1036, 1006, 958, 920, 841, 730, 578, 536, 428 cm^{-1}.

(*R*)-5-(2-Hydroxyethyl)-*N*-((*S*)-1-(methoxymethoxy)-3-methylbutan-2-yl)-2,6-dimethyl-4,7-dioxo-2,3,4,7-tetrahydro-1*H*-indene-2-carboxamide ((*R*,*S*)-433):

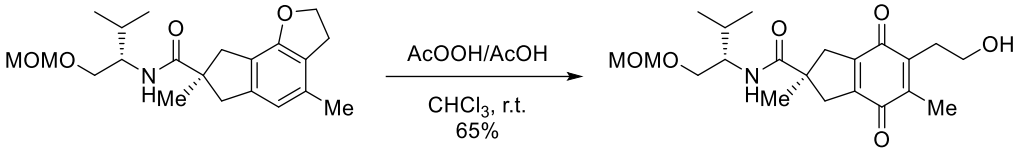

Peracetic acid (39% in AcOH, 50 µl) was added to a solution of amide **(*R*,*S*)-432** (10 mg, 0.028 mmol) in $CHCl_3$ (1 mL). The reaction stirred at r.t. for 10 hours. The reaction was then diluted with sat. $NaHCO_{3(aq)}$ (1 mL) and extracted with DCM (3 × 2 mL). Combined organic extracts were dried over Na_2SO_4, filtered, and concentrated to afford a yellow residue. The residue was purified by preparative TLC (230-400 mesh silica, 2% MeOH in DCM) to afford quinone **(*R*,*S*)-433** as a yellow film (7.2 mg, 65%). Spectra agreed with previous reports.[20] **^{1}H NMR** (400 MHz, $CDCl_3$) δH 5.96 (1H, d, *J* = 9.1 Hz, D_2O exch.), 4.60 (2H, m), 3.85 (1H, m), 3.75 (3H, m), 3.47 (1H, dd, *J* = 10.3, 3.5 Hz), 3.37 (3H, s), 3.36 (1H, m), 3.32 (1H, m), 2.79 (2H, t, *J* = 6.5 Hz) 2.73 (1H, d, *J* = 3.3 Hz), 2.68 (1H, d, *J* = 3.4 Hz), 2.07 (3H, s), 1.91 (1H, m), 1.38 (3H, s), 0.97 (3H, d, *J* = 6.7 Hz), 0.93 (3H, d, *J* = 6.8 Hz); **^{13}C NMR** (101 MHz, $CDCl_3$) δC 186.4, 185.9, 175.8, 145.9, 145.5, 142.7, 141.4, 97.0, 68.5, 61.5, 55.5, 54.3, 47.8, 42.7, 42.6, 29.9, 29.6, 26.5, 19.5, 19.1, 12.2; **HRMS (ESI) m/z**: $[M+Na]^+$ calculated for $[C_{21}H_{31}O_6NNa]^+$ 416.2044, found 416.2049.

(*R*)-4-Methoxy-2-methyl-2,3-dihydro-1*H*-indene-2-carboxylic acid (437):

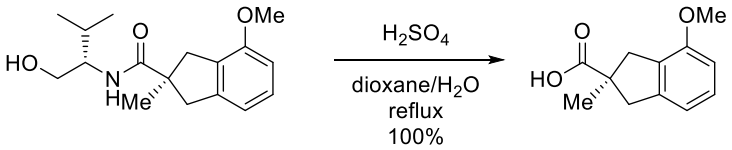

4 M $H_2SO_{4(aq)}$ (6 mL) was added dropwise to a solution of amide **353** (118 mg, 0.40 mmol) in 1,4-dioxane (6 mL). The solution stirred at reflux for 4 hours. The reaction was cooled to r.t., diluted

with H_2O (20 mL), and extracted with Et_2O (3 × 25 mL). Combined organic extracts were dried over $MgSO_4$, filtered, and concentrated to afford carboxylic acid **437** as a yellow-brown solid. **^{1}H NMR** (500 MHz, $CDCl_3$) δH 11.59 (1H, br. s, D_2O exch.), 7.15 (1H, dd, *J* = 7.8, 7.8 Hz), 6.81 (1H, d, *J* = 7.8 Hz), 6.69 (1H, d, *J* = 7.8 Hz), 3.82 (3H, s), 3.53 (1H, d, *J* = 16.0 Hz), 3.42 (1H, d, *J* = 16.4 Hz), 2.86 (1H, d, *J* = 16.4 Hz), 2.84 (1H, d, *J* = 16.0 Hz), 1.41 (3H, s); **^{13}C NMR** (126 MHz, $CDCl_3$) δC 183.8, 156.1, 143.0, 128.7, 128.1, 117.0, 108.1, 55.2, 49.2, 44.2, 40.7, 25.1; **HRMS (APCI) m/z**: $[M-H]^-$ calculated for $[C_{12}H_{13}O_3]^-$ 205.0870, found 205.0862; **IR** (neat) $\tilde{\nu}$ = 3080, 2933, 2706, 2607, 1699, 1590, 1485, 1471, 1439, 1312, 1290, 1261, 1231, 1124, 1120, 1076, 941, 926, 763, 737 cm^{-1}.

Isopropyl ((*R*)-4-methoxy-2-methyl-2,3-dihydro-1*H*-indene-2-carbonyl)-*L*-prolinate ((*R,S*)-435):

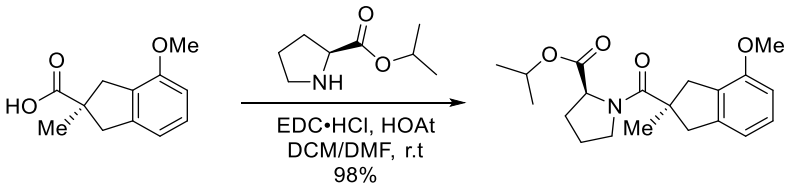

EDC•HCl (14.4 mg, 0.075 mmol, 1.5 equiv) and HOAt (10.2 mg, 0.075 mmol, 1.5 equiv) were added to a solution of carboxylic acid **437** (10.0 mg, 0.05 mmol, 1 equiv) in a 1:1 solution of DCM and DMF (0.5 mL) at 0 °C. The solution was stirred at 0 °C for 15 min before isopropyl-*L*-proline (60 mg, 0.38 mmol, 7.6 equiv) was added dropwise as a solution in DCM and DMF (1:1, 0.6 mL). After being left to stir at r.t overnight, the reaction was diluted with sat. $NH_4Cl_{(aq)}$ (2.5 mL) and H_2O (2.5 mL) with the resulting solution extracted with Et_2O (2 × 20 mL). Combined organic extracts were dried over Na_2SO_4, filtered, and concentrated to afford an off-white solid. The solid was purified by column chromatography (10 g SiO_2, 40% EtOAc in hexanes) to provide amide (***R,S*)-435** as a white solid (17 mg, 98%). Spectra are in agreement with data reported for the

product.[22] **^{1}H NMR** (500 MHz, $CDCl_3$) δH 7.15 (1H, dd, *J* = 8.1, 7.4 Hz), 6.82 (1H, d, *J* = 7.4 Hz), 6.68 (1H, d, *J* = 8.1 Hz), 5.03 (1H, qq, *J* = 6.3, 6.2), 4.50 (1H, dd, *J* = 8.4, 4.0 Hz), 3.82 (1H, s), 3.75 (1H, m), 3.69 (1H, m), 3.61 (1H, d, *J* = 16.3 Hz), 3.33 (1H, d, *J* = 16.1 Hz), 2.95 (1H, d, *J* = 16.1 Hz), 2.87 (1H, d, *J* = 16.3 Hz), 2.15 (1H, m), 2.06 (1H, m), 1.96 (1H, m), 1.90 (1H, m), 1.37 (3H, s), 1.26 (3H, d, *J* = 6.3 Hz), 1.21 (3H, d, *J* = 6.2 Hz); **^{13}C NMR** (126 MHz, $CDCl_3$) δC 175.8, 172.1, 156.1, 143.0, 128.3, 128.0, 117.1, 107.8, 68.1, 60.7, 55.1, 49.7, 47.6, 44.8, 40.1, 28.1, 25.6, 25.0, 21.8, 21.7; **HRMS (APCI) m/z**: $[M+H]^+$ calculated for $[C_{20}H_{28}O_4N]^+$ 346.2013, found 346.2016; **IR** (neat) $\tilde{\nu}$ = 2976, 2937, 2877, 1734, 1625, 1592, 1485, 1401, 1372, 1265, 1108, 1076, 922, 767, 729, 707 cm^{-1}.

Isopropyl ((*R*)-4-methoxy-2-methyl-2,3-dihydro-1*H*-indene-2-carbonyl)-*D*-prolinate (*R*,*R*)-435):

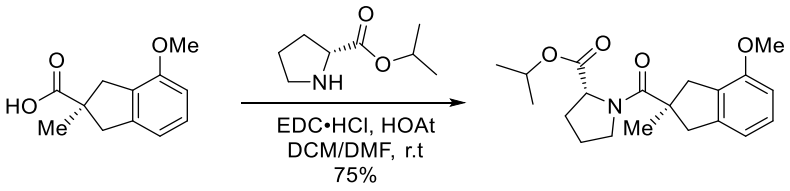

EDC•HCl (24 mg, 0.12 mmol, 1.5 equiv) and HOAt (17 mg, 0.12 mmol, 1.5 equiv) were added to a solution of carboxylic acid **437** (17 mg, 0.082 mmol, 1 equiv) in a 1:1 solution of DCM and DMF (0.5 mL) at 0 °C. The solution was stirred at 0 °C for 15 min before isopropyl-*D*-proline (52 mg, 0.33 mmol, 4.0 equiv) was added dropwise as a solution in DCM and DMF (1:1, 0.6 mL). After being left to stir at r.t for 12 h, the reaction was diluted with sat. $NH_4Cl_{(aq)}$ (2.5 mL) and H_2O (2.5 mL) with the resulting solution extracted with Et_2O (2 × 20 mL). Combined organic extracts were dried over Na_2SO_4, filtered, and concentrated to afford an off-white solid. The solid was purified by column chromatography (10 g SiO_2, 10 to 30% EtOAc in hexanes) to provide amide (***R*,*R*)-435** as a colourless film (15 mg, 75%). Spectra are in agreement with data reported for the product.[22]

^{1}H NMR (500 MHz, $CDCl_3$) δH 7.15 (H, dd, *J* = 8.1, 7.5 Hz), 6.82 (1H, d, *J* = 7.5 Hz), 6.68 (1H, d, *J* = 8.1 Hz), 5.03 (1H, qq, *J* = 6.3, 6.2 Hz), 4.50 (1H, dd, *J* = 8.6, 4.8 Hz), 3.82 (3H, s), 3.73 (1H, m), 3.64 (1H, m), 3.61 (1H, d, *J* = 16.3 Hz), 3.39 (1H, d, *J* = 16.3 Hz), 2.94 (1H, d, *J* = 16.3 Hz), 2.87 (1H, d, *J* = 16.3 Hz), 2.17 (1H, m), 2.06 (1H, m), 1.85 – 1.97 (2H, m), 1.36 (3H, s), 1.26 (3H, d, *J* = 6.3 Hz), 1.19 (3H, d, *J* = 6.2 Hz); **^{13}C NMR** (126 MHz, $CDCl_3$) δC 175.8, 172.1, 156.2, 143.0, 128.5, 128.0, 117.1, 68.1, 60.8, 55.1, 49.5, 47.6, 44.6, 40.5, 28.1, 25.7, 25.2, 21.8, 21.7; **HRMS (APCI) m/z**: $[M+H]^+$ calculated for $[C_{20}H_{28}O_4N]^+$ 346.2013, found 346.2016; **IR** (neat) $\tilde{\nu}$ = 2976, 2937, 2877, 1734, 1625, 1592, 1485, 1401, 1372, 1265, 1185, 1108, 1076, 922, 767, 729, 707 cm^{-1}.

5.4 Procedures for Chapter 4

5.4.1 Synthesis of Hybrid Inhibitors

2-(4-Bromophenyl)acetaldehyde (492):

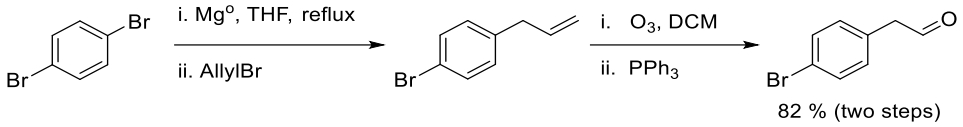

Four small chips of I_2 were added to a suspension of magnesium turnings (2.55 g, 105 mmol) in anhydrous THF (300 mL). The solution was then heated to reflux under an argon atmosphere until the brown colour had dissipated to a light yellow. The solution was cooled to r.t. and 1,4-dibromobenzene (23.6 g, 100 mmol) was added causing an exotherm which continued for approximately 1 h. Allyl bromide (15.6 mL, 180 mmol) was then added and the reaction headed to reflux for 6 h. The reaction was quenched with sat. $NH_4Cl_{(aq)}$ (200 mL) and H_2O (50 mL) and extracted with Et_2O (1 × 250 mL) and EtOAc (2 × 250 mL). Combined organic extracts were dried over Na_2SO_4 and concentrated to afford a yellow-orange liquid. The liquid was the subjected to distillation using a 15 cm vigreux column (4 mmHg, 58 °C). This afforded 4-allyl bromobenzene (**491**, contaminated with 1,4-diallyl benzene) as a colourless oil which was used without further purification. A stream of O_3 was passed through a solution of crude 4-allyl bromobenzene in DCM at −78 °C until a vivid blue colour persisted. The stream of $O_3$was then replaced with a stream of O_2 until the solution became colourless. The solution was then warmed to r.t. and placed in a water bath before PPh_3 was added in small portions. PPh_3 addition was continued until a signal at −6.0 ppm could be observed in the ^{31}P NMR spectrum (14.3 g, 54.6 mmol, 1 equiv). All volatiles were then removed by rotary evaporation affording a thick residue. Et_2O/pentane were then added to force the precipitation of triphenylphosphine oxide as a white solid. The solid was filtered through

a glass frit and the filtrate concentrated before being subjected to short-path distillation (6 mmHG, 104-106 °C). This afforded **492** as a waxy white solid (8.91 g, 82%). Spectra are in agreement with data reported for the product.[23] **^{1}H NMR** (400 MHz, $CDCl_3$) δH 9.74 (1H, t, *J* = 2.1 Hz), 7.50 (2H, m), 7.09 (2H, m), 3.66 (2H, d, *J* = 2.1 Hz).

Ethyl (*E*)-4-(4-bromophenyl)but-2-enoate (523):

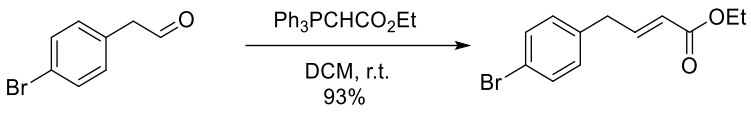

Ethyl (triphenylphosphoranylidene)acetate (12.7 g, 36.5 mmol, 1.0 equiv) was added to a solution of **492** in DCM (150 mL) at r.t. and left to stir under argon overnight. All volatiles were removed, and the resulting residue passed through a plug of SiO_2 eluting with 4% EtOAc in hexanes. The filtrate was concentrated and subjected to column chromatography (50 g SiO_2, 0 – 5% EtOAc in hexanes) to provide ester **523** as a colourless oil (9.13 g, 93%). **^{1}H NMR** (500 MHz, $CDCl_3$) δH 7.44 (2H, m), 7.05 (3H, m), 5.79 (1H, dt, *J* = 15.6, 1.7 Hz), 4.18 (2H, q, *J* = 7.0 Hz), 3.47 (2H, dd, *J* = 6.7, 1.4 Hz), 1.27 (3H, t, *J* = 7.0 Hz).

(*E*)-4-(4-Bromophenyl)but-2-en-1-ol (493):

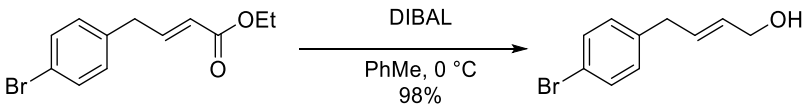

DIBAL-H (25 wt%, 1.74 mL, 2.61 mmol, 2.35 equiv) was added dropwise to a solution of ethyl (*E*)-4-(4-bromophenyl)but-2-enoate (**523**) in PhMe (10 mL) at 0 °C under argon. After 2.5 h the reaction was quenched with H_2O (100 µL) followed by $KOH_{(aq)}$ (15 wt%, 100 µL) and finally H_2O (260 µL). The solution was then warmed to r.t. and stirred vigorously until a white solid had formed then filtered through a pad of celite. The filtrate was concentrated, and the resulting residue

subjected to column chromatography (24 g SiO_2, 0 – 40% EtOAc in hexanes over 15 min). Fractions of interest were combined and concentrated to afford **493** as a colourless oil (300 mg, 98%). **^{1}H NMR** (400 MHz, $CDCl_3$) δH 7.41 (2H, m), 7.06 (2H, m), 5.82 (1H, m), 5.69 (1H, m), 4.13 (2H, d, *J* = 5.0 Hz), 3.34 (2H, d, *J* = 6.5 Hz), 1.34 (1H, br. s, D_2O exch.); **^{13}C NMR** (126 MHz, $CDCl_3$) δC 138.9, 131.5, 130.8, 130.7, 130.3, 119.9, 63.4, 38.0.

((2*R*,3*R*)-3-(4-Bromobenzyl)oxiran-2-yl)methanol (495):

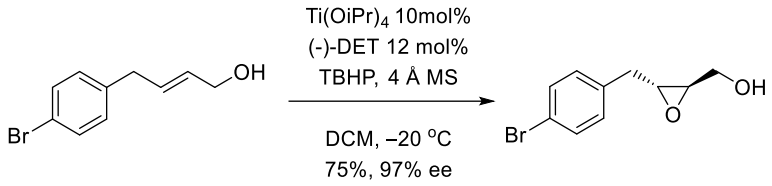

Ti(O*i*Pr)$_4$ (185 μL, 0.616 mmol, 5.50 mol%) was added to a solution of allylic alcohol **493** (2.54 g, 11.2 mmol, 1 equiv), (−)-diethyl D-tartrate (130 μL, 0.748 mmol, 6.60 mol%), and crushed molecular sieves (4 Å, 3 g) in anhydrous DCM (25 mL) at −25 °C under an argon atmosphere. The solution was allowed to age for 15 min before TBHP (7.13 mL, 39.2 mmol, 3.5 equiv) was added dropwise over 5 min. The reaction was then stirred at −25 °C for 12 h before being filtered through a pad of celite (2 g) and H_2O (10 mL) added. The biphasic solution was stirred vigorously at 0 °C for 1 h before $NaOH_{(aq)}$ (1M, 50 mL) was added and the stirring continued for an additional 30 min at 0 °C. The phases were then separated, and the aqueous phase extracted with DCM (5 × 50 mL). Combined organic extracts were dried over Na_2SO_4 and concnetarted to afford a colourless oil which was subjected to column chromatography (24g SiO_2, 0 – 50% EtOAc in hexanes over 30 min) to afford epoxide **495** as a colourless oil (2.05 g, 75%, 97% ee). **^{1}H NMR** (400 MHz, $CDCl_3$) δH 7.44 (2H, m), 7.12 (2H, m), 3.91 (1H. ddd. *J* = 12.7, 5.1, 2.6 Hz), 3.65 (1H, ddd, *J* = 12.7, 7.4, 4.1 Hz), 3.19 (1H, ddd, *J* = 8.2, 4.9, 2.2 Hz), 2.96 (1H, ddd, *J* = 4.0 2.4, 2.4 Hz), 2.90 (1H, dd, *J* = 14.7, 4.9 Hz), 2.84 (1H, dd, *J* = 14.7, 6.1 Hz), 1.57 (1H, dd, *J* = 7.3, 5.6 Hz, D_2O

exch); **^{13}C NMR** (126 MHz, $CDCl_3$) δC 135.9, 131.6, 130.7, 120.7, 61.2, 58.0, 55.4, 37.1; **Chiral HPLC:** OD column 5 to 15% iPrOH in hexanes over 20 min, major enantiomer:13.5 min, minor enantiomer: 14.9 min.

(2*S*,3*S*)-3-Azido-4-(4-bromophenyl)butane-1,2-diol (496):

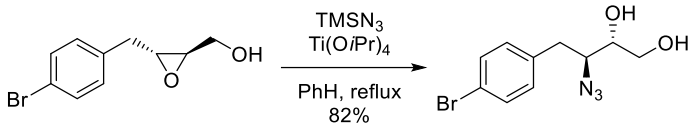

$TMSN_3$ (6.60 mL, 49.7 mmol, 3.0 equiv) was added to a solution of Ti(O*i*Pr)$_4$ (7.40 mL, 24.9 mmol, 1.5 equiv) in anhydrous PhH (34 mL) at r.t. under an argon atmosphere. The reaction was then heated to reflux for 4 h then cooled to r.t. and epoxide **495** (4.03 g, 16.6 mmol, 1 equiv) added as a solution in PhH (8 mL). The reaction was stirred for an additional 30 min before being quenched with $H_2SO_{4(aq)}$ (5% v/v, 100 mL) and the resulting biphasic mixture extracted with DCM (3 × 100 mL). Combined organic extracts were dried over Na_2SO_4 and concentrated to afford a slightly yellow solid. The solid was subjected to recrystallisation from hot DCM to afford diol **496** as a white solid (3.89 g, 82%). **^{1}H NMR** (400 MHz, DMSO-d_6) δH 7.51 (2H, m), 7.24 (2H, m), 5.21 (1H, d, *J* = 5.21, D_2O exch.), 4.72 (1H, dd, *J* = 5.5, 5.5, D_2O exch.), 3.61 (2H, m), 3.47 (2H, m), 2.95 (1H, dd, *J* = 14.1, 3.2 Hz), 2.69 (1H, dd, 14.2, 9.9 Hz); **^{13}C NMR** (126 MHz, DMSO-d_6) δC 138.1, 131.4, 131.2, 119.4, 73.1, 64.7, 62.5, 34.0.

(2*S*,3*S*)-3-Azido-4-(4-bromophenyl)-2-hydroxybutyl 4-methylbenzenesulfonate (498):

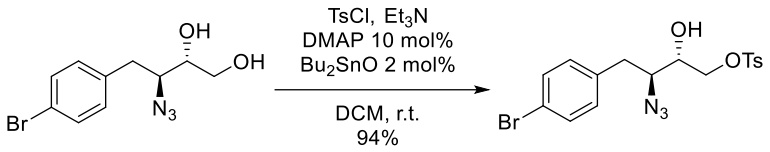

TsCl (1.20 g, 6.31 mmol, 1.1 equiv) was added to a solution of diol **496** (1.64 g, 5.74 mmol, 1 equiv), Et_3N (1.60 mL, 11.5 mmol, 2.0 equiv), Bu_2SnO (29 mg, 0.12 mmol, 2.0 mol%), and DMAP (70 mg, 0.57 mmol, 10 mol%) in anhydrous DCM (30 mL) at 0 °C under an argon atmosphere. The reaction was then warmed to r.t. and left to stir for 3.5 h then adsorbed onto SiO_2 and subjected to column chromatography (24 g SiO_2, 0 – 100% EtOAc over 20 min) affording azide **498** as a colourless oil (2.365 g, 94%). **^{1}H NMR** (500 MHz, $CDCl_3$) δH 7.80 (2H, m), 7.44 (2H, m), 7.38 (2H, m), 7.11 (2H, m), 4.21 (1H, dd, *J* = 10.7, 3.1 Hz), 4.09 (1H, dd, *J* = 10.8, 6.0 Hz), 3.72 (1H, m), 3.64 (1H, m), 3.03 (1H, dd, *J* = 14.2, 3.8 Hz), 2.75 (1H, dd, *J* = 14.2, 8.7 Hz), 2.48 (1H, d, *J* = 5.8 Hz, D_2O exch), 2.46 (3H, s); **^{13}C NMR** (126 MHz, $CDCl_3$) δC 145.5, 135.6, 132.2, 131.8, 131.2, 130.1, 128.0, 121.0, 70.8(4), 70.8(1), 64.1, 36.1, 21.7.

(2*R*,3*S*)-3-Azido-4-(4-bromophenyl)-1-(isobutylamino)butan-2-ol (531):

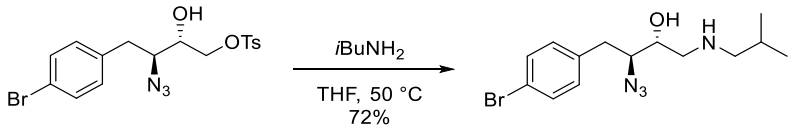

i$BuNH_2$ (230 μL, 2.30 mmol, 6 equiv) was added to a solution of azide **498**(169 mg, 0.384 mmol, 1 equiv) in THF (2 mL). The reaction was then warmed to 50 °C and left to stir overnight. An additional portion of *i*$BuNH_2$ (230 μL, 2.30 mmol, 6 equiv) was added and the reaction left for another 10 h before being adsorbed onto SiO2 and subjected to column chromatography (10 g SiO_2, 12 – 100% EtOAc in hexanes). Fractions of interest were combined and concentrated to

afford amine **531** as an oil (95 mg, 72%). (**^{1}H NMR** (400 MHz, $CDCl_3$) δH 7.45 (2H, m), 7.14 (2H, m), 3.59 (2H, m), 2.98 (1H, dd, *J* = 14.3, 3.7 Hz), 2.90 (1H, dd, *J* = 12.1, 3.4 Hz), 2.71 (2H, dd, *J* = 12.6, 8.4 Hz), 2.48 (2H, m), 1.78 (1H, qq, *J* = 6.7, 6.7 Hz), 0.94(2) (3H, d, *J* = 6.7 Hz), 0.93(9) (3H, d, *J* = 6.6 Hz); **^{13}C NMR** (126 MHz, $CDCl_3$) δC 136.6, 131.6, 131.1, 120.7, 70.0, 66.6, 57.5, 50.7, 36.4, 28.3, 20.4(6), 20.4(5).

***N*-((2*R*,3*S*)-3-Azido-4-(4-bromophenyl)-2-hydroxybutyl)-*N*-isobutyl-4-nitrobenzene-sulfonamide (499):**

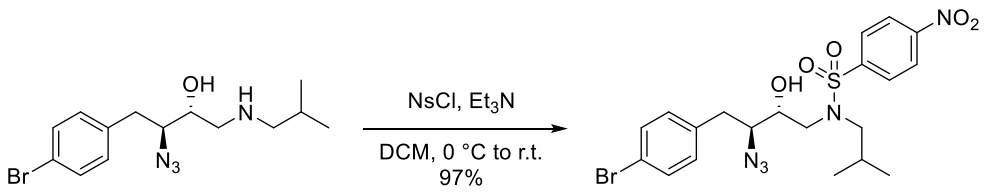

NsCl (673 mg, 3.04 mmol, 1.1 equiv) was added to a solution of amine **531** (943 mg, 2.76 mmol, 1 equiv) and Et3N (770 µL, 5.53 mmol, 2.0 equiv) in anhydrous DCM (10 mL) at 0 °C under an argon atmosphere. The reaction was warmed to r.t. and left to stir for 4.5 h then adsorbed onto SiO_2 and subjected to column chromatography (24 g SiO_2, 0 – 40% EtOAc in hexanes over 15 min). Fractions of interest were combined and concentrated to afford azide **499** as a viscous yellow oil (1.41 g, 97%). **^{1}H NMR** (500 MHz, $CDCl_3$) δH 8.40 (2H, m), 8.00 (2H, m), 7.46 (2H, m), 7.16 (2H, m), 3.74 (1H, m), 3.56 (1H, m), 3.28 (1H, dd, *J* = 15.3, 9.2 Hz), 3.19 (2H, dd, *J* = 13.6, 2.6 Hz), 3.07 (2H, m), 2.92 (1H, dd, *J* = 13.4, 6.6 Hz), 2.78 (1H, dd, *J* = 14.3, 9.2 Hz), 1.84 (1H, qq, *J* = 6.6, 6.6 Hz), 0.93 (3H, d, *J* = 6.6 Hz), 0.88 (3H, d, *J* = 6.6 Hz); **^{13}C NMR** (126 MHz, $CDCl_3$) δC 150.2, 144.3, 135.8, 131.8, 131.1, 128.5, 124.5, 121.0, 71.5, 66.2, 58.5, 52.7, 36.2, 27.1, 20.0, 19.7.

***N*-((2*R*,3*S*)-3-amino-4-(4-bromophenyl)-2-hydroxybutyl)-*N*-isobutyl-4-nitrobenzene-sulfonamide (500)**

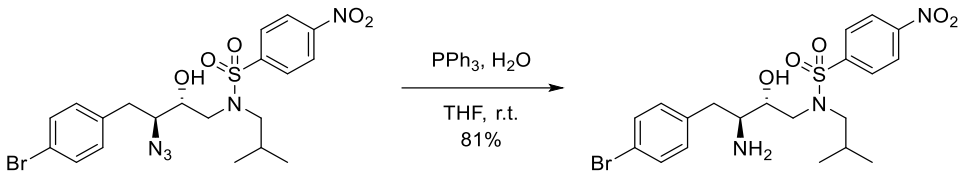

PPh_3 (384 mg, 1.46 mmol, 1.1 equiv) was added to a solution of azide **499** (700 mg, 1.33 mmol, 1 equiv) in THF (15 mL). The reaction was left to stir at r.t. for 30 min before H_2O (400 μL) was added and the reaction left overnight. An additional volume of H_2O (200 μL) was added and the reaction left at r.t. overnight. The reaction was diluted with H_2O (15 mL) and sat. $NaHCO_3$(aq) (5 mL) and extracted with EtOAc (3 × 50 mL). Combined organic extracts were dried over Na_2SO_4 and concentrated to afford a yellow oil which was purified by column chromatography (40 g SiO_2, 1.5/0.5/98 v/v/v MeOH to Et_3N to DCM) to provide amine **500** (540 mg, 81%). **^{1}H NMR** (500 MHz, DMSO-d_6) δH 8.37 (2H, m), 8.06 (2H, m), 7.45 (2H, m), 7.17 (2H, m), 4.72 (1H, d, *J* = 6.3 Hz, D_2O exch.), 3.51 (1H, dd, *J* = 14.8, 2.2 Hz), 3.38 (1H, m), 3.12 (2H, dd, *J* = 14.2, 8.7 Hz), 2.94 (1H, dd, *J* = 13.8, 6.7 Hz), 2.78 (1H, dd, *J* = 13.4, 4.1 Hz), 2.71 (1H, m), 2.33 (1H, dd, *J* = 13.4, 9.2), 1.96 (1H, qq, *J* = 6.7, 6.7 Hz), 1.30 (2H, br. s, D_2O exch.), 0.84 (3H, d, *J* = 6.6 Hz), 0.80 (3H, d, *J* = 6.7 Hz); **^{13}C NMR** (126 MHz, $CDCl_3$) δC 150.0, 145.0, 137.5, 131.8, 131.0, 128.5, 124.4, 120.5, 72.7, 57.7, 55.5, 52.0, 38.6, 26.9, 20.0, 19.9.

(*S*)-2-Acetamido-*N*-((2*S*,3*R*)-1-(4-bromophenyl)-3-hydroxy-4-((*N*-isobutyl-4-nitrophenyl)-sulfonamido)butan-2-yl)-3-methylbutanamide (501):

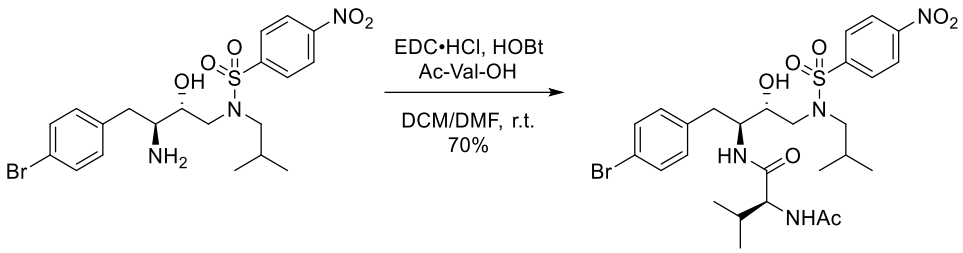

To a flask charged with HOBt (88 mg, 0.66 mmol, 1.2 equiv), *N*-acyl valine (104 mg, 0.66 mmol, 1.2 equiv), and EDC·HCl (126 mg, 0.66 mmol, 1.2 equiv) cooled to 0 °C was added anhydrous DMF (1 mL) and anhydrous DCM (1 mL). The solution was left to stir at 0 °C for 15 min before amine **500** (273 mg, 0.55 mmol, 1 equiv) was added as a solution in 1:1 DMF to DCM (3 mL) *via* canula. The reaction was then left to stir at 0 °C for another 15 min before being warmed to r.t. and left overnight. DCM was removed by rotary evaporation and H_2O (10 mL) added to the remaining residue and the resulting solution extracted with EtOAc (3 × 15 mL) to afford a cloudy solution. The solution was made homogeneous by addition of MeOH then dried over Na_2SO_4 and concentrated to afford a white solid. Compound **501** was isolated as a white powder by precipitation from DCM/hexanes (244 mg, 70%). **^{1}H NMR** (500 MHz, DMSO-d_6) δH 8.37 (2H, m), 8.06 (2H, m), 7.81 (1H, d, *J* = 9.3 Hz, D_2O exch.) 7.69 (1H, d, *J* = 9.0 Hz, D_2O exch.), 7.34 (1H, m), 7.10 (1H, m), 4.97 (1H, d, *J* = 6.7 Hz, D_2O exch.), 3.95 (1H, dd, *J* = 8.7, 8.7 Hz), 3.82 (1H, m), 3.52 (1H, m), 3.09 (2H, m), 2.94 (2H, m), 2.45 (1H, dd, *J* = 13.9, 11.0 Hz), 1.95 (1H, qq, *J* = 6.6, 6.6 Hz), 1.81 (3H, s), 1.75 (1H, qq, *J* = 7.1, 7.1 Hz), 0.82 (3H, d, *J* = 6.1 Hz), 0.81 (3H, d, *J* = 6.1 Hz), 0.70 (3H, d, *J* = 6.7 Hz), 0.67 (3H, d, *J* = 6.7 Hz); **^{13}C NMR** (126 MHz, $CDCl_3$) δC 181.8, 170.4, 150.0, 144.7, 136.3, 131.8, 130.9, 128.7, 124.3, 120.8, 59.9, 57.4, 48.9, 45.3, 41.9, 37.0, 30.4, 27.0, 22.9, 19.8, 19.7, 19.5, 18.2.

(*S*)-2-Acetamido-*N*-((2*S*,3*R*)-4-((4-amino-*N*-isobutylphenyl)sulfonamido)-1-(4-bromophenyl) -3-hydroxybutan-2-yl)-3-methylbutanamide (508):

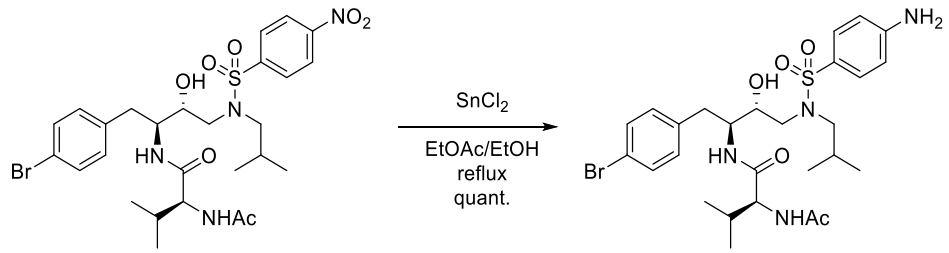

$SnCl_2$ (379 mg, 2.00 mmol, 4.0 equiv) was added to a solution of nitro arene **501** (320 mg, 0.50 mmol, 1 equiv) in EtOAc (7 mL) and EtOH (2 mL). The reaction was heated to reflux and left to stir for 4.5 h before being diluted with sat. $NaHCO3_{(aq)}$ (40 mL) and H_2O (10 mL). The resulting solution was extracted with EtOAc (3 × 15 mL). Combined organic extracts were dried over Na_2SO_4 and concentrated to afford aniline **508** as a white solid (306 mg, 100%). **^{1}H NMR** (500 MHz, DMSO-d_6) δH 7.77 (1H, d, *J* = 9.4 Hz, D_2O exch.), 7.66 (1H, d, *J* = 9.2 Hz, D_2O exch.), 7.39 (2H, m), 7.34 (2H, m), 7.13 (2H, m), 6.60 (2H, m), 5.95 (2H, s, D_2O exch.), 4.91 (1H, d, *J* = 6.1 Hz, D_2O exch.), 4.00 (1H, dd, *J* = 9.0, 7.6 Hz), 3.91 (1H, m), 3.59 (1H, m), 3.22 (1H, dd, *J* = 14.5, 4.3 Hz), 2.98 (1H, dd, *J* = 13.7, 3.0 Hz), 2.85 (1H, dd, *J* = 13.6, 8.4 Hz), 2.74 (1H, dd, *J* = 14.4, 8.3 Hz), 2.68 (1H, dd, *J* = 13.6, 6.6 Hz), 2.48 (1H, dd, *J* = 13.6, 10.8 Hz), 1.90 (1H, m), 1.82 (3H, s), 1.76 (1H, m), 0.81 (3H, d, *J* = 6.6 Hz), 0.78 (3H, d, *J* = 6.6 Hz), 0.70 (3H, d, *J* = 6.6 Hz), 0.69 (3H, d, *J* = 6.6 Hz); **^{13}C NMR** (126 MHz, DMSO-d_6) δC 171.0, 169.3, 153.2, 139.1, 132.1, 131.0, 129.5, 124.2, 119.3, 113.1, 72.0, 58.4, 57.6, 53.4, 53.0, 35.0, 30.6, 26.9, 23.0, 20.5(4), 20.4(9), 19.7, 18.7.

Methyl 5-(4-((2*S*,3*R*)-2-((*S*)-2-acetamido-3-methylbutanamido)-4-((4-amino-*N*-isobutylphenyl) sulfonamido)-3-hydroxybutyl)phenyl)pentanoate (509):

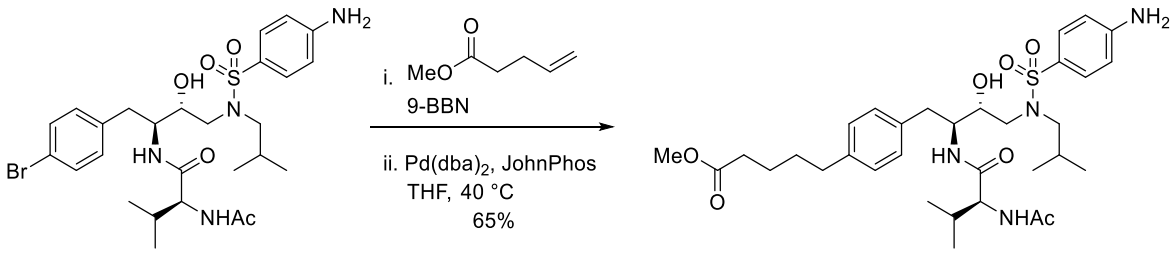

9-BBN (0.5 M in THF, 1.7 mL, 0.85 mmol, 5.0 equiv) was added dropwise over 5 min to a solution of methyl 4-pentenoate (97 mg, 0.85 mmol, 5.0 equiv) in anhydrous THF (0.5 mL) at 0 °C under an atmosphere of argon. The solution was then left at r.t. for 9 hours. The resulting solution was then cannulated into a second flask charged with aryl bromide **508** (104 mg, 0.17 mmol, 1 equiv), Cs_2CO_3 (277 mg, 0.85 mmol, 5.0 equiv), $Pd(dba)_2$ (9.8 mg, 0.017 mmol, 10 mol%), and JohnPhos (5.1 mg, 0.017 mmol, 10 mol%) in anhydrous THF (1 mL) under an atmosphere of argon. The resulting mixture was heated to 40 °C for 2 days with the addition of additional anhydrous THF (1 mL) when needed. The reaction was diluted with sat. $NH_4Cl_{(aq)}$ (13 mL) and H_2O (2 mL) and the resulting solution extracted with EtOAc (4 × 15 mL). Combined organic extracts were dried over Na_2SO_4 and concentrated. The resulting residue was purified by column chromatography (5 g SiO_2, 25% – 40% acetone in hexanes) to afford ester **509** as a white solid (71 mg, 65%). **^{1}H NMR** (500 MHz, $CDCl_3$) δH 7.55 (2H, m), 7.13 (2H, m), 7.06 (2H, m), 6.67 (2H, m), 6.34 (1H, d, *J* = 7.8 Hz, D_2O exch.), 5.84 (1H, d, *J* = 8.3 Hz, D_2O exch.), 4.10 – 4.21 (4H, m), 3.89 (1H, m), 3.81 (1H, m), 3.65 (3H, s), 3.00 – 3.04 (3H, m), 2.87 (2H, m), 2.78 (1H, dd, *J* = 13.4, 7.0 Hz), 2.57 (2H, m), 2.32 (2H, m), 2.02 (1H, m), 1.96 (3H, s), 1.80 (1H, m), 1.62 (4H, m), 0.89 (3H, d, *J* = 6.8 Hz), 0.87 (3H, d, *J* = 6.6 Hz), 0.83 (3H, d, *J* = 6.8 Hz), 0.74 (3H, d, *J* = 6.8 Hz); **^{13}C NMR** (126 MHz,

$CDCl_3$) δC 174.2, 171.5, 170.2, 150.6, 140.2, 135.1, 129.5, 129.3, 128.5, 126.4, 114.1, 72.6, 59.0, 58.6, 54.1, 53.5, 51.5, 35.2, 35.1, 33.9, 30.7, 30.1, 27.3, 24.4, 23.2, 20.1, 19.9, 19.3, 17.6.

Methyl 7-(4-((2*S*,3*R*)-2-((*S*)-2-acetamido-3-methylbutanamido)-4-((4-amino-*N*-isobutyl-phenyl)sulfonamido)-3-hydroxybutyl)phenyl)heptanoate (510):

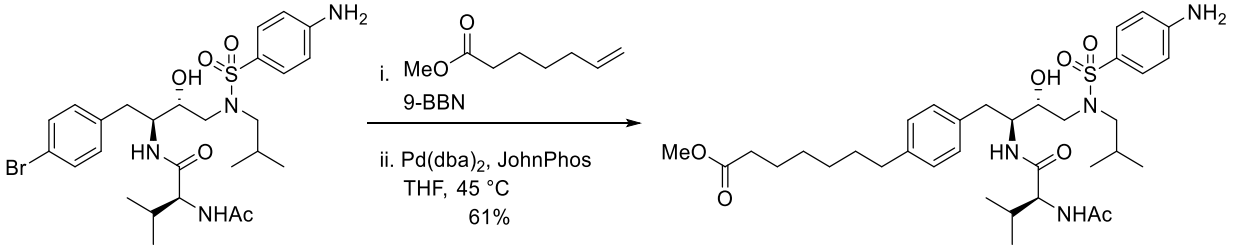

9-BBN (0.5 M in THF, 2.0 mL, 1.0 mmol, 5.0 equiv) was added dropwise over 5 min to a solution of methyl 6-heptenoate (160 μL, 1.0 mmol, 5.0 equiv) in anhydrous THF (0.5 mL) at 0 °C under an atmosphere of argon. The solution was then left to slowly warm to r.t. overnight. The resulting solution was then cannulated into a second flask charged with aryl bromide **508** (122 mg, 0.2 mmol, 1 equiv), Cs_2CO_3 (326 mg, 1.0 mmol, 5.0 equiv), $Pd(dba)_2$ (11.5 mg, 0.02 mmol, 10 mol%), and JohnPhos (6 mg, 0.02 mmol, 10 mol%) in anhydrous THF (1.5 mL) under an atmosphere of argon. The resulting mixture was heated to 45 °C for 3 days with the addition of additional anhydrous THF (1 mL) when needed. The reaction was diluted with sat. $NH_4Cl_{(aq)}$ (12 mL) and H_2O (2 mL) and the resulting solution extracted with EtOAc (4 × 15 mL). Combined organic extracts were dried over Na_2SO_4 and concentrated. The resulting residue was purified by column chromatography (20 g SiO_2, 40% acetone in hexanes) to afford ester **510** as a white solid (82 mg, 61%). **^{1}H NMR** (500 MHz, $CDCl_3$) δH 7.55 (2H, m), 7.12 (2H, m), 7.05 (2H, m), 6.67 (2H, m), 6.41 (1H, d, *J* = 8.6 Hz, D_2O exch.), 5.78 (1H, d, *J* = 8.6 Hz, D_2O exch.), 4.16 (4H, m), 4.01 (1H, d, *J* = 3.2 Hz), 3.82 (1H, m),3.66 (3H, s), 2.98 – 3.09 (3H, m), 2.87 (2H, m), 2.79 (1H, dd, *J* = 13.4, 7.0 Hz), 2.53 (2H, m), 2.29 (2H, m), 2.04 (1H, m), 1.95 (3H, s), 1.82 (1H, m), 1.59 (4H, m),

1.32 (4H, m) 0.88 (3H, d, *J* = 6.7 Hz), 0.86 (3H, d, *J* = 6.7 Hz), 0.84 (3H, d, *J* = 6.8 Hz), 0.75 (3H, d, *J* = 6.8 Hz); **^{13}C NMR** (126 MHz, $CDCl_3$) δC 174.3, 171.6, 170.2, 150.7, 140.8, 134.9, 129.5, 129.3, 128.5, 126.5, 114.1, 72.6, 59.0, 58.6, 54.2, 53.4, 51.5, 35.5, 35.1, 34.1, 31.3, 30.3, 28.9(4), 28.8(9), 27.3, 24.8, 23.2, 20.0, 19.3, 17.7.

5-(4-((2*S*,3*R*)-2-((*S*)-2-Acetamido-3-methylbutanamido)-4-((4-amino-*N*-isobutylphenyl) sulfonamido)-3-hydroxybutyl)phenyl)-*N*-hydroxypentanamide (488):

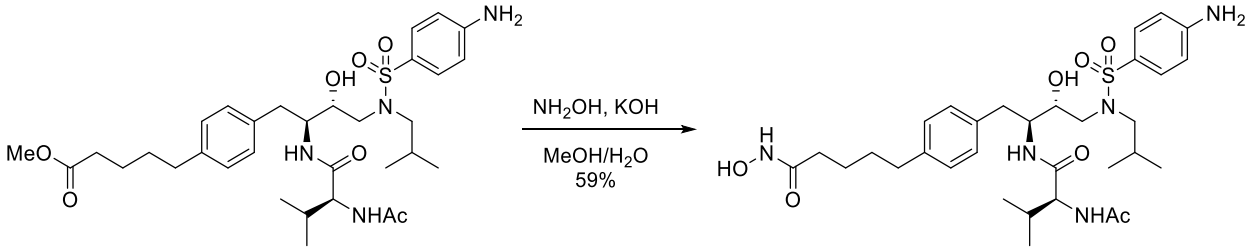

NH_2OH (50 wt% in H_2O, 1.53 mL, 25 mmol, 500 equiv) was added to solution of ester **509** (32 mg, 0.05 mmol, 1 equiv) in THF (0.2 mL) at 0 °C. The solution was allowed to stir at 0 °C for 15 min before KOH (15 wt% or 2.67 M, 170 μL, 7 equiv) was added dropwise followed by enough MeOH to result in a homogeneous mixture. Stirring was continued at 0 °C for 30 min before the reaction was warmed to r.t. and left overnight. The reaction was then brought to pH 7 with $HCl_{(aq)}$ (10% v/v) and extracted with EtOAc (3 × 20 mL). Combined organic extracts were dried over Na_2SO_4 and concentrated and adsorbed onto celite the subjected to reversed phase column chromatography (5.5 g C-18 SiO2, 10% – 100% MeOH in H_2O). Fractions of interest were combined and MeOH removed by rotary evaporation. Hydroxamic acid **488** was isolated as a fluffy white solid from the resulting aqueous solution by lyophilisation (19 mg, 59%). Aliquots were subjected to semi-prep HPLC purification prior to use in HDAC inhibition assays. (Zorbax SB-C18, 50 – 80% MeOH in H_2O, 3 mL/min over 30 min). **^{1}H NMR** (400 MHz, DMSO-d_6) δH 10.33 (1H, s, D_2O exch.), 8.65 (1H, s, D_2O exch.), 7.73 (1H, d, *J* = 9.2 Hz, D_2O exch.), 7.66 (1H,

d, *J* = 9.2 Hz, D_2O exch,), 7.39 (2H, m), 7.09 (2H, m), 6.99 (2H, m), 6.60 (2H, m), 5.96 (1H, s), 4.86 (1H, d, *J* = 6.0 Hz), 4.04 (1H, m), 3.92 (1H, m), 3.59 (1H, m),3.30 (3H, s), 3.21 (1H, dd, *J* = 14.6, 3.8 Hz), 2.95 (1H, dd, *J* = 13.8, 3.1 Hz), 2.85 (1H, dd, *J* = 13.8, 8.4 Hz), 2.76 (1H, dd, *J* = 14.6, 8.4 Hz), 2.67 (1H, dd, *J* = 13.6, 6.8 Hz), 1.91 (3H, m), 1.82 (3H, s), 1.80 (1H, m), 1.48 (4H, m), 0.81 (3H, d, *J* = 6.5 Hz), 0.78 (3H, d, *J* = 6.6 Hz), 0.70 (3H, d, *J* = 6.6 Hz), 0.69 (3H, d, *J* = 6.5 Hz).

7-(4-((2*S*,3*R*)-2-((*S*)-2-Acetamido-3-methylbutanamido)-4-((4-amino-*N*-isobutylphenyl)sulfonamido)-3-hydroxybutyl)phenyl)-*N*-hydroxyheptanamide (489):

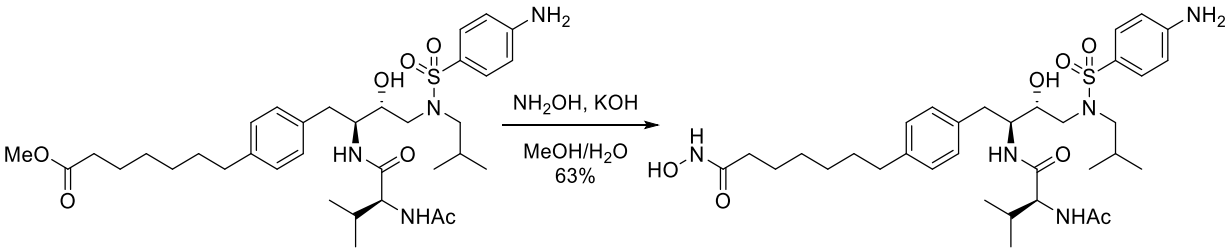

NH_2OH (50 wt% in H_2O, 3.7 mL, 60 mmol, 500 equiv) was added to solution of ester **510** (81 mg, 0.12 mmol, 1 equiv) in THF (0.4 mL) at 0 °C. The solution was allowed to stir at 0 °C for 15 min before KOH (15 wt% or 2.67 M, 315 µL, 7 equiv) was added dropwise followed by enough MeOH to result in a homogeneous mixture (1.3 mL). Stirring was continued at 0 °C for 30 min before the reaction was warmed to r.t. and left for 2 days. The reaction was then brought to pH 7 with $HCl_{(aq)}$ (10% v/v) and extracted with EtOAc (4 × 20 mL). Combined organic extracts were dried over Na_2SO_4 and concentrated and adsorbed onto celite the subjected to reversed phase column chromatography (5.5 g C-18 SiO_2, 10% – 100% MeOH in H_2O). Fractions of interest were combined and MeOH removed by rotary evaporation. Hydroxamic acid **489** was isolated as a fluffy white solid from the resulting aqueous solution by lyophilisation (51 mg, 63%). Aliquots were subjected to semi-prep HPLC purification prior to use in HDAC inhibition assays (Zorbax

SB-C18, 50 – 80% MeOH in H_2O, 3 mL/min over 30 min). **^{1}H NMR** (500 MHz, DMSO-d_6) δH 10.31 (1H, s), 8.64 (1H, s), 7.72 (1H, d, *J* = 9.3 Hz), 7.66 (1H, d, *J* = 9.1 Hz), 7.39 (2H, m), 7.09 (2H, m), 7.00 (2H, m), 6.61 (2H, m), 5.96 (1H, s), 4.86 (1H, d, *J* = 6.0 Hz), 4.04 (1H, m), 3.92 (1H, m), 3.59 (1H, m),3.30 (3H, s), 3.21 (1H, dd, *J* = 14.6, 3.8 Hz), 2.95 (1H, dd, *J* = 13.8, 3.1 Hz), 2.85 (1H, dd, *J* = 13.8, 8.4 Hz), 2.76 (1H, dd, *J* = 14.6, 8.4 Hz), 2.67 (1H, dd, *J* = 13.6, 6.8 Hz), 1.91 (3H, m), 1.82 (3H, s), 1.80 (1H, m), 1.48 (4H, m), 1.26 (4H, m), 0.81 (3H, d, *J* = 6.5 Hz), 0.78 (3H, d, *J* = 6.6 Hz), 0.70 (3H, d, *J* = 6.6 Hz), 0.69 (3H, d, *J* = 6.5 Hz).

(*S*)-2-Acetamido-*N*-((2*S*,3*R*)-4-((4-amino-*N*-isobutylphenyl)sulfonamido)-3-hydroxy-1-(4-vinylphenyl)butan-2-yl)-3-methylbutanamide (511):

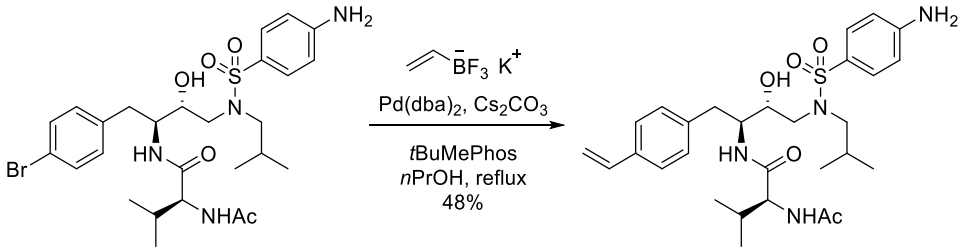

Degassed *n*PrOH (5 mL) and H_2O (0.5 mL) were added to a flask equipped with a reflux condenser containing aryl bromide **508** (92 mg, 0.15 mmol, 1 equiv), $Pd(dba)_2$ (17.4 mg, 0.03 mmol, 20 mol%), tBuMePhos (9.4 mg, 0.03 mmol, 20 mol%), and Cs_2CO_3 (62 mg, 0.45 mmol, 3.0 equiv). The reaction was then brought to reflux and left overnight. *n*PrOH was removed by rotary evaporation, sat. $NH_4Cl_{(aq)}$ (10 mL) and H_2O (2 mL) added, and the resulting solution was extracted with EtOAc (3 × 10 mL). Combined organic extracts were dried over Na_2SO_4 and the resulting residue purified by column chromatography (15 g SiO_2, Et_3N/acetone/hexanes 1/40/59 v/v/v) to afford styrene **511** as a yellow residue (40 mg, 48%). **^{1}H NMR** (400 MHz, $CDCl_3$) 7.54 (2H, m), 7.30 (2H, m), 7.18 (2H, m), 6.67 (2H, m), 6.50 (1H, d, *J* = 8.8 Hz, D_2O exch.), 5.77 (1H, m), 5.70 (1H, d, *J* = 17.6 Hz), 5.20 (1H, d, *J* = 10.9 Hz), 4.22 (1H, m), 4,14 (2H, m), 3.99 (1H, m),

3.83 (1H, m), 3,05 (2H, m), 2.88 (2H, m), 2.77 (1H, dd, *J* = 13.2, 6.7 Hz), 2.00 (1H, m), 1.91 (3H, s), 1.82 (2H, m), 0.89 (3H, d, *J* = 6.6 Hz), 0.87 (3H, d, *J* = 6.7 Hz), 0.84 (3H, d, *J* = 6.8 Hz), 0.77 (3H, d, *J* = 6.8 Hz); **^{13}C NMR** (101 MHz, $CDCl_3$) δC 171.4, 170.1, 150.6, 137.5, 136.5, 135.8, 129.6, 129.5, 126.4, 126.3, 114.1, 113.4, 72.6, 58.9, 58.7, 53.7, 53.6, 35.3, 30.4, 29.3, 27.3, 23.2, 20.1, 19.9, 19.2.

Methyl (*E*)-3-(4-((2*S*,3*R*)-2-((*S*)-2-acetamido-3-methylbutanamido)-4-((4-amino-*N*-isobutyl-phenyl)sulfonamido)-3-hydroxybutyl)phenyl)acrylate (512):

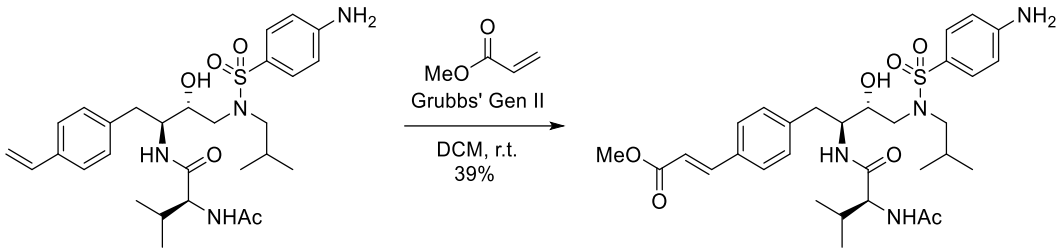

Grubbs' second-generation catalyst (8.5 mg, 0.010 mmol, 14 mol%) was added to a solution of styrene **511** (40 mg, 0.072 mmol, 1 equiv) and freshly distilled methyl acrylate (65 μL, 0.72 mmol, 10 equiv) in anhydrous DCM under an argon atmosphere. The flask was equipped with a reflux condenser, heated to reflux and left overnight. An addition portion of methyl acrylate (65 μL, 0.72 mmol, 10 equiv) was added and the reaction left at reflux for a second night. At this point DCM was removed by rotary and the resulting residue was purified by column chromatography (10 g SiO_2, Et_3N/acetone/hexanes 1/50/49 v/v/v) to afford ester **512** as a thin film (17 mg, 39%). **^{1}H NMR** (500 MHz, $CDCl_3$) δH 7.65 (1H, d, *J* = 16.0 Hz), 7.54 (2H, m), 7.42 (2H, m), 7.26 (2H, m), 6.67 (2H, m), 6.40 (1H, d, *J* = 16.0 Hz), 6.32 (1H, d, *J* = 8.9 Hz, D_2O exch.), 5.66 (1H, d, *J* = 8.5 Hz, D_2O exch.), 4.23 (1H, m), 4.08 (1H, dd, *J* = 8.5, 6.9 Hz), 4.01 (1H, d, *J* = 2.9, D_2O exch.), 3.82 (1H, m), 3.80 (3H, s), 3.08 (1H, dd, *J* = 14.2, 4.9 Hz), 3.02 (2H, d, *J* = 6.1 Hz), 2.92 (1H, dd, *J* = 12.2, 9.7 Hz) 2. 88 (1H, m), 2.77 (1H, dd, *J* = 13.4, 6.9 Hz), 2.00 (1H, m), 1.92 (3H, s), 1,81

(1H, m), 1.31 (1H, broad s, D_2O exch.), 0.88 (3H, d, *J* = 6.6 Hz), 0.87 (3H, d, *J* = 6.7 Hz), 0.83 (3H, d, *J* = 6.7 Hz), 0.75 (3H, d, *J* =6.9 Hz); **^{13}C NMR** (126 MHz, $CDCl_3$) δC 171.5, 170.1, 167.5, 150.7, 144.5, 140.6, 132.7, 130.0, 129.5, 128.2, 126.2, 117.3, 114.1, 72.7, 59.1, 58.8, 53.7, 53.6, 51.7, 35.4, 30.2, 27.3, 20.1, 19.9, 19.2, 17.7.

Methyl 3-(4-((2*S*,3*R*)-2-((*S*)-2-acetamido-3-methylbutanamido)-4-((4-amino-*N*-isobutyl-phenyl)sulfonamido)-3-hydroxybutyl)phenyl)propanoate (513):

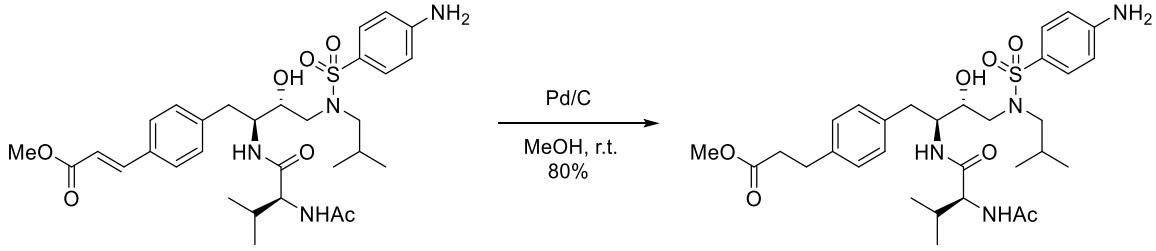

Pd/C (5 wt%, 7.5 mg, 10 mol%) was added to a solution of ester **512** (20 mg, 0.032 mmol, 1 equiv) in MeOH (1 mL) under a hydrogen atmosphere. The reaction was stirred vigorously for 1 h before being filtered through a small plug of celite and the filtrate concentrated to afford ester **513** (16 mg, 80%). **^{1}H NMR** (500 MHz, $CDCl_3$) 7.54 (2H, m), 7.14 (2H, m), 7.07 (2H, m), 6.67 (2H, m), 6.49 (1H, d, *J* = 8.9 Hz, D_2O exch.), 5.88 (1H, d, *J* = 8.5 Hz, D_2O exch.), 4.19 (3H, m), 4.13 (1H, dd, *J* = 8.6, 6.7 Hz), 4.03 (1H, s, D_2O exch.), 3.82 (1H, m), 3.66 (3H, s), 2.99 – 3.09 (3H, m), 2.83 – 2.9 (4H, m), 2.79 (1H, dd, *J* = 13.4, 7.1 Hz), 2.59 (2H, dd, *J* = 8.0, 8.0), 2.00 (1H, m), 1.95 (3H, s), 1.82 (1H, m), 1.73 (1H, broad s, D_2O exch.),0.88 (3H, d, *J* = 6.6 Hz), 0.87 (3H, d, *J* = 6.6 Hz), 0.82 (3H, d, *J* = 6.7 Hz), 0.74 (3H, d, *J* = 6.8 Hz); **^{13}C NMR** (126 MHz, $CDCl_3$) δC 173.4, 171.5, 170.3, 150.7, 138.5, 135.7, 129.4(8), 129.4(6), 128.3, 126.3, 114.1, 72.6, 58.9, 58.6, 54.0, 53.4, 51.6, 35.7, 35.1, 31.7, 30.5, 30.1, 27.2, 23.2, 20.1, 19.9, 19.2, 17.7.

5.4.2 Preparation of HDAC Inhibitor Assay Substrate

Acetyl-*L*-leucine (524):

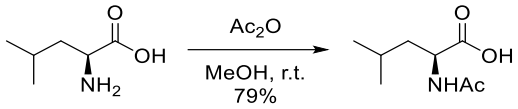

Acetic anhydride (4.8 mL, 51 mmol, 3.4 equiv) was added to a solution of L-leucine (2.0 g, 15 mmol, 1 equiv) in dry MeOH (9 mL). The reaction was then left to stir at r.t. overnight. All volatiles were then removed and the resulting solid suspended in EtOAc (15 mL) and stirred for 2 hours before being filtered. Acetyl-L-leucine (**524**) was obtained through recrystallisation of the solid from DCM/hexanes (2.1 g, 79%). Spectra are in agreement with data reported for the product.[24] **^{1}H NMR** (500 MHz, DMSO-d_6) δH 12.46 (1H, broad s, D_2O exch.), 8.08 (1H, d, J = 7.9 Hz, D_2O exch.), 4.20 (1H, m), 1.84 (3H, s), 1.63 (1H, m), 1.44 – 1.53 (2H, m), 0.89 (3H, d, J = 6.4 Hz), 0.84 (3H, d, J = 6.6 Hz).

Benzyl acetyl-*L*-leucylglycinate (525):

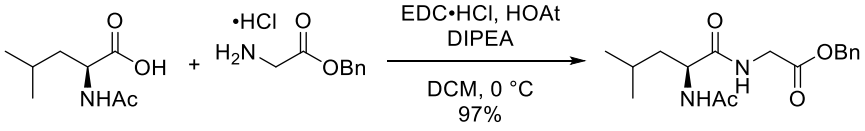

EDC•HCl (538 mg, 2.75 mmol, 1.1 equiv) was added to a solution of acetyl-L-leucine (**524**, 433 mg, 2.50 mmol, 1 equiv), and HOAt (364 mg, 2.68 mmol, 1.07 equiv) in dry DCM (5 mL) at 0 °C. The solution was stirred at 0 °C for 12 min before benzyl glycinate hydrochloride (554 mg, 2.75 mmol, 1.1 equiv) and DIPEA (466 µl, 2.68 mmol, 1.07 equiv) were added as a solution in dry DCM (7.5 mL). The reaction was stirred at 0 °C 4.5 h then quenched with sat. NH_4Cl (20 mL) and H_2O (5 mL) and extracted with DCM (4 × 40 mL). Combined organic extracts were dried over Na_2SO_4 and concentrated. Chromatography (16 g SiO_2, 40 to 100% EtOAc in hexanes) provided

525 (780 mg, 97%). **^{1}H NMR** (500 MHz, $CDCl_3$) δH 7.35 (5H, m), 6.70 (1H, broad s, D_2O exch.), 5.96 (1H, d, *J* = 8.2 Hz, D_2O exch.), 5.30 (2H, s), 4.51 (1H, m), 4.09 (1H, dd, *J* = 18.3, 5.6 Hz), 4.03 (1H, dd, *J* = 18.3, 5.3 Hz), 1.99 (3H, s), 1.65 (2H, m), 1.51 (1H, m), 0.93 (3H, d, *J* = 6.4 Hz), 0.91 (3H, d, *J* = 6.4 Hz).

Acetyl-*L*-leucylglycine (526):

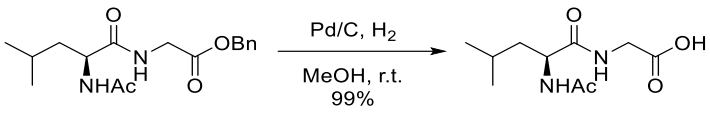

Pd/C (37 mg, 0.017 mmol, 2 mol%) was added to a solution of acetyl-L-leucylglycine (**525**, 280 mg, 0.87 mmol, 1 equiv) in MeOH (4 mL). The flask was then equipped with a balloon of H_2 and left to stir at r.t. for 2.5 hours. The reaction was filtered through a pad of Celite-® and washed with excess MeOH. Concentration of the filtrate provided amide **526** as a white foam (200 mg, 99%). **^{1}H NMR** (500 MHz, DMSO-d_6) δH 12.56 (1H, broad s, D_2O exch.), 8.15 (1H, dd, *J* = 5.7, 5.7 Hz, D_2O exch.), 7.98 (1H, d, *J* = 8.4 Hz, D_2O exch.), 4.32 (1H, m), 3.71 (2H, m), 1.84 (3H, s), 1.60 (1H, m), 1.45 (2H, m), 0.89 (3H, d, *J* = 6.5 Hz), 6.5 (3H, d, d, *J* = 6.5 Hz).

N^6-Acetyl-*L*-lysine (527):

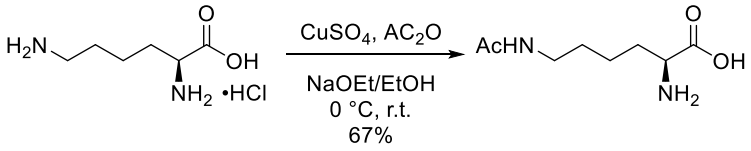

Sodium metal (920 mg, 40 mmol, 2.0 equiv) was added to dry EtOH (35 mL) under argon. Upon consumption of the sodium L-lysine hydrochloride (3.65 g, 20 mmol, 1 equiv) was added and the resulting solution stirred for 1.5 hours before $CuSO_4$ (1.63 g, 10.2 mmol, 0.51 equiv) and sat. $NaHCO_{3(aq)}$ (20 mL) were added. The reaction was left to stir at r.t for 5 hours at which time it was

diluted with H_2O to a total volume of 175 mL (to allow for adequate stirring) before Ac_2O (3.7 mL, 40 mmol, 2 equiv) and left stirring overnight. Filtering of the reaction afforded a blue solid which was resuspended in H_2O (200 mL) with 8-hydroxyquinoline (3.2 g, 22 mmol, 1.1 equiv) then added and the solution stirred at 45 °C overnight. The resulting yellow solid was filtered off and washed with EtOAc (3 × 300 mL) with amino acid **527** afforded by concentration of the filtrate (2.53 g, 67%). Spectra are in agreement with data reported for the product.[25] **^{1}H NMR** (500 MHz, D_2O) δH 3.63 (1H, dd, *J* = 6.5, 5.8 Hz), 3.08 (2H, dd, *J* = 6.9, 6.9 Hz), 1.88 (3H, s), 1.77 (2H, m), 1.45 (2H, m), 1.31 (2H, m); **^{13}C NMR** (126 MHz, D_2O) δC 174.8, 174.0, 54.6, 39.0, 30.0, 27.9, 21.8, 21.7.

***N*^{6}-Acetyl-*N*^{2}-(tert-butoxycarbonyl)-*L*-lysine (528):**

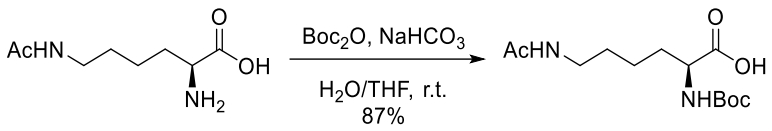

Boc_2O (600 mg, 2.75 mmol. 1.1 equiv) was added to a solution of *N*^{6}-acetyl-*L*-lysine (470 mg, 2.5 mmol, 1 equiv) and $NaHCO_3$ (788 mg, 9.38 mmol, 3.75 equiv) in 2:1 H_2O:THF (18 mL) at r.t. and left to stir for 44 hours. THF was removed *via* rotary evaporation and the aqueous phase washed with Et_2O (2 × 15 mL) then acidified to pH 3 with conc. $HCl_{(aq)}$. The aqueous phase was then extracted with DCM (5 × 30 mL). Combined organic extracts were dried over Na_2SO_4 and concentrated to afford acid **528** as a white foam (627 mg, 87%). **^{1}H NMR** (500 MHz, $CDCl_3$) δH 10.17 (1H, broad s, D_2O exch.), 6.11 (1H, s, D_2O exch.), 5.34 (1H, d, *J* = 7.8 Hz, D_2O exch.), 3.27 (1H, ddd, *J* = 6.8, 6.8, 6.8 Hz), 2.75 (2H, m), 2.02 (3H, s), 1.88 (2H, m), 1.57 (2H, m), 1.47 (9H, s), 1.44 (2H, m).

***tert*-Butyl (*S*)-(6-acetamido-1-((4-methyl-2-oxo-2H-chromen-6-yl)amino)-1-oxohexan-2-yl)-carbamate (529):**

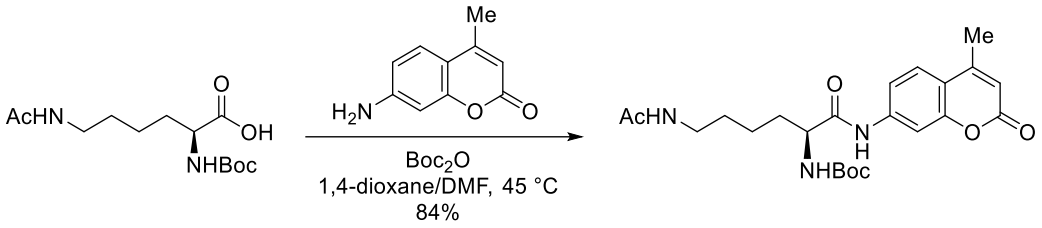

N^6-acetyl-N^2-(tert-butoxycarbonyl)-*L*-lysine (630 mg, 2.18 mmol, 1 equiv), as a solution in 1,4-dioxane (10 mL) and DMF (3 mL), was added *via* canula to a flask charged with Boc_2O (596 mg, 2.73 mmol, 1.25 equiv) under argon. To this was added pyridine (169 µl, 2.10 mmol, 0.96 equiv) and 7-amino-4-methyl cumarin (478 mg, 2.73 mmol, 1.25 equiv) and the reaction then heated to 40 °C for 20 hours. The resulting solution was concentrated to one third its volume, diluted with sat. $NH_4Cl_{(aq)}$ (40 mL) and H_2O (10 mL), then extracted with EtOAc (5 × 60 mL). Combined organic extracts were filtered to remove a fine suspended powder then dried over Na_2SO_4 and concentrated to afford a yellow-orange liquid. The liquid was subjected to column chromatography (35 g SiO_2, 4% MeOH in DCM) to provide amide **529** which was further purified by recrystallisation from DCM/hexanes (820 mg, 84%). Spectra are in agreement with data reported for the product.[26] **^{1}H NMR** (400 MHz, $CDCl_3$) δH 9.20 (1H, broad s, D_2O exch.), 7.68 (1H, s), 7.53 (2H, m), 6.20 (1H, d, *J* = 1.1 Hz,), 5.74 (1H, dd, *J* = 5.9, 5.9 Hz, D_2O exch.), 5.32 (1H, d, *J* = 5.0 Hz, D_2O exch.), 4.27(1H, m), 3.22 – 3.39 (2H, m), 2.43 (3H, d, *J* = 1.2 Hz), 2.05 (1H, m), 2.02 (3H, s), 1.75 (1H, m), 1.61 (3H, m), 1.52 (2H, m), 1.49 (9H, s).

(*S*)-6-Acetamido-2-amino-*N*-(4-methyl-2-oxo-2*H*-chromen-7-yl)hexanamide (530):

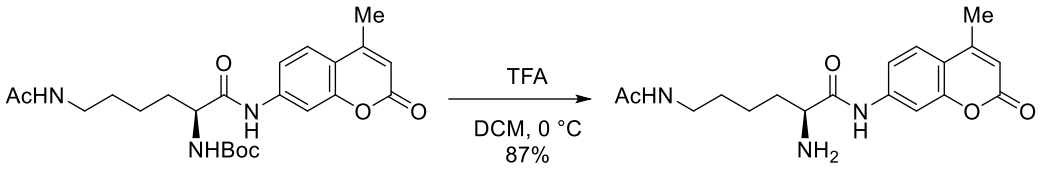

TFA (3 mL, 39 mmol) was added to a solution of ***tert***-butyl (*S*)-(6-acetamido-1-((4-methyl-2-oxo-2H-chromen-6-yl)amino)-1-oxohexan-2-yl)carbamate (**529**, 445 mg, 1.0 mmol, 1 equiv) in DCM (10 mL) at 0 °C. The reaction stirred at 0 °C for 2 hours at which point all volatiles were removed by passing a stream of air over the solution. Sat. $NaHCO_{3(aq)}$ (20 mL) was added to the resulting residue and the solution extracted with DCM (4 × 50 mL). Combined organic extracts were dried over Na_2SO_4 and concentrated to afford amine **530** as a white solid (300 mg, 87%). **^{1}H NMR** (500 MHz, DMSO-d_6) δH 7.84 (1H, d, *J* = 2.0 Hz), 7.77 (1H, d, *J* = 4.5 Hz, D_2O exch.), 7.73 (1H, d, *J* = 8.7 Hz), 7.57 (1H, dd, *J* = 8.7, 2.0 Hz), 6.27 (1H, d, *J* = 1.2 Hz), 3.18 (1H, d, *J* = 5.2 Hz), 3.01 (2H, ddd, *J* = 6.6, 6.6, 6.6 Hz), 2.41 (3H, d, *J* = 1.2 Hz), 1.77 (3H, s), 1.65 (1H, m), 1.28 – 1.50 (5H, m).

(*S*)-6-Acetamido-2-(2-((*S*)-2-acetamido-4-methylpentanamido)acetamido)-*N*-(4-methyl-2-oxo-2*H*-chromen-7-yl)hexanamide (518):

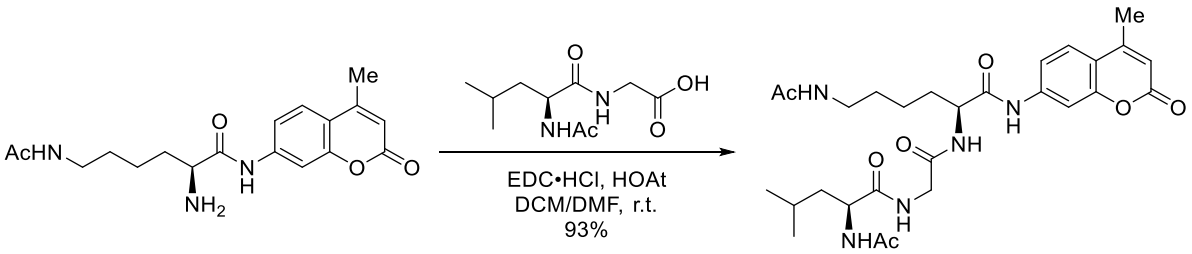

EDC•HCl (187 mg, 0.955 mmol, 1.1 equiv) was added to a solution of Acetyl-L-leucylglycine (**530**, 200 mg, 0.869 mmol, 1 equiv) and HOAt (126 mg, 0.929 mmol, 1.07 equiv) in a 1:1 solution

of DCM:DMF (4 mL) at 0 °C). The mixture was stirred at 0 °C for 10 min before (*S*)-6-acetamido-2-amino-*N*-(4-methyl-2-oxo-2*H*-chromen-7-yl)hexanamide (**530**, 300 mg, 0.869, 1.0 equiv) as a solution in 1:1 DCM:DMF (8 mL). The reaction was then left to stir at r.t. for 15 hours. DCM was removed by rotary evaporator with the resulting solution diluted with sat. $NaCl_{(aq)}$ (25 mol) and extracted with DCM (2 × 30 mL). Combined organic extracts were dried over Na_2SO_4 and concentrated to afford a yellow residue. The residue was subjected to column chromatography (30 g SiO_2, 9 to 10% MeOH in DCM) to provide **518** as a slightly yellow foam (453 mg, 93%). Spectra are in agreement with data reported for the product.[27] **^{1}H NMR** (400 MHz, DMSO-d_6) δH 10.37 (1H, s, D_2O exch.), 8.33 (1H, dd, *J* = 5.8, 5.8 Hz, D_2O exch.), 8,09 (1H, d, *J* = 7.3 Hz, D_2O exch.), 8.01 (1H, d, , *J* = 7.5 Hz, D_2O exch.), 7.80 (1H, d, *J* = 2.0 Hz), 7.78 (1H, dd, *J* = 5.3, 5.3 Hz, D_2O exch.), 7.74 (1H, d, *J* = 8.7 Hz), 7.54 (1H, dd, *J* = 8.7, 2.0 Hz), 6.28 (1H, d, *J* = 1.2 Hz), 4.38 (1H, m), 4.23 (1H, m), 3.73 (2H, m), 3.01 (2H, ddd, *J* = 6.8, 6.8, 6.8 Hz), 2.41 (3H, d, *J* = 1.2 Hz), 1.85 (3H, s), 1.77 (3H, s), 1.24 – 1.76 (3H, m), 1.46 (2H, m), 1.39 (2H, m), 1.24 – 1.35 (2H, m), 0.89 (3H, d, *J* = 6.6 Hz), 0.85 (3H, d, *J* = 6.5 Hz).

5.4.3 HDAC Inhibitor Assay

In Vitro Histone Deacetylase Inhibition Assays

For inhibition of recombinant human HDAC3 and HDAC6, dose−response experiments with internal controls were performed in black low-binding Nunc 96-well microtiter plates. Dilution series (8 concentrations) were prepared in HDAC assay buffer with 1.7 % v/v DMSO. The appropriate dilution of inhibitor (10 μL of 5 times the desired final concentration) was added to each well followed by HDAC assay buffer (25 μL) containing substrate [Ac-Leu-Gly-Lys(Ac)-AMC, 40 or 30 μM for HDAC 3 and 80 or 60 μM for HDAC 6]. Finally, a solution of the appropriate HDAC (15 μL) was added [HDAC3, 10 ng/well; HDAC 6, 60 ng/well] and the plate

incubated at 37 °C for 30 min with mechanical shaking (270 rpm). Then trypsin (50 μL, 0.4 mg/mL) was added and the assay developed for 30 min at room temperature with mechanical shaking (50 rpm). Fluorescence measurements were then taken on a Molecular Devices SpectraMax i3x plate reader with excitation at 360 (9 nm bandwidth) nm and detecting emission at 460 nm (15 nm bandwidth). Each assay was performed in triplicate at two different substrate concentrations. Baseline fluorescence emission was accounted for using blanks, run in triplicate, containing substrate (25 μL), HDAC assay buffer (15 μL), HDAC assay buffer with 1.7 % v/v DMSO (10 μL), and trypsin (50 μL). Fluorescence emission was normalized using controls, run in triplicate, containing substrate (25 μL), HDAC (15 μL), HDAC assay buffer with 1.7 % v/v DMSO (10 μL), and trypsin (50 μL). The data were analyzed by nonlinear regression with GraphPad Prism to afford IC_{50} values from the dose−response experiments. K_i values were determined from the Cheng−Prusoff equation [$K_i = IC_{50}/(1+[S]/K_m)$] with the assumption of a standard fast-on−fast-off mechanism of inhibition.

Assay Materials

HDAC3−"NCoR1" complex [(purity 90% by SDS−PAGE according to supplier; fusion protein of GST-tagged HDAC3 with the deacetylase activation domain (DAD) of NCoR1 (nuclear receptor corepressor)], HDAC6 (purity >90% by SDS−PAGE according to the supplier), The HDAC assay buffer consisted of 50 mM Tris-HCl, 137 mM NaCl, 2.7 mM KCl, 1 mM $MgCl_2$, and bovine serum albumin (0.5 mg/mL), pH was adjusted to 8 using 6 M NaOH and 1 M HCl as needed. Trypsin [25 mg/mL, from porcine pancreas, in 0.9% sodium chloride, from Sigma Aldrich]. All inhibitors were purified (>95% purity at 254 nm) by reversed-phase preparative or semi-preparative HPLC. Stock solutions of inhibitors and substrate were obtained by dissolution in DMSO and addition of HDAC assay buffer to afford solutions containing 1.7 % v/v DMSO.

Serial dilution using HDAC buffer contacting 1.7 % v/v DMSO was used to obtain all requisite inhibitors and substrate solutions.

5.5 References

1. Hill, R. R.; Rychnovsky, S. D., Generation, Stability, and Utility of Lithium 4,4′-Di-Tert-Butylbiphenylide (Lidbb). *The Journal of Organic Chemistry* **2016,** *81* (22), 10707-10714.

2. Meyers, A. I.; Dickman, D. A.; Bailey, T. R., Asymmetric Synthesis of 2-Alkyl Pyrrolidines and Piperidines. Synthesis of (+)-Metazocine. *Journal of the American Chemical Society* **1985,** *107* (26), 7974-7978.

3. Arpin, A.; Manthorpe, J. M.; Gleason, J. L., A Practical Chiral Bicyclic Thioglycolate Lactam Auxiliary for Stereoselective Quaternary Carbon Formation. *Organic Letters* **2006,** *8* (7), 1359-1362.

4. Bieszczad, B.; Barbasiewicz, M., The Key Role of the Nonchelating Conformation of the Benzylidene Ligand on the Formation and Initiation of Hoveyda–Grubbs Metathesis Catalysts. *Chemistry – A European Journal* **2015,** *21* (29), 10322-10325.

5. Gingrich, D. E.; Lisko, J. G.; Curry, M. A.; Cheng, M.; Quail, M.; Lu, L.; Wan, W.; Albom, M. S.; Angeles, T. S.; Aimone, L. D.; Haltiwanger, R. C.; Wells-Knecht, K.; Ott, G. R.; Ghose, A. K.; Ator, M. A.; Ruggeri, B.; Dorsey, B. D., Discovery of an Orally Efficacious Inhibitor of Anaplastic Lymphoma Kinase. *Journal of Medicinal Chemistry* **2012,** *55* (10), 4580-4593.

6. Dowd, P.; Weber, W., Preparation and Diels-Alder Reaction of (1e)-1,3-Dimethoxybutadiene. *The Journal of Organic Chemistry* **1982,** *47* (24), 4774-4777.

7. Singh, A. K.; Khade, P. K., 7-Methoxy-3-Nitro-2-Naphthalenemethanol—a New Phototrigger for Caging Applications. *Tetrahedron Letters* **2011,** *52* (38), 4899-4902.

8. Tolbert, L. M.; Haubrich, J. E., Photoexcited Proton Transfer from Enhanced Photoacids. *Journal of the American Chemical Society* **1994,** *116* (23), 10593-10600.

9. Williams, F. J.; Relles, H. M.; Manello, J. S.; Donahue, P. E., Reactions of Phenoxides with Nitro-Substituted Phthalate Esters. *The Journal of Organic Chemistry* **1977,** *42* (21), 3419-3425.

10. Su, C.; Ye, Y.; Xu, L.; Zhang, C., Synthesis and Properties of Novel Sulfide-Containing Aniline Copolymers as a Cathode Material for Li-Ion Batteries. *Macromolecular Chemistry and Physics* **2011,** *212* (22), 2487-2492.

11. Heiszman, J.; Bitter, I.; Harsányi, K.; Töke, L., A Facile Synthesis of Dialkyl Cyclopropane-1,1-Dicarboxylates and Alkyl 1-Cyanocyclopropanecarboxylates by Phase-Transfer Alkylation. *Synthesis* **1987,** (08), 738-739.

12. White, D. A., Alkylations with Potassium Carbonate in Dimethylformamide. *Synthetic Communications* **1977,** *7* (8), 559-568.

13. Donnelly, J. A.; Keegan, J. R., Cyclopropyloxetanes - Reactions of 5-Oxaspiro[2.3]Hexane with Hydrogen Halides. *Monatshefte Fur Chemie* **1982,** *113* (2), 209-212.

14. Velcicky, J.; Bodendorf, U.; Rigollier, P.; Epple, R.; Beisner, D. R.; Guerini, D.; Smith, P.; Liu, B.; Feifel, R.; Wipfli, P.; Aichholz, R.; Couttet, P.; Dix, I.; Widmer, T.; Wen, B.; Brandl, T., Discovery of the First Potent, Selective, and Orally Bioavailable Signal Peptide Peptidase-Like 2a (Sppl2a) Inhibitor Displaying Pronounced Immunomodulatory Effects in Vivo. *Journal of Medicinal Chemistry* **2018,** *61* (3), 865-880.

15. Wade, P. A.; Kondracki, P. A., Thermolytic Rearrangements of 1,1-Cyclopropanedimethanol Disulfonates: Cyclopropylcarbinyl Cations Revisited. *The Journal of Organic Chemistry* **1993,** *58* (11), 3140-3147.

16. Hoover, J. M.; Stahl, S. S., Highly Practical Copper(I)/Tempo Catalyst System for Chemoselective Aerobic Oxidation of Primary Alcohols. *Journal of the American Chemical Society* **2011,** *133* (42), 16901-16910.

17. Szymańska, E.; Frydenvang, K.; Contreras-Sanz, A.; Pickering, D. S.; Frola, E.; Serafimoska, Z.; Nielsen, B.; Kastrup, J. S.; Johansen, T. N., A New Phenylalanine Derivative Acts as an Antagonist at the Ampa Receptor Glua2 and Introduces Partial Domain Closure: Synthesis, Resolution, Pharmacology, and Crystal Structure. *Journal of Medicinal Chemistry* **2011,** *54* (20), 7289-7298.

18. Vuoti, S.; Autio, J.; Laitila, M.; Haukka, M.; Pursiainen, J., Palladium-Catalyzed Suzuki–Miyaura Cross-Coupling of Various Aryl Halides Using Ortho-Alkyl-Substituted Arylphosphanes and (Ortho-Alkylphenyl)Alkylphosphanes under Microwave Heating. *European Journal of Inorganic Chemistry* **2008,** (3), 397-407.

19. Cooper, S. P.; Booker-Milburn, K. I., A Palladium(Ii)-Catalyzed C-H Activation Cascade Sequence for Polyheterocycle Formation. *Angewandte Chemie International Edition* **2015,** *54* (22), 6496-6500.

20. Tiong, E. A.; Rivalti, D.; Williams, B. M.; Gleason, J. L., A Concise Total Synthesis of (R)-Puraquinonic Acid. *Angewandte Chemie International Edition* **2013,** *52* (12), 3442-3445.

21. Becker, U.; Erkel, G.; Anke, T.; Sterner, O., Puraquinonic Acid, a Novel Inducer of Differentiation of Human Hl-60 Promyelocytic Leukemia Cells from Mycena Pura (Pers. Ex Fr.). *Natural Product Letters* **1997,** *9* (3), 229-236.

22. Melot, R.; Craveiro, M. V.; Bürgi, T.; Baudoin, O., Divergent Enantioselective Synthesis of (nor)Illudalane Sesquiterpenes Via Pd^0-Catalyzed Asymmetric $C(Sp^3)$–H Activation. *Organic Letters* **2019,** *21* (3), 812-815.

23. Misal Castro, L. C.; Li, H.; Sortais, J.-B.; Darcel, C., Selective Switchable Iron-Catalyzed Hydrosilylation of Carboxylic Acids. *Chemical Communications* **2012,** *48* (85), 10514-10516.

24. Barratt, B. J. W.; Easton, C. J.; Henry, D. J.; Li, I. H. W.; Radom, L.; Simpson, J. S., Inhibition of Peptidylglycine A-Amidating Monooxygenase by Exploitation of Factors Affecting the Stability and Ease of Formation of Glycyl Radicals. *Journal of the American Chemical Society* **2004,** *126* (41), 13306-13311.

25. Liu, Y.; Jia, G.; Ling, X.; Lan, N.; Zheng, Y.; Li, S.; Zhang, L.; Liu, L.; Zhang, R.; Xue, Y., Decomposition of Copper – Amino Acid Complexes by Oxalic Acid Dihydrate. *Canadian Journal of Chemistry* **2012,** *90* (6), 557-559.

26. Reddy, D. N.; Ballante, F.; Chuang, T.; Pirolli, A.; Marrocco, B.; Marshall, G. R., Design and Synthesis of Simplified Largazole Analogues as Isoform-Selective Human Lysine Deacetylase Inhibitors. *Journal of Medicinal Chemistry* **2016,** *59* (4), 1613-1633.

27. Madsen, A. S.; Olsen, C. A., Substrates for Efficient Fluorometric Screening Employing the Nad-Dependent Sirtuin 5 Lysine Deacylase (Kdac) Enzyme. *Journal of Medicinal Chemistry* **2012,** *55* (11), 5582-5590.

Appendix

^{1}H NMR (500 MHz, $CDCl_3$, ppm) for Compound 277

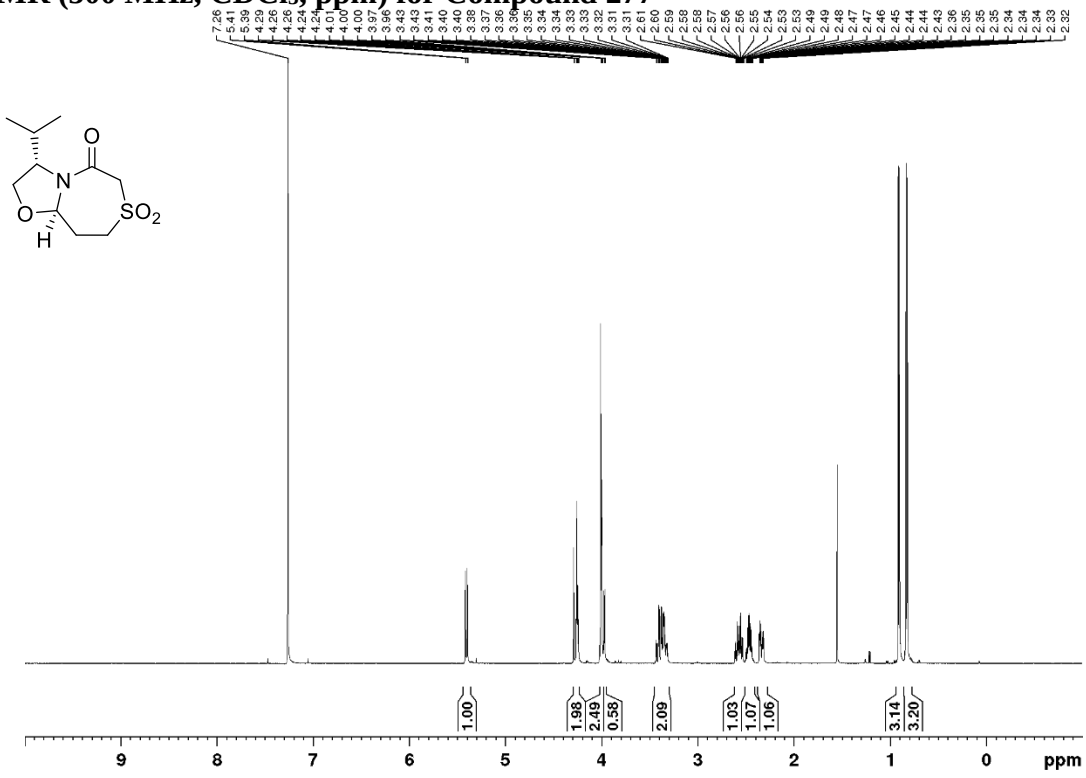

^{13}C NMR (126 MHz, $CDCl_3$, ppm) for Compound 277

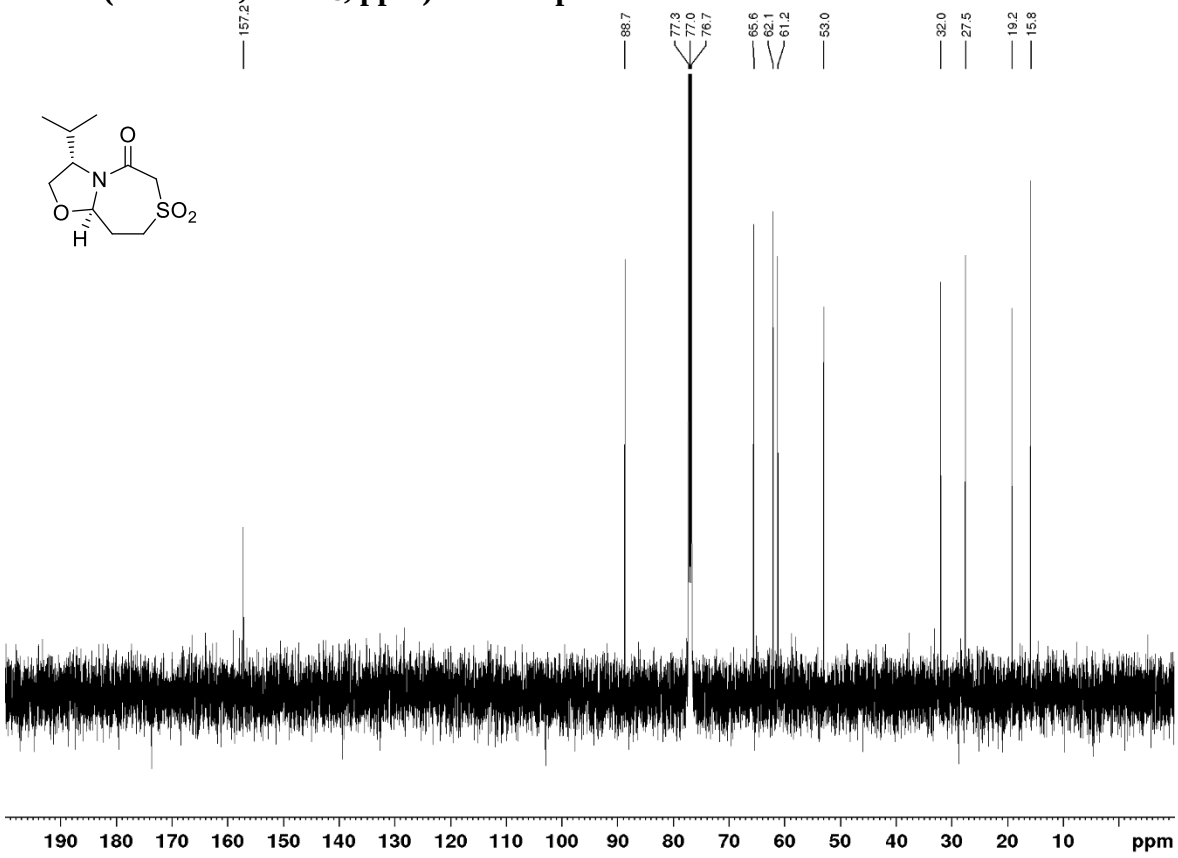

^{1}H NMR (500 MHz, DMSO-d_6, ppm) for Compound 277

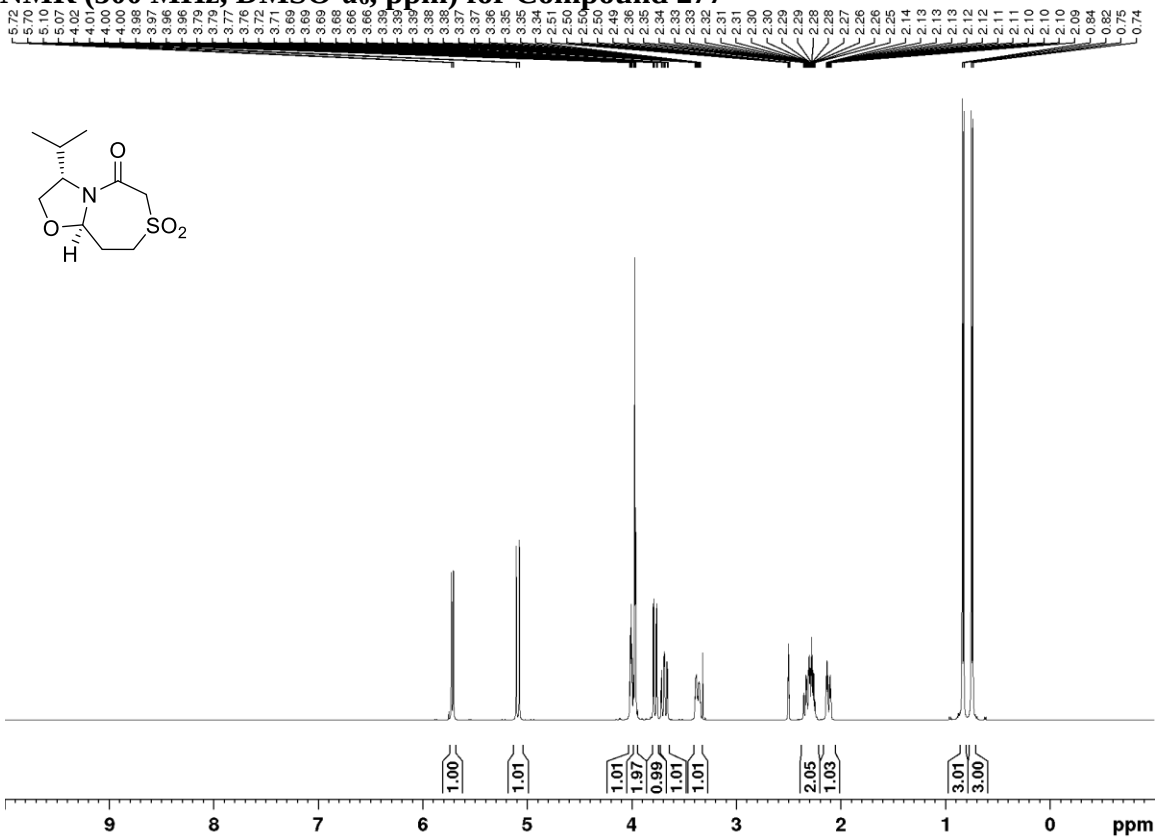

^{13}C NMR (126 MHz, DMSO-d_6, ppm) for Compound 277

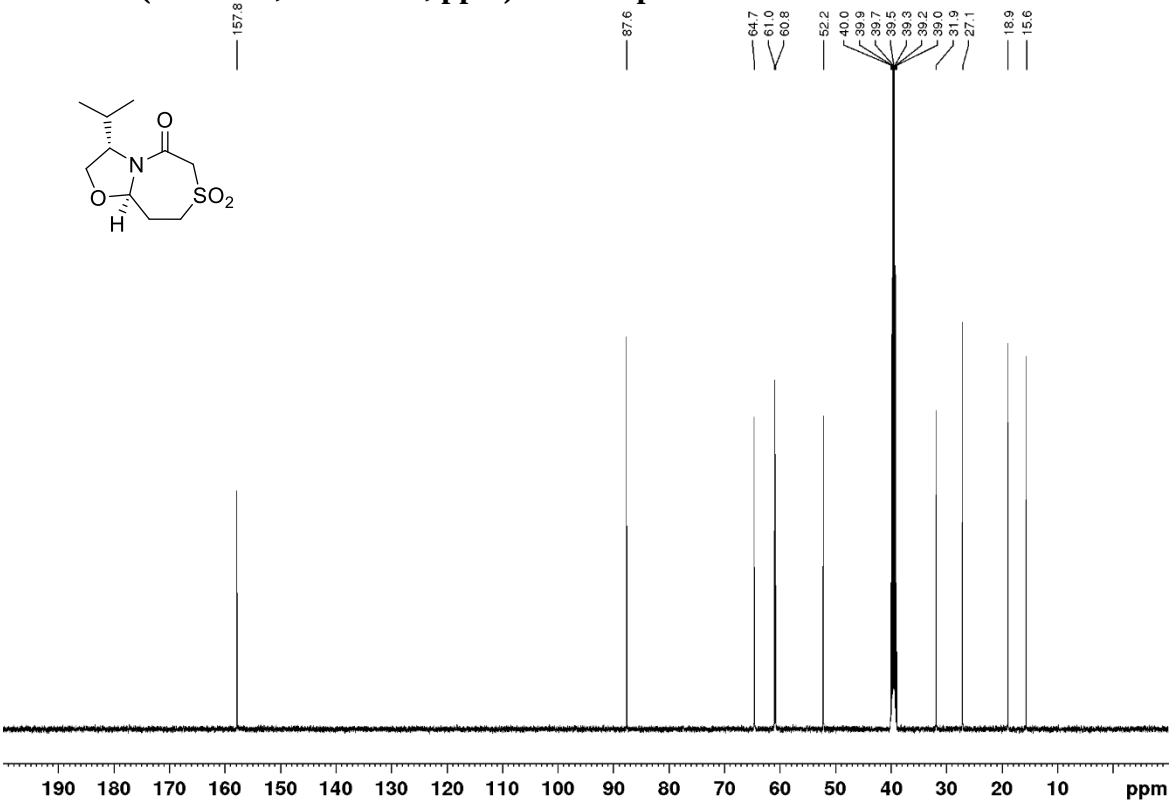

^{1}H NMR (500 MHz, $CDCl_3$, ppm) for Compound 271

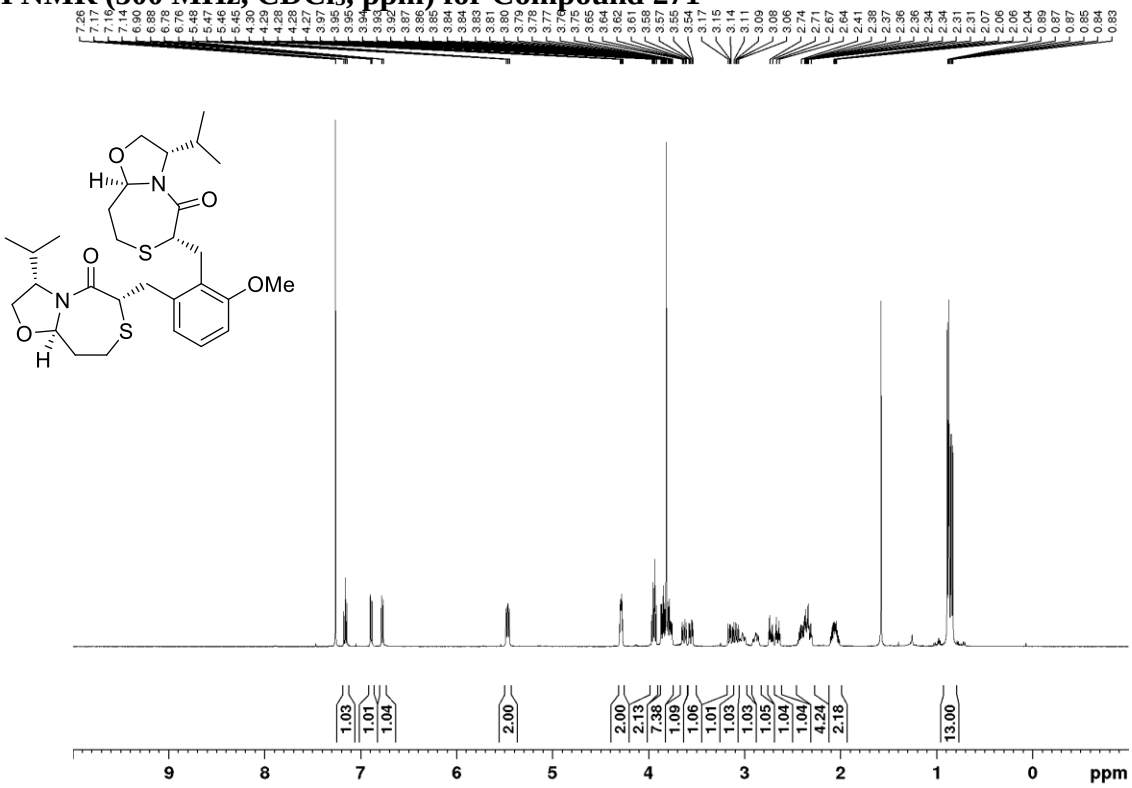

^{13}C NMR (126 MHz, $CDCl_3$, ppm) for Compound 271

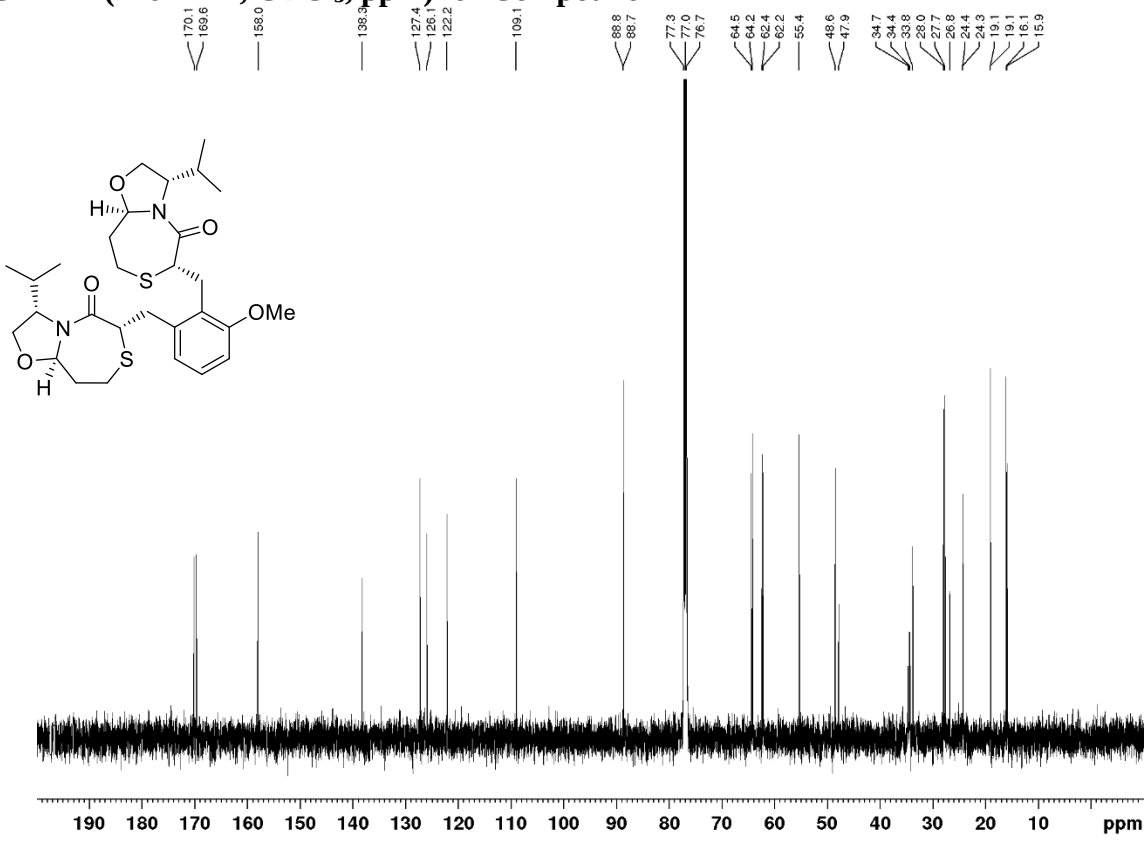

HSQC (500 MHz, $CDCl_3$, ppm) for Compound 271

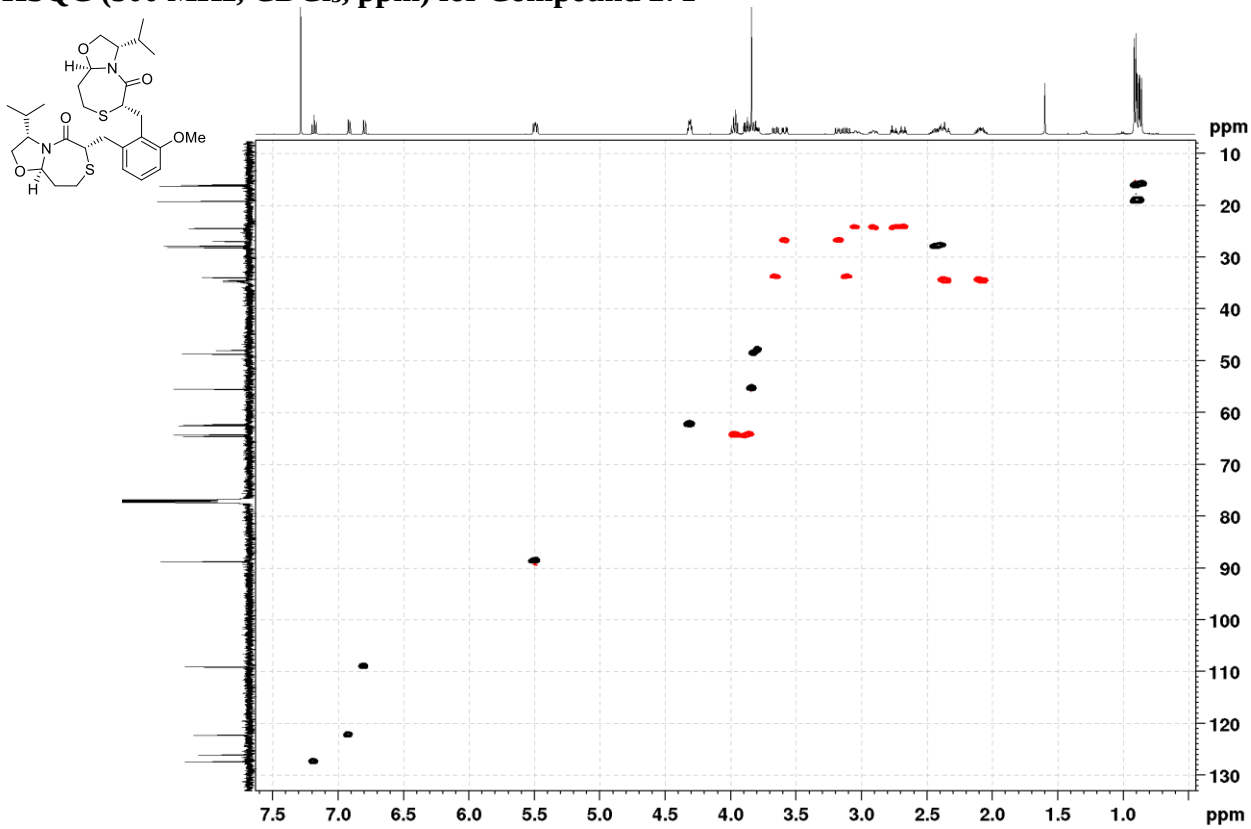

NOESY (500 MHz, $CDCl_3$, ppm) for Compound 271

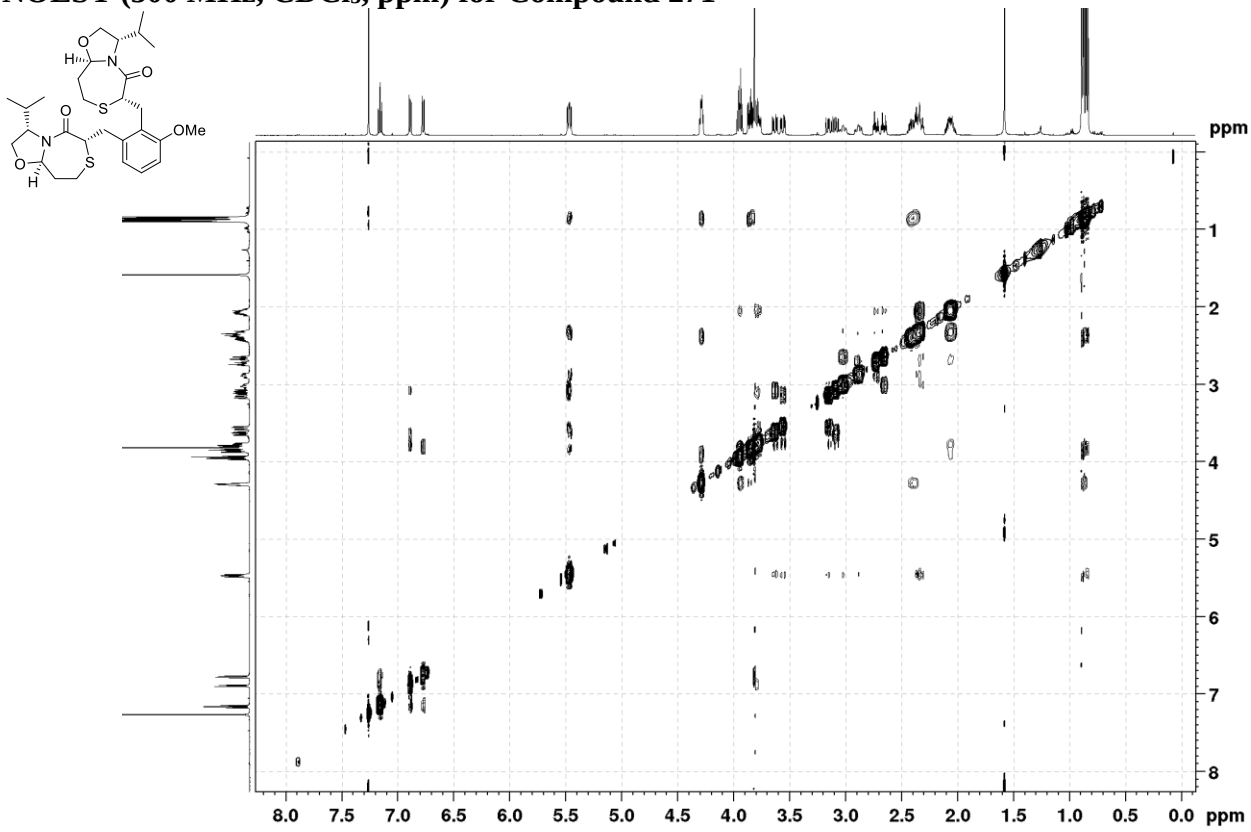

NOE (500 MHz, $CDCl_3$, ppm) for Compound 271

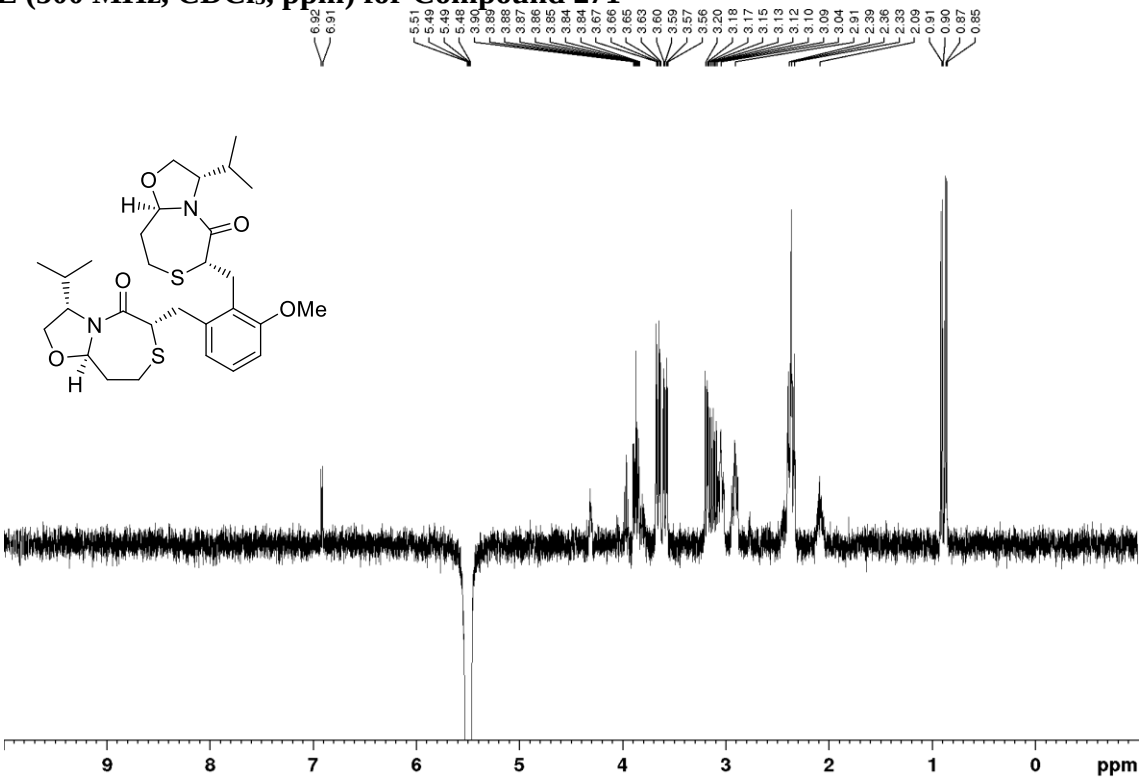

^{1}H NMR (500 MHz, $CDCl_3$, ppm) for Compound 310a

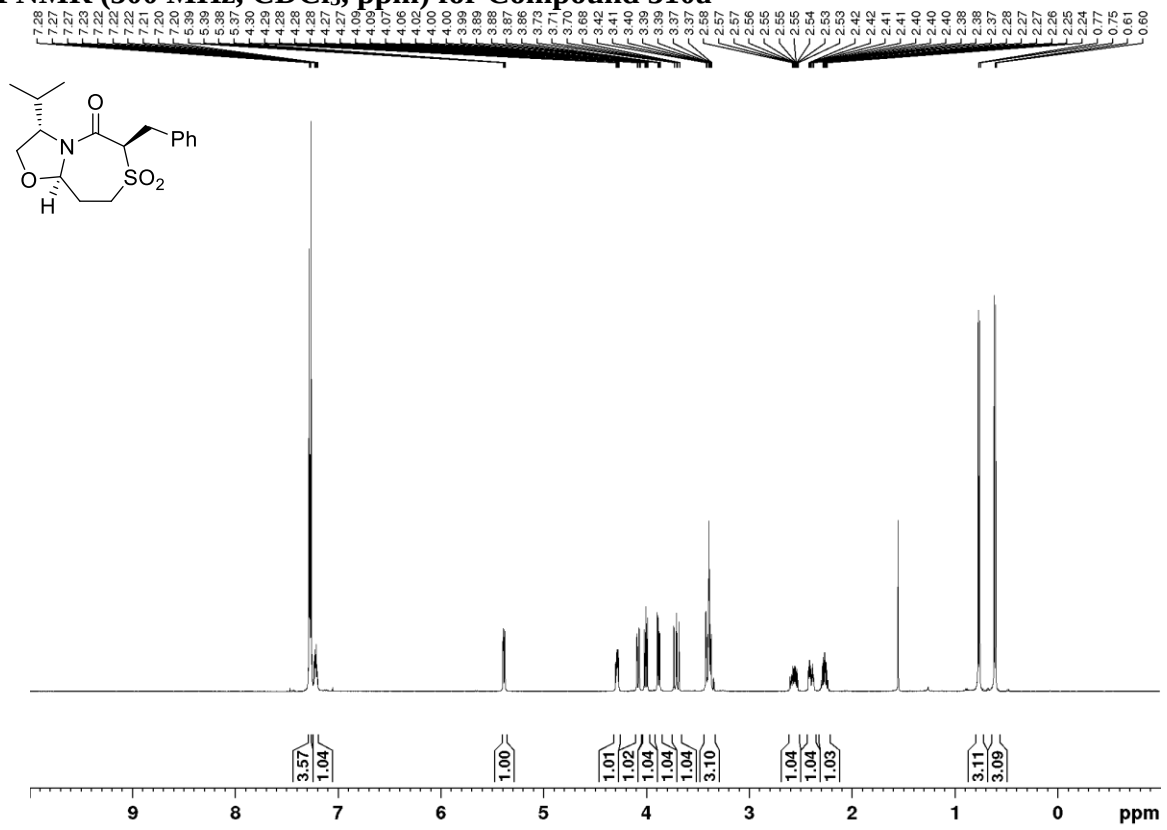

^{13}C NMR (126 MHz, $CDCl_3$, ppm) for Compound 310a

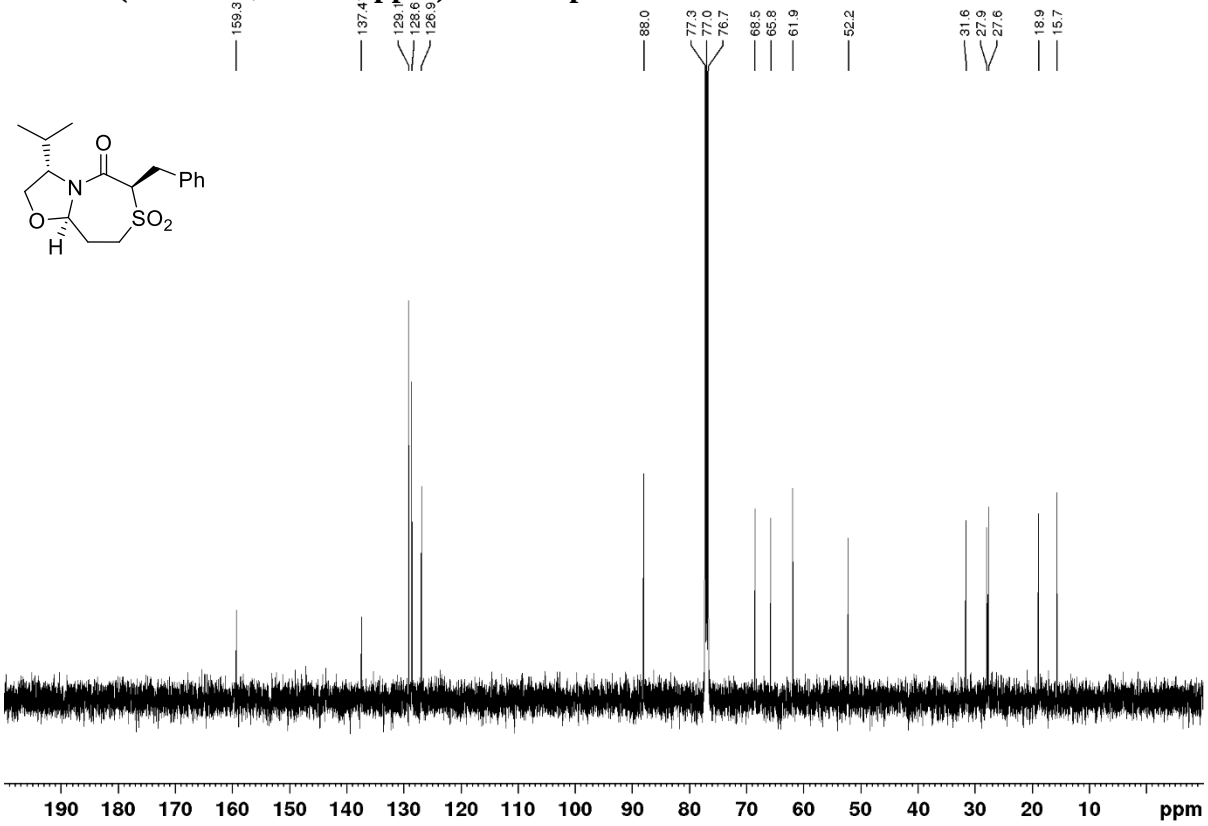

COSY (500 MHz, $CDCl_3$, ppm) for Compound 310a

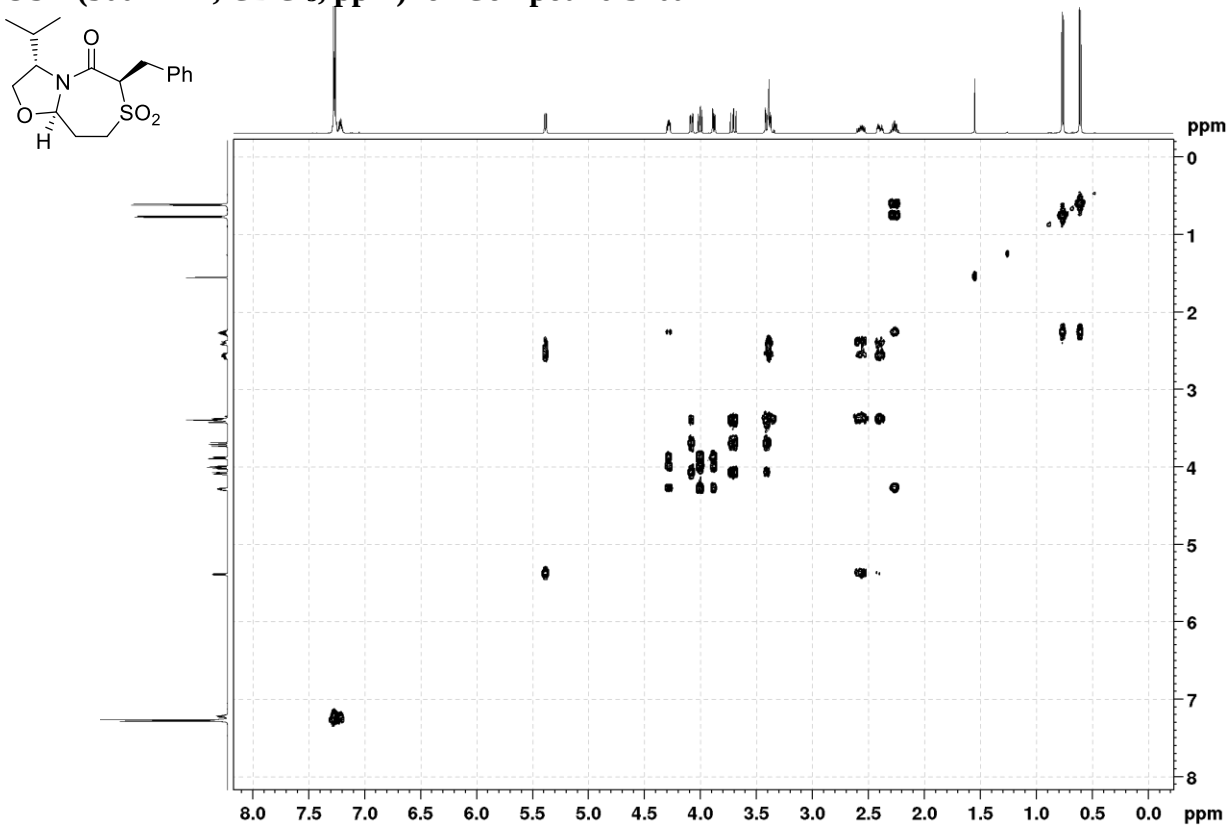

HSQC (500 MHz, $CDCl_3$, ppm) for Compound 310a

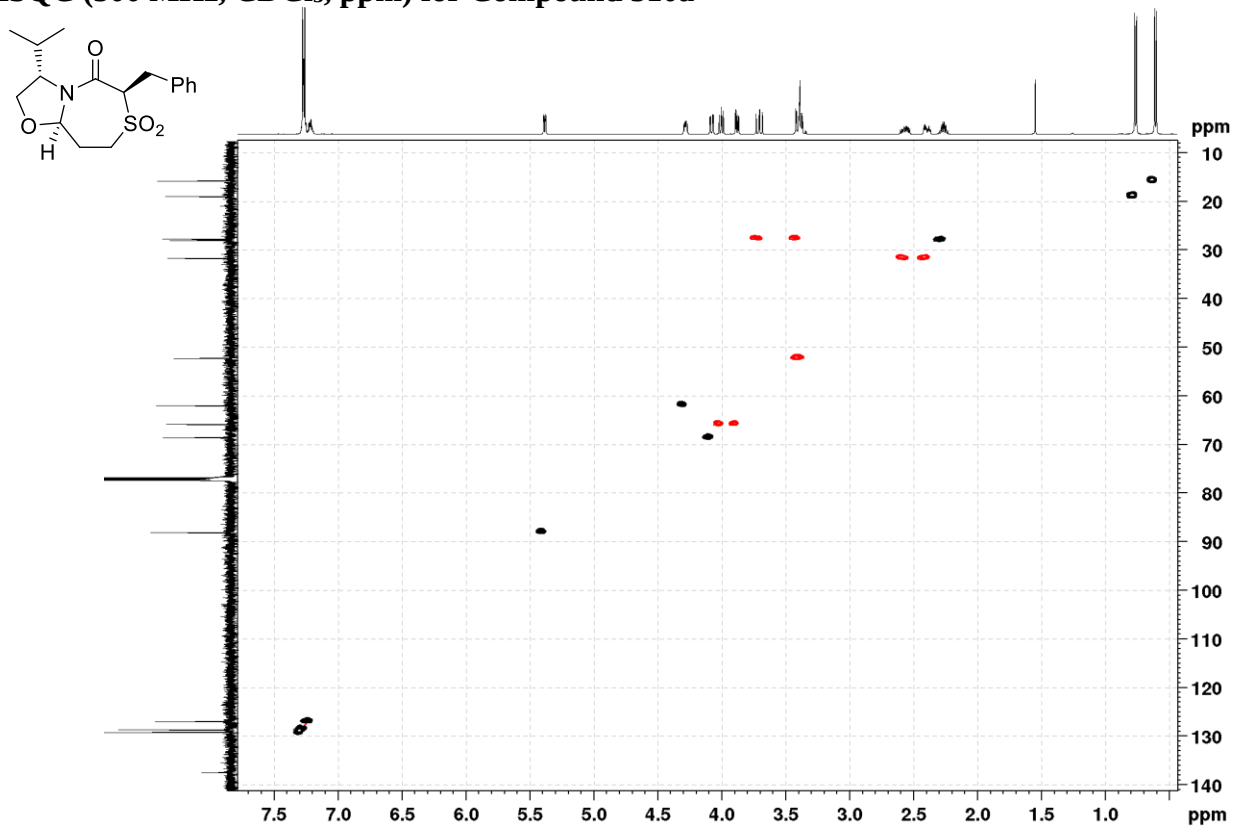

NOESY (500 MHz, $CDCl_3$, ppm) for Compound 310a

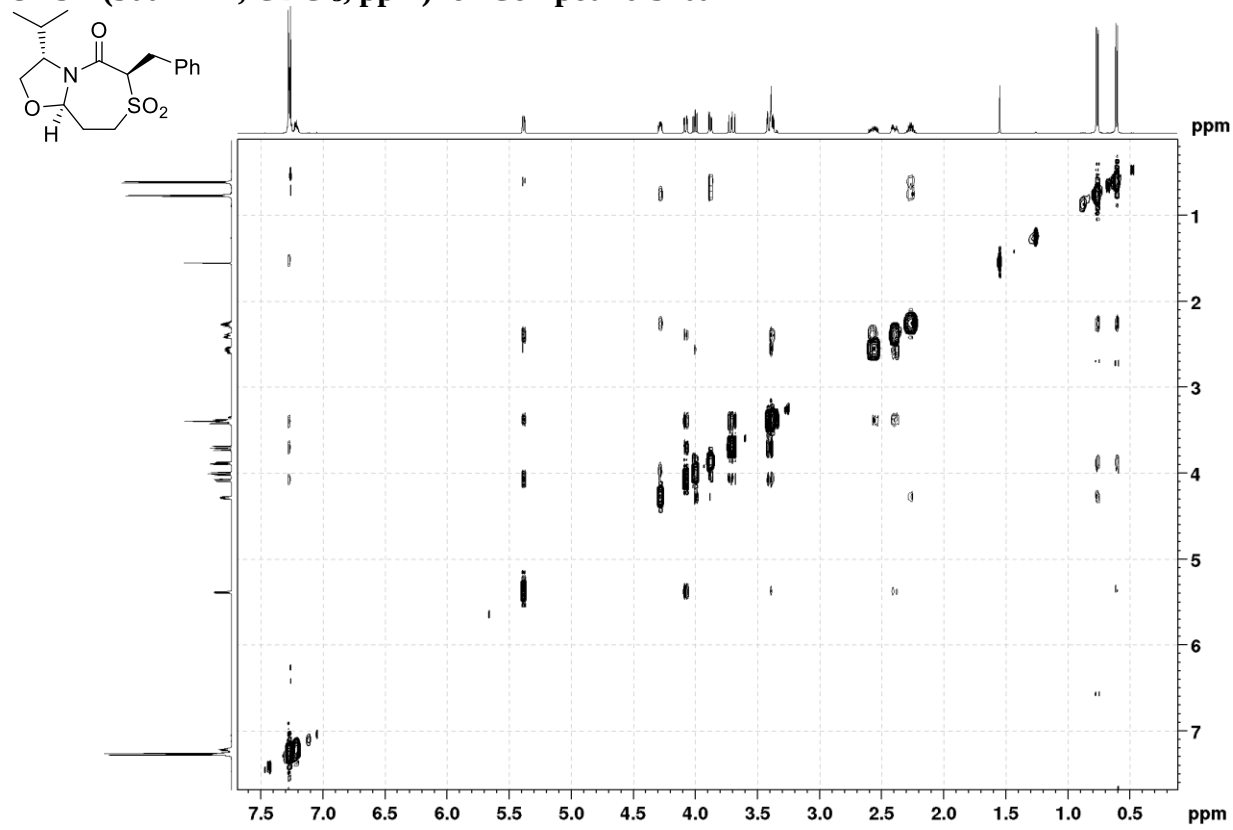

^{1}H NMR (500 MHz, $CDCl_3$, ppm) for Compound 310b

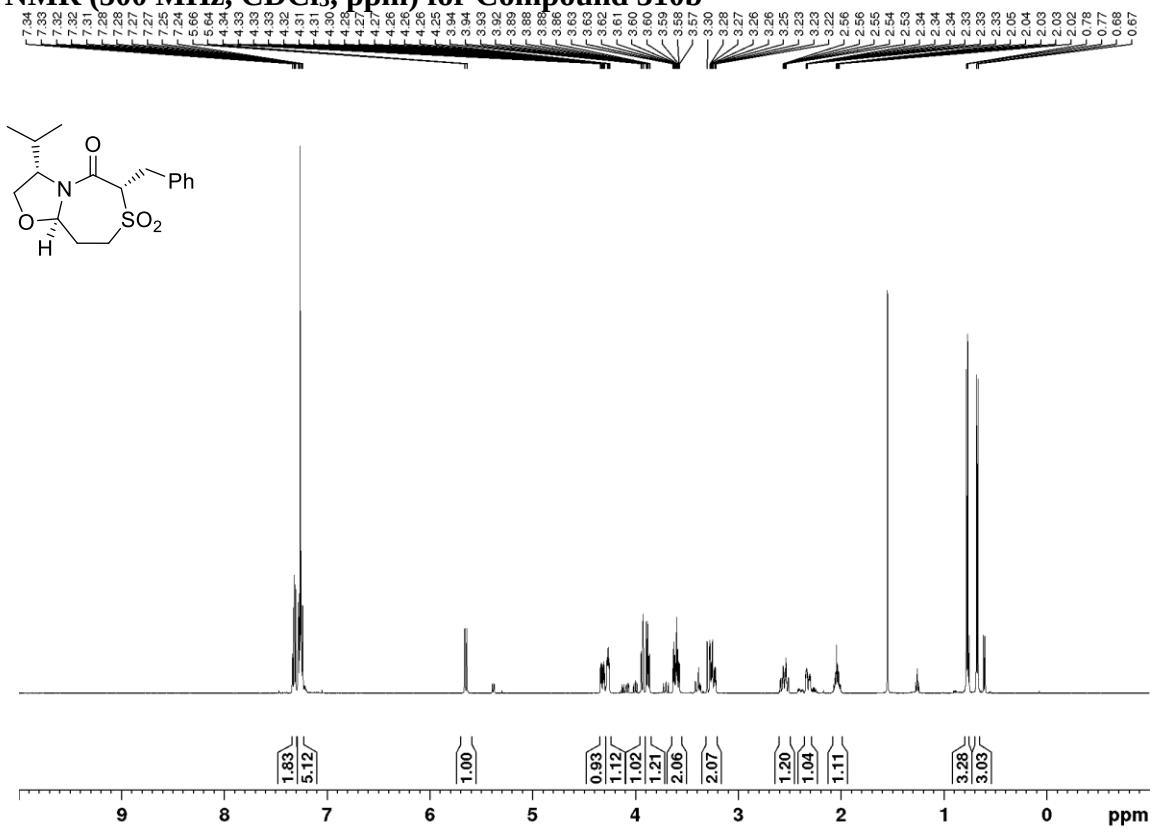

^{13}C NMR (126 MHz, $CDCl_3$, ppm) for Compound 310b

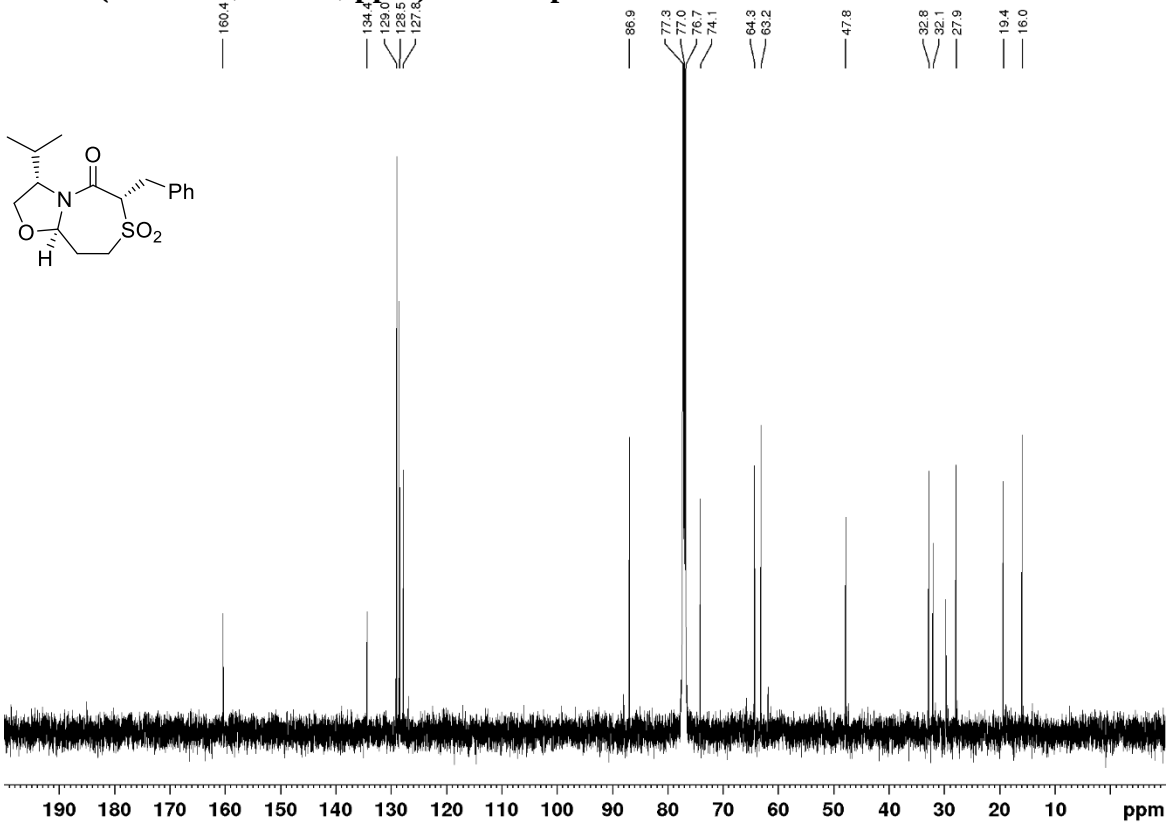

COSY (500 MHz, $CDCl_3$, ppm) for Compound 310b

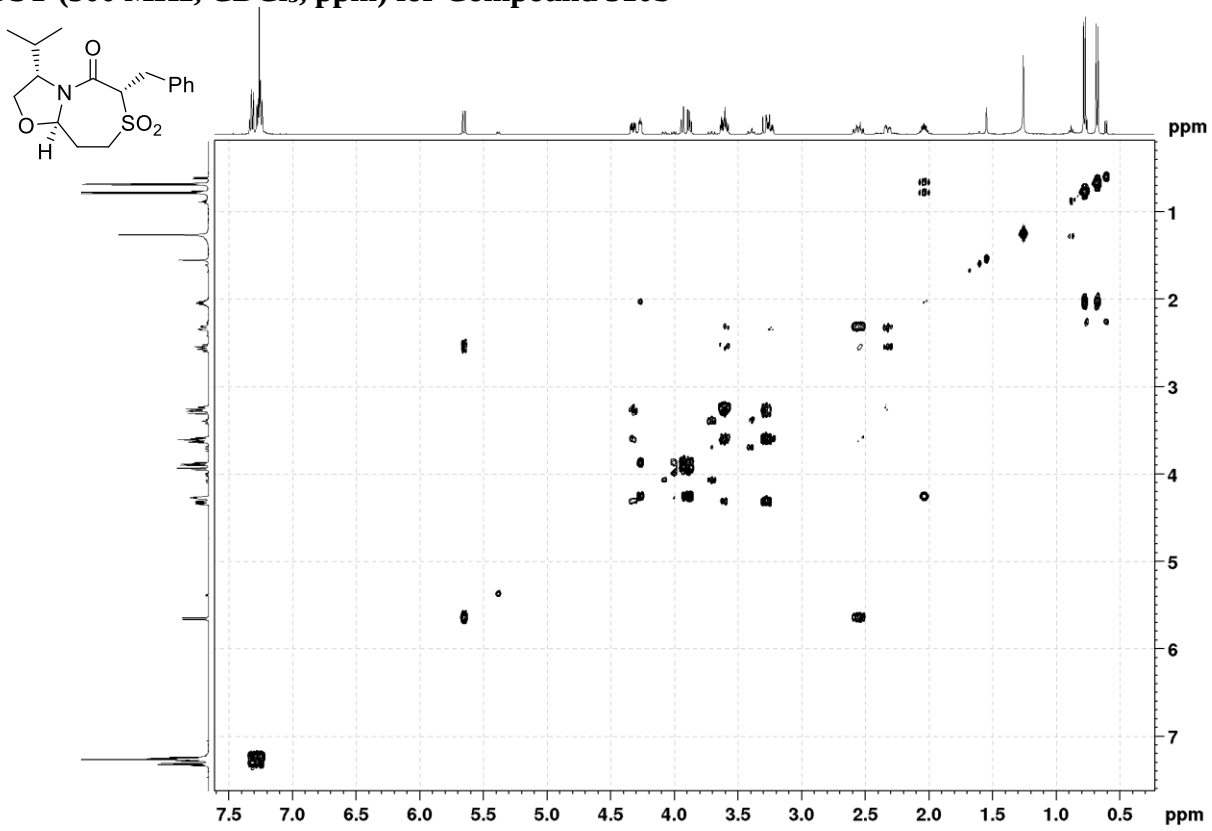

HSQC (500 MHz, $CDCl_3$, ppm) for Compound 310b

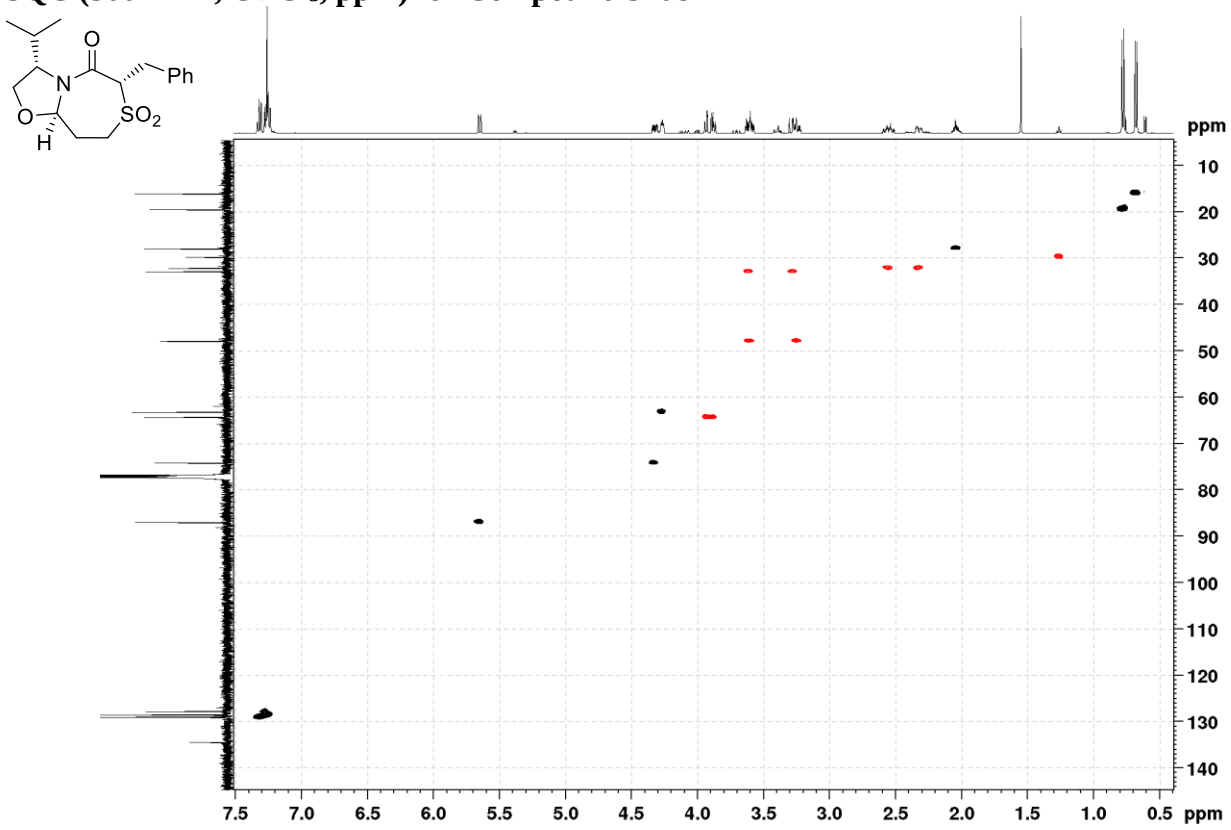

NOESY (500 MHz, $CDCl_3$, ppm) for Compound 310b

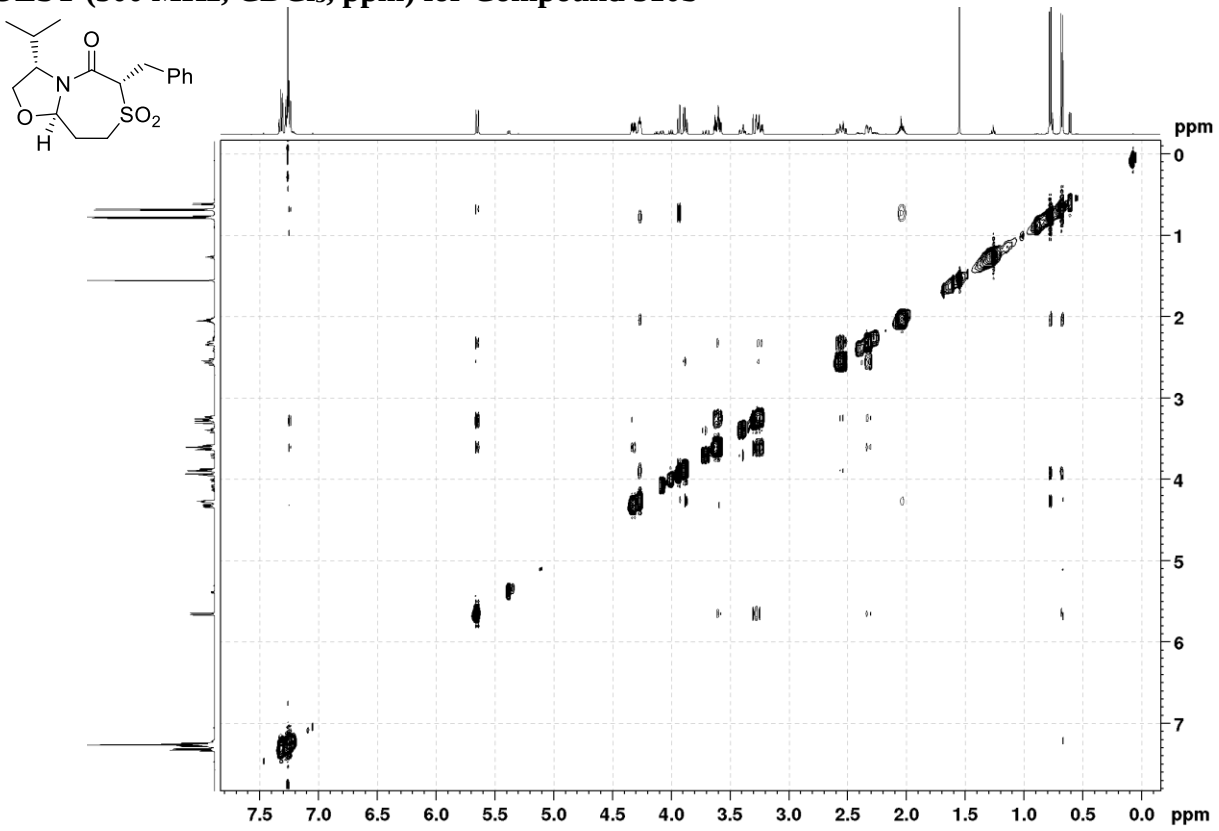

^{1}H NMR (500 MHz, $CDCl_3$, ppm) for Compound 311

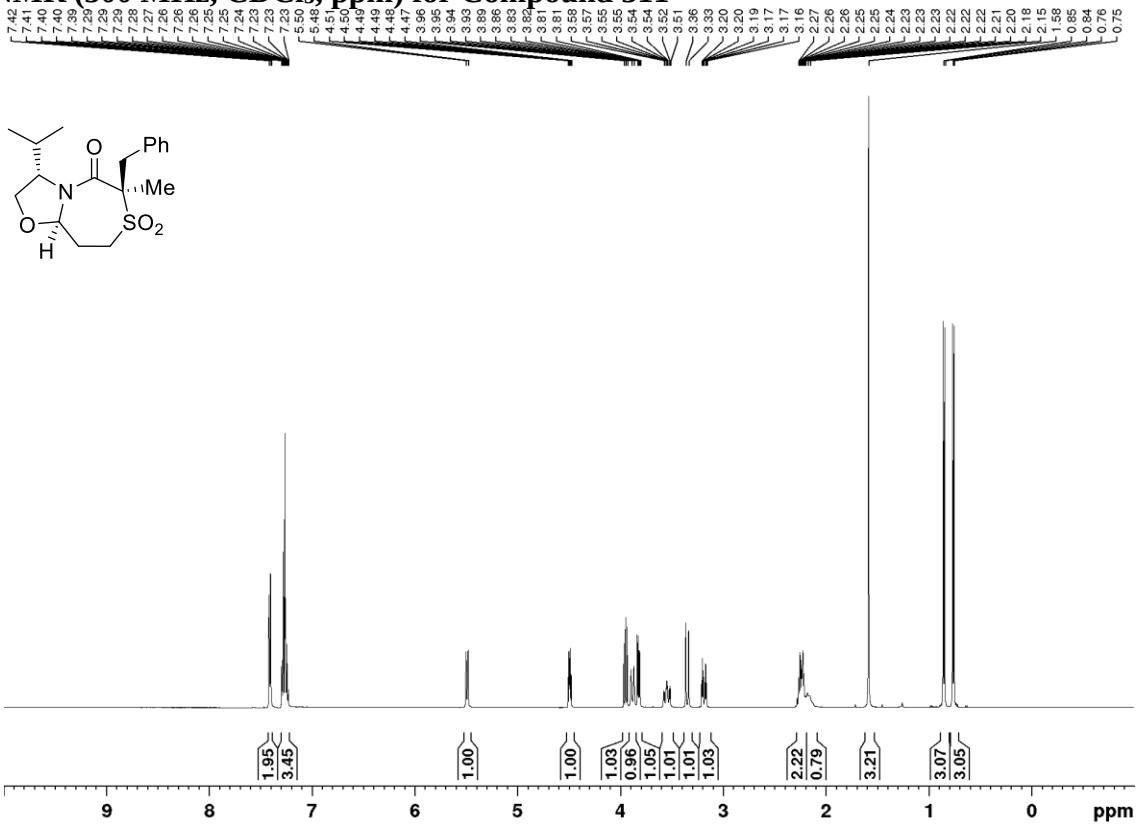

^{13}C NMR (126 MHz, $CDCl_3$, ppm) for Compound 311

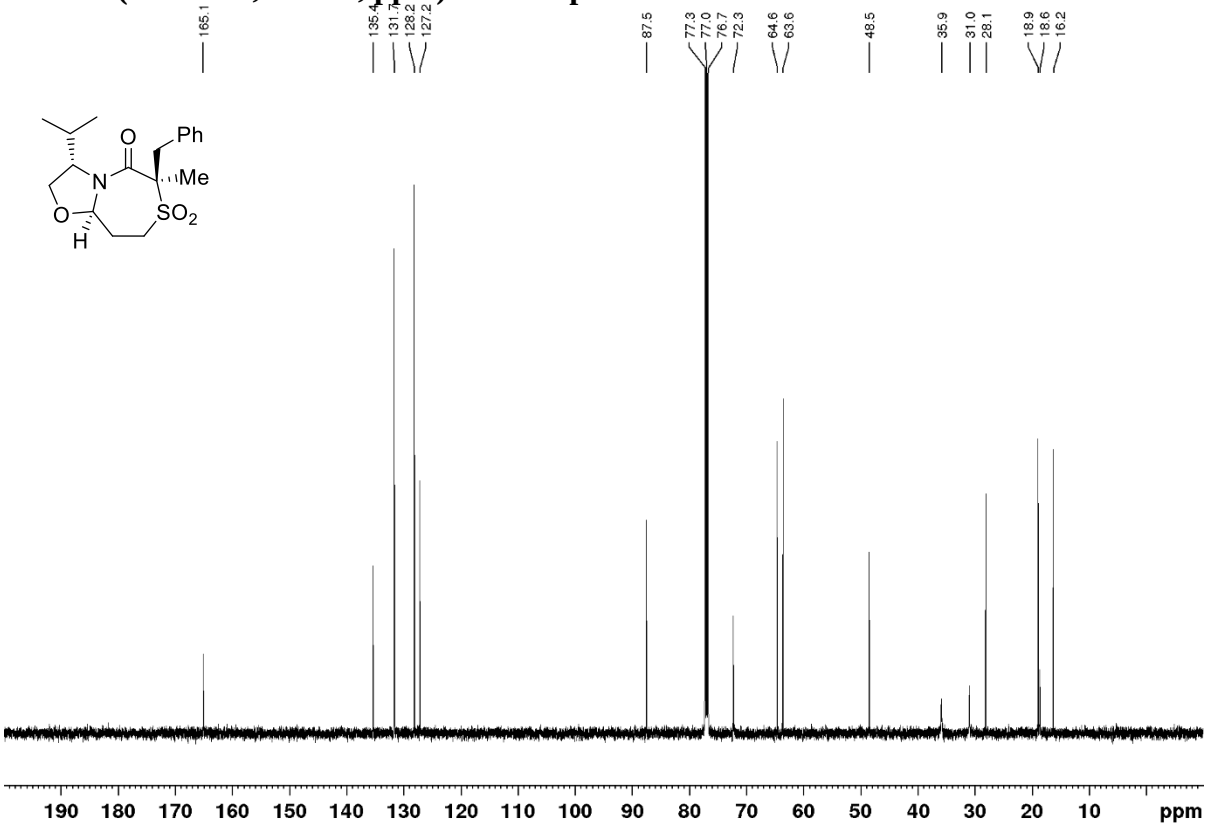

(500 MHz, $CDCl_3$, ppm) for Compound 311

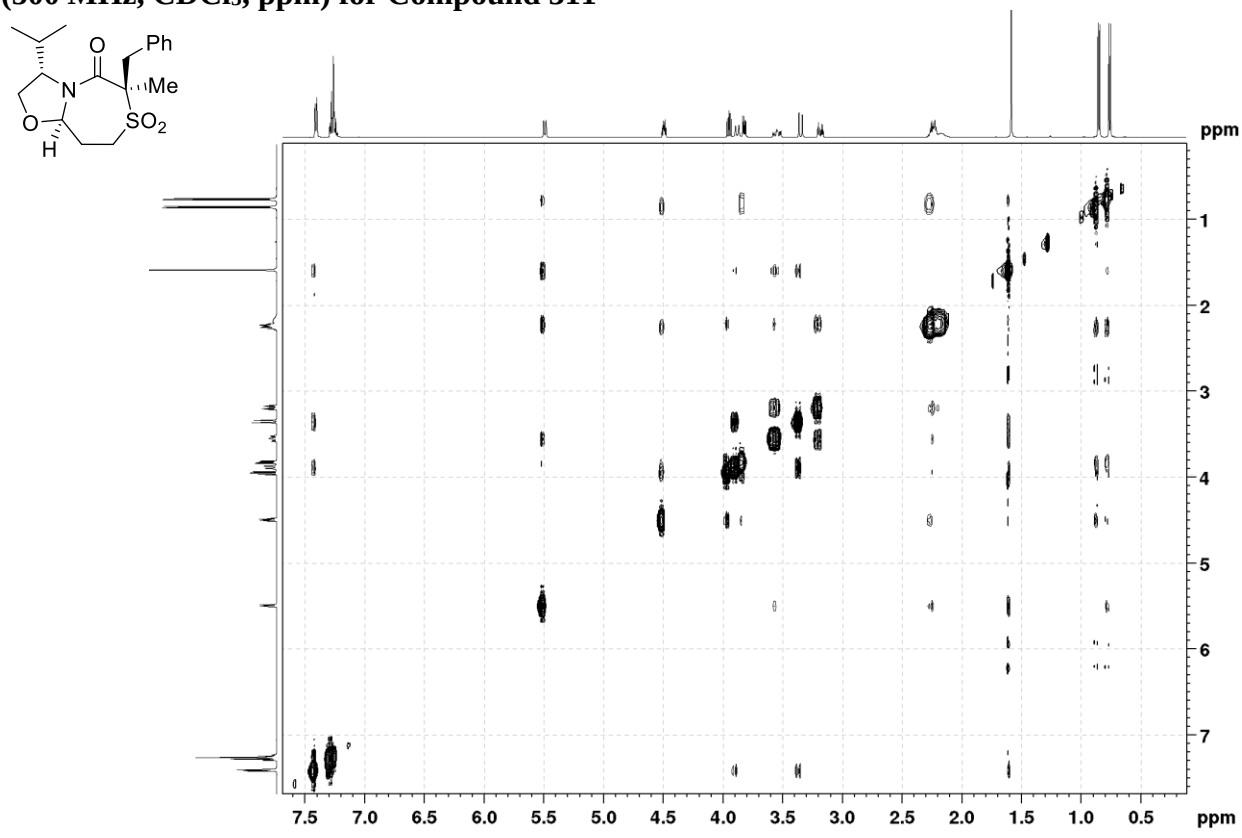

^{1}H NMR (500 MHz, $CDCl_3$, ppm) for Compound 317

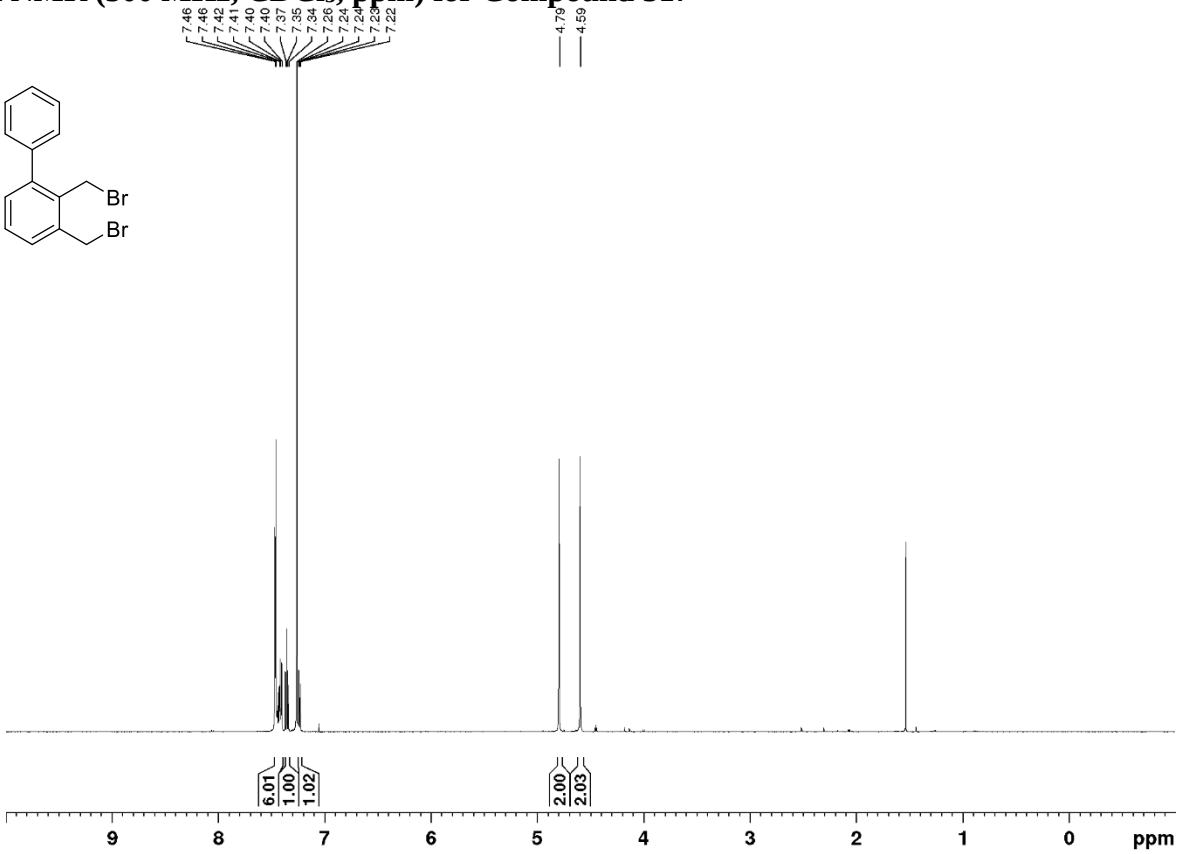

^{13}C NMR (126 MHz, $CDCl_3$, ppm) for Compound 317

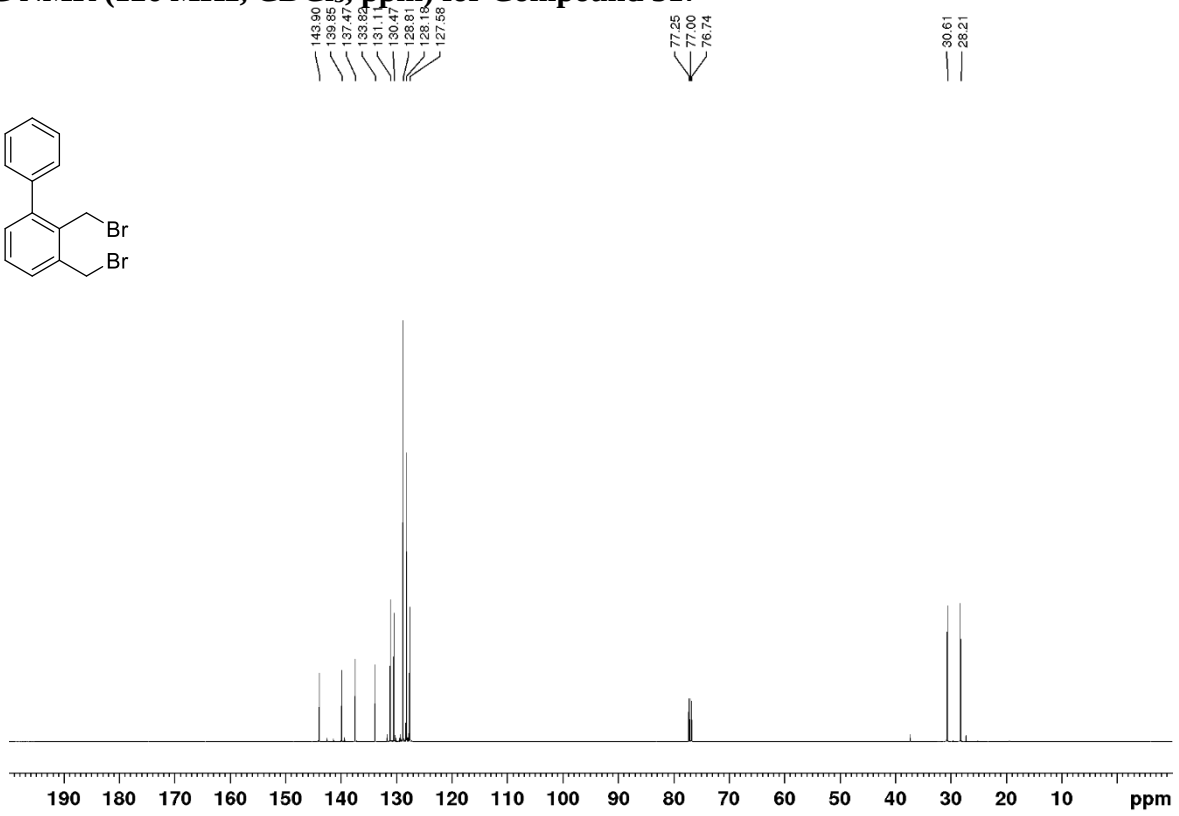

^{1}H NMR (500 MHz, $CDCl_3$, ppm) for Compound 342

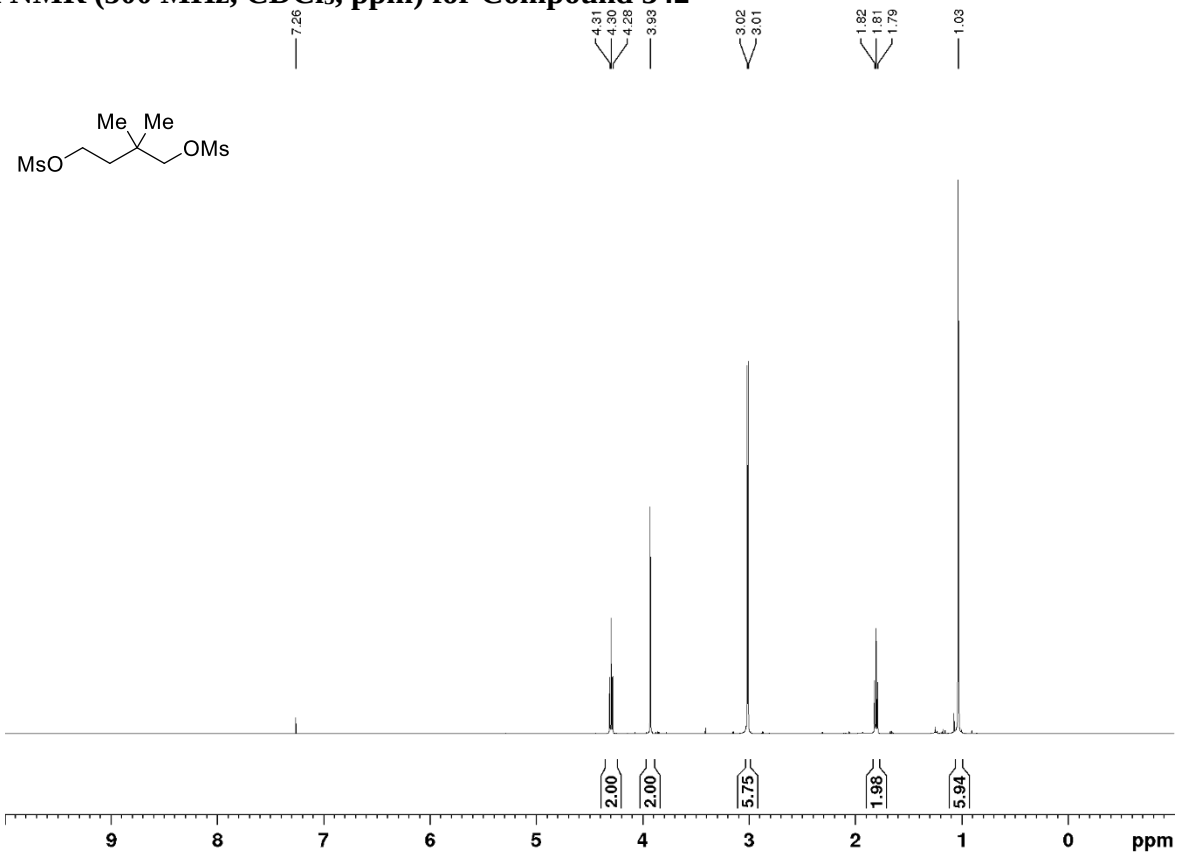

^{13}C NMR (126 MHz, $CDCl_3$, ppm) for Compound 342

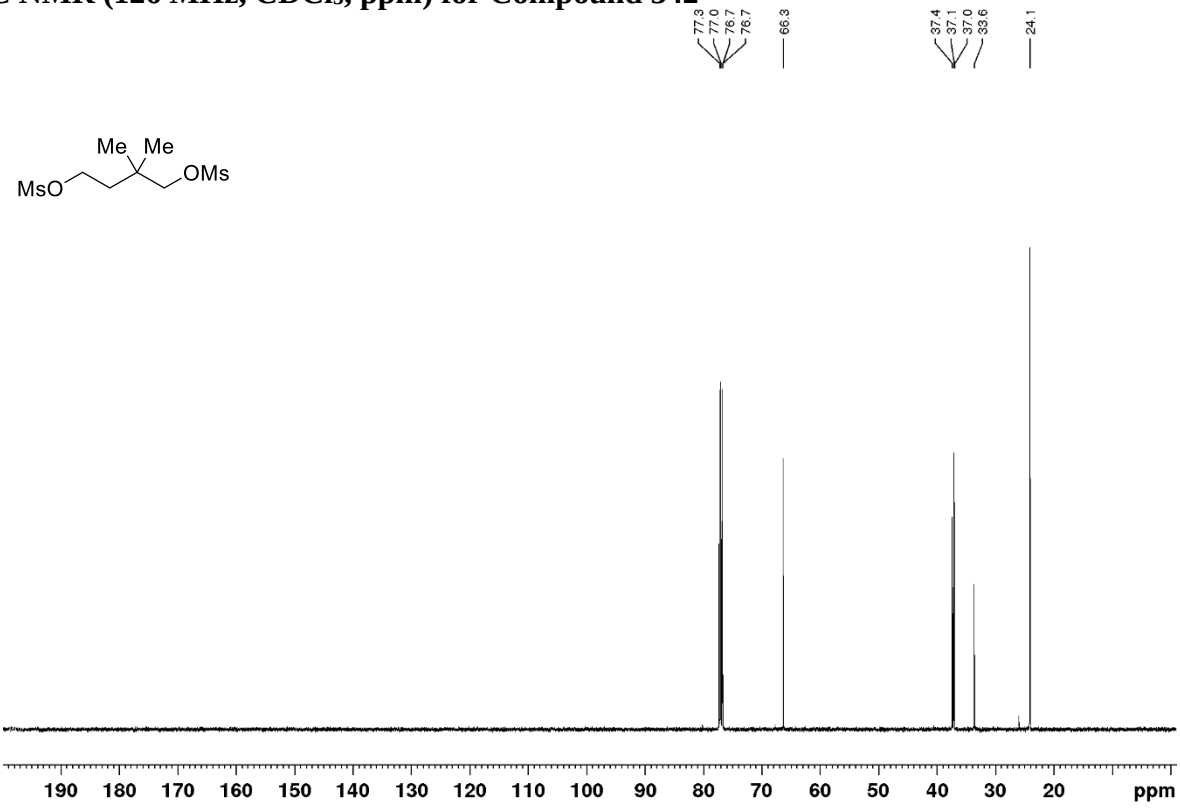

^{1}H NMR (500 MHz, $CDCl_3$, ppm) for Compound 287

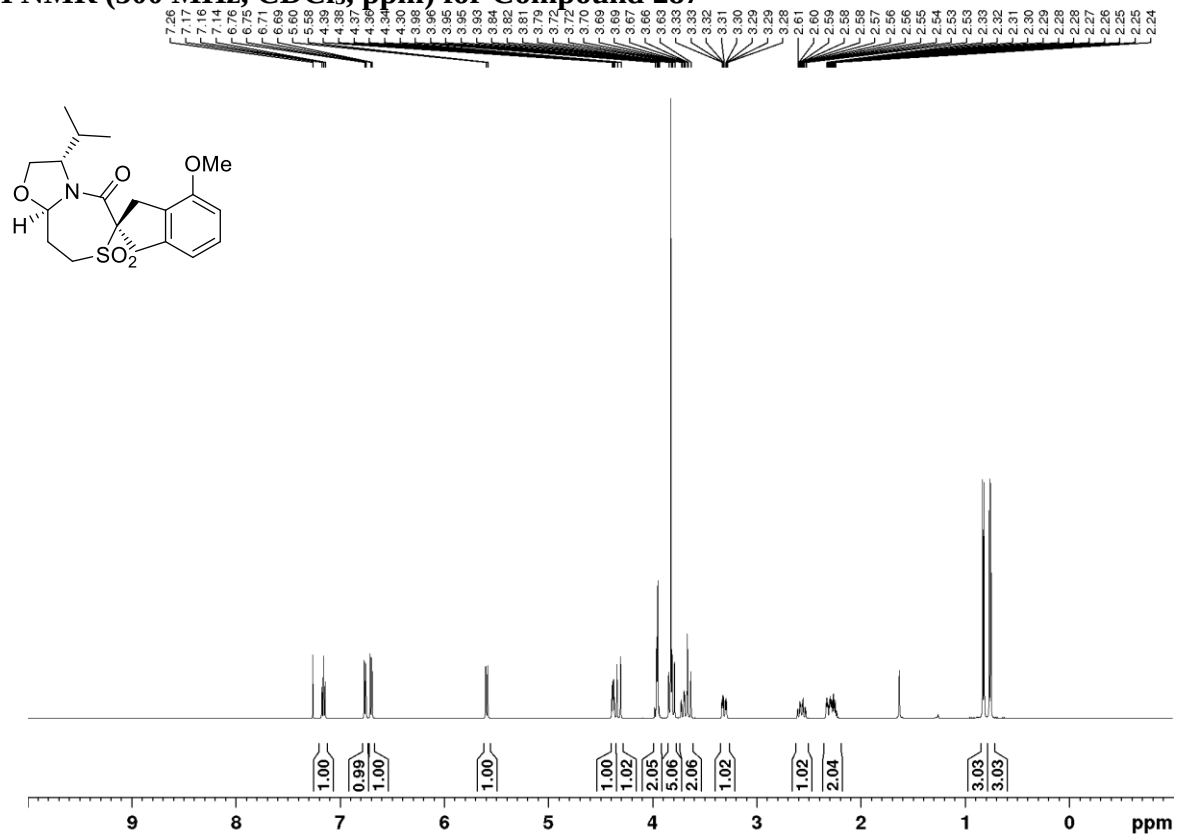

^{13}C NMR (126 MHz, $CDCl_3$, ppm) for Compound 287

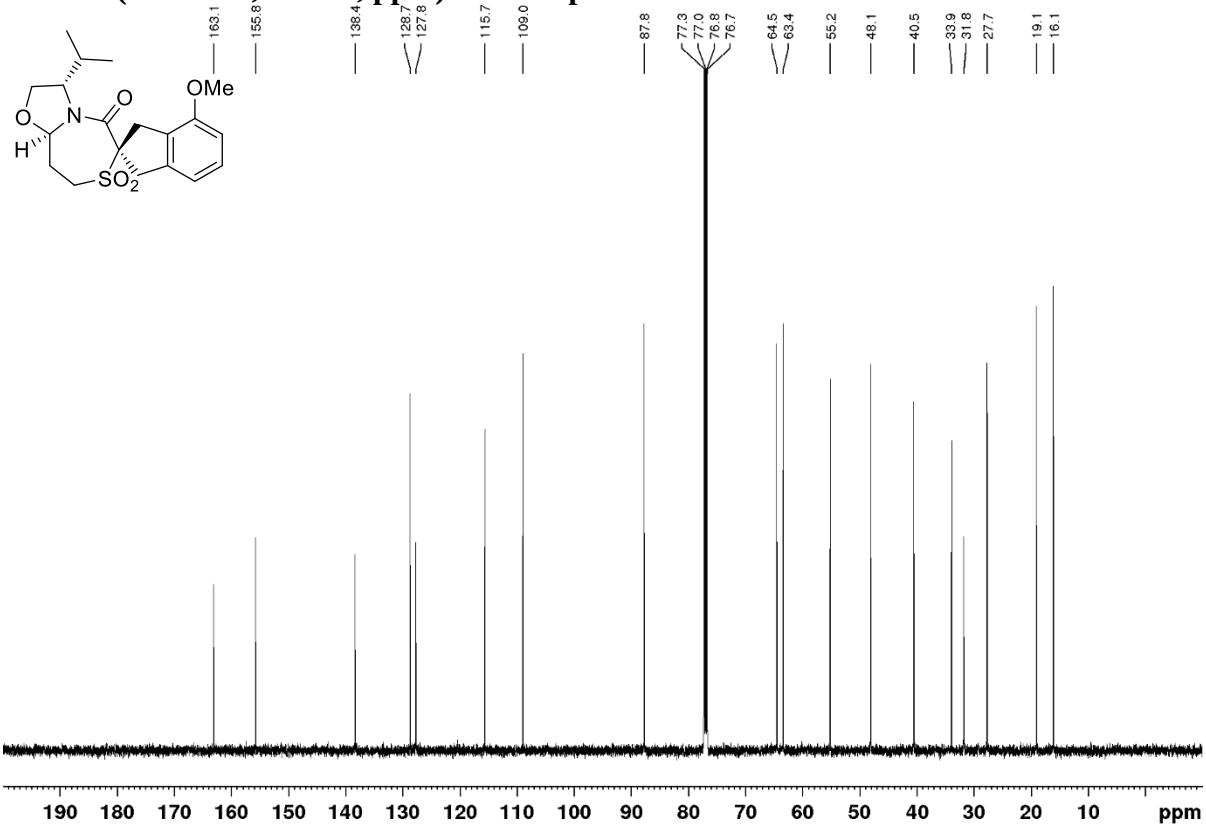

COSY (500 MHz, $CDCl_3$, ppm) for Compound 287

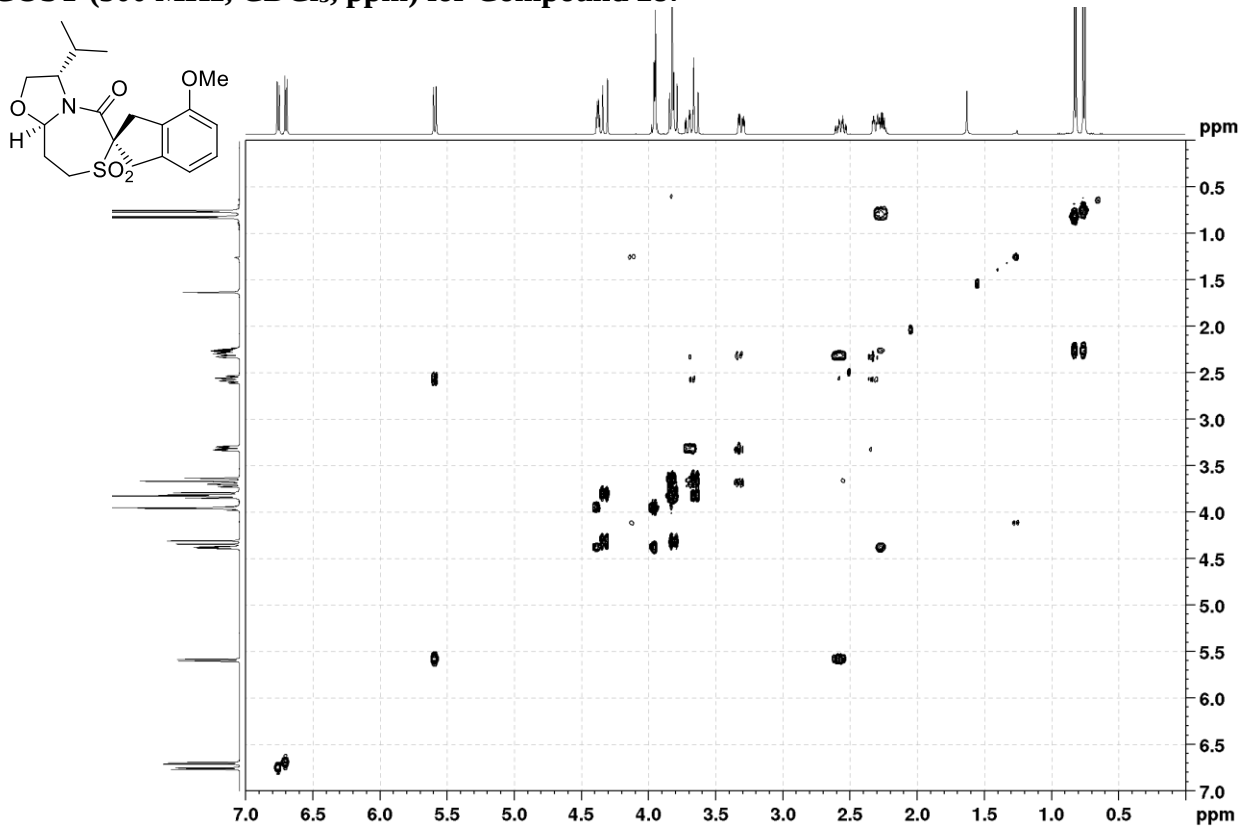

HSQC (500 MHz, $CDCl_3$, ppm) for Compound 287

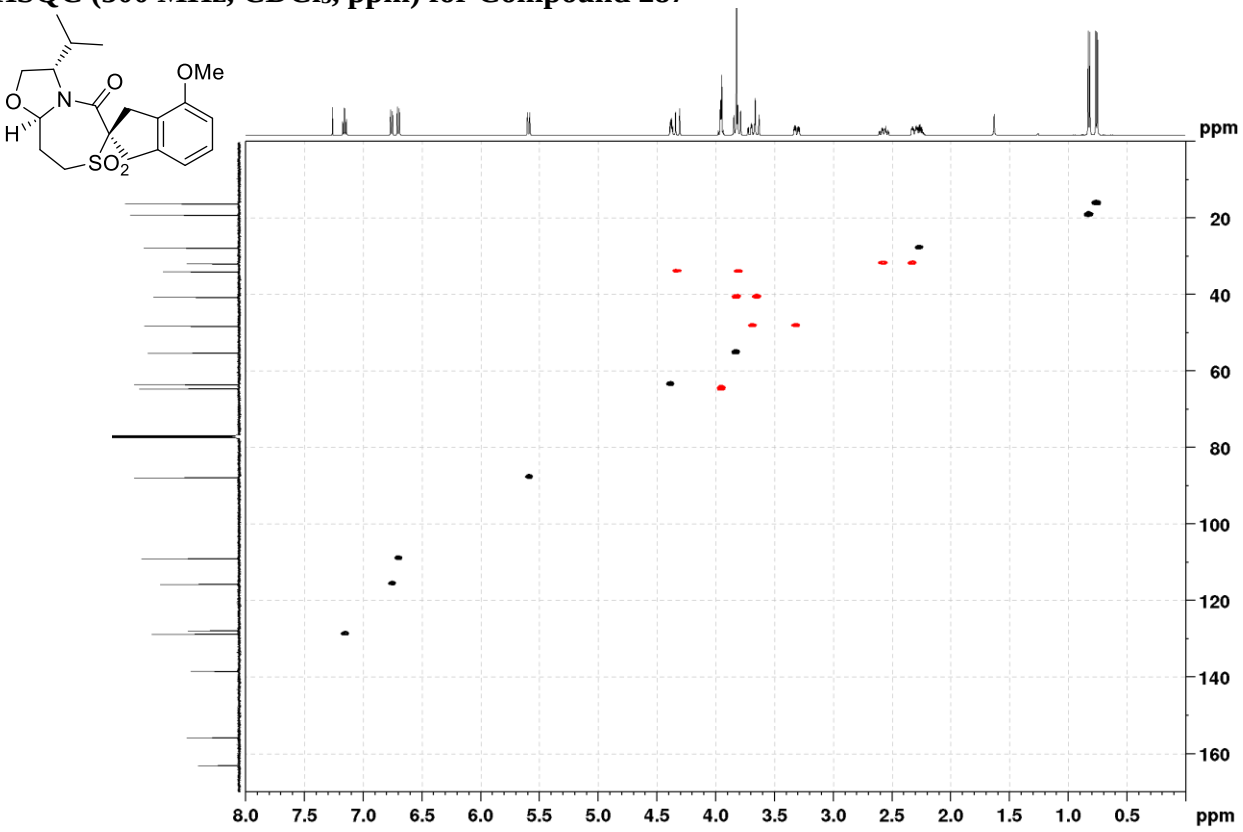

HMBC (500 MHz, $CDCl_3$, ppm) for Compound 287

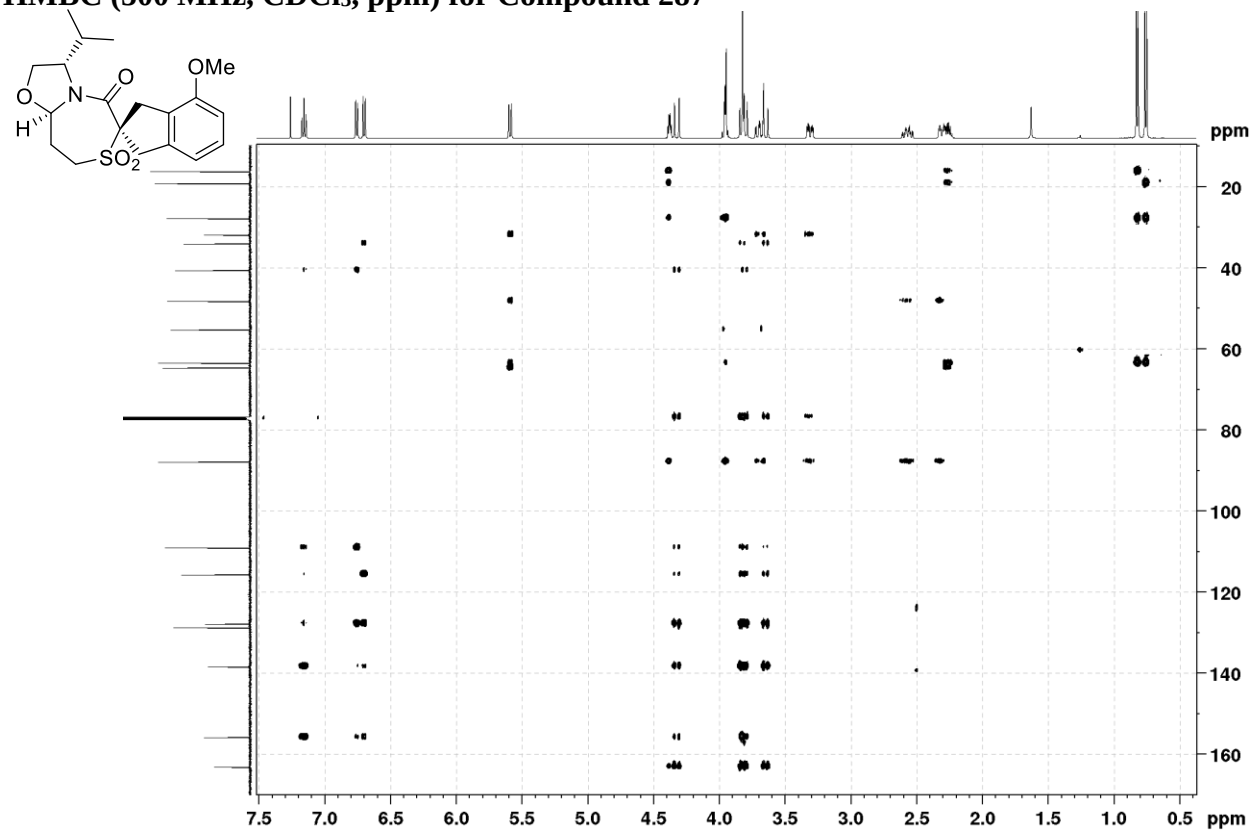

NOESY (500 MHz, $CDCl_3$, ppm) for Compound 287

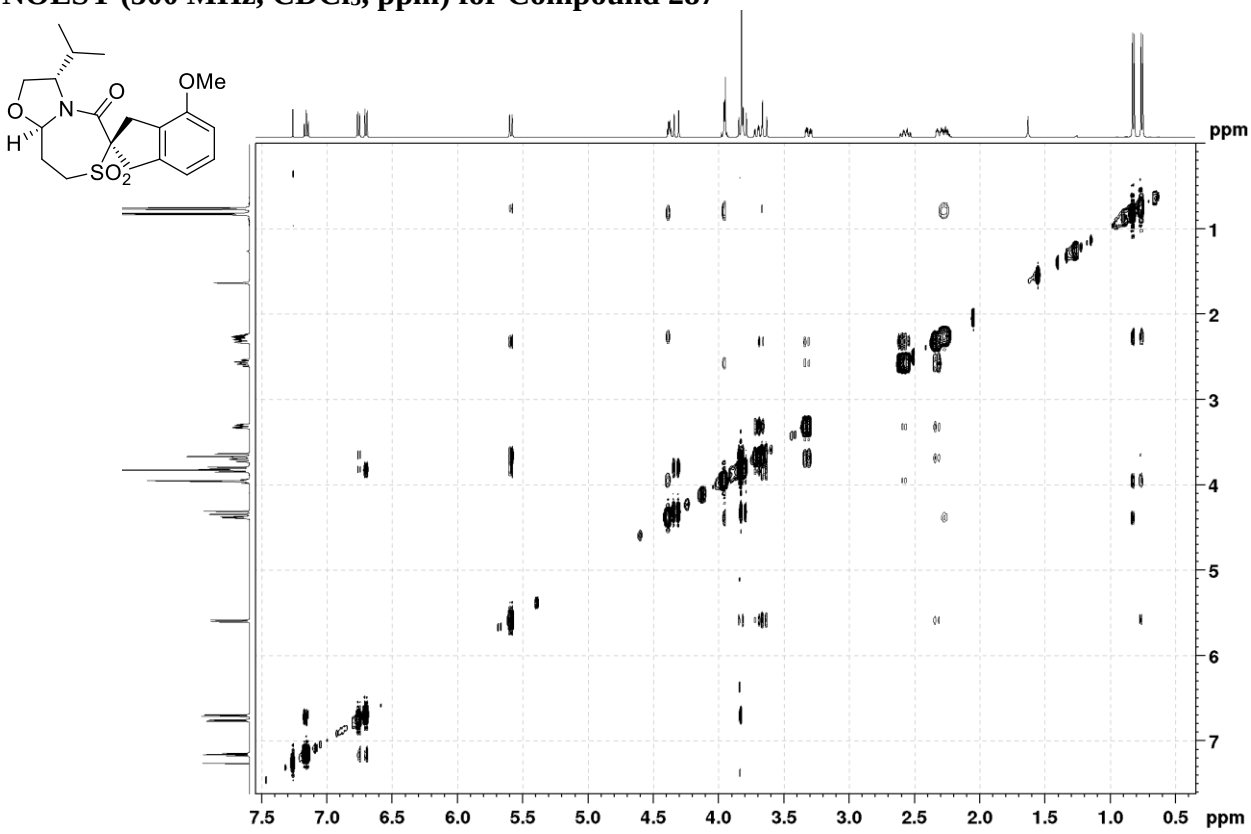

^{1}H NMR (500 MHz, $CDCl_3$, ppm) for Compound 345

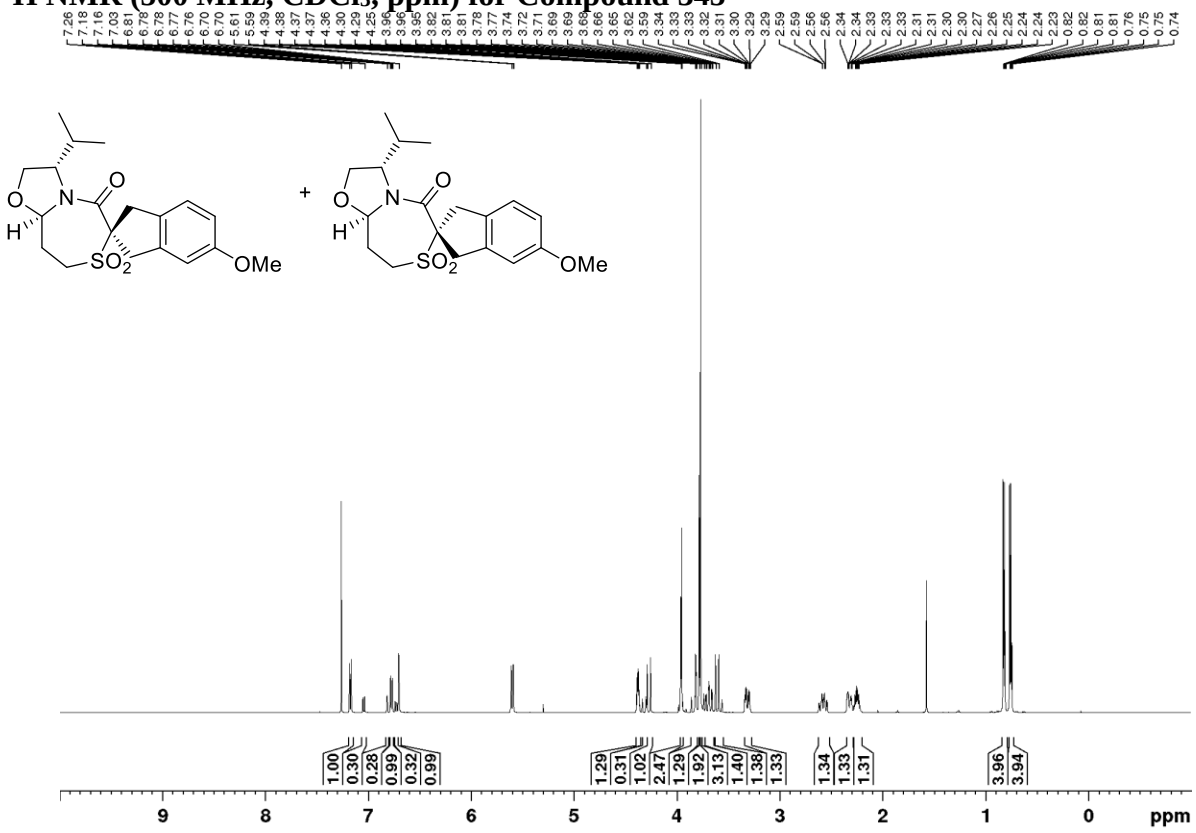

^{13}C NMR (126 MHz, $CDCl_3$, ppm) for Compound 345

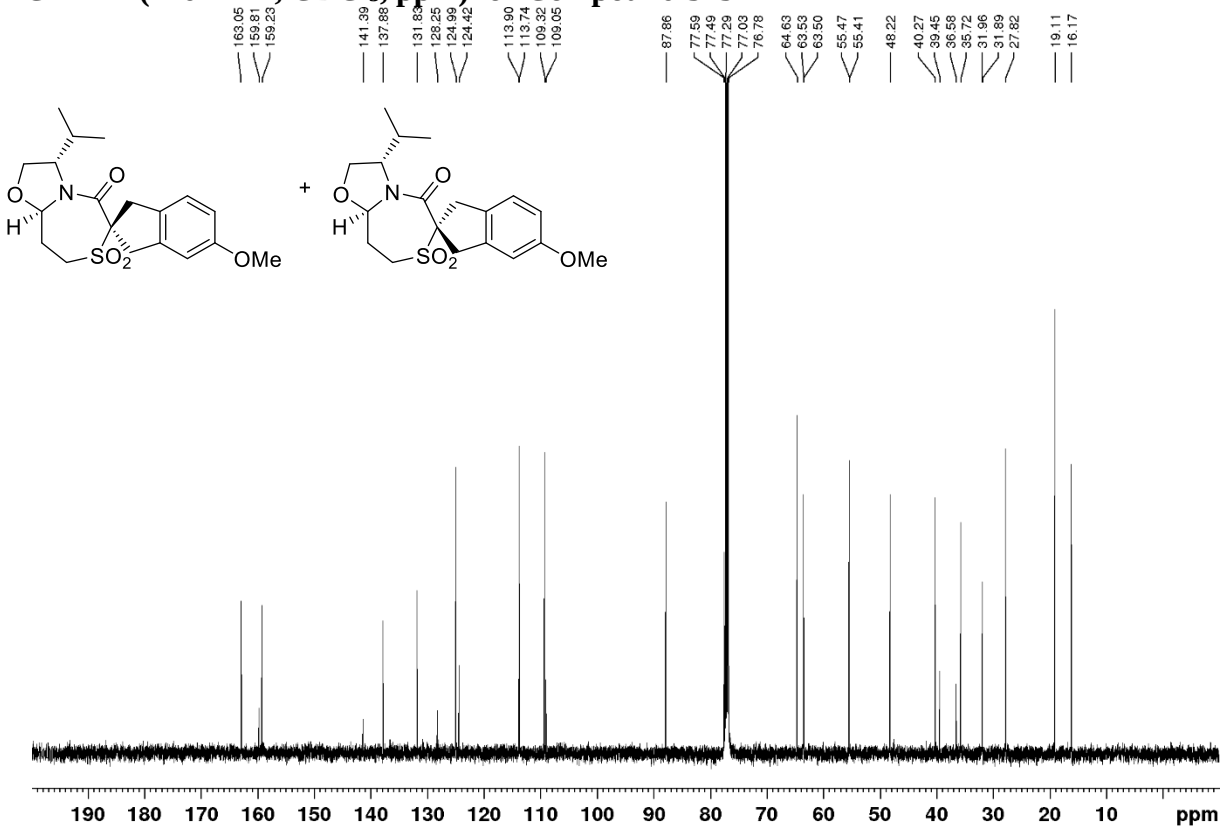

COSY (500 MHz, $CDCl_3$, ppm) for Compound 345

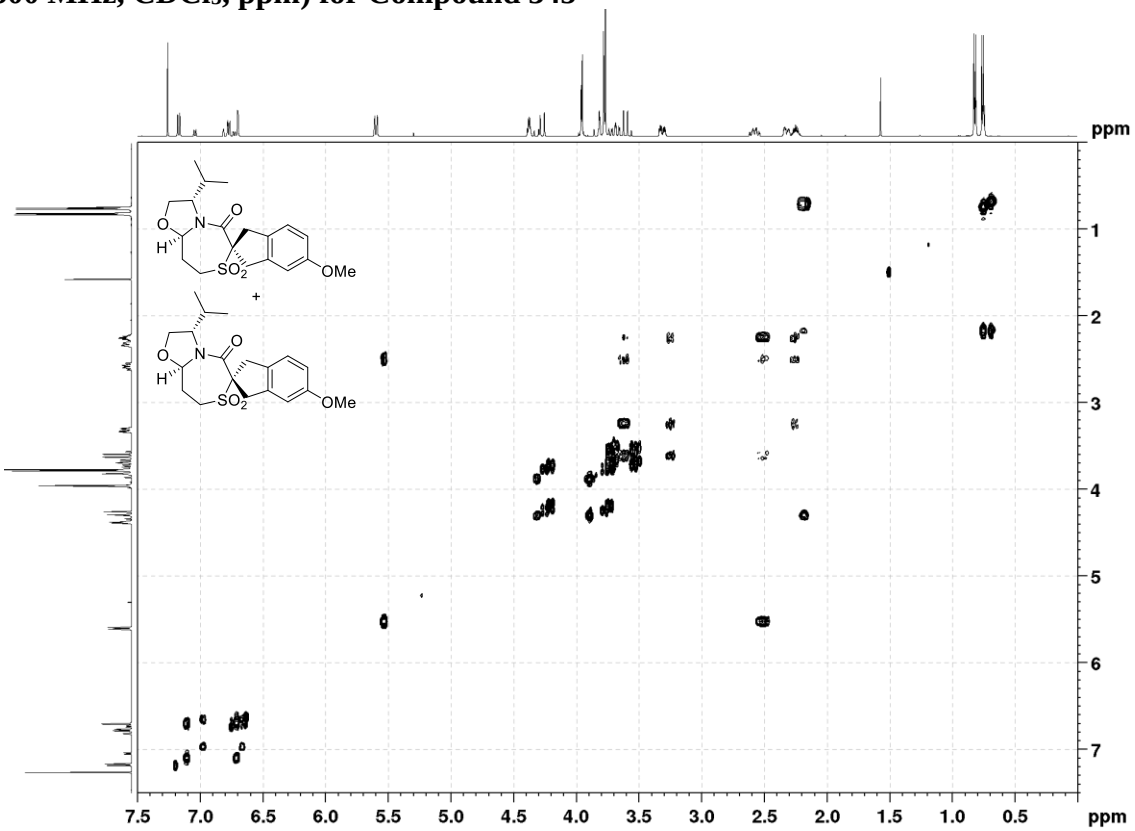

HSQC (500 MHz, $CDCl_3$, ppm) for Compound 345

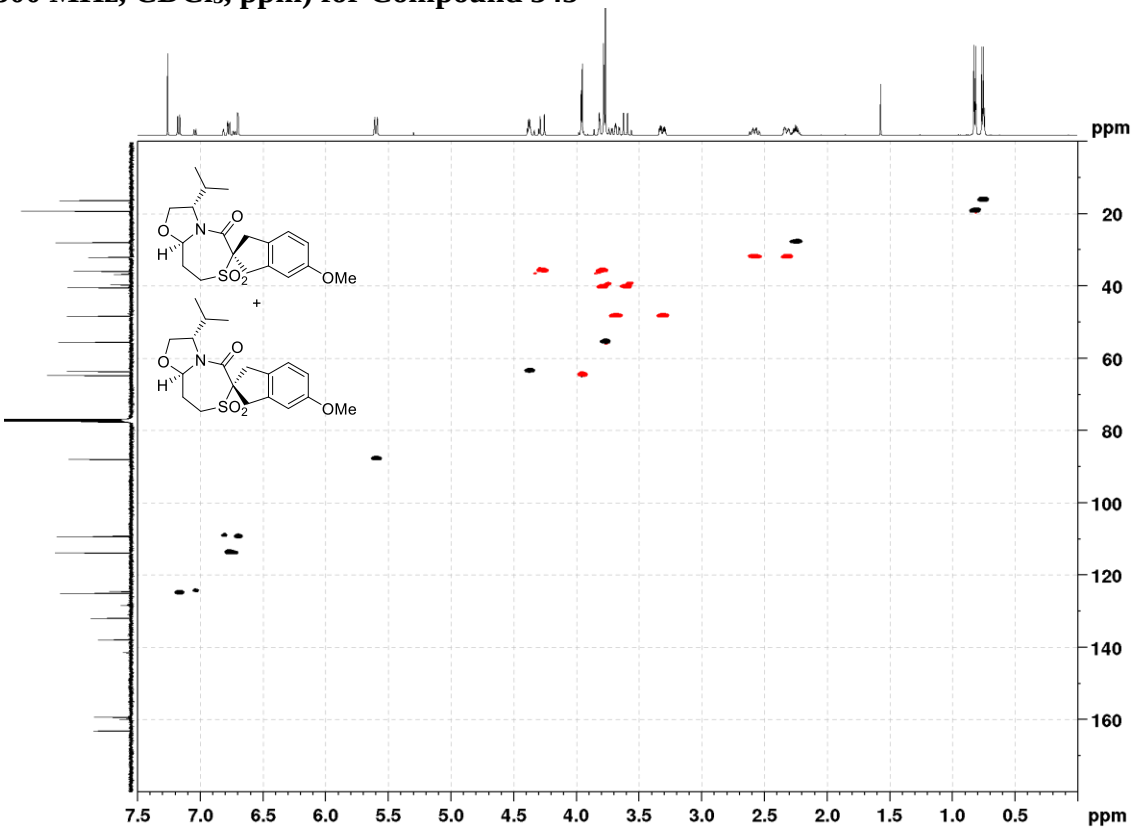

HMBC (500 MHz, $CDCl_3$, ppm) for Compound 345

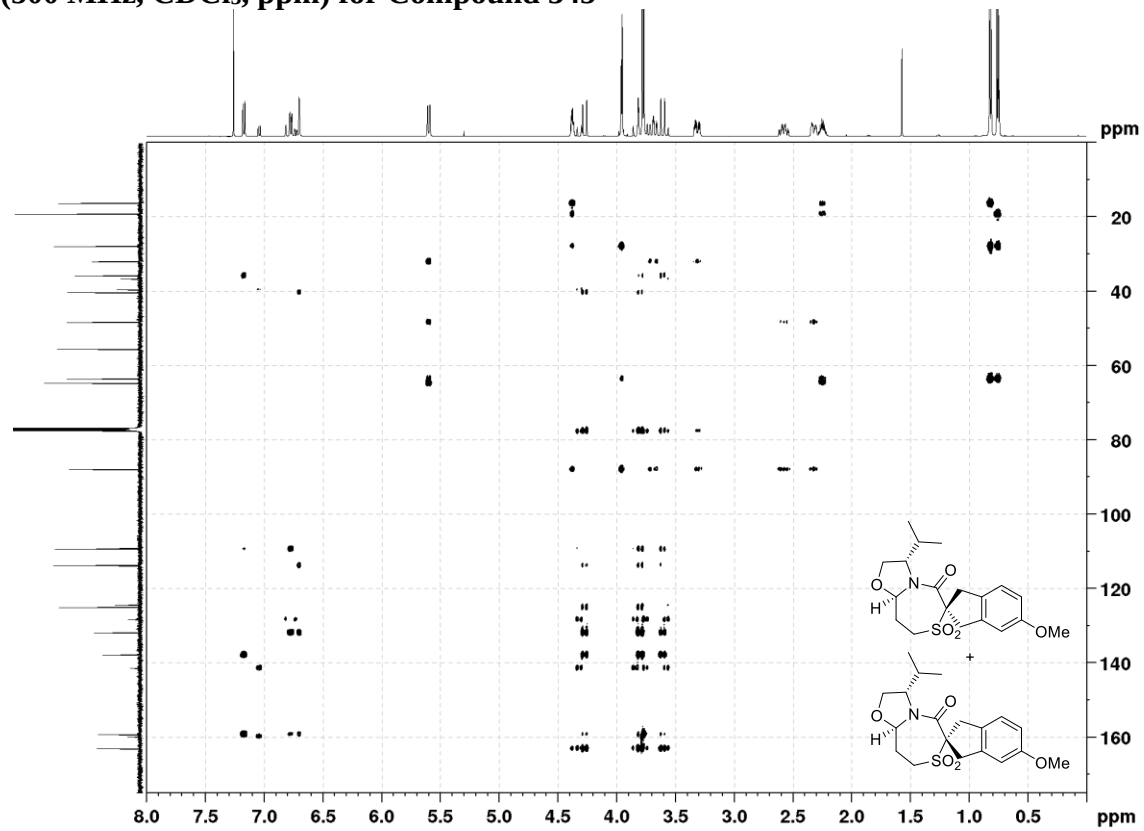

NOESY (500 MHz, $CDCl_3$, ppm) for Compound 345

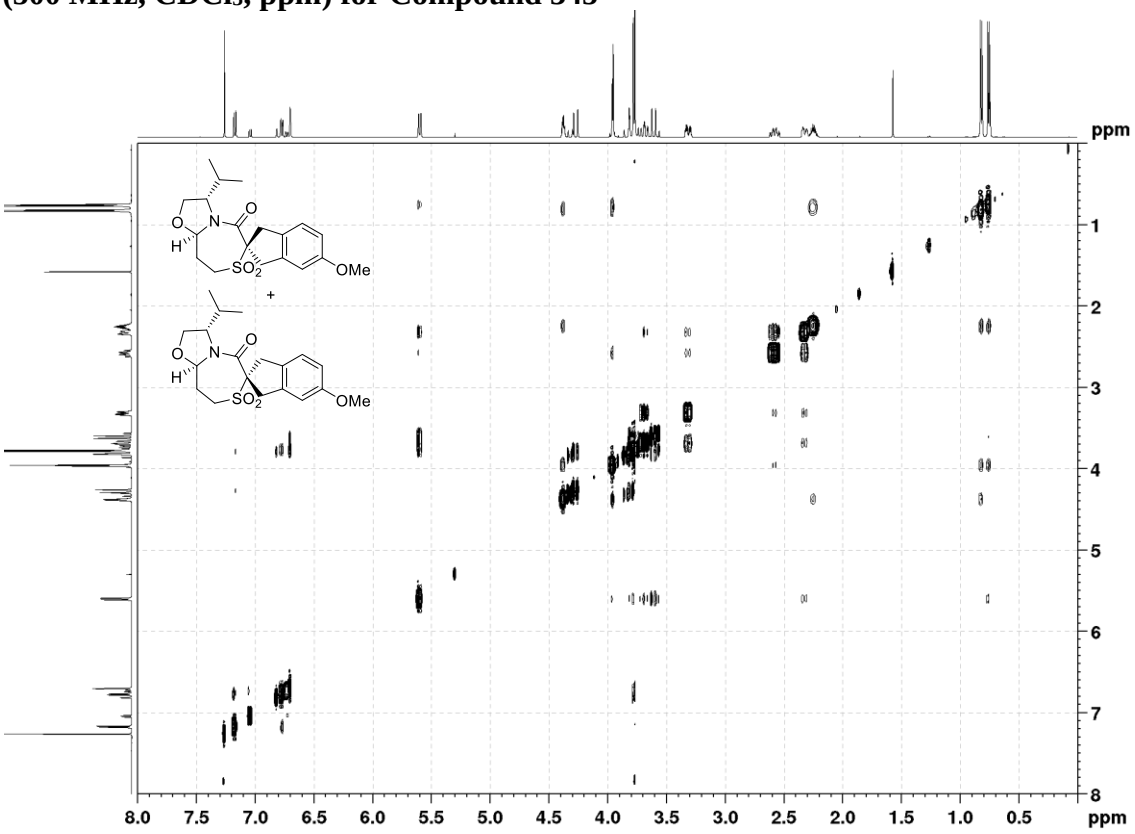

^{1}H NMR (500 MHz, $CDCl_3$, ppm) for Compound 346

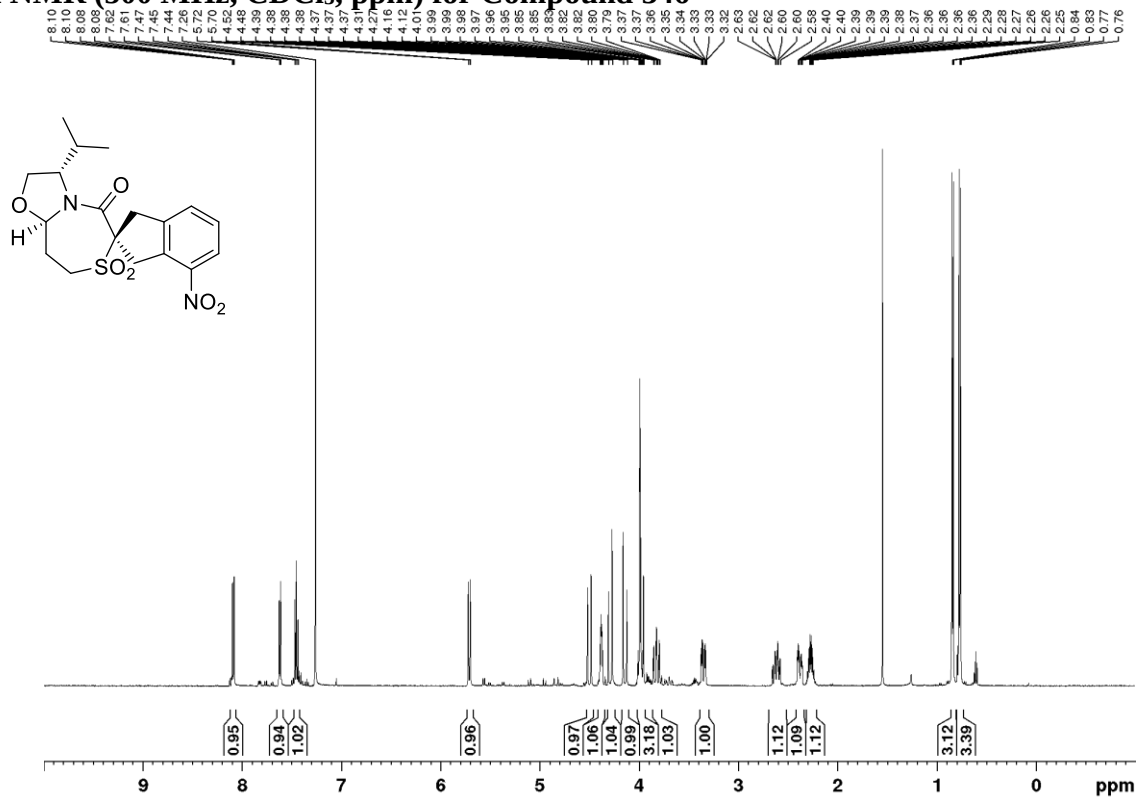

^{13}C NMR (126 MHz, $CDCl_3$, ppm) for Compound 346

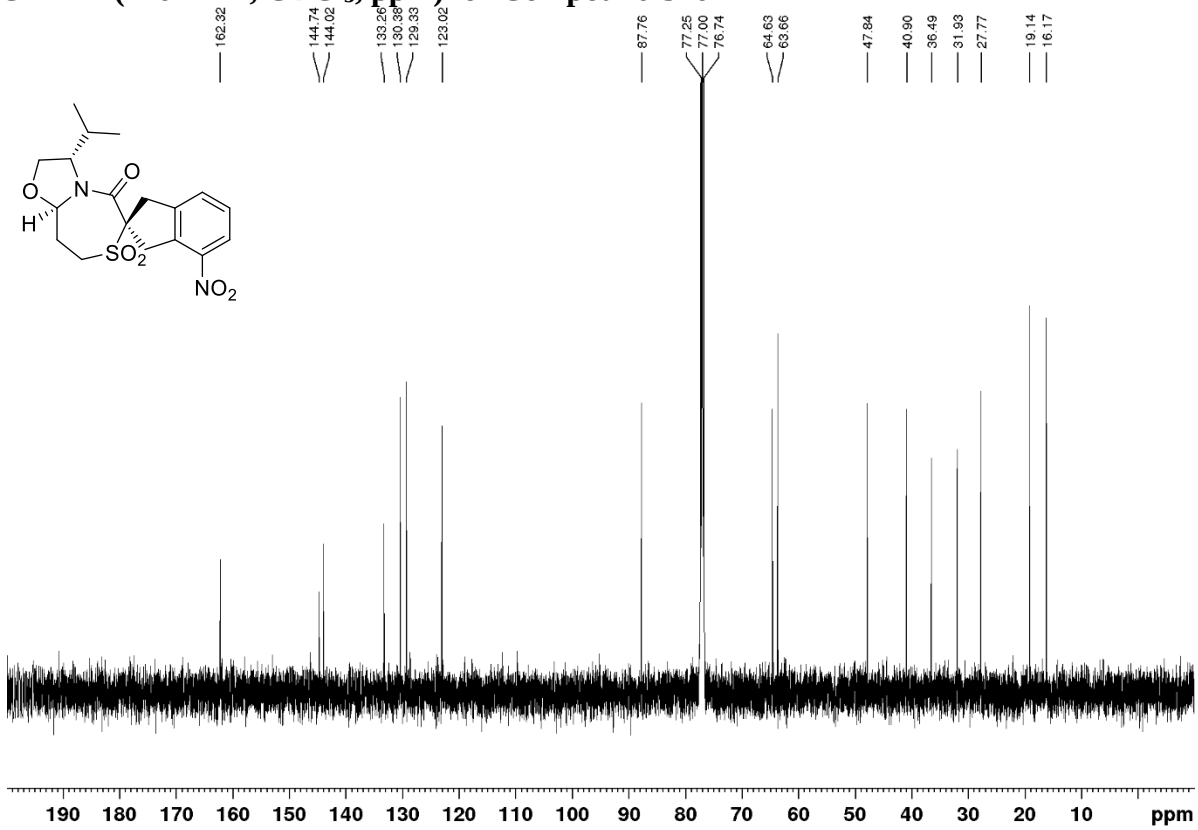

HSQC (500 MHz, $CDCl_3$, ppm) for Compound 346

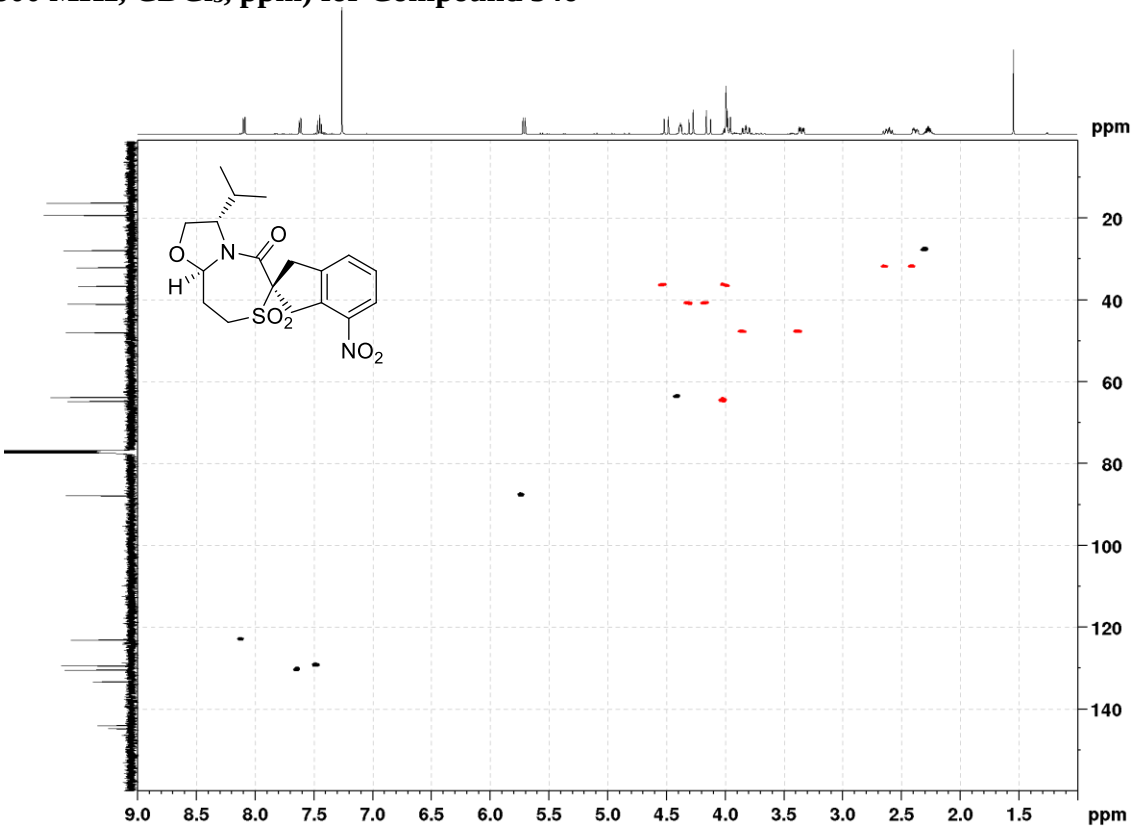

HMBC (500 MHz, $CDCl_3$, ppm) for Compound 346

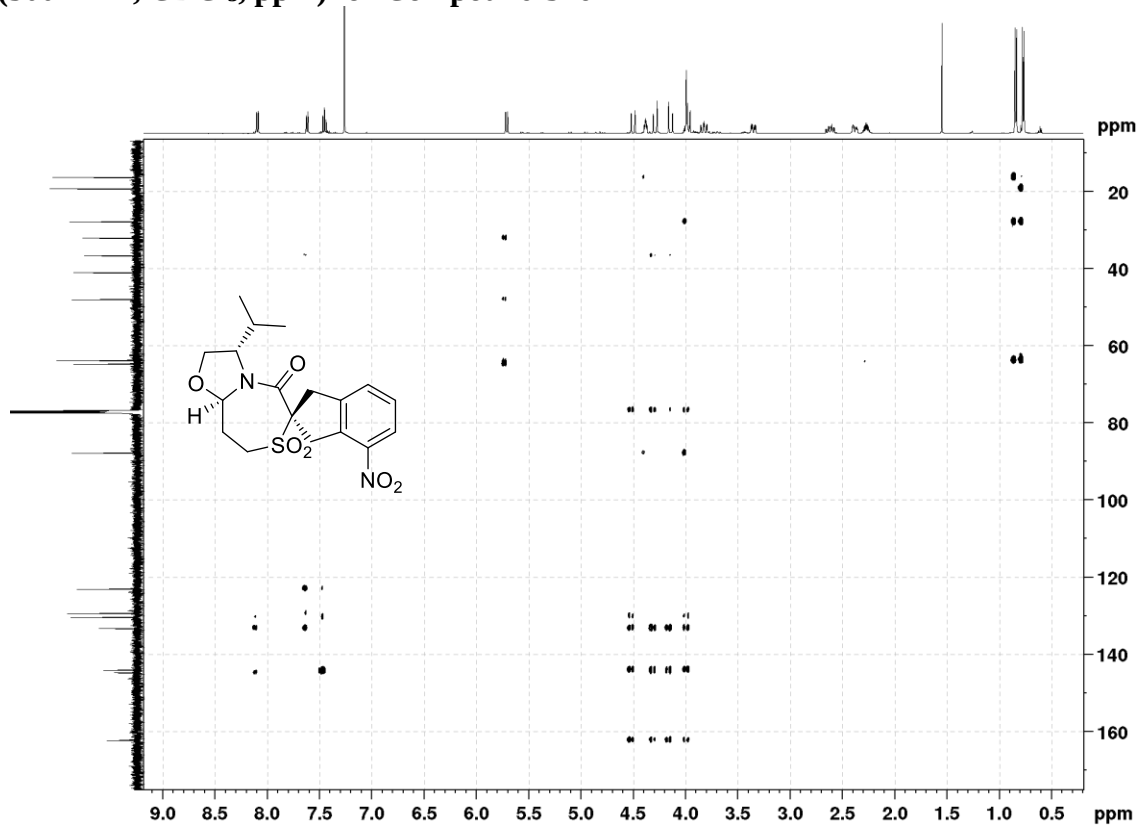

NOESY (500 MHz, $CDCl_3$, ppm) for Compound 346

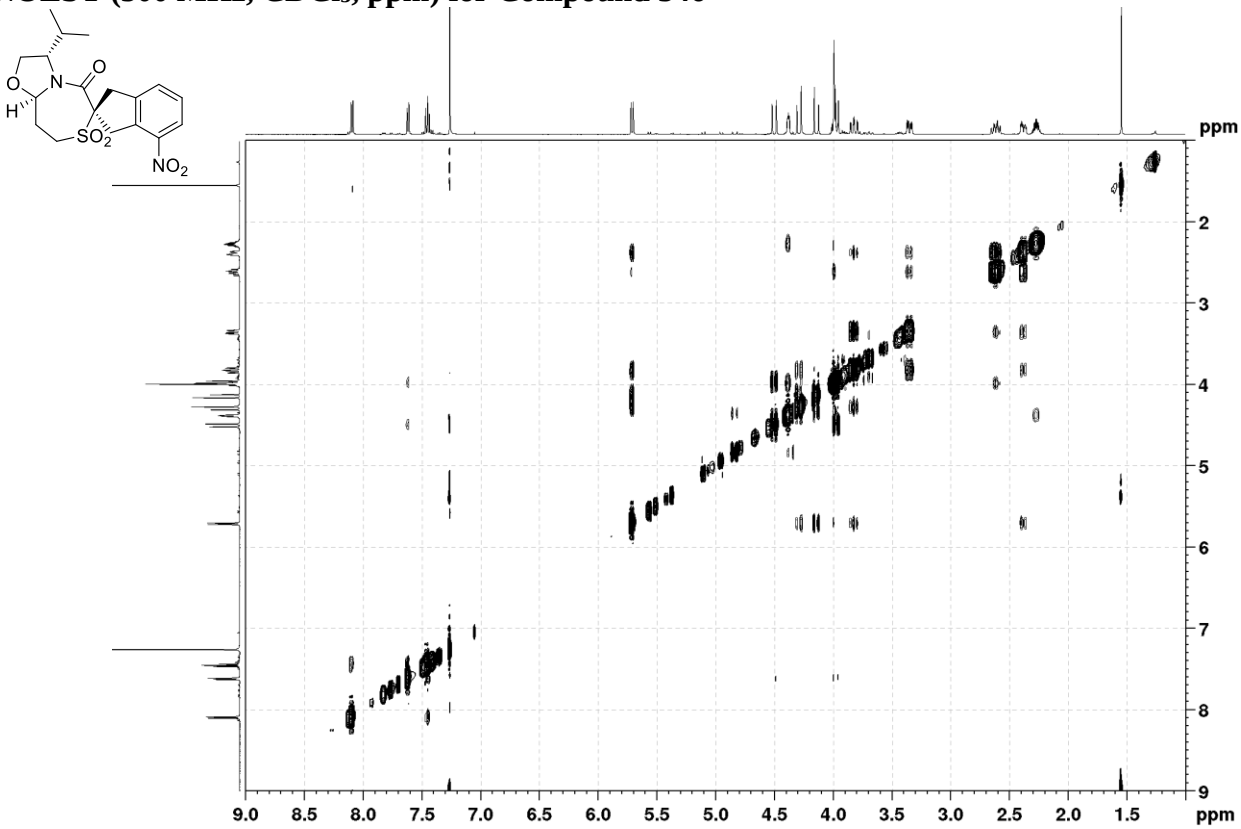

^{1}H NMR (500 MHz, $CDCl_3$, ppm) for Compound 347

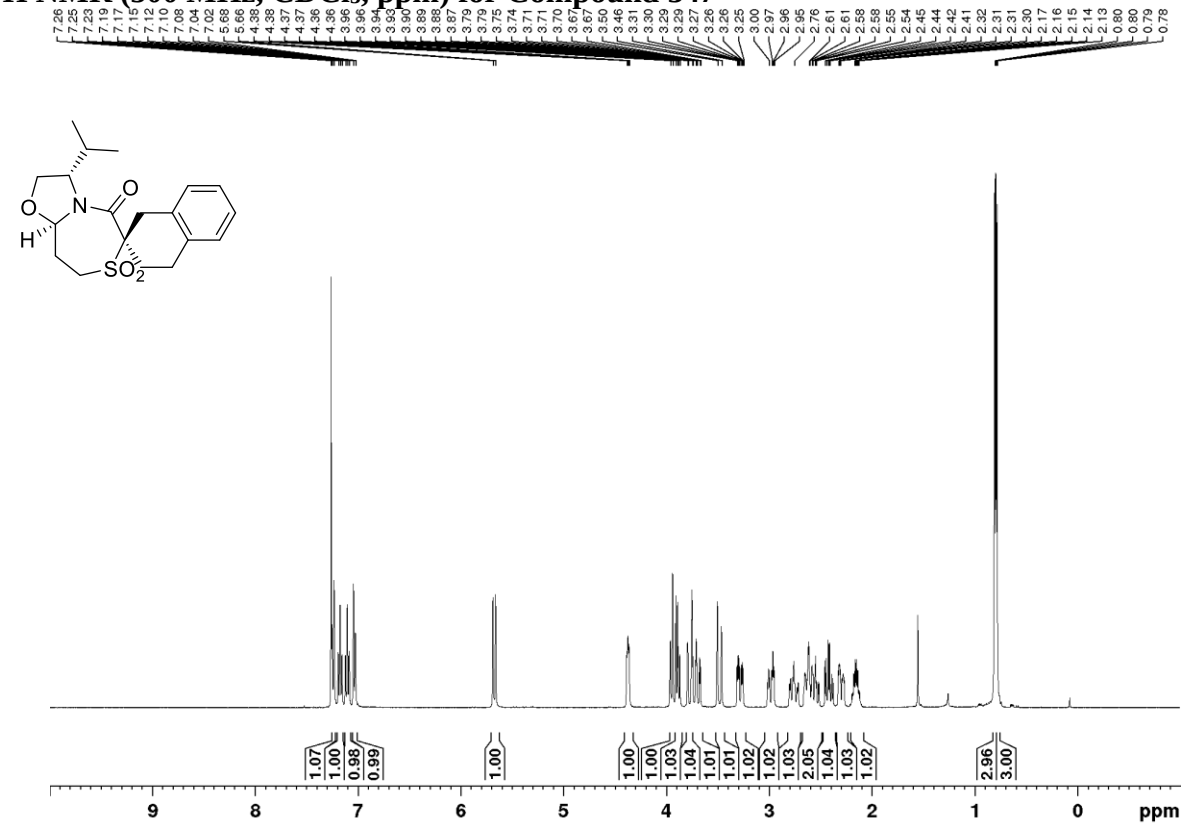

^{13}C NMR (500 MHz, $CDCl_3$, ppm) for Compound 347

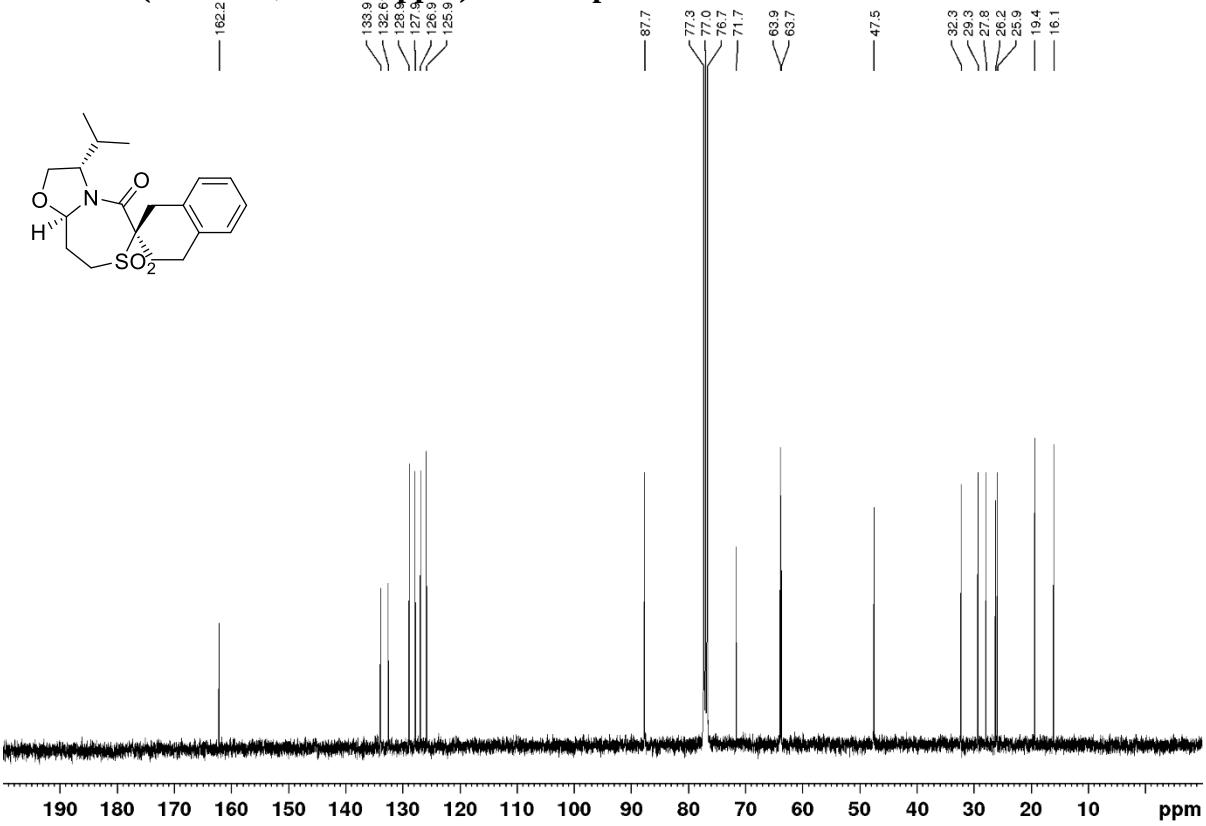

COSY (500 MHz, $CDCl_3$, ppm) for Compound 347

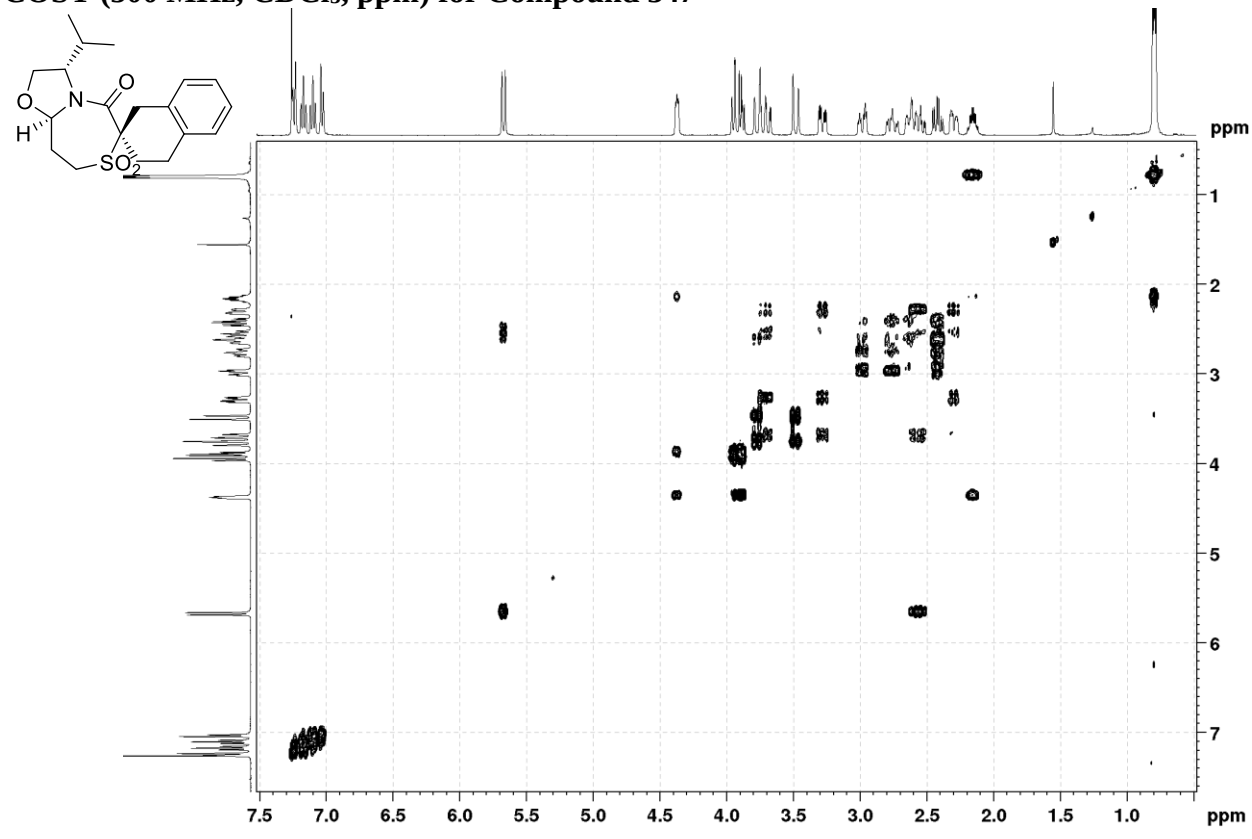

HSQC (500 MHz, $CDCl_3$, ppm) for Compound 347

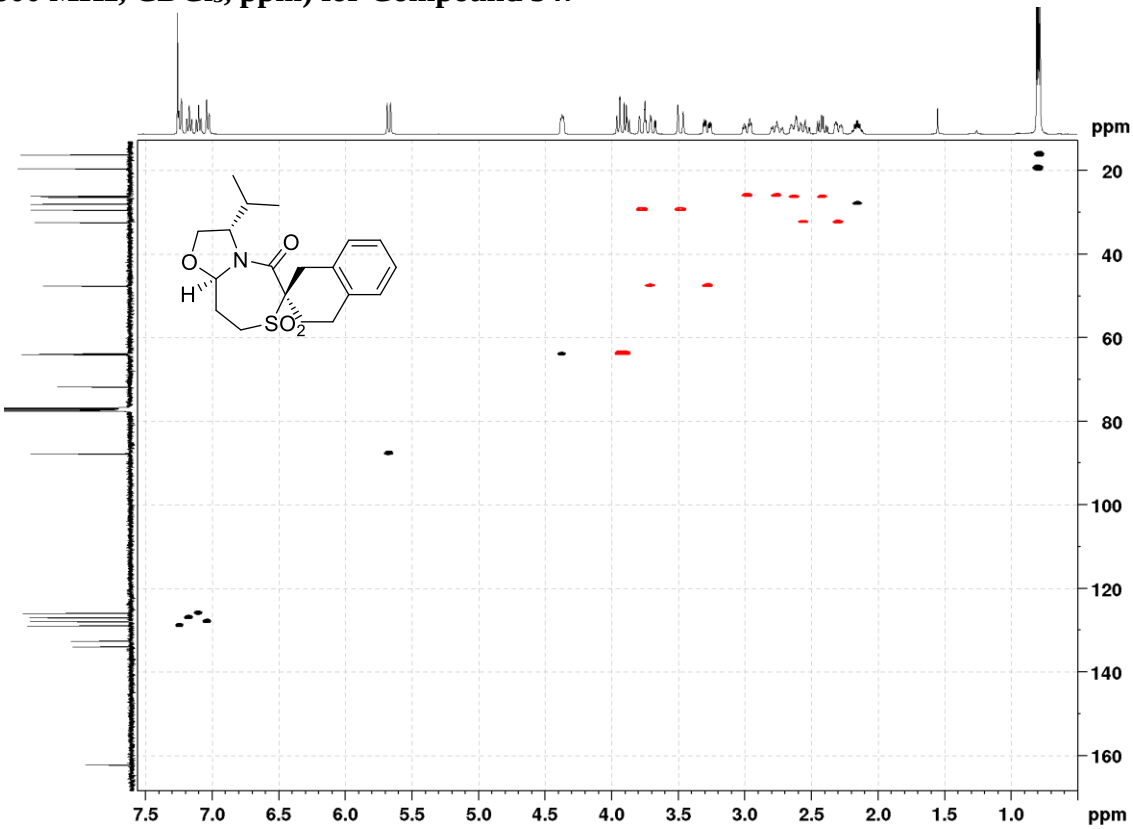

HMBC (500 MHz, $CDCl_3$, ppm) for Compound 347

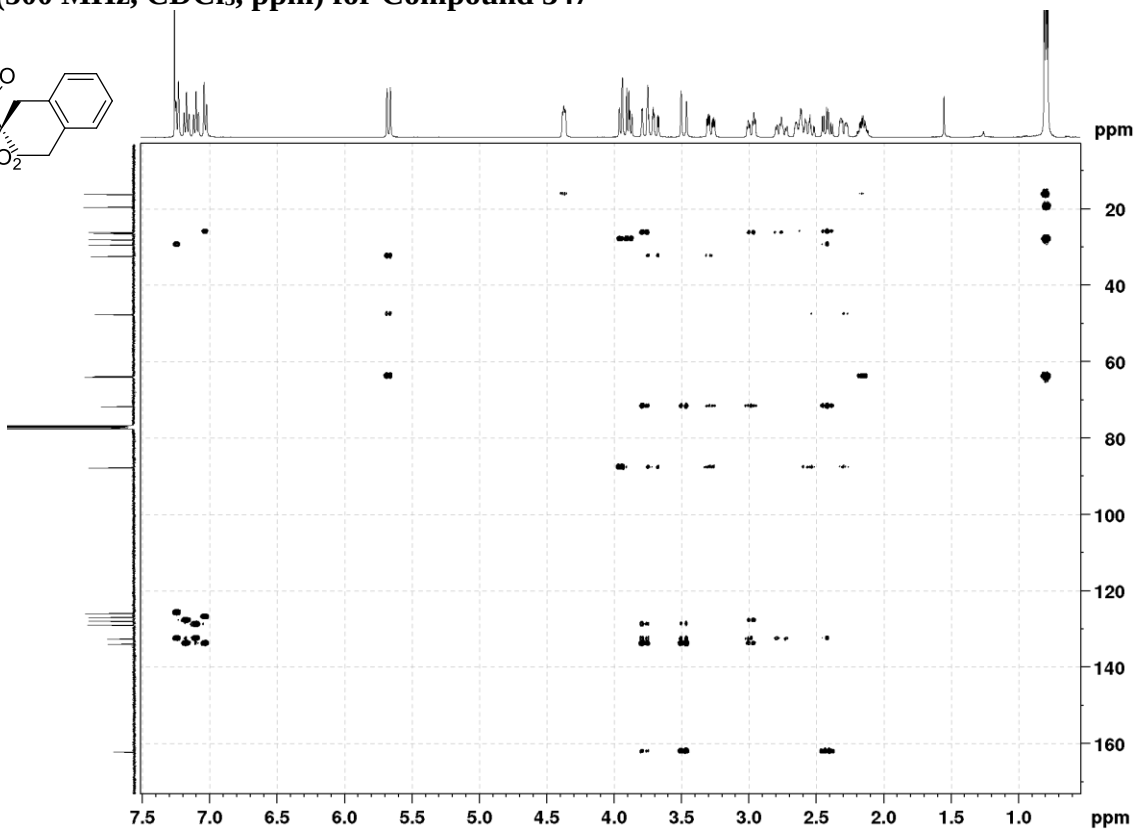

NOESY (500 MHz, $CDCl_3$, ppm) for Compound 347

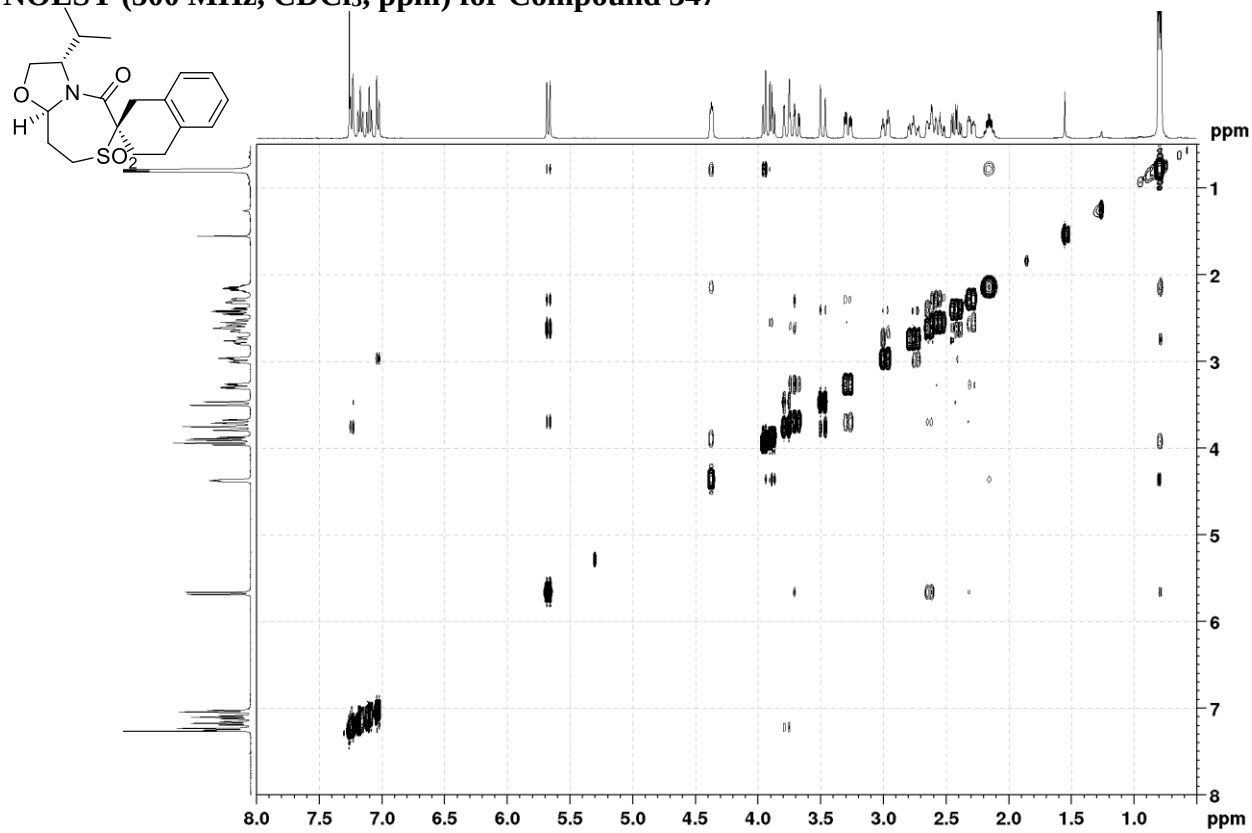

^{1}H NMR (500 MHz, $CDCl_3$, ppm) for Compound 348

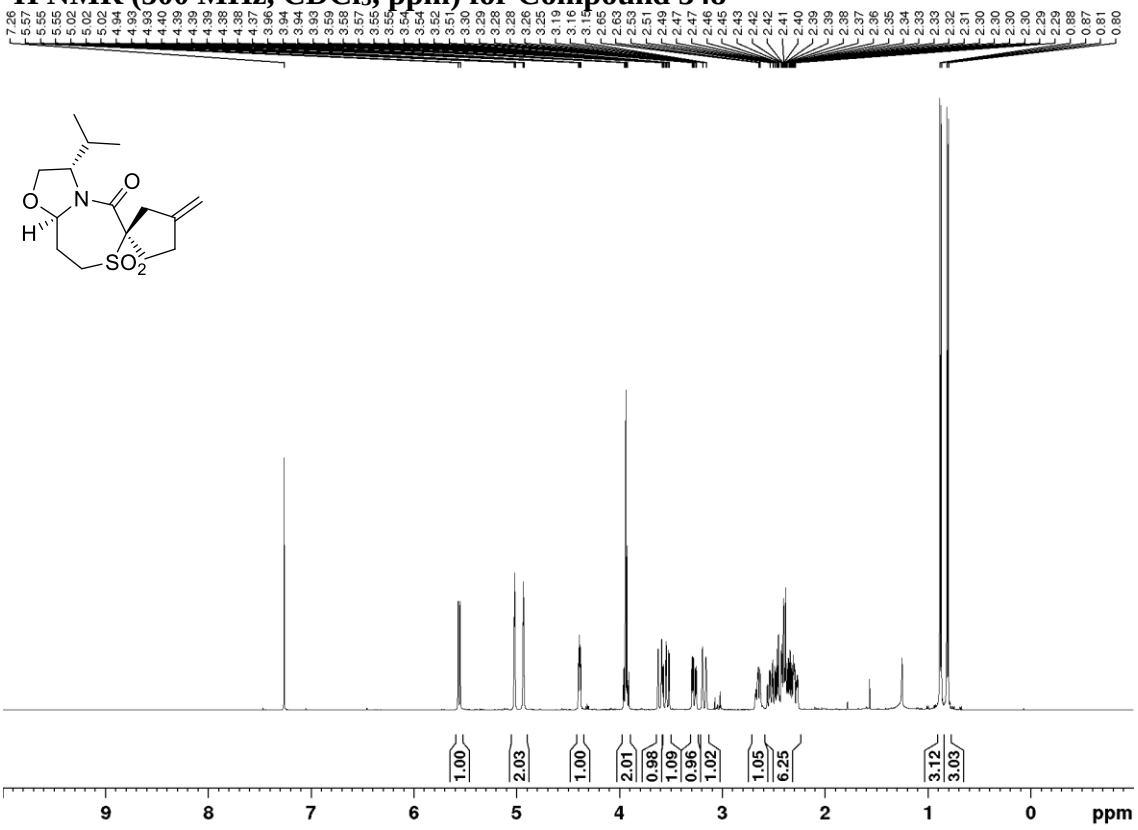

^{13}C NMR (126 MHz, $CDCl_3$, ppm) for Compound 348

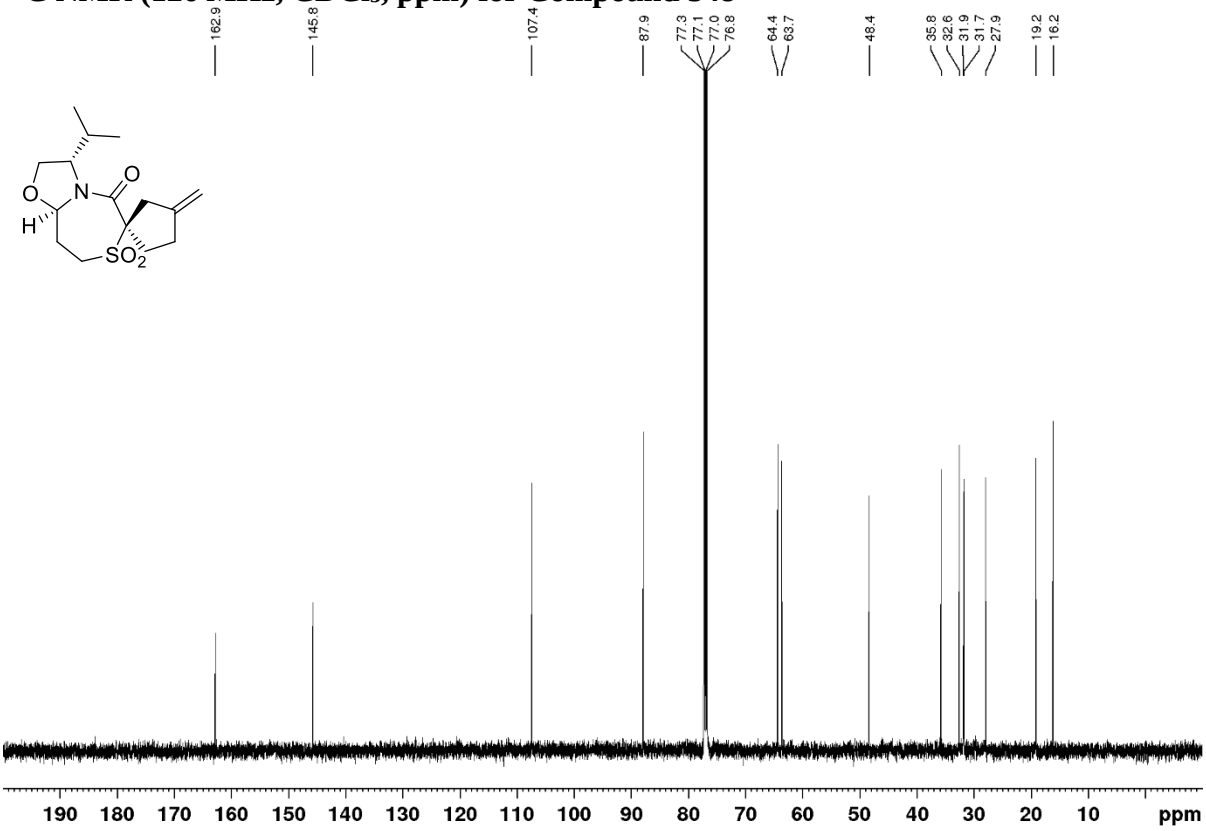

COSY (500 MHz, $CDCl_3$, ppm) for Compound 348

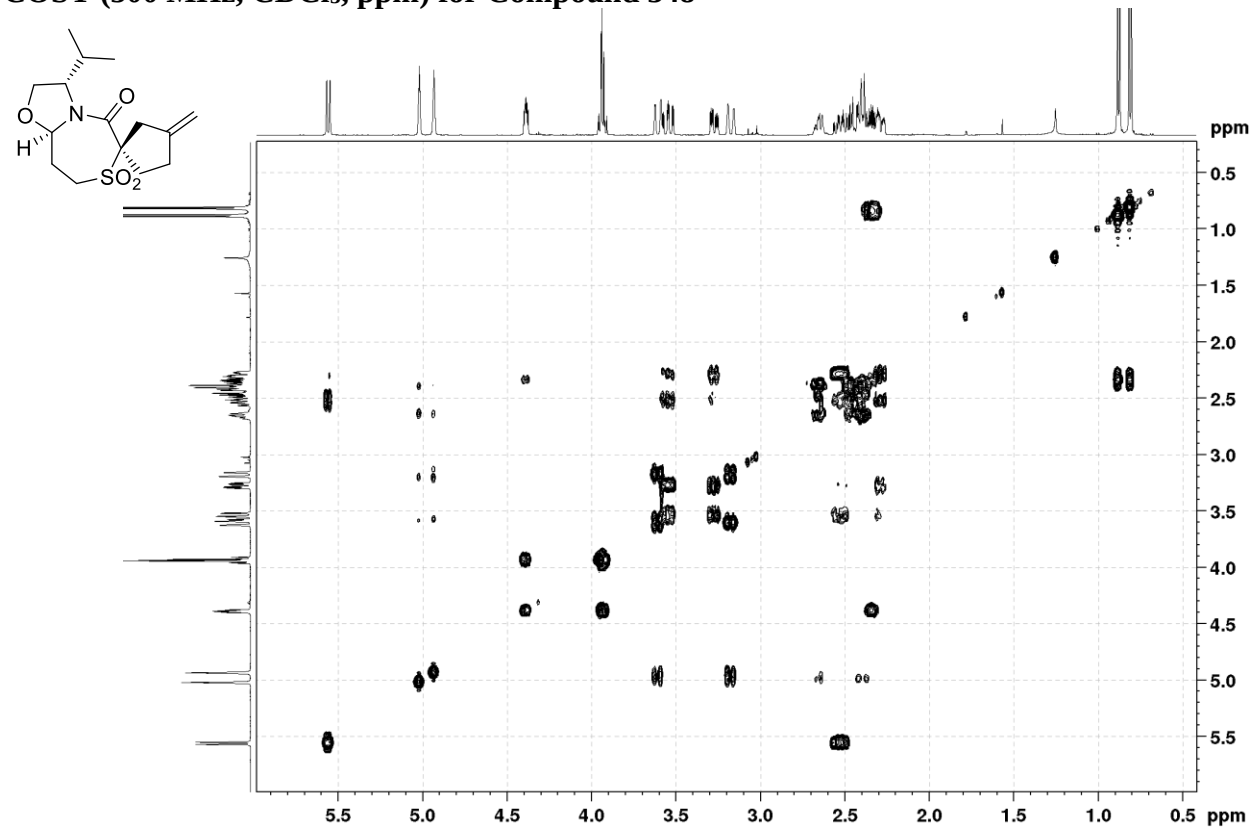

HSQC (500 MHz, $CDCl_3$, ppm) for Compound 348

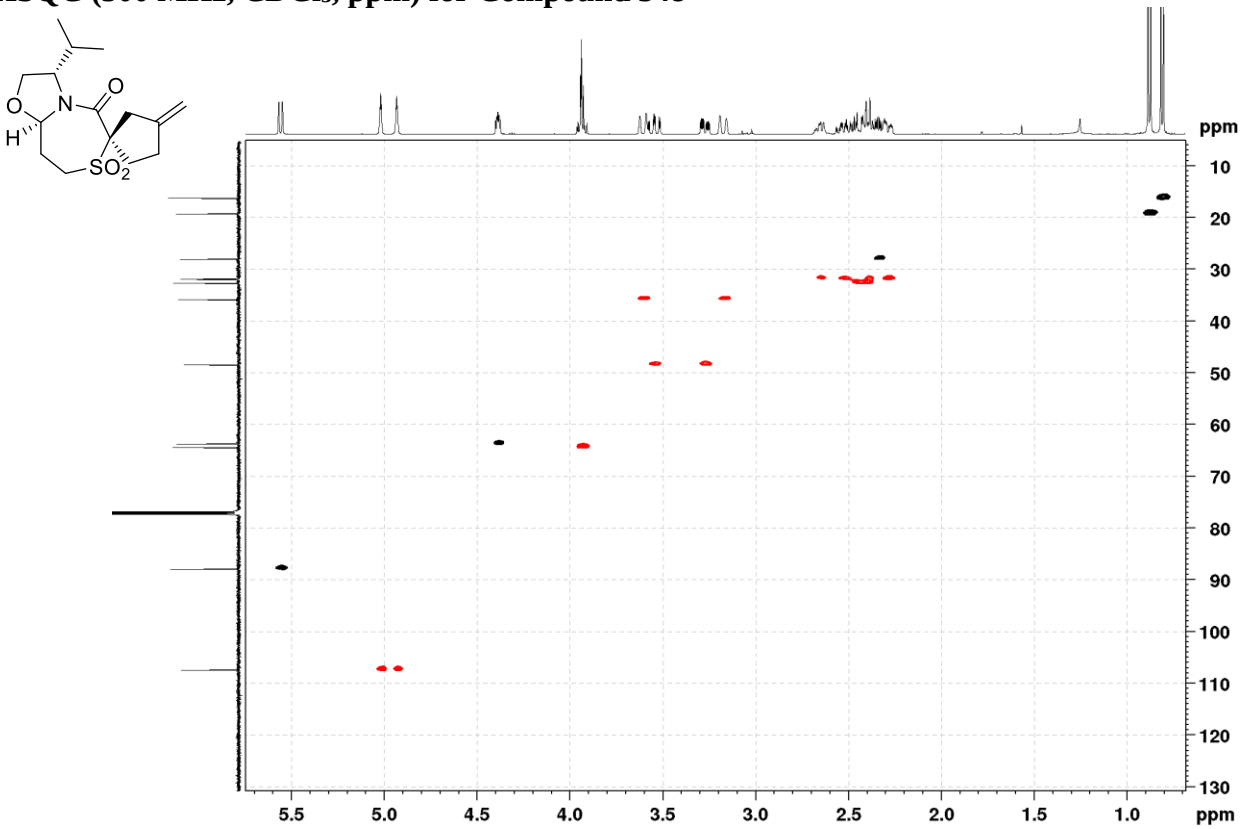

HMBC (500 MHz, $CDCl_3$, ppm) for Compound 348

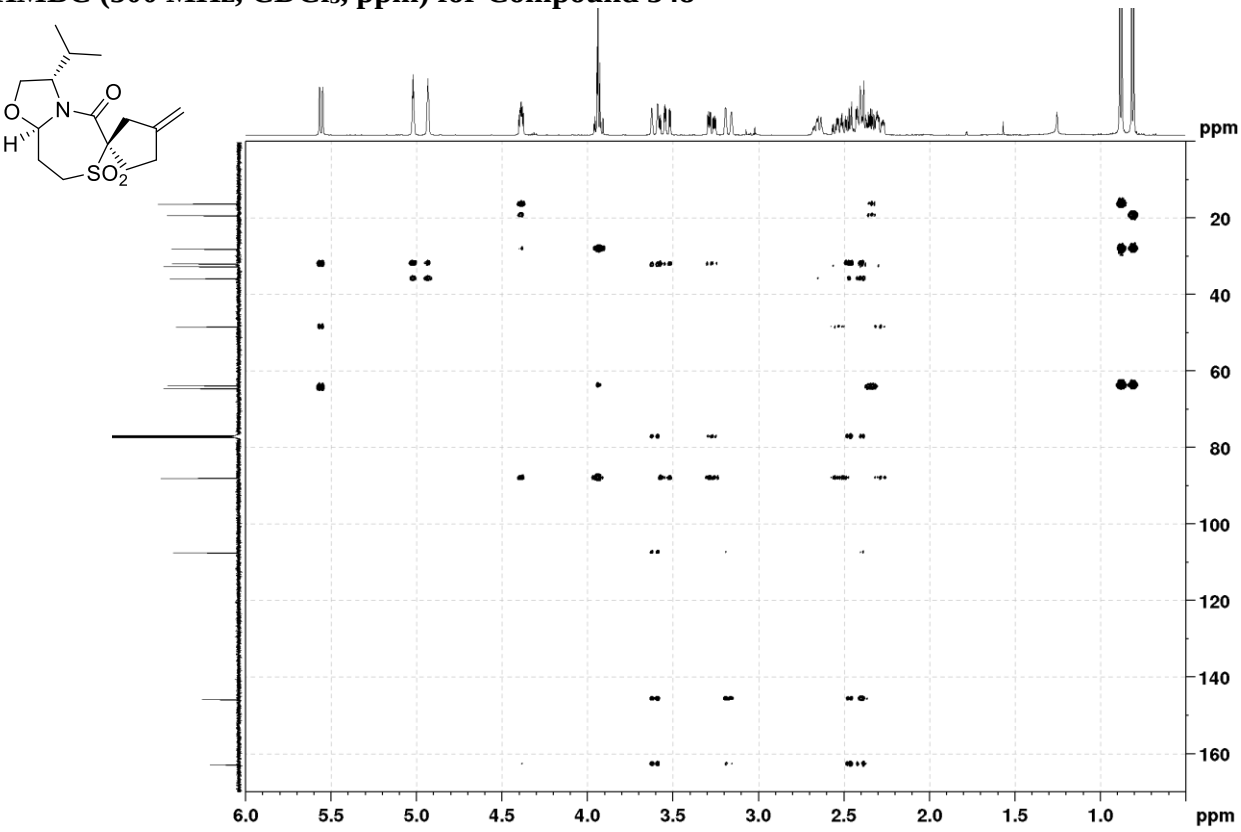

NOESY (500 MHz, $CDCl_3$, ppm) for Compound 348

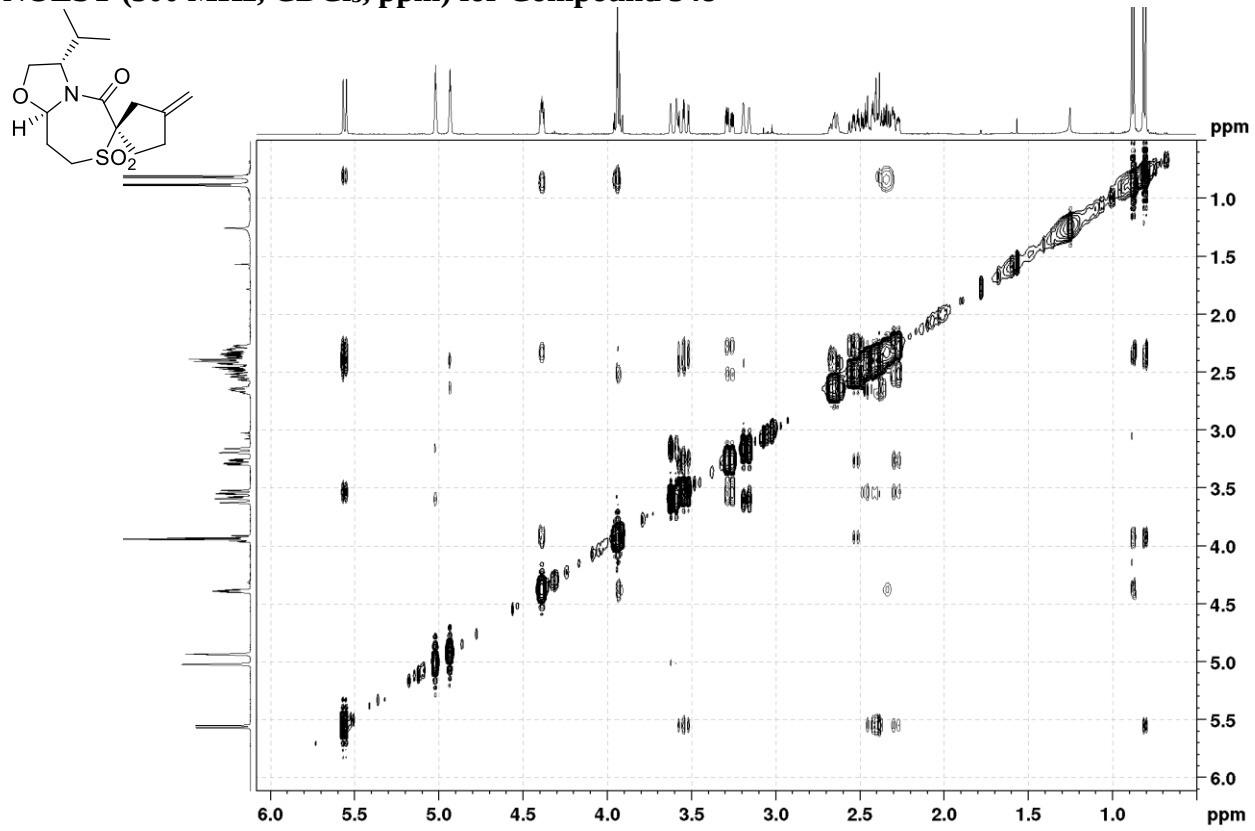

^{1}H NMR (500 MHz, $CDCl_3$, ppm) for Compound 349

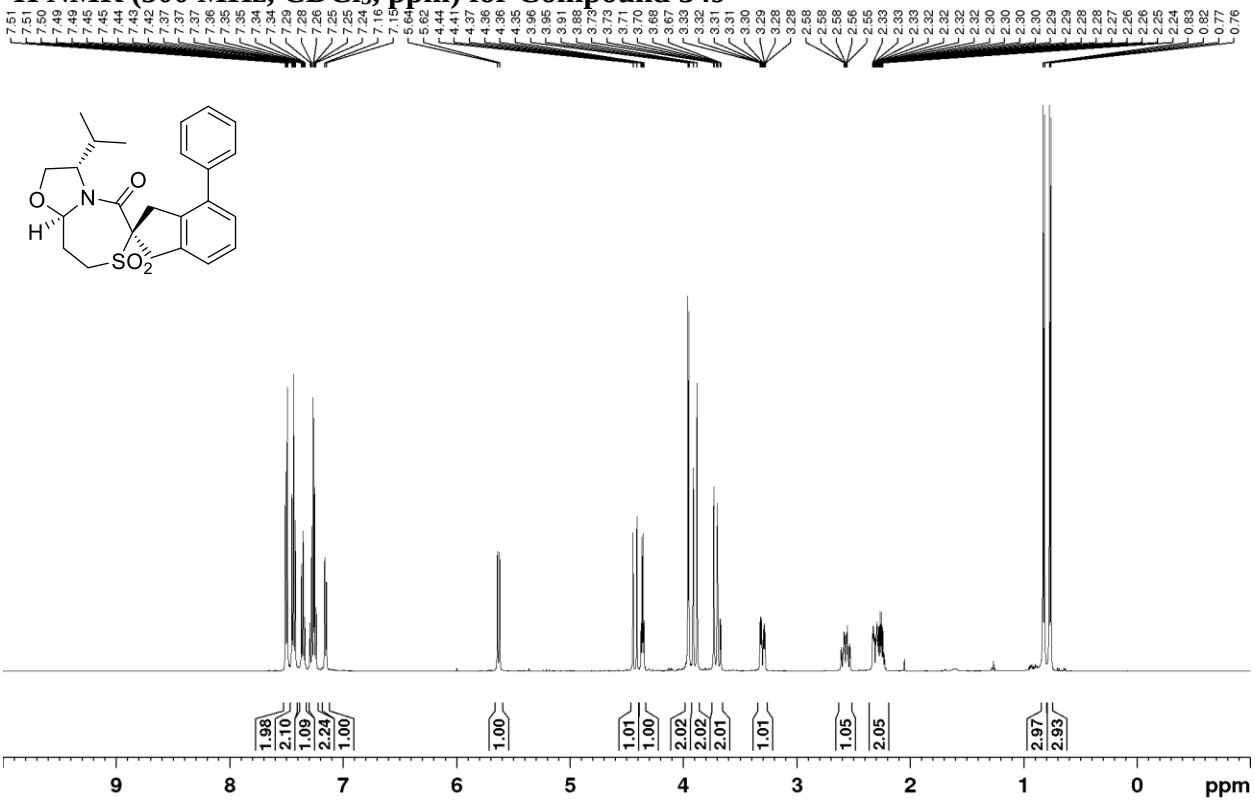

^{13}C NMR (126 MHz, $CDCl_3$, ppm) for Compound 349

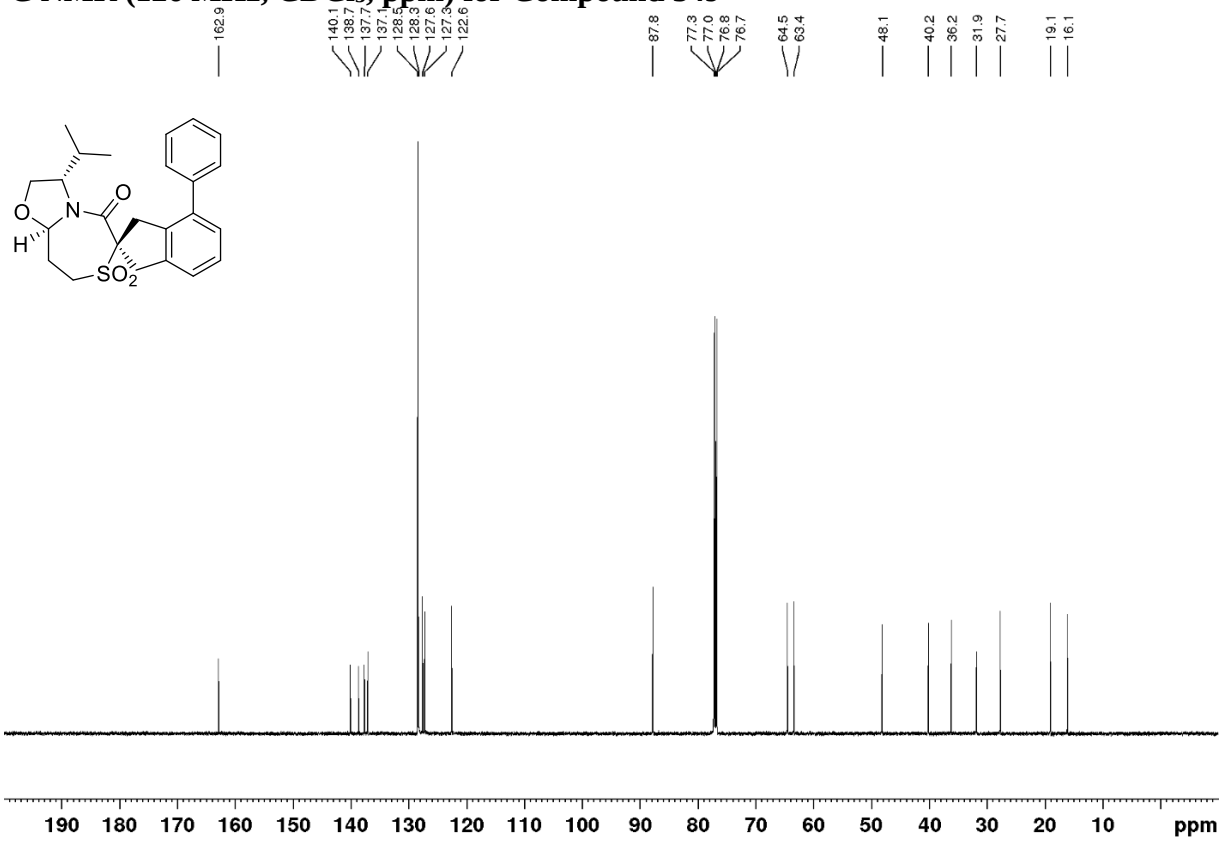

COSY (500 MHz, $CDCl_3$, ppm) for Compound 349

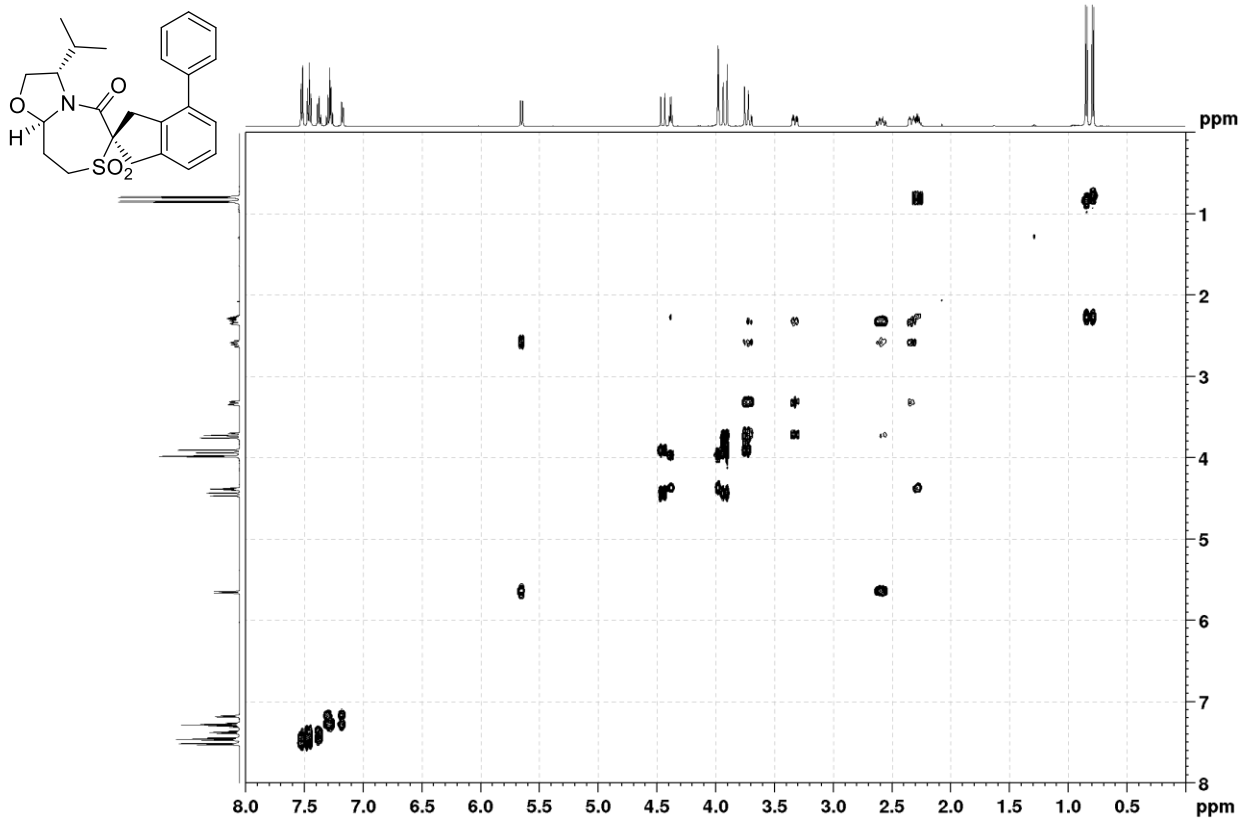

HSQC (500 MHz, $CDCl_3$, ppm) for Compound 349

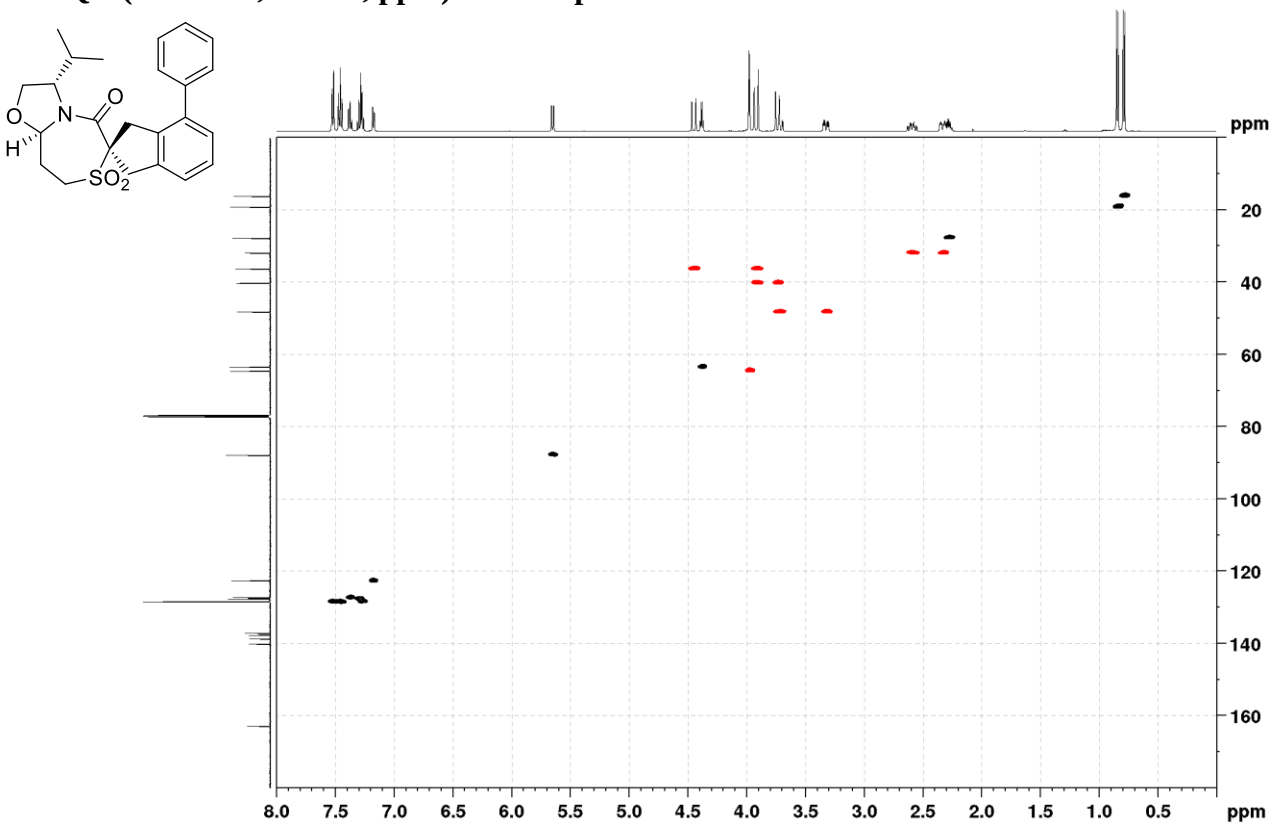

HMBC (500 MHz, $CDCl_3$, ppm) for Compound 349

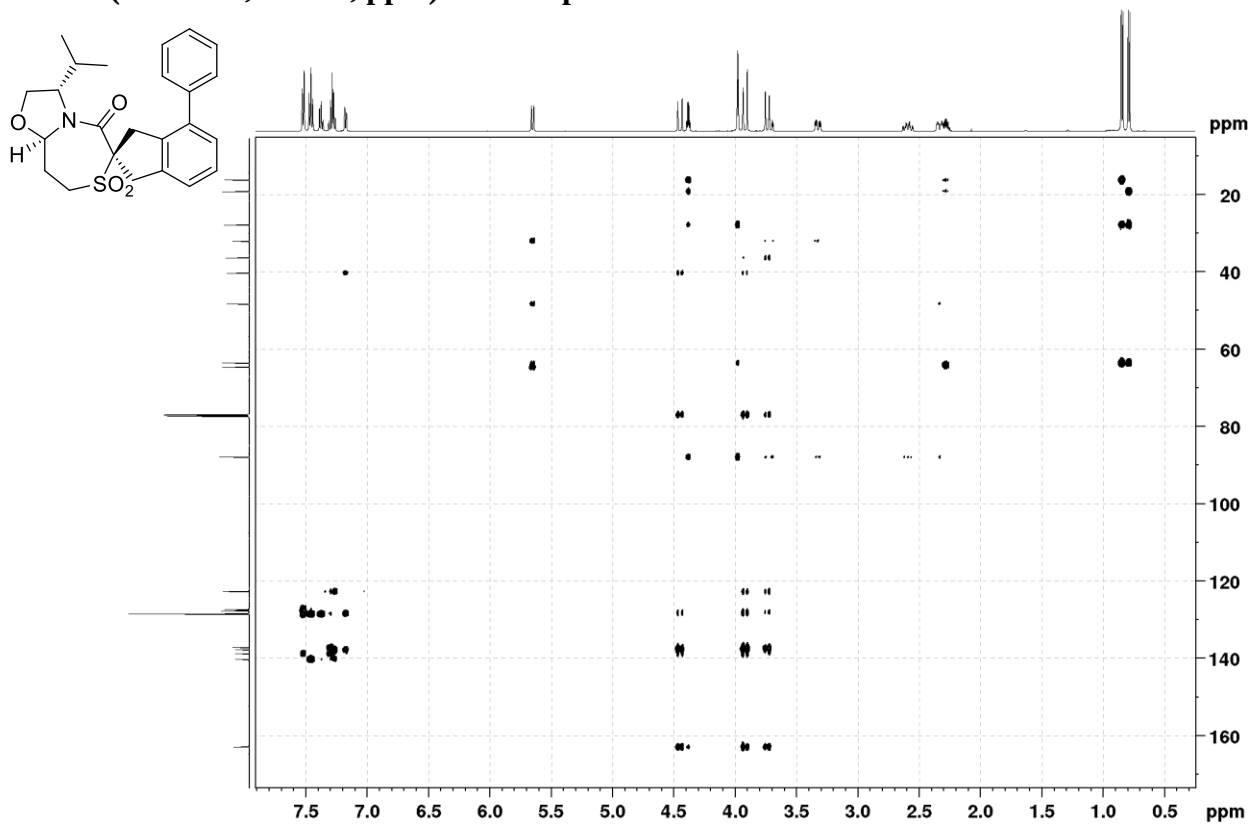

NOESY (500 MHz, $CDCl_3$, ppm) for Compound 349

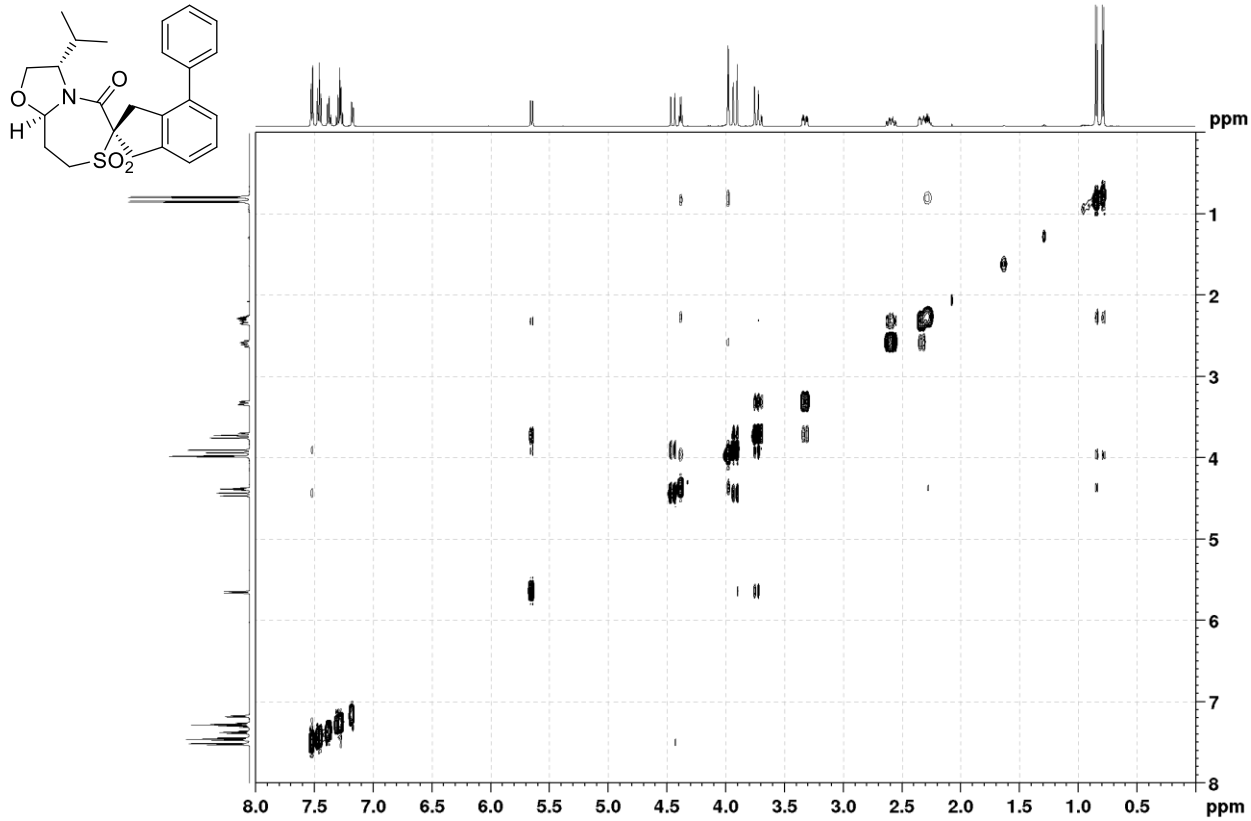

^{1}H NMR (500 MHz, $CDCl_3$, ppm) for Compound 350

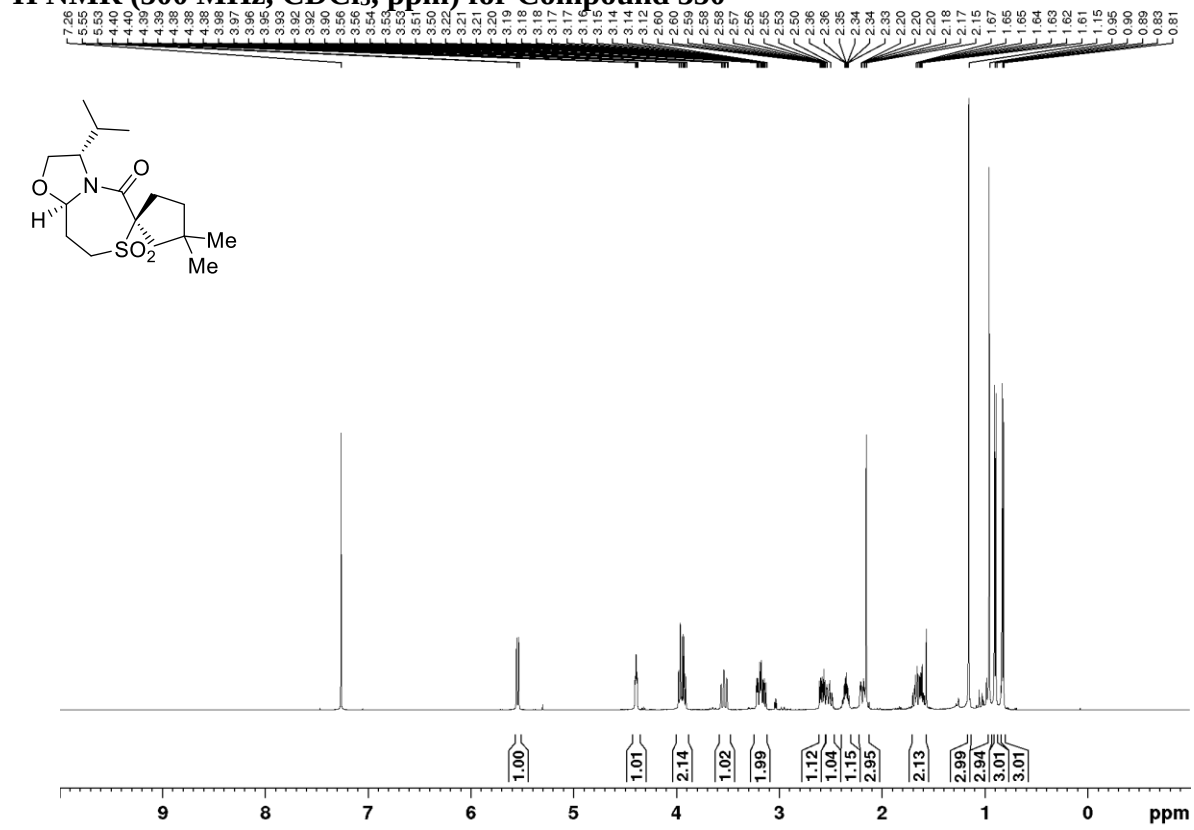

^{13}C NMR (126 MHz, $CDCl_3$, ppm) for Compound 350

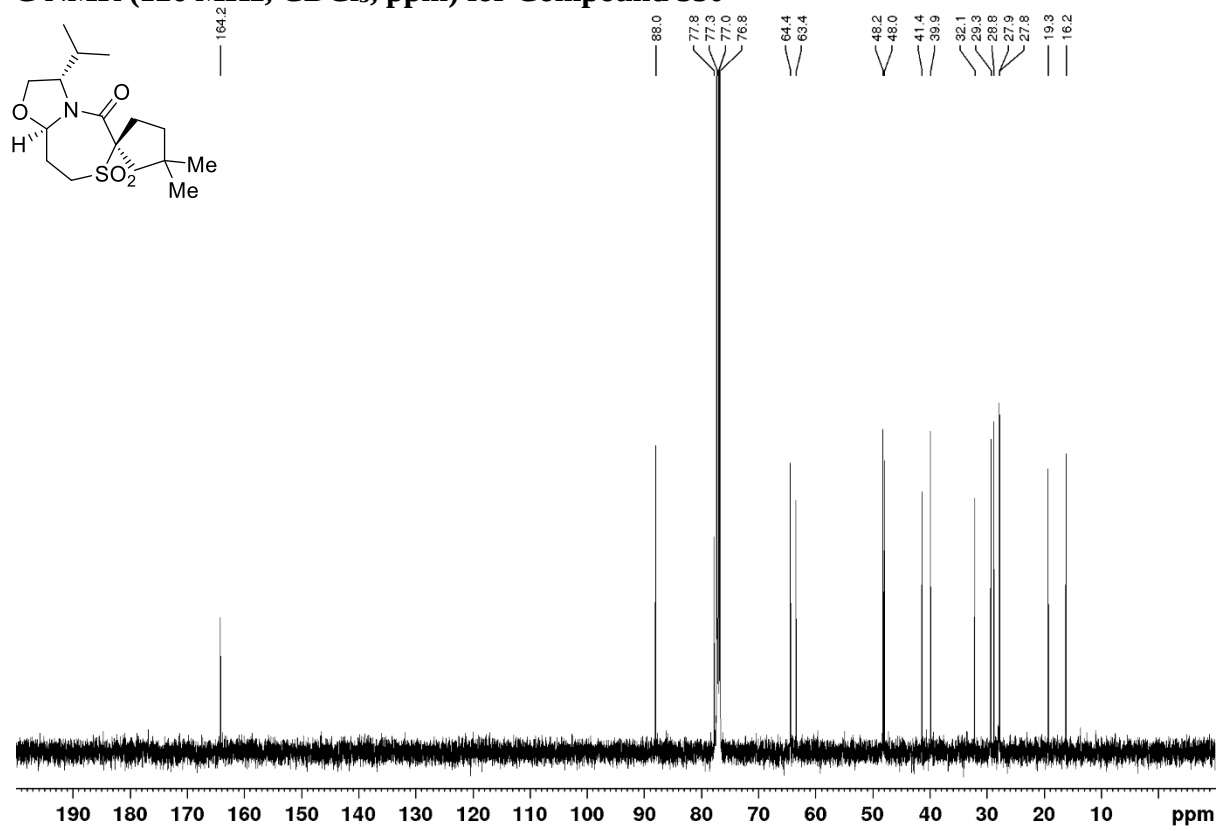

HSQC (500 MHz, $CDCl_3$, ppm) for Compound 350

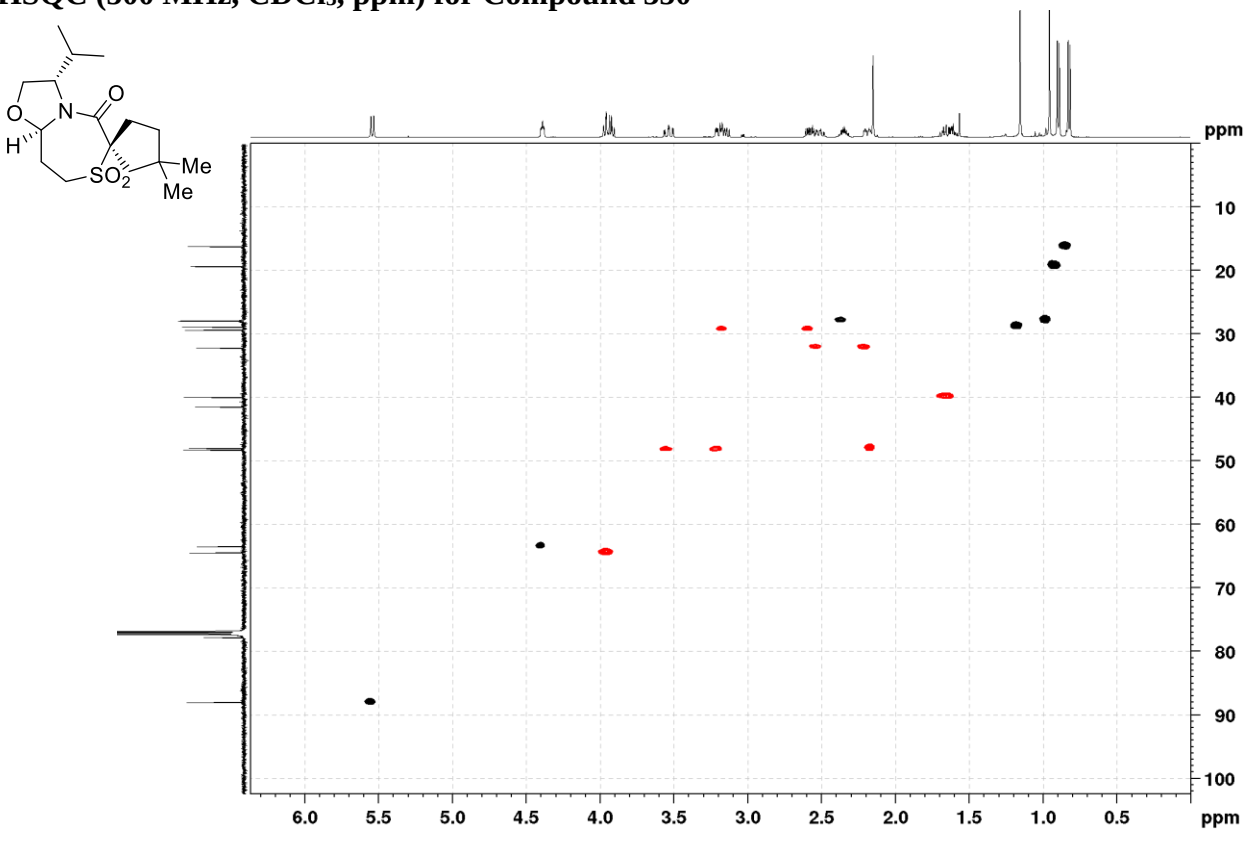

NOESY (500 MHz, $CDCl_3$, ppm) for Compound 350

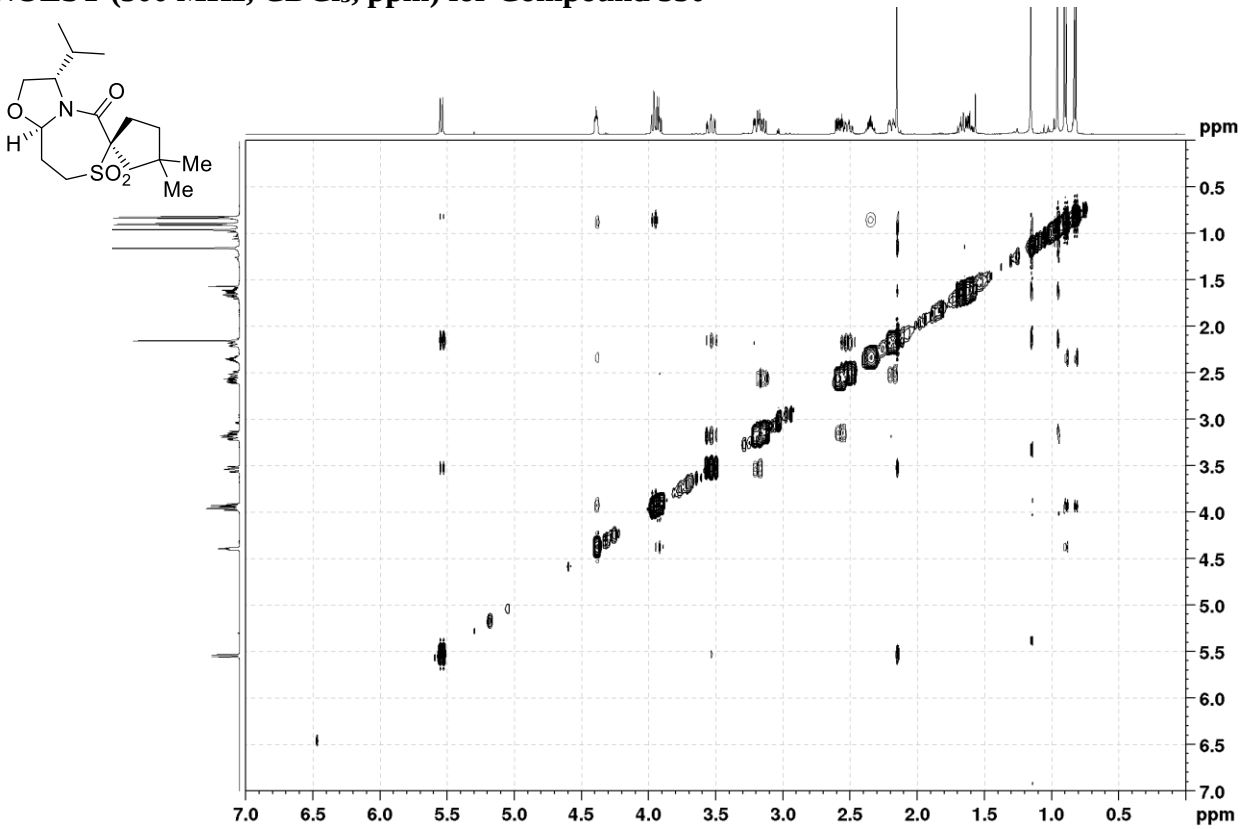

^{1}H NMR (500 MHz, $CDCl_3$, ppm) for Compound 353

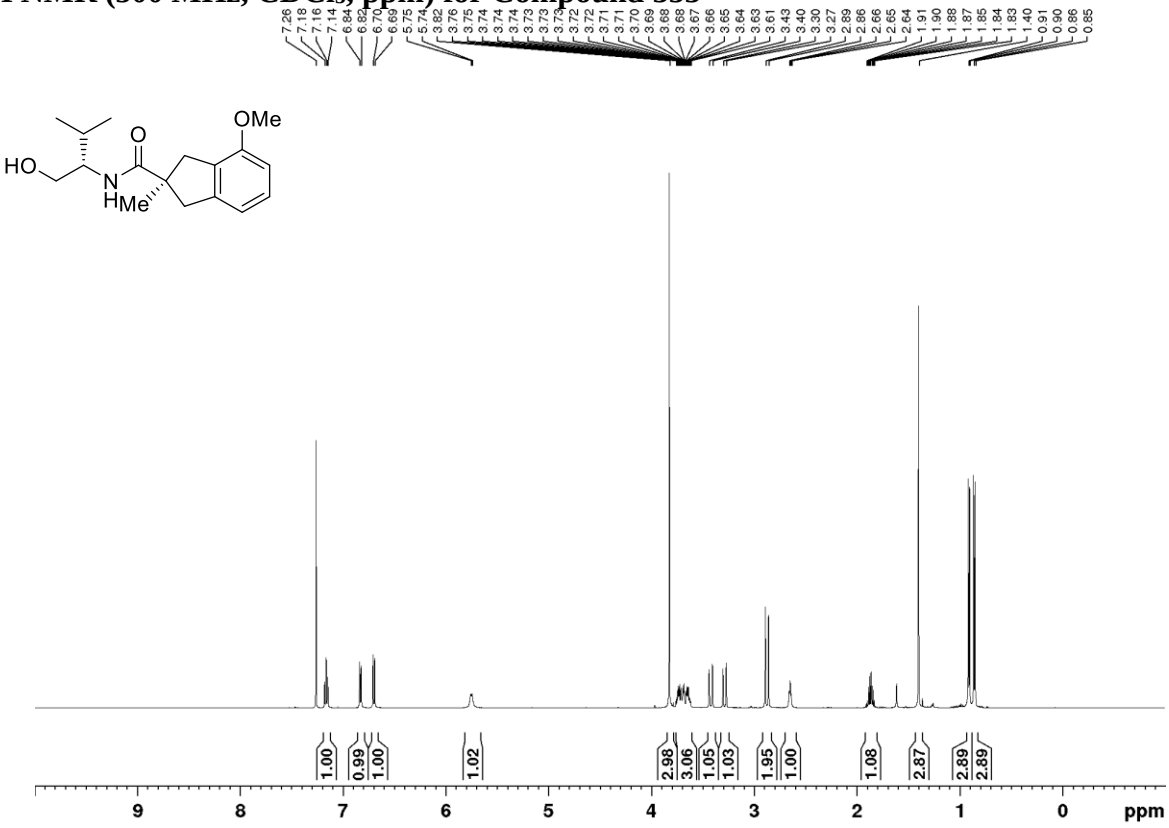

^{13}C NMR (126 MHz, $CDCl_3$, ppm) for Compound 353

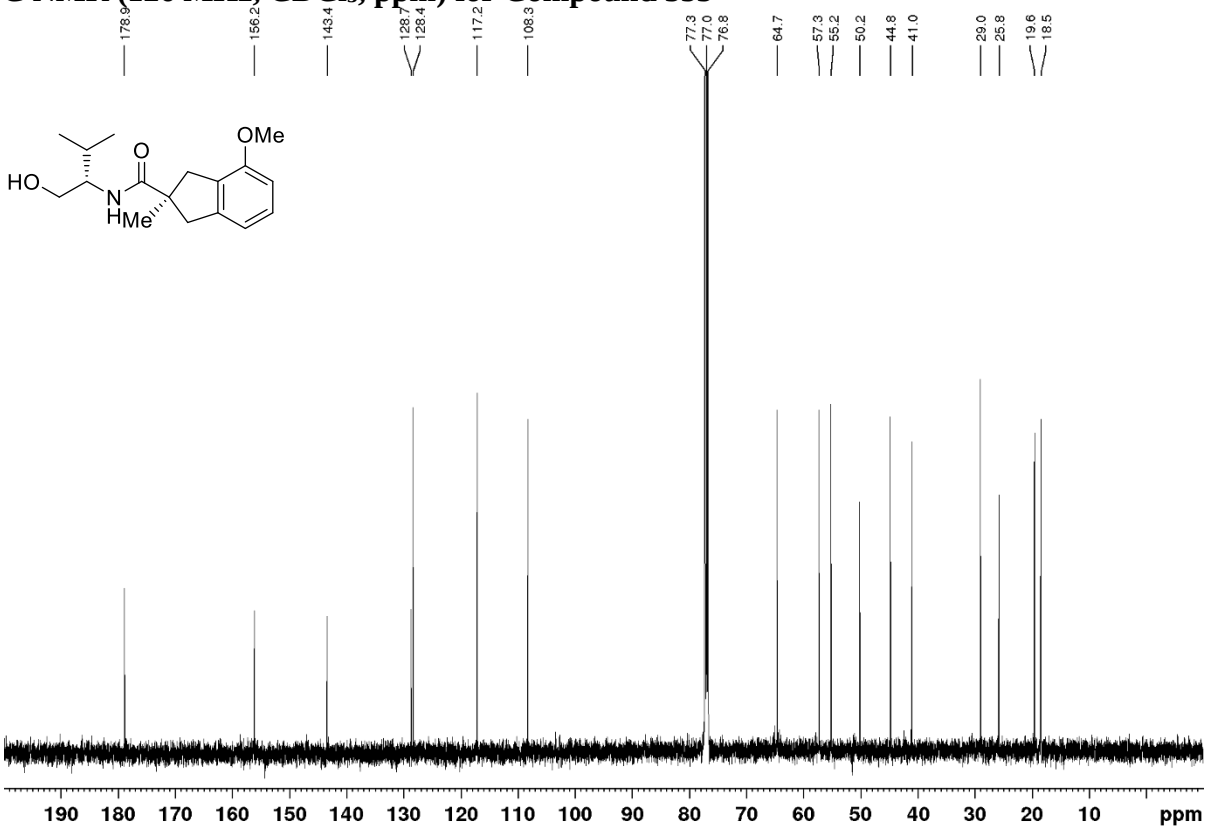

^{1}H NMR (500 MHz, $CDCl_3$, ppm) for Compound 354

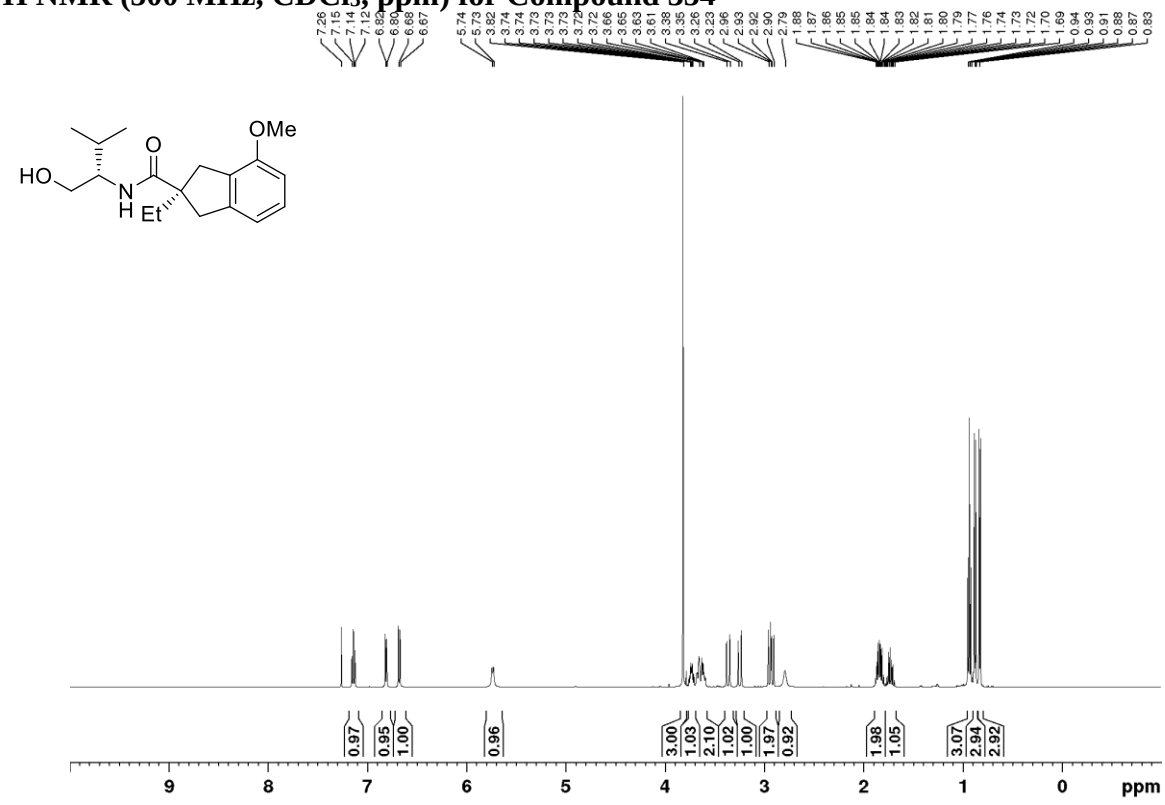

^{13}C NMR (126 MHz, $CDCl_3$, ppm) for Compound 354

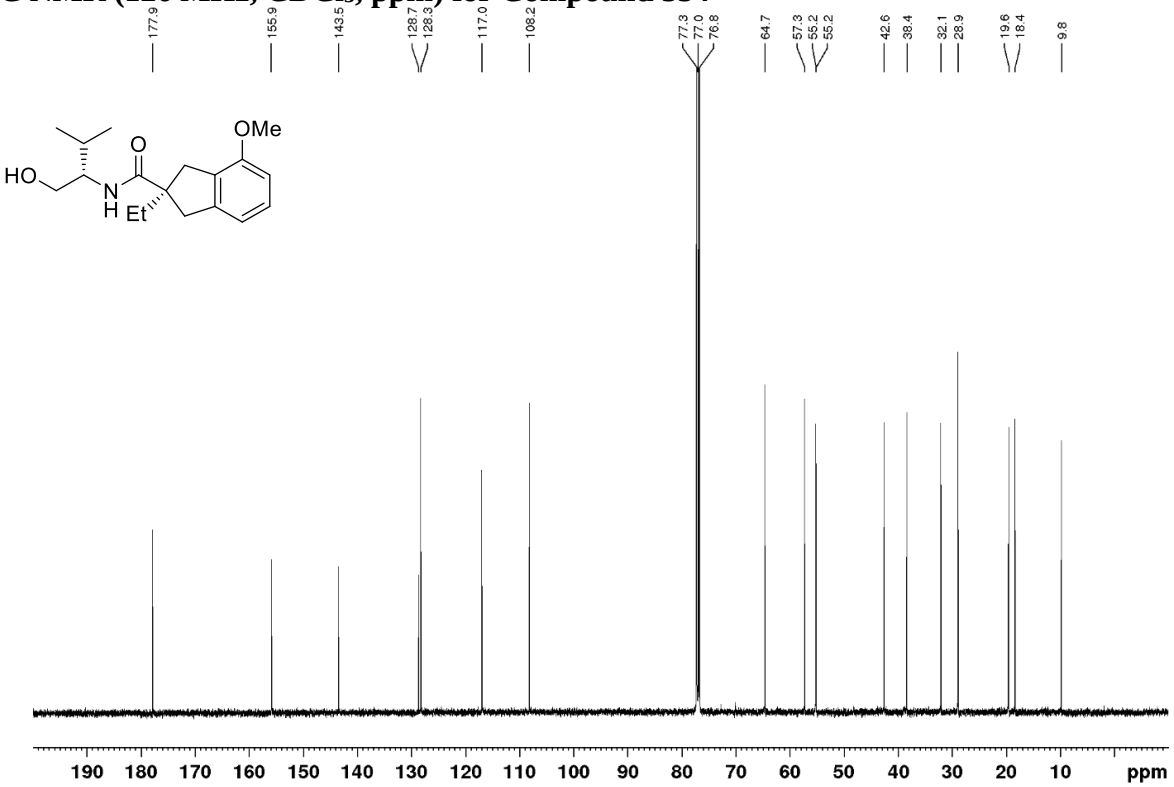

^{1}H NMR (500 MHz, $CDCl_3$, ppm) for Compound 355

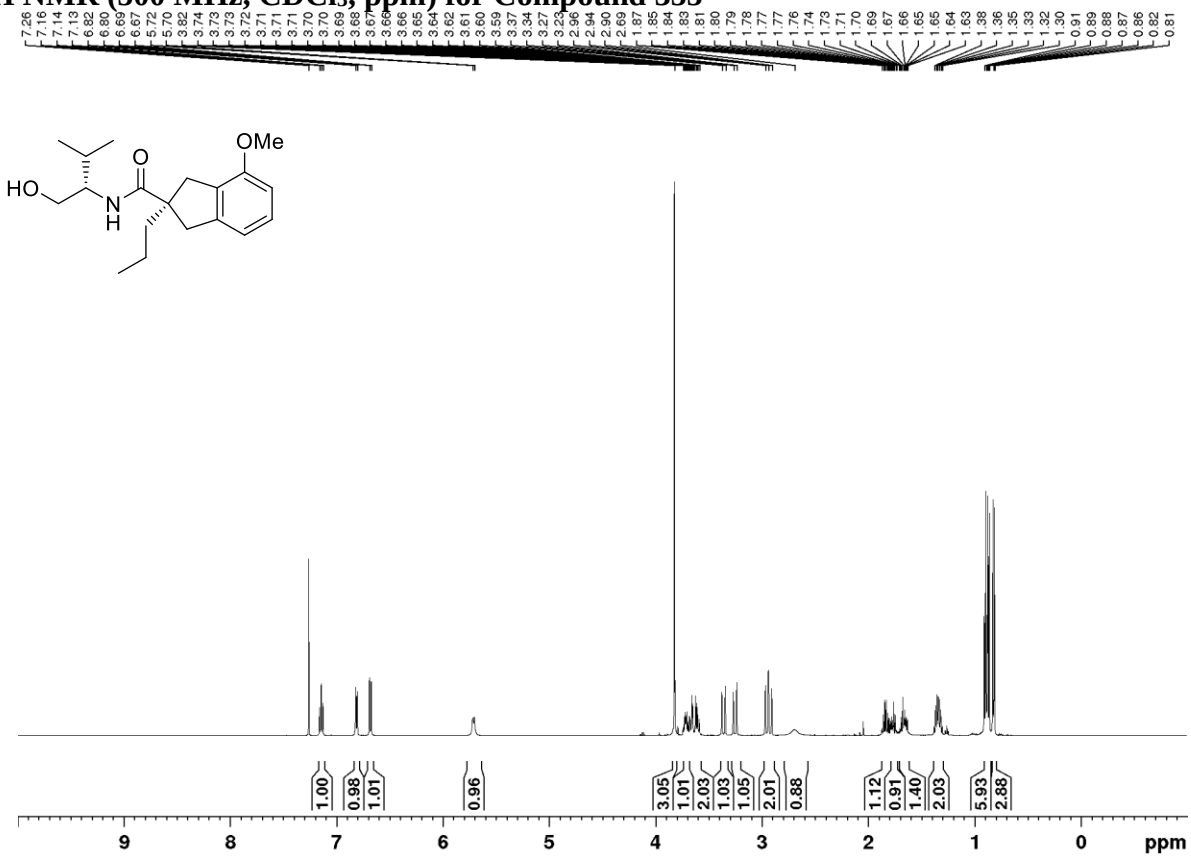

^{13}C NMR (126 MHz, $CDCl_3$, ppm) for Compound 355

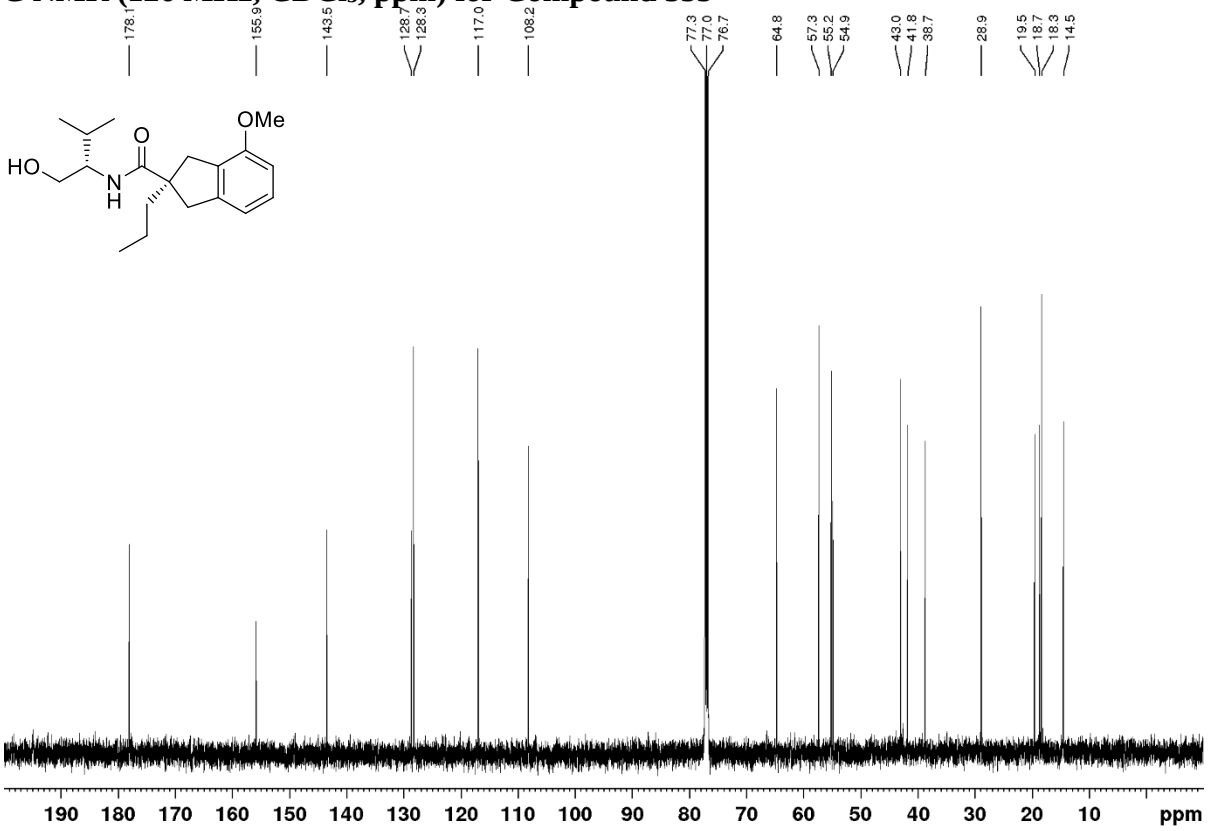

^{1}H NMR (500 MHz, $CDCl_3$, ppm) for Compound 356

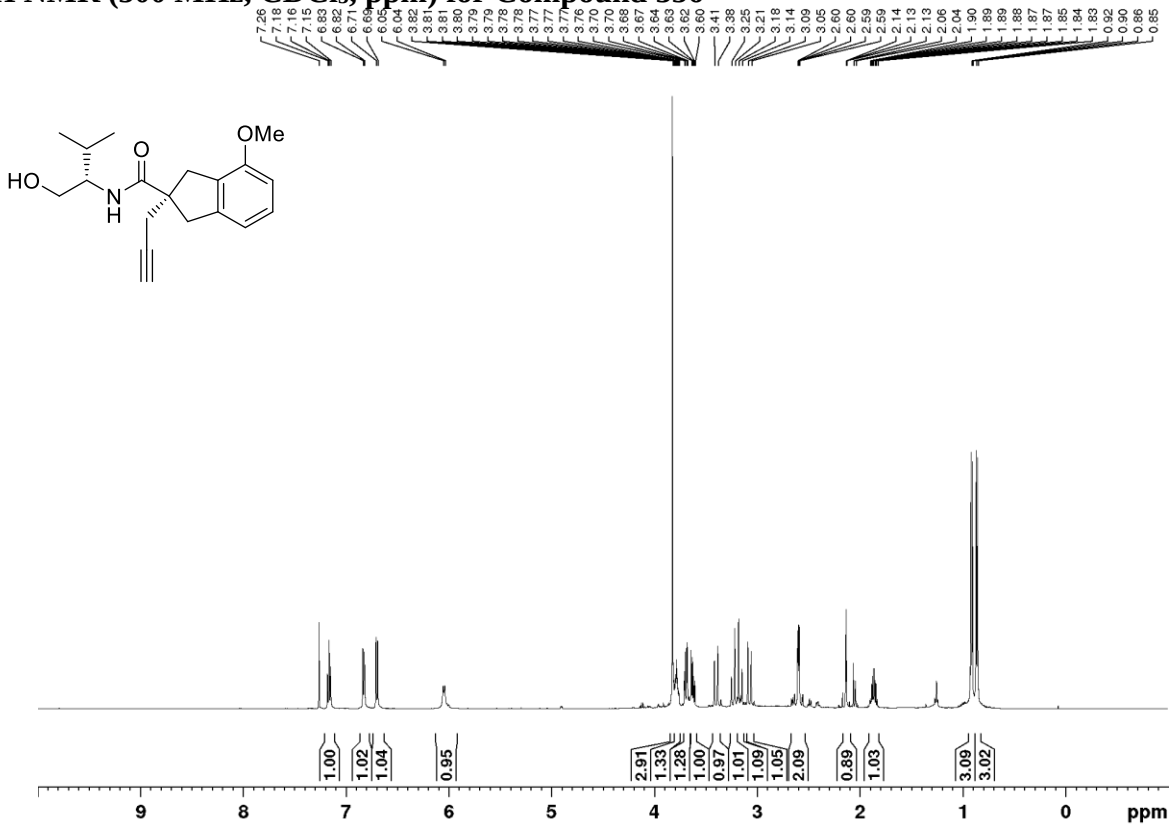

^{13}C NMR (126 MHz, $CDCl_3$, ppm) for Compound 356

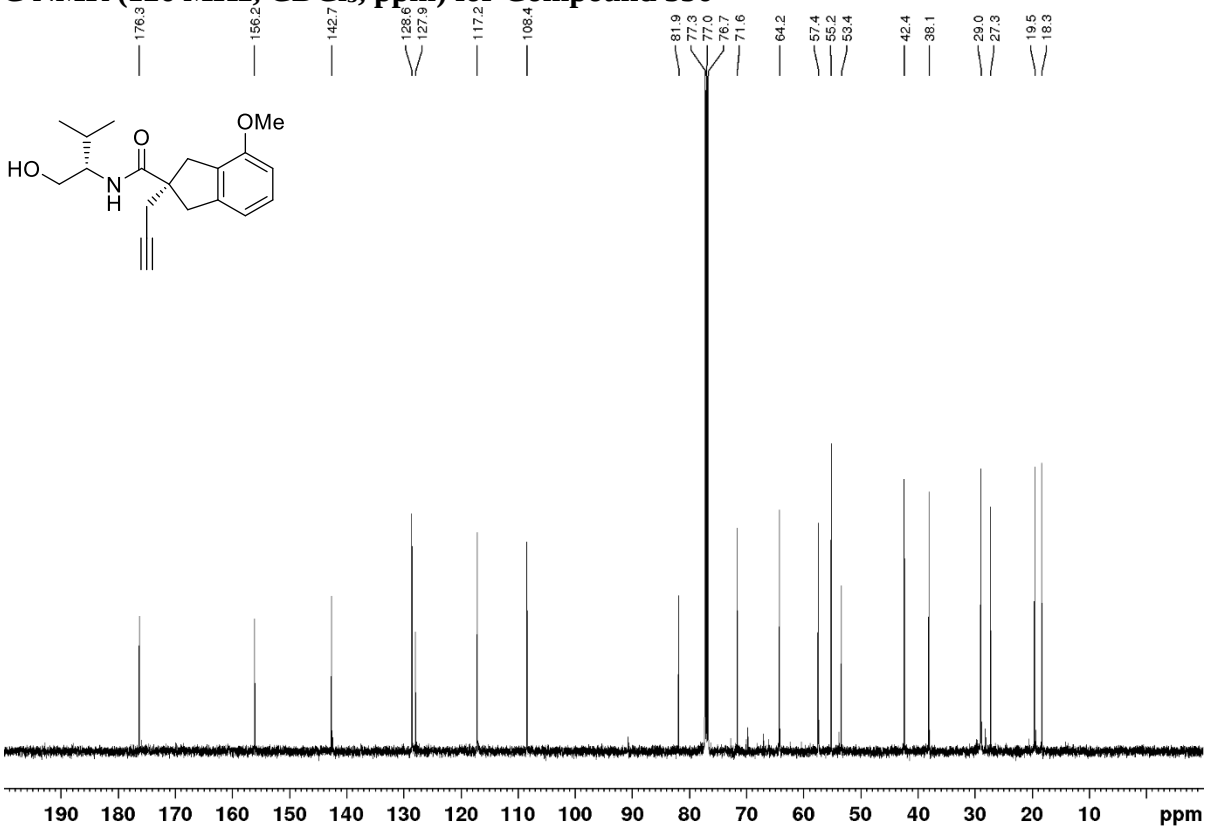

^{1}H NMR (500 MHz, $CDCl_3$, ppm) for Compound 357

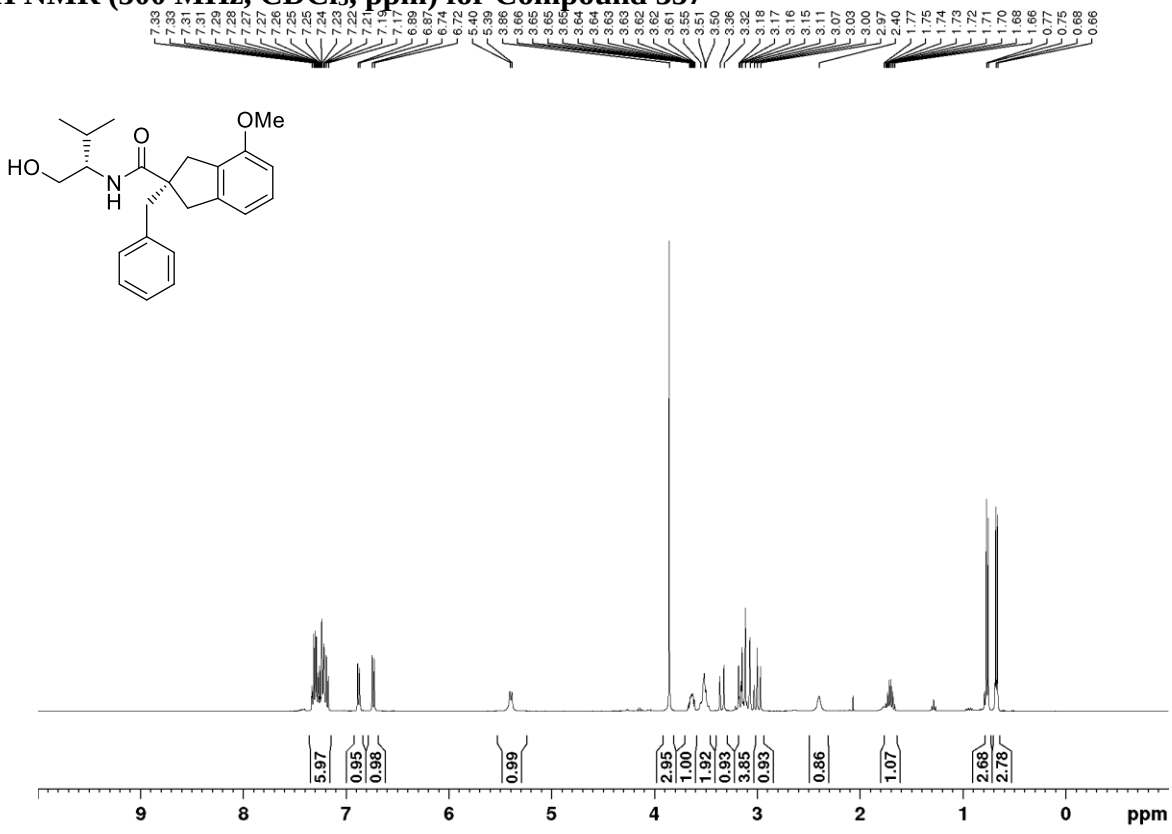

^{13}C NMR (126 MHz, $CDCl_3$, ppm) for Compound 357

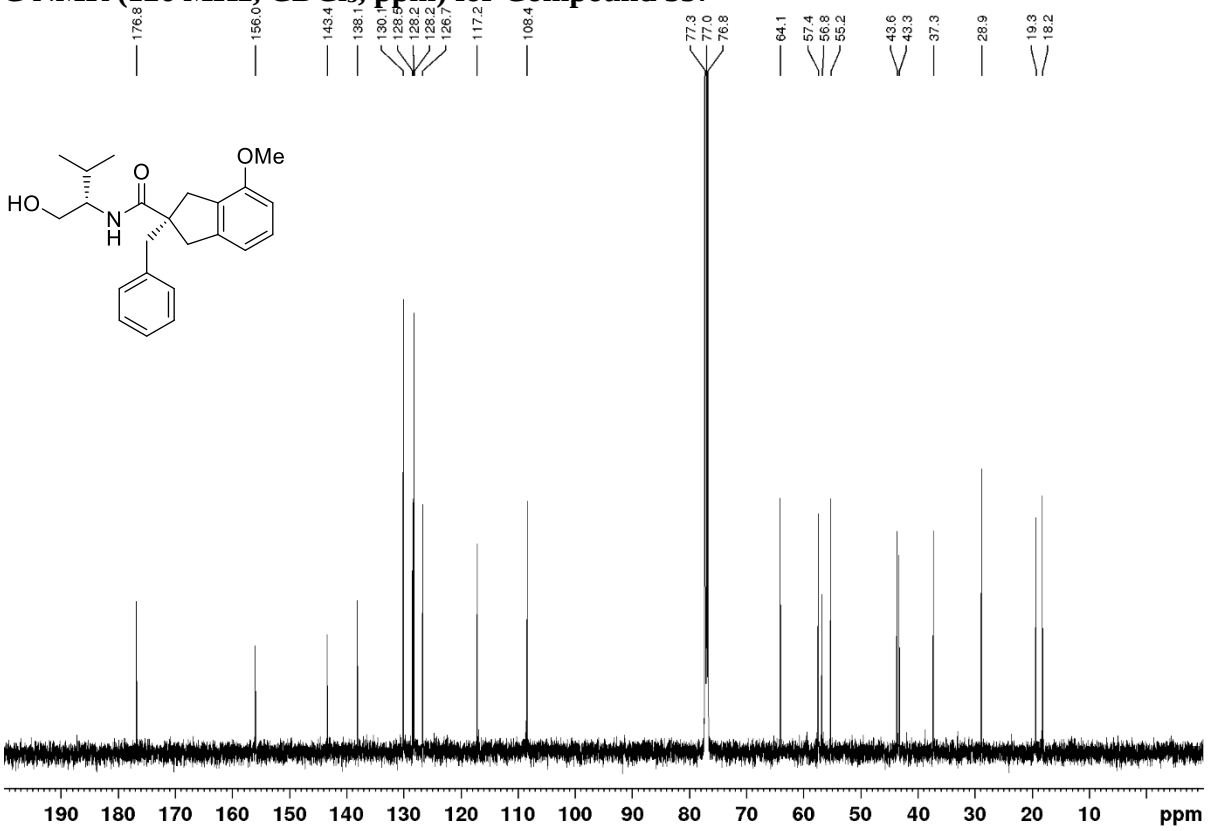

^{1}H NMR (500 MHz, $CDCl_3$, ppm) for Compound 358

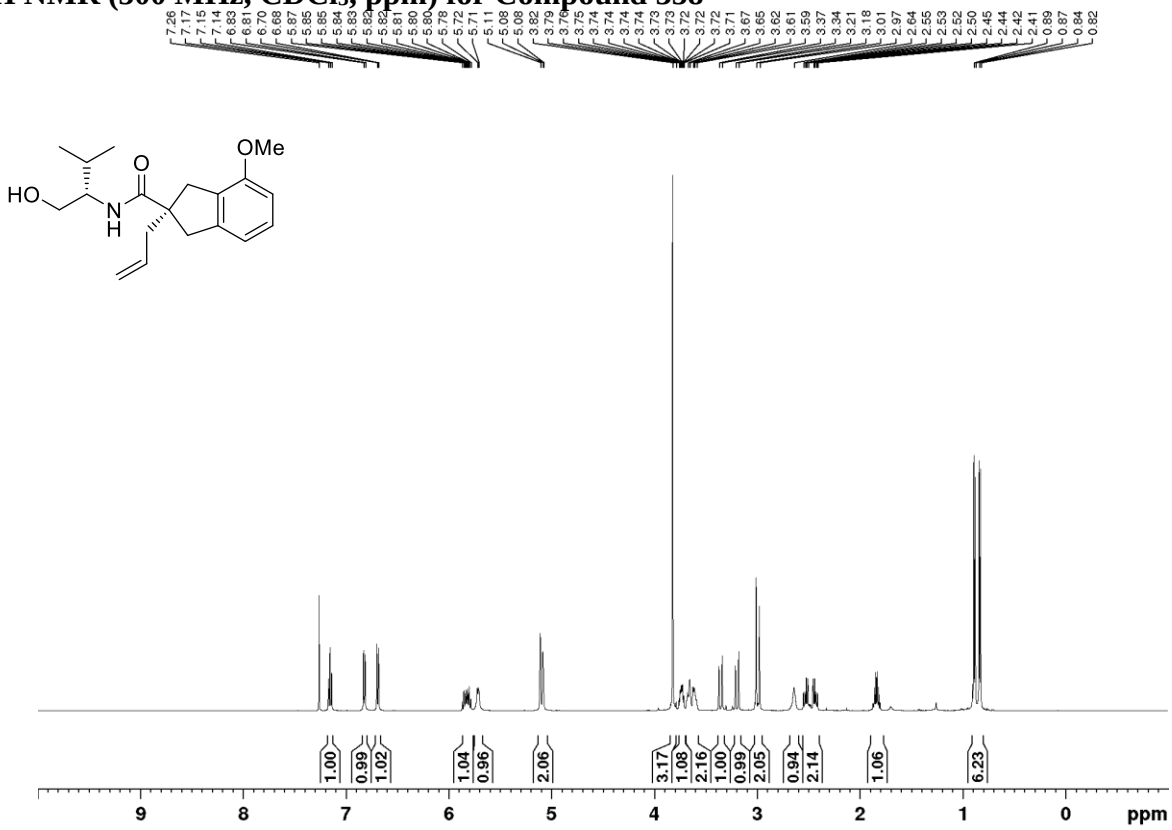

^{13}C NMR (126 MHz, $CDCl_3$, ppm) for Compound 358

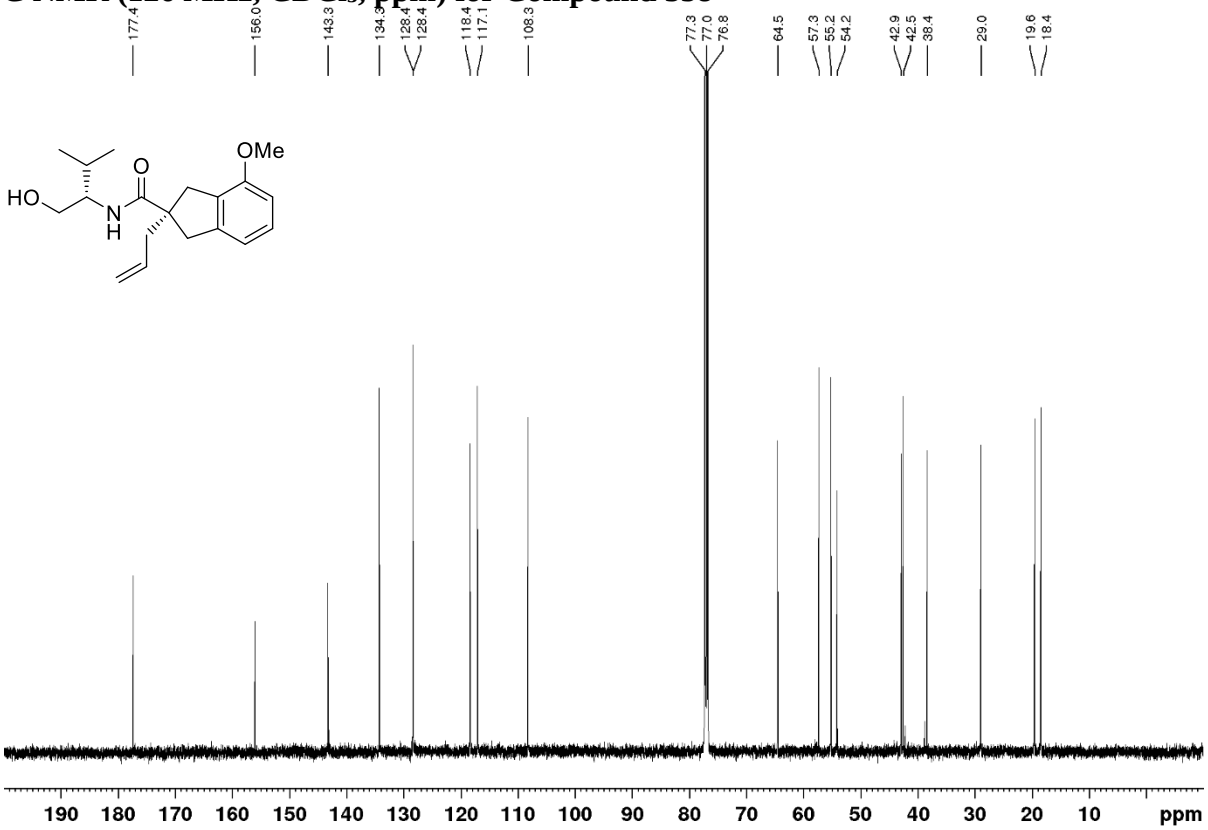

^{1}H NMR (500 MHz, $CDCl_3$, ppm) for Compound 359

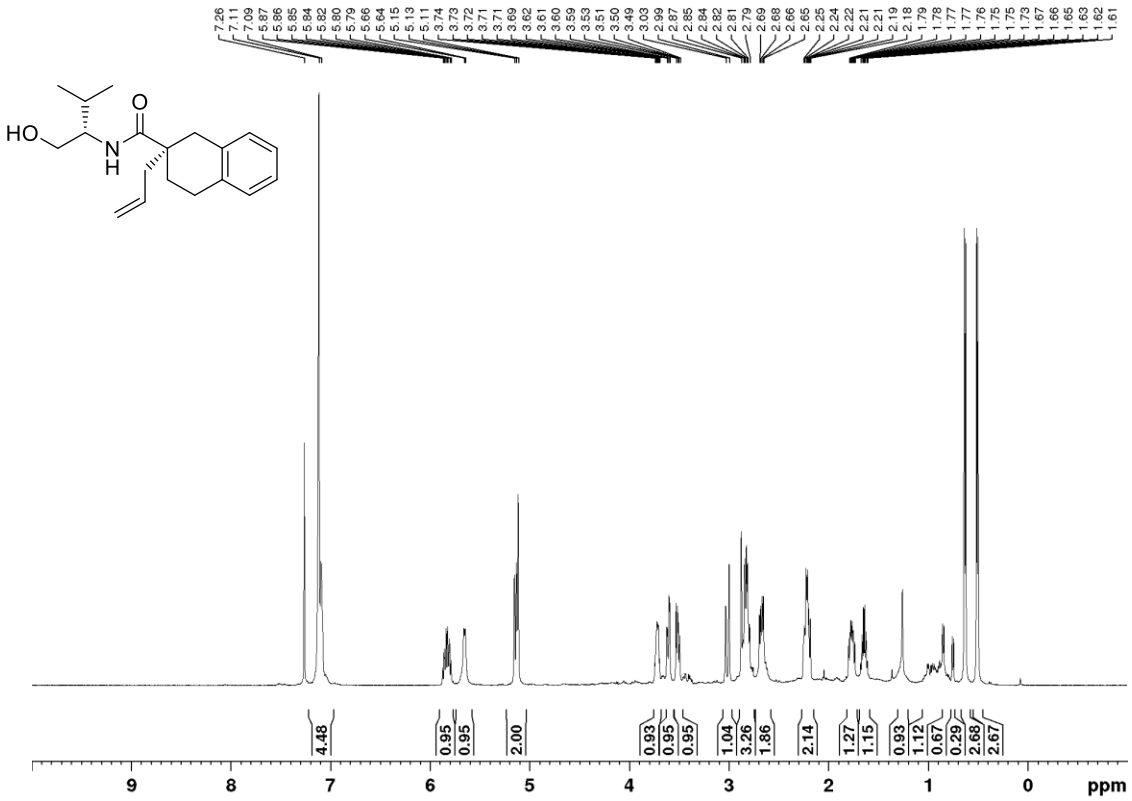

^{13}C NMR (126 MHz, $CDCl_3$) for Compound 359

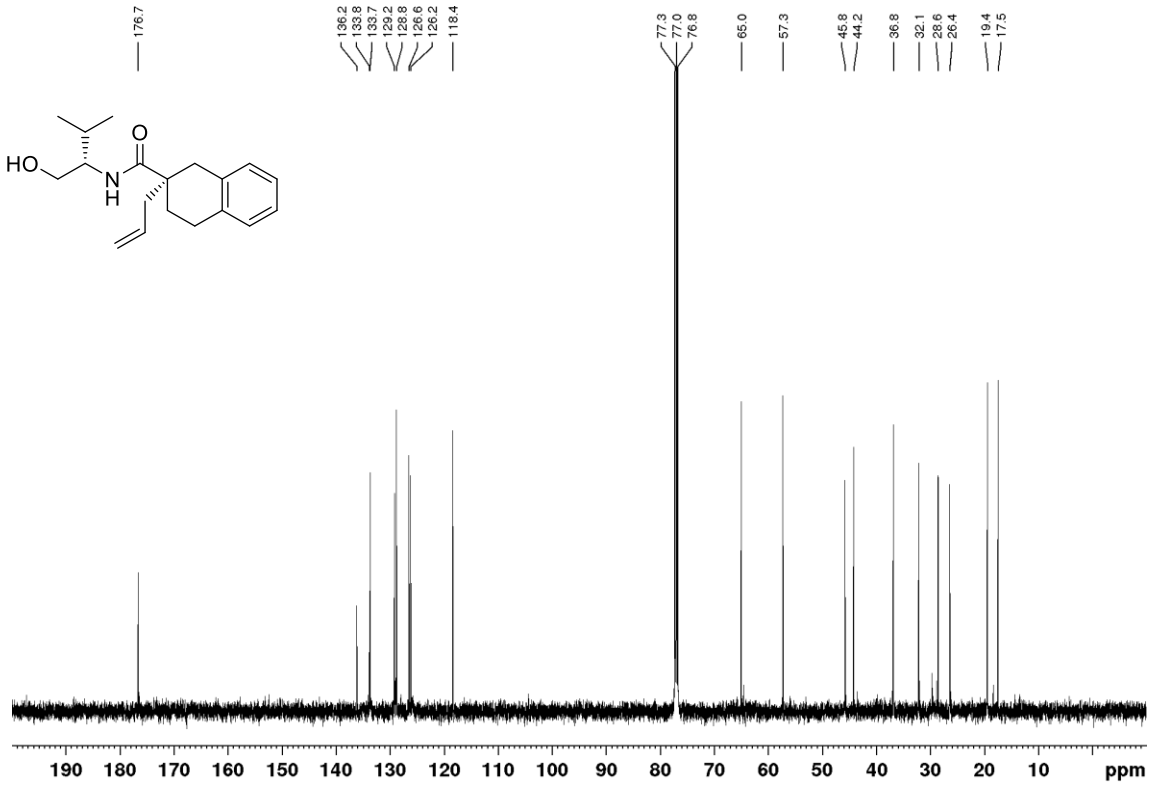

^{1}H NMR (500 MHz, $CDCl_3$, ppm) for Compound 361

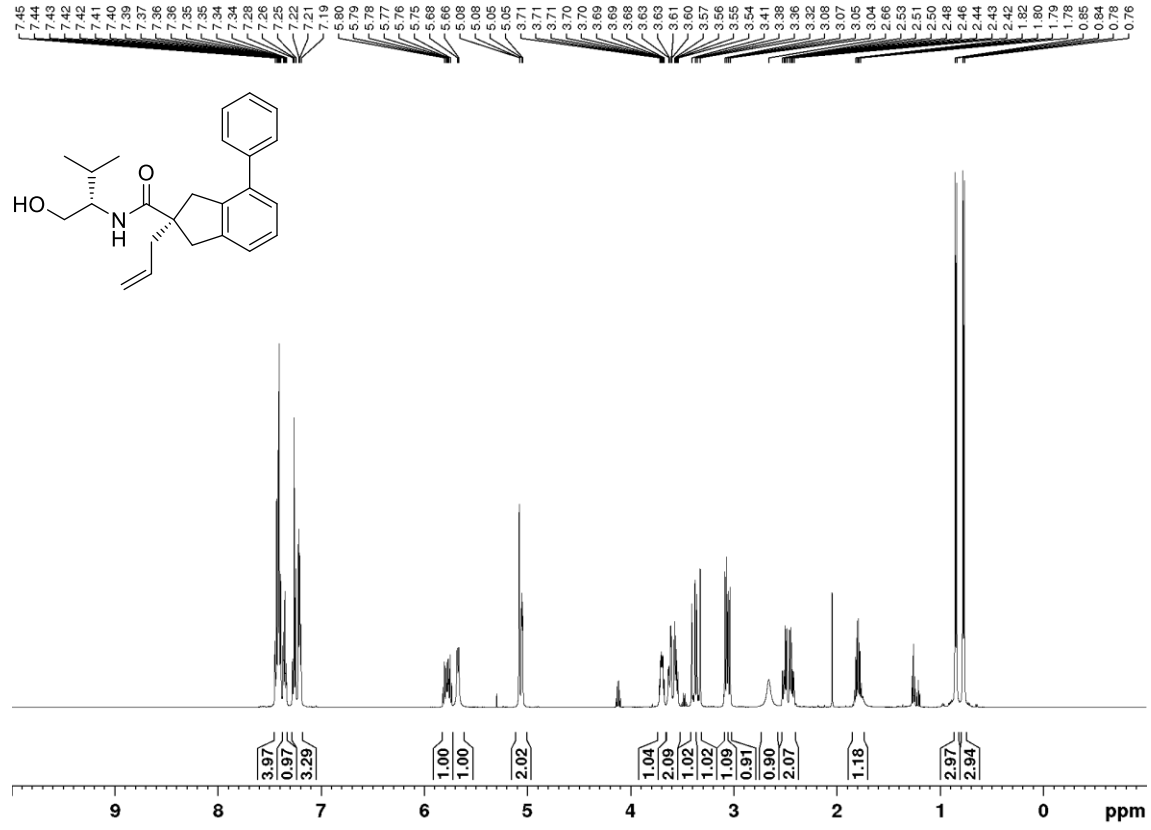

^{13}C NMR (126 MHz, $CDCl_3$, ppm) for Compound 361

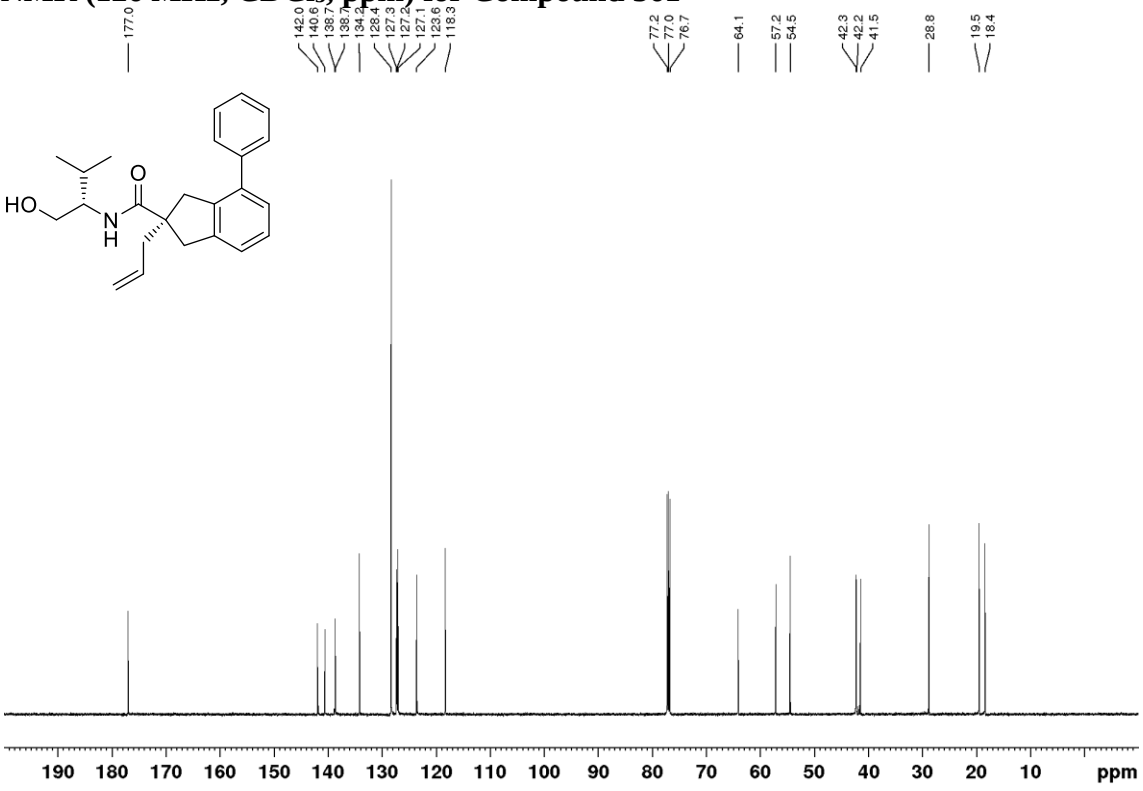

^{1}H NMR (500 MHz, $CDCl_3$, ppm) for Compound 362

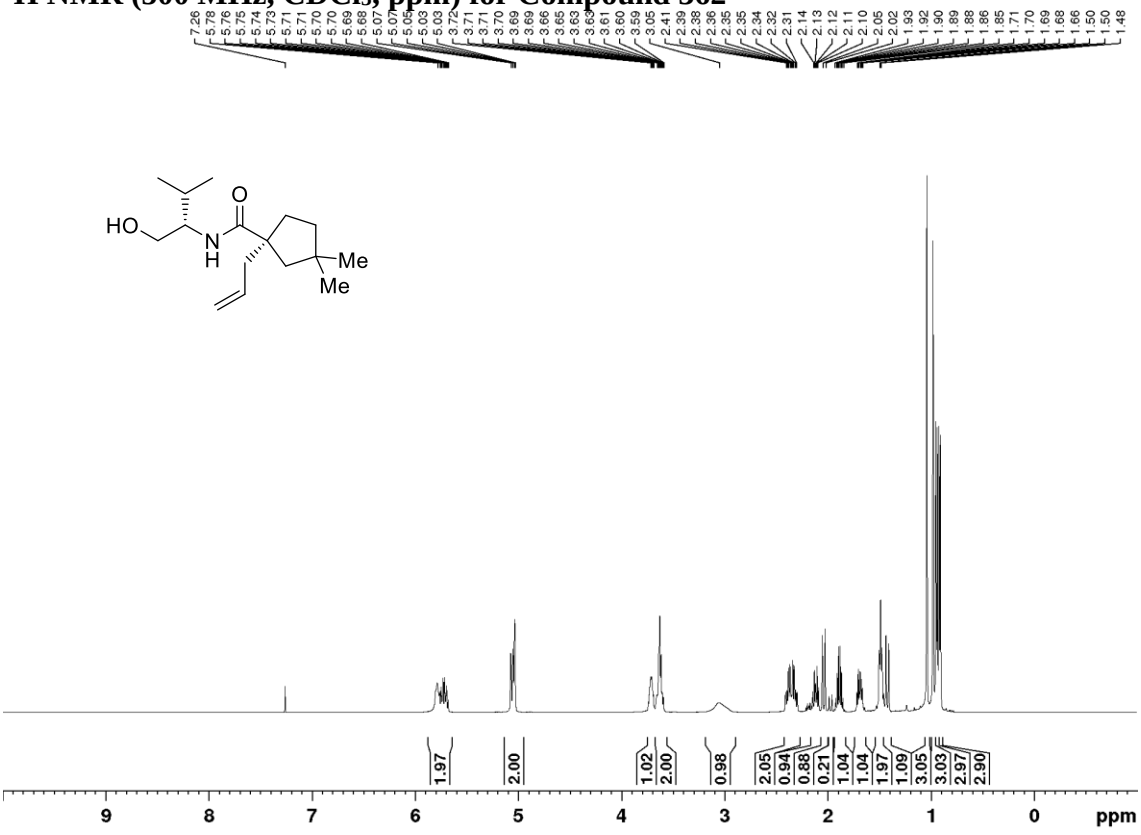

^{13}C NMR (126 MHz, $CDCl_3$, ppm) for Compound 362

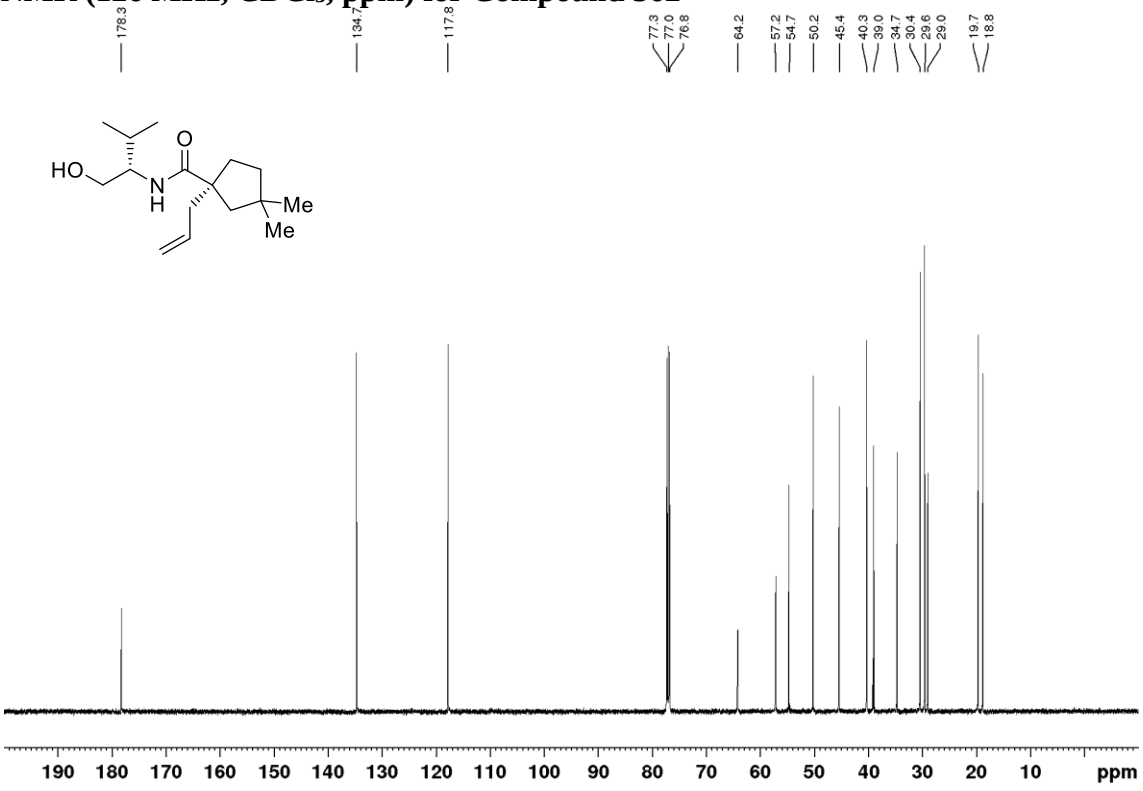

^{1}H NMR (500 MHz, $CDCl_3$, ppm) for Compound 363

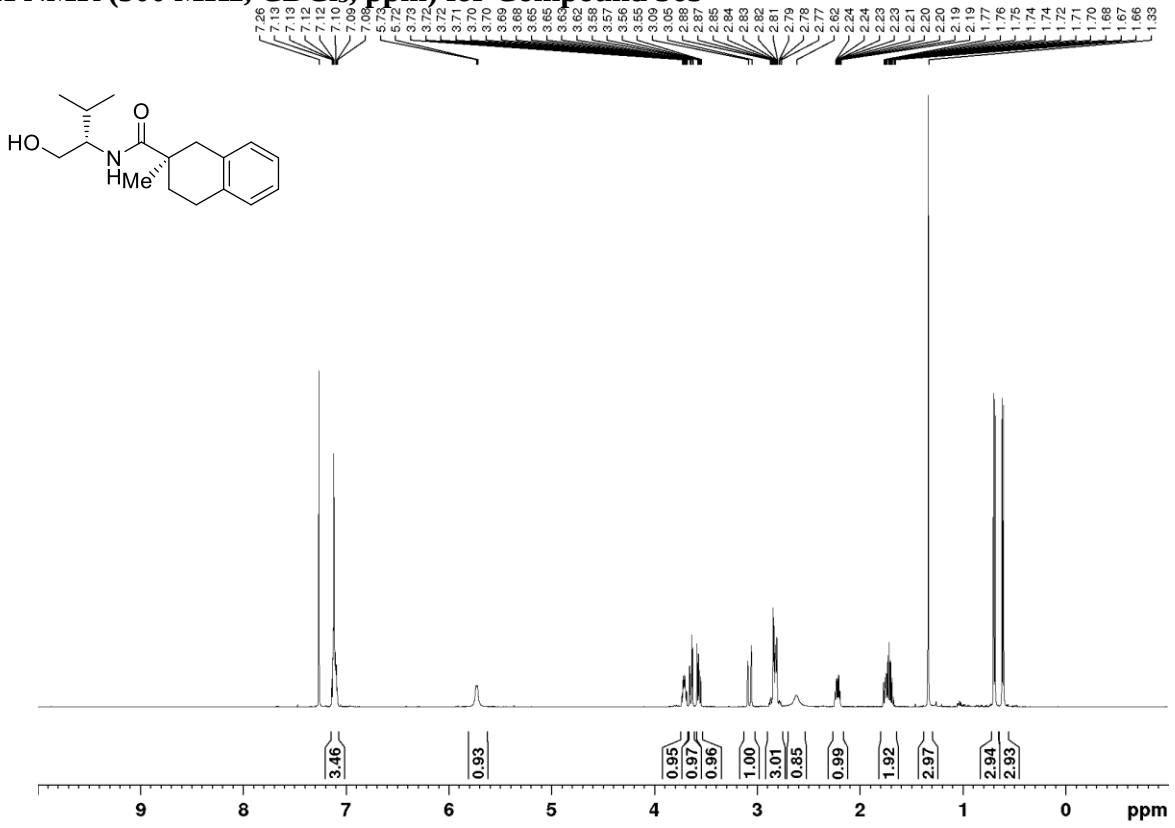

^{13}C NMR (126 MHz, $CDCl_3$, ppm) for Compound 363

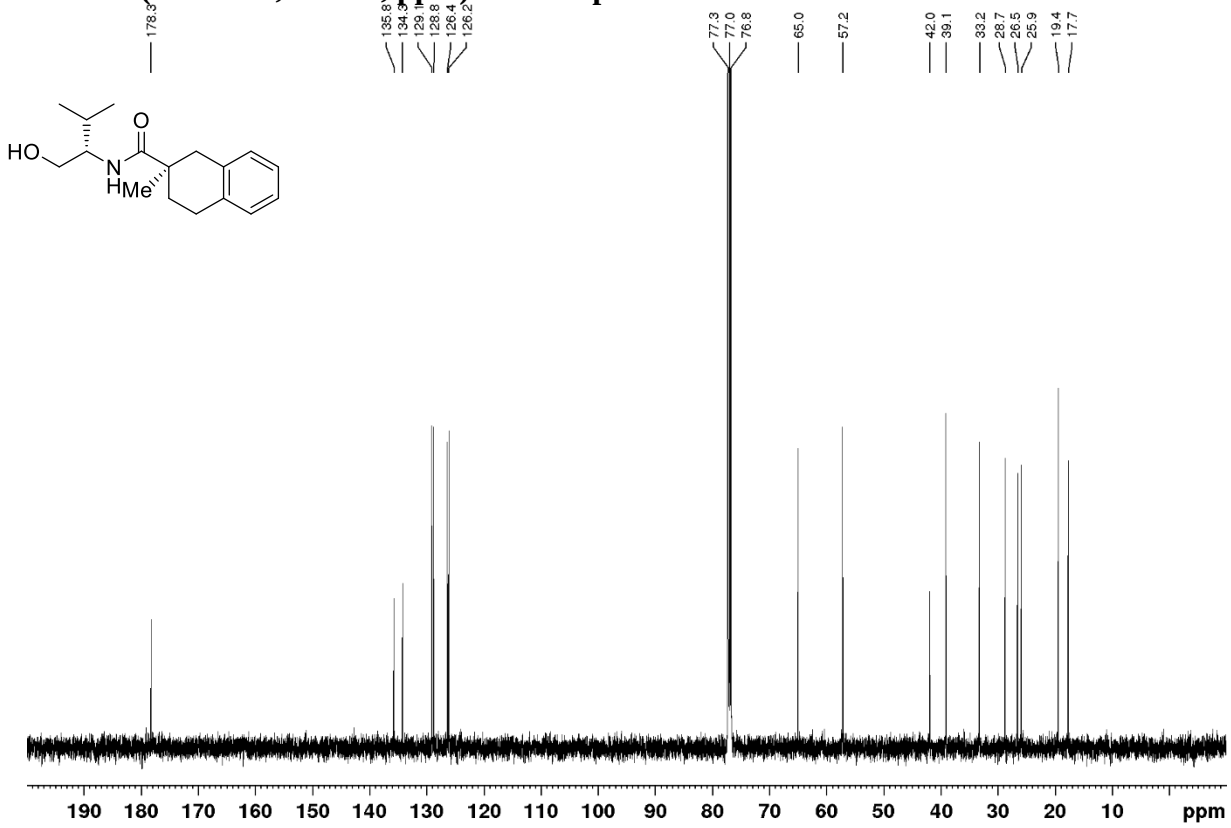

^{1}H NMR (500 MHz, $CDCl_3$, ppm) for Compound 364

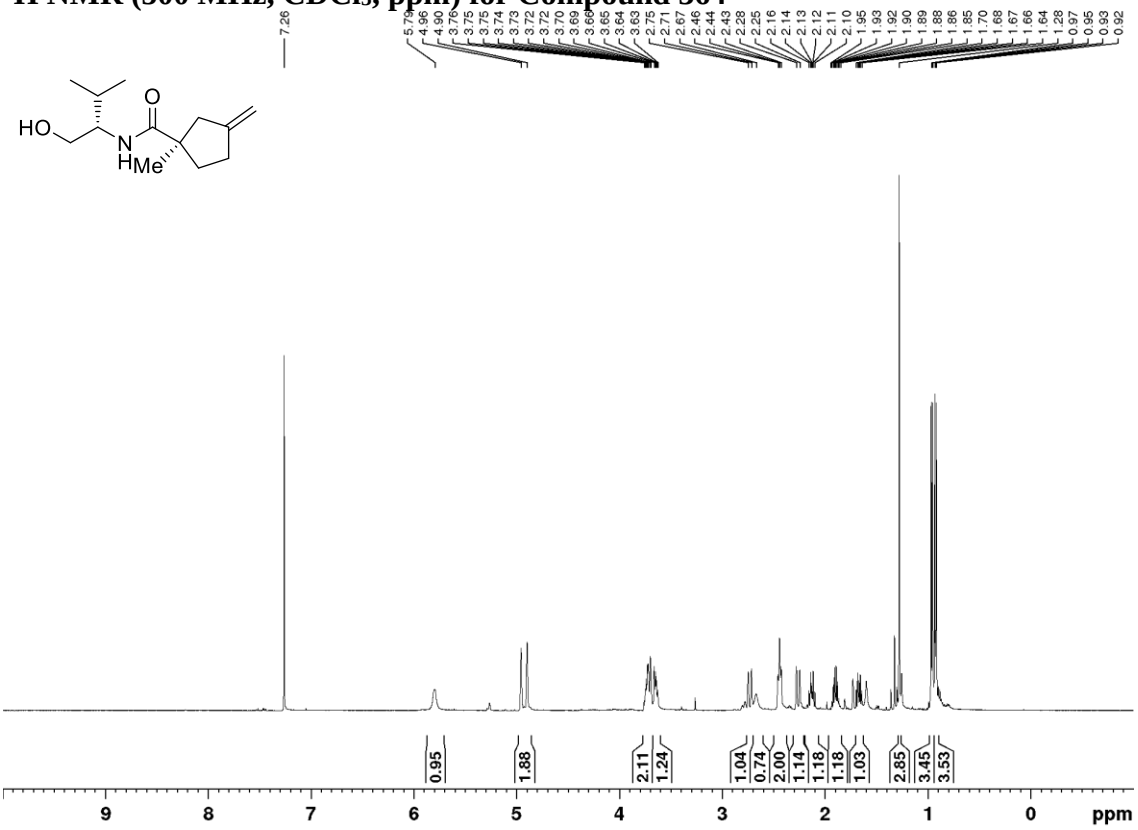

^{13}C NMR (126 MHz, $CDCl_3$, ppm) for Compound 364

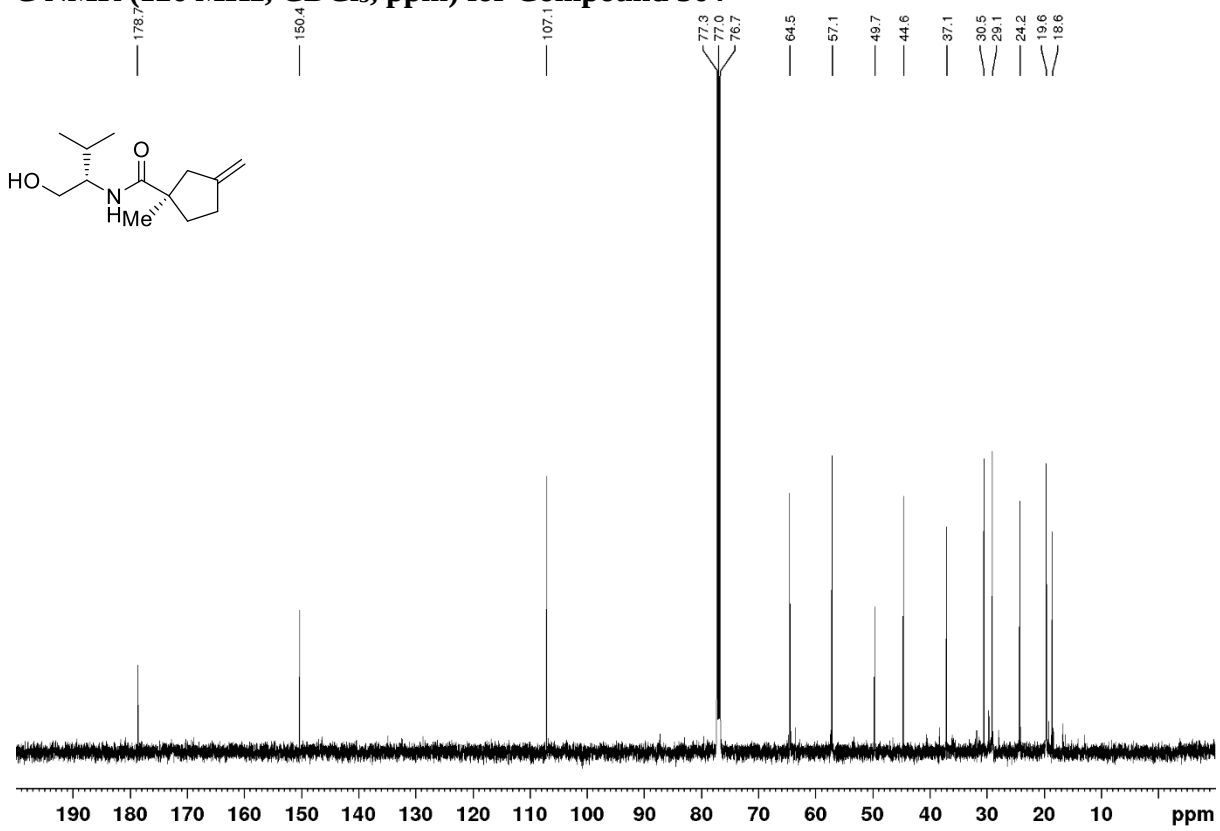

^{1}H NMR (500 MHz, $CDCl_3$, ppm) for Compound 365

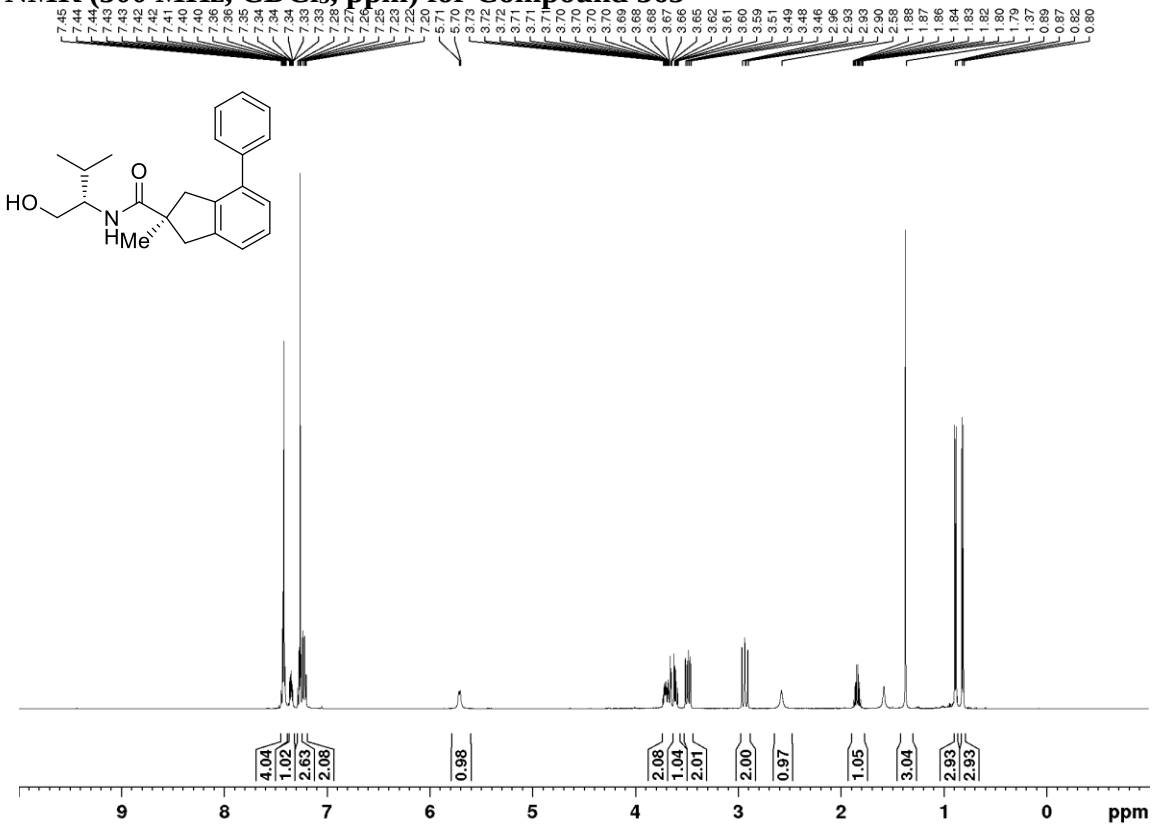

^{13}C NMR (126 MHz, $CDCl_3$, ppm) for Compound 365

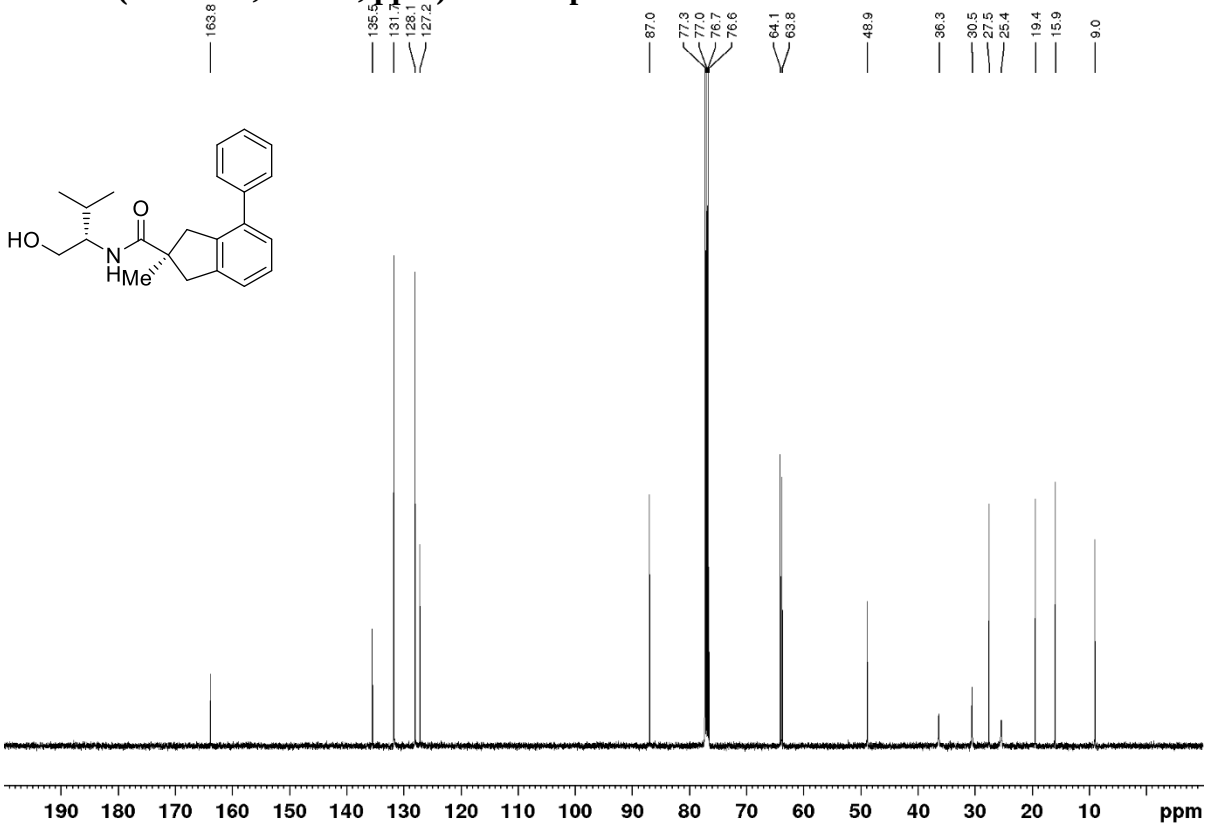

^{1}H NMR (500 MHz, $CDCl_3$) for Compound 366

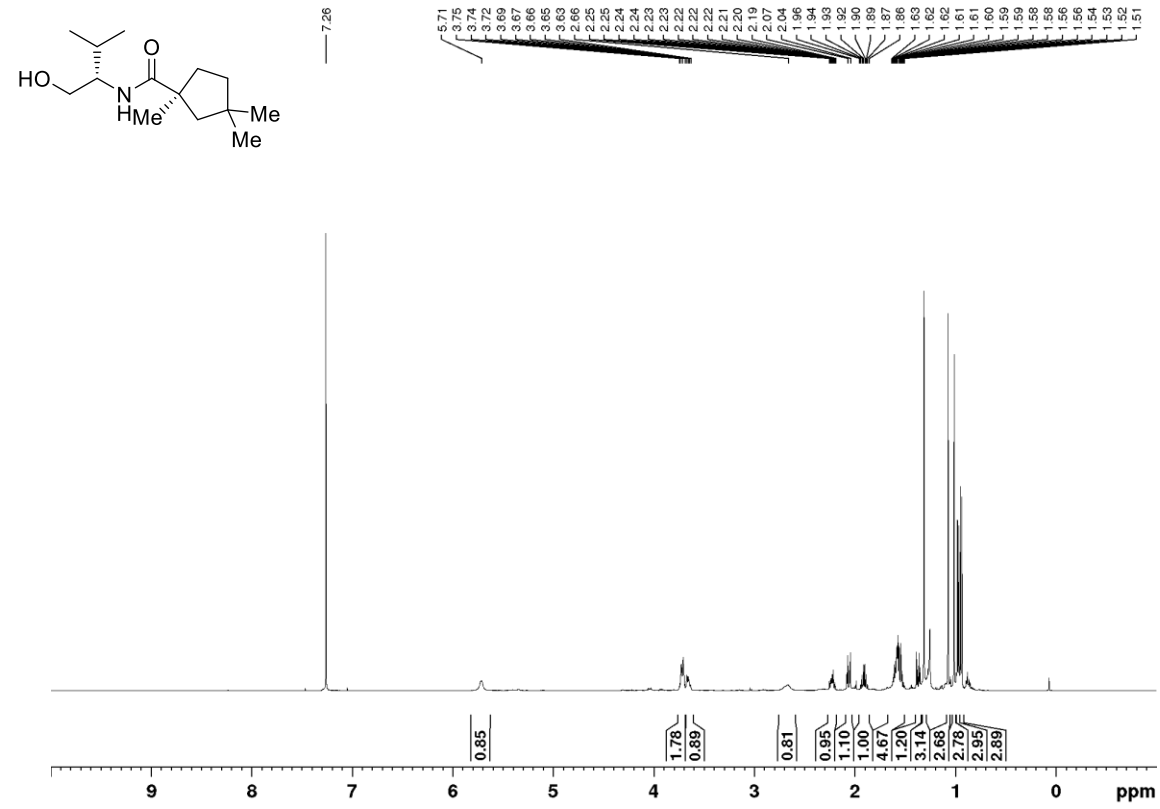

^{13}C NMR (126 MHz, $CDCl_3$, ppm) for Compound 366

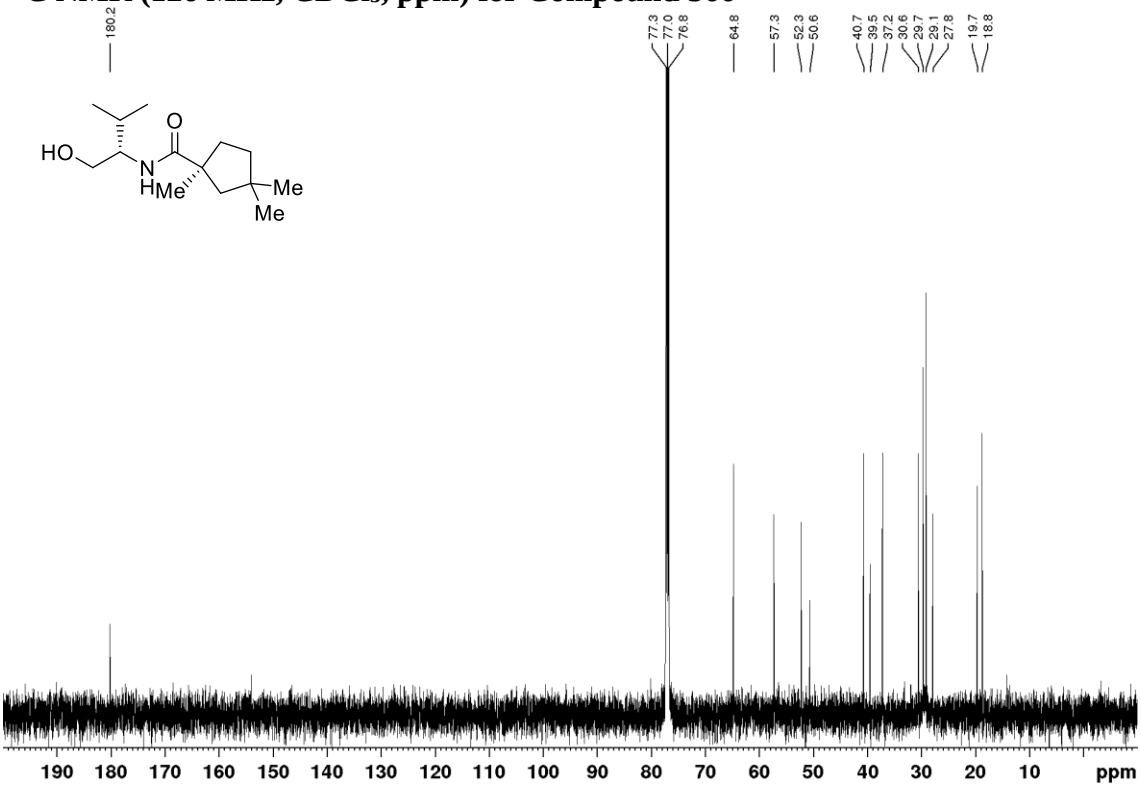

^{1}H NMR (500 MHz, $CDCl_3$, ppm) for Compound 367

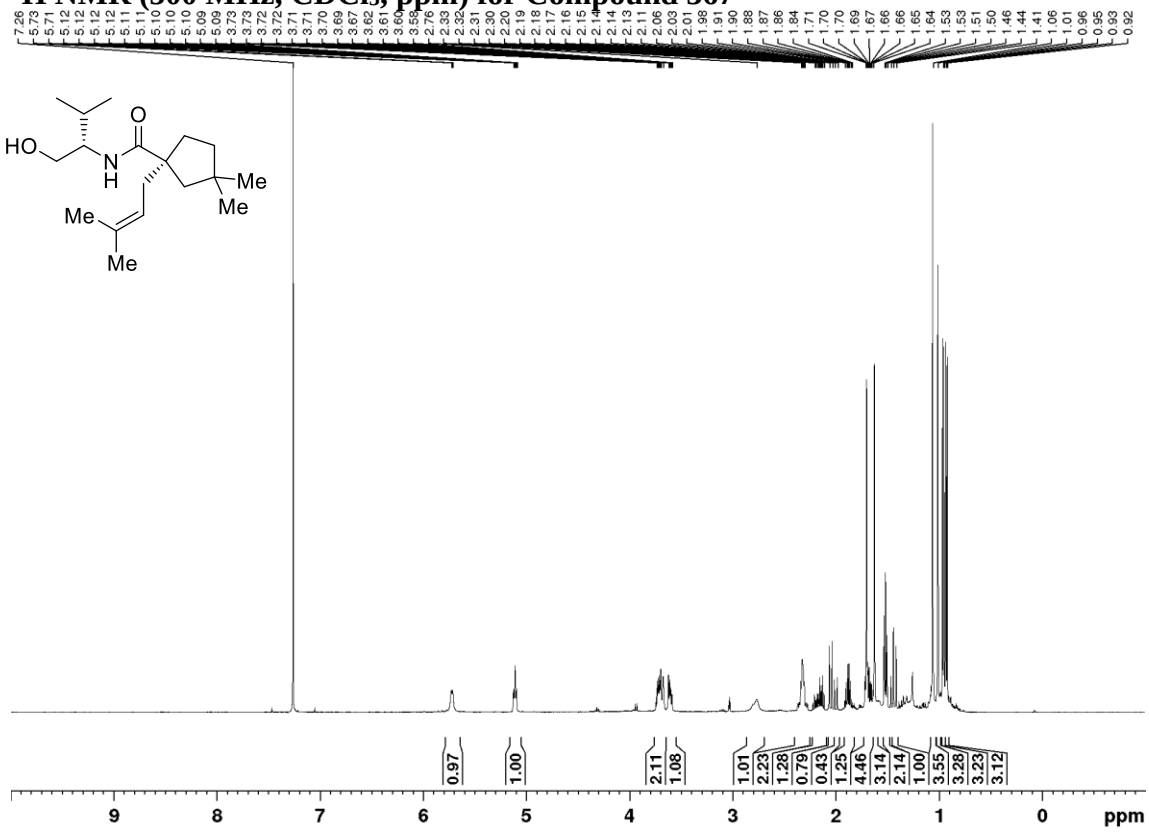

^{13}C NMR (126 MHz, $CDCl_3$, ppm) for Compound 367

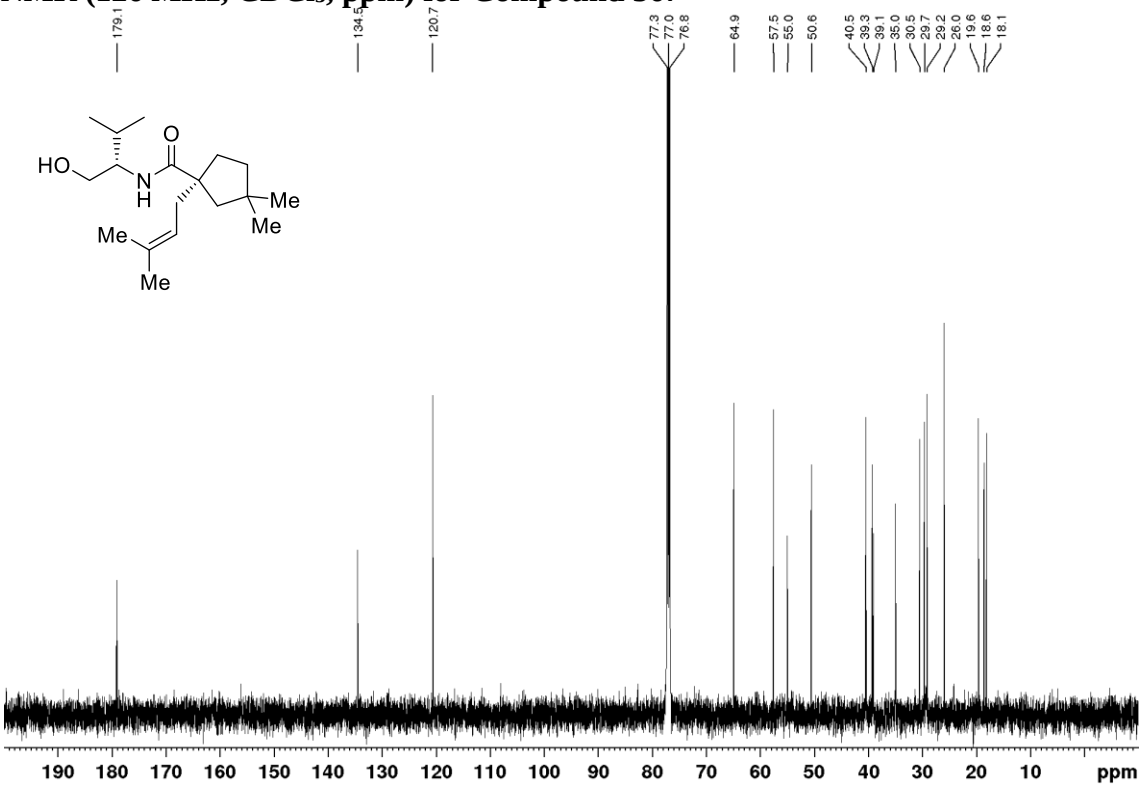

^{1}H NMR (500 MHz, $CDCl_3$, ppm) for Compound 399

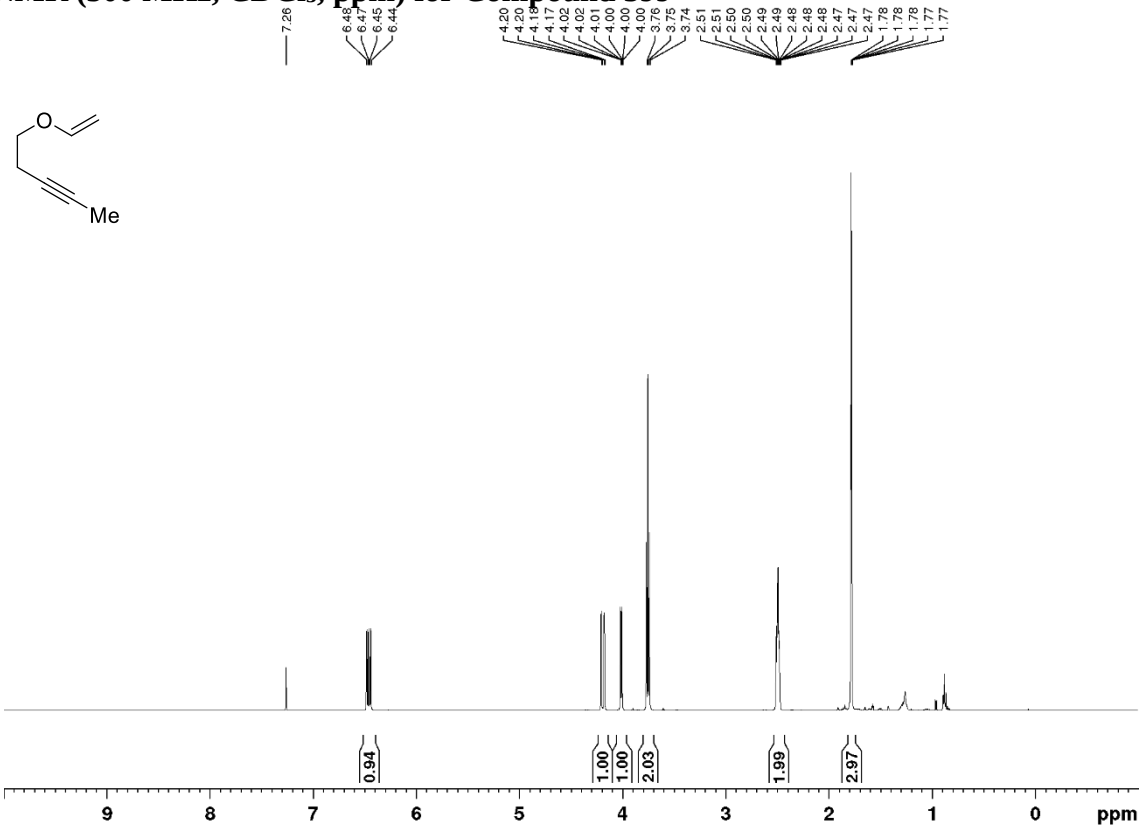

^{13}C NMR (126 MHz, $CDCl_3$, ppm) for Compound 399

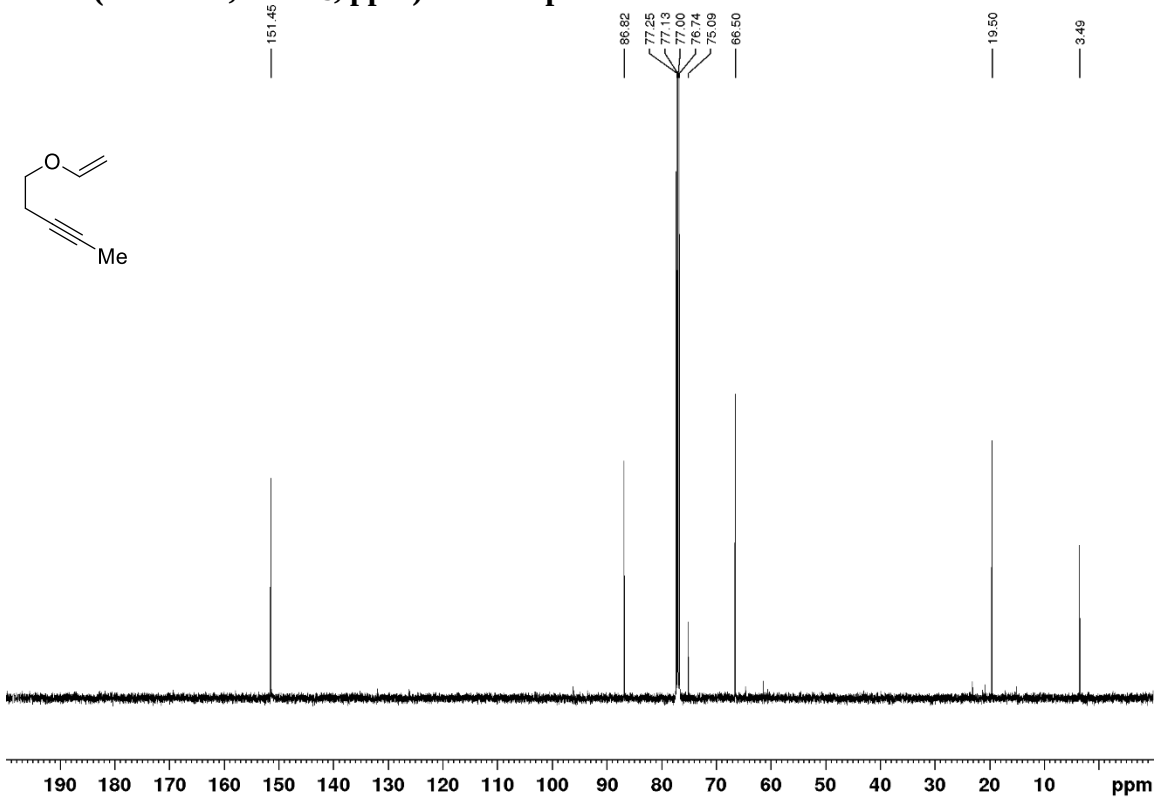

^{1}H NMR (500 MHz, $CDCl_3$, ppm) for Compound 398

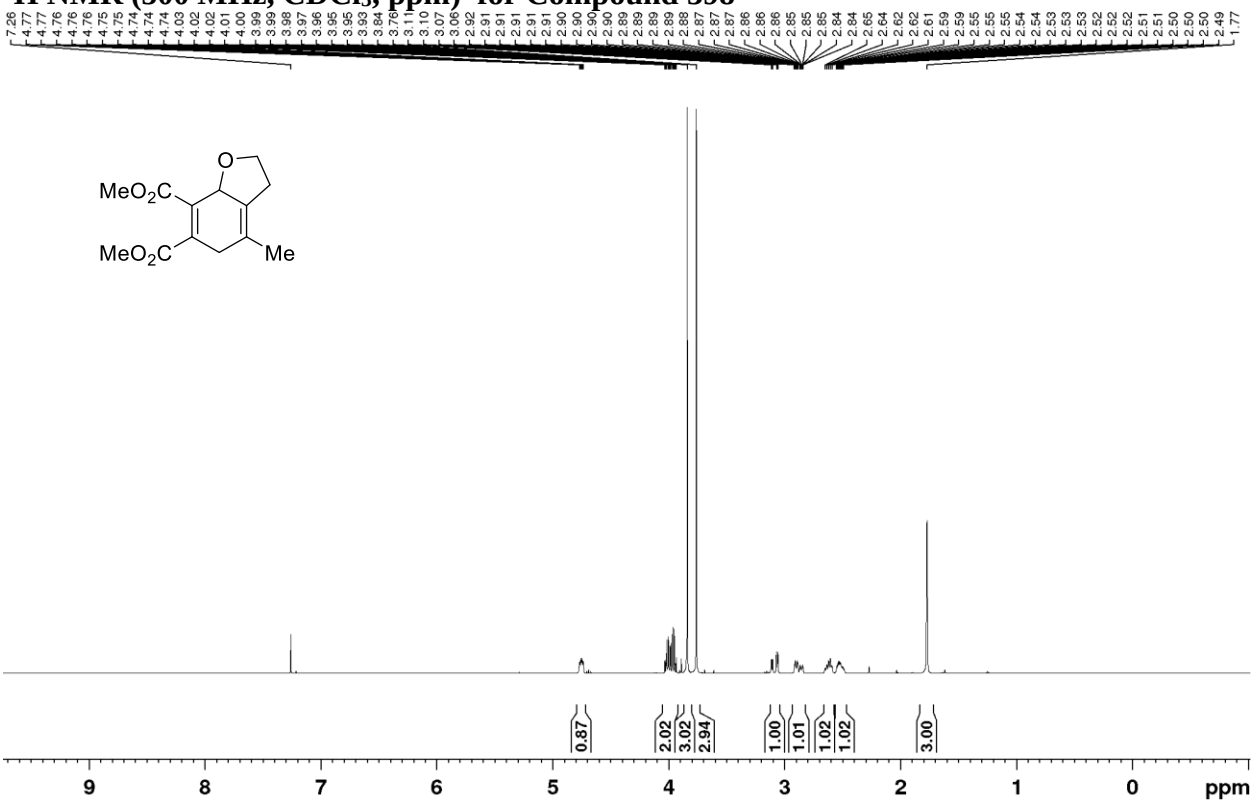

^{13}C NMR (126 MHz, $CDCl_3$, ppm) for Compound 398

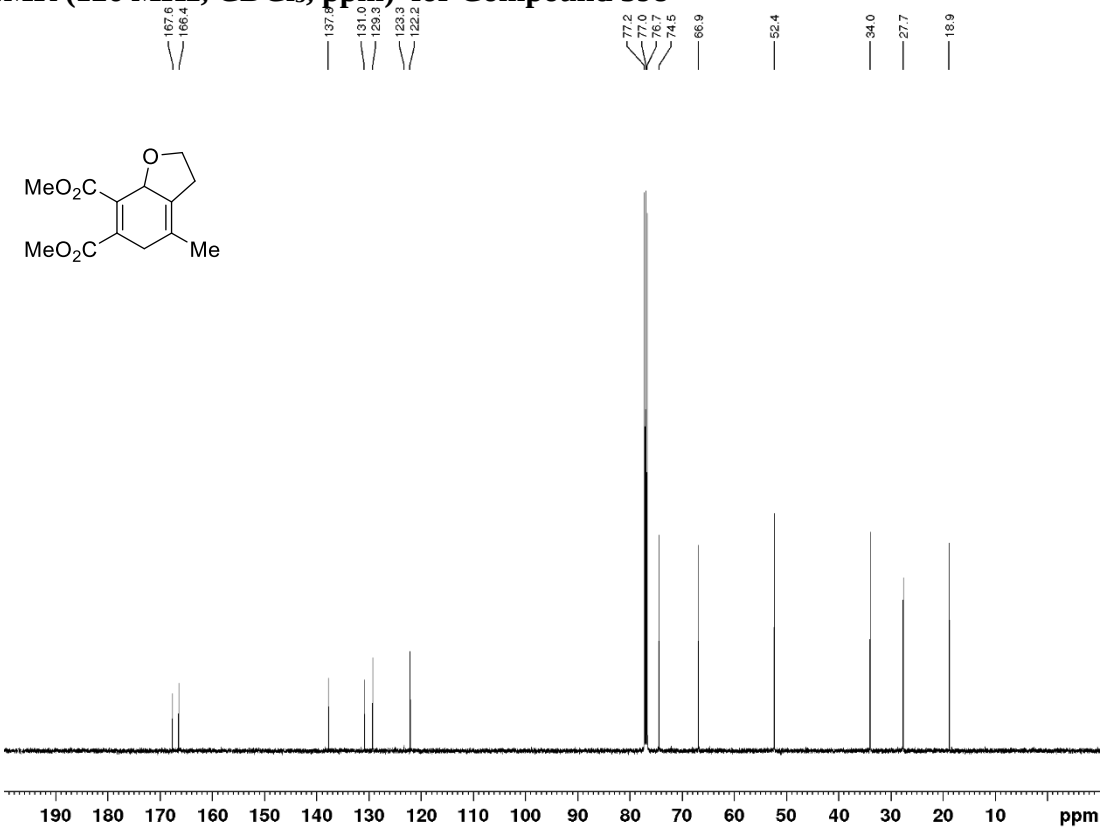

^{1}H NMR (500 MHz, $CDCl_3$, ppm) for Compound 376

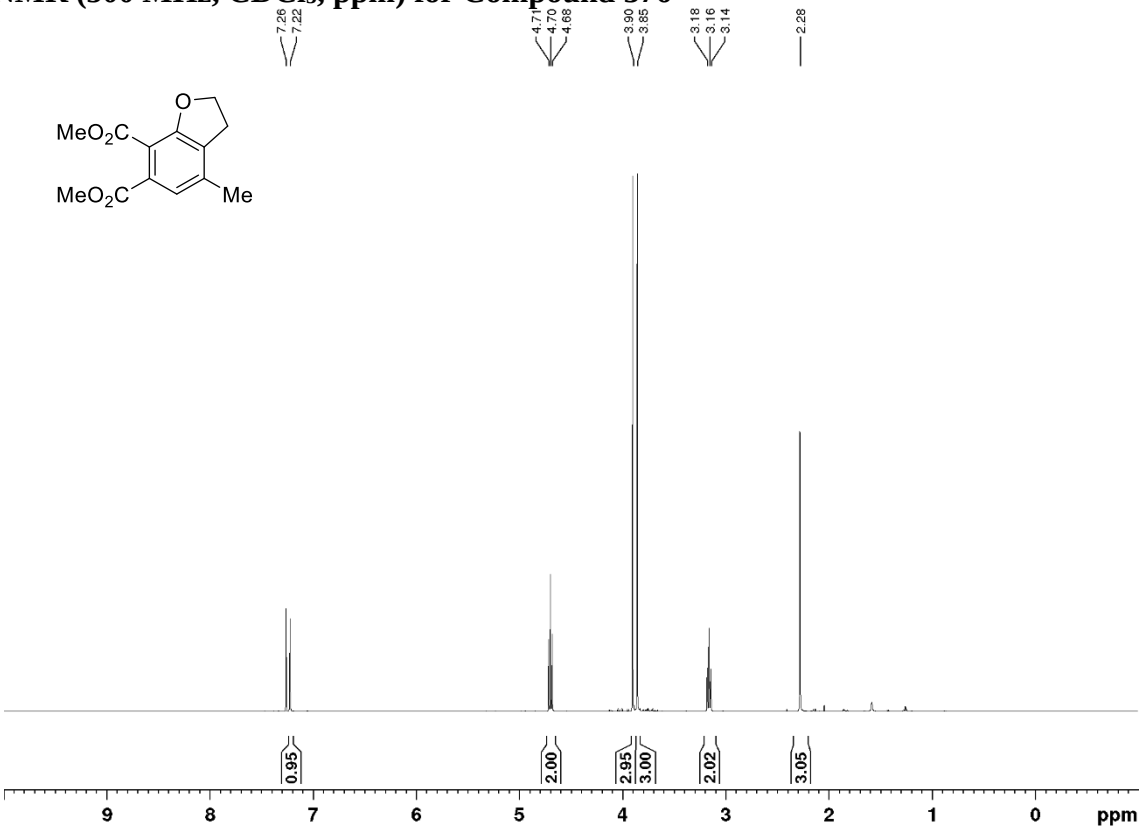

^{13}C NMR (126 MHz, $CDCl_3$, ppm) for Compound 376

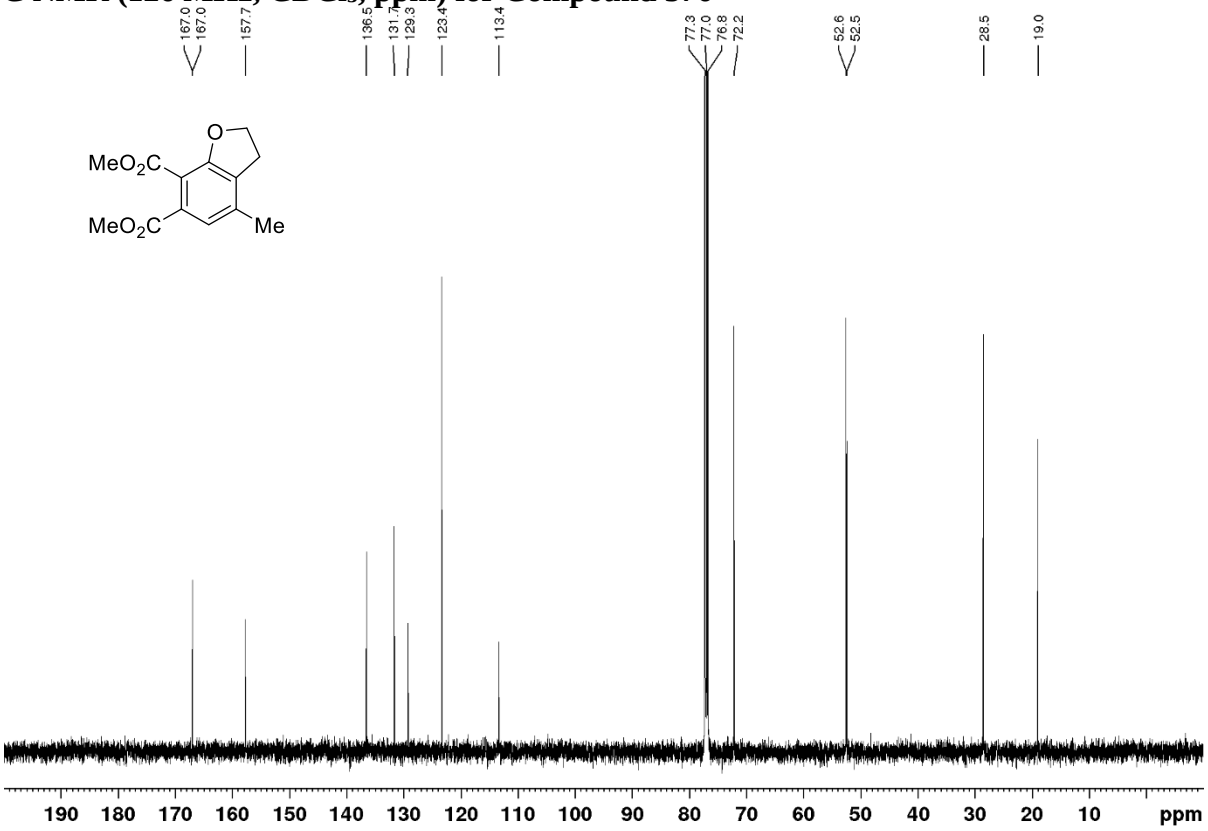

^{1}H NMR (500 MHz, DMSO-d_6, ppm) for Compound 415

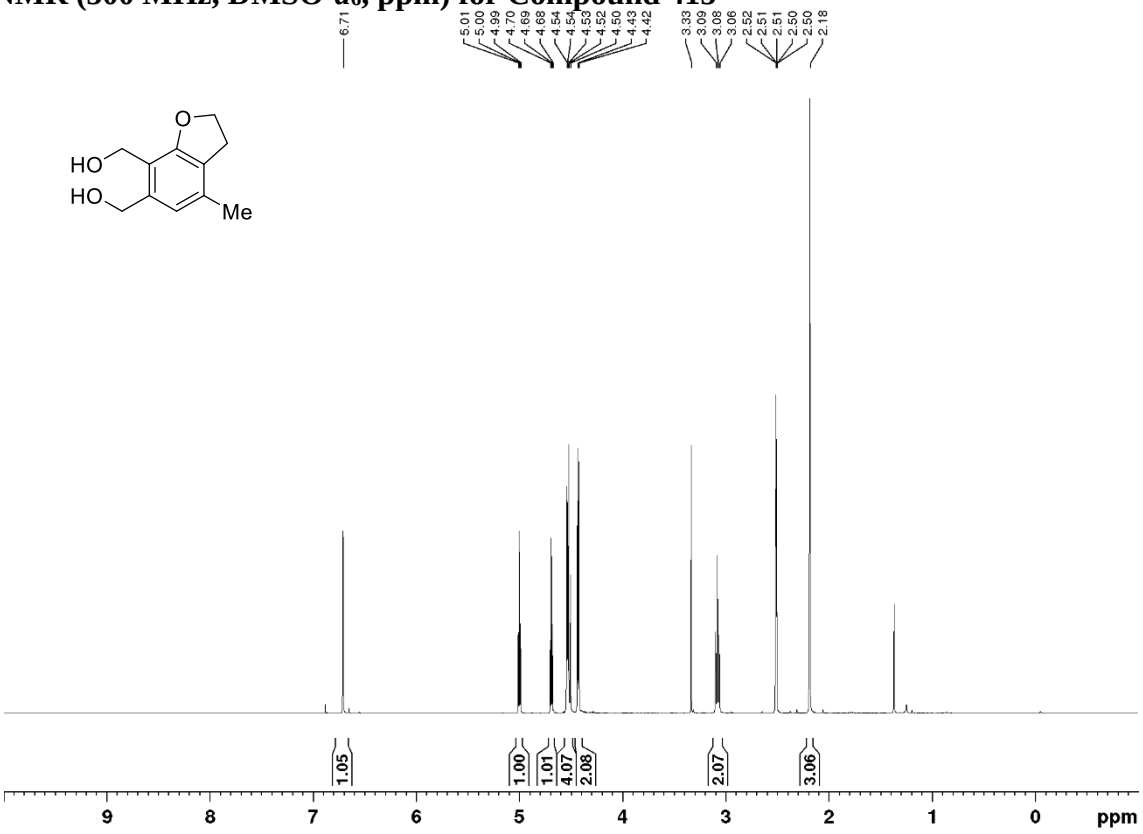

^{13}C NMR (126 MHz, DMSO-*d*$_6$, ppm) for Compound 415

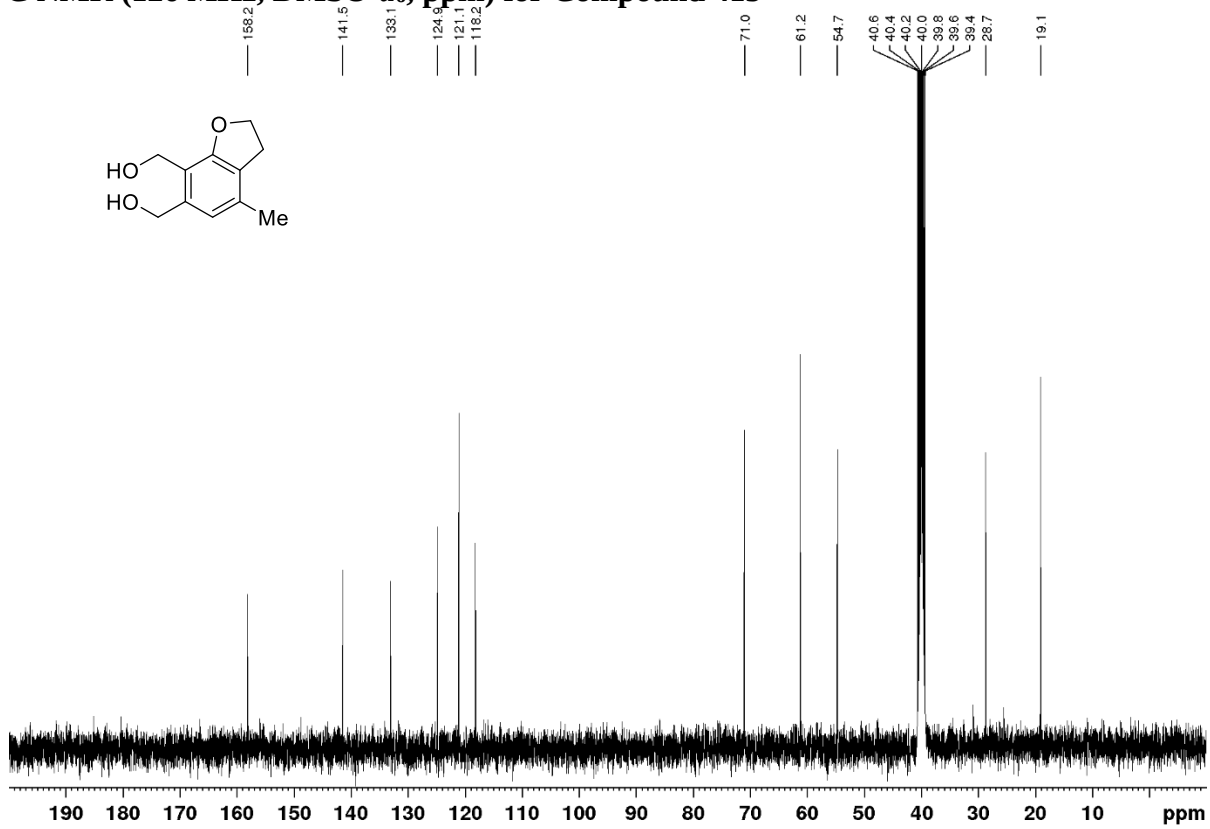

^{1}H NMR (500 MHz, CDCl$_3$, ppm) for Compound 415

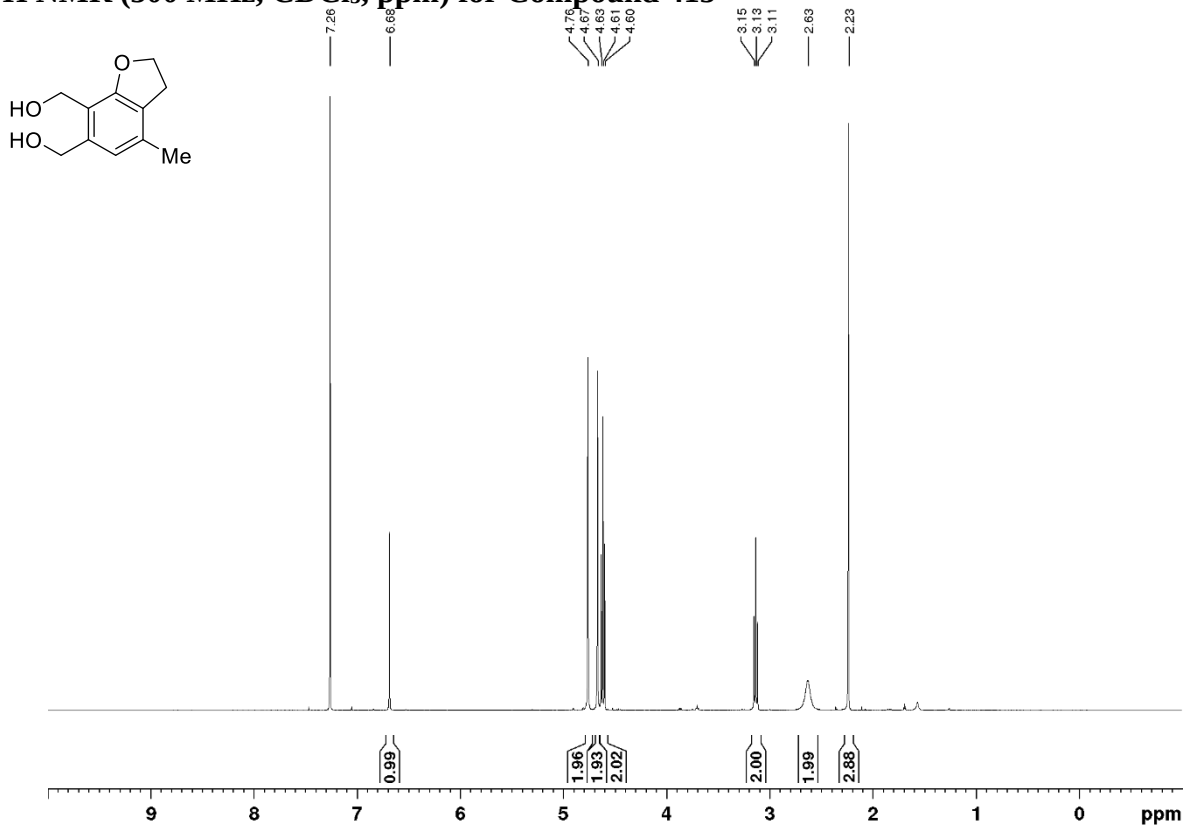

^{13}C NMR (126 MHz, $CDCl_3$, ppm) for Compound 415

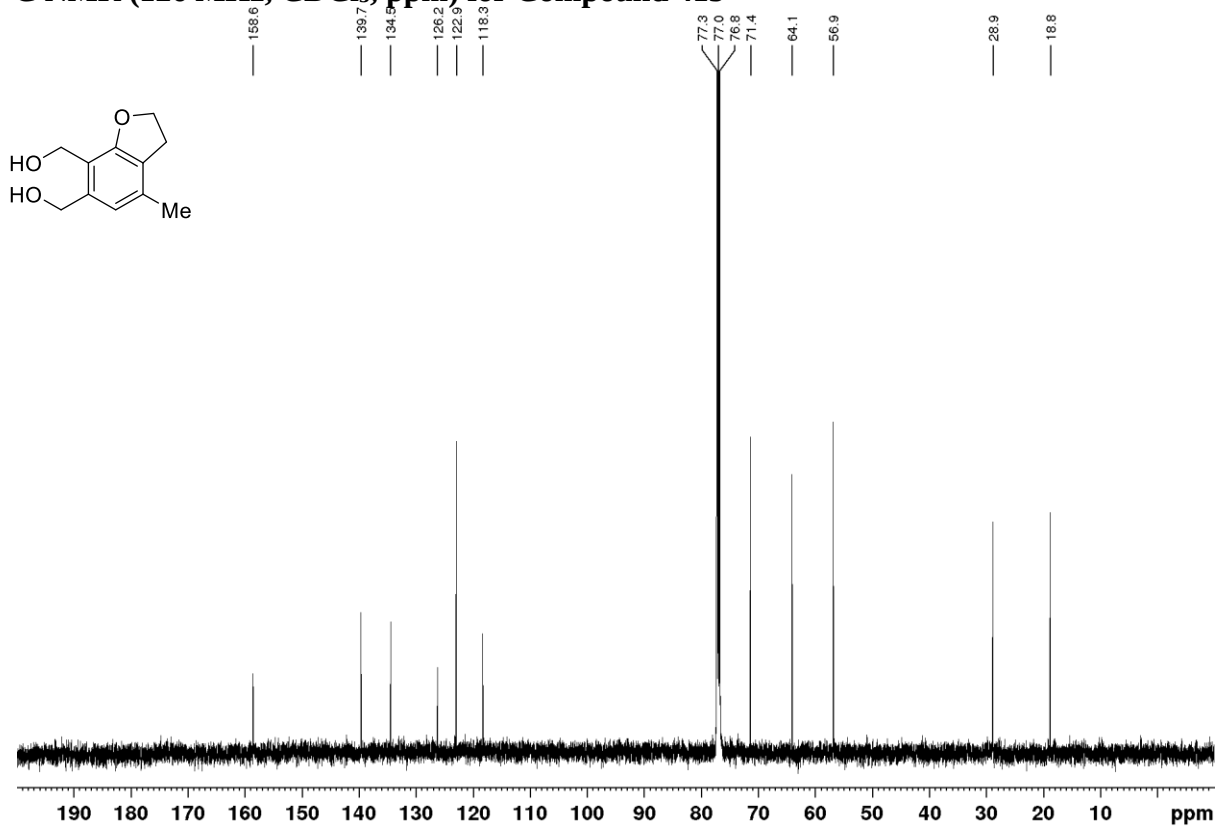

^{1}H NMR (500 MHz, $CDCl_3$, ppm) for Compound 375

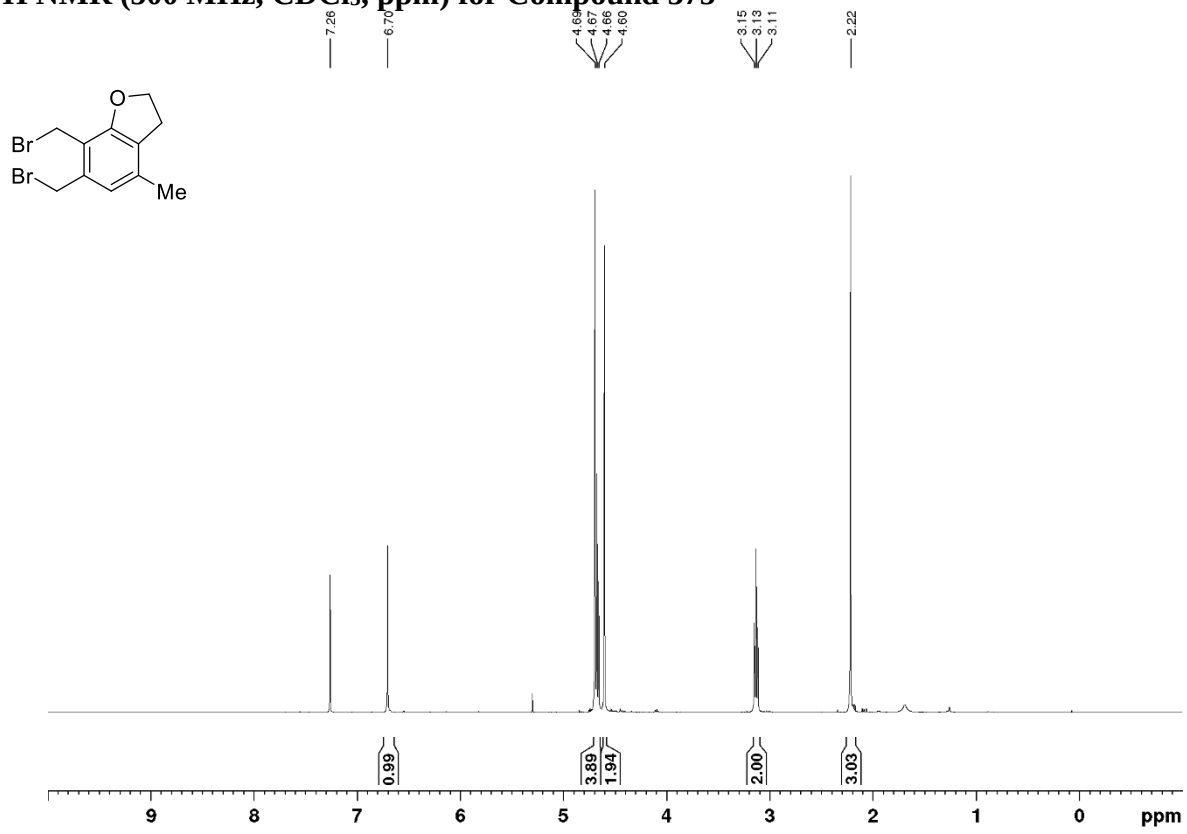

^{13}C NMR (126 MHz, $CDCl_3$, ppm) for Compound 375

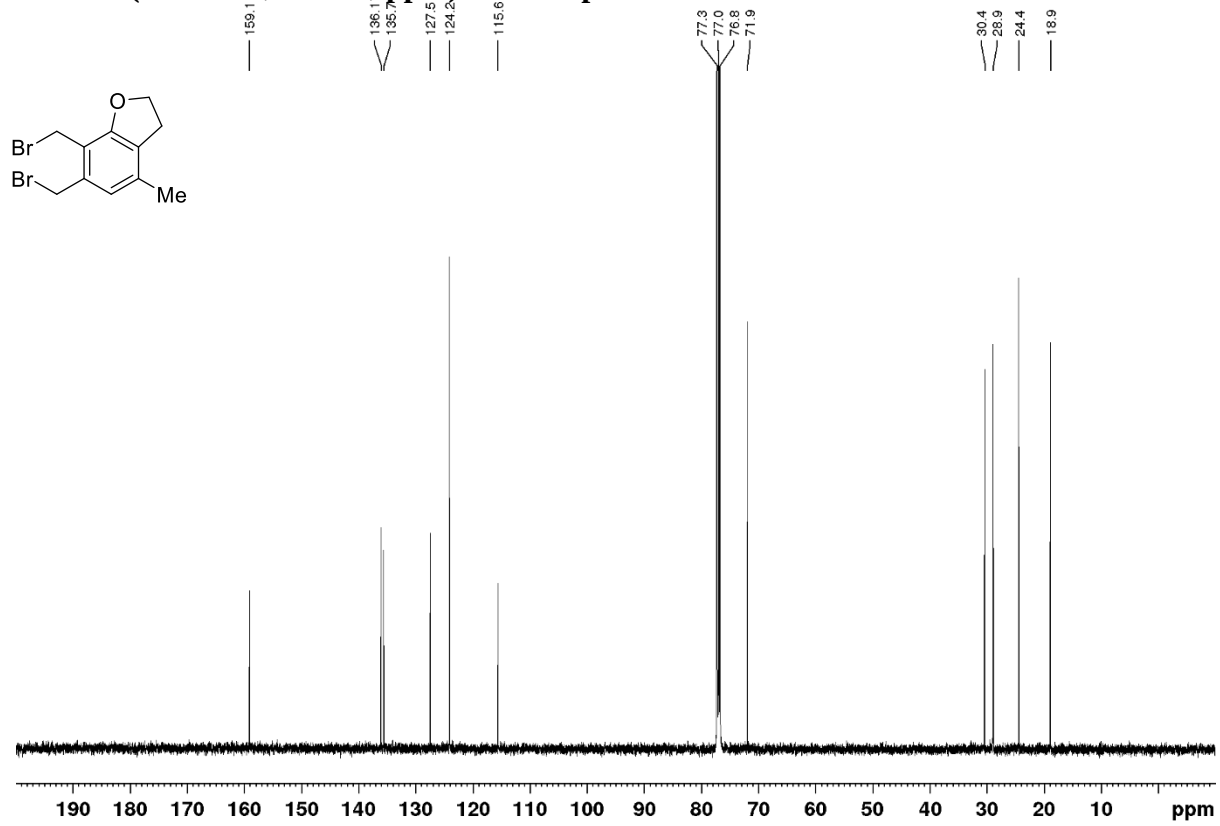

^{1}H NMR (500 MHz, $CDCl_3$, ppm) for Compound 374

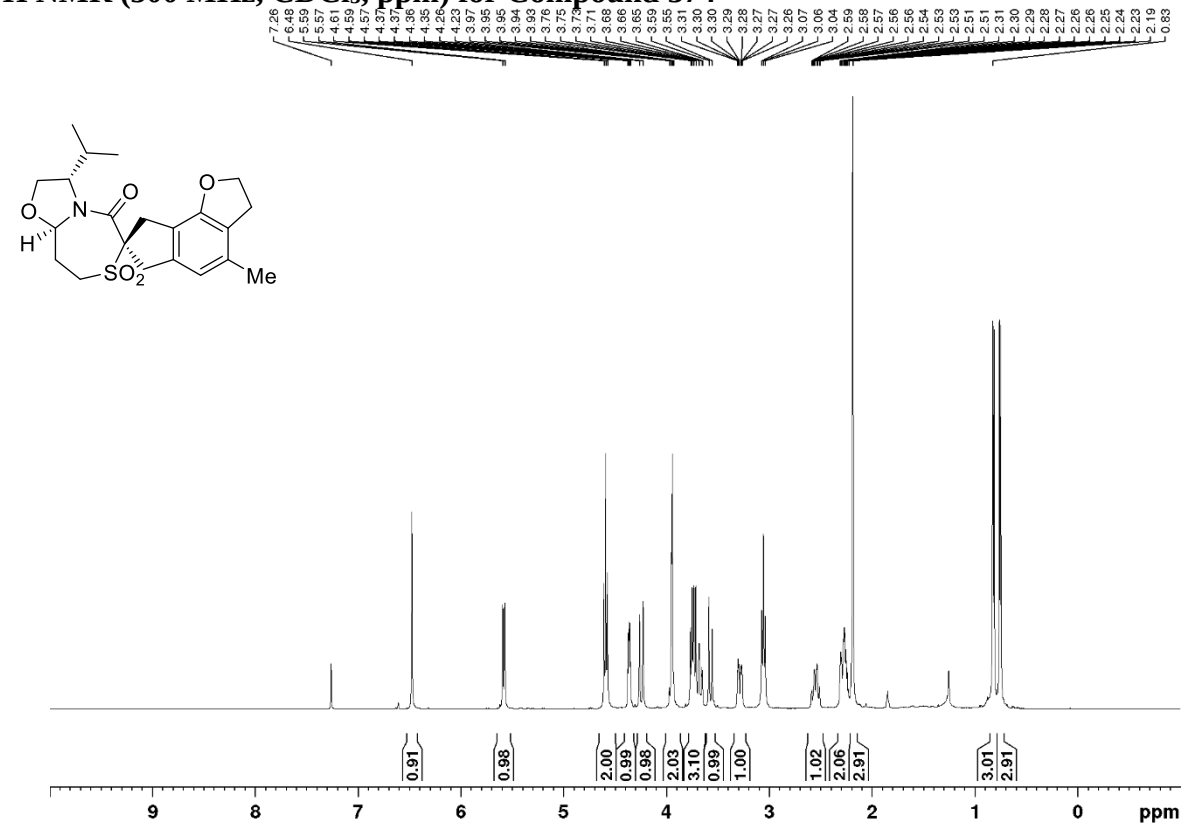

^{13}C NMR (126 MHz, $CDCl_3$, ppm) for Compound 374

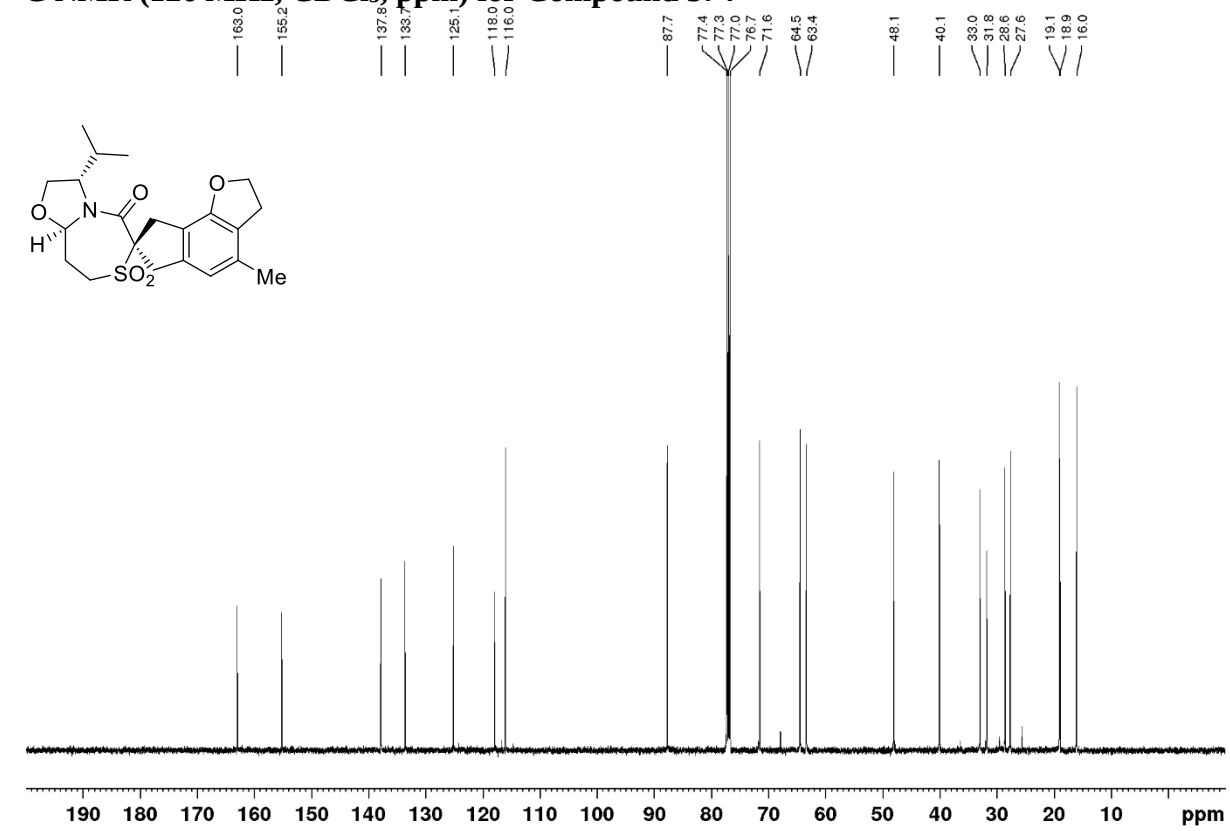

HSQC (126 MHz, $CDCl_3$, ppm) for Compound 374

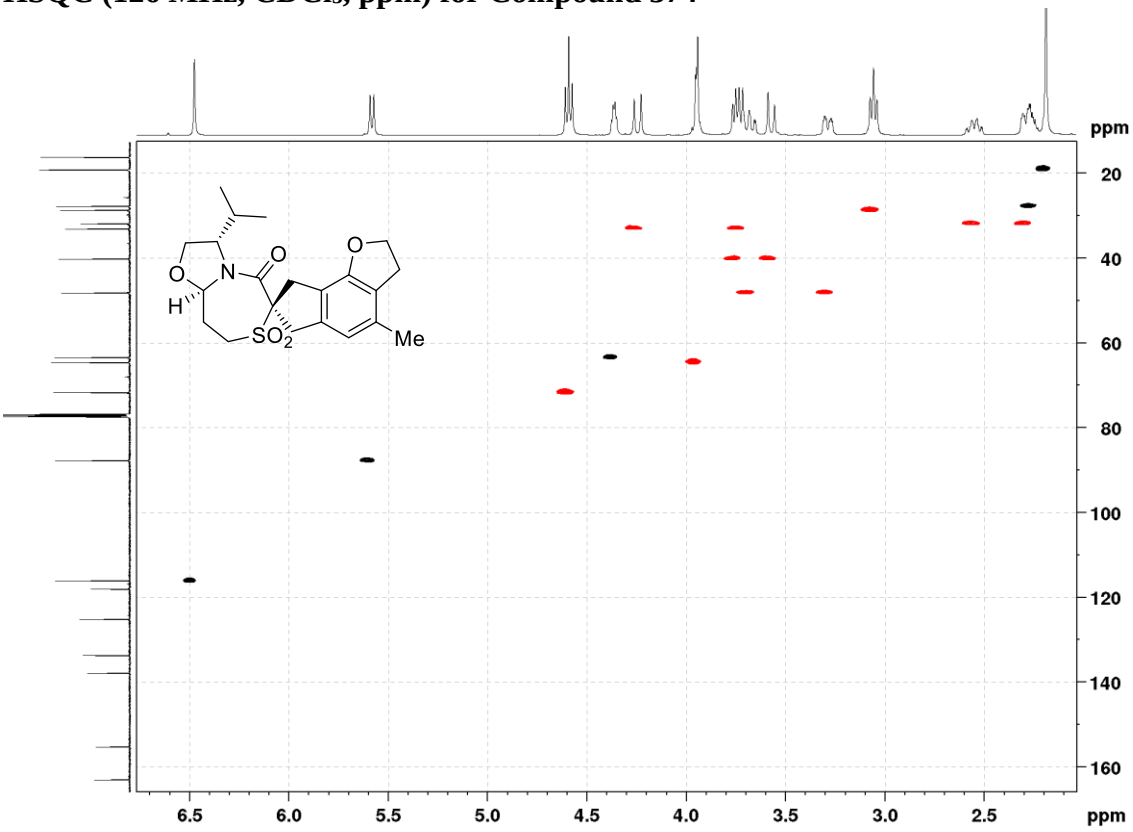

NOESY (126 MHz, $CDCl_3$, ppm) for Compound 374

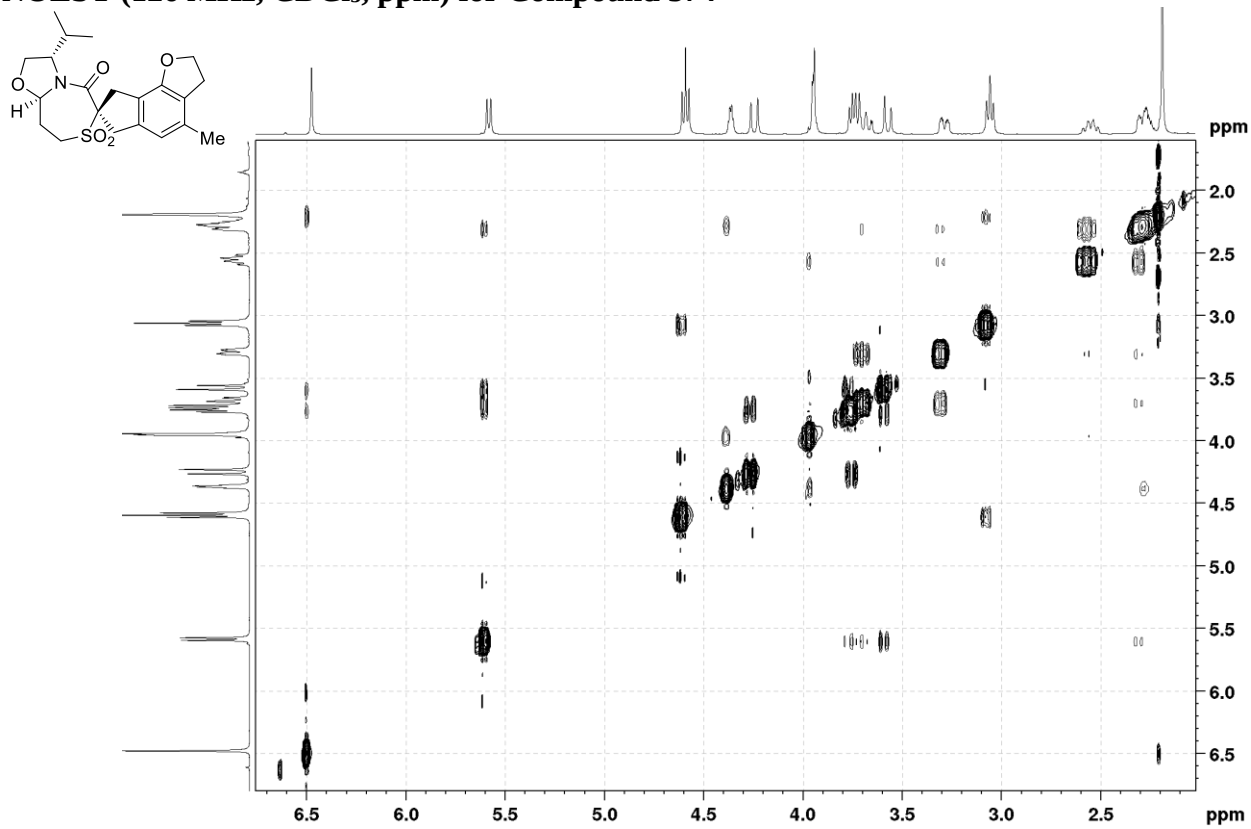

^{1}H NMR (500 MHz, $CDCl_3$, ppm) for Compound 416

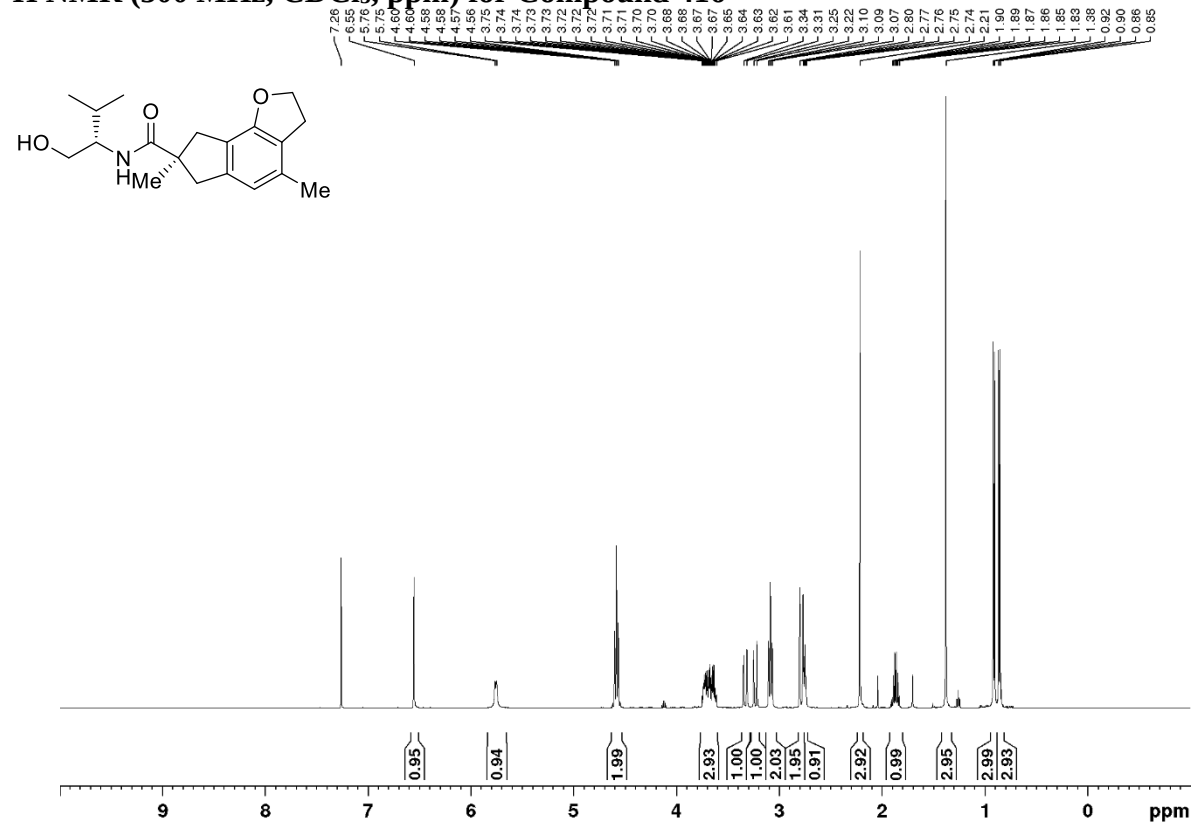

^{13}C NMR (126 MHz, $CDCl_3$, ppm) for Compound 416

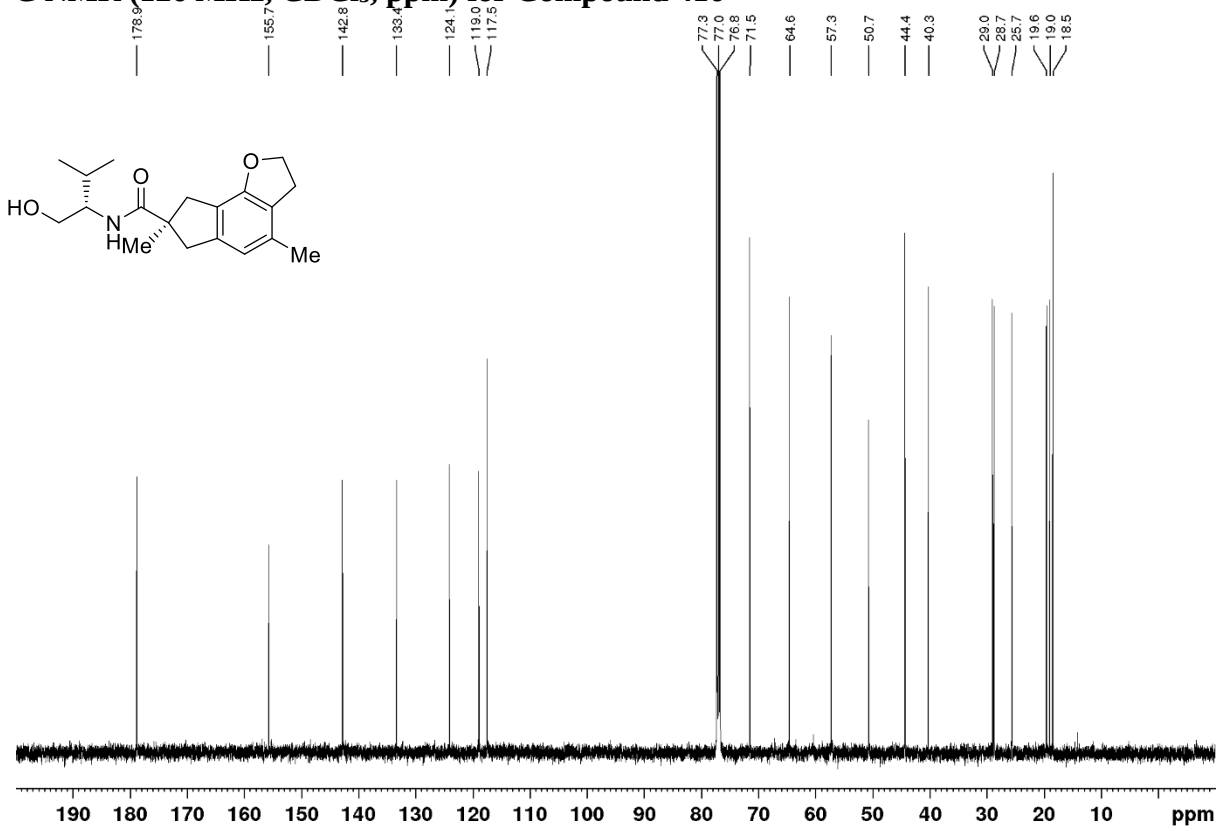

^{1}H NMR (500 MHz, $CDCl_3$, ppm) for Compound 417

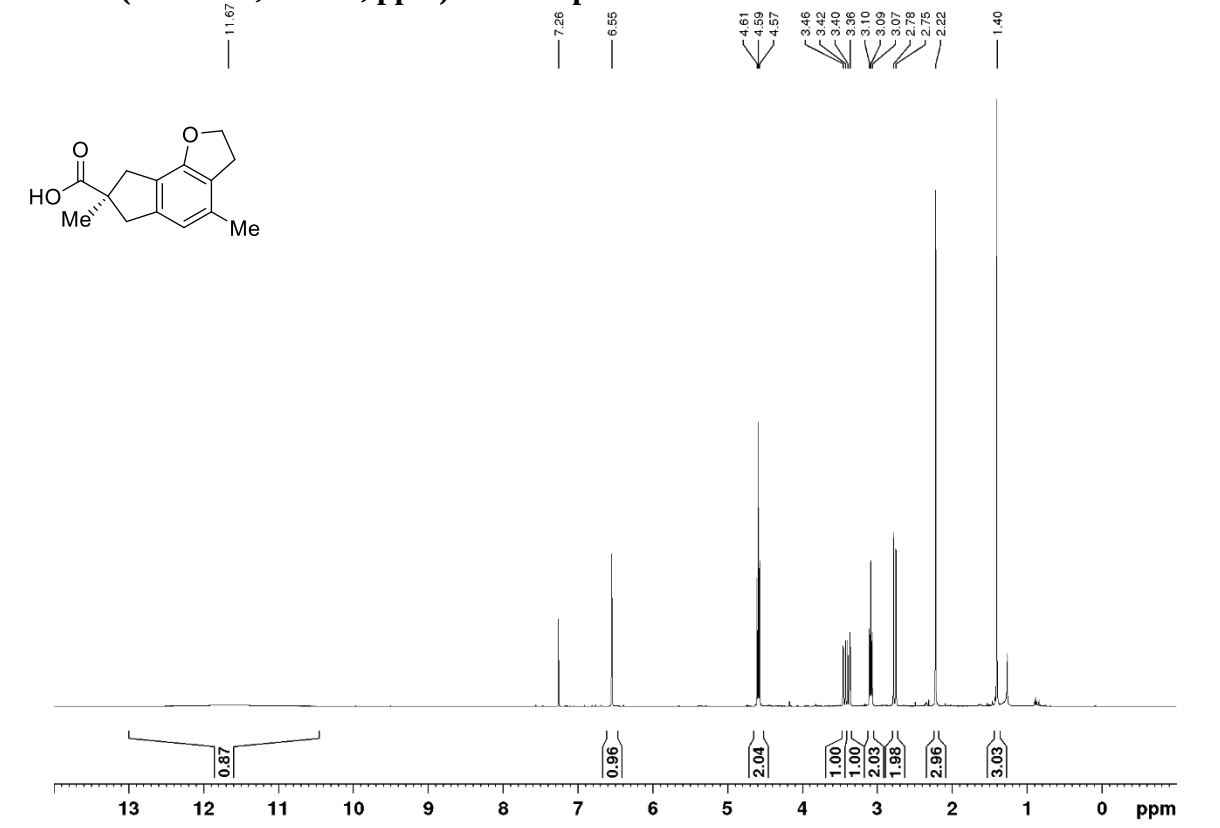

^{13}C NMR (126 MHz, $CDCl_3$, ppm) for Compound 417

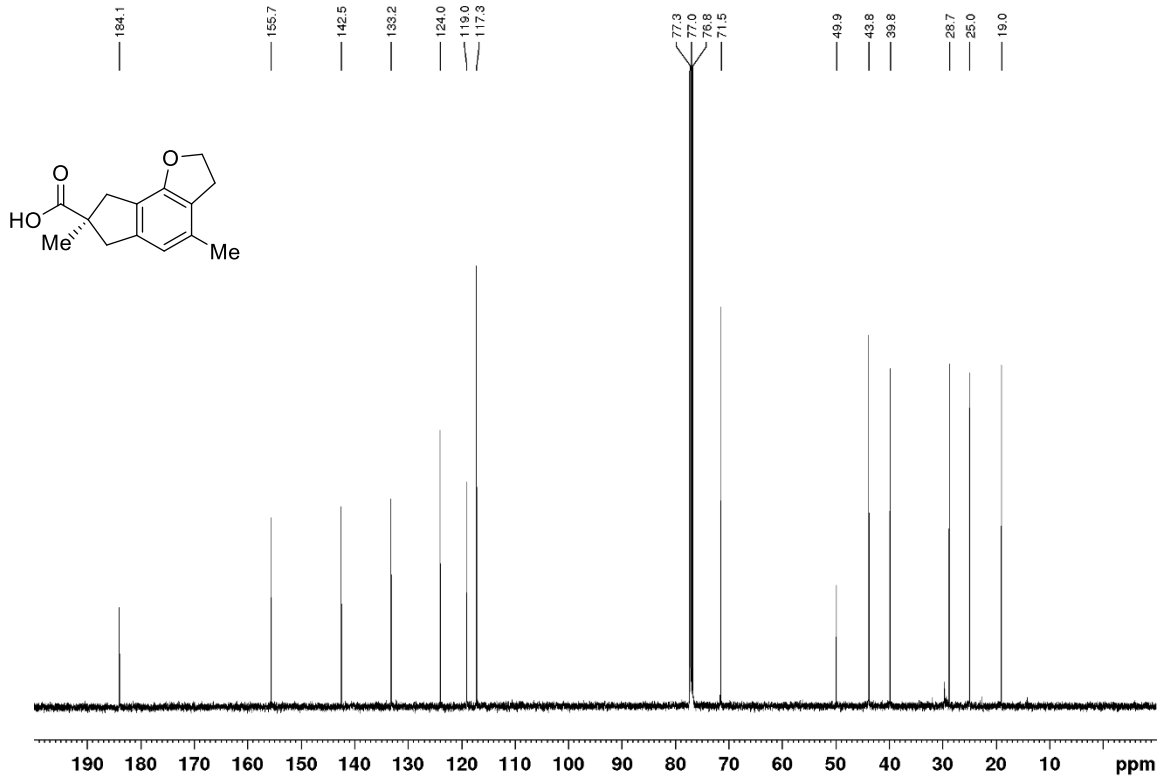

^{1}H NMR (500 MHz, $CDCl_3$, ppm) for Compound (*R*)-164 ((*R*)-puraquinonic acid)

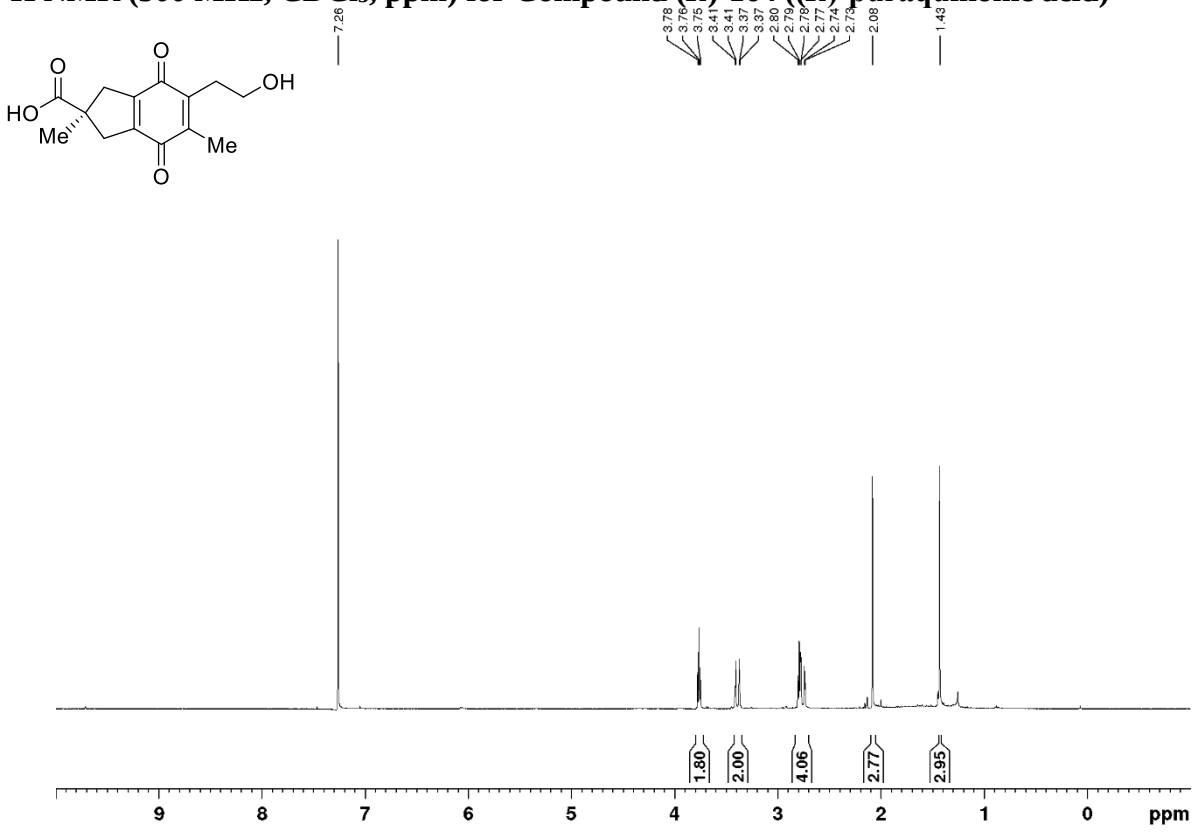

^{13}C NMR (101 MHz, $CDCl_3$, ppm) for Compound (*R*)-164 ((*R*)-puraquinonic acid)

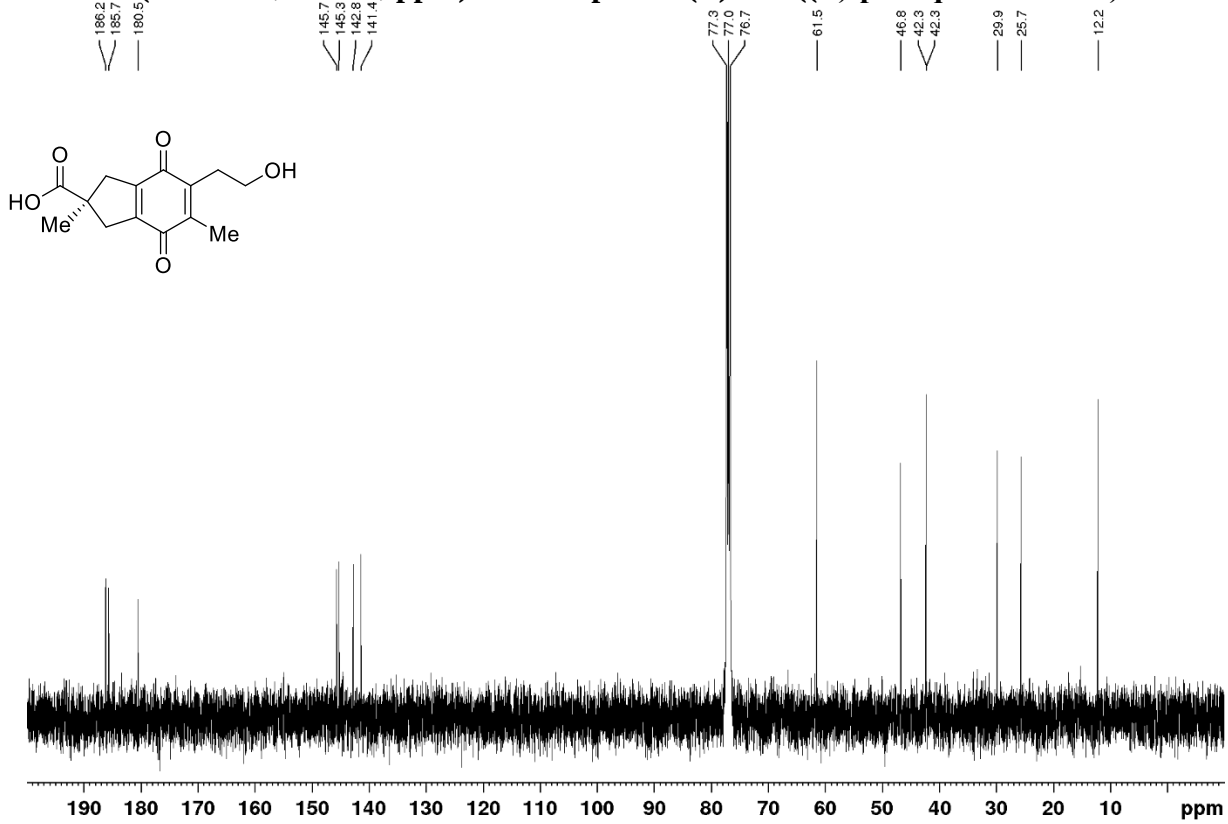

^{1}H NMR (500 MHz, DMSO-*d*$_6$, ppm) for Compound 430

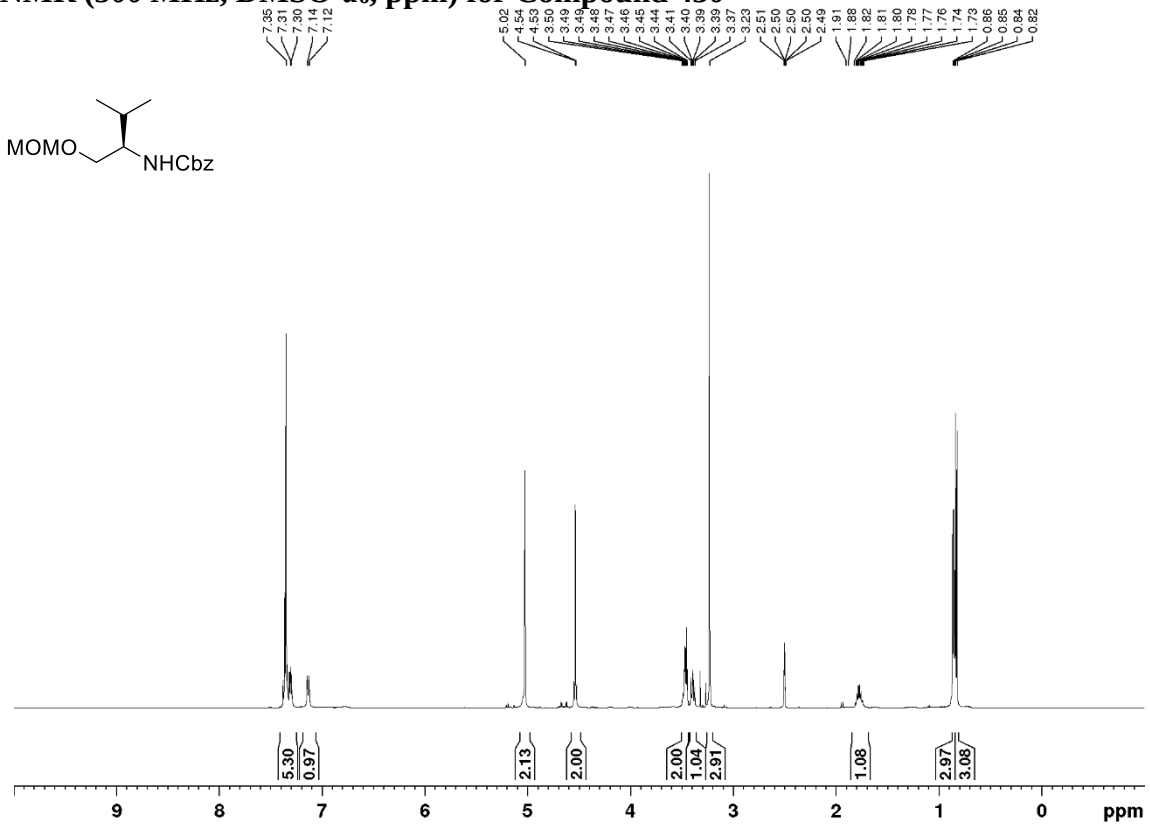

^{13}C NMR (126 MHz, DMSO-d_6, ppm) for Compound 430

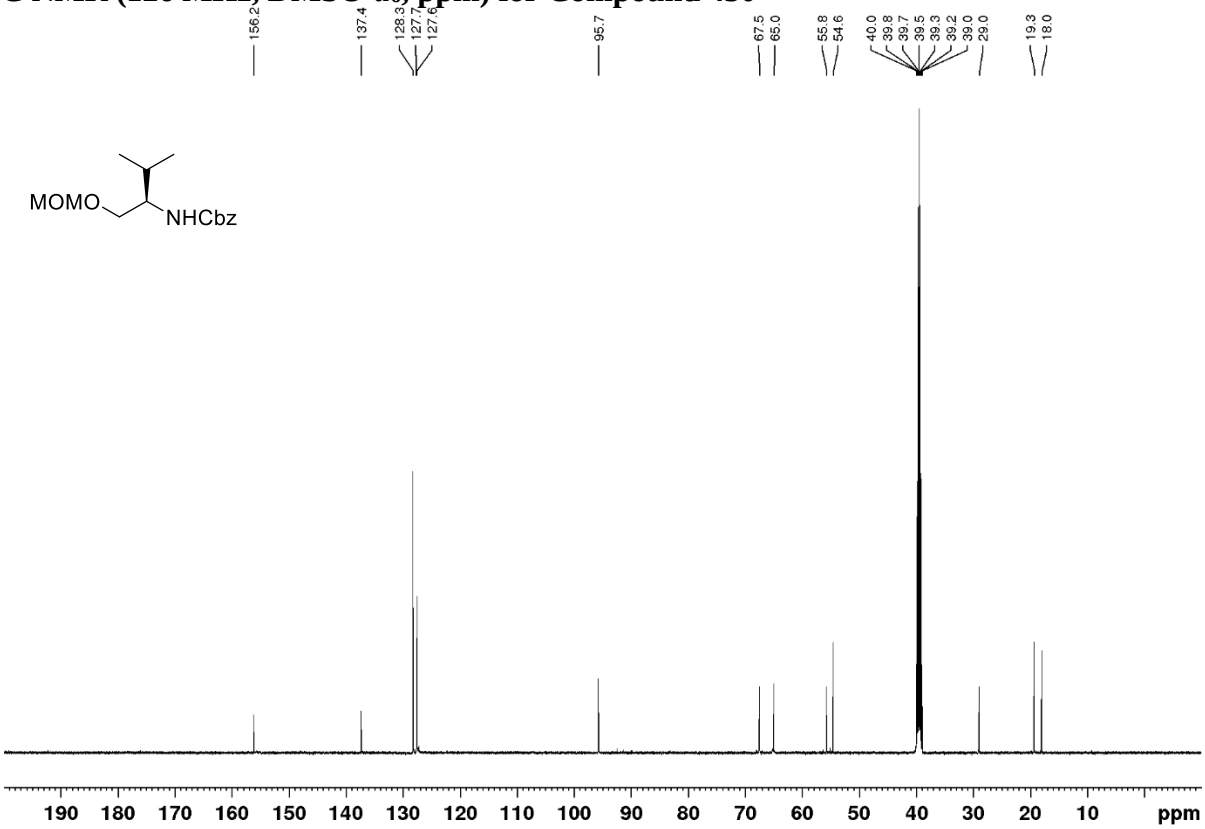

^{1}H NMR (500 MHz, $CDCl_3$, ppm) for Compound 431

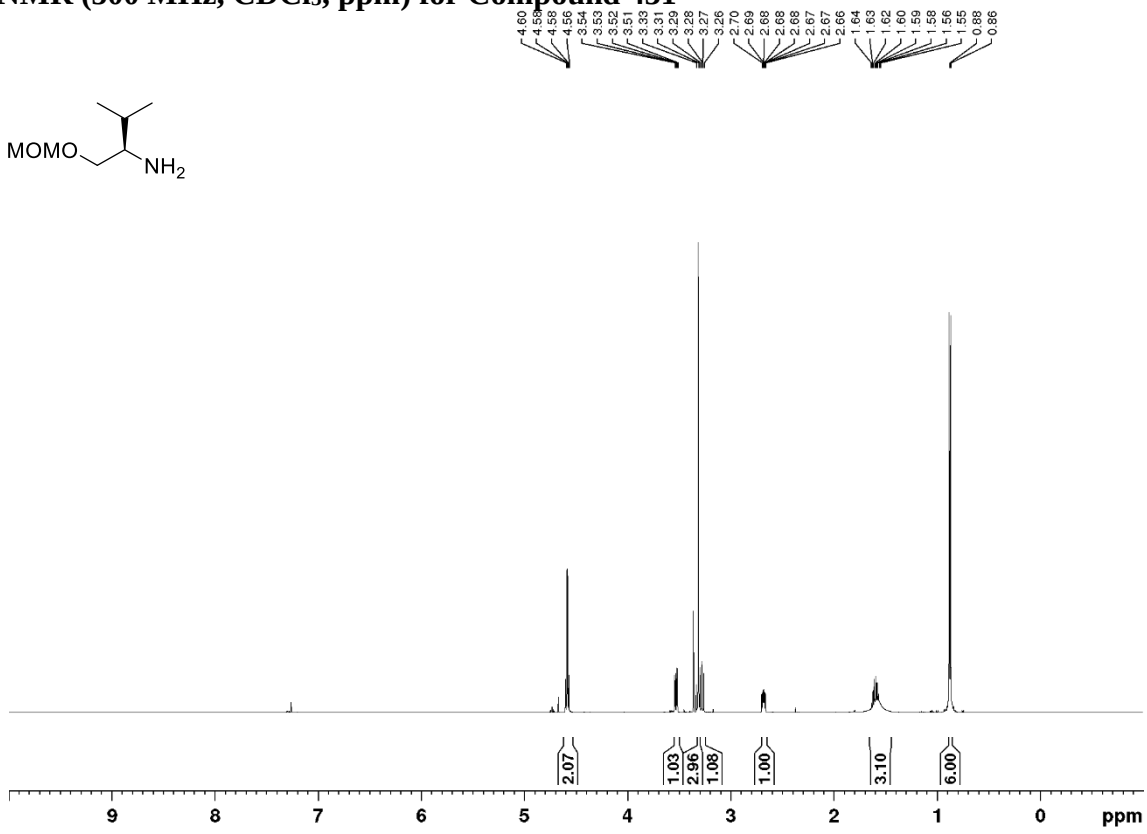

^{13}C NMR (126 MHz, $CDCl_3$, ppm) for Compound 431

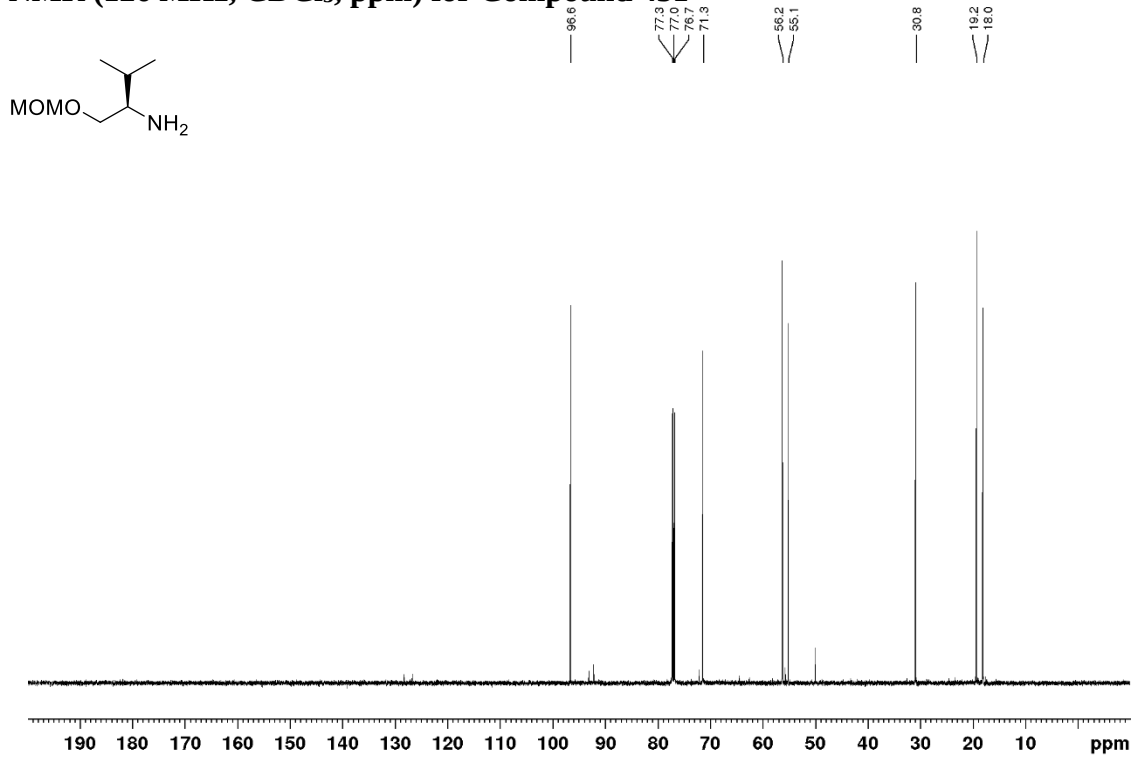

^{1}H NMR (500 MHz, $CDCl_3$, ppm) for Compound (*R*,*R*)-432

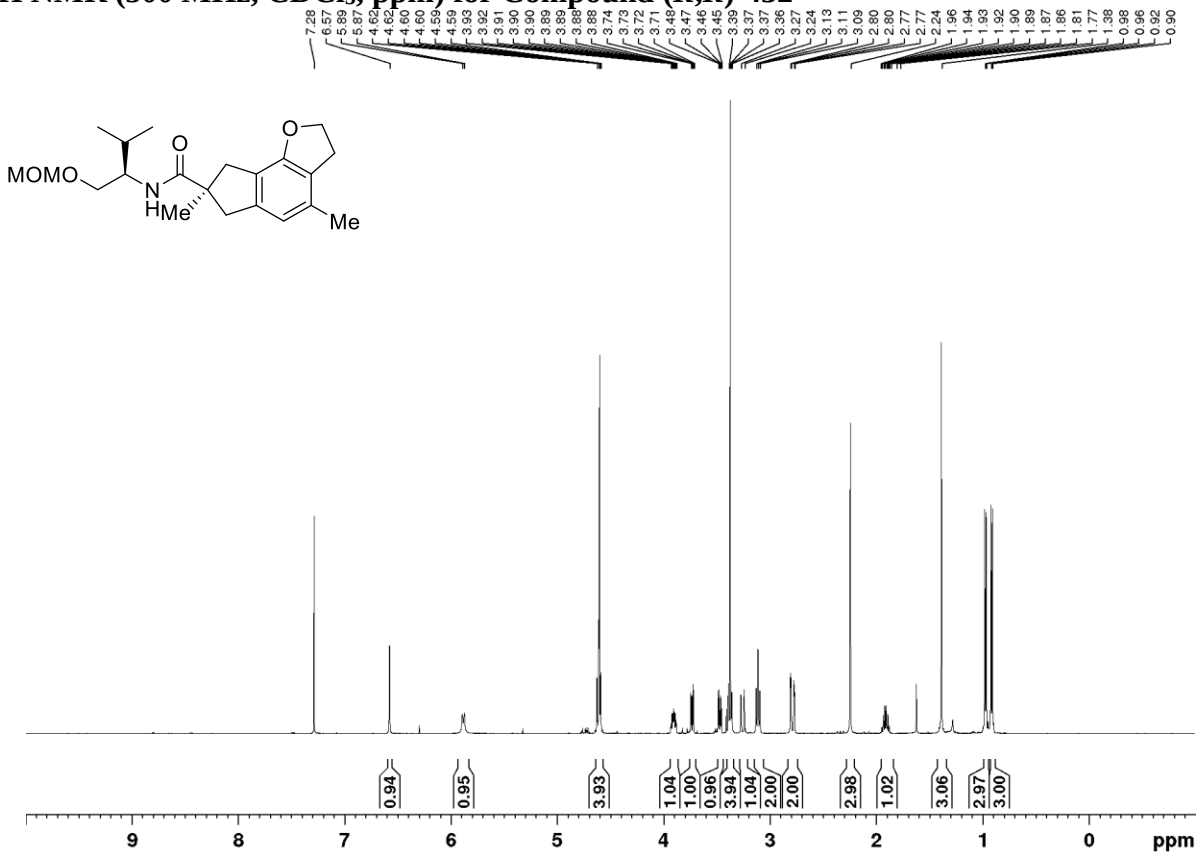

^{13}C NMR (126 MHz, $CDCl_3$, ppm) for Compound (*R*,*R*)-432

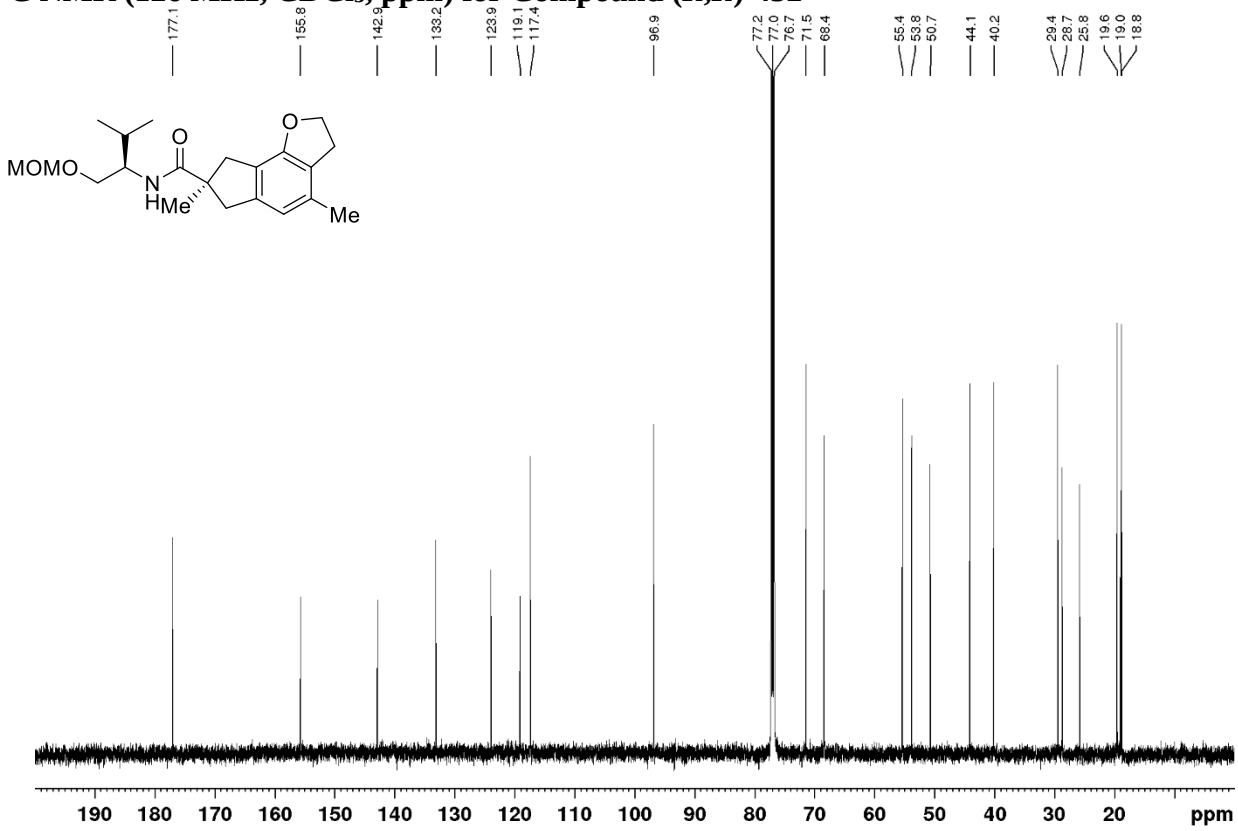

^{1}H NMR (500 MHz, $CDCl_3$, ppm) for Compound (*R*,*R*)-433

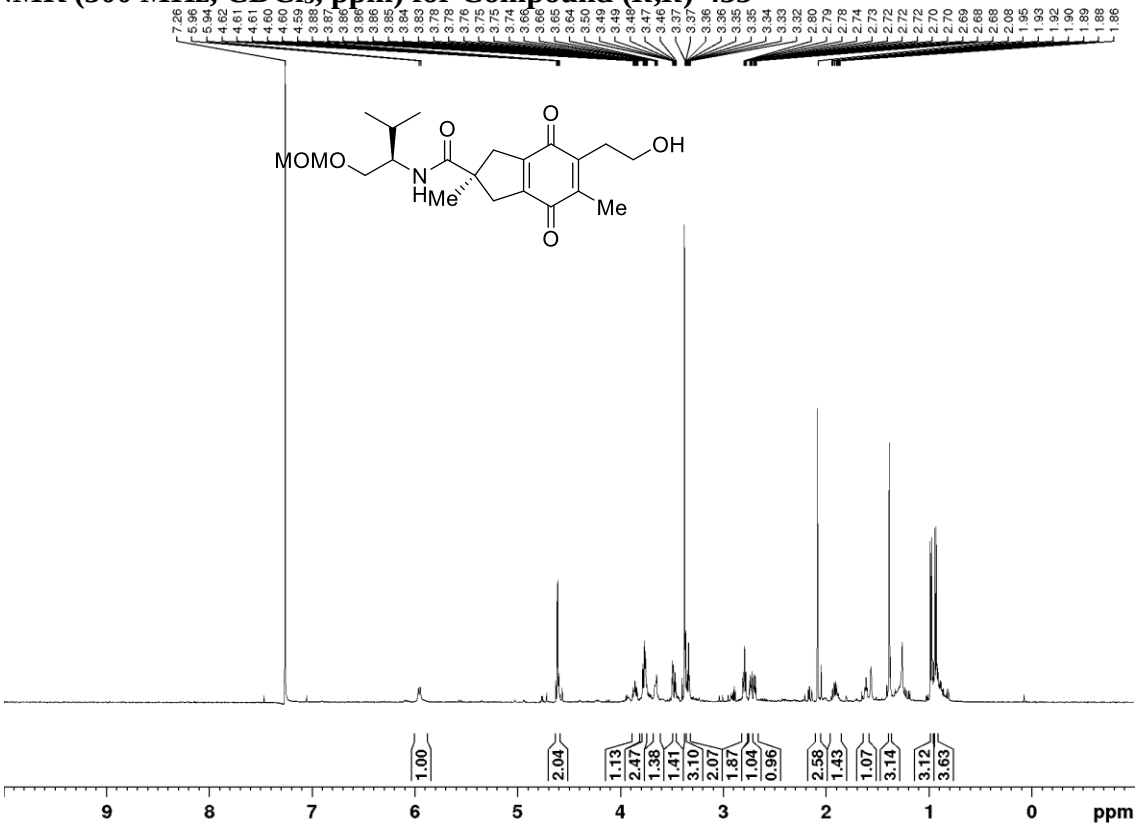

^{13}C NMR (101 MHz, $CDCl_3$, ppm) for Compound (*R*,*R*)-433

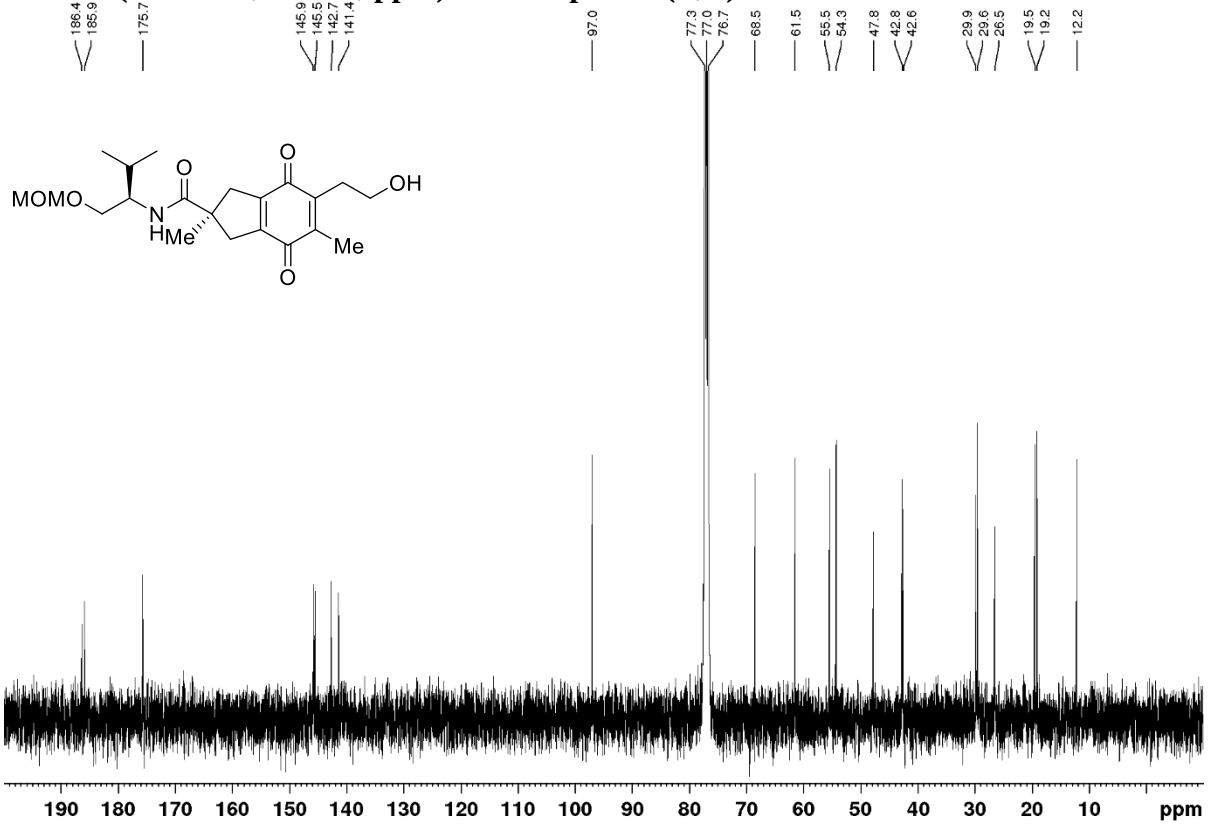

^{1}H NMR (500 MHz, $CDCl_3$, ppm) for Compound (*R*,*S*)-432

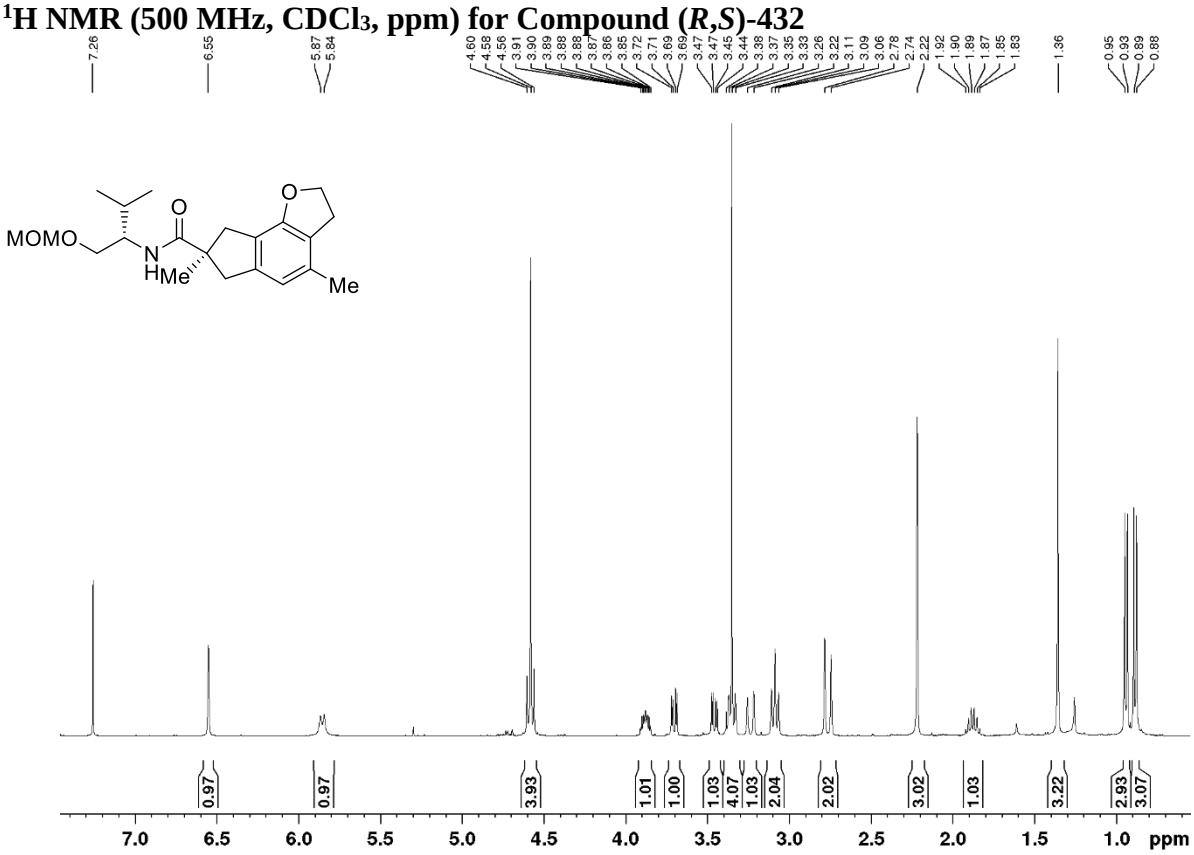

^{13}C NMR (126 MHz, $CDCl_3$, ppm) for Compound (*R*,*S*)-432

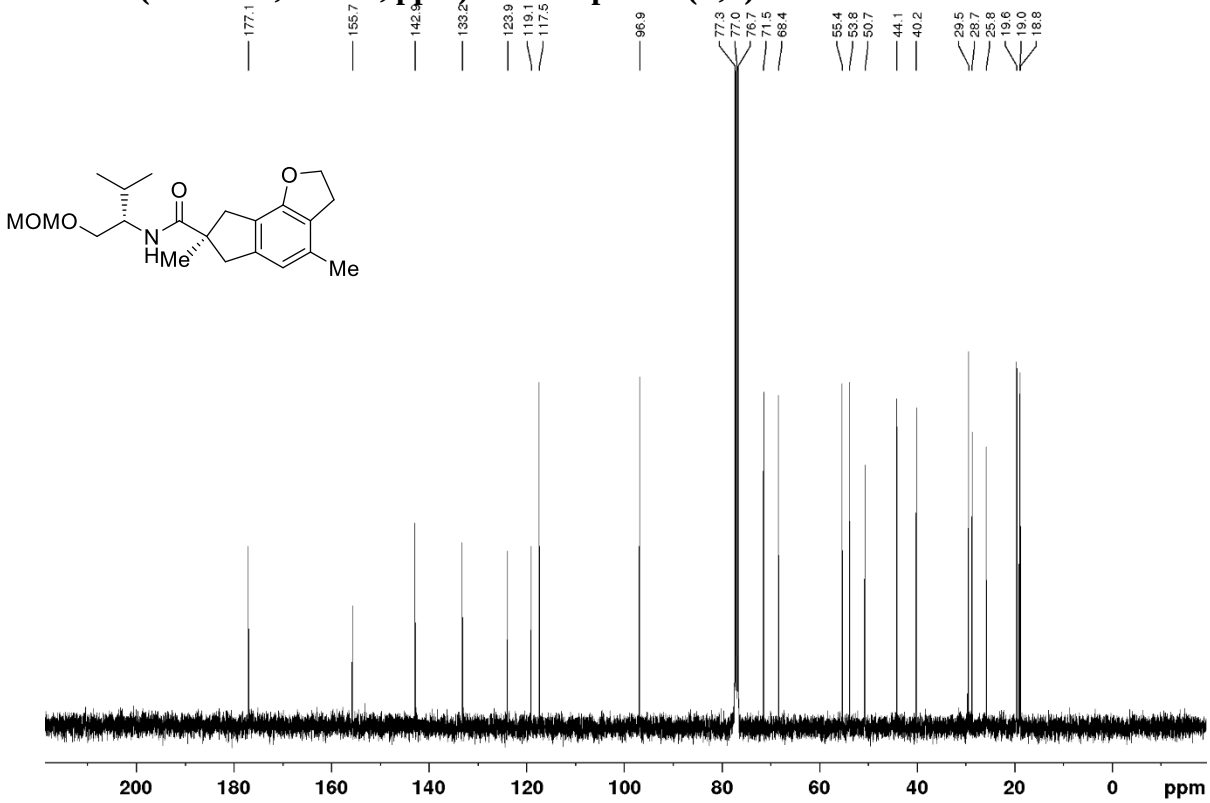

^{1}H NMR (500 MHz, $CDCl_3$, ppm) for Compound 437

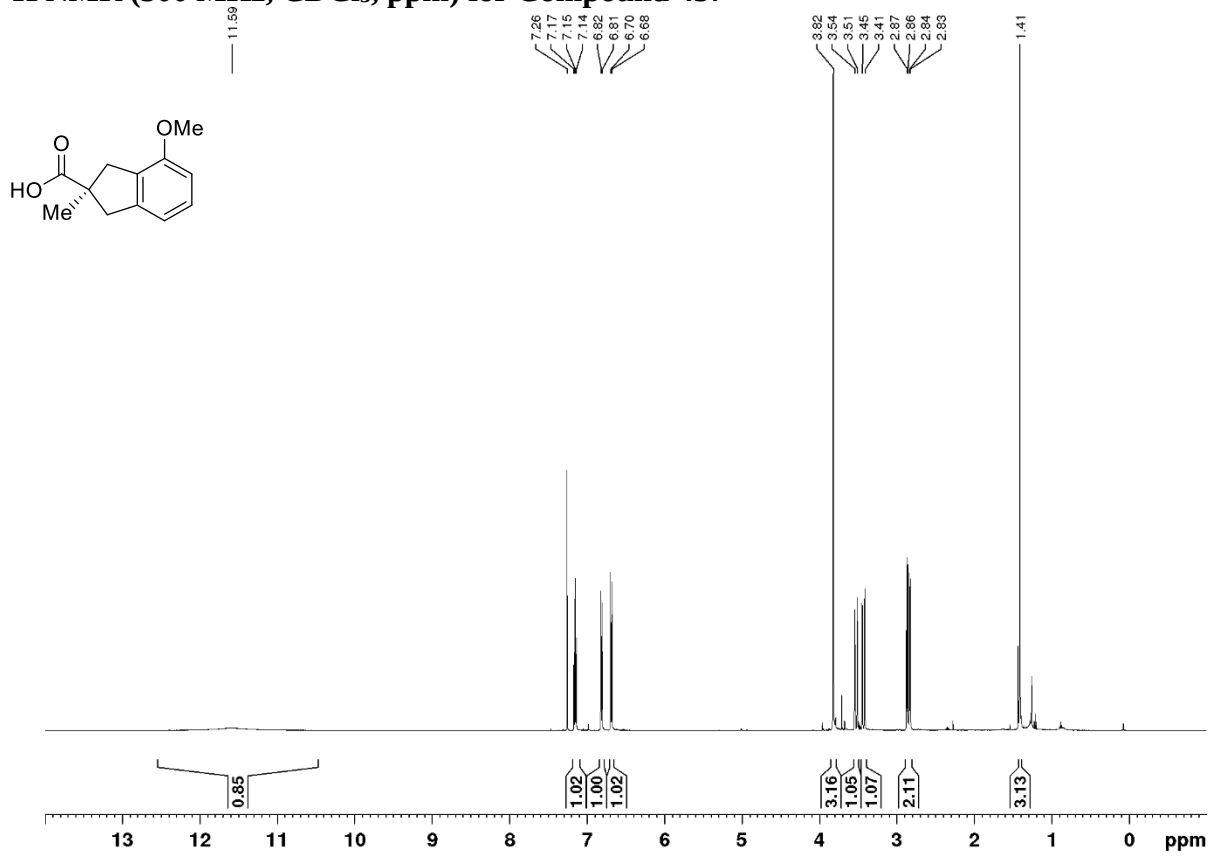

^{13}C NMR (126 MHz, $CDCl_3$, ppm) for Compound 437

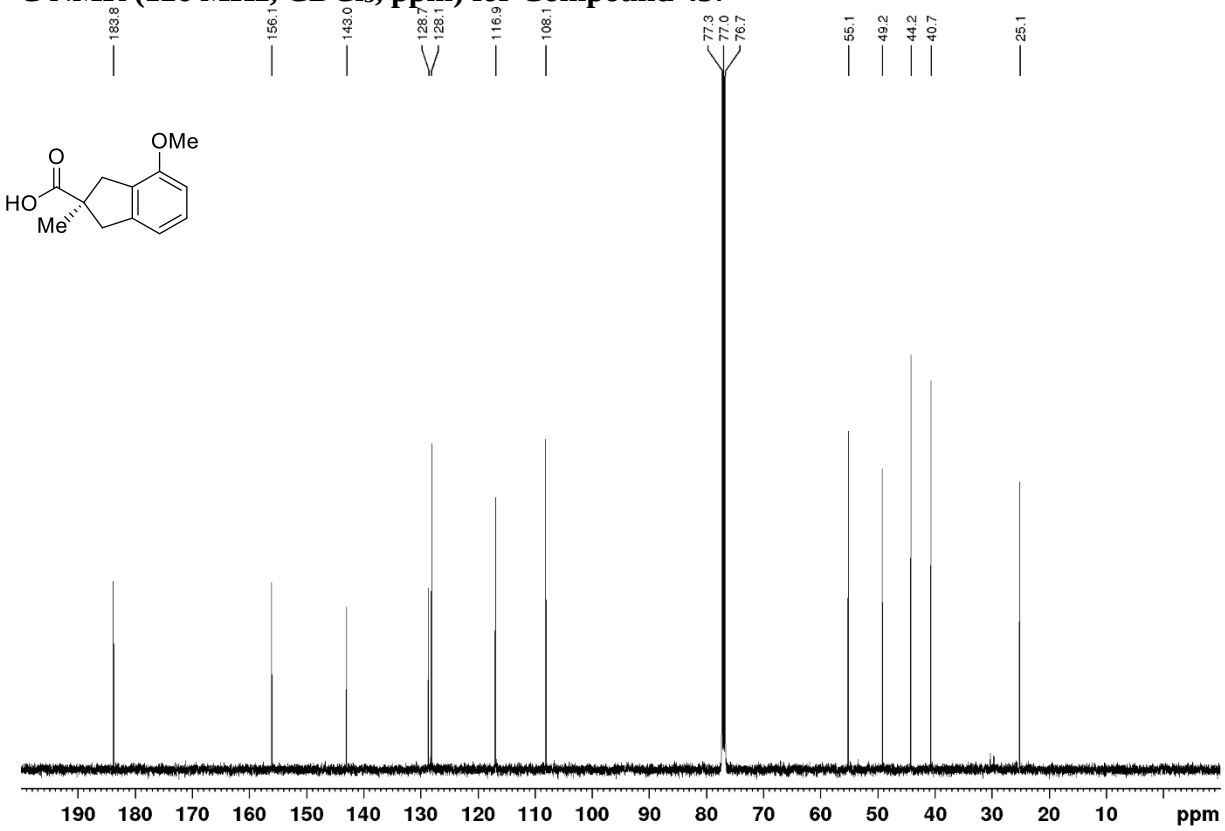

^{1}H NMR (500 MHz, $CDCl_3$, ppm) for Compound (*R*,*S*)-435

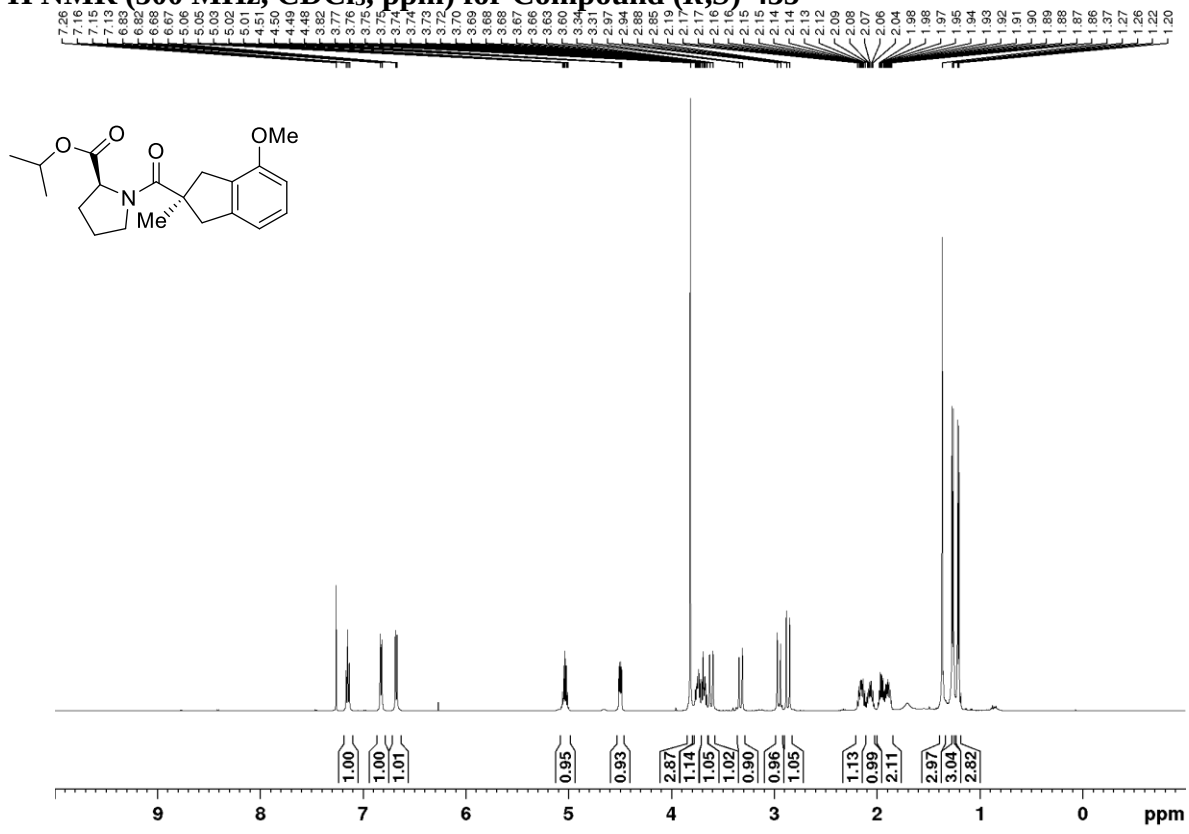

^{13}C NMR (126 MHz, $CDCl_3$, ppm) for Compound (*R*,*S*)-435

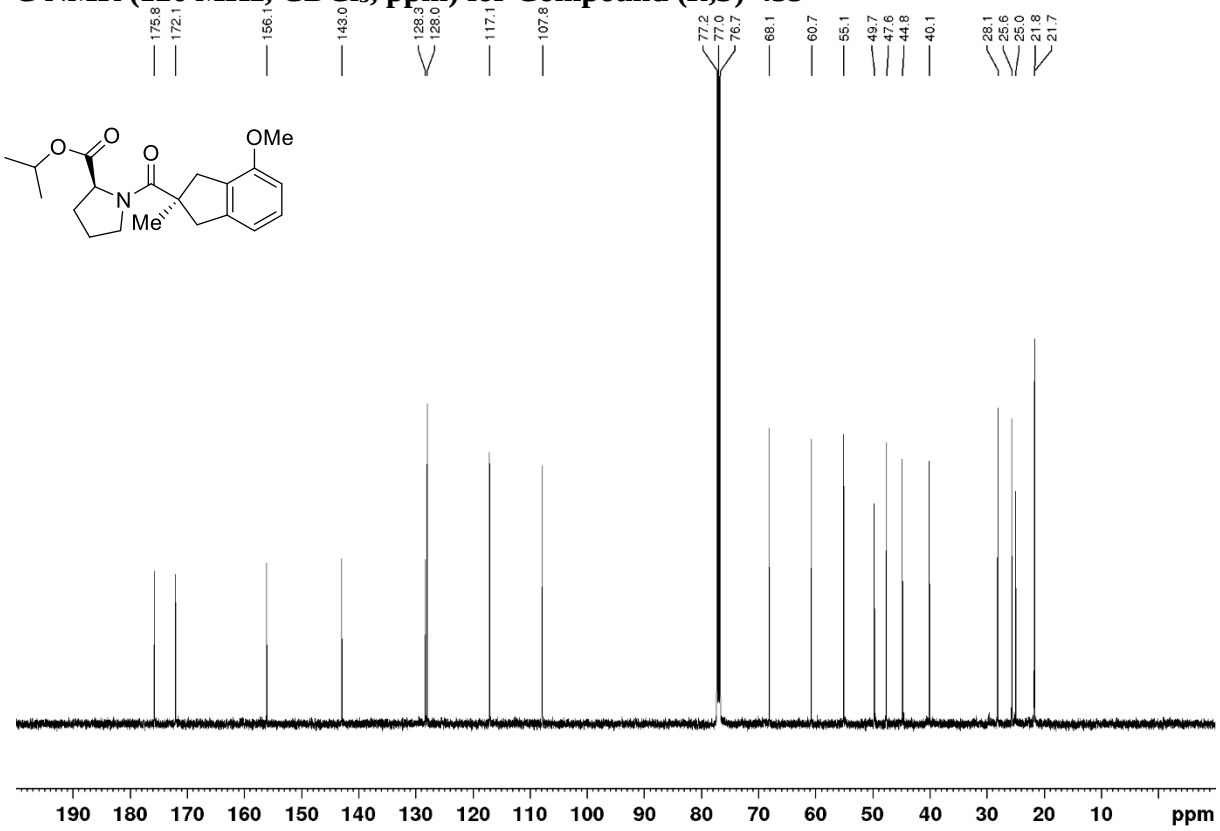

^{1}H NMR (500 MHz, $CDCl_3$, ppm) for Compound (*R*,*R*)-435

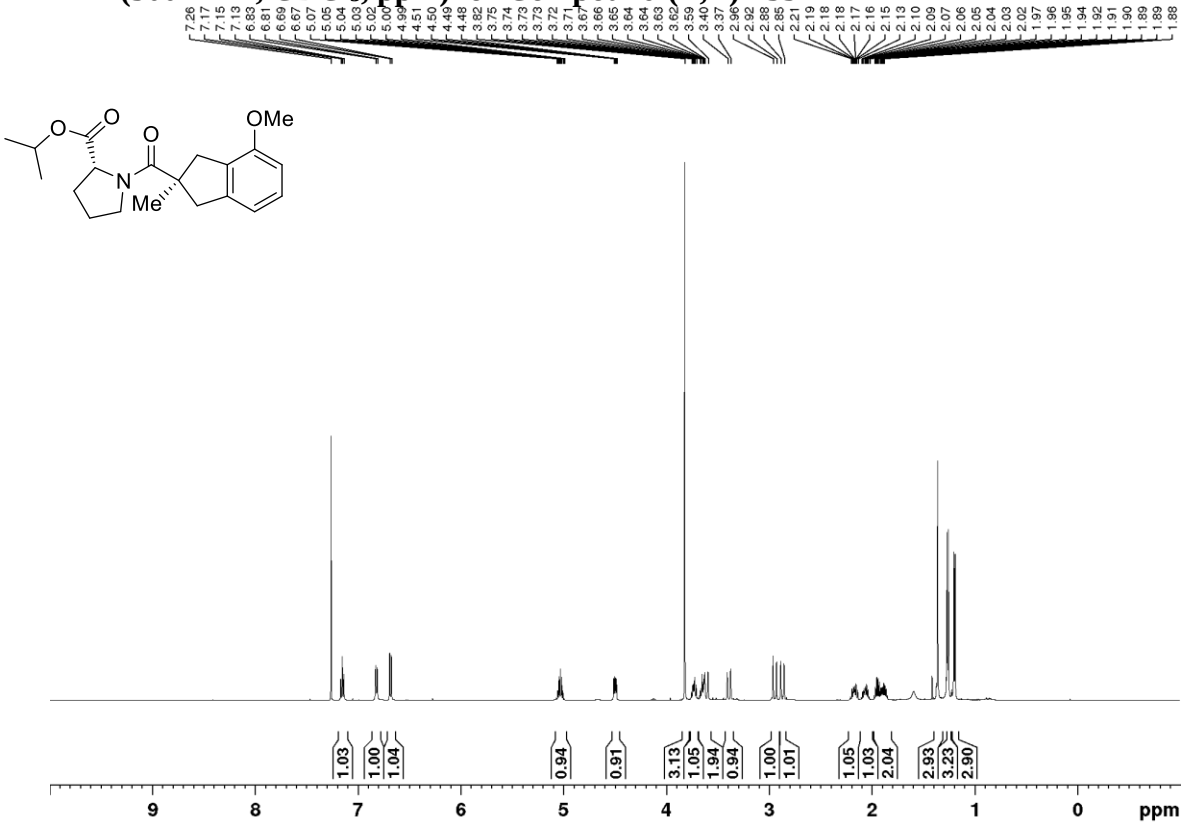

^{13}C NMR (126 MHz, $CDCl_3$, ppm) for Compound (*R*,*R*)-435

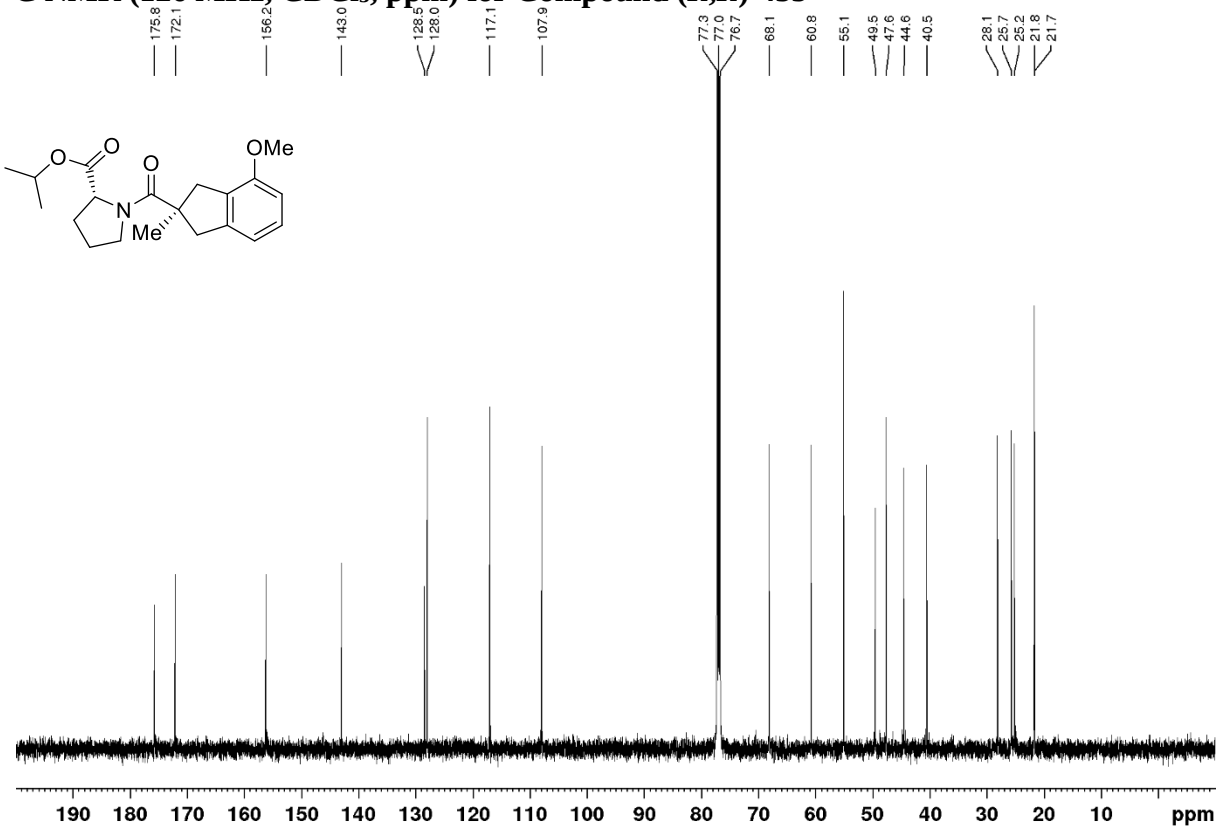

^{1}H NMR (400 MHz, $CDCl_3$, ppm) for Compound 493

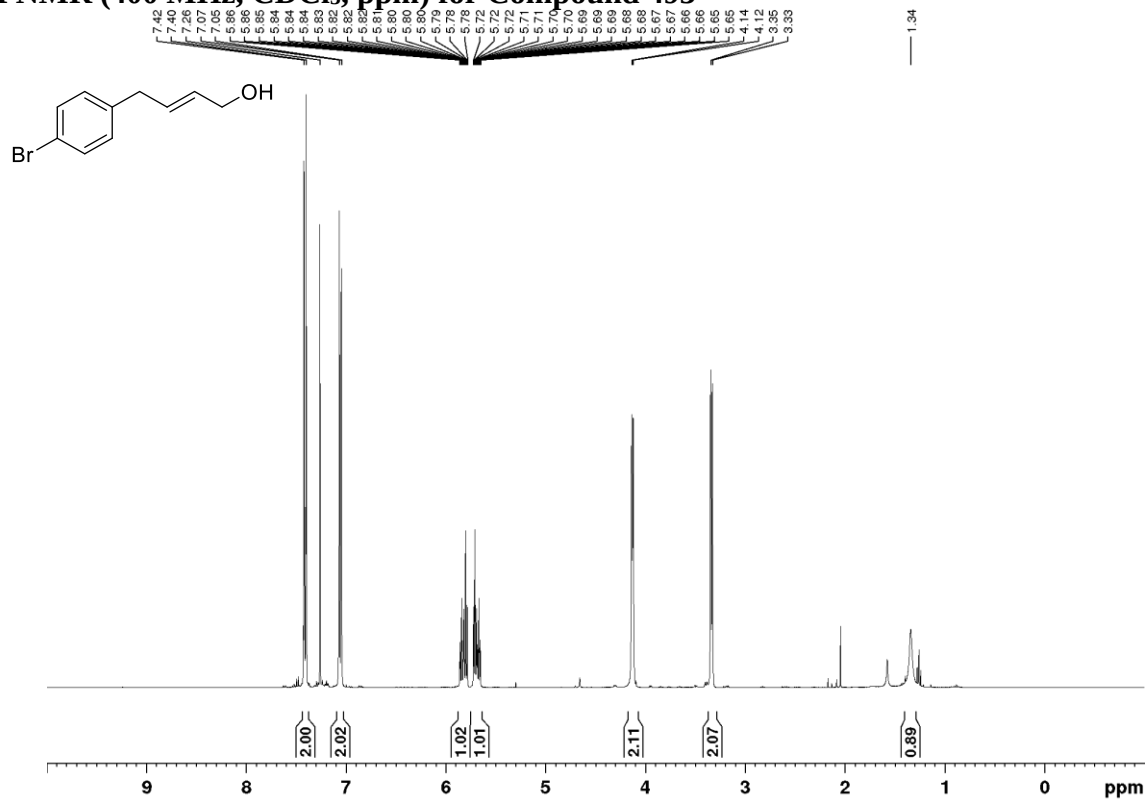

^{13}C NMR (126 MHz, $CDCl_3$, ppm) for Compound 493

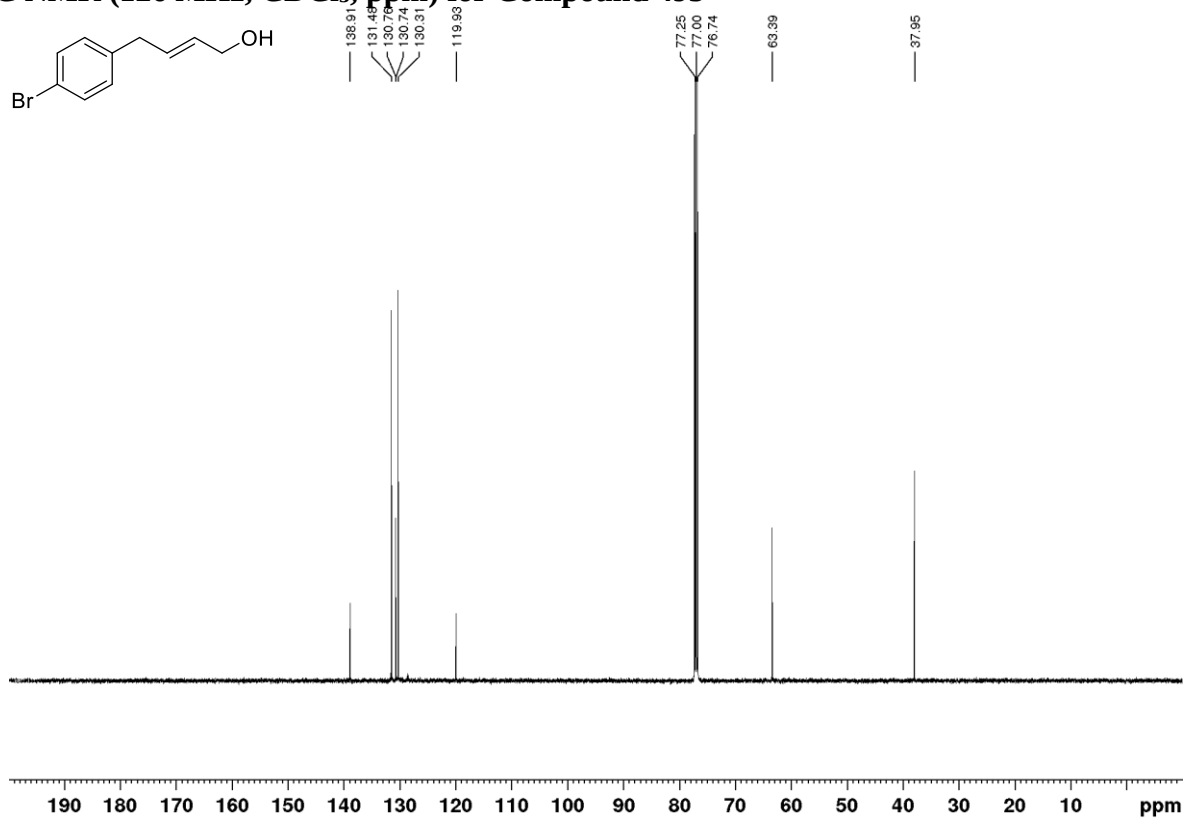

^{1}H NMR (400 MHz, $CDCl_3$, ppm) for Compound 495

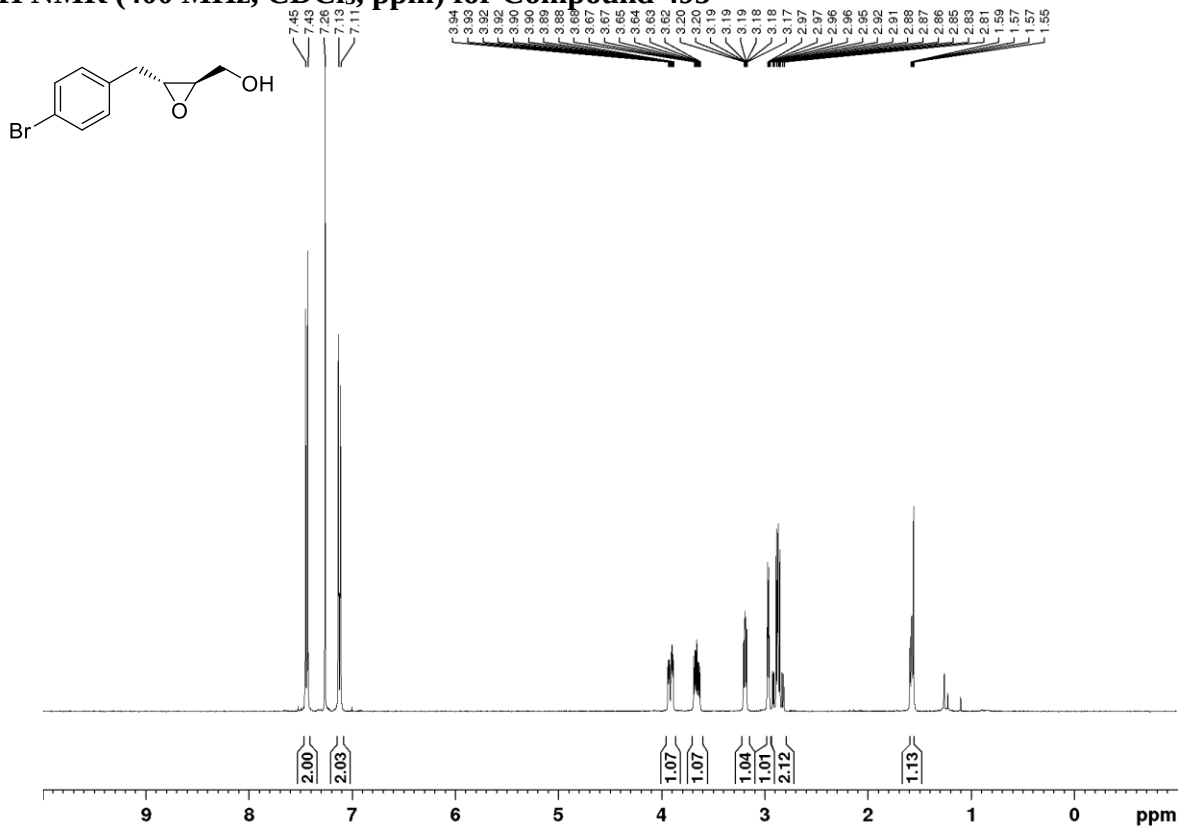

^{13}C NMR (126 MHz, $CDCl_3$, ppm) for Compound 495

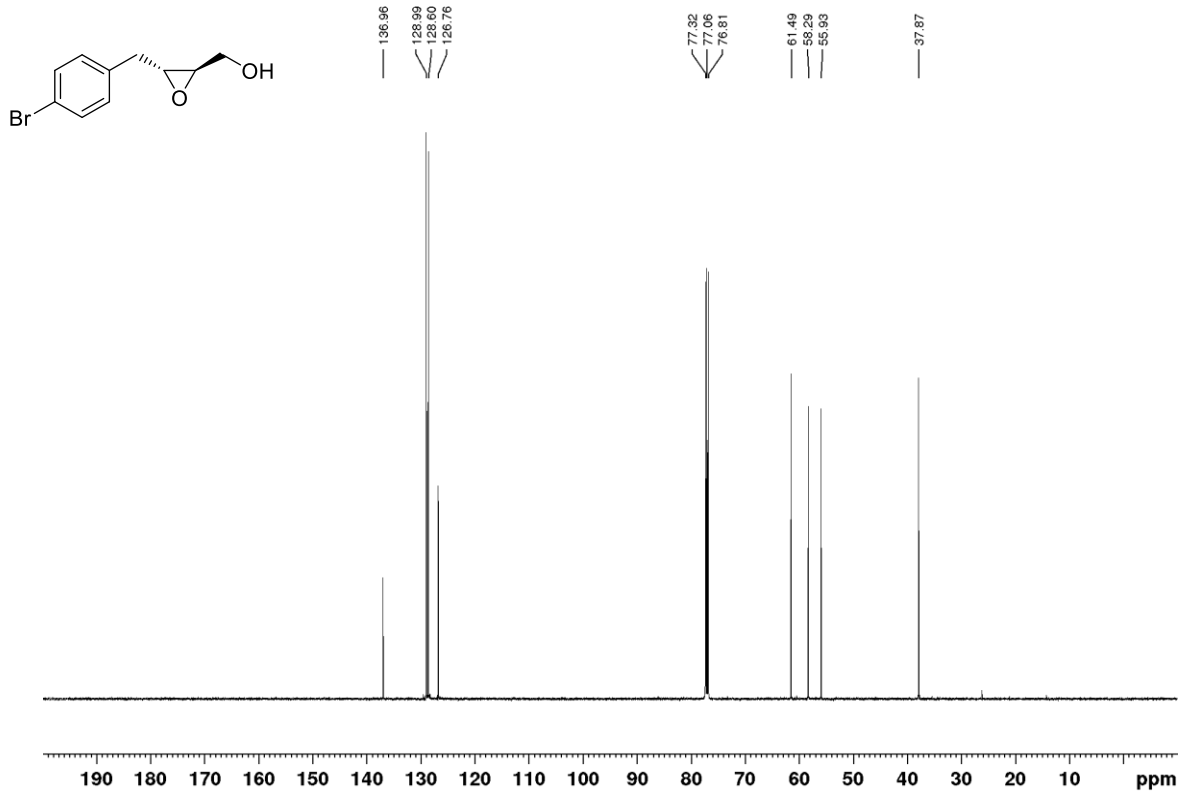

^{1}H NMR (400 MHz, DMSO-d_6, ppm) for Compound 496

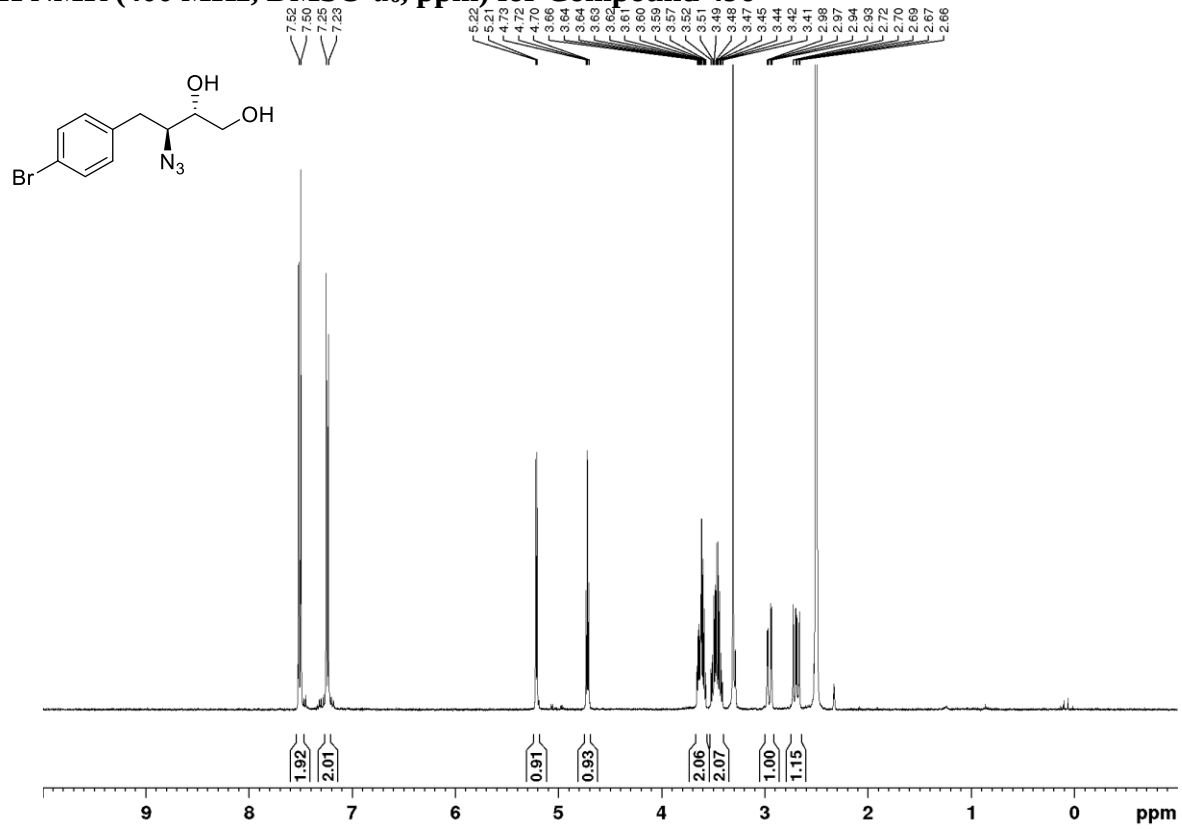

^{13}C NMR (126 MHz, DMSO-d_6, ppm) for Compound 496

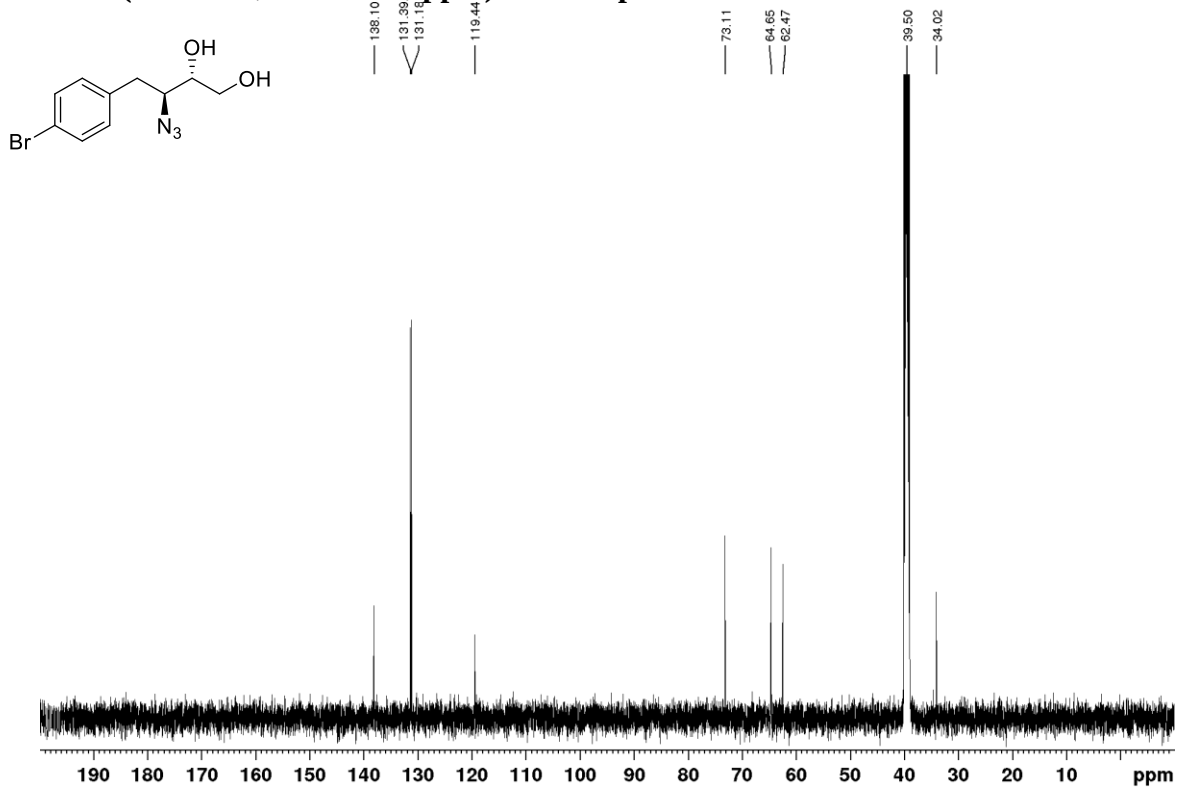

^{1}H NMR (500 MHz, $CDCl_3$, ppm) for Compound 498

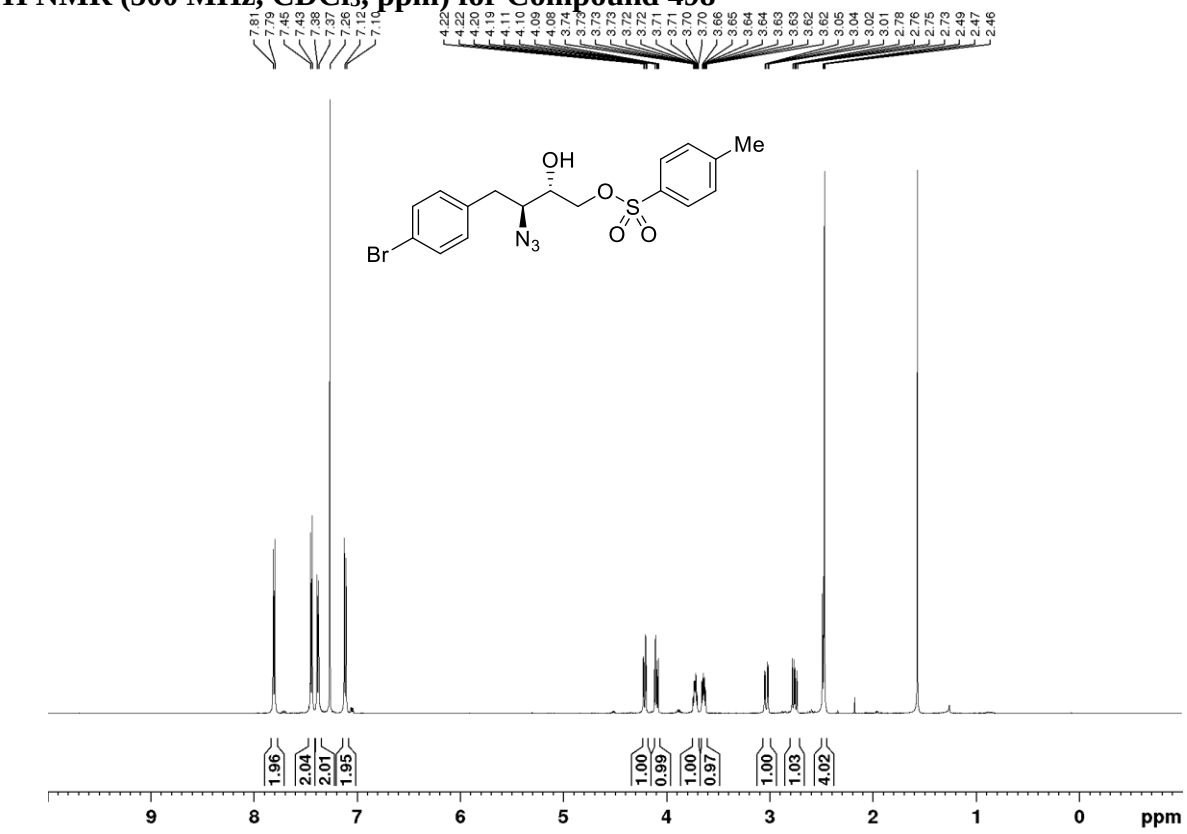

^{13}C NMR (126 MHz, $CDCl_3$, ppm) for Compound 498

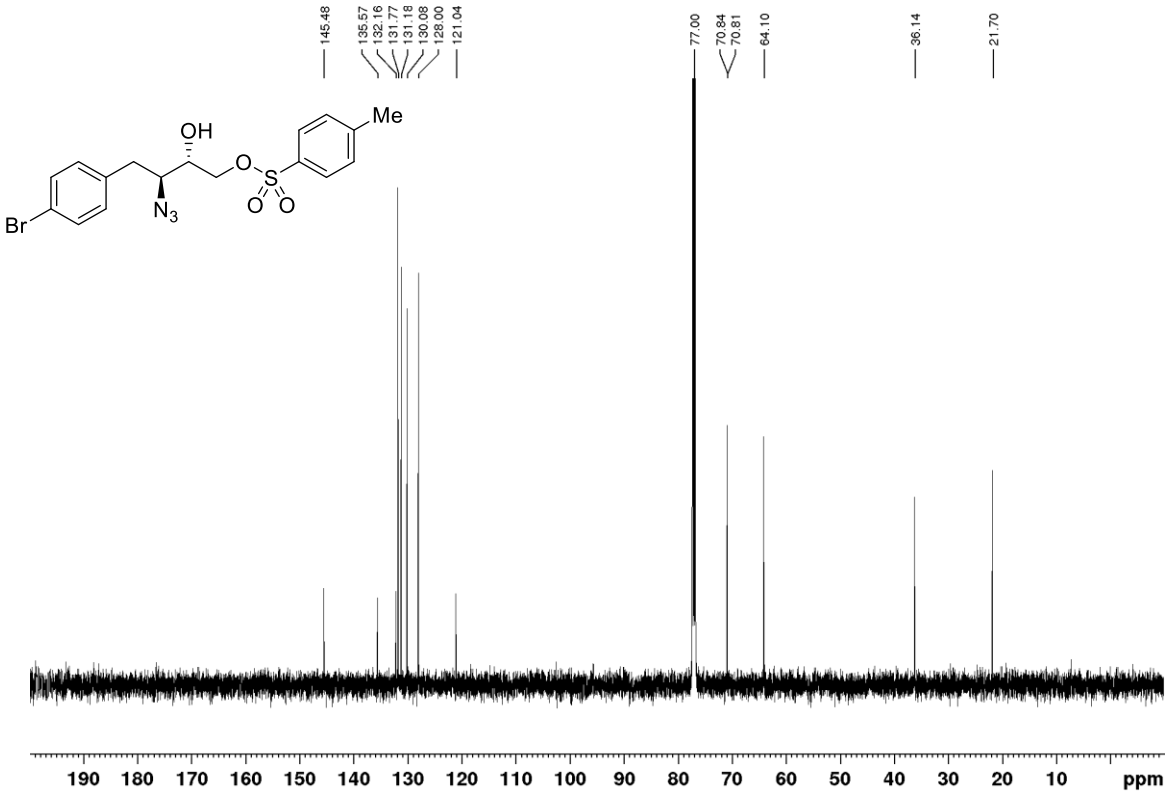

^{1}H NMR (400 MHz, $CDCl_3$, ppm) for Compound 531

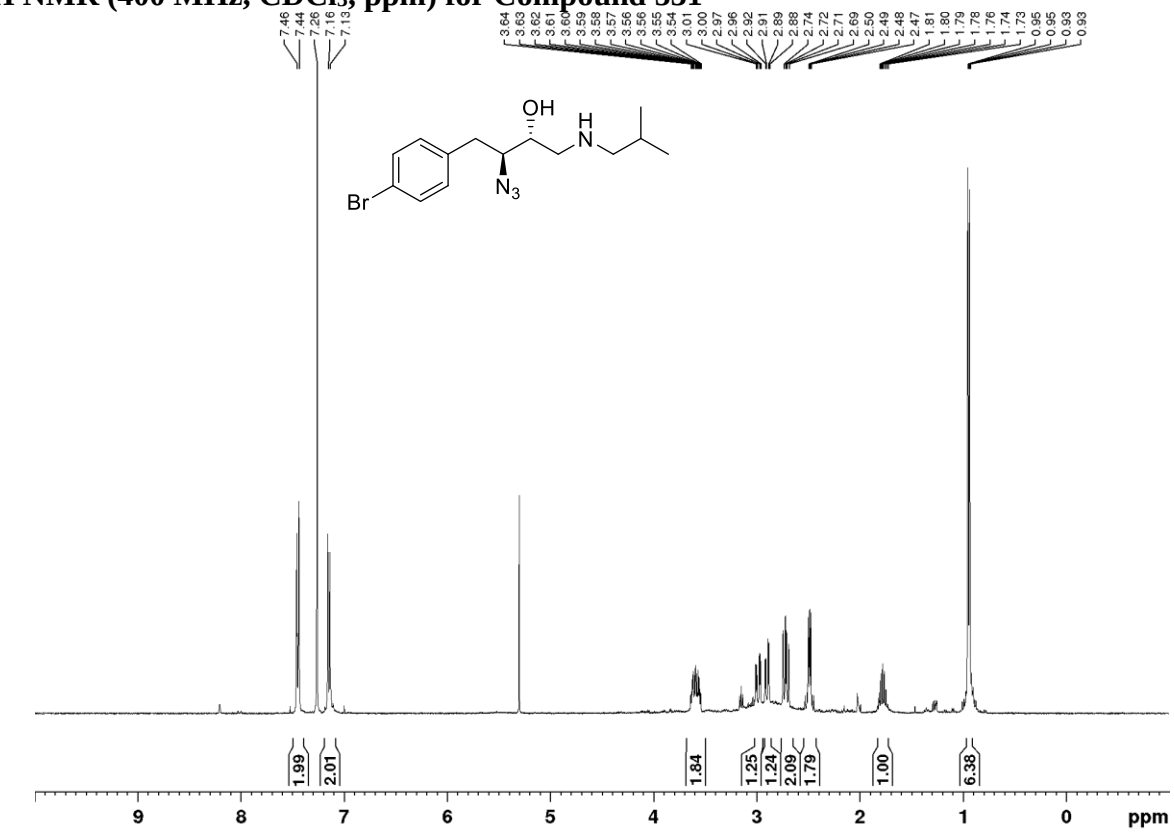

^{13}C NMR (126 MHz, $CDCl_3$, ppm) for Compound 531

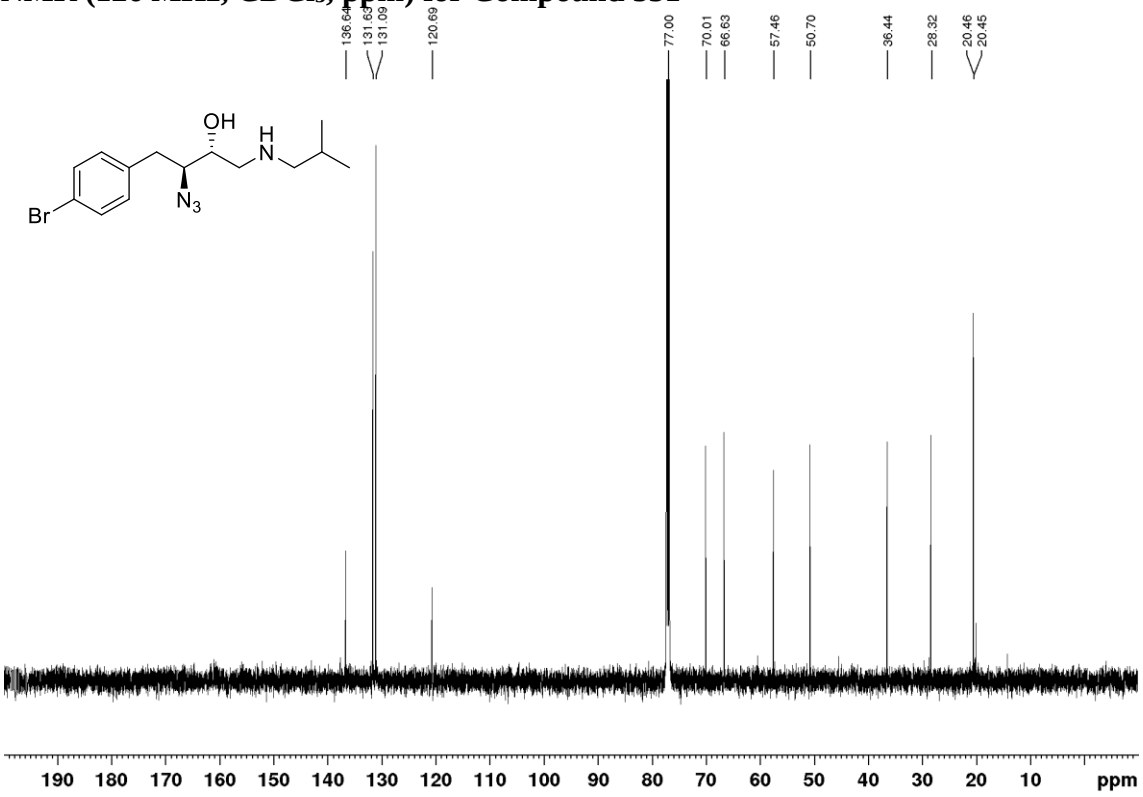

^{1}H NMR (500 MHz, $CDCl_3$, ppm) for Compound 499

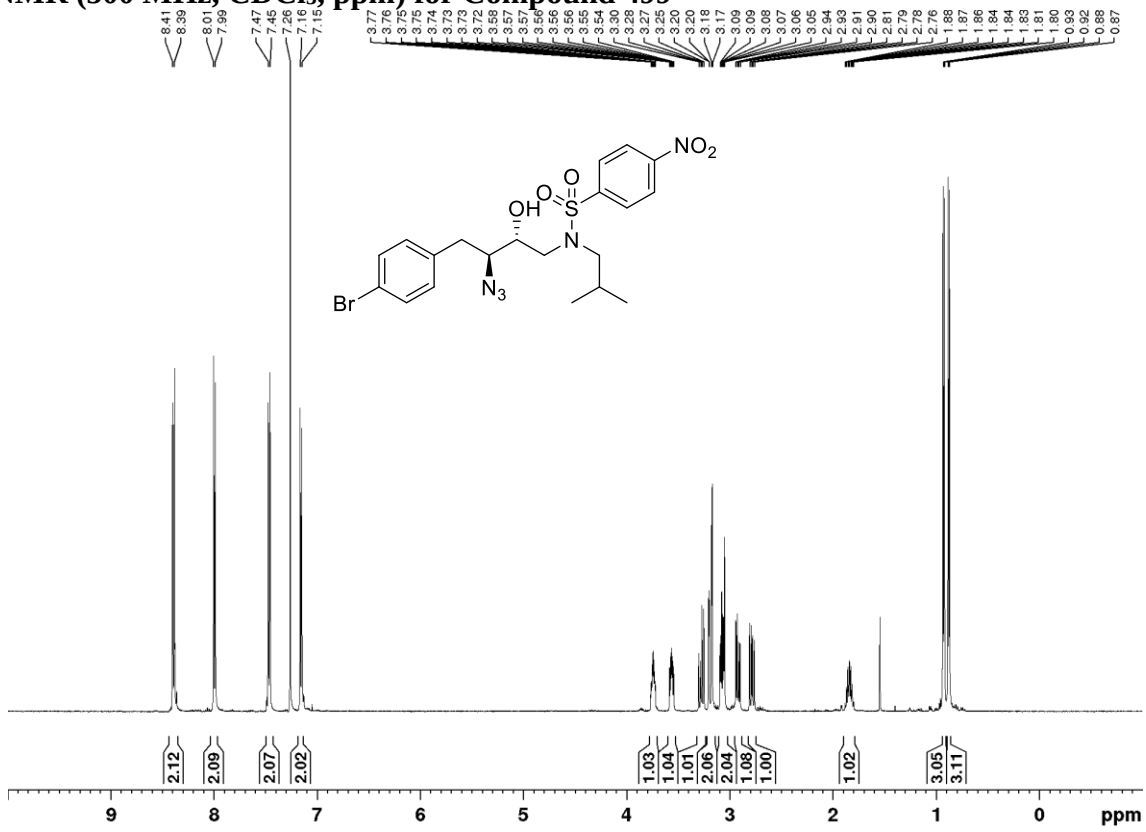

^{13}C NMR (126 MHz, $CDCl_3$, ppm) for Compound 499

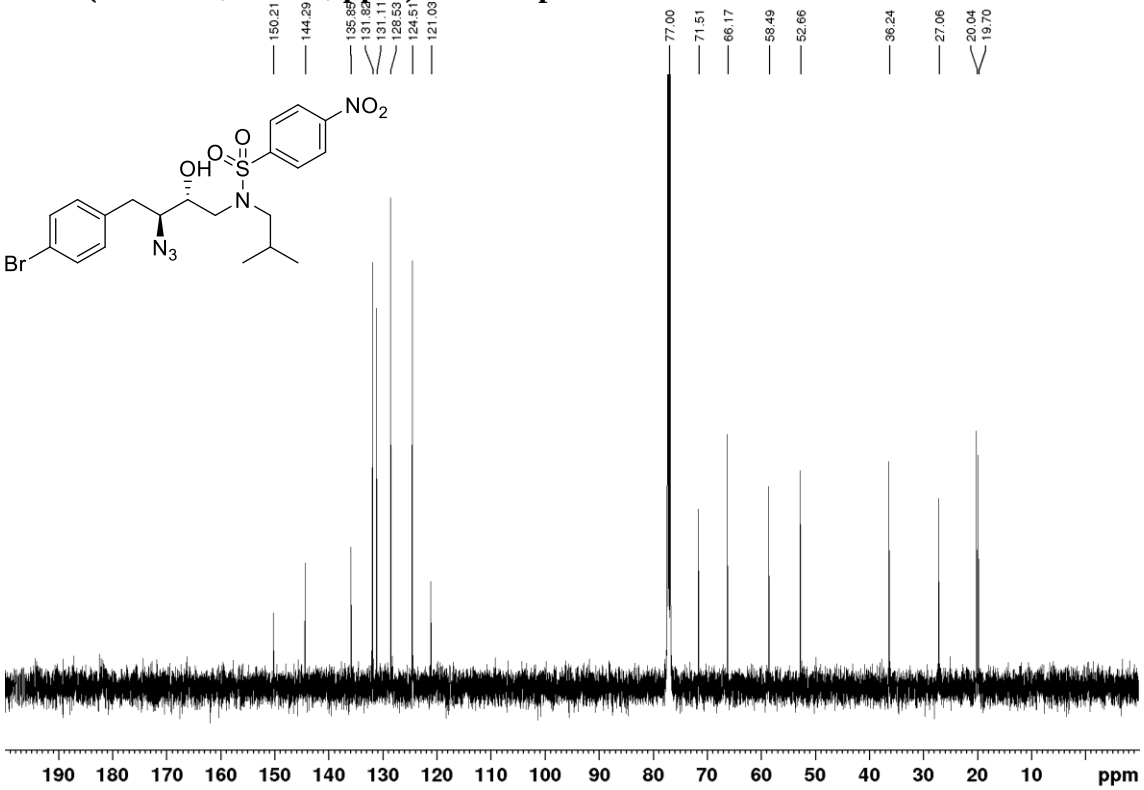

^{1}H NMR (500 MHz, DMSO-d_6, ppm) for Compound 500

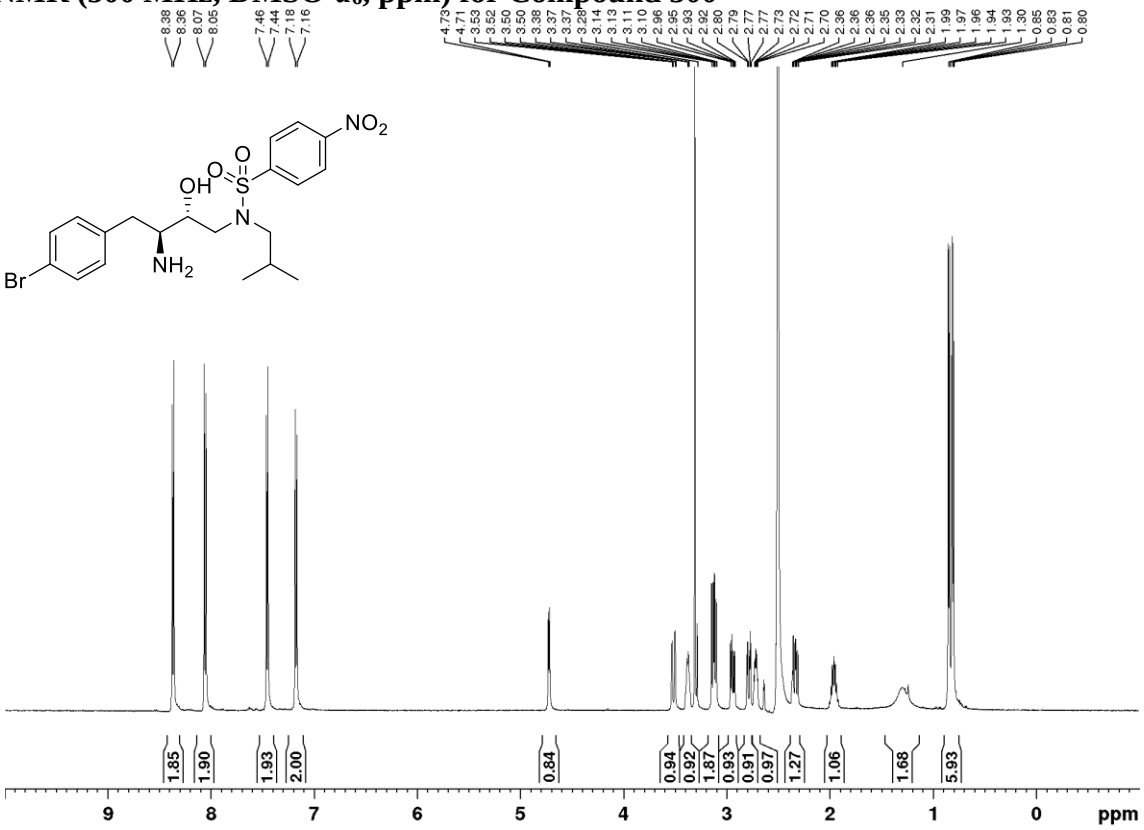

^{13}C NMR (126 MHz, $CDCl_3$, ppm) for Compound 500

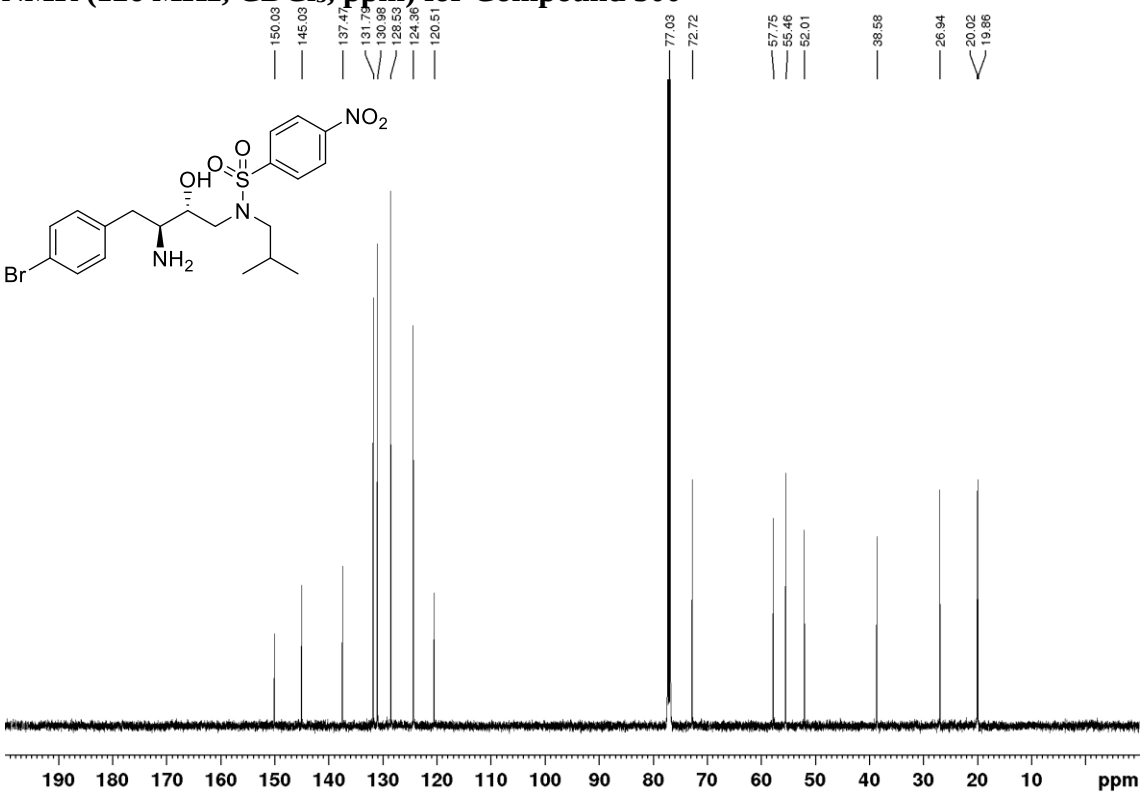

^{1}H NMR (500 MHz, DMSO-*d*$_6$, ppm) for Compound 501

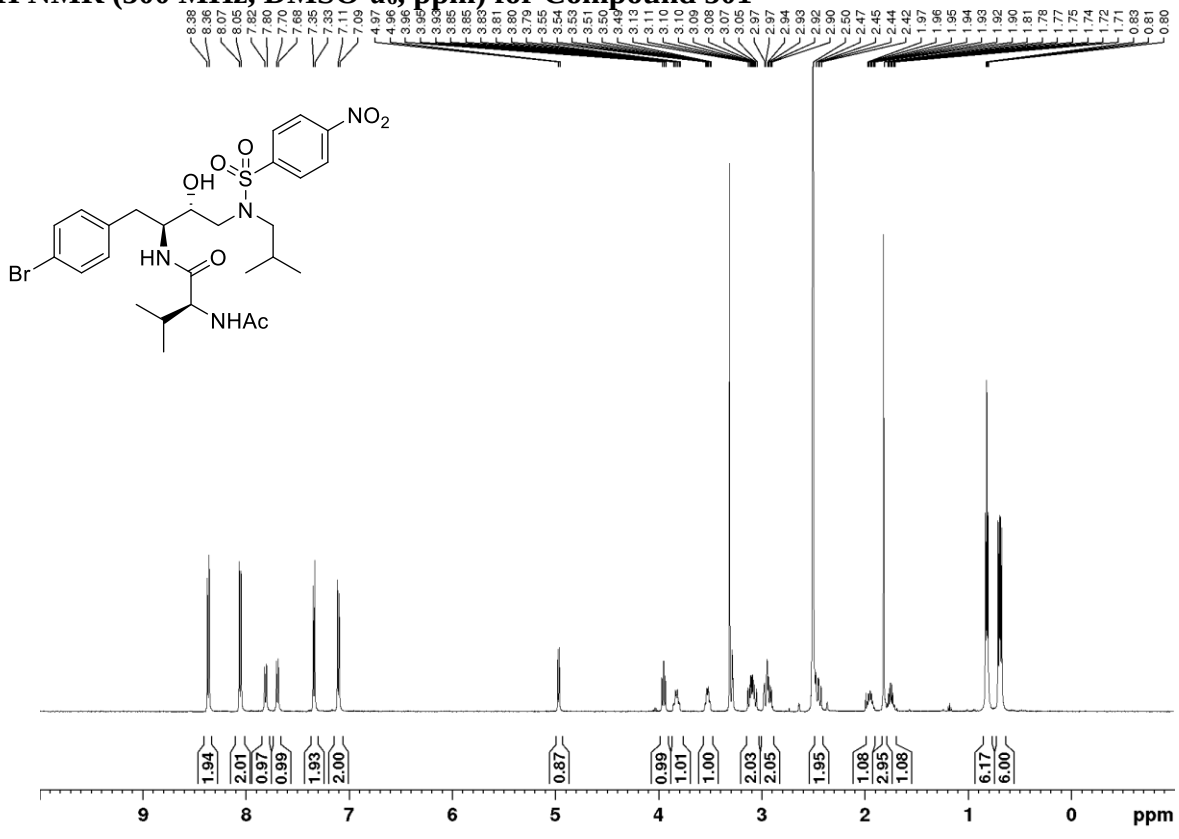

^{13}C NMR (126 MHz, $CDCl_3$, ppm) for Compound 501

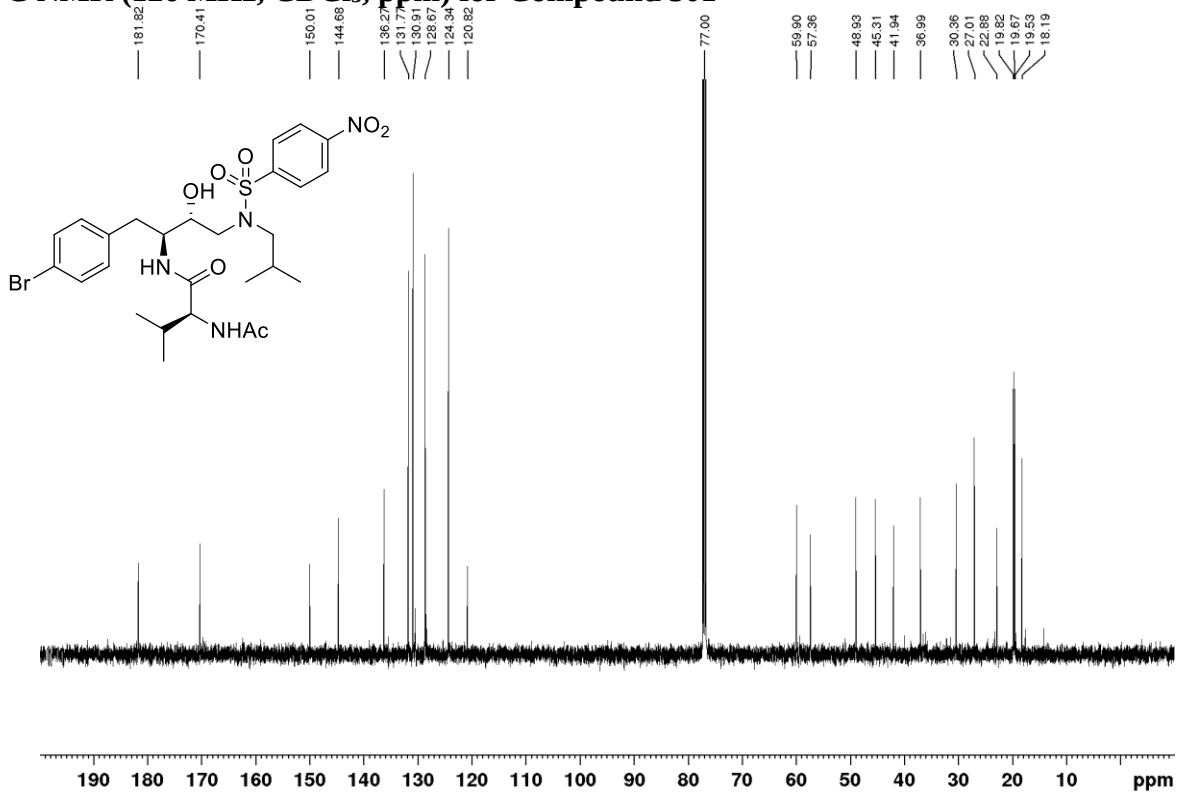

^{1}H NMR (500 MHz, DMSO-d_6, ppm) for Compound 508

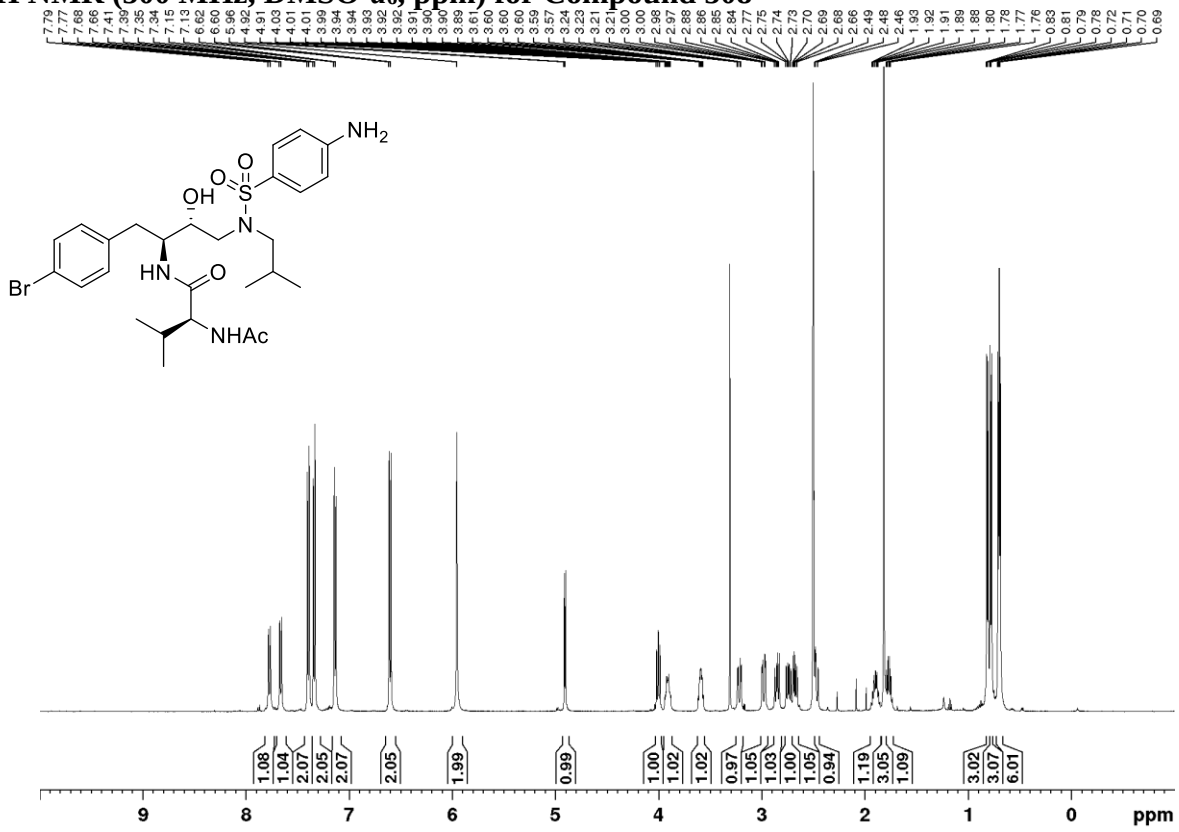

^{13}C NMR (126 MHz, DMSO-*d*$_6$, ppm) for Compound 508

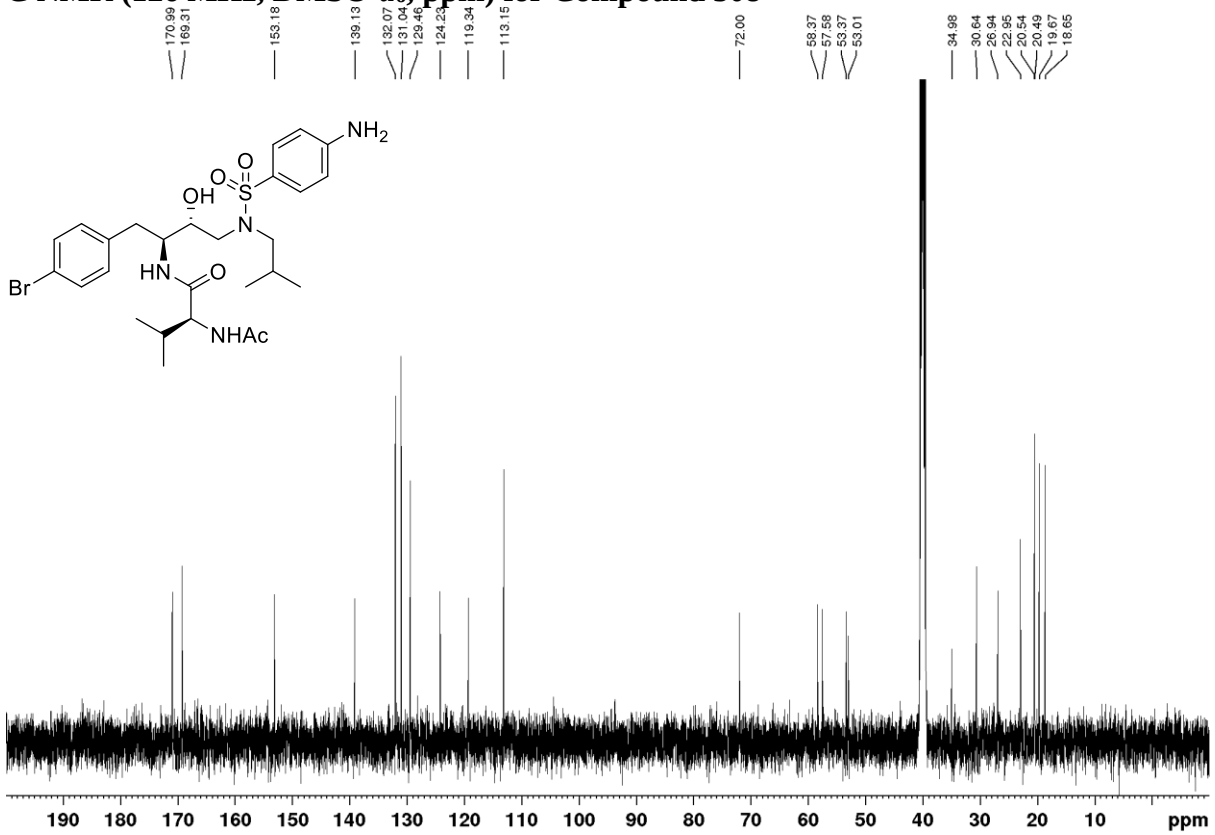

^{1}H NMR (500 MHz, CDCl$_3$, ppm) for Compound 509

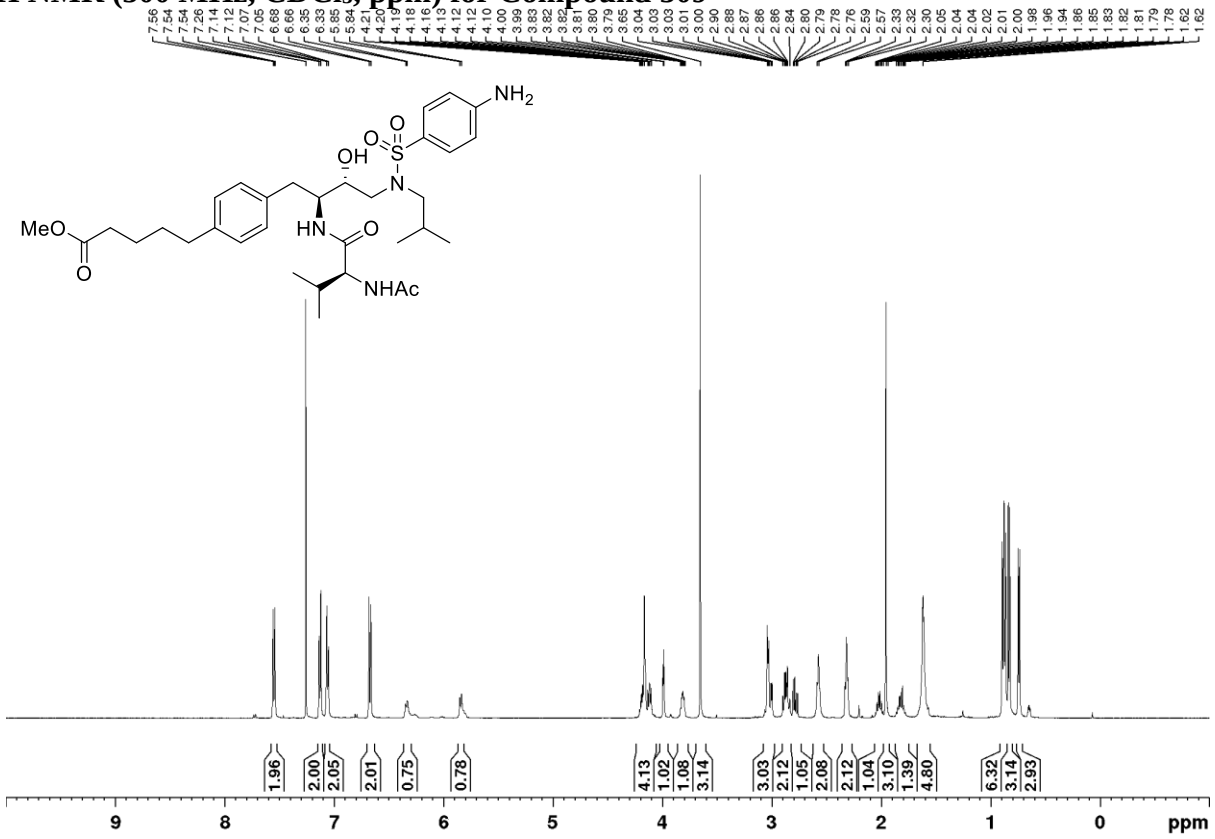

^{13}C NMR (126 MHz, $CDCl_3$, ppm) for Compound 509

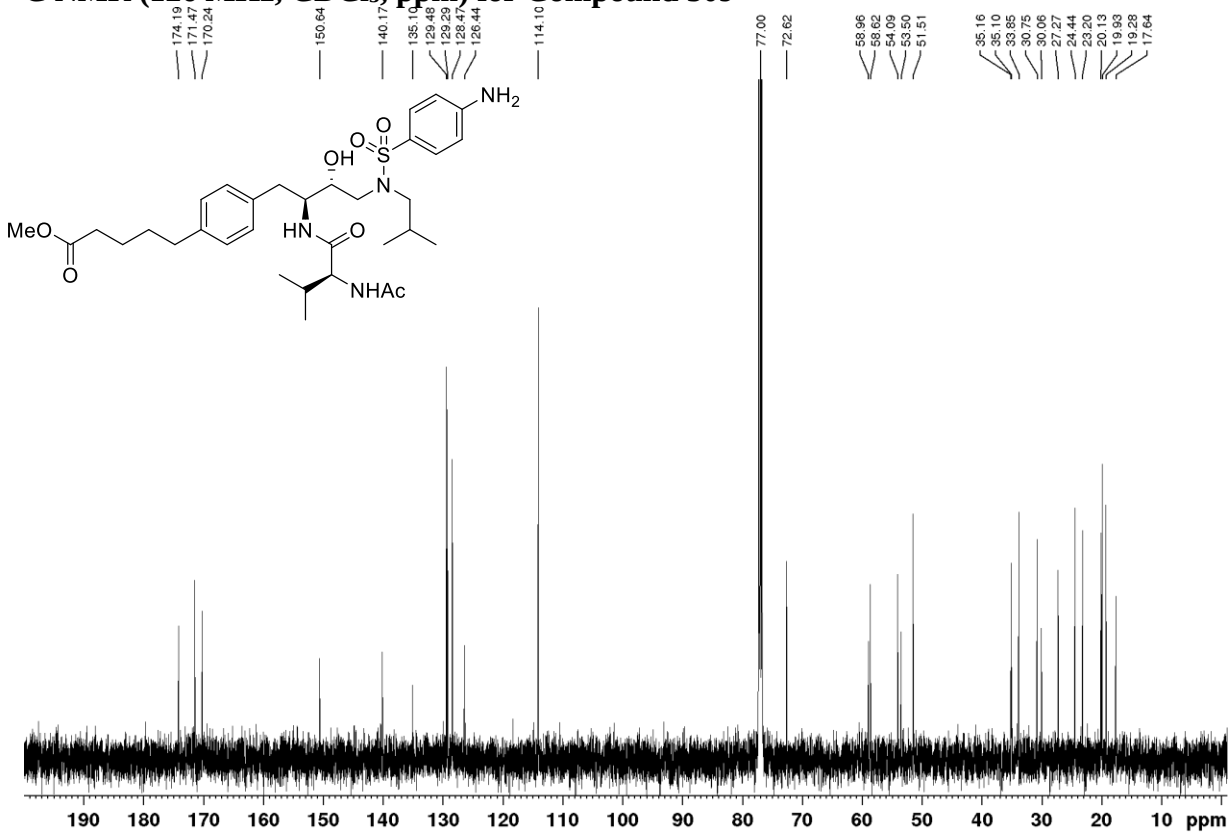

^{1}H NMR (500 MHz, $CDCl_3$, ppm) for Compound 510

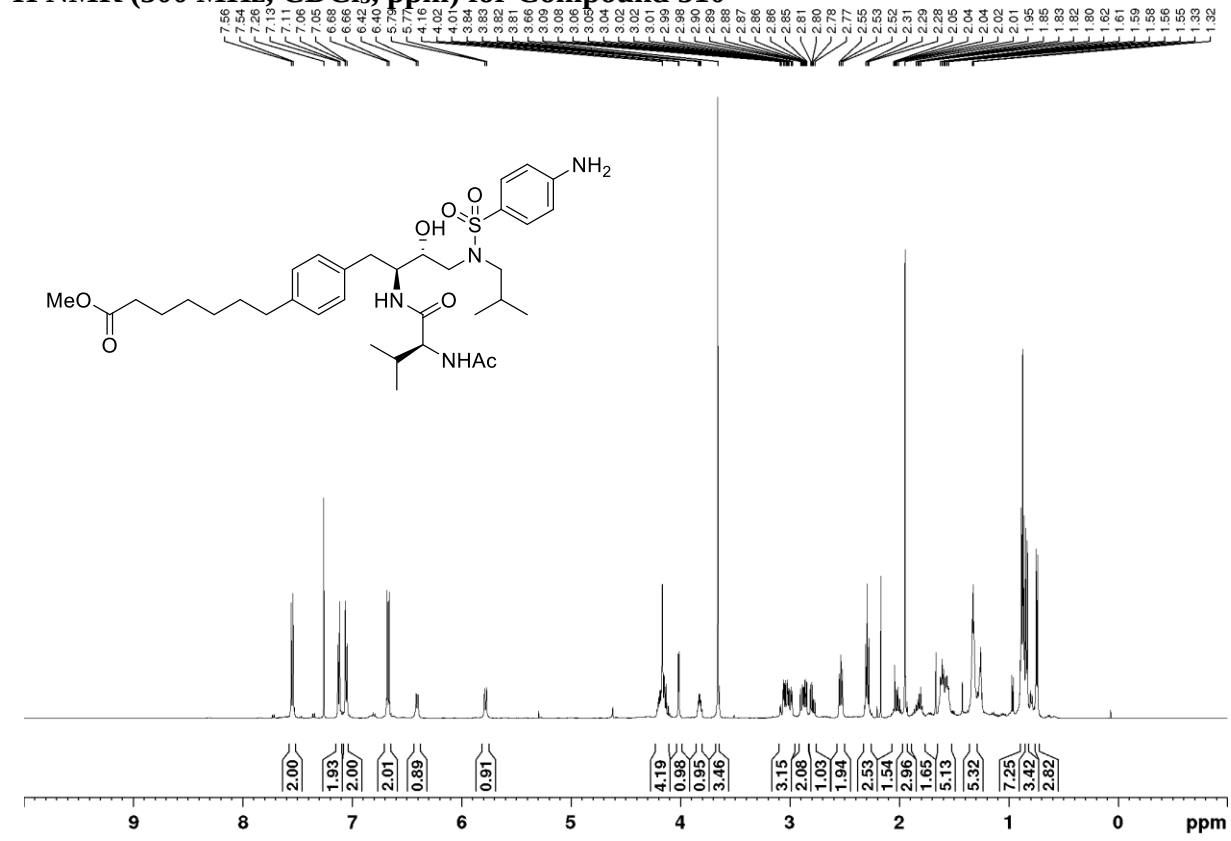

^{13}C NMR (126 MHz, $CDCl_3$, ppm) for Compound 510

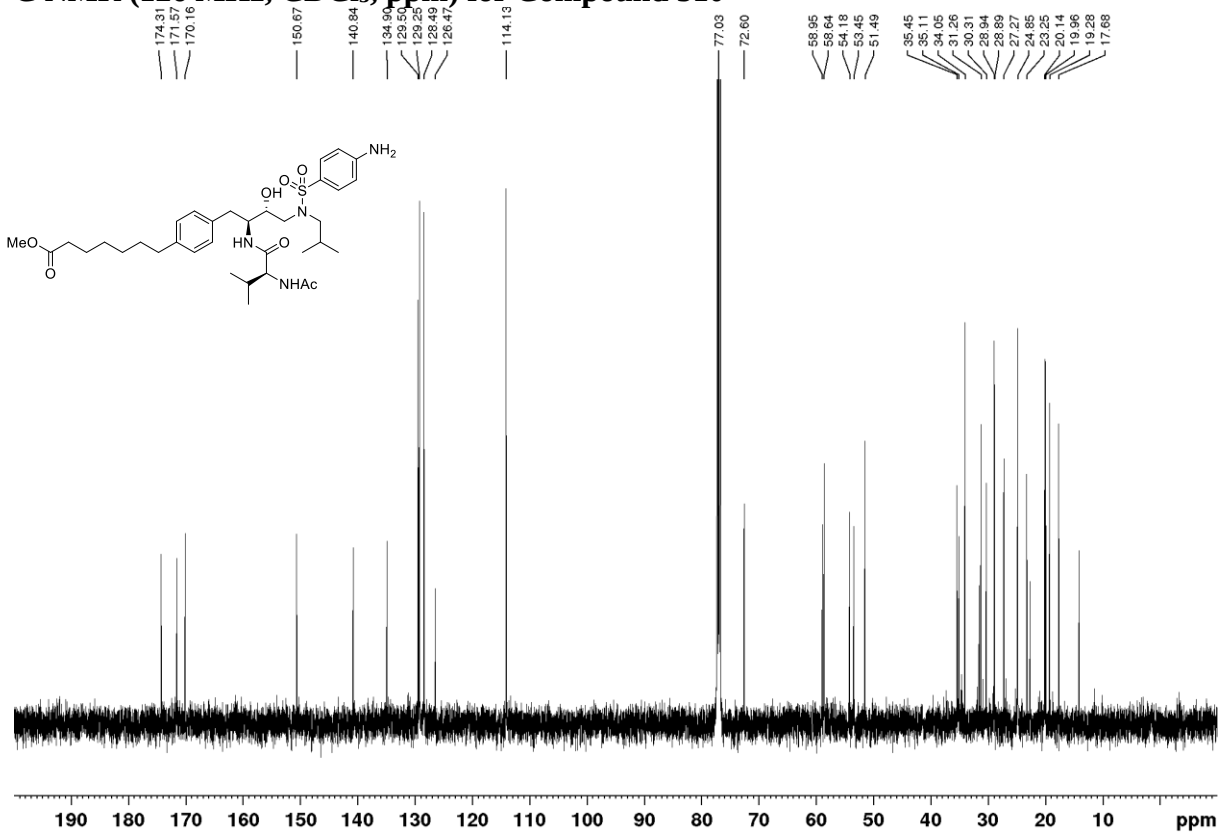

^{1}H NMR (400 MHz, DMSO-d_6, ppm) for Compound 488

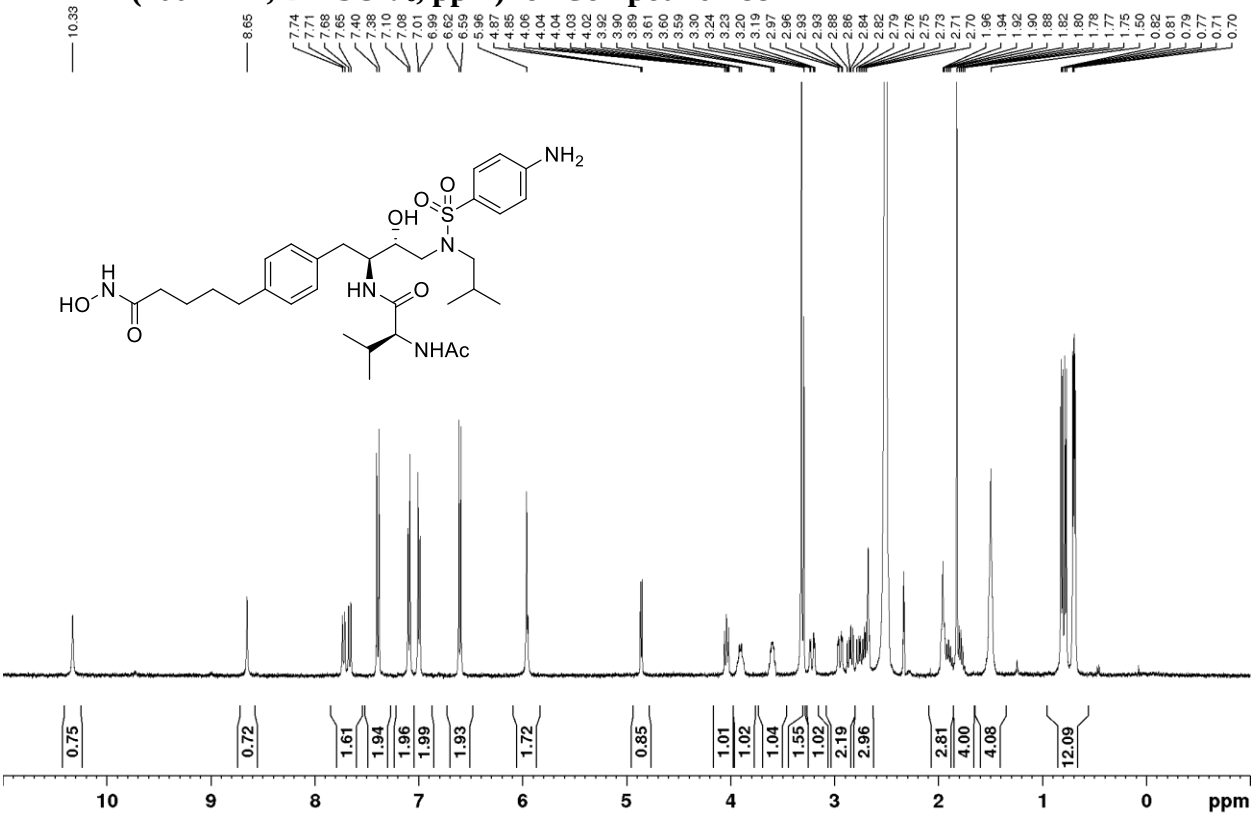

^{1}H NMR (400 MHz, DMSO-d_6, ppm) for Compound 489

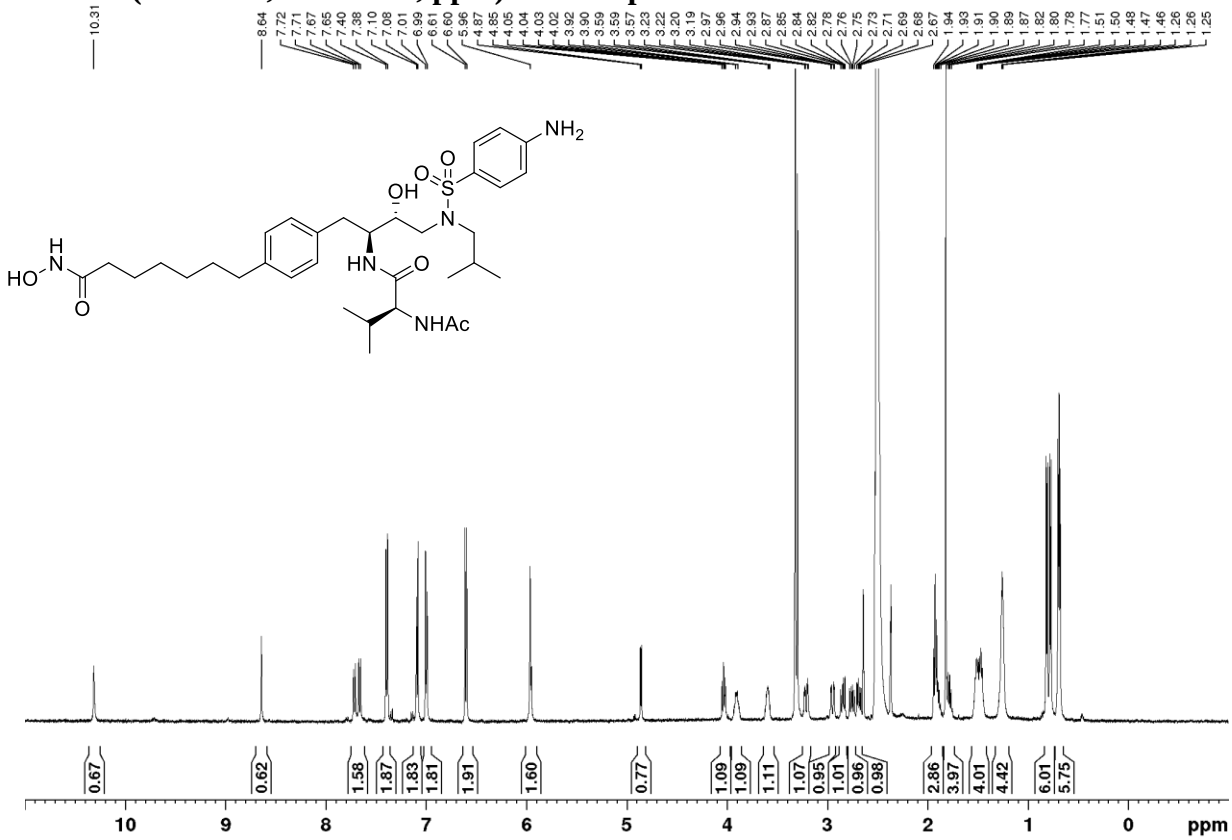

^{1}H NMR (400 MHz, $CDCl_3$, ppm) for Compound 511

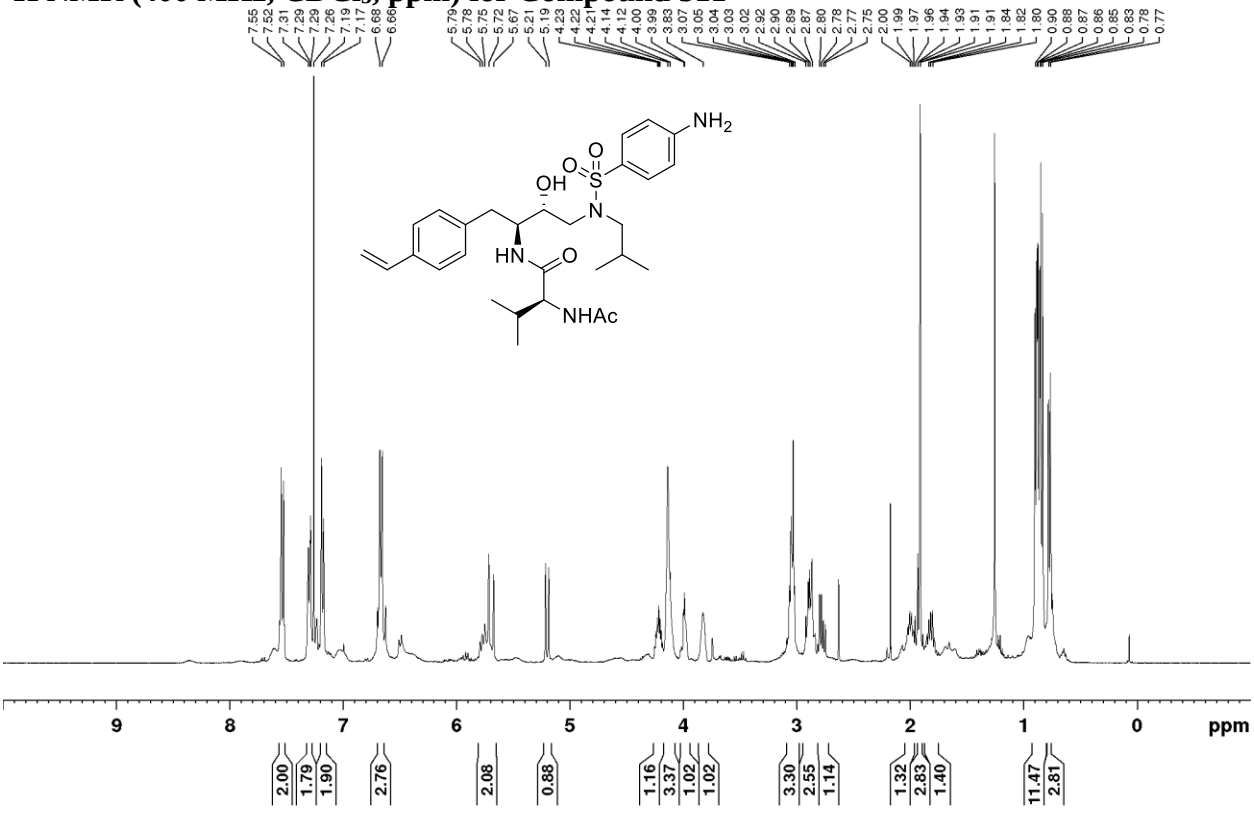

^{13}C NMR (101 MHz, $CDCl_3$, ppm) for Compound 511

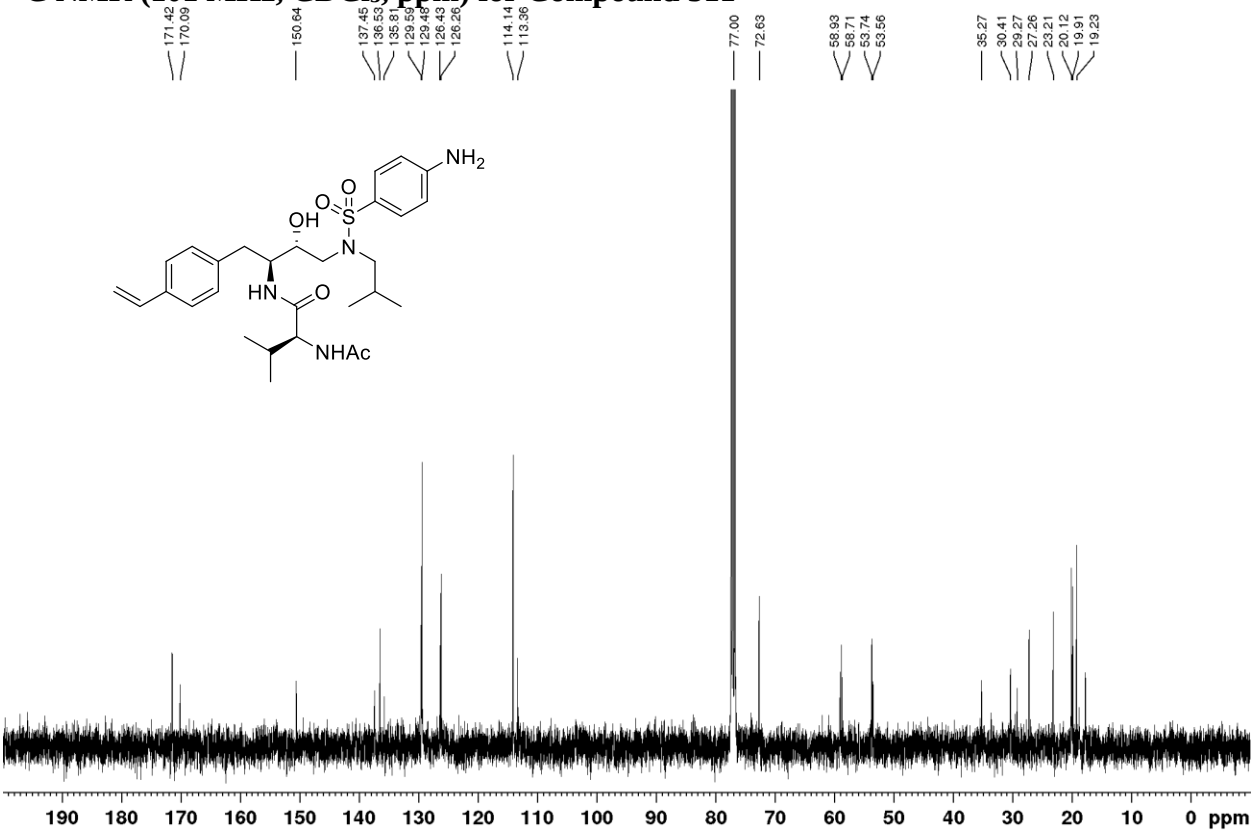

^{1}H NMR (500 MHz, $CDCl_3$, ppm) for Compound 512

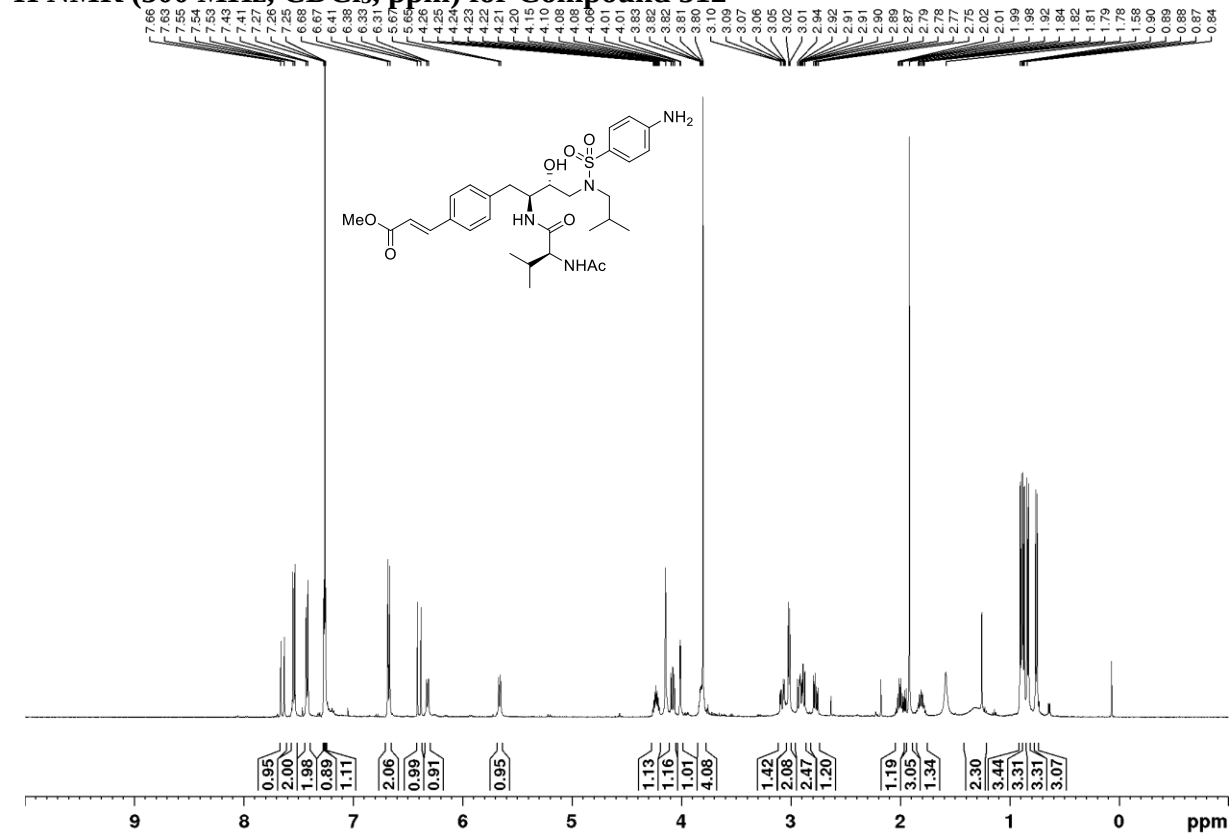

^{13}C NMR (126 MHz, $CDCl_3$, ppm) for Compound 512

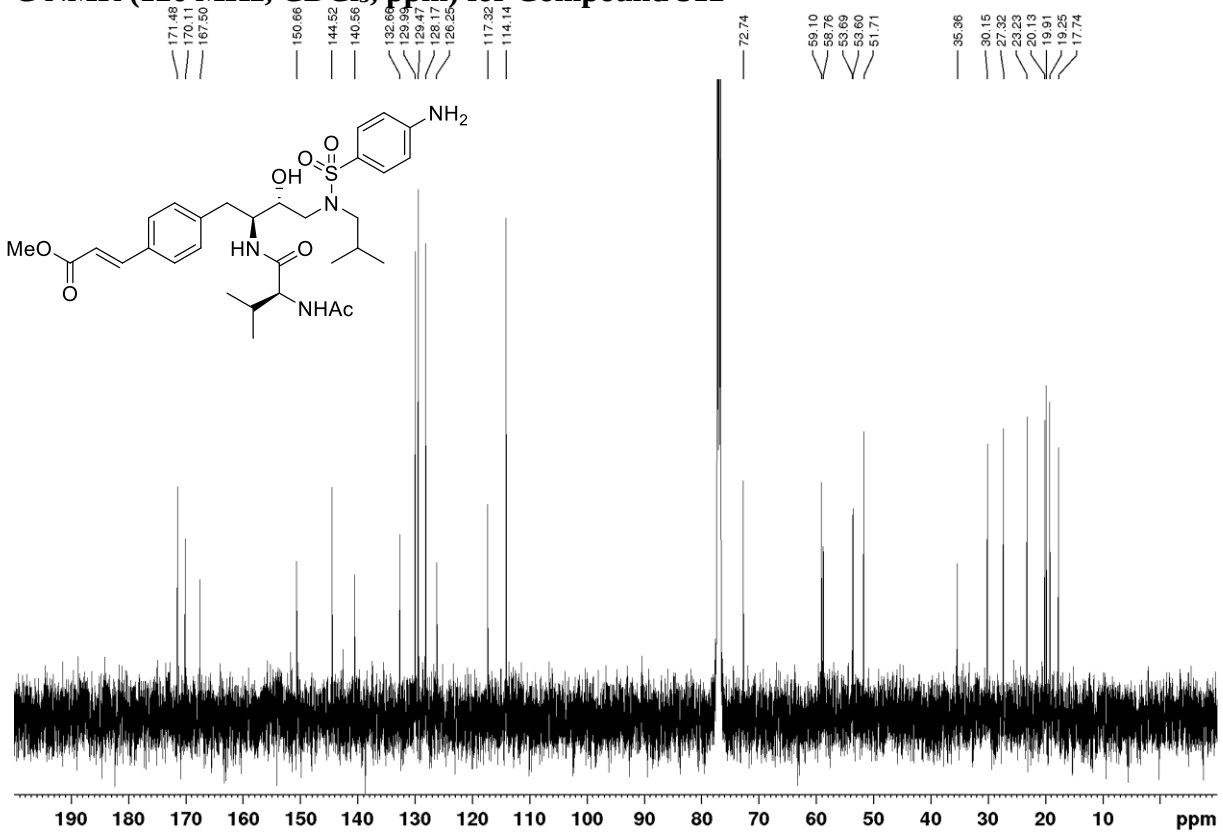

^{1}H NMR (126 MHz, $CDCl_3$, ppm) for Compound 513

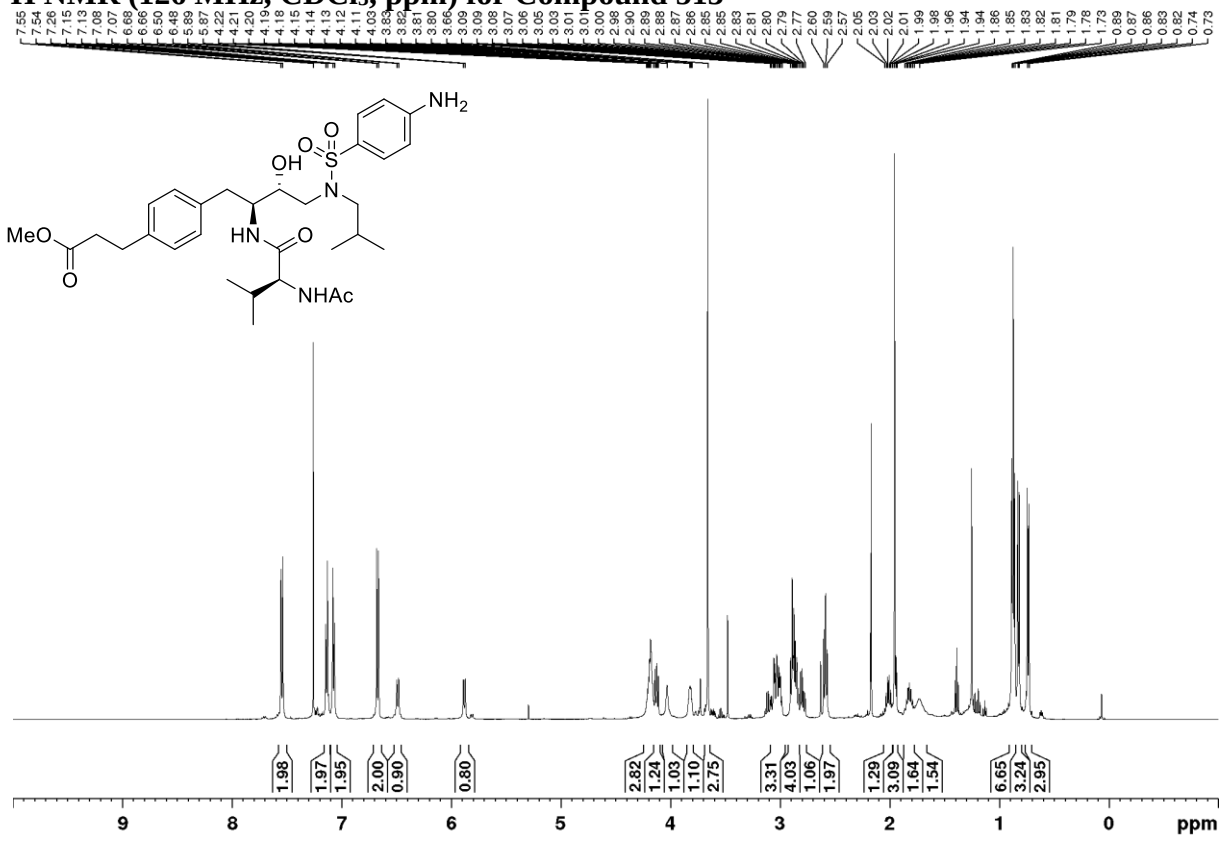

^{13}C NMR (126 MHz, $CDCl_3$, ppm) for Compound 513

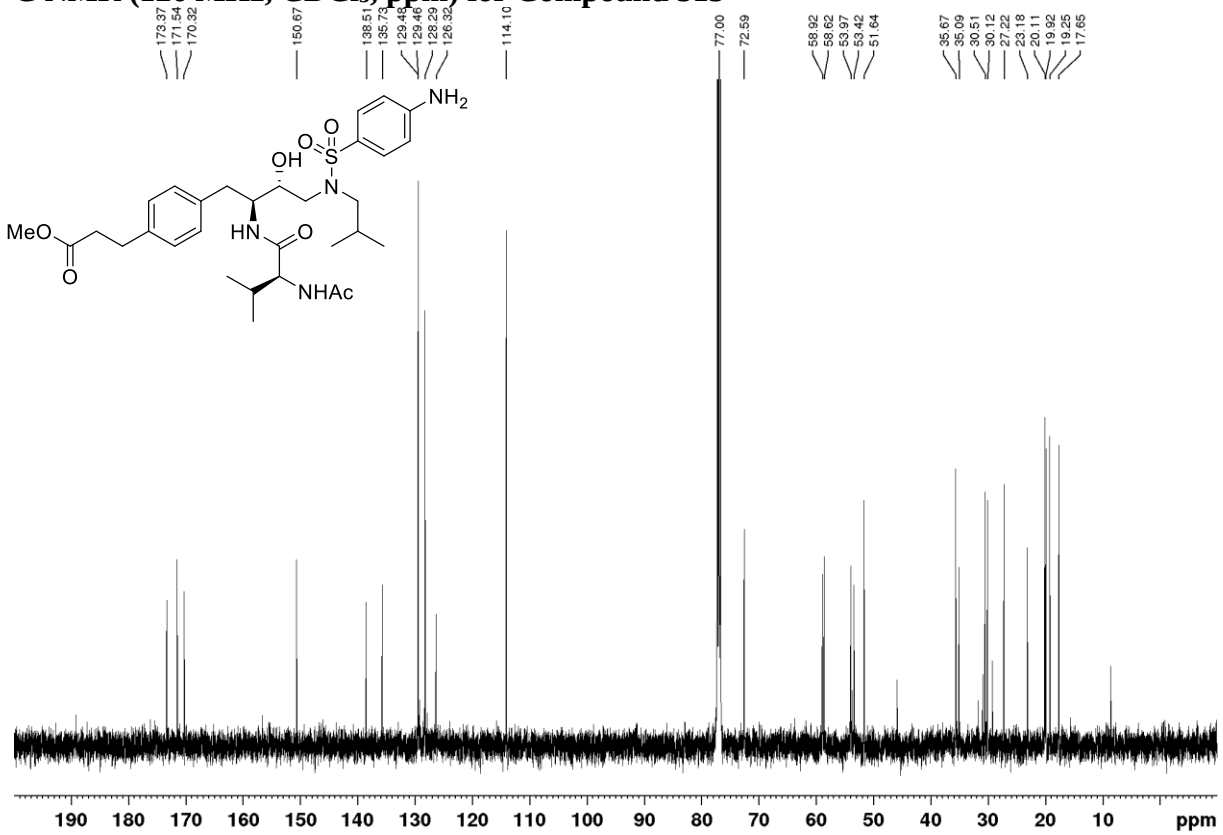

^{1}H NMR (500 MHz, $CDCl_3$, ppm) for Compound 524

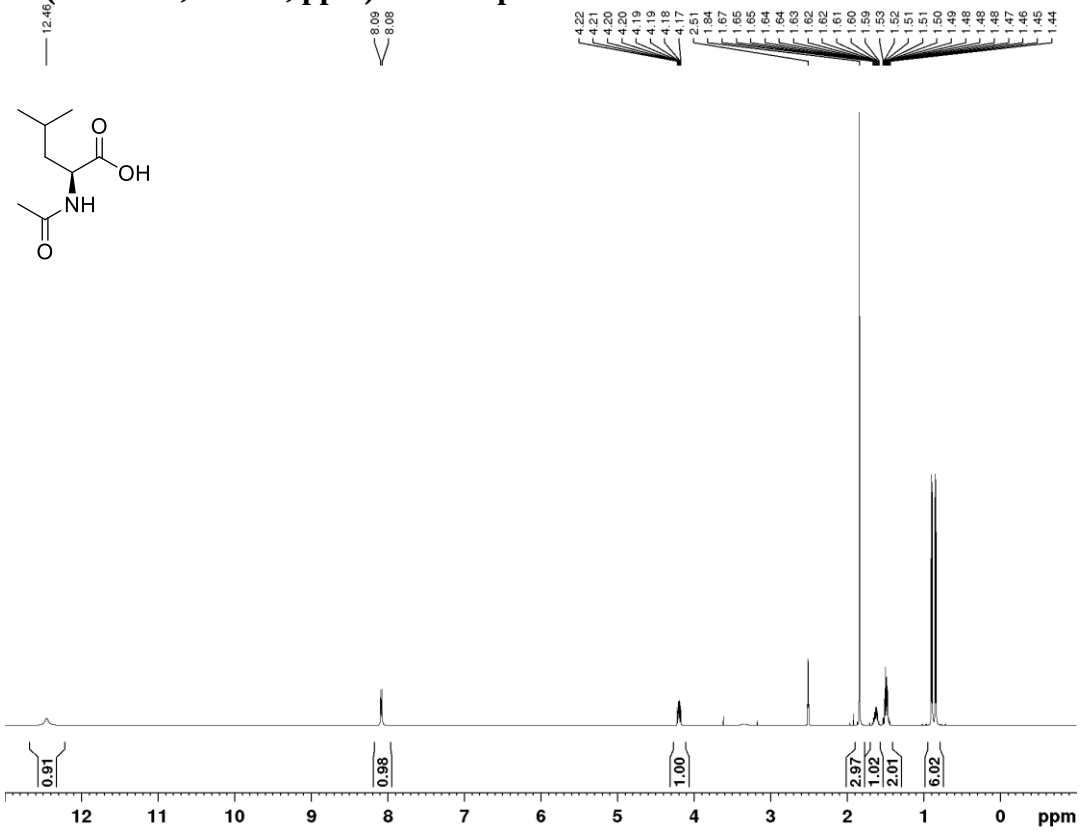

^{1}H NMR (500 MHz, $CDCl_3$, ppm) for Compound 525

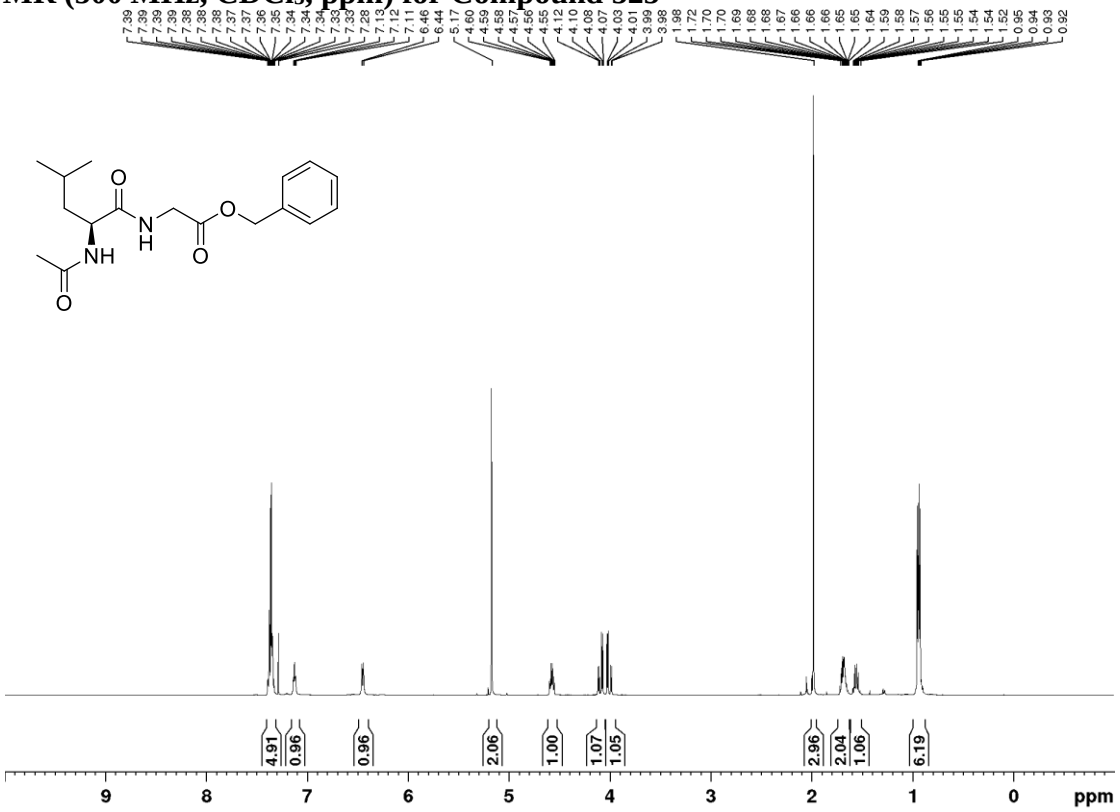

^{1}H NMR (500 MHz, $CDCl_3$, ppm) for Compound 528:

^{1}H NMR (400 MHz, DMSO-d_6, ppm) for Compound 518